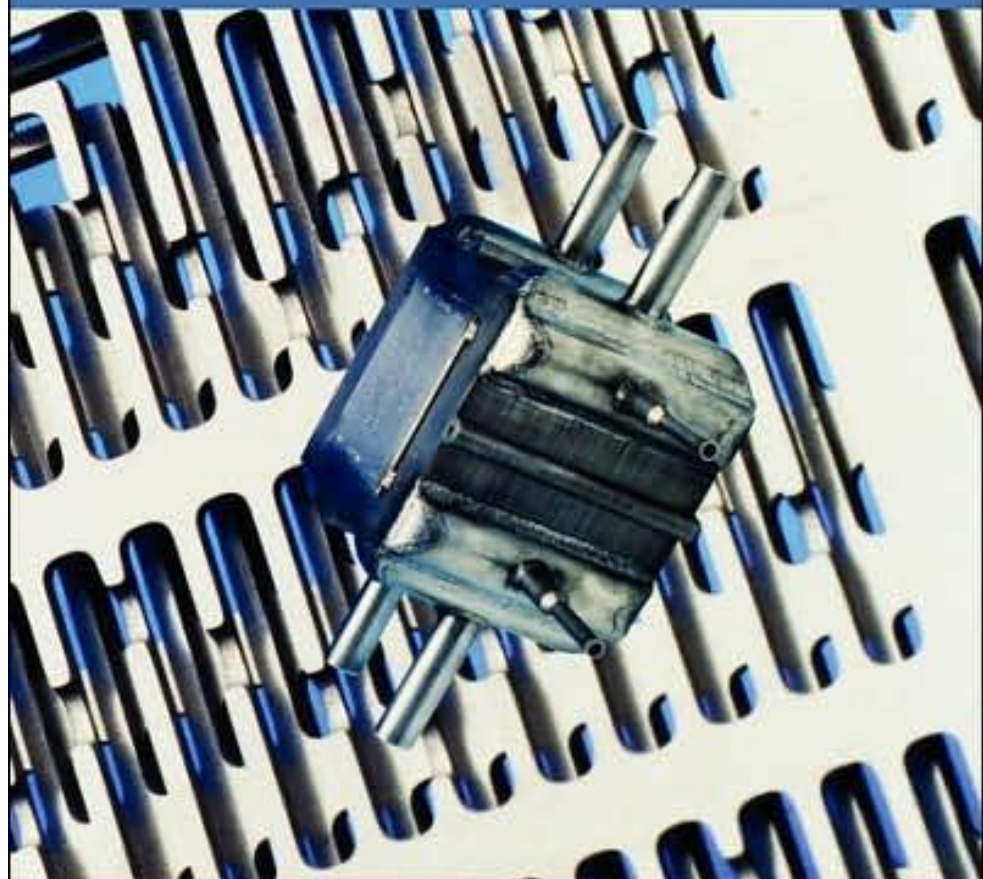


COMPACT HEAT EXCHANGERS

Selection, Design and Operation



J.E. Hesselgreaves

PERGAMON

- ISBN: 0080428398
- Pub. Date: January 2001
- Publisher: Elsevier Science & Technology Books

FOREWORD

The importance of compact heat exchangers (CHEs) has been recognized in aerospace, automobile, gas turbine power plant, and other industries for the last 50 years or more. This is due to several factors, for example packaging constraints, sometimes high performance requirements, low cost, and the use of air or gas as one of the fluids in the exchanger. For the last two decades or so, the additional driving factors for heat exchanger design have been reducing energy consumption for operation of heat exchangers and process plants, and minimizing the capital investment in process and other industries. As a result, in process industries where not-so-compact heat exchangers were quite common, the use of plate heat exchangers and other CHEs has been increasing owing to some of the inherent advantages mentioned above. In addition, CHEs offer the reduction of floor space, decrease in fluid inventory in closed system exchangers, use as multifunctional units, and tighter process control with liquid and phase-change working fluids.

While over 100 books primarily on heat exchangers have been published worldwide in English, no systematic treatment can be found on many important aspects of CHE design that an engineer can use as a comprehensive source of information. Dr Hesselgreaves has attempted to provide a treatment that goes beyond dimensionless design data information. In addition to the basic design theory, this monograph includes descriptions of industrial CHEs (many new types of CHEs being specifically for process applications); specification of a CHE as a part of a system using thermodynamic analysis; and broader design considerations for surface size, shape and weight. Heat transfer and flow friction single-phase design correlations are given for the most commonly used modern heat transfer surfaces in CHEs, with the emphasis on those surfaces that are likely to be used in the process industries; design correlations for phase-change in CHEs; mechanical design aspects; and finally some of the operational considerations including installation, commissioning, operation, and maintenance, including fouling and corrosion.

One of the first comprehensive books on design data for compact heat exchangers having primarily air or gases as working fluids was published by Kays and London through their 24-year project sponsored by the Office of Naval Research. While this book is still very widely used worldwide, the most recent design data referenced date from 1967. Because manufacturing technology has progressed significantly since the 1970s, many new and sophisticated forms of heat transfer surfaces have been in use in CHEs. The design data for these surfaces are scattered in the worldwide literature. Dr Hesselgreaves has drawn from these extensive data sources in this systematic modern compilation.

In addition to design data and correlations for modern CHE surfaces in Chapter 5, the highlights of this book are: (1) Exergy analysis applied to heat exchangers and entropy generation minimization criteria presented for design choices in Chapter 3. (The author has provided for the first time the thermodynamic analysis important for the design and optimization of process and other heat exchangers - an analysis extended to heat exchanger networks.) (2) How to select a CHE surface for a given application. Chapter 4 presents a comprehensive treatment of a number of quantitative criteria and methods for selecting a heat transfer surface from the many possible configurations for a given application.

An extensive appendix section provides thermophysical and mechanical property data for a wide variety of working fluids and construction materials, in addition to information on CHE manufacturers and help organizations.

It is essential for newcomers to the field to have a reliable guide to the important design considerations of CHEs. This book provides for the first time an in-depth coverage of CHEs, and it will promote and accelerate the use of CHEs in the process industries, as well as provide a comprehensive source of modern information for many others.

Ramesh K. Shah
Delphi Automotive Systems
Lockport, NY, USA

Preface

Happy is the man who finds wisdom, and the man who gets understanding.

Proverbs 3, 13

The purpose of this book is to attempt to bring together some of the ideas and industrial concepts that have been developed in the last 10 years or so. Historically, the development and application of compact heat exchangers and their surfaces has taken place in a piecemeal fashion in a number of rather unrelated areas, principally those of the automotive and prime mover, aerospace, cryogenic and refrigeration sectors. Much detailed technology, familiar in one sector, progressed only slowly over the boundary into another sector. This compartmentalisation was a feature both of the user industries themselves, and also of the supplier, or manufacturing industries. These barriers are now breaking down, with valuable cross-fertilisation taking place.

One of the industrial sectors that is waking up to the challenges of compact heat exchangers is that broadly defined as the process sector. If there is a bias in the book, it is towards this sector. Here, in many cases, the technical challenges are severe, since high pressures and temperatures are often involved, and working fluids can be corrosive, reactive or toxic. The opportunities, however, are correspondingly high, since compacts can offer a combination of lower capital or installed cost, lower temperature differences (and hence running costs), and lower inventory. In some cases they give the opportunity for a radical re-think of the process design, by the introduction of *process intensification* (PI) concepts such as combining process elements in one unit. An example of this is reaction and heat exchange, which offers, among other advantages, significantly lower by-product production.

The intended users of this book are practising engineers in user, contractor and manufacturing sectors of industry. It is hoped that researchers, designers and specifiers will find it of value, in addition to academics and graduate students. The core emphasis is one of design, especially for situations outside conventional ranges of conditions. Because of this emphasis, I have tried to make the book within reasonable limits a 'one-stop shop', to use current jargon. Thus up-to-date correlations have been provided for most practical surface types, to assist in the now-normal computer-aided design techniques. In addition, physical property data are given for many fluids particular to the key industrial sectors.

In order to keep the book within a reasonable size, some topics of relevance to compact exchanger applications have been omitted, in particular those of transients (for regenerators) and general enhancement methods. In addition mechanical

design, and hence materials aspects, are treated only insofar as they impinge on thermal design aspects (although materials property data are provided). Most omitted topics, fortunately, are treated superbly in other accessible books, such as *Compact Heat Exchangers* by Kays and London (1998), *Principles of Enhanced Heat Transfer* by Webb (1994), *Enhanced Boiling Heat Transfer* by Thome (1990), *Heat Exchanger Design Handbook* by Hewitt et al. (1992), and papers. Conversely, I have included some approaches which I feel have been under-developed, and which may stimulate interest. One of these is the Second Law (of Thermodynamics), pioneered by Bejan and co-workers. The justification for this is that there is increasing interest in life-cycle and sustainable approaches to industrial activity as a whole, often involving exergy (Second Law) analysis. Heat exchangers, being fundamental components of energy and process systems, are both savers and spenders of exergy, according to interpretation.

The book is structured loosely in order according to the subtitle Selection, Design and Operation. After the Introduction, which examines some of the concepts fundamental to compactness, the main compact exchanger types are described briefly in chapter 2. As mentioned, the definition of 'compact' is chosen as a wide one, encompassing exchangers with surface area densities of upwards of about $200\text{m}^2/\text{m}^3$. This chapter includes a table of operating constraints and a short section to aid the selection process.

The third chapter takes a wider view of the function of the exchanger in its system, introducing the Exergy approach based on the Second Law of Thermodynamics, which although not new is normally only found in thermodynamics texts and advanced monographs. The development in the second part of this chapter introduces, within given conditions, an approach to optimisation of a heat exchanger in its system when pressure drop is taken into account.

In the fourth chapter the implications of compactness are examined analytically, from the point of view of their impact on the size and shape of one side. A feature of this chapter is the separate treatment of the conventional heat transfer approach (that of non-dimensional Colburn j factor and Fanning friction factor), and of a fully-developed laminar approach, yielding some surprising differences. Some typical industrial surfaces are examined in relation to their compactness attributes in given conditions of operating, as a fundamental aid to selection.

Chapter 5 provides heat transfer and pressure drop correlations for most major types of surface for the exchanger types described in chapter 2, as far as possible in usable (that is, algorithmic) form. Simplified forms are given for cases in which a correlation is either very complex or not available, as applies for many proprietary types. These simplified forms should be treated with caution and only used for estimation purposes.

In chapter 6 the design process is described in what might be called the 'conventional' approach, with the application of allowances to handle such aspects as the variation of physical properties, fin efficiency, and longitudinal wall conduction. Evaporation and condensation in compact passages is also surveyed, and recommended correlations given. A worked example of a (single- phase) design is given.

The final chapter (7), largely contributed by my friend and colleague David Reay, examines some of the important issues connected with installation, operation and maintenance, mainly from the standpoint of process exchangers, but relevant in principle to all types. An important aspect of operation is naturally fouling, and a summary of fouling types and procedures for operational handling of them is given. Naturally, there is a link between fouling and how to allow for it in design, and some approaches are offered from a consideration of the system design. In particular a rational approach based on scaling the traditional (and sometimes disastrous) application of fouling factors is argued, and opportunities for changing (where possible) the pump or fan characteristics to reduce fouling propensity are outlined.

The appendices are included to aid exchanger selectors and users (list of manufacturers), and designers and developers (software organisations, awareness groups and property data).

I have drawn heavily on much existing information, especially the theories and methods embodied in well known texts such as those of Kays and London, Kakac, Shah and Aung (1987), Rohsenow, Hartnett and Ganic (1985), and Kakac, Shah and Bergles (1983). More recent texts such as those of Webb (loc. cit.), Hewitt, Bott and Shires (1994), Hewitt, and Smith (1997) have also been referred to extensively. Much recent knowledge has been accumulated in Shah, Kraus and Metzger, *Compact Heat Exchangers: A Festschrift for A.L. London* (1990), and two proceedings of conferences specifically called to promote compact process exchangers, edited by Shah (1997, 1999).

I have used the nomenclature recommended by the ISO throughout. This differs from that currently used by many, if not most books in a few important respects, which are worth noting at this point. Dynamic viscosity is denoted by η instead of the common μ . Thermal conductivity is denoted by λ instead of k . The symbol k is used, largely in chapter 4, for the product fRe which is constant in fully- developed laminar duct flow. Heat transfer coefficient is denoted by α instead of h . A further related point is that the friction factor used is that of Fanning, which is one quarter of the Moody factor used predominantly in the USA.

Acknowledgements

I am greatly indebted to my wife, June, for her unfailing support and patience during the writing of this book, and to my daughters Julie and Hannah for help with several drawings. My colleague Professor David Reay wrote the bulk of chapter 7, provided the index and was a constant source of encouragement and information. Mary Thomson's help and guidance in typing and in preparing the script for camera-readiness was invaluable. I am most grateful to Dr. Ramesh Shah for agreeing to write the Foreword. Dr. Peter Kew read the part of chapter 6 on evaporation and condensation in compact passages, and Dr. Eric Smith read chapters 4 and 6, both providing valuable comments. Mr Tim Skelton of the Caddett organisation generously gave permission to use information from the Caddett guide: Learning from experiences with Compact Heat Exchangers. Others supplying valuable information were Dr. Chris Phillips of BHR, Mr. Keith Symonds of Chart Heat Exchangers, and Drs. B. Thonon, V. Wadekar and F. Aguirre. I am indebted to the Department of Mechanical and Chemical Engineering at Heriot-Watt University for library and other facilities given. Finally, I would like to thank Mr. Keith Lambert of Elsevier Science for his unfailing support and encouragement during the preparation of the book.

Lanark
October 2000

John E Hesselgreaves
j.e.hesselgreaves@hw.ac.uk

References

Hewitt, G.F., Bott, T.R. and Shires, G.L., (1994), Process Heat Transfer, Begell House & CRC Press.

Hewitt, G.F. ed., (1992) Heat Exchanger Design Handbook, Begell House, New York.

Kays, W.M and London, A.L. (1984), Compact Heat Exchangers, 3rd edn., McGraw Hill.

Kakac, S., Shah, R. K. and Bergles, A.E., (1983), eds., Low Reynolds number Flow Heat Exchangers, Hemisphere, New York.

Kakac, S., Shah, R.K. and Aung, W., (1987). Handbook of Single Phase Convective Heat Transfer, John Wiley, New York.

Rohsenow, W.M., Hartnett, J.P. and Ganic, (1985), *Handbook of Heat Transfer Applications*, McGraw Hill, New York.

Shah, R.K. (ed.), (1997), *Compact Heat Exchangers for the Process Industries*, Snowbird, Utah, Begell House, inc. New York.

Shah, R.K. (ed.), (1999), *Compact Heat Exchangers and enhancement Technologies for the Process Industries*, Banff, Canada, Begell House, inc. New York.

Shah, R.K., Kraus, A.D. and Metzger, D., (1990), *Compact Heat Exchangers: A Festschrift for A.L. London*, Hemisphere, New York.

Smith, E.M., (1997), *Thermal Design of Heat Exchangers, a Numerical Approach*, John Wiley and Sons, New York.

Thome, J.R. (1990), *Enhanced Boiling Heat Transfer*, Hemisphere, New York.

Webb, R. L., (1994), *Principles of Enhanced Heat Transfer*, John Wiley & Sons, New York.

Chapter 1

INTRODUCTION

I only make progress because I make a leap of faith.

A. Einstein

One of the encouraging aspects of heat exchanger developments in the last decade or so has been that the historical sectorial divisions utilising compact heat exchangers (CHEs), have been breaking down. These sectors, loosely defined as refrigeration, power, automotive, aerospace, process and cryogenic, are experiencing increasing cross-fertilisation of technology. Thus the advances in development and understanding in the well-established application areas of different types of plate-fin exchangers for gas separation (cryogenic) exchangers, gas turbine recuperators and the automotive sectors have come together, and have impacted on the power generation, refrigeration and process sectors. It is appropriate to review some of these advances.

Recent developments in compact heat exchanger technology

The well-known Plate and Frame Heat Exchanger (PHE) has undergone two such developments. The first of these is that of the Brazed Plate Exchanger (see chapter 2), originally developed by SWEP in Sweden, and now widely adopted by other manufacturers. Its success has been such that brazed plate exchangers now dominate the low to medium (100kW) capacity range of refrigeration and central air conditioning equipment, almost completely replacing shell- and tube exchangers.

Another, more recent derivative of the PHE is the welded plate exchanger, which utilises specialised seams to enable the welding of the plates together either as pairs or as a whole unit. These units are offered both in 'stand-alone' form or in a modified frame to contain higher pressures or differential pressures. Because of the (normally stainless steel) plate material they are suitable for a wide variety of process applications of moderate pressures.

In the automotive and domestic air conditioning sector, there has been steady progress, largely cost and space-driven, to reduce the size of evaporators and condensers. This progress is graphically demonstrated in Figure 1.1 which shows the evolutionary progress of condensers since 1975. Whilst still retaining a tubular refrigerant side to contain the condensing pressure (now significantly higher than before with the replacement of R12 by R134a), development has progressed simultaneously on both sides. On the air side, louvred plate fins have replaced, in turn, wavy fins and plane fins, thus decreasing the air side flow

length. On the tube side the diameter has decreased and grooves have been introduced. The consequence is a three-fold reduction in volume - largely in the depth (air side flow length).

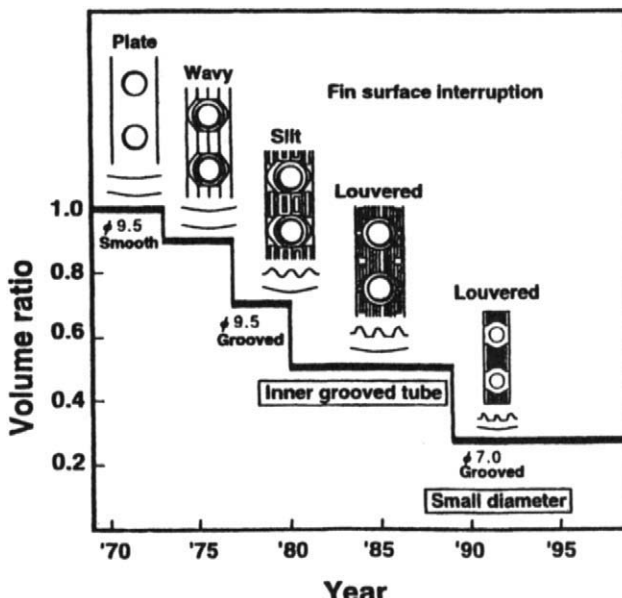


Figure 1.1 Progress in air conditioning condenser technology, showing simultaneous air side and refrigerant side improvements.
(Torikoshi and Ebisu (1997), reproduced by permission of Begell House, inc.)

Various forms of diffusion bonded heat exchangers, pioneered by Meggitt Heatic, have appeared in the process heat exchanger market. These are more fully described in chapter 2, and offer the combination of compactness (hydraulic diameters of the order of 1mm) and great structural integrity. Their main applications so far have been in high-pressure gas processing, both on and offshore, although their potential is in principle considerable owing to the uniformity of the metallic structure, and their compactness. They and their developments such as compact reactors are likely to play a large role in the next generation of process plant, which will utilise concepts of Process Integration (PI). An outline of the principles of reactor exchangers is given at the end of this chapter, and thermal design aspects are discussed in chapter 6.

Finally, there is renewed interest in compact recuperators for gas turbines. Although some earlier development took place, driven by efficiency considerations following the oil crises of the early 1970s, this was largely suspended and development is only recently re-stimulated by the growing

concern over carbon dioxide and other emissions. Ironically, the finite and politically fickle hydrocarbon resource issue is now relegated in importance. Part of the growing interest is centred on land-based electrical generation sets using natural gas, where recuperation improves the economics of operation in addition to reducing emissions. Two of the recent developments are the spiral recuperator of Rolls Royce, and the proposals of McDonald described in chapter 2.

Basic aspects of compactness

Preparatory to a more complete description in chapter 4, it is useful to investigate briefly some of the basic elements of compactness and its relationship with enhancement. To simplify the approach we will deal only with one side.

Geometrical aspects

The fundamental parameter describing compactness is the hydraulic diameter d_h , defined as

$$d_h = \frac{4A_c L}{A_s} \quad (1.1)$$

For some types of surface the flow area A_c varies with flow length, so for these an alternative definition is

$$d_h = \frac{4V_s}{A_s} \quad (1.2)$$

where V_s is the enclosed (wetted) volume.

This second definition enables us to link hydraulic diameter to the surface area density β , which is A_s/V , also often quoted as a measure of compactness. Here, the overall surface volume V is related to the surface porosity σ by

$$\sigma = \frac{V_s}{V}, \quad (1.3)$$

so that the surface area density β is

$$\beta = \frac{A_s}{V} = \frac{4\sigma}{d_h}. \quad (1.4)$$

A commonly accepted lower threshold value for β is $300 \text{ m}^2/\text{m}^3$, which for a typical porosity of 0.75 gives a hydraulic diameter of about 10 mm. For tubes this represents the inside tube diameter, and for parallel plates it represents a plate spacing of 5 mm - typical of the plate and frame generation of exchangers. An informative figure given by Shah (1983) shows the 'spread' of values and representative surfaces - mechanical and natural.

It should be noted at this point that the porosity affects the actual value of surface density, independently of the active surface. In Figure 1.2, the value of 0.83 is chosen which is typical of high performance plate-fin surfaces with aluminium or copper fins. As hydraulic diameter is progressively reduced, it is less easy to maintain such a high value, especially for process exchangers. This is for two reasons, both associated with the effective fin thickness. Firstly, for high temperature and high pressure containment, stainless steel or similar materials are necessary for construction, and diffusion bonding is the preferred bonding technique. This in turn requires significantly higher fin thicknesses to contain the pressure. Secondly, the lower material thermal conductivity calls for higher thicknesses to maintain an adequate fin efficiency and surface effectiveness. Thus typical values for porosity for diffusion bonded exchangers are from 0.5 to 0.6, so having a strong effect on surface density and exchanger weight. Brazed stainless steel plate-fin exchangers have intermediate porosities of typically 0.6 to 0.7. The aspects of shape and size are more thoroughly reviewed in chapter 4.

Heat transfer aspects of compactness

The heat transfer coefficient α is usually expressed, in compact surface terminology, in terms of the dimensionless j , or Colburn, factor by the definition

$$j = \frac{Nu}{RePr^{1/3}} = StPr^{2/3}, \quad (1.5)$$

where Nu = Nusselt number $Nu = \frac{\alpha d_h}{\lambda}$, and (1.6)

$$St = \text{Stanton number } St = \frac{\alpha}{Gc_p}. \quad (1.7)$$

Thus α is non-dimensionalised in terms of the mass velocity G : for a fixed G , j is proportional to α .

For a single side, a specified heat load, \dot{Q} , is given by the heat transfer and rate equations

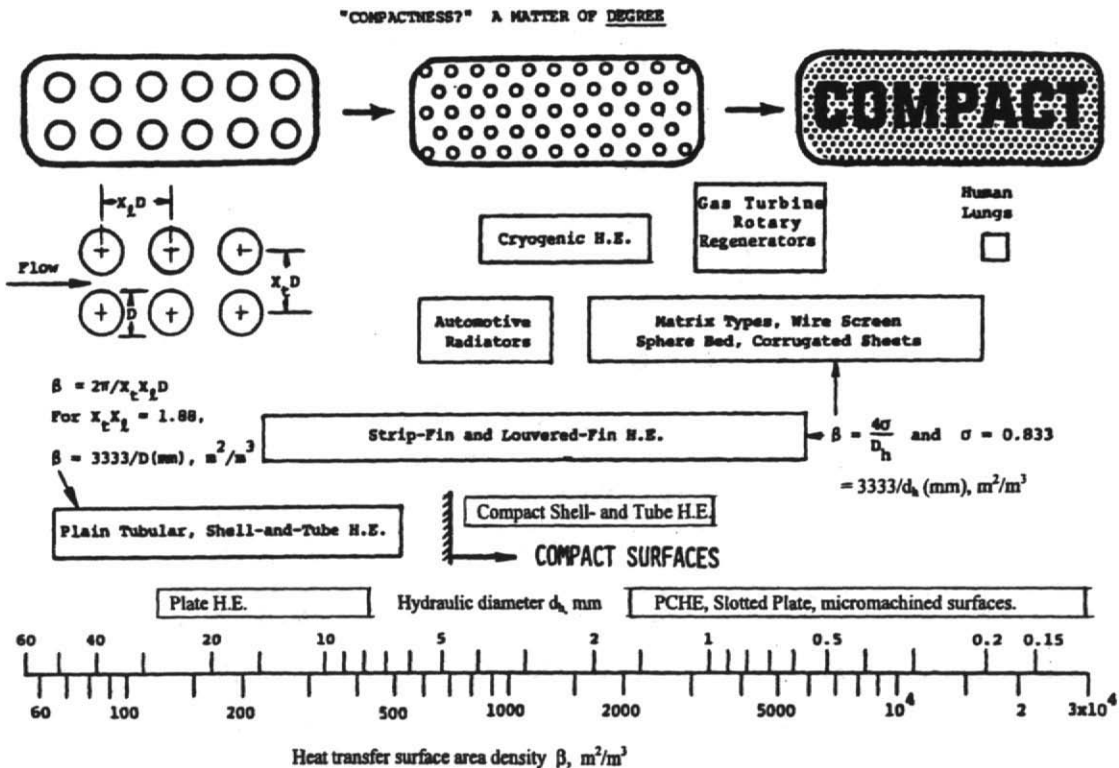


Figure 1.2 Overview of compact heat transfer surfaces, adapted from Shah (1983) with permission

$$\dot{Q} = \alpha A_s \overline{\Delta T} = \dot{m} C_p (T_2 - T_1), \quad (1.8)$$

neglecting for convenience the influences of wall resistance and surface efficiency on α .

The first part of equation 1.8 can be written, using equation 1.4

$$\dot{Q} = \alpha \frac{4\sigma V}{d_h} \Delta T. \quad (1.9)$$

Thus for a specified heat load \dot{Q} , to reduce the volume V means that we must increase the ratio α/d_h . The choice therefore is to increase heat transfer coefficient α or to decrease hydraulic diameter (increase *compactness*), or both. We will make the distinction that *enhancement* implies increasing α with no change of compactness.

In fully-developed laminar flow, the Nusselt number is constant, that is, importantly, independent of Reynolds number, giving

$$\alpha = \frac{Nu\lambda}{d_h}. \quad (1.10)$$

Substituting this into equation 1.9 gives

$$\dot{Q} = \frac{4\sigma V N u \lambda \Delta T}{d_h^2}. \quad (1.11)$$

Hence for a given \dot{Q} and temperature difference, the exchanger volume required is proportional to the inverse square of the hydraulic diameter, for laminar flows. This volume requirement is unchanged whatever the specified pressure drop, as is shown later (although the *shape* does change).

The situation for flows other than fully-developed laminar is more complex, needing compatibility of both thermal and pressure drop requirements. It is shown in chapter 4 that the thermal requirement (the heat load \dot{Q}) is linked to the surface performance parameter j by

$$j = \frac{A_c}{A_s} Pr^{2/3} N, \quad (1.12)$$

where N = NTU (Number of Thermal Units) for the side

$$= (T_2 - T_1) / \overline{\Delta T} \quad \text{for this case.} \quad (1.13)$$

Alternatively, in terms of the hydraulic diameter and flow length,

$$j = \frac{d_h}{4L} Pr^{2/3} N. \quad (1.14)$$

For given conditions the product $Pr^{2/3}N$ is fixed, so the required j factor is proportional to the aspect ratio d_h/L of the surface. Thus from the thermal requirement, the flow length element of size and shape is reduced directly by reducing hydraulic diameter and maintaining the j factor. Put another way, the same heat transfer coefficient is obtained if G and the ratio d_h/L are fixed. The latter condition also implies that the surface area to flow area ratio is fixed, through equation 1.1.

The equivalent expression to equation 1.11 for a surface described by a j factor is

$$\dot{Q} = \frac{4\sigma V j Re Pr^{1/3} \lambda \Delta T}{d_h^2} \quad (1.15)$$

Here, although the superficial square law relationship with hydraulic diameter is retained, the hydraulic diameter affects the Reynolds number, as will be seen in chapter 4: this in turn influences the j factor. The Reynolds number is constrained in addition by the mass velocity, which depends on pressure drop, unlike the fully-developed laminar case.

The required pressure drop is thus a significant factor in the shape and size of exchangers. Neglecting, for many practical exchangers, the relatively small contributions of entry and exit losses and flow acceleration, the pressure drop Δp of fluid through a surface is given by

$$\Delta p = \frac{1}{2} \rho u^2 \frac{4L}{d_h} f, \quad (1.16)$$

f being the Fanning friction factor.

Relating the mean velocity u to the mass flow rate, we have

$$\frac{2\rho\Delta p}{\dot{m}^2} = f \frac{4L}{d_h A_c} = \text{constant for given conditions.} \quad (1.17)$$

We can now combine the thermal and pressure drop requirements in the core mass velocity equation, after London (1983), which can now be derived from equations 1.14 and 1.17:

$$\frac{2\rho\Delta p}{\dot{m}^2} = \frac{f Pr^{2/3} N}{j A_c^2}, \quad (1.18)$$

and

$$\frac{G^2}{2\rho\Delta p} = \frac{j/f}{Pr^{2/3} N}, \quad (1.19)$$

For given conditions of Pr , N , ρ and Δp , it is clear that G is only a function of j/f , and most importantly is independent of hydraulic diameter of the surface. As pointed out by London, j/f is only a weak function of Reynolds number, being of the order of 0.2 to 0.3 for most compact surfaces. Thus G , and hence flow area, can be closely estimated from the design specification.

Examination of the pressure drop and thermal requirements together thus shows that the mass velocity G and hence the flow area are closely circumscribed by the specification. If the aspect ratio of the *surface* (not the exchanger), d_h/L , is maintained, then both the heat transfer coefficient and the surface area are also the same between two cases, hence giving the same performance.

We have now established the basic elements of the effect of the surface on the thermal design of a non-laminar flow exchanger, with the normal (but not the invariable) specification of both heat load and pressure drop. These are:

- that flow length decreases as hydraulic diameter decreases
- that flow area is largely independent of hydraulic diameter

The straightforward implication of this is that exchanger *cores* are changed in their aspect ratio as they are made more compact, whilst their internal *surfaces* maintain a constant or nearly constant ratio d_h/L . The heat transfer coefficient and surface area change according to the change in consequent Reynolds number. These aspects are more thoroughly discussed in chapter 4.

Scaling laws for heat exchangers

A natural question to ask following the above development is: "how does this relate to the issue of simply scaling a heat exchanger up (i.e. less compact) or down (more compact) by its linear dimensions?" By making a number of assumptions and simplifications it is possible to develop a series of scaling relationships to describe how performance is affected by size with different operational conditions. In order to do so we consider the simple case of the scaling of a heat exchanger tube of given length and diameter, shown in Figure 1.3, representative of a heat exchanger tube.

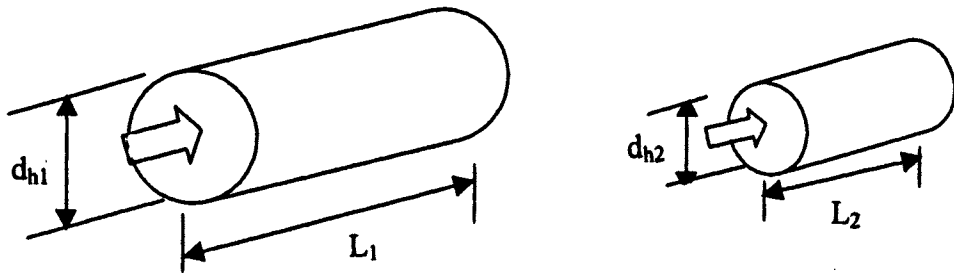


Figure 1.3 Heat exchanger tube scaled by a factor N

For geometrical similarity in this case we only require that the length and diameter are scaled by the same factor N. Then the following ratios apply to the geometric parameters:

Hydraulic diameter	Length	Surface area	Flow area	Volume
$d_{h2} = d_{h1}/N$	$L_2 = L_1/N$	$A_{s,2} = A_{s,1}/N^2$	$A_{c2} = A_{c1}/N^2$	$V_2 = V_1/N^3$

Note that the area and volume scaling factors apply equally to complete cores as well as single tubes, the only proviso being that the number of tubes (the *tube count*) is the same.

Thus a factor N of 25 represents the scaling from a tube diameter of, say, 25mm (1inch) down to 1mm, equivalent to reducing a typical shell and tube exchanger dimension to a compact dimension (which may still be of shell and tube form).

In the analysis the assumptions made are that

1. The physical properties are fixed, based for example on the inlet conditions

2. The inlet temperatures are fixed.
3. Each flow stream is treated the same

We now examine four scenarios for the scaled heat exchanger, on the further assumption that the tube is representative of both sides. Thus a shell and tube exchanger would have the scaling factor applied to all linear dimensions, including baffle pitch. The four scenarios are:

1. Same mass flow \dot{m} (for each stream, as above).
2. Same Reynolds number.
3. Same flow velocity.
4. Same pressure drop.

The resultant parameters required are the heat load \dot{Q} and the pressure drop Δp . For interest we examine the common limiting flow conditions of fully-developed laminar and fully-developed turbulent. For brevity only the first scenario is analysed in full, the others being equally simple to derive and thus merely quoted.

Scenario 1. Same mass flow ($\dot{m}_2 = \dot{m}_1$)

The ratio of mass velocities is the same as the ratio of throughflow velocities and is given by

$$\frac{G_2}{G_1} = \frac{u_2}{u_1} = \frac{\dot{m}_2}{\dot{m}_1} \frac{A_{c1}}{A_{c2}} = N^2 \quad (1.20)$$

and the ratio of Reynolds numbers is thus (since the relative fluid viscosities are the same)

$$\frac{Re_2}{Re_1} = \frac{G_2}{G_1} \frac{d_{h2}}{d_{h1}} = \frac{N^2}{N} = N. \quad (1.21)$$

The case of fully-developed laminar flow is first examined. This is characterised by constant Nusselt number Nu and constant product f/Re . We also need to assume that the scaling process does not change the flow regime because of the change in Reynolds number.

The ratio of overall heat transfer coefficients (which by assumption 3 is given by the ratio of side coefficients) is

$$\frac{U_2}{U_1} = \frac{\alpha_2}{\alpha_1} = \frac{Nu_2}{Nu_1} \frac{d_{h1}}{d_{h2}} = \frac{d_{h1}}{d_{h2}} = N \quad (1.22)$$

The heat load ratio is given in terms of the effectiveness by

$$\frac{\dot{Q}_2}{\dot{Q}_1} = \frac{\dot{m}_2 c_{p2} \varepsilon_2 (T_{h,in} - T_{c,in})_2}{\dot{m}_1 c_{p1} \varepsilon_1 (T_{h,in} - T_{c,in})_1} = \frac{\varepsilon_2}{\varepsilon_1}, \quad (1.23)$$

by the application of the assumptions. This can only be evaluated if the (starting) value of effectiveness of the un-scaled exchanger and its flow arrangement are known. In order to find these we would need the ratio of Ntus:

$$\frac{Ntu_2}{Ntu_1} = \frac{(UA_s)_2}{(UA_s)_1} \frac{\dot{m}_1}{\dot{m}_2} = \frac{N}{N^2} = \frac{1}{N}. \quad (1.24)$$

Without further knowledge as above no firm conclusions can be drawn. Two observations can, however, be made. Firstly, if the initial Ntu is high, a scaling factor higher than unity will make relatively little difference to the effectiveness, so that in this event the heat loads will be very similar. Secondly, for Ntus very much smaller than unity (say up to about 0.2), the effectiveness is closely approximated by Ntu, with the result that the heat load is directly proportional to scaling factor N.

The ratio of pressure drops is given by

$$\frac{\Delta p_2}{\Delta p_1} = \frac{u_2^2}{u_1^2} \frac{f_2}{f_1} \frac{(L/d_h)_2}{(L/d_h)_1} = N^3, \quad (1.25)$$

$$\text{since } \frac{f_2}{f_1} = \frac{Re_1}{Re_2} = \frac{1}{N} \text{ for fully-developed laminar flow.} \quad (1.26)$$

For the case of fully-developed turbulent flow, we assume for simplicity that the power law relationships $Nu \propto Re^{0.8}$ and $f \propto Re^{-0.2}$ apply, representing commonly-used heat transfer and friction correlations. A similar analysis to that above yields

$$\frac{\dot{Q}_2}{\dot{Q}_1} = \frac{\dot{m}_2 c_{p2} \varepsilon_2 (T_{h,in} - T_{c,in})_2}{\dot{m}_1 c_{p1} \varepsilon_1 (T_{h,in} - T_{c,in})_1} = \frac{\varepsilon_2}{\varepsilon_1} \quad (1.27)$$

as above but with the Ntus in the ratio

$$\frac{Ntu_2}{Ntu_1} = \frac{1}{N^{0.2}}, \quad (1.28)$$

so that the heat load is less affected than for the laminar case. The ratio of pressure drops is

$$\frac{\Delta p_2}{\Delta p_1} = N^{3.8}. \quad (1.29)$$

It is perhaps this strong (cubic or above) relationship of pressure drops for unchanged mass flows that has given rise to the often- expressed misunderstanding that a compact exchanger (for $N \gg 1$ compared with conventional dimensions) has a higher pressure drop than a non- compact one, for comparable thermal performance. The misconception centres on the implicit assumption of scaling all of the dimensions simultaneously ('making it smaller'). We have seen in the previous section that a specified pressure drop can be maintained in a compact exchanger by keeping the flow area approximately the same, whilst reducing the flow length in proportion to the hydraulic diameter. More generally, a compact exchanger can be designed for a specified pressure drop, but it will have a different shape, which in many cases has important implications for the best flow configuration. These aspects are dealt with more thoroughly in chapters 4 and 6.

The remaining scenarios are summarised in Table 1.1, which shows the consequent ratios of mass flow, heat flow, Ntu and pressure drop for the fully-developed laminar and turbulent flow cases respectively.

It can be seen in this table that, for each limiting case, the performance parameters follow a definite progression as the imposed constraints progress through constant mass flow, Reynolds number, throughflow velocity and pressure drop. Only in the case of a fixed Reynolds number is there a definite result for the ratio of heat flows. This arises from no change in Ntu. Note especially, following the above observations on pressure drop, that to scale in this way for fixed pressure drop has similar dramatic consequences on the heat flow as does maintaining a fixed mass flow on the pressure drop.

Clearly, for the intermediate case of developing laminar flow, the results would be intermediate between the limits examined.

Table 1.1 Scaling parameters for heat exchangers

Fixed	Fully Developed Laminar				Fully Developed Turbulent			
	$\frac{\dot{m}_2}{\dot{m}_1}$	$\frac{\dot{Q}_2}{\dot{Q}_1}$	$\frac{Ntu_2}{Ntu_1}$	$\frac{\Delta p_2}{\Delta p_1}$	$\frac{\dot{m}_2}{\dot{m}_1}$	$\frac{\dot{Q}_2}{\dot{Q}_1}$	$\frac{Ntu_2}{Ntu_1}$	$\frac{\Delta p_2}{\Delta p_1}$
\dot{m}	1	$\frac{\epsilon_2}{\epsilon_1}$	$\frac{1}{N}$	N^3	1	$\frac{\epsilon_2}{\epsilon_1}$	$N^{-0.2}$	$N^{3.8}$
Re	$\frac{1}{N}$	$\frac{1}{N}$	1	N^2	$\frac{1}{N}$	$\frac{1}{N}$	1	N^2
\bar{u}	$\frac{1}{N^2}$	$\frac{1}{N^2} \frac{\epsilon_2}{\epsilon_1}$	N	N	$\frac{1}{N^2}$	$\frac{1}{N^2} \frac{\epsilon_2}{\epsilon_1}$	$N^{-0.2}$	$N^{0.2}$
Δp	$\frac{1}{N^3}$	$\frac{1}{N^3} \frac{\epsilon_2}{\epsilon_1}$	N^2	1	$\frac{1}{N^{19/9}}$	$\frac{1}{N^{19/9}} \frac{\epsilon_2}{\epsilon_1}$	$N^{2/9}$	1

Size and compactness

Before examining some further aspects of enhancement we can now see that an exchanger with both compact surfaces (that is, a compact heat exchanger, or CHE) is not necessarily small. The flow areas, and hence face areas, are proportional to the flow rates of the streams, and the length is proportional to the Ntu (and heat load) for a selected hydraulic diameter. Thus both face area and length, defining the size of a CHE, can be large. Figure 1.4 shows a large CHE for a cryogenic duty with large flows and high Ntu.

Conversely, it is clear that a shell and tube exchanger can be both compact and small, as shown in Figure 1.5. This exchanger has enhanced (dimpled) tubes of about 1.7mm internal (hydraulic) diameter, and is used in aircraft for fuel/oil heat exchange, with moderate Ntu. Finally, for completeness, a shell- and tube exchanger can have non- compact surfaces and be small, as shown in Figure 1.6. This exchanger is used for exhaust gas recirculation from truck diesel engines to reduce emissions. It has a high hydraulic diameter to avoid fouling problems, and a very low Ntu.

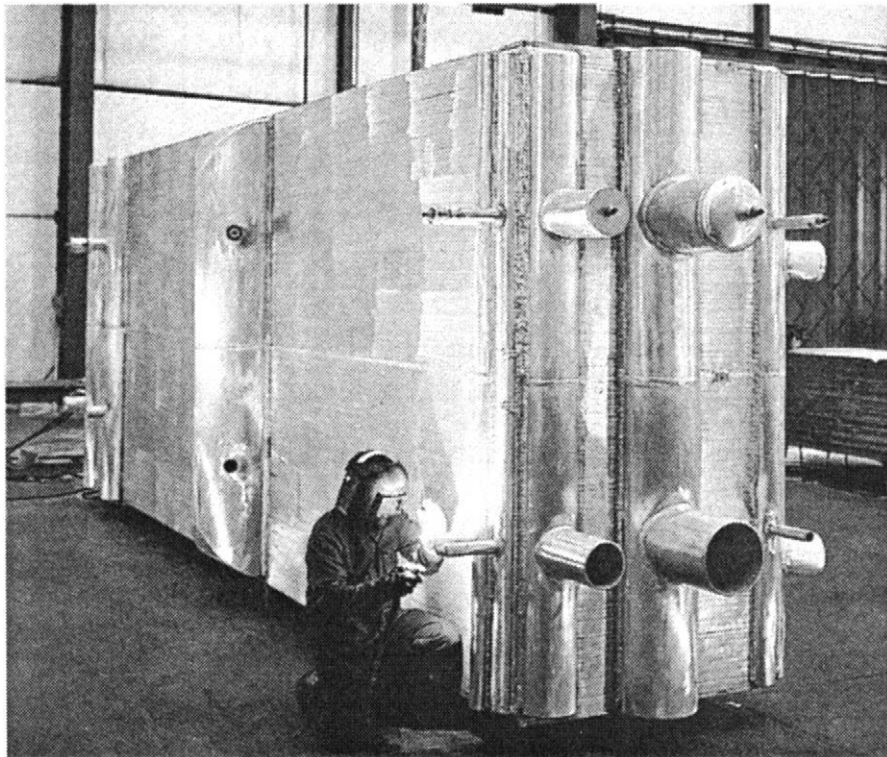


Figure 1.4 Large compact heat exchanger for cryogenic duty
(courtesy Chart Heat exchangers).

The relationship of compactness and enhancement

In the above sections it is shown (and developed in chapter 4) that for a given thermal and pressure drop specification, the size- principally volume- of an exchanger is a function of both geometrical compactness of the surface(s) and of the performance parameters independently of the surface. Although the compactness and performance parameters appear in separated form in the volume expression, they are indirectly linked in that the operating parameter is a function of Reynolds number, which is proportional to hydraulic diameter. The performance parameters described, for example, by the ratio j/f (for flow or face area), or j^3/f (for volume), in turn depend on the Reynolds number, as shown in chapter 4.

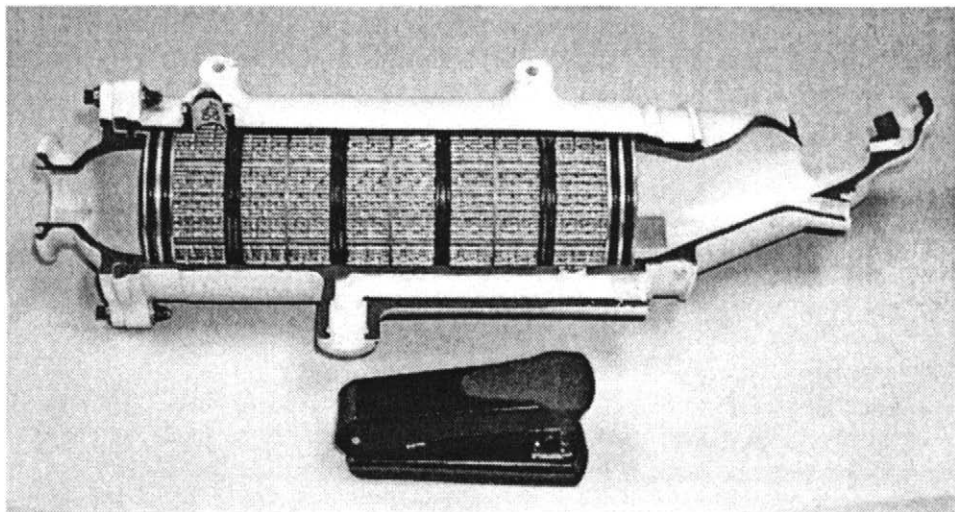


Figure 1.5 A compact, small shell and tube exchanger for oil/fuel heat exchange (courtesy Serck Aviation)

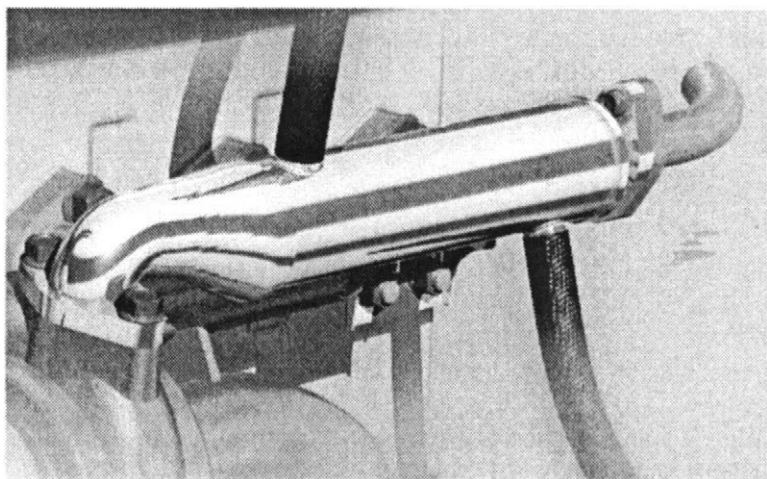


Figure 1.6 A non-compact, small shell and tube exchanger for exhaust gas recirculation (courtesy Serck Heat Transfer)

One of the clearest ways of illustrating the inter-relationship of compactness and performance is by considering the basic concept of the offset strip fin (OSF). The simplest approach is that of Kays (1872), who utilised the Blasius solution for the developing laminar flow over a flat plate of length l , giving for the average Stanton number:

$$\bar{St} = 0.664 Re_l^{-0.5} Pr^{-2/3}, \quad (1.30)$$

and the corresponding relationship for the skin friction:

$$\bar{f} = 1.328 Re_l^{-0.5}. \quad (1.31)$$

This simple form reflects the Reynolds analogy of $f/j = 2$. The j factor expression is remarkably close to experimental data for most plate fin surfaces, as will be seen in chapter 5. Kays modified the friction factor to take into account the contribution of the finite thickness of a practical fin, postulating a drag coefficient equal to that of a flat plate normal to the incident flow and giving

$$f = 1.328 Re_l^{-0.5} + \frac{C_d}{2} \frac{t}{l}, \quad (1.32)$$

where $C_d = 0.88$. This value generally under-estimates the friction factor.

If the strip fins form the dominant proportion of a surface, the Stanton number can be expressed as a j factor in terms of the surface hydraulic diameter-based (instead of the strip length-based) Reynolds number as

$$j = 0.664 Re_{dh}^{-0.5} \left(\frac{d_h}{l} \right)^{0.5}. \quad (1.33)$$

Thus for a surface of given hydraulic diameter, the j factor is increased progressively as the strip length is reduced, especially if $l \ll d_h$. (the surfaces with highest augmentation in fact have a strip length of the same order as the hydraulic diameter, each being about 1mm). This effect is illustrated in Figure 1.7.

Noting also that the heat transfer coefficient is also given as Nusselt Number in terms of Prandtl number by equation 1.5, we see that

$$Nu = 0.664 Re^{0.5} Pr^{1/3} \left(\frac{d_h}{l} \right)^{0.5}. \quad (1.34)$$

For length to hydraulic diameter ratios larger than about 2, the boundary layer displacement thickness affects the free stream flow, which then effectively becomes a *channel* or *duct flow* and the corresponding relationship is described in terms of the Graetz Number G_z .

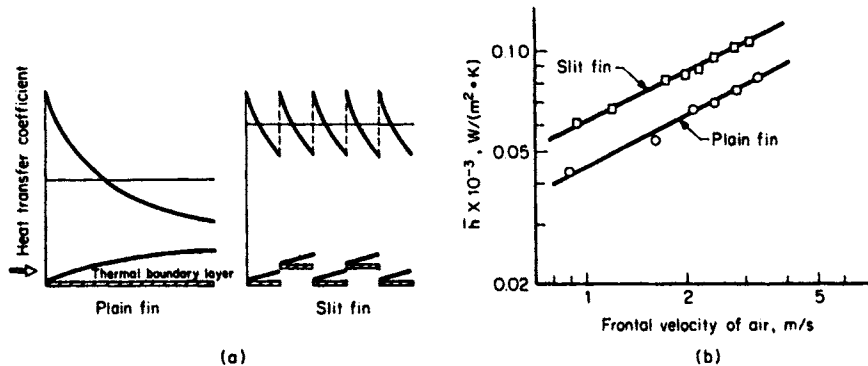


Figure 1.7 The effect of reducing strip (fin) length, shown schematically for an offset strip fin (OSF) geometry in an automotive air conditioning core, with a) local heat transfer coefficients for plain and strip fin, and b) average heat transfer coefficients for plain fin and strip fin.

(From Techniques to Augment Heat Transfer, A.E. Bergles, in Handbook of Heat Transfer Application, ed. Rohsenow et al, 1985, McGraw Hill, reproduced by permission of the McGrawHill Companies)

Channel flows at low Reynolds number would normally have fully-developed laminar flow with a Nusselt number which is constant (usually being about 5 for a typical rectangular channel) and independent of Prandtl number. The importance of equation 1.34 is that a strip fin or any interruption giving a developing boundary layer will give a Nusselt number dependent on Prandtl number, which for high Prandtl number fluids such as oils will yield a high heat transfer enhancement. This explains why oil coolers often have very fine surface enhancement such as looped wire or strip bonded inserts on the oil side. The normally very low Reynolds number characteristic of oil flows means that the contribution of the looped wire to the pressure drop is not excessive, since the flow over the wires does not separate to give high form drag. For the same reason folded tape surfaces are also very effective for low Reynolds number, high Prandtl number flows. Clearly the influence of Prandtl number is low for gases ($Pr = \text{about } 0.7$).

A related mechanism to direct surface interruption is that of the mixing of otherwise deeply laminar tube flows provided by turbulators or inserts of the

coiled wire type (Figure 1.8). These are normally drawn into the tube with a 'dry' wire- to- wall contact. Thus there is little or no conduction between coil and wall, and hence no secondary surface or fin effect. The mixing generated by the coil instead re-distributes the thermal energy, thereby flattening the temperature distribution and giving a high wall temperature gradient. This gradient, and the heat transfer coefficient, approximates to the equivalent turbulent profile, and reinstates the Prandtl number dependence. Bejan (1995) has shown from physical reasoning that the underlying heat transfer mechanism in the eddy structure of a turbulent flow has a direct analogy with simultaneously developing laminar flow, and hence the same Prandtl number dependence.

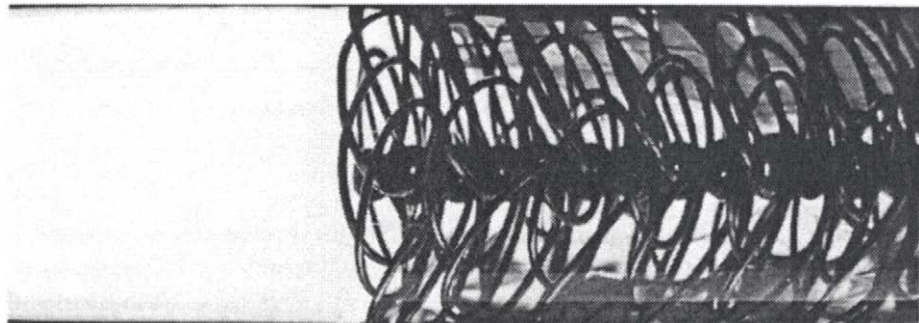


Figure 1.8 Coiled wire insert in laminar flow
(Courtesy Cal Gavin)

As pointed out by Webb (1994), for enhancement at low Reynolds numbers, it is necessary to apply mixing through the whole duct cross- section since substantial temperature gradients exist here. These are of course parabolic in profile for both circular tube and parallel plate geometries. In contrast, the highest temperature gradients in turbulent flows exist very close to the wall, so it is only necessary to mix there to increase the wall temperature gradient. Mixing outside the wall area is ineffective thermally but gives high parasitic pressure drops. Typical enhancements for turbulent flows are simple wire coils and rib roughnesses (transverse microfins, fluting or corrugation).

Many compact surfaces operate in the transitional flow regime when using gases or viscous liquids, with hydraulic diameter- based Reynolds number in the range of 1000 to 4000. Enhancement devices such as inserts or shaped (e.g. dimpled, knurled, or corrugated) ducts are used to 'trip' the boundary layer into turbulent behaviour, thus giving the desired high wall temperature gradient. The effective mechanism is not so much to *increase* the effective Reynolds number, but to *reduce* the Reynolds number at which instabilities can be

maintained. The transitional Reynolds number range is also reduced. Plate Heat Exchanger (PHE) surfaces are often operated in this range and effectively turbulent boundary layer behaviour is observed down to $Re = 200$, depending on corrugation angle: the higher the angle, the lower the tripped Reynolds number.

The function of secondary surfaces (fins)

It is instructive, in view of the above, to examine the principles of secondary or extended surfaces in exchanger design, since superficially an exchanger can be made indefinitely compact with primary surfaces. Secondary surfaces have one or two functions in compact exchangers, depending on the surface type.

The first function is to enable the balancing of stream, or side, resistances, especially for tubular surfaces (see chapter 6), to give a low overall resistance $1/UA_s$. This means equalising, as far as is realistic, the product αA_s on each side. If the tube side fluid is a liquid and the outside (usually called the shell side) fluid is a low or medium pressure gas, the liquid side heat transfer coefficient (typically about $2000\text{W/m}^2\text{K}$) is very much greater than that of the gas (about $60\text{W/m}^2\text{K}$). To balance the design to obtain an economic heat exchanger thus requires the shell side to have a much greater surface area, and the transverse annular or plate fins provide this. A factor of up to 20 is commonplace for fins on circular tubes. It should be noted at this point that this applies independently of the form of secondary surface. It is not necessary for balancing in itself that the fins are thinner than the primary surface: the fins could be thick but closely-spaced, giving an effective hydraulic diameter of approximately twice the fin spacing. The balancing process is one of equalising, within practical limits, the resistances of the two sides 1 and 2, giving an overall resistance $(1/UA_s)_o$ as

$$\frac{1}{(UA_s)_o} = \frac{1}{(\alpha A_s)_1} + \frac{1}{(\alpha A_s)_2}. \quad (1.35)$$

The closer the two components are, the lower is the overall resistance and the more economical is the exchanger. For the above example the areas would have to be in the ratio of about 33 to achieve this; in fact it is rare for sides to be fully balanced in, for instance, water to air exchangers. These exchangers thus tend to be compact on the extended (finned) side, but non-compact on the tube side. If the product αA on the air side is substantially lower than that on the water side, (thus its resistance component is higher), the exchanger is said to be air side dominated. It is clear that any improvements should target the air-side, and that enhancement to the water side would be largely ineffective in improving overall performance.

The second function of fins, both for tubular and plate surfaces, is to enable a low hydraulic diameter, with its advantage for heat transfer coefficient, to be obtained without the secondary surface having to serve a function of separating the two fluids. In the case of plate-fin surfaces the fins also serve to carry mechanical load arising from the differential pressure between streams. This does not apply for a fin-tube surface.

Arising from both of the above functions, the consequence is that the fin can be made thinner than the primary surface, thus saving weight and cost. Since the heat transferred by the fin has to be conveyed by conduction to the primary surface, however, there is necessarily a drop in temperature along the fin, and a degradation of performance of the surface as a whole. This is characterised by the fin efficiency and surface effectiveness, (chapter 6), which has to be allowed for by an increase in surface area. Thus the thinner the fin is, the lower is the weight per unit length, but conversely the larger the increment in area and thus the greater the weight. In practice manufacturing, material and handling factors put constraints on the actual fin thickness used: in air to fluid crossflow configurations the fins rarely provide full side balancing. One consequence of this is that only in recent years, with the steady progression of air-side improvements, has the need arisen to augment water or refrigerant-side surfaces in automotive and related equipment, with its unending demands of cost and space reduction.

To summarise, finning is not always appropriate, even if possible for one or both sides of a heat exchanger. Where both appropriate and possible, it can reduce the size. For exchangers which are already compact (e.g. with hydraulic diameter of the order of 1mm) it can be more difficult to introduce finning economically, although some very fine fin spacings are manufactured for specialised applications such as cryo-coolers for infra-red detection systems.

Compactness and its relationship to enhanced boiling surfaces, rib roughnesses etc.

It is mentioned in chapter 6 that at present, enhanced boiling or condensing surfaces are not utilised for compact evaporators and condensers. These surfaces have now an established place in refrigeration equipment, and are making inroads in process applications. Boiling surfaces consist of matrices of re-entrant cavities produced by some form of machining followed by rolling, or of a porous structure sintered onto the tube, as shown in Figure 1.9.

Condensing surfaces consist of fine, tapered fins with well-defined grooves for condensate drainage. The point to note in both cases is that the *local heat transfer surface*, whether of fins or internal pores, is *compact*, and is superimposed on a tubular surface which is *not compact*. In consequence the bulk of the space between tubes is inactive thermally, only serving to allow passage of the two-phase fluid (this space may be necessary to keep pressure drops in

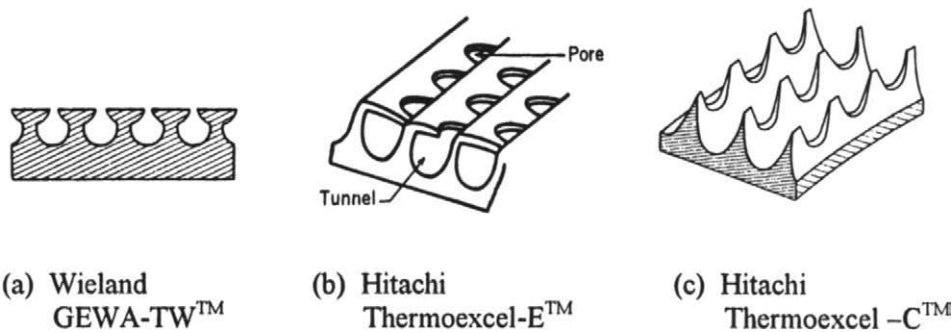


Figure 1.9 Detail of proprietary enhanced boiling (a) and (b) and condensing (c) surfaces

check, but that is another matter). The function of the re-entrant cavities in the boiling surfaces is to prevent the too-rapid removal of superheated liquid from the surface. This then promotes the formation and growth of bubbles. A typical hydraulic diameter of a boiling surface is less than 1mm, which is close to the hydraulic diameter of the more compact of industrial compact exchangers. It is likely, then, that this *confinement* (see chapter 6), characteristic of the whole surface of a compact exchanger acts in an analogous way to that of a proprietary boiling surface. There may be differences of detail with regard to the bulk fluid flow, and both mechanistic processes are very complex.

Similar arguments may be made for the analogy between proprietary condensing surfaces and compact (e.g. plate-fin) exchanger surfaces. Webb (1994) gives an extensive treatment of both boiling and condensing surfaces.

The relationship to rib-roughnesses and similar surface treatments to a tube, whether intrinsically compact or not, has different aspects, although the basic principle is the same: to increase the wall temperature gradient. Roughness elements, as remarked above, have two functions: to provide an extended surface, and to thin the boundary layer on both extended and primary surface. It could thus be argued that there are elements of local compactness and boundary layer interruption in this function, although the latter is more of the form of mixing and generation of turbulence than of re-starting the boundary layer in an otherwise largely laminar flow.

Surface optimisation

Much has been written about surface optimisation (e.g. Webb (1994), Shah (1983)), and it is not necessary to expand on this unduly. What is clear logically and from the literature is that it is rarely possible to define how to optimise: in most selection processes there are several, often conflicting, criteria that have to be met with regard to the exchanger. Some of these are cost (first and life cycle), frontal area, size and weight, and they impact very differently on selection choices according to the application sector. They are often expressed, either singly or in combined form, as *objective functions* in optimisation or search procedures. A summary of guidelines for selection, principally for process exchangers, is given in chapter 2, whilst some aspects of surface comparison are discussed in chapter 4.

One clear common requirement, although having varying priority according to sector, is the reduction of material quantity, which reflects in cost and weight particularly. We have seen above that secondary surfaces are used, independently or in combination with compactness, to save weight, through material content, and thereby the first (capital) cost and the installation cost, although size implications are more complex. The arguments in the previous section show that reducing the fin thickness has two opposing effects on weight. This raises the ideal question: "is there a fin thickness which yields a minimum weight, and if so, is it realistic from the point of view of mechanical and other criteria?" For the case of plate fins there is in fact a minimum condition, investigated by the present author (Hesselgreaves (1992, 1993)). An example of the calculations from the analysis is shown in Figure 1.10, for a plain fin of rectangular section of 5/1 aspect ratio, and for a separating plate- to gap ratio of 0.1. The controlling parameter in the set of curves is the Biot number, defined in this case by

$$Bi = \frac{\alpha b}{\lambda_m}, \quad (1.36)$$

where b is the effective plate gap and λ_m is the material conductivity.

The material volume, for a given duty, is non-dimensionalised by the theoretical minimum represented by a fin of zero thickness and infinite conductivity (zero Biot number). At low Biot numbers, representing high conductivity (e.g. aluminium or copper), there is a clear minimum at a dimensionless thickness parameter $t^* = t/b$ of about 0.007 to 0.013. The values correspond to high fin efficiency values. Thus if the plate gap b is 10mm the minimum thickness is about 0.1mm, or 100 μ m. To the right of the minimum the higher weight represents the cost of extra fin thickness not being compensated for by higher efficiency. To the left the lower efficiency necessitates extra flow

length. These values are not far from, and explain the basis for, the very thin fins found in automotive applications such as radiator and heater cores, for

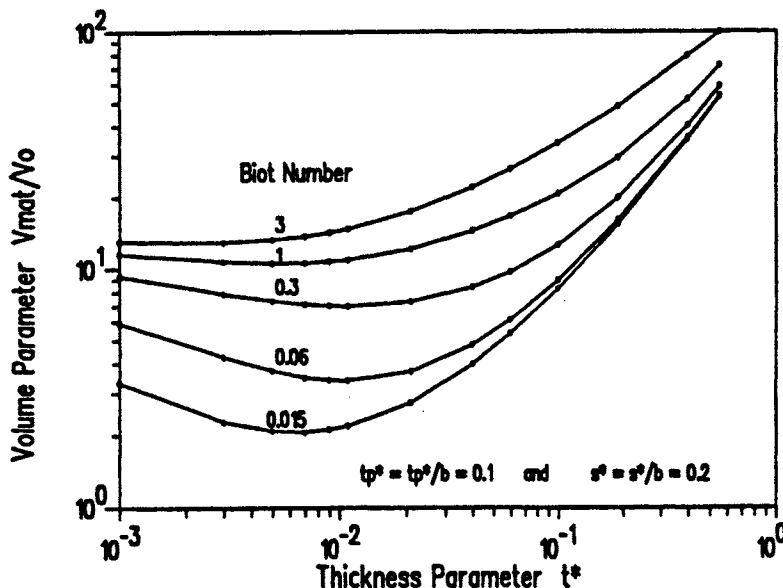


Figure 1.10 Material volume parameter as a function of fin thickness parameter and Biot number, showing a minimum.

which the cost of material is a significant, if not dominating, component in the manufacturing cost. For stainless steel plate-fin types, the corresponding Biot numbers would be two orders of magnitude higher for gases, and a further order of magnitude higher for liquids. The figure shows that although the 'optimum' shifts to the right (greater fin thickness) initially, it then shifts back again towards very low thickness at these high Biot numbers, whilst becoming progressively weaker. The corresponding fin efficiency is very low, indicating the low *heat transfer* function of fins for process exchangers. Their mechanical function, however, remains.

Heat exchanger reactors

The chemical process industry is showing a rapidly growing interest in combining reaction with heat exchange (see also chapter 6), as part of an overall drive towards Process Intensification (P.I.), and heat exchanger manufacturers are developing variants of their exchangers to meet the demand. The BHR group at Cranfield in the UK has had an active role in the development of design

technology for such reactors. Studies of flow structures using powerful Computational Fluid Dynamics (CFD) codes are being conducted at GRETh in Grenoble (Thonon and Mercier (1997)), and various aspects of reactor technology are active at Newcastle and Birmingham Universities in the UK, and elsewhere.

Many, if not most, of process reactions for high added-value products are conducted in stirred tank reactors, consisting of a large tank with rotating paddle. The mixing process has a high energy demand and yet, because of its highly non-uniform nature, is not efficient. When reactions with a high intrinsic speed are undertaken in such reactors, the rate of mixing is insufficient to match the reaction rate. Hence the reaction is slowed down and by-product formation is increased (Hearn and McGrath (1994)). The importance of the latter can be judged from the statement that fast exothermic reactions such as alkylations, emulsifications, nitrations and polymerisations, produce by-products of up to 5kg/kg of desired products for bulk chemicals, and up to 50kg/kg of products for fine chemicals (Phillips et al. (1999)).

The benefits of utilising heat exchanger reactors are threefold (Phillips et al.(1997)):

1. Energy savings: the heat of reaction in batch reactors, although often removed by coils around the tank periphery, is not normally recovered, owing to the transient nature of the process.
2. Increased selectivity of competing reactions: the maintenance of near-isothermal conditions can give significant reductions in by-product formation, thus reducing waste and improving productivity.
3. Improved plant safety: this comes both from the possibility of preventing runaway reactions by removing the heat of reaction, and also from potentially a much-reduced inventory- by up several orders of magnitude.

In theory any heat exchanger becomes a heat exchanger reactor when the reacting fluids are introduced at entry on one side. Heat of reaction will then be added or removed as appropriate by the other fluid, but without any control of the rate of removal, which often depends on the rate of mixing.

The effectiveness of a heat exchanger reactor, in addition to its capability of removing the heat of reaction, relies on the nature of the flow in the passages in which the reaction is to take place. The desired flow has a high degree of turbulent (called micro-) mixing, allowing mixing of the reactants, characterised by a high proportion of the overall dissipation rate in the total pressure drop being converted to turbulent energy dissipation. This proportion varies widely in different heat exchanger passage geometries. It has been shown that an exchanger specifically designed for reaction- heat exchange (the Marbond, see chapter 2) has greater micro- mixing than, for example, an equivalent plate-fin

exchanger, and hence the capability of significant reductions in by- product formation (Phillips et al. (1999)).

Some principles of the thermal design of reactor heat exchangers are given in chapter 6.

References

Bejan, A. (1995), *Convection Heat Transfer*, 2nd ed., John Wiley, New York.

Hearn, S.J. and McGrath, G., (1994), Compact Heat Exchanger: Research Needs and Commercial Opportunities, 10th Int. Heat Transfer Conf., Industrial Session on Process Optimisation and Fouling, Brighton, UK.

Hesselgreaves J.E. (1993), Optimising Size and Weight of Plate-Fin Heat Exchangers, 1st. Int, Conf. on Aerospace Heat Exchanger Technology, Palo Alto; Elsevier, New York.

Hesselgreaves, J.E. (1993), Fin Thickness Optimisation for Plate-Fin Heat Exchangers, Conf. on Heat Exchanger Engineering: Advances in Design and Operation, Leeds 1993.

Kays, W.M., (1972), Compact Heat Exchangers, ACARD Lecture Series on Heat Exchangers, No.57, J.J. Ginoux, Ed., AGARD-LS-57-72.

London, A.L., (1983), Compact Heat Exchangers- Design Methodology, in Low Reynolds Number Flow Heat Exchanger, ed. Kakac, S., Shah, R.K. and Bergles, A.E., Hemisphere, New York.

Phillips, C.H., Lauschke, G. and Peerhossaini, H, (1997), Intensification of Batch Chemical Processes by using Integrated Chemical Reactor-Heat Exchangers, *Applied Thermal Engineering*, Vol. 17, nos. 8-10, pp 809-824.

Phillips, C.H., (1999), Development of a Novel Compact Chemical Reactor-Heat Exchanger, 3rd International Conference on Process Intensification for the Chemical Industry, Antwerp, BHR Group Conference Series Publication No.38, Professional Engineering Publishing Ltd, Bury St Edmunds, London.

Shah, R.K. (1983), Classification of Heat Exchangers, in Low Reynolds number Flow Heat Exchanger, ed. Kakac et al. Hemisphere, New York.

Shah, R.K. (1983), Compact Heat Exchanger Surface Selection, Optimisation and Computer- aided Design, in Low Reynolds number Flow Heat Exchanger, ed. Kakac et al. Hemisphere, New York.

Thonon, B and Mercier, P., (1999), Flow Structure, Thermal and Hydraulic Performances of Compact Geometries used as Integretated Heat Exchanger-Reactor, 3rd International Process Intensification Conference, Antwerp.

Torikoshi, K. and Ebisu, T., (1979), Japanese Advanced Technologies of Heat Exchanger in Air-Conditioning and Refrigeration Application, in Proceedings of Int. Conf. on Compact Heat Exchangers and Enhancement Technologies for the Process Industries, Banff, Canada.

Webb, R.L. (1994), Principles of Enhanced Heat Transfer, John Wiley, New York.

Chapter 2

INDUSTRIAL COMPACT EXCHANGERS

*It takes a lot of discipline not to jump to the obvious non-creative solution.
But practice helps.*

P. Evans and G. Deehan

INTRODUCTION

In this chapter the basic physical features and construction of the principal industrial compact heat exchanger types are described. The definition of 'compact' in this respect is consciously chosen as a wide one, implying surface area densities upwards of about $200\text{m}^2/\text{m}^3$, representing hydraulic diameters lower than about 14 mm. The reason for this is twofold. Firstly, several generic types have area densities that span the accepted definition of $700\text{ m}^2/\text{m}^3$ (hydraulic diameter ≈ 4 mm). Secondly, some of these types are relatively new entrants into the process exchanger market, and offer the possibility of significant reductions in size over shell- and tube types.

The descriptions given are as far as possible in the form of the generic type (e.g. plate- fin heat exchanger), and thus may have many variants by manufacturers for a wide range of industrial sectors. The manufacturers of these are not therefore listed in the main description section, but can be found in the list of manufacturers in Appendix 4. Some exchangers, however, are specific to one manufacturer. These are necessarily identified by their manufacturer's name, directly or indirectly. The exchanger types described and their manufacturers are those available to the author, and clearly are not exhaustive. Any clear omission is regretted and is not intended.

Applications and case studies are not given here. They have been very adequately described elsewhere (Reay et al.(1995), Reay (1999), Berntsson et al. (1995), ETSU et al.(1994, 1996, 1998)), and the reader is recommended to consult these sources for further information.

Several new developments are described in the last descriptive section. A distinction is made between sensible heat exchangers and heat exchanger reactors, the latter being the subject of rapidly increasing industrial interest.

The characteristics of each exchanger are summarised in Table 2.2 later in the chapter, and some pointers towards relative costs are given in Table 2.3. A short section is appended on selection criteria.

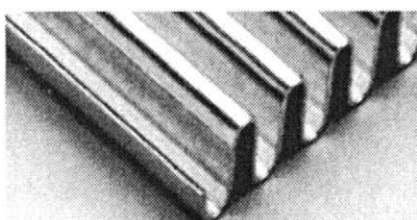
THE PLATE-FIN HEAT EXCHANGER (PFHE)

This group of exchangers is characterised by having secondary surfaces, or fin structures, between plane parting, or stream separation, plates. The fins have two functions, firstly to act as the secondary heat transfer surface and thus to obtain a low hydraulic diameter, and secondly to contain the pressure differential between the streams. The types of fin are more fully described in the following sections.

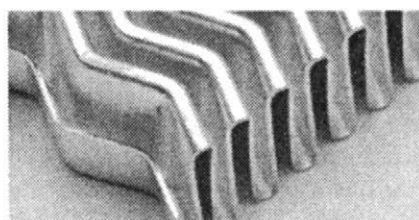
The Brazed Aluminium PFHE

Vacuum brazed exchangers

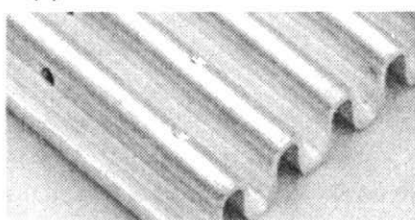
Originally developed for the aircraft industry in the 1940's, for use in environmental control and oil-fuel heat exchange duties, the aluminium PFHE is extensively used in the cryogenics, or gas separation and liquification, industries, where the good low temperature properties of aluminium are paramount. Widespread use is also made in ethylene production plant. The vacuum-brazed construction technique also allows for multi-streaming, of up to 12 streams, to be incorporated into a single core, saving much weight and cost of the system. The high area density (hydraulic diameter of the order of 1 to 2 mm) also allows for the low temperature differences necessary for efficient operation, especially at cryogenic temperatures, at which the power requirements are strongly influenced by Second Law constraints (see chapter 3). The various fin types used are illustrated in Figure 2.1, and the basic structure is shown in Figure 2.2.



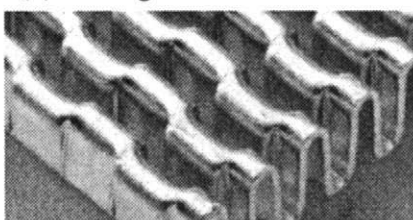
(a) Plain



(b) Herringbone



(c) Perforated



(d) Offset Strip Fin (OSF)

Figure 2.1 PFHE Fin types (courtesy Chart Heat Exchangers)

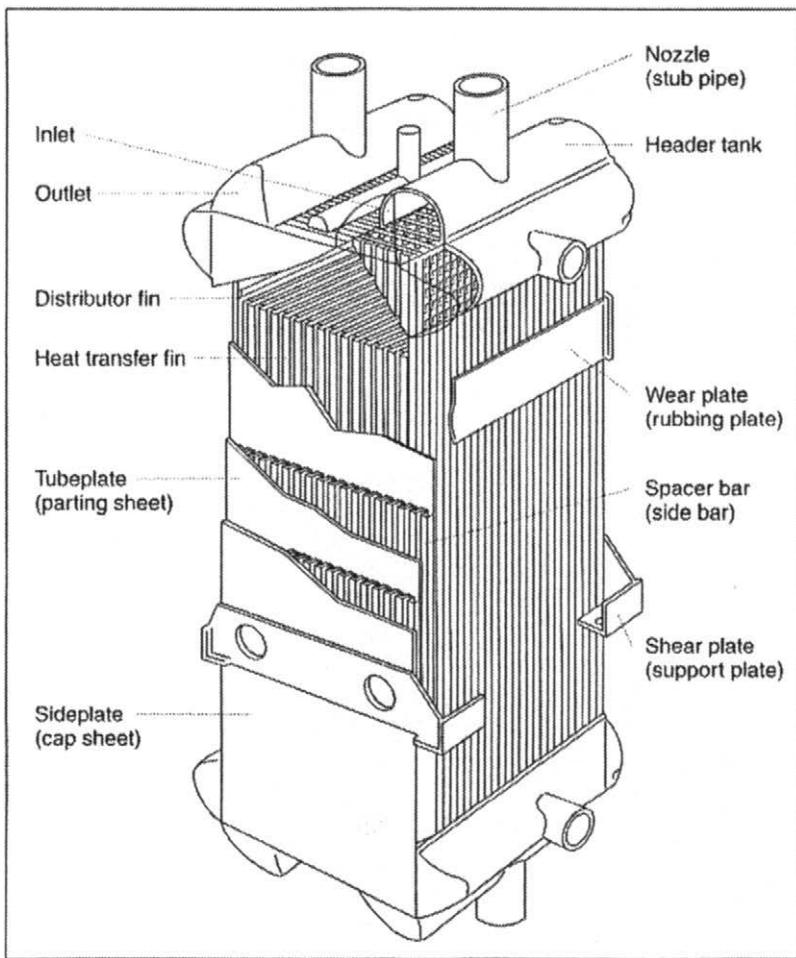


Figure 2.2 Basic structure of Plate Fin Heat Exchanger (PFHE)
(courtesy Chart Heat Exchangers)

A feature of the typically large PFHEs for cryogenic and ethylene applications (Figures 1.4 and 2.3) is that they are nearly invariably one-off units custom-designed for a given plant.

Aerospace PFHEs may be constructed in stainless steel, nickel and inconel in addition to aluminium. They are also tailored designs for specific applications - usually to fit in a closely-defined space. A typical aluminium exchanger for an air conditioning system is shown in Figure 2.4

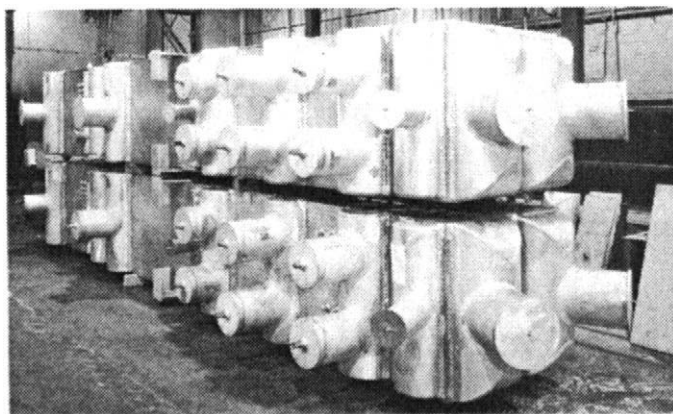


Figure 2.3 Aluminium PFHE for ethylene plant (courtesy Chart Heat Exchangers)

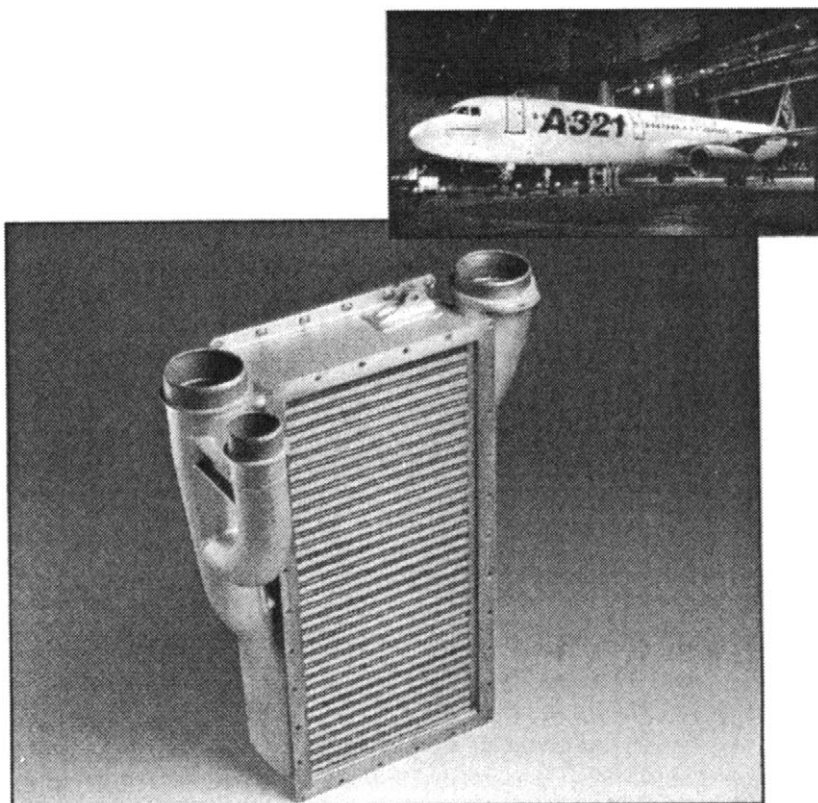
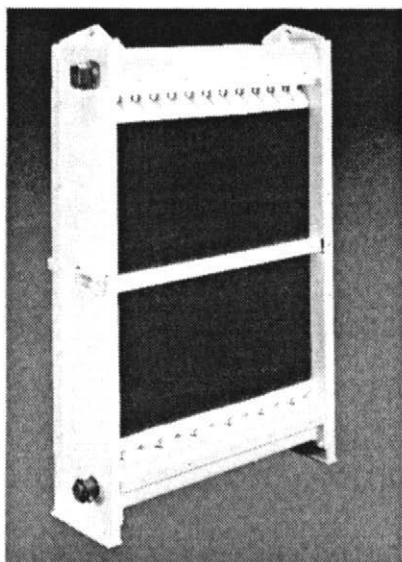


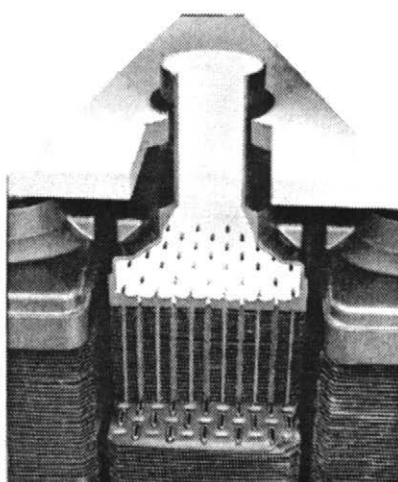
Figure 2.4 Primary air-air heat exchanger, Airbus A320
(Courtesy Secan/Allied Signal)

Dip brazed and solder-bonded exchangers

A second group of plate-fin exchangers, very similar in surface form and construction, but developed for an entirely different market area, is that used for many decades for a variety of prime mover applications. These applications range from automotive cooling (radiators) and heating to charge air or oil cooling for compressors. In this form, the plain, corrugated or louvred fin is bonded onto a series of flat tubes. Aluminium dip-brazing is the most common material of construction, but copper has also been extensively used. The units are almost invariably crossflow in configuration, most being for air-water or oil-water heat exchange with atmospheric air. Production numbers vary from the order of 10's (generation set and air compressor applications) to millions (car heaters, radiators). Not surprisingly, such variation is strongly reflected in the production method, the unit cost and expected lifetime. An example of a radiator for the former group of applications is shown in Figure 2.5.



(a) View of radiator



(b) Detail of element

Figure 2.5 Removable element radiator
(courtesy Serck Heat Transfer)

A further new development is in the field of air conditioning, especially for automotive applications. The traditional round tube (previously needed to withstand the high condensing pressures) with helical or plain plate fin is replaced by flat, internally-supported tubes and louvred fins (the arrangement being called "tube- and centre"). These can be either headered, as shown in

Figure 2.6a or wound as a single tube in serpentine form (Figure 2.6b). These developments have taken place simultaneously in Europe, the USA and Japan (Cowell and Achaichia (1997), Ohara (1999)). Figure 2.7 shows typical variants of the augmented galleried tubes.

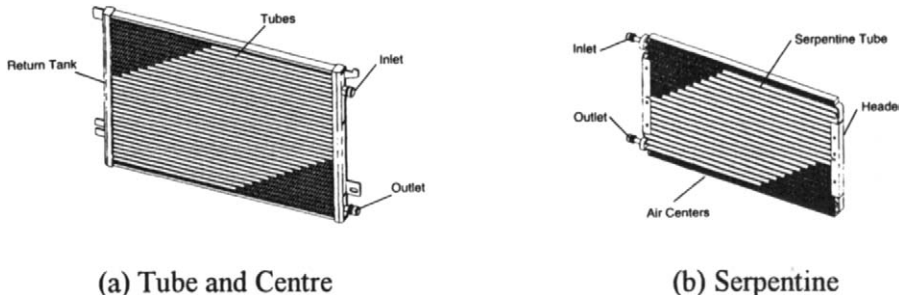


Figure 2.6 Vehicular air-cooled condenser types (Cowell and Achaichia (1997)), (reproduced by permission of Begell House, inc.)



Figure 2.7 Flat condenser tubes (courtesy Hitachi Cable)

The brazed stainless steel/ titanium heat exchanger

For temperatures above about 200°C aluminium is unsuitable for process exchanger use as it rapidly loses strength; in addition it is incompatible with many process chemicals. Stainless steel PFHEs, which can operate at temperatures up to 800°C, have been developed for these more demanding applications. The braze material is nickel, cupronickel, silver or copper according to process stream compatibility (largely temperature) and other considerations. Figures 2.8 and 2.9 show typical examples.

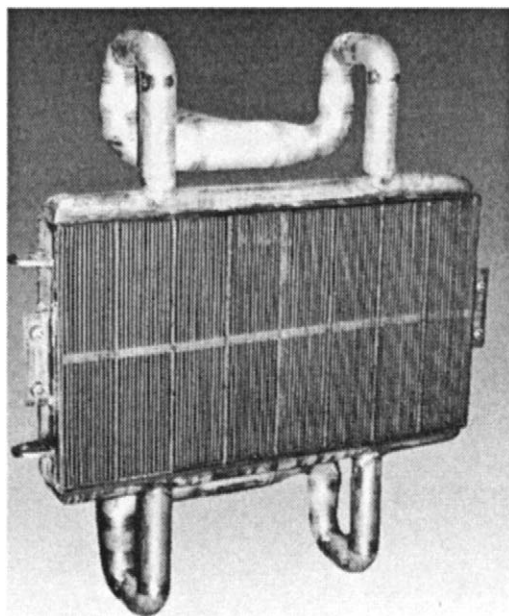


Figure 2.8 Brazed stainless steel polymer heater (courtesy Sumitomo)

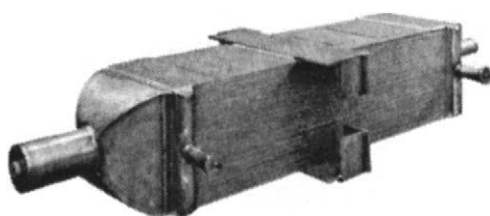


Figure 2.9 Brazed stainless steel exchanger (courtesy Chart Heat Exchangers)

TUBE-FIN HEAT EXCHANGERS

Tube-fin exchangers, with either individual fins or plate-fins, have been used for many years for locomotive radiators, charge air cooling, steam condensers and other applications. The tubes are commonly expanded onto the fins or fin block to effect the thermal contact. This is unsuitable for the thick or hard materials required for tubes and fins in many process applications. One method which has been developed to overcome this problem is the Elfin™ system of Britannia Heat Transfer in the UK, which uses an interlocking collar on each fin to provide a high quality tube contact in addition to very close control of the fin spacing. This procedure allows the use of stainless steel and exotic materials such as titanium and Hastalloy®. In addition, it allows the use of extruded internally-finned tube for compactness on both sides- especially important for oil coolers. A selection of finned surfaces is shown in Figure 2.10.

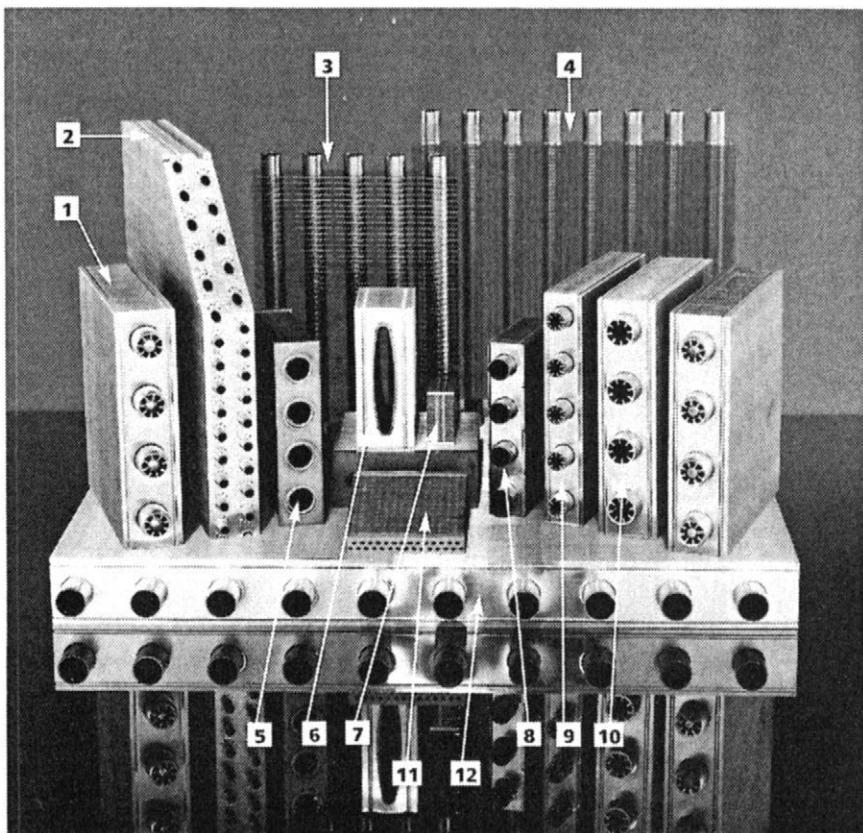


Figure 2.10 Tube and fin exchanger surfaces
(courtesy Britannia Heat Transfer)

DIFFUSION BONDED HEAT EXCHANGERS

Many processes, especially those involving corrosive or reactive chemicals, or actual reactions, do not tolerate dissimilar materials in fabrication. Diffusion-bonded heat exchangers have been developed to meet the increasing demand for compact alternatives to shell and tube exchangers traditionally used for these processes. Three such types are now described.

The Printed Circuit Heat Exchanger (PCHE)

This exchanger, originally developed for refrigeration applications, is formed by the diffusion bonding of a stack of plates with fluid passages photochemically etched on one side of each plate using technology adapted from that used for electronic printed circuit boards - hence the name. It is manufactured in the UK by Heatic Ltd. The diffusion bonding process includes a thermal soaking period to allow grain growth, thereby enabling an interface-free join between the plates. This gives base-material strength and very high pressure containment capability, in addition to the avoidance of corrosion cells. A typical cross section of a plate stack is shown in Figure 2.11. The fluid passages are

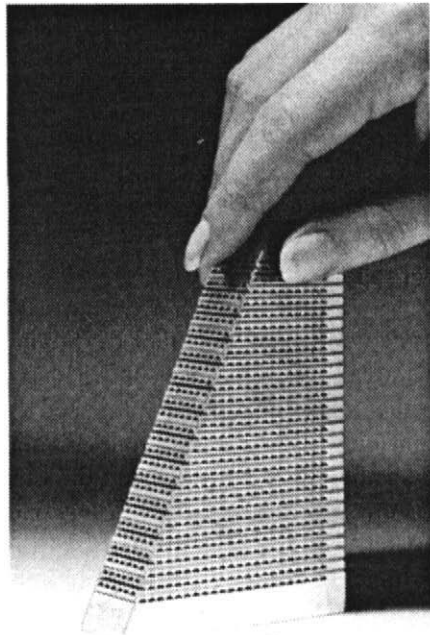


Figure 2.11 Section of PCHE
(courtesy Heatic)

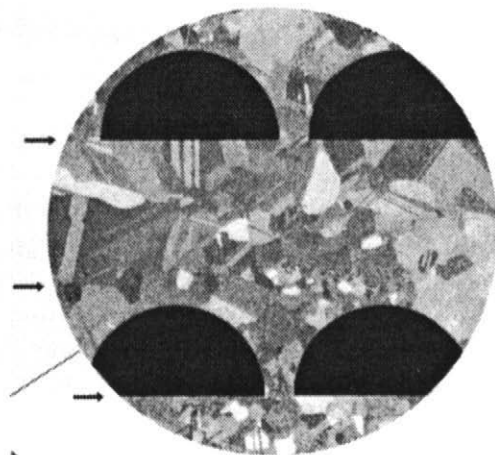


Figure 2.12 Photomicrograph of duct cross section (courtesy Heatic)

approximately semicircular in cross-section, being typically 1.0-2.0 mm wide and 0.5-1.0 mm depth, and giving hydraulic diameters of 1.5 to 3.0 mm, as shown in Figure 2.12. The passage shape may be corrugated as shown in Figure 2.13, or straight, depending on a number of factors such as the fluid used (liquid or gas, and Prandtl number if liquid), and the heat load and pressure drop relationship. The 'land' between passages is about 0.5 mm, the actual value being dependent on the pressure containment requirements of the exchanger.

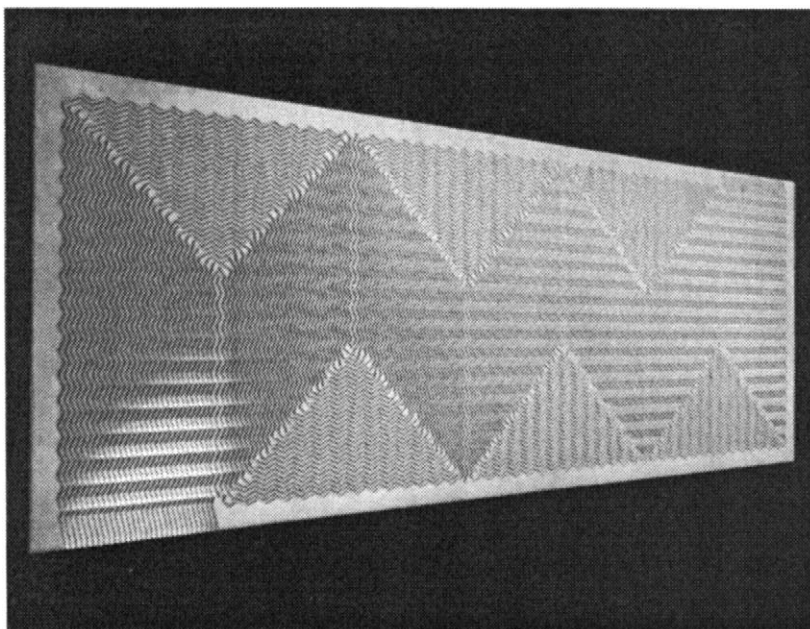


Figure 2.13 Detail of passage shapes (courtesy Heatic)

After bonding, any number of core blocks can be welded together to provide flow capacity to any level: units with surface areas in excess of 2500 m^2 have been manufactured. As can be inferred from the cross-counterflow plate shown in Figure 2.14, any desired flow stream configuration can be provided, and multi-streaming is easily incorporated. Headers and nozzles are welded directly onto the final core block. A typical finished unit, for a high pressure gas-gas duty, is shown in Figure 2.15. Note the 'short, fat' shape, a characteristic of the low hydraulic diameter, for duties involving high gas flow rates with pressure drop constraint (see chapters 4 and 6).

It can be seen from Figure 2.12 that the surface form of this exchanger is strictly-speaking of the plate-fin type, but with the fin of decreasing thickness towards the tip (at the plate join). The consequence of this fin shape is that even with the low conductivity materials frequently used for process exchangers, such

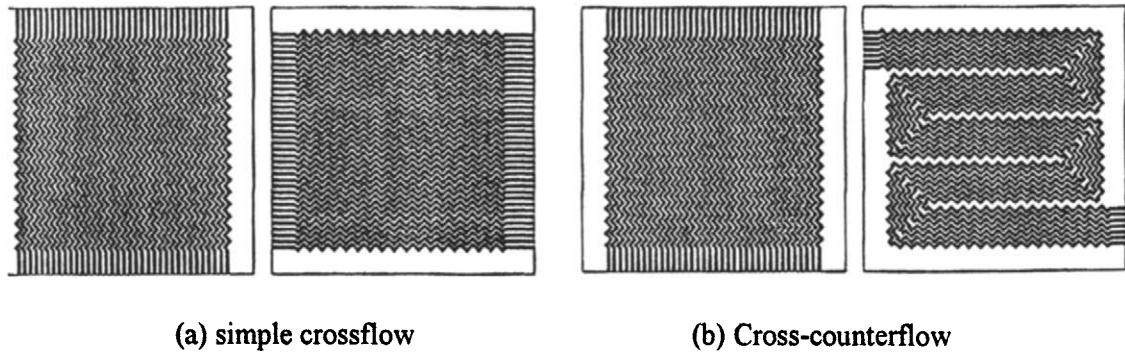


Figure 2.14 Illustrating the flexibility of the concept for simple crossflow, and for cross-counterflow with unbalanced capacity rates.

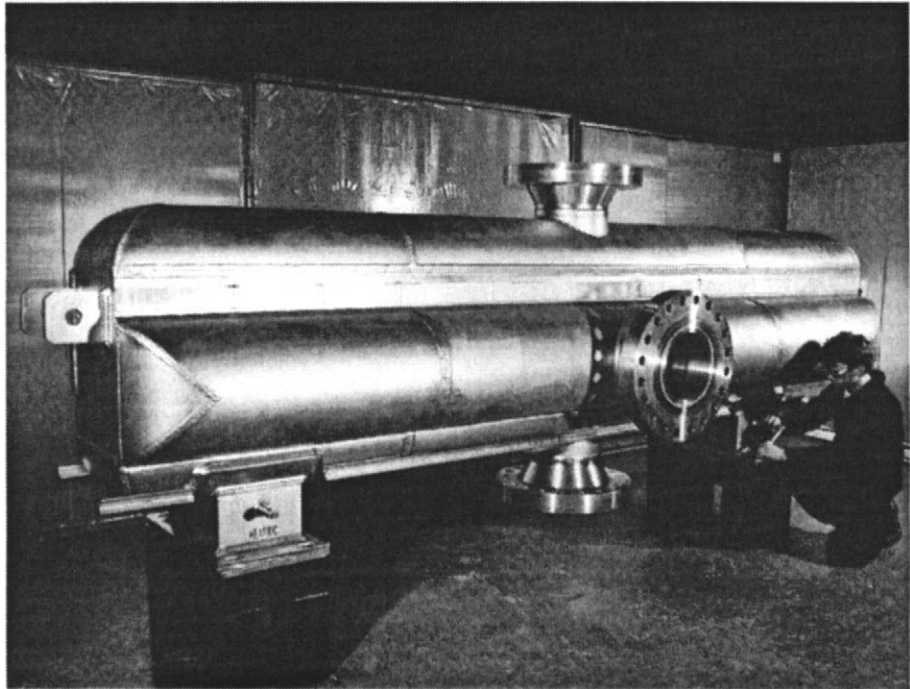


Figure 2.15 PCHE for high pressure gas duty (courtesy Heatric)

as stainless steel, Inconel etc, the fin efficiency is very high and surface effectiveness (see chapter 6) is usually implicitly taken as unity in design calculations. In other words the surface is treated as a primary surface.

A further consequence of the surface form is that the porosity of the exchanger is low-of the order of 0.4 to 0.55, compared with 0.6- 0.75 as a typical range for a plate-fin exchanger of similar material. This normally means higher weight and lateral dimensions for similar hydraulic diameters.

The MarbondTM heat exchanger

The MarbondTM heat exchanger, manufactured by Chart Heat Exchangers, is formed of slotted flat plates, that is, plates which have been chemically etched through. The plate pack is then diffusion- bonded together. In contrast with the PCHE, several, thinner, slotted plates are typically stacked to form a single sub-stream, thus giving the potential for very low hydraulic diameters, depending on the width of the slots and the plate thickness (variants with hydraulic diameters down to 0.33 mm have been tested). The porosity is typically 0.6 to 0.7. A representative form of the surface is shown schematically in Figure 2.16, and a cutaway view is shown in Figure 2.17. It is clear that the form of surface is very versatile, giving precise passage shapes from a form very similar to that of a plate- fin (PFHE) surface, to one similar to a PCHE surface. As with the PCHE, the range of constructional materials is only limited by their ability to be diffusion-bonded.

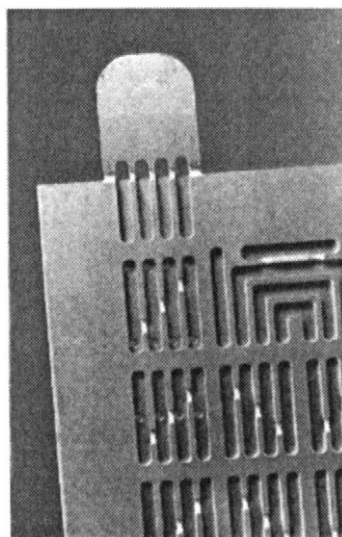


Figure 2.16 Detail of MarbondTM surface

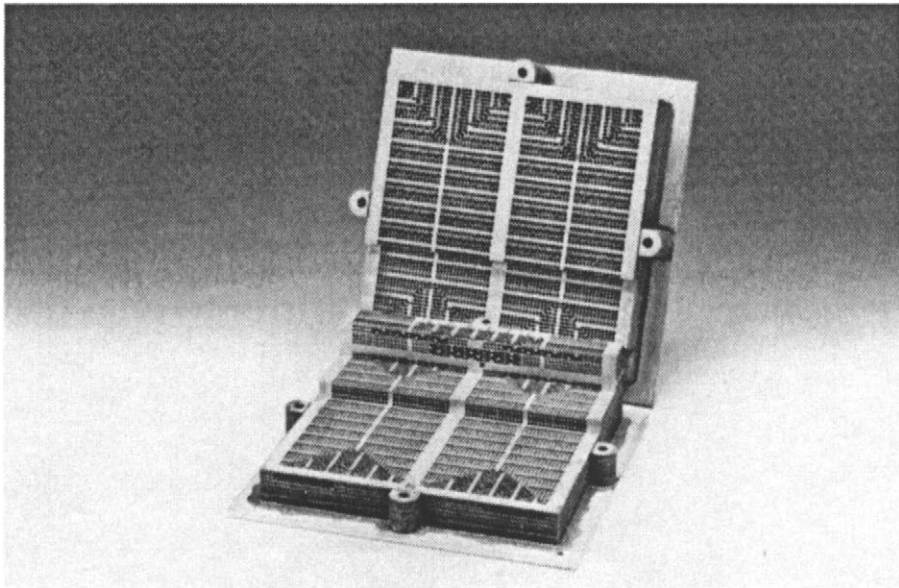


Figure 2.17 Cutaway of Marbond™ exchanger

The Rolls Laval super-plastically formed/ diffusion bonded (SPF/DB) heat exchanger

This exchanger was developed by Rolls Laval Heat Exchangers, a collaborative venture between Rolls Royce PLC and Alfa Laval Ltd. The exchanger, as with the PCHE, is also formed by the diffusion bonding of flat plates. The surface is formed, however, by an adaptation of the technique developed by Rolls Royce to form high integrity gas turbine blades. The basic construction process is shown in Figure 2.18. An element is formed by diffusion bonding three sheets of material (currently titanium) with the inner sheet to finally form the fin. A bond inhibitor is applied to the inward facing surfaces of the parting (outer) sheets using an appropriate pattern for the final fin passage shape (typically corrugated), and the unit is diffusion bonded at high temperature and pressure. The element is then placed in a die, and high pressure gas is injected at the edge to separate the sheets which are heated, the central sheet deforming super-plastically to form the fin, after which an increase of pressure flattens the element. Similar elements formed in this way are then diffusion bonded together to form a core. A completed unit is shown in Figure 2.19a, and a cutaway showing the internal structure is shown in Figure 2.19b

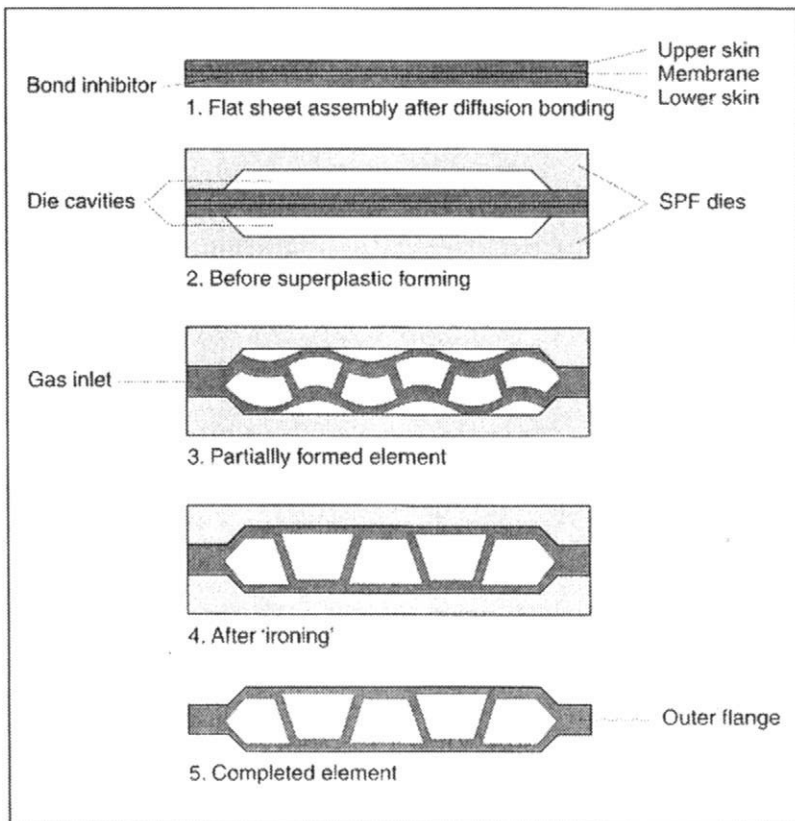
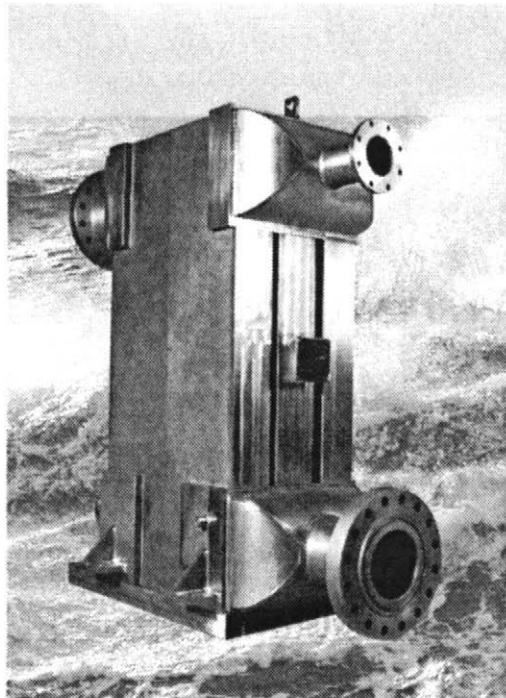


Figure 2.18 Basic construction process of a SPFDB element
 (courtesy Rolls Laval)

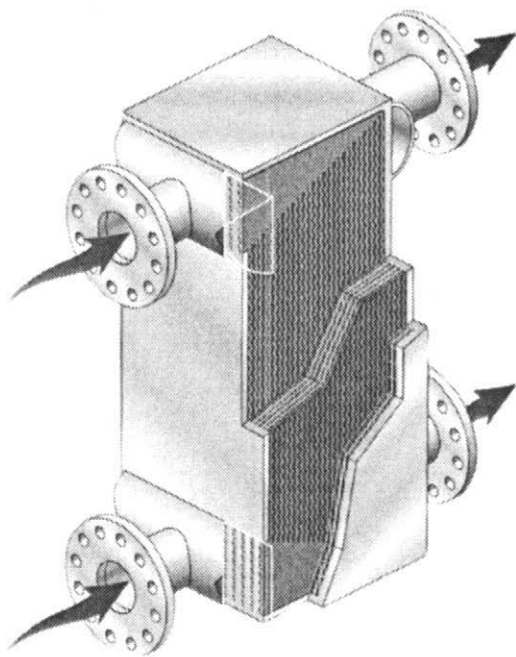
As with the PCHE fabrication method, the bond strength of the SPF/DB core is that of the parent metal, and very high containment pressures (up to 400 bar with titanium) can be sustained. Since the fin is formed by the superplastic stretching process, however, the porosity is similar to the brazed PFHE, typically about 0.6 to 0.75.

This exchanger, being of 100% titanium fabrication, is very suitable for offshore oil and gas duties, because of its corrosion resistance and low weight.

A typical range of hydraulic diameters is from 3-5 mm.



(a) Complete exchanger



(b) Cutaway view

Figure 2.19 A Rolls Laval Compact Heat Exchanger

WELDED PLATE HEAT EXCHANGERS

Several welded plate exchanger types are currently available for process applications. These have a similar advantage to that of plate and frame exchangers in that they use standard ranges of plate sizes, so that for a given application the 'design' process consists simply of selection of the number and size of the plates to meet the thermal and pressure drop requirements. This reduces the cost. A disadvantage is that present exchangers fall only marginally into the compact category, having hydraulic diameters in the range of 5-10 mm. An exchanger for a given specification will thus be smaller than a shell- and tube unit but larger than, for example, a PFHE. This section deals with types not related to a PHE derivative, the latter being described in the next section.

Manufacturers: Barriquand (Platular), Vicarb (Compabloc, Compaplate), Packinox, Hunt Engineering

The Platular Heat Exchanger

This exchanger consists of a series of flattened plate channels welded into header plates. The channels (side 'A') are of several configurations, and the spacing between them, forming the other stream (side 'B') channel can be adjusted to match the stream capacity rates. The plate channel configurations are shown in Figure 2.20.

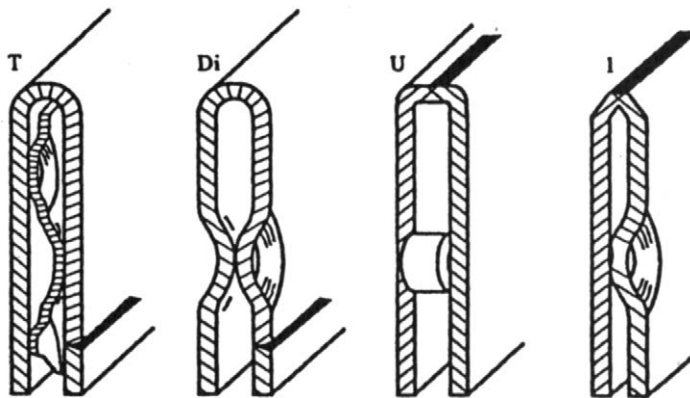


Figure 2.20 Platular channels (side A), types T, DI, U, I, showing plate contact points (courtesy Barriquand)

Type T is formed of a flat plate folded and welded longitudinally, and containing a turbulator which also acts as a secondary surface, thus reducing the hydraulic diameter of the channel side. It is thus especially suitable for gases and viscous (high Prandtl number) fluids. Type D1 is formed of plates stamped with opposed dimples, which are spot-welded together. The resulting containment pressure is thus high. Type U has flat plates separated by welded studs, which enables a rather wider plate spacing and allows mechanical cleaning through flanged end covers. Type I has one flat plate and one stamped plate. Both types U and I can handle high pressure fluids. If a highly contaminated fluid is used the channel shape can be arranged as shown in Figure 2.21, with no contact points. Side B is used for the contaminated fluid, and is cleanable. In general, the channels with contact points (types T, DI, and I) are not cleanable by mechanical means.

Several different streams can be accommodated by appropriate porting arrangements, and the basic surface type allows for any combination of flow configurations.

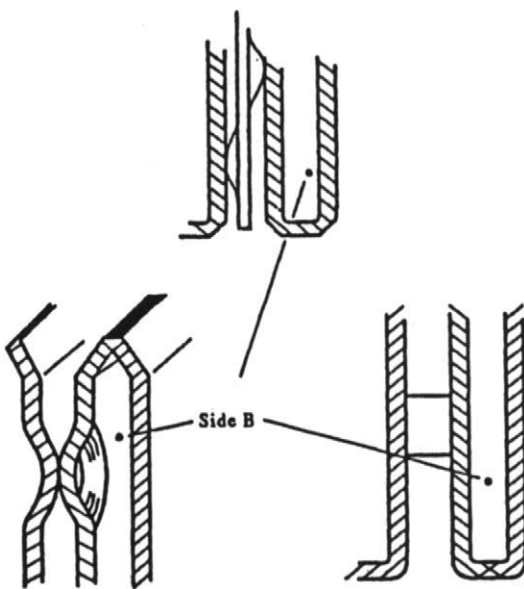


Figure 2.21 Platular channels (side B), without contact points
(courtesy Barriquand)

A typical assembly is shown in Figure 2.22, for two streams.

Typical hydraulic diameters of this exchanger are 4 to 8 mm (type I) to 28 mm (type U) for side A, and from 6 mm to 80 mm for side B.

The Compabloc^R and Compaplate^R Heat Exchangers

The Compabloc^R Heat Exchanger

This exchanger consists of a stack of pressed plates automatically welded at alternate edges to provide a crossflow configuration as shown in Figure 2.23.

A column liner is resistance welded to each corner of the stack, and head liners are also welded on without filler material. The column liner supports both a bolted frame, top and bottom heads and nozzle panels, as shown in the exploded diagram in Figure 2.24. As can be seen in this example, multi-passing of either or both streams is possible by means of baffle assemblies between the plate stack and panels. Gaskets are used to seal the nozzle panels. These limit the maximum operational temperature to 300°C.

The form of the plates is clearly similar to that of the gasketed plate heat exchanger (PHE) so will have broadly similar thermal performance characteristics. The hydraulic diameter is typically about 7 mm, based on the plate spacing of 5 mm.

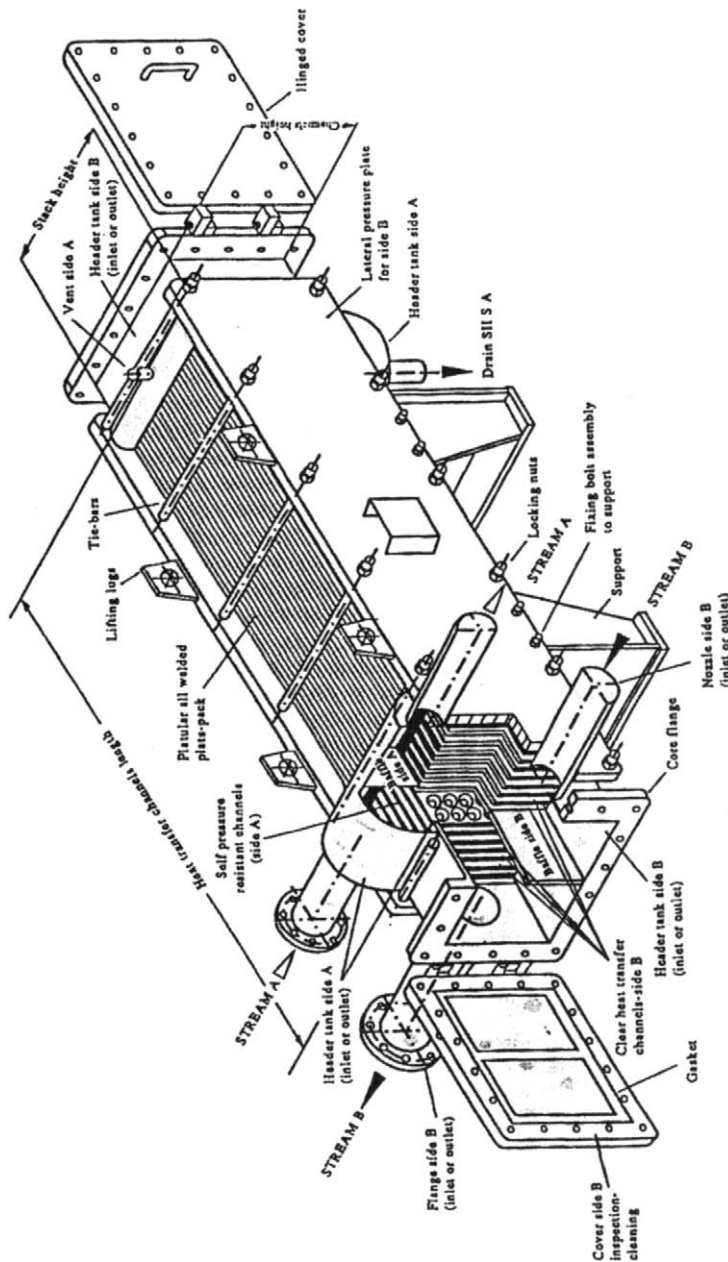
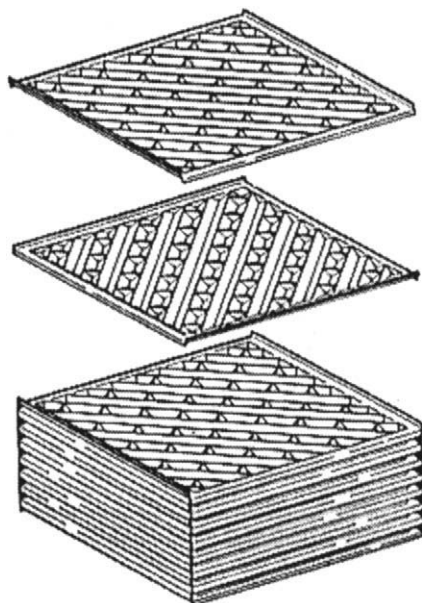


Figure 2.22 Assembly of Platular unit (courtesy Barriquand)



Precision pressing and welding of plate pack in automated machines.

Figure 2.23 Compabloc configuration (Courtesy Vicarb)

The Compabloc^R Wide Gap Welded Heat Exchanger

This exchanger is especially designed to handle dirty fluids on one side (the process side), which is fully accessible for mechanical cleaning. It consists of a stack of welded dimpled plates (Figures 2.25 and 2.26) mounted in a bolted frame in an essentially counterflow configuration, as shown in Figure 2.27. Up to four fluid streams can be accommodated. A range of plate dimple sizes is available, and the plate gap (i.e. between the plates) is variable between 4 mm and 20 mm. to accommodate a range of fouling streams. No inter-plate gaskets are used, but the process side employs a cover plate seal, limiting operating temperatures to 260°C. An exploded view is shown in Figure 2.28.

The hydraulic diameter of the clean side is about 5 mm and that of the process side from 8 mm to 40 mm, thus within the strict definition of 'compact' on one side.

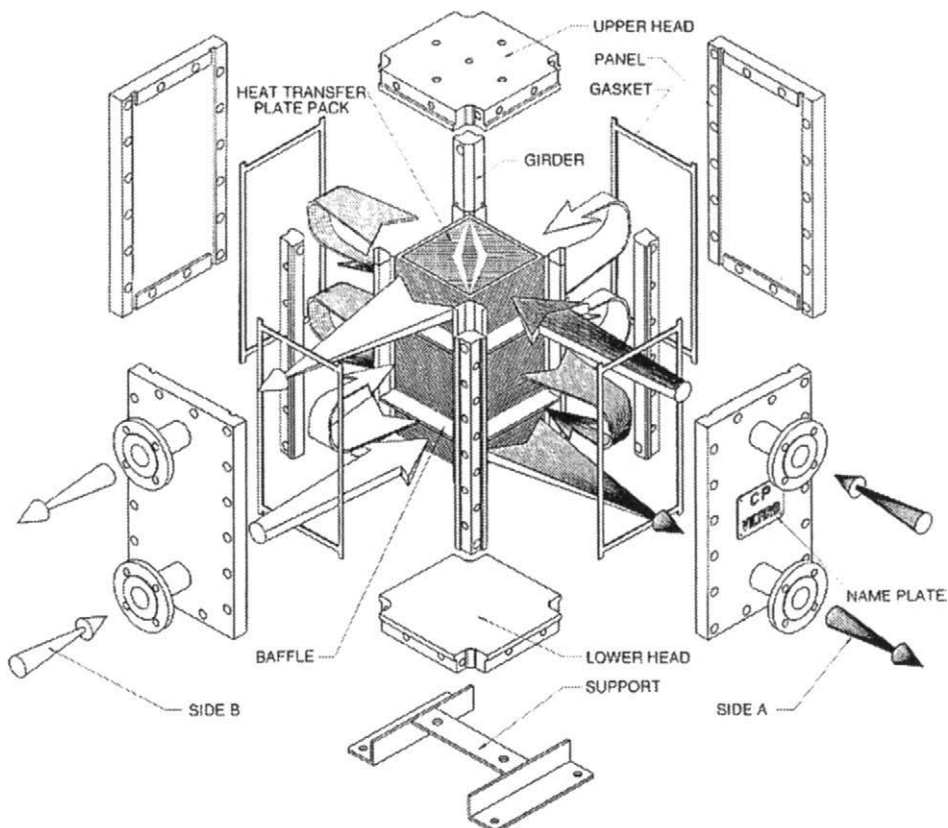


Figure 2.24 Exploded view of Compabloc, showing cross-counterflow arrangement (Courtesy Vicarb)

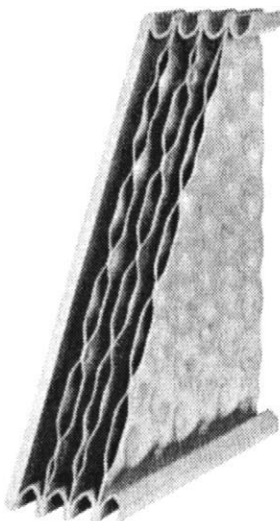


Figure 2.25 Compaplate Wide Gap plate assembly

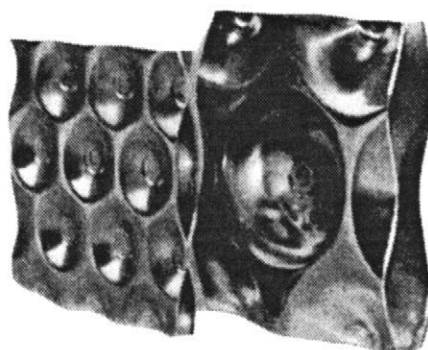


Figure 2.26 Compaplate Wide Gap Dimple configurations
(courtesy Vicarb)

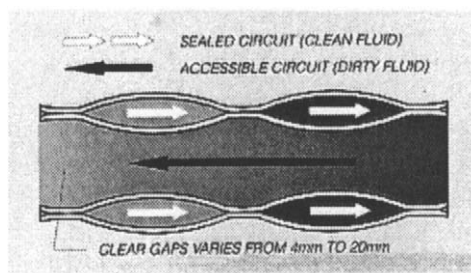


Figure 2.27 Compaplate Wide Gap flow arrangement (courtesy Vicarb)

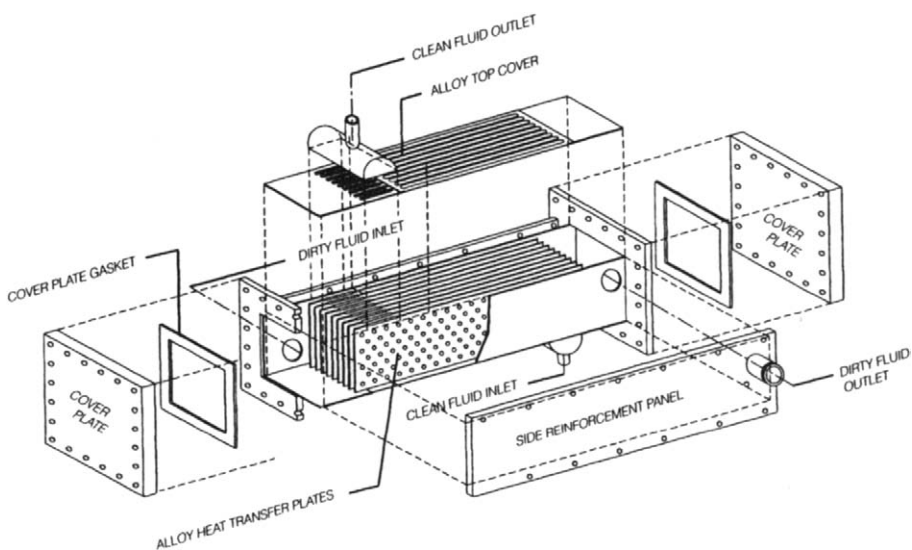


Figure 2.28 Compaplate Wide Gap exploded view (courtesy Vicarb)

The Packinox Welded Plate Heat Exchanger

(Manufacturer Framatome)

This exchanger has plates explosively formed in a corrugated chevron pattern in a counterflow configuration similar to that of a PHE. Very large bundles are possible, an example being shown in Figure 2.29. Edge welding is accomplished in the world's largest press, as shown in Figure 2.30. They are inserted into pressure vessels, with bellows on the internal fluid ducting to allow for differential expansion. A development, used especially for in-column vaporisers and overhead condensers, is the Ziepack. These units are crossflow units as shown in Figure 2.31, with a near-tubular stream flow on the "double-plate" side, which is formed by laser-welding two plates back-to-back along the

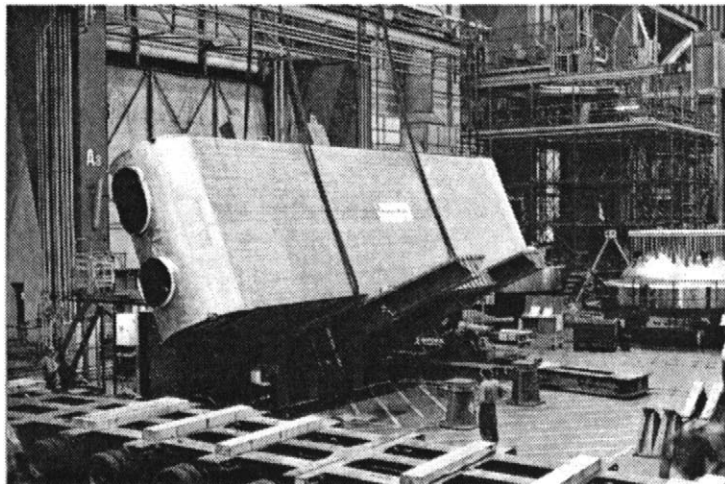


Figure 2.29 A Packinox exchanger of $16,000\text{m}^2$ surface area
(courtesy Alain de Baudus/Framatome)

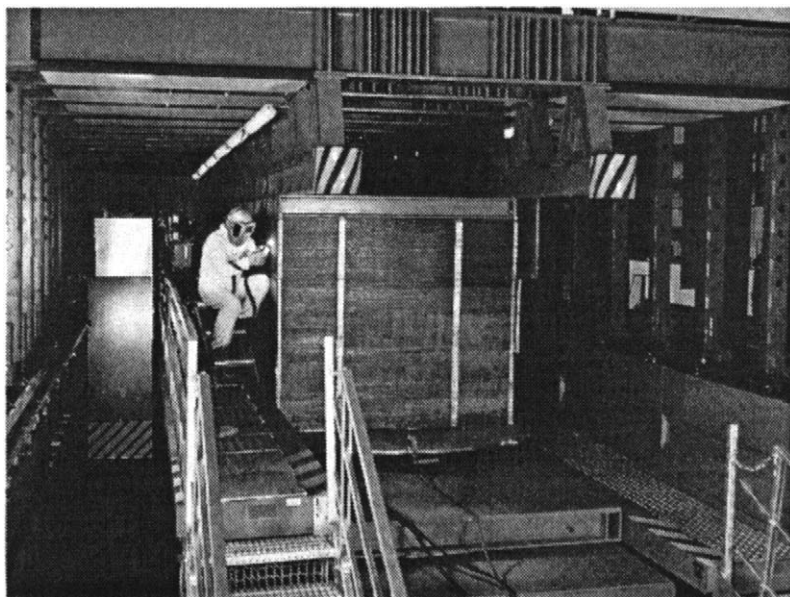


Figure 2.30 Stack welding of a Packinox block
(courtesy René Quatrain/Framatome)

contact lines, then expanding hydraulically. The other side is corrugated to give a flow path in a similar form to that of the shell-side of a shell- and tube exchanger. Bundles are often assembled to operate in a cross-counter configuration.

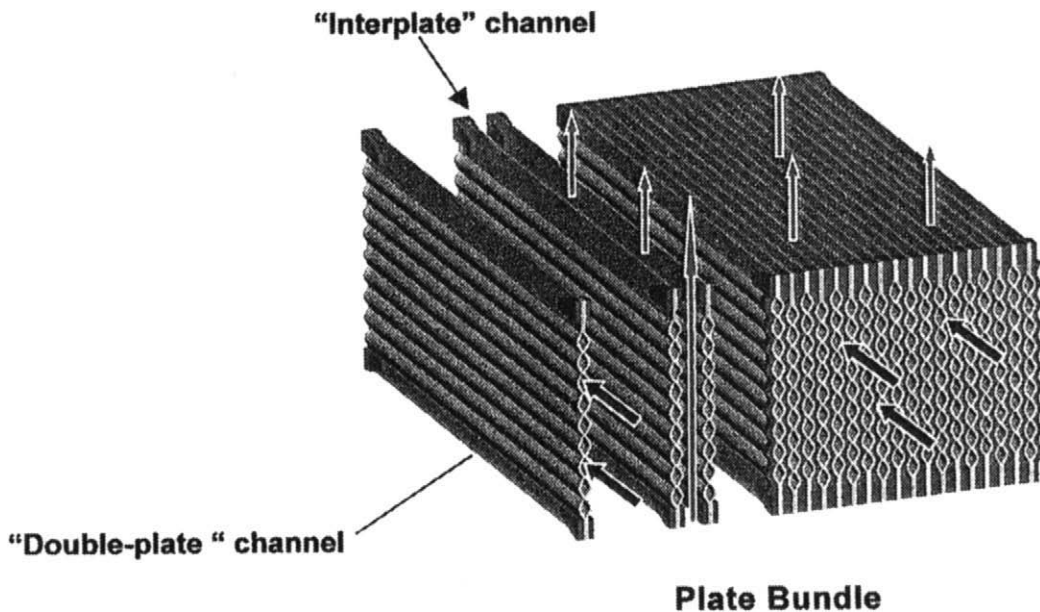


Figure 2.31 The Ziepack plate pack (courtesy Framatome)

Hydraulic diamters for both variants are of the order 6-10 mm.

The Hybrid Heat Exchanger

Manufacturer: Balcke-Durr (plates, Hunt Thermal Engineering

In this exchanger the plates are pressed in a corrugated form with transverse 'shapings' at intervals. Pairs of plates are welded back to back, as shown in Figure 2.32, so forming the shape of tubes on one side. The other side (necessarily in crossflow configuration), is of a parallel corrugated shape, with the shapings providing spacing and support (Figure 2.33). The exchanger surface structure thus embodies elements of the corrugated plate form and the tubular form, the latter giving advantages of containment pressure and some heat transfer enhancement from the internal corrugated effect of the transverse

shapings. The corrugated (crossflow) side has parallel channels and, probably, a superior performance to the equivalent shell side of a tubular unit.

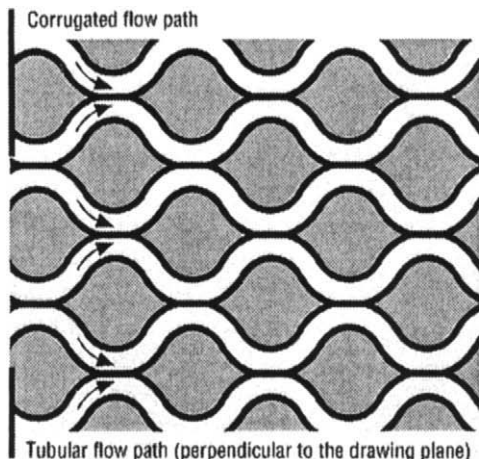


Figure 2.32 Flow path of Hybrid Heat Exchanger

(both figures courtesy Balcke-Durr)

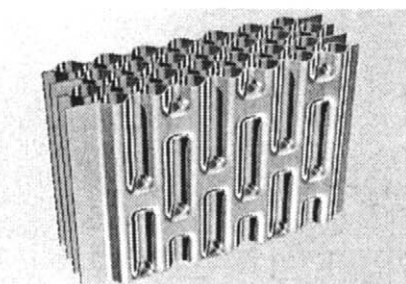


Figure 2.33 Plate pack configuration

Plate packs are assembled and welded with transverse and seam welds, together with supporting framework, and mounted inside a pressure vessel containing headers: the vessel may contain baffles to allow cross-counterflow configuration as shown in Figure 2.34. Pass variation can also be achieved on the tube side.

The equivalent tube diameters range from 6 to 9 mm depending on the depth of the shaping, thus giving a size advantage over a tubular unit. The hydraulic diameter of the plate side is of the same order, but can be made larger by special lateral shaping. The basic plate element is 330 mm wide, with a length from 450 to 8000 mm, which together with stack height variation (plate number) gives considerable flexibility in capacity.

PLATE AND FRAME HEAT EXCHANGERS (PHE) AND DERIVATIVES

This section deals with the original plate and frame exchanger type and its direct derivatives, that is those with ports integral with each plate; some are totally brazed, and some are welded, either totally or in pairs.

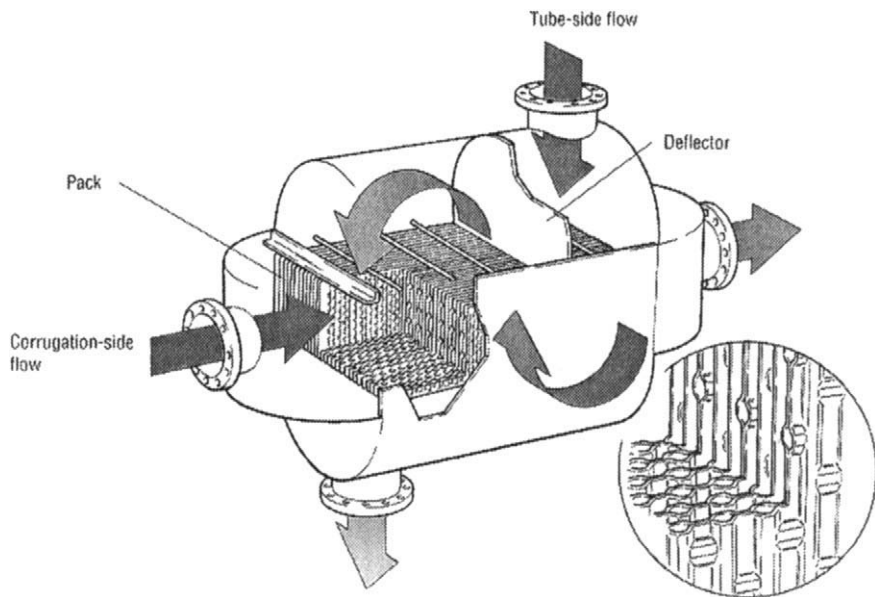


Figure 2.34 Section of Hybrid Heat Exchanger (courtesy Balcke-Durr)

Plate and Frame Heat Exchangers (PHE)

Manufacturers: Alfa Laval, APV Baker, Barriquand, GEA, HRS, SWEP, VICARB, Schmitt, Funke.

The PHE is the best known of all alternatives to the shell and tube exchanger, having been introduced in 1923 for milk pasteurisation. It is widely used in the food and drink processing industries, and is selectively used in the chemical processing industries.

This heat exchanger, which provided the generic form for many of the above welded plate forms, consists of a stack of pressed plates (Figure 2.35) in a bolted frame (Figure 2.36), including stiff end plates to contain the stream pressure. Registration is facilitated on assembly by means of shaped slots in top and bottom edges of the plates. The slots engage in an upper carrying bar and a

lower guiding bar mounted in the frame. Sealing between streams is accomplished by means of gaskets - usually elastomeric - trapped in grooves in the plates. These are either clipped or glued in place, and except in the distribution regions any leakage caused by failure of the seals will be to the environment and not between streams. In the distribution regions there is a double seal.

A special feature of the PHE is that the ports for the hot and cold streams are incorporated in the plate form, thus obviating the need for header arrangements. In addition, by the use of blanking plates within the stack, multi-passing can be accommodated, as illustrated in Figure 2.37, allowing for increased flow length and hence reduced temperature approach.

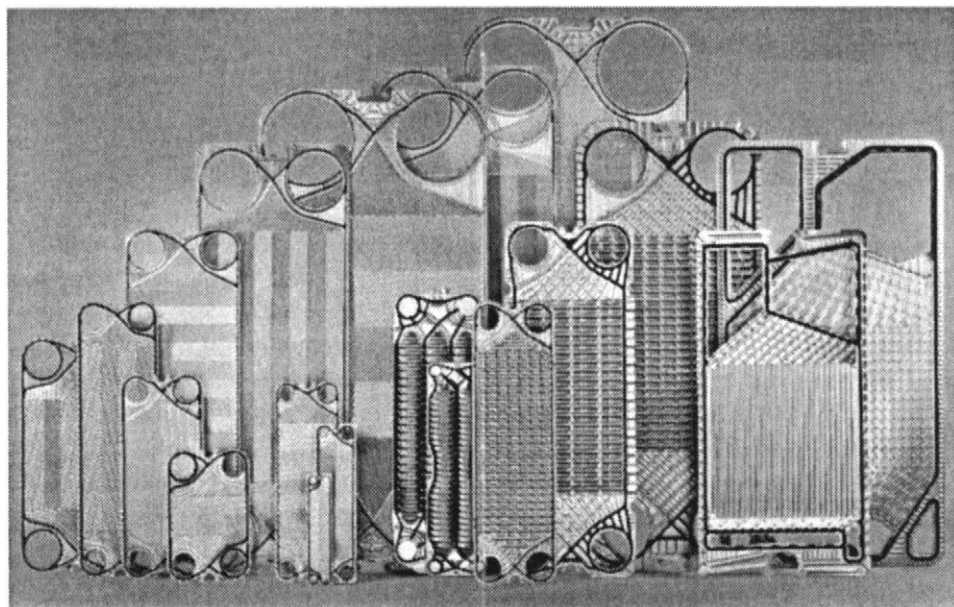
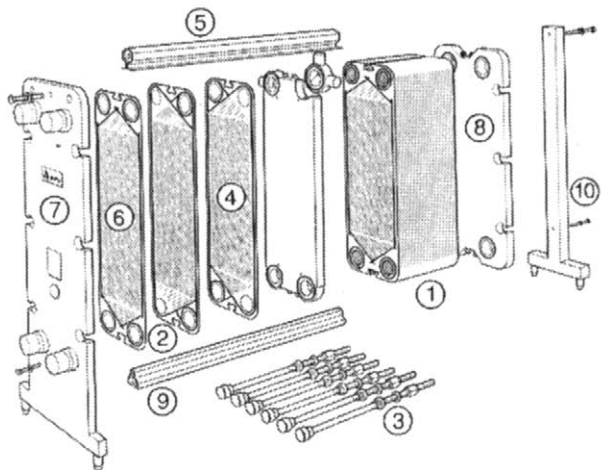


Figure 2.35 Typical range of plate forms
(courtesy GEA)



Parts of a whole

1. Plate pack
2. Corrugated plates with inlet and outlet
3. Tie bar
4. Gasket and gasket groove
5. Top bar
6. Flow plate
7. Fixed head with inlet and outlet ports
8. Followerplate with four ports
9. Bottom bar (guide bar)
10. Column

Figure 2.36 Plate stack assembly (courtesy APV)

Apart from the inherent modular nature of the PHE (the facility to vary the number of plates in the stack), the performance can be regulated by the use of different patterns of plate pressing - in other words the form of corrugation. The corrugations are normally of chevron type, and are characterised by the angle (θ) of the corrugations to the overall direction of flow. High θ designs have high thermal performance and high pressure drop, to a limit of 90° , giving a so-called 'hard' surface, and low θ designs have moderate thermal performance and low pressure drop (Figure 2.38). Some manufacturers combine low and high plate types back to back for intermediate performance ratings. In addition, some specialist designs are offered, for example for fouling fluids (Figure 2.39), with non-contacting plate channels of 5-12 mm spacing, and for asymmetrical duties (Figure 2.38). GEA have also introduced a new design (the Ecoflex, Figure 2.39) which obviates the need for a gasket groove in the distribution area, thus increasing the effective thermal length. A saving of up to 25% of surface cost is claimed for this development.

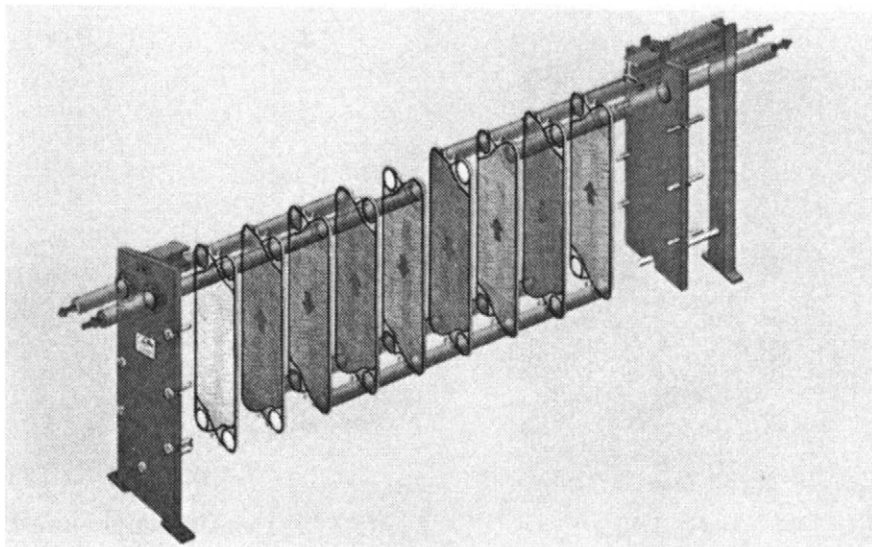


Figure 2.37 Multi-passing flow arrangement (courtesy GEA)

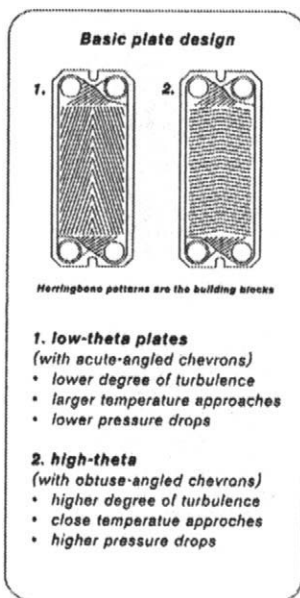


Figure 2.38 Basic plate corrugations (courtesy SWEP)

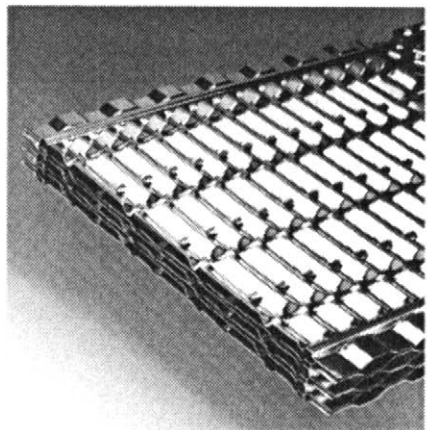


Figure 2.39 The GEA Free-Flow plate structure
(courtesy GEA)

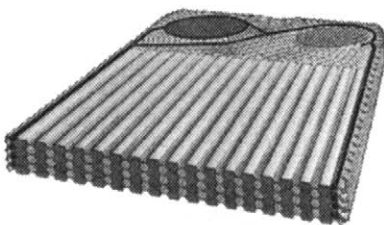


Figure 2.40 The Alfa Laval Flow-Flex plate structure
(courtesy Alfa Laval)

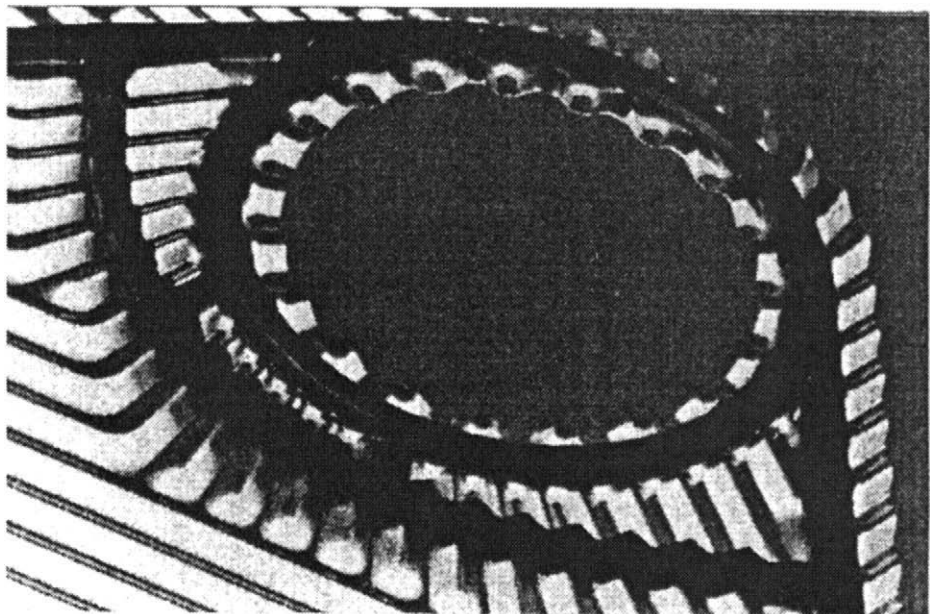


Figure 2.41 Ecoflex port geometry (courtesy GEA)

Brazed Plate Exchangers

Manufacturers: Alfa Laval, SWEP, GEA, HRS, Schmitt, Funke

These exchangers (Figure 2.42) were developed in the 1970's for the refrigeration industry and rapidly replaced shell and tube types in the low to medium capacity range. They are making steady inroads in other application areas.

The basic plate form is the same as the gasketed type, but the gasket is omitted and the seal is effected by folding the edge of each plate over to overlap that of the adjacent plate (see Figure 2.43). The assembly is then vacuum brazed, so that bonding is achieved over both edges and each contact point of the herringbone corrugation. In this way leak tightness is obtained up to 30 bar operating pressure.

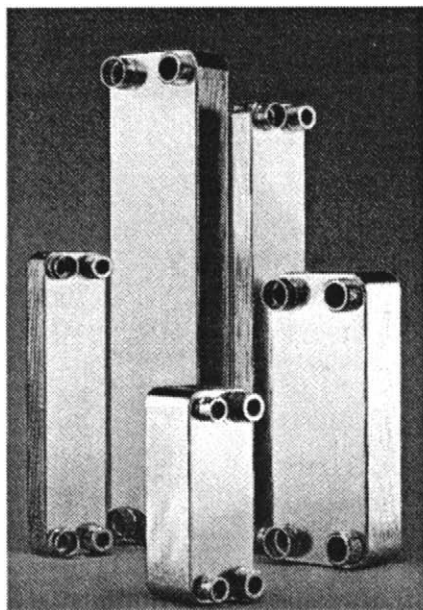


Figure 2.42 A range of brazed exchangers (courtesy SWEP)

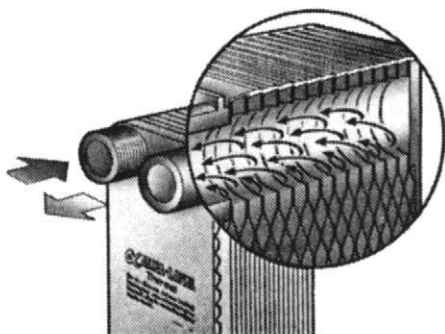


Figure 2.43 Method of edge sealing (courtesy Alfa Laval)

The normal brazing metal for halogen refrigerants is copper. For refrigeration duties with ammonia, and for process applications with corrosive fluids, most manufacturers now offer versions with a nickel braze, giving an 'all stainless' exchanger.

Welded Plate Heat Exchanger (PHE types)

Manufacturers: Alfa Laval, Schmitt, GEA

This is an all-welded exchanger in which the plates are laser welded along two contact lines in the plane of the plates which are equivalent to the gasket grooves in a conventional PHE, as illustrated in Figure 2.44. The two dimensional welding allows expansion and high thermal cycling protection. The pack is mounted in a frame and accommodates containment pressures of up to 40 barg. The absence of gaskets allows operational temperatures to 350°C.

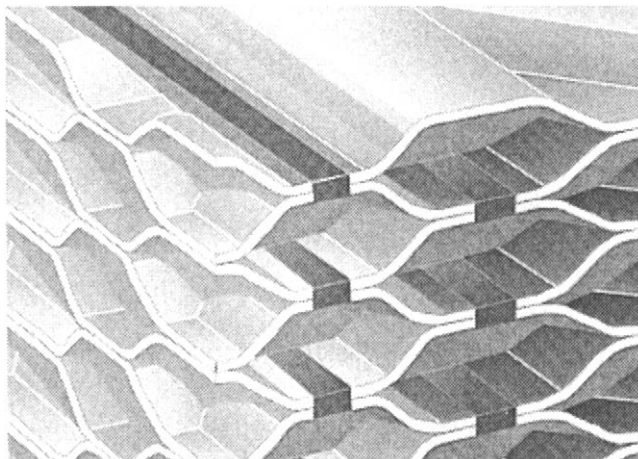


Figure 2.44 Welded Plate exchanger (AlfaRex) (courtesy Alfa Laval)

Welded Plate Pair Heat Exchanger

Manufacturers: Alfa Laval, APV

This form of exchanger was developed for safe heat exchange where one of the fluids is highly corrosive. Pairs of plates are welded along the channels, as shown in Figure 2.45, and each pair is separated with a gasket to provide the other fluid path. Thus the only contact of the aggressive medium with gasket material is with the port gasket between the welded plate pairs.

Because the only internal support is that of the edge weld, the pressure rating is lower than that of the brazed exchanger, and is typically 25 bar.

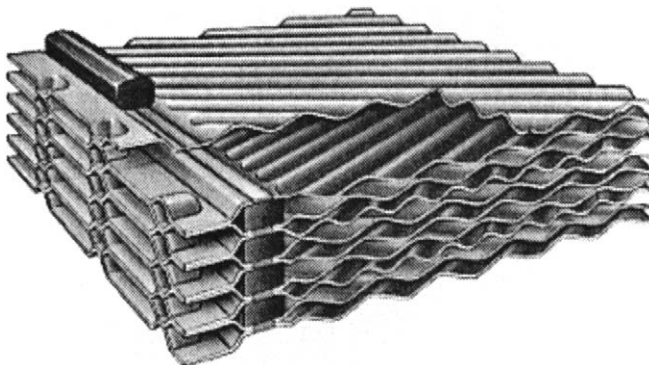


Figure 2.45 Welded Plate Pair exchanger (courtesy Alfa Laval)

Other specialised PHE types

Various manufacturers offer special types for exceptional applications, including a graphite/fluoroplastic composite plate type (Figure 2.46) for exceptional corrosion resistance, and a double wall type (Figure 2.47) designed to avoid the hazard of reaction if the two media should mix. SWEP have introduced two brazed types (Figure 2.48) for relatively 'short' duties, one with crossflow, to accommodate applications with strongly asymmetrical flows (to 1:5).

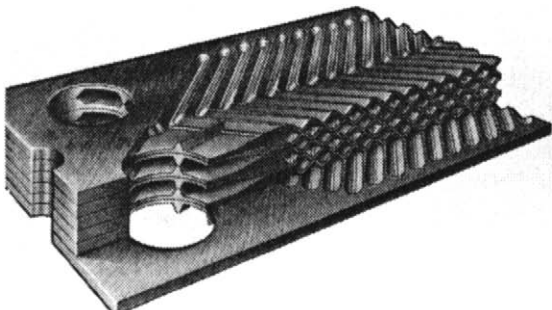


Figure 2.46 The Diabon F Graphite Plate exchanger

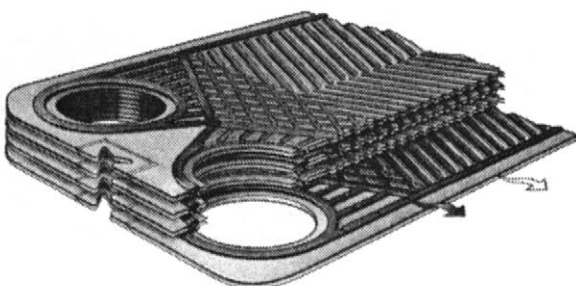


Figure 2.47 The Double-Wall plate exchanger

(both courtesy Alfa Laval)

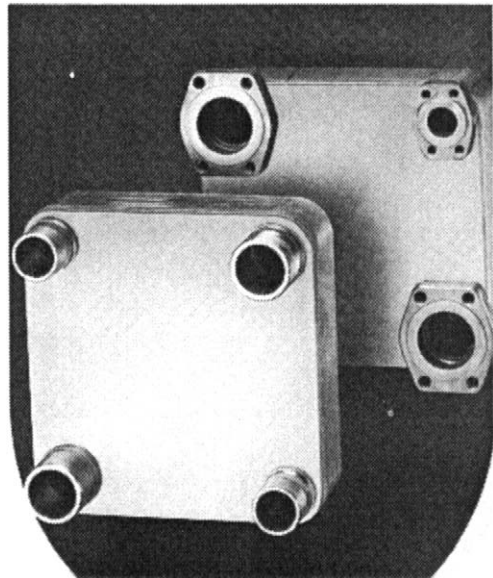


Figure 2.48 The SWEP B60 brazed plate exchanger, for asymmetrical flows (courtesy SWEP)

THE PLATE AND SHELL HEAT EXCHANGER (PSHE)

Manufacturers: APV, Vahterus, Kapp

This exchanger utilises a welded pack of corrugated plate pairs of circular planform (developed in Finland by Vahterus) with ports for one fluid at the extremes of a diameter, so that this fluid finds its own flow path within the plate planform. The other fluid is introduced through ports in the cylindrical shell and is ducted across the plate pack in counterflow, as shown in Figure 2.49. Other flow configurations can be achieved by baffling, as illustrated in Figure 2.50. The plate pack can be made removable for shell side cleaning. Because of the feature of a cylindrical shell, the containment pressures are higher than for other plate types, with design pressures to 100 bar being quoted.

Hydraulic diameters are of the same order as other plate types, i.e. 5- 10 mm.

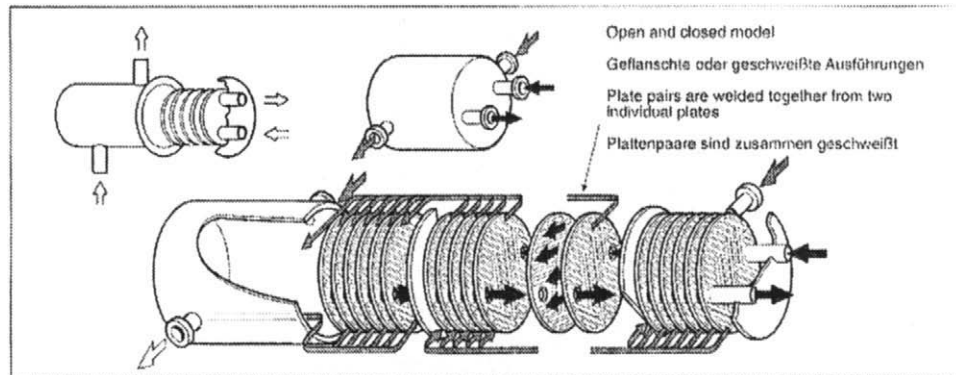


Figure 2.49 Schematic of PSHE (courtesy Vahterus)

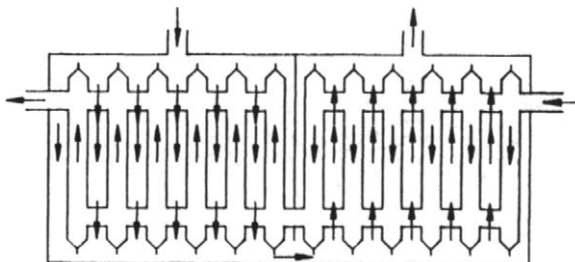


Figure 2.50 Two pass configuration, shell and tube side (courtesy Vahterus)

SPIRAL HEAT EXCHANGERS (SHE)

The spiral heat exchanger (SHE) has a long history as an exchanger type, being used extensively for heat exchange for fluids containing suspended materials such as slurries: the common application is for heating sewage sludge

for digestion. Most of these types are strictly speaking not compact, but some more recent developments are compact (Figure 2.51).

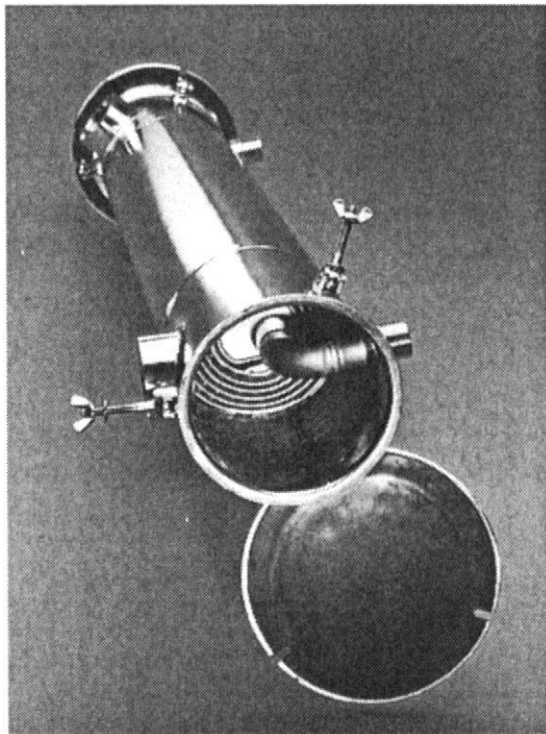


Figure 2.51 A compact Spiral Heat Exchanger (courtesy Occo Coolers)

The (SHE) operates in nearly complete counterflow, and is assembled from two long strips of plate wrapped to form a pair of concentric spirals, as visible in the schematic in Figure 2.52. Alternate edges of the passages are closed so that the fluid streams flow through continuous sealed channels. Studs are normally welded onto one side of each strip for support. Covers are fitted to each end to complete the unit. It is clear from the single channel spiral form that the typical Ntu is high, implying 'long' thermal duties.

The unit can be made of any metal which can be cold-formed and welded. Available sizes range up to 500 m^2 in one body. Typical applications cover liquid-liquid duties, condensers and gas coolers. A variant has one medium in crossflow and the other in spiral flow. This type can be used for condensing duties, and as an effective thermosyphon reboiler in distillation columns.

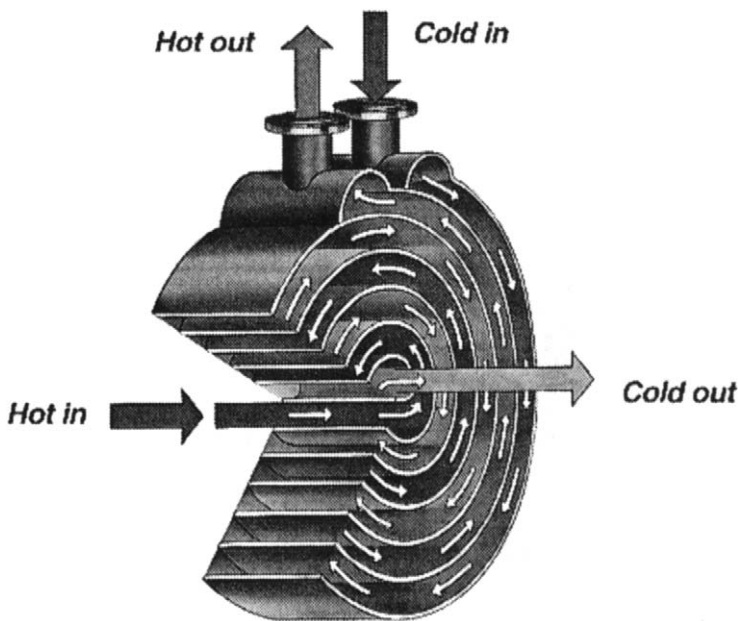


Figure 2.52 Schematic of Spiral Heat Exchanger (courtesy Alfa Laval)

Channel spacings range between 5 mm and 25 mm (representing hydraulic diameters of 10 to 50 mm) being available, so that the potential user can trade off between high heat transfer surface area density and a low propensity for blockage by fouling. This is enabled by the scouring action of secondary flows in the passages. Access for cleaning via removable flanges is provided, and chemical cleaning is also suitable.

COMPACT SHELL AND TUBE HEAT EXCHANGERS

As shown in chapter 1, shell- and tube exchangers can be both compact and small. Some polymer types have area densities of up to $500 \text{ m}^2/\text{m}^3$, while the aluminium fuel heater/oil coolers used in most aircraft engines can exceed this figure by several times. This is achieved by the use of large numbers of small diameter (typically 3 mm o.d.) tubes, which are often augmented, for example by dimples. An example is shown in Figure 2.53.

There are also various developments affecting shell-side behaviour, such as novel baffle types and twisted tapes. Disc- and ring baffle systems are often used instead of segmental systems as they have been shown to offer superior performance.

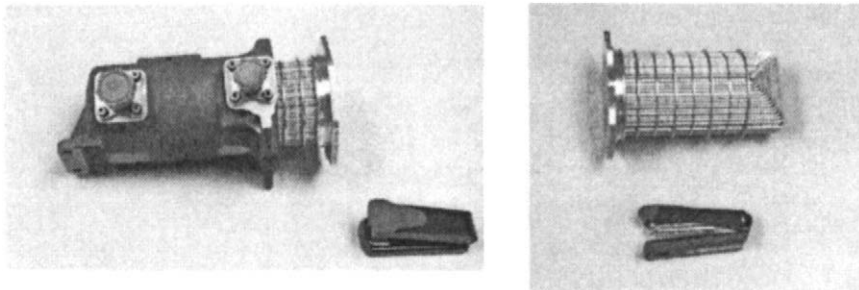


Figure 2.53 A compact shell and tube exchanger for fuel heating/oil cooling, and a typical two-pass tube bundle. (courtesy Serck Aviation Ltd.)

POLYMER EXCHANGERS

The use of polymers in heat exchangers has become increasingly popular as an alternative to the use of exotic materials for combating corrosion in process duties involving strong acid solutions, (here competing with exotic metals and graphite). Perhaps the most familiar variant is the Du Pont (now Ametec) Teflon shell and tube heat exchanger, where tubes of 4.45mm o.d. can be used. An example of this is shown in Figure 2.54.

The smooth surface finish obtainable with polymers reduces the adhesion of deposits, making fouling less likely and mechanical removal by flushing easier.

As higher temperature polymers become available, and fibre reinforcement gives increased pressure capabilities, the application of polymer CHEs may be expected to grow significantly. Tube inserts for enhancement can also be used.



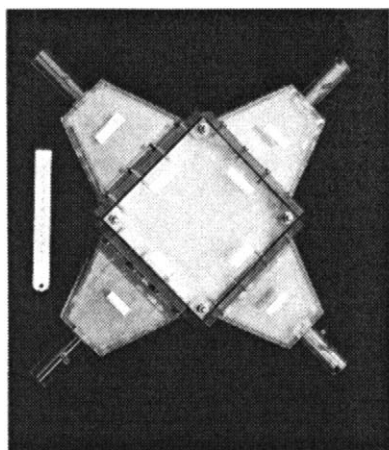
Figure 2.54 A polymer tubular exchanger (courtesy Ametec)

SOME RECENT DEVELOPMENTS

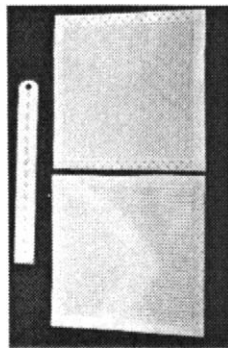
Polymer exchanger development

Most of the plastic heat exchangers use the conventional shell - tube configuration where the tube wall thickness offers a significant thermal resistance. However the heat exchanger developed by Newcastle University (Figure 2.55) addresses this issue by using flow channels consisting of 100 μm thick cross corrugated films. The films have a corrugation width of 2mm and height of 1mm. The corrugated films are crossed at 90°, and the edges are bonded by using a laser technique. The flow layers are stacked to form a cross flow configuration. Such heat exchangers are ideal for gas/gas and gas/liquid duties where fouling, corrosion and weight savings are important. Very high heat transfer coefficients can be achieved in these modules, as the cross-corrugated configuration is very effective in creation and destruction of boundary layers. Also all the surface of the heat exchanger is primary and it has a surface area density of approximately $1600 \text{ m}^2/\text{m}^3$. These exchangers have

been shown to be very energy efficient, light in weight and resistant to fouling. Various configurations using different angles of cross corrugation have been studied extensively for fluids with different Prandtl number.



(a) Test arrangement



(b) corrugated plates

Figure 2.55 Polymer exchanger development (courtesy Newcastle University)

Gas turbine recuperator developments

As it becomes more economical, in view of ever-rising emissions legislation, to operate small scale gas turbines for decentralised power production, as well as for marine and, ultimately, aircraft propulsion, the challenge to develop effective recuperators is increasing (McDonald (1999, 2000)). One recent development (Oswald et al. (1999)) is that of Rolls Royce, which is a spiral exchanger with a very low parts count. The flow is counterflow for high thermal efficiency, but is axial in contrast with the spiral form normal for conventional spiral formats. The general construction is shown in Figure 2.56.

The gas (high temperature) side is finned with plain fins of 14 f.p.i., the air side being dimpled. The fins are not bonded to the primary surface, thus facilitating relief of cyclic stresses. Thermal contact is maintained instead by the high pressure of the air side acting on the fin structure through the parting sheet, as shown in Figure 2.57. The assembly and edge welding process is highly automated, with the potential for low cost. Thermal and cyclic stress performance tests so far have been successful. This type of recuperator has significant advantages for gas turbine systems of relatively low-pressure ratio (characteristic of lower power systems of up to 4MW), for which recuperation

gives a considerable increase in cycle efficiency. The hydraulic diameter is of order of 1.5 mm. on the air side, and 2.3 mm on the gas side.

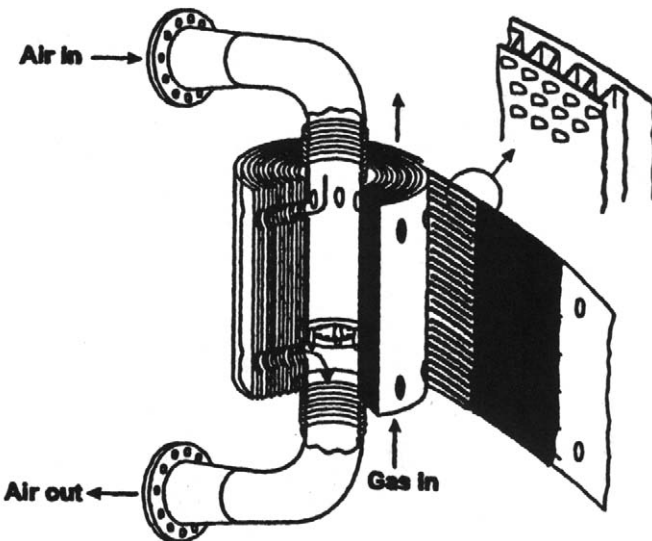


Figure 2.56 Schematic of construction of spiral recuperator
(courtesy Rolls Royce)

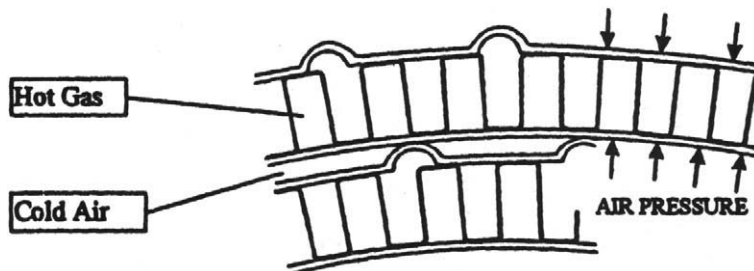


Figure 2.57 Section through recuperator matrix (courtesy Rolls Royce)

A further proposal, which has had considerable background development, is the folded primary surface concept of McDonald (2000), based on an earlier development of Foerster and Kleeman (1978). This construction has similarities

to many oil coolers used for automotive applications, the flow paths being essentially counterflow with "U" form entry and exit. The basic construction and flow paths are shown in the schematic of Figure 2.58, and the welded end sealing method is shown in Figure 2.59.

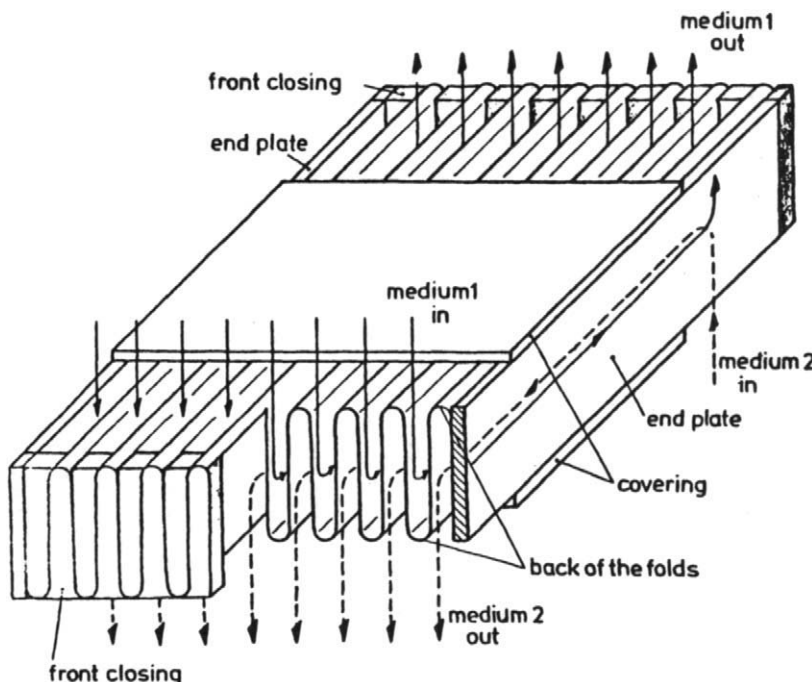


Figure 2.58 Schematic of primary surface recuperator
(courtesy M. Kleeman and S Foerster)

It is envisaged that the stamping, assembly and welding process would ultimately be totally automated, necessary to bring the cost of the core down to the target of about \$500 for a 50kW unit. A further development of this (basically rectangular) concept is to fold the surface into an annular form to surround a microturbine. The hydraulic diameter of the projected unit, given by McDonald (2000) is 0.75 to 1.85 mm.

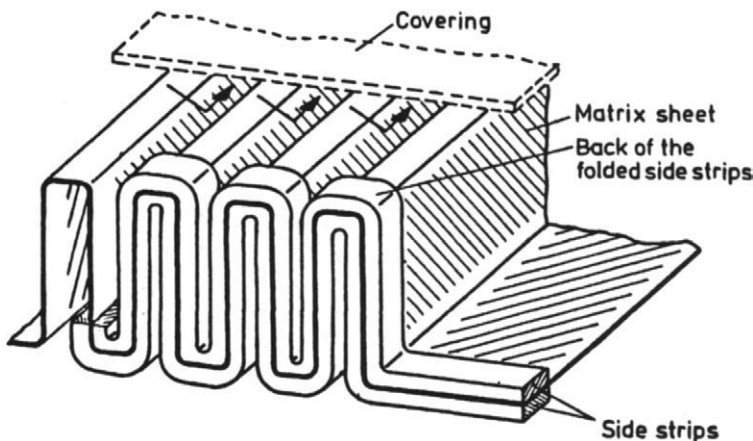


Figure 2.59 Method of end seal closure (courtesy M. Kleeman and S. Foerster)

HEAT EXCHANGER REACTORS

The two types of exchanger reactor being developed are those with a controlled rate of reactant injection, and those with, in addition, an internal catalyst. These are now described in turn.

Heat exchangers with reactant injection

The Marbond™ heat exchanger reactor

In this reactor the plate pack, similar in form to that of the Marbond™ exchanger, is designed to allow the controlled injection of a reactant into the primary, or process, stream, in order for mixing and reaction to be dispersed along the flow length, for non-catalytic chemistry. The heat of reaction is matched by heat addition or removal by the secondary stream. As shown in chapter 6, a close approximation to constant temperature conditions can thereby be achieved, giving several benefits especially in minimising by-product formation. The special feature of this design is its high degree of microscopic mixing owing to the high turbulence levels generated. The plate pack is illustrated in Figure 2.60, which shows the variation possible in stream areas, and an example of the reactor is shown in Figure 2.61.

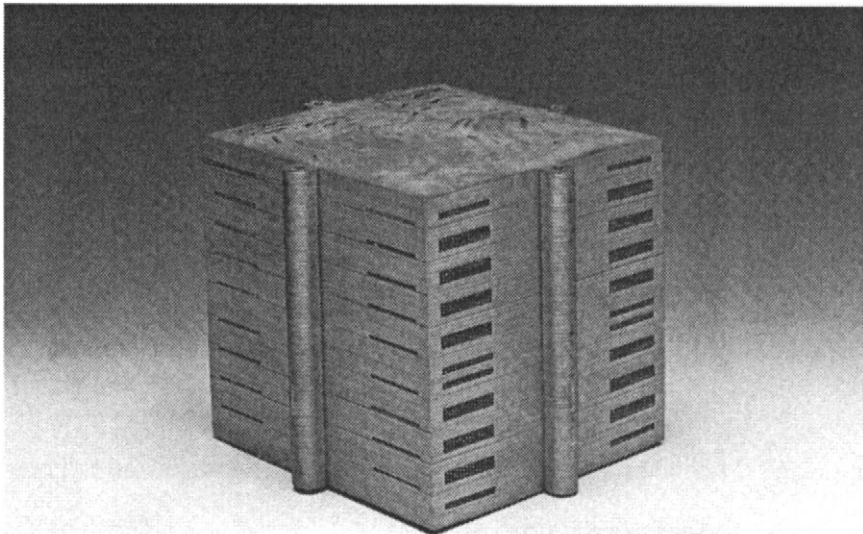


Figure 2.60 Marbond™ plate stack (courtesy Chart Heat Exchangers)

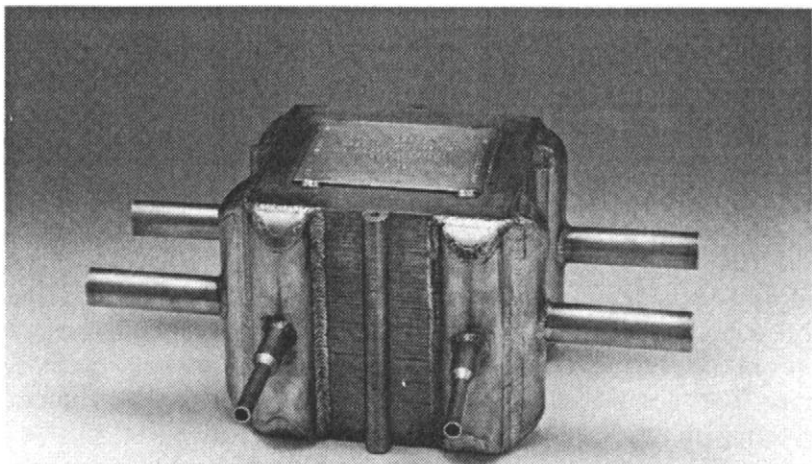


Figure 2.61 Marbond™ reactor (courtesy Chart Heat Exchangers)

Catalytic reactor exchangers

The Sumitomo plate fin heat exchanger reactor

This stainless steel exchanger reactor, of PFHE form, has been developed with a catalyst coating, and is shown in Figure 2.62.

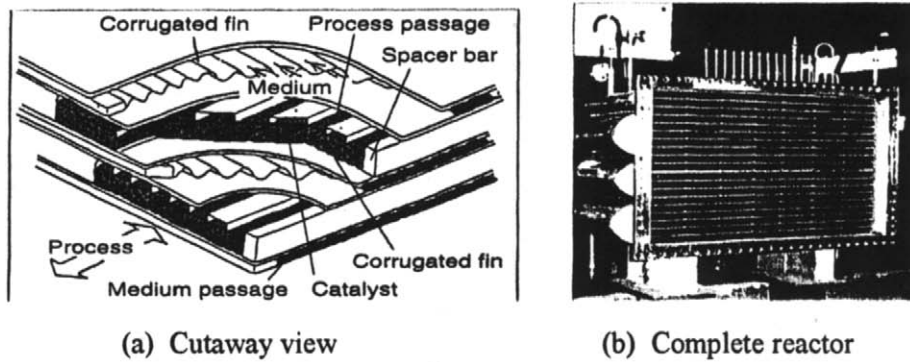


Figure 2.62 Cutaway schematic of Sumitomo plate-fin reactor
(courtesy Sumitomo)

The manufacturers expect applications in hydrogen generation plant.

The Chart-Pak heat exchanger reactor

This reactor, developed specifically for gas processes, incorporates a bed of granulated catalyst through which the process stream passes and into which the reactant is injected. A third stream, adjacent to the process stream acts as the coolant stream. The reactor thus consists of a large number of layer sequences of Coolant-Process-Injection. Each layer consists of a number of etched shims stacked to high precision to give a pin-fin structure with the desired layer height, the whole being bonded together. A sectioned view of the pin + ligament secondary stream (injection) surface is shown in Figure 2.63, and a close-up of the surface showing injection holes into the process stream is shown in Figure 2.64. The ligaments are etched to half the plate thickness and give both rigidity to the pin structure and extra heat transfer surface. The baffle visible is to aid distribution of the flow between ports. At each end of the process stream ducts there is a mesh (not shown) to retain the catalyst. This is mounted between the flanges of the unit, which is shown in an overall view in Figure 2.65. The

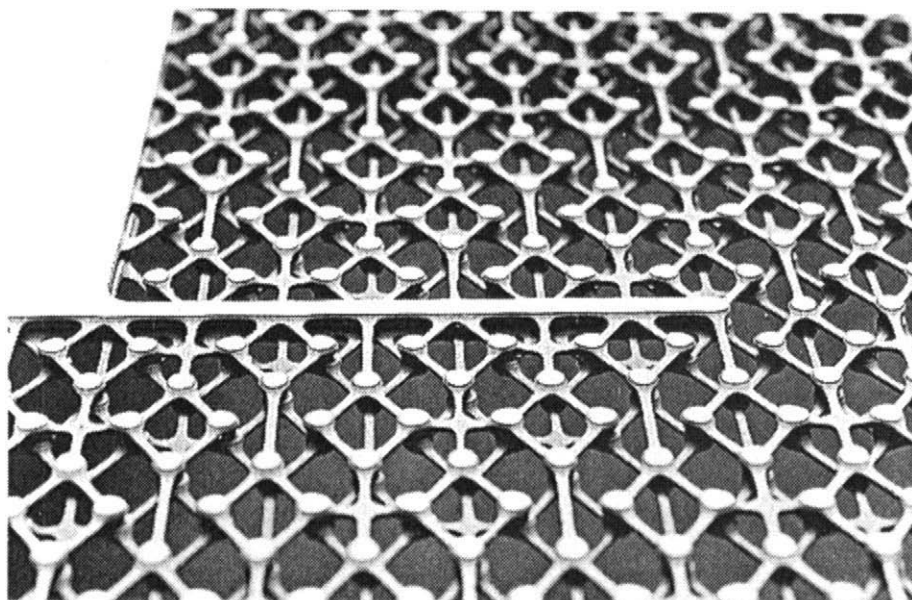


Figure 2.63 Chart-Pak: section of secondary (injected) stream surface showing pin fins (courtesy Chart Heat Exchangers)

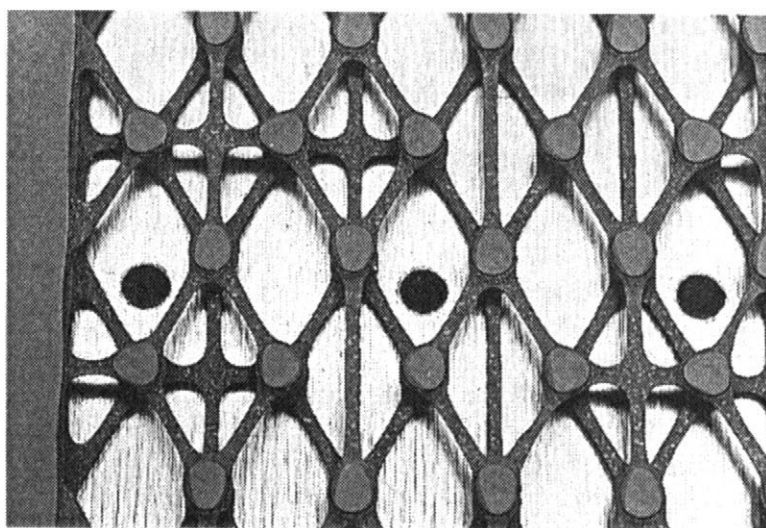


Figure 2.64 Chart-Pak: detail of pins and ligaments showing injection holes (courtesy Chart Heat Exchangers)

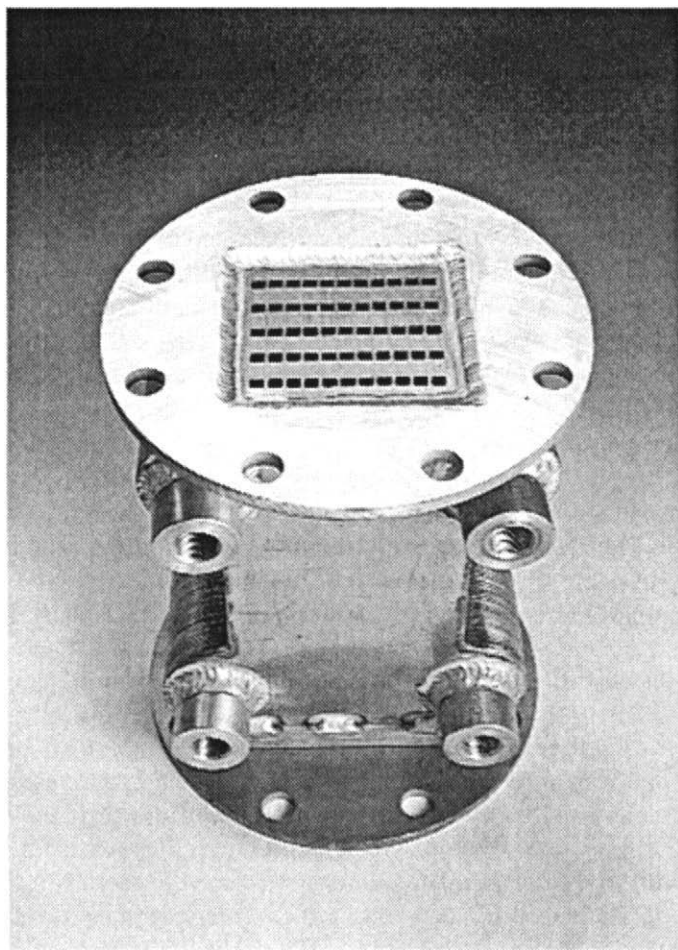


Figure 2.65 Chart-Pak: overview of reactor showing ducts for process fluid and catalyst (courtesy Chart Heat Exchangers)

arrangement allows for the ready removal of the catalyst when exhausted. The concept, clearly offering great flexibility of design in terms of pin size, geometry etc., is appropriate for manufacture either in aluminium (with a brazed bond) or in stainless steel for diffusion bonding.

Other variants of the concept are being developed for liquid reactions and for high pressure duties.

Variants of the Marbond exchanger are being developed in which a catalyst is deposited on one surface of the exchanger, either in coating form or in the form of embedded granules.

SURFACE SELECTION

The selection of surfaces for a given thermal application is firstly determined by the basic exchanger *type*, as described in this chapter. This is most strongly influenced by the industrial sector, with its individual requirements for cost, size, reliability and maintenance, expected life etc. The experienced designer or specifier in each sector will normally know quite closely what type, or close range of types, is most suited to his/her needs, given of course adequate awareness of the available types.

The industrial sectors and their preferred generic types are best treated separately, bearing in mind the growing fuzziness of the inter-sector boundaries. Emphasis will be placed here on the process sector, partly because of the current steady growth in application of compact exchangers, and partly because the selection criteria in the other sectors are more established (Shah (1983)).

Process exchangers

For many process and other applications the choices are conveniently highlighted by Table 2.1 summarising the principal features. This indicates the temperature, pressure and material ranges available for each type. Often, the operational conditions largely confine the choice of type and its surface to a small selection.

Clearly, the cost of an exchanger is an important item in its choice, and this is often expressed in the form of a cost per unit surface area of heat transfer. This is necessarily affected by the heat transfer coefficient on that surface, which in turn is dependent upon the compactness (either expressed as m^2/m^3 or as hydraulic diameter) and the degree of enhancement of the surface. These latter aspects are discussed in chapter 4. With this in mind, the area costs summarised in table 2.2 will give some guidance. When advanced materials (stainless steels and higher) are necessary for construction, the more compact types assume a greater advantage, which increases with duty. This is a direct reflection of the cost of material: for large duties with exotic materials, the cost relationship would typically be, in order of ascending cost, and assuming both feasibility and availability: Slotted plate (Marbond); PFHE; PCHE; plate and frame (PHE); welded plate; shell- and tube. For small duties, provided that sealing requirements were met, the 'proprietary' exchangers such as double pipe, and PHE, will be cheapest because of their assembly from off-the-shelf components rather than being specifically designed.

Further information on first cost is given by Reay (1999) based on the extensive data compiled by ESDU (1992, 1997) and by Hewitt and Pugh (1998).

As a cautionary qualification to the above it has often been noted that by far the most important feature of exchangers used for core applications in the process industries, for example in petrochemical production, is that of reliability.

The cost of unscheduled downtime in terms of lost production for repair or replacement of a failed exchanger can be several orders of magnitude higher than the first, or capital, cost. It is for this reason that the chemical process industry has an understandable conservatism with regard to specification (Hills (1997)), especially if a relatively untried exchanger type is offered by a manufacturer or contractor as an alternative to a conventional one (usually a shell- and-tube type). An alleviating factor for these vital processes is that the much smaller size may make it economical to install two compact exchangers in parallel (as noted in chapter 7), thus giving the opportunity for switching, both for routine maintenance and as a safeguard against failure. User confidence will grow with experience. It should also be noted here that the description shell-and-tube does not necessarily imply non-compact, as was indicated in chapter 1. The aerospace industries routinely use compact shell-and-tube exchangers for oil/fuel heat exchange and related duties. The essential difference, apart from the obvious one of fouling susceptibility, is that the tube- to tubeplate bond is almost always by mechanical expansion and brazing, which is adequate to provide leak-tightness for the fluids and pressures used. The process industries, on the other hand, normally specify a welded joint because of the requirements of safety related to the danger of mixing of the fluids, the possibility of corrosion cells arising from the use of dissimilar metals, or the leak of a toxic fluid to the environment. This carries implications for the minimum size of tube.

When the use of a compact exchanger is a possibility in a process application, it is preferable that this is highlighted early in the plant design, at which point much can be saved in terms of installation costs. These are typically 2 to 5 times the capital costs, depending on type: a factor of 2 is typical of a PHE, whilst 5 is typical of shell-and-tube applications. Other aspects of installation are dealt with more fully in chapter 7.

It is clear from the above arguments that the capital cost, although not irrelevant, is not the dominant factor determining heat exchanger selection.

Significant other factors concerning the choice are

- Expected reliability, including ease of cleaning. Aspects of industry experience, partly in the form of a selection of case studies, are described by Reay (1999).
- Size, both in terms of overall volume and shape.
- Weight (with size especially important for offshore and aerospace applications, and for cost of installation).
- Fluid inventory (an increasingly important factor for environmental and safety considerations). This of course depends on the size.

Increasing attention is being paid to the life- cycle cost of operating plant including its heat exchangers. Fundamental to such approaches is the exergy cost of both manufacture and operation: aspects of the latter are examined in chapter 3.

Table 2.1 Process exchangers: features and operational ranges - Cadet table 2.1 (from CADDET Analysis Series No.25: Learning from experience with Compact Heat Exchangers, copyright CADDET Energy Efficiency, reproduced with permission.)

Type of heat exchanger Features	Plate-and-frame (Gaskets)	Partially welded plate	Fully welded plate (AlfaReX)	Brazed plate	Platular plate	Compabloc plate
Compactness (m ² /m ³)	→ 200	→ 200	→ 200	→ 200	200	→ 300
Stream types ¹	liquid-liquid gas-liquid 2-phase	liquid-liquid gas-liquid 2-phase	liquid-liquid gas-liquid 2-phase	liquid-liquid 2-phase	gases liquids 2-phase	liquids
Materials ²	s/s, Ti, Incoloy Hastelloy graphite polymer	s/s Ti Incoloy Hastelloy	s/s Ti Ni alloys	s/s	s/s Hastelloy Ni alloys	s/s Ti, Incoloy
Temperature range (°C)	-35 to +200	-35 to +200	-50 to +350	-195 to +220	→ 700	→ 300
Maximum pressure (bar) ³	25	25	40	30	40	32
Cleaning methods	Mech. ¹⁹	Mech. ^{4,19} Chem. ⁶	Chemical	Chem. ⁵	Mech. ^{12,19}	Mech. ¹⁹
Corrosion resistance	Good ⁷	Good ⁷	Excellent	Good ⁸	Good	Good
Multi-stream capability	Yes ⁹	No	No	No	Yes ¹³	Not usually
Multi-pass capability	Yes	Yes	Yes	No ¹⁰	Yes	Yes

s/s = stainless steel, c/s = carbon steel, Ti = titanium, Ni = nickel, Cu = copper, Chem. = chemical, Mech. = mechanical

Notes

- 1 Two-phase includes boiling and condensing duties.
- 2 Other special alloys are frequently available.
- 3 The maximum pressure capability is unlikely to occur at the higher operating temperatures, and assumes no pressure/stress-related corrosion.
- 4 On gasket side.
- 5 Ensure compatibility with copper braze.
- 6 On welded side.
- 7 Function of gasket as well as plate material.
- 8 Function of braze as well as plate material.
- 9 Not common.
- 10 Not in a single unit.
- 11 On tube side.

Packinox plate	Spiral	Brazed plate-fin	Diffusion-bonded plate-fin	Printed-circuit	Polymer (e.g. channel plate)	Plate-and-shell	Marbond
→ 300	→ 200	800-1,500	700-800	200-5,000	450	-	→ 10,000
gases liquids 2-phase	liquid-liquid 2-phase	gases liquids 2-phase	gases liquids 2-phase	gases liquids 2-phase	gas-liquid (14)	liquids	gases liquids 2-phase
s/s, Ti Hastelloy Inconel	c/s, s/s, Ti, Incoloy Hastelloy	Al, s/s Ni alloy	Ti s/s	s/s, Ni, Ni alloys Ti	PVDF ²⁰ PP ²¹	s/s, Ti (shell also in c/s) ¹⁵	s/s, Ni, Ni alloys, Ti
-200 to +700	→ 400	Cryogenic to +650	→ 550	-200 to +900	→ 150 ¹⁸	→ 350	-200 to +900
300	25	90	>200	>400	6	70	>400
Mech. ^{16,19}	Mech. ¹⁹	Chemical	Chemical	Chemical	Water wash	Mech. ^{16,19} Chem. ¹⁷	Chemical
Good	Good	Good	Excellent	Excellent	Excellent	Good	Excellent
Yes ⁹	No	Yes	Yes	Yes	No	No	Yes
Yes	No	Yes	Yes	Yes	Not usually	Yes	Yes

12 Only when flanged access provided, otherwise chemical cleaning.

13 Five fluids maximum.

14 Condensing on gas side.

15 Shell may be composed of polymeric material.

16 On shell side.

17 On plate side.

18 PEEK (polyetheretherketone) can go to 250°C.

19 Can be dismantled.

20 Polyvinylidene difluoride.

21 Polypropylene.

Table 2.2 Cost per unit area of process heat exchanger types
 (from CADDET Analysis Series No.25: Learning from experience with
 Compact Heat Exchangers, copyright CADDET Energy Efficiency, reproduced
 with permission.)

Heat Exchanger	Q/ΔT (W/K)	Cold Stream	Hot Stream	U (W/m ² K)	C (GBP/W/K)
S+THX	1,000	Water	Water	938	1.12
PHE ¹ (Gasket)	1,000	Water	Water	3,457	0.036
S+THX	30,000	Water	Water	938	0.14
PHE ¹ (Gasket)	30,000	Water	Water	3,457	0.033
PFHE ³	100,000	Medium pressure gas	Condensing hydrocarbon	402	0.227
PCHE ⁴	100,000	Medium pressure gas	Condensing hydrocarbon	1090	0.55
PHE (Welded)	100,000	Medium pressure gas	Condensing hydrocarbon	1518	0.186
S+THX	30,000	Water	Water	938	0.14
PHE (Welded)	30,000	Water	Water	9,100	0.147
PHE ² (Gasket)	30,000	Water	Water	3,500	0.02
PCHE ⁵	30,000	Water	Water	3,230	0.4
Notes:					
1 & 2 Different sources of data.					
3 Aluminium. Stainless steel costs are 3 times greater. Titanium costs are greater by a factor of 5.					
4 Stainless steel.					
5 Treated water on one side, 30% triethylene glycol on other side.					

Refrigeration exchangers

The process of choice of surfaces for commercial and industrial refrigeration applications is relatively straightforward, simply reflecting the exchanger type. Large duties (e.g. heat loads over about 100 kW) normally require shell- and tube condensers and flooded evaporators. The former often have low-finned tubes and the latter an enhanced surface on the bottom few rows of tubes. Smaller duties, as mentioned in chapter 1, are nearly exclusively now the domain of the brazed-plate exchanger.

In the closely-related field of air conditioning, especially for the space and cost-conscious transport and domestic sectors, development is progressing of variants of flat and galleried tube-fin exchangers for both evaporation and condensation, to replace the round tube and fin exchangers historically used.

Automotive and prime mover sector

In this sector the heat transferred is normally from atmospheric air to water, oil, refrigerant or compressed air, and louvred fin surfaces are used for the air-side. In the case of automobiles, with production runs in the millions, first cost is paramount. Thus material quantity and speed of production are dominant factors in the selection, and louvred fin, flat tube surfaces are almost invariably used. This is because they are the highest performers from the point of view of compactness and enhancement (see chapter 4), and also because the fins are produced by a very rapid rolling process. A crossflow arrangement is standard for these exchangers. The flat tubes (when carrying cooling water) are normally used without augmentation, since the air side usually dominates the overall heat transfer resistance. Oil coolers, on the other hand, as mentioned in chapter 1, require oil side enhancement to balance resistances.

Aerospace sector

This sector has some features in common with the process sector, in requiring reliability and integrity as top priority. In addition, light weight is desired and size constraints are usually imposed. Because of these demanding factors, and low production runs (exchangers being specifically designed for each aircraft type) the cost is often high, and manufacture is undertaken by a very few specialist companies. For the vulnerable duties of oil cooling (often combined with fuel preheating) compact brazed shell and tube units are made, with augmented (e.g. dimpled) tubes. Environmental control exchangers are frequently plate-fin units.

References

Berntsson, T, Franck, P-A., Hilbert, L. and Horgby, K., (1995), Learning from Experiences with Heat Exchangers in Aggressive Environments, CADDET Analysis Series No. 16, CADDET, Sittard, Netherlands.

ESDU (1992), Data item 92013: Selection and Costing of Heat Exchangers. Engineering Sciences Data Unit, London.

ESDU (1997), Data item 97006: Costing of Plate-Fin Heat Exchangers. Engineering Sciences Data Unit, London.

ETSU, Reay, D.A., and Pritchard, A., (1998), Experience in the Operation of Compact Heat Exchangers, Good Practice Guide 198, ETSU, Harwell, UK.

ETSU, Linden Consulting Partnership, (1996), Waste Heat Recovery from High Temperature Gas Streams, Good Practice Guide 13, ETSU, Harwell, UK.

ETSU, Simulation Engineering, (1994), Guide to Compact Heat Exchangers, Good Practice Guide 89, ETSU, Harwell, UK.

Foerster, S. and Kleeman, M. (1978), Compact Metallic and Ceramic Recuperators for Gas Turbines, ASME paper 78-GT- 62.

Hewitt, G.F. and Pugh, S.J., (1998), Approximate Design and Costing Methods for Heat Exchangers, Int. Conf. on Heat Exchangers for Sustainable Development, Lisbon, Portugal.

Hills, P.D., (1997), So What's Wrong with a Shell & Tube Heat Exchanger? Proceedings of the International Conference on Compact Heat Exchangers for the Process Industries, Snowbird, Utah: Begell House, New York.

Jachuk, R.J.J. and. Ramshaw, C. Process Intensification: Polymer Film Compact Heat Exchanger (PFCHE), Trans IChemE, Vol. 72, Part A, March 1994.

McDonald, C.F. (1999), Emergence of Recuperated Gas Turbines for Power Generation, ASME paper 99-GT-67, presented at the International Gas Turbine & Aeroengine Congress & Exhibition, Indianapolis, Indiana, USA.

McDonald, C.F. (2000), Low- Cost Compact Primary Surface Recuperator Concept for Microturbines, Applied Thermal Engineering, Vol. 20 no. 5.

Oswald, J.I., Dawson, D.A. and Clawley, L.A., (1999), A New Durable Gas Turbine Recuperator, ASME paper 99-GT-369, presented at the International Gas Turbine & Aeroengine Congress & Exhibition, Indianapolis, Indiana, USA.

Reay, D.A., Osprey Environmental Technologies Ltd, (1996), Waste Heat Recovery in the Process Industries, Good Practice Guide 141, ETSU, Harwell, UK.

Reay, D.A., (1999), Learning from Experiences with Compact Heat Exchangers, CADDET Analysis Series No. 25, CADDET, Sittard, Netherlands.

Shah, R.K. (1983), Compact Heat Exchanger Surface Selection, Optimisation, and Computer-aided Thermal Design, in Low Reynolds Number Flow Heat Exchangers, ed. Kakaç et al. Hemisphere, New York.

Shah, R.K. (1983), Compact Heat Exchanger Surface Selection, Optimisation, and Computer-aided Thermal Design, in Low Reynolds Number Flow Heat Exchangers, ed. Kakaç et al. Hemisphere, New York.

Chapter 3

THE HEAT EXCHANGER AS PART OF A SYSTEM: EXERGETIC (SECOND LAW) ANALYSIS

All heat energy is equal, but some heat energy is more equal than other heat energy.

Author not known, adapted from G. Orwell.

INTRODUCTION

Heat exchangers in systems are used for:

1. recovering heat directly from one flowing medium to another or via a storage system, or indirectly via a heat pump or heat transformer.
2. heating or cooling a process stream to the required temperature for a chemical reaction (this can also be direct or indirect).
3. enabling, as an intrinsic element, a power, refrigeration or heat pumping process, that is interchanging heat between a hot source or stream with the working fluid and with the low temperature heat sink (or source). Clearly both power and refrigeration systems need both hot and cold streams: some (heat transformers and absorption refrigeration systems) need 2 or more sources or sinks.

In all applications of heat exchangers mechanical power is necessarily expended to pump the working fluids through each exchanger by virtue of pressure losses in its ducting or heat exchange passages. For liquids this power is usually relatively small. In the case of air or other gaseous (i.e. compressible fluid) systems, however, the pumping power is often a significant design variable, and its value- relative to the heat rate (or power) transferred- is a commonly used (Kays and London (1984)) measure of the cost of primary energy. The driving energy for pumps, fans and compressors is usually electricity, which is of course produced with an efficiency less than the Carnot efficiency.

Many systems in the process industries have multiple streams exchanging heat with each other and with "service" streams, that is, with streams of water, steam or air specifically introduced to heat or cool. Some streams have the

express function of absorbing power, or delivering power, as is the case with compressors or turbines. In all cases a stream absorbs power as noted above.

These concepts point to the need for a rational way of analysing systems, especially those involving both heat and power exchange, to enable operation at minimum total energy consumption. Exergy analysis, a natural extension to classical thermodynamic Second Law (entropy) analysis, is the unifying tool for this purpose, and the basic concepts are developed in this chapter. The tool is increasing being used in extended forms to include life- cycle analyses, that is, to include the exergy cost of producing the (capital) equipment and its ultimate disposal, but such development is beyond the scope of this book. The reader wishing to take the subject further is recommended to study papers including aspects of Thermoeconomics such as those by Witte (1988), Ranasinghe and Reistad (1990), and books by Aherne, Szargut and Bejan et al (1996).

In this chapter the basic principles of exergy analysis are first outlined. Their application to heat exchangers is then developed, firstly for zero pressure drop and then for finite pressure drop for which an entropy generation minimum criterion is derived, and its implications for design choices is discussed. Finally, a brief discussion is given of the application of the principles to heat exchanger networks.

BASIC PRINCIPLES OF EXERGY ANALYSIS

First and Second Law (Open Systems)

Consider the open system (open because it has flows in and out), which in the present case is a heat exchanger, shown schematically in Figure 3.1.

The First Law of thermodynamics is a statement of conservation of energy and is expressed by:

$$\begin{aligned}
 \text{1st Law } \underbrace{\sum_{in} \dot{m} \left(h + \frac{1}{2} u^2 + gZ \right) - \sum_{out} \dot{m} \left(h - \frac{1}{2} u^2 + gZ \right) + \dot{Q} - \dot{W}_{sh}}_{\text{Energy rate (power) transferred}} &= \frac{\partial E}{\partial t} \\
 &= 0 \text{ for steady flow .} \tag{3.1}
 \end{aligned}$$

The expressions in parentheses are readily recognisable as Bernoulli's equation, and it will be recognised that the contribution of the potential energy term is often negligible.

The Second Law equation is a statement describing the irreversibility of the process within the system boundary (within the heat exchanger between inlet and outlet ducts):

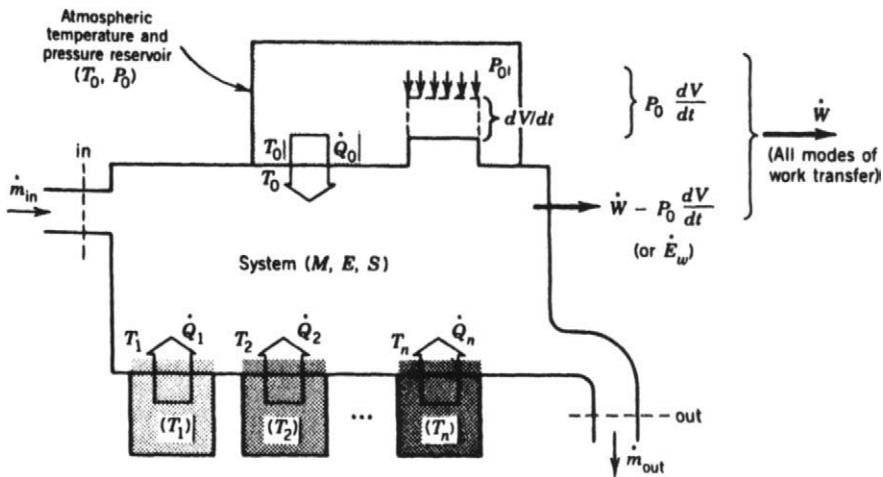


Figure 3.1 An open system exchanging heat (and, in general, work)

From Advanced Engineering Thermodynamics, Bejan, A., Copyright © (1997, John Wiley & sons inc.). Reprinted by permission of John Wiley & Sons inc.

$$\text{2nd Law } \underbrace{\sum_{in} \dot{m}s - \sum_{out} \dot{m}s + \frac{\dot{Q}}{T}}_{\text{Entropy rate transfer}} \leq \frac{\partial S}{\partial t} \quad \text{Note entropy transfer rate associated only with } \dot{Q}, \text{ not } \dot{W} \quad (3.2)$$

↓
Rate of entropy change
(extensive)

The inequality can be re-arranged to give the entropy generation rate:

$$\dot{S}_{gen} = \frac{\partial S}{\partial t} - \frac{\dot{Q}}{T} + \sum_{in} \dot{m}s - \sum_{out} \dot{m}s \geq 0 \quad \left(\frac{\partial S}{\partial t} = 0 \text{ for steady flow} \right) \quad (3.3)$$

The entropy generation rate \dot{S}_{gen} is zero for a reversible system and positive for any real system (i.e. one involving friction or temperature gradients).

Hence \dot{S}_{gen} is conveniently a measure of reversibility.

Availability, exergy, lost work

If a system has several heat transfer interactions \dot{Q}_i , $i = 0$ to n , including an interaction with the environment¹ $i = 0$, we can re-write (3.1) as

$$\frac{dE}{dt} = \sum_{i=0}^n \dot{Q}_i - \dot{W} + \sum_{in} \dot{m}h_t - \sum_{out} \dot{m}h_t \quad (3.4)$$

with $h_t = h + \frac{u^2}{2} + gz$,
= total enthalpy or generalised enthalpy group,

and the second law (3.3) as

$$\dot{S}_{gen} = \frac{dS}{dt} - \sum_{i=0}^n \frac{\dot{Q}_i}{T_i} - \sum_{in} \dot{m}s + \sum_{out} \dot{m}s \geq 0. \quad (3.6)$$

This system is shown diagrammatically in Figure 3.1, after Bejan (1988). Although only one mass flow inlet and exit each is shown, equation (3.6) allows for multiple flows.

Isolating the atmospheric interaction the two laws become

$$\frac{dE}{dt} = \dot{Q}_o + \sum_{i=1}^n \dot{Q}_i - \dot{W} + \sum_{in} \dot{m}h_t - \sum_{out} \dot{m}h_t \quad (3.7)$$

and $\dot{S}_{gen} = \frac{dS}{dt} - \frac{\dot{Q}_o}{T_o} - \sum_{i=1}^n \frac{\dot{Q}_i}{T_i} - \dot{W} + \sum_{in} \dot{m}h_t - \sum_{out} \dot{m}h_t \quad (3.8)$

Suppose we wish to maximise the work rate output \dot{W} from a given system with fixed total enthalpy fluxes. The 1st Law (3.7), which is an equality, tells us that one or more of the heat flows \dot{Q} has to change. We choose \dot{Q}_o on the basis that heat interaction to the atmosphere is characteristic of power and

¹ The environment is at an arbitrary also called the “dead state” which can vary. The Standard Atmosphere condition is normally chosen (Bejan (1988)), enabling exergy relationships to be related to the same basis as other thermodynamic properties. It is: $T_o = 25^\circ\text{C}$ (298.15K), and $p_o = 1\text{bar}$ (0.101325Mpa).

refrigeration (or heat pump) systems and accordingly now eliminate \dot{Q}_o from equation (3.7) and (3.8):

$$\dot{W} = -\frac{d}{dt}[E - T_o S] + \sum_{i=1}^n \left(1 - \frac{T_o}{T_i}\right) \dot{Q}_i + \sum_{in} \dot{m} (h_i - T_o s) - \sum_{out} \dot{m} (h_i - T_o s) - T_o \dot{S}_{gen} \quad (3.9)$$

This representation now gives us the condition for maximum possible work from the system, since by the second law \dot{S}_{gen} cannot be negative. By definition this is also the reversible process condition, since $\dot{S}_{gen} = 0$ represents the isentropic process. We put, accordingly,

$$\dot{W}_{rev} = \dot{W}_{max} = -\frac{d}{dt}[E - T_o S] + \sum_{i=1}^n \left(1 - \frac{T_o}{T_i}\right) \dot{Q}_i + \sum_{in} \dot{m} (h_i - T_o s) - \sum_{out} \dot{m} (h_i - T_o s) \quad (3.10)$$

Clearly, from (3.9) and (3.10)

$$\dot{W} = \dot{W}_{rev} - T_o \dot{S}_{gen} \quad (3.11)$$

and now, re-asserting the second law,

$$\dot{W}_{rev} - \dot{W} = T_o \dot{S}_{gen} \geq 0 \quad (3.12)$$

Thus the system loses work $(\dot{W}_{rev} - \dot{W})$ at a rate proportional to the rate of entropy generation in the system, given by

$$\dot{W}_{lost} = \dot{W}_{rev} - \dot{W} = T_o \dot{S}_{gen} \quad (3.13)$$

This work is unavailable to the user, and is thus called lost available work. The result is the lost work theorem, is also known as the Gouy-Stodola theorem.

Two observations are worthy of mention at this point.

Firstly, the choice of the atmospheric conditions suffix o is mathematically arbitrary: we could have chosen any of the $i (= n + 1)$ thermal interaction states as the reference state, and the \dot{W}_{rev} and \dot{W}_{lost} relationships would then be referred

to $T_i \dot{S}_{gen}$, \dot{S}_{gen} itself being unchanged. A further consequence of this is that \dot{W}_{rev} and \dot{W} could both be negative, it only being necessary that \dot{W}_{lost} is positive. Note also that lost work is proportional to the reference absolute temperature, so in the case of an above atmospheric temperature system producing power, the lost work is a minimum (giving maximum available work), when the final (lowest) heat interaction is with the atmosphere. In addition it is clear that the atmosphere is (ideally) the only reservoir which can exchange heat within a process without undergoing a change of temperature itself. We say ideally because any actual temperature changes are on a time scale (including global warming!) up to many orders of magnitude higher than those appropriate to the analysis of engineering systems.

The second point arises from invoking a steady state cyclic process, so that the time derivatives vanish, and also taking a single (other than atmospheric) heat interaction Q_i . Hence $\dot{m}_{in} = \dot{m}_{out}$, and similarly for s and h_i .

Equation (3.8) now becomes simply, on dropping the now redundant subscript I

$$\dot{W}_{rev} = \dot{W}_{max} = \left(1 - \frac{T_o}{T}\right) \dot{Q} \quad (3.14)$$

where $1 - \frac{T_o}{T}$ is the easily recognisable Carnot efficiency of a system exchanging heat \dot{Q} at a temperature T and rejecting it at the ambient T_o . Thus any given heat flow \dot{Q} has the potential for delivering power via a heat engine up to the limit defined by equation 3.14. Clearly, the higher the temperature T of the heat exchange, the higher the possible power extractable.

Exergy

A consequence of the generality of the system so far examined is that \dot{W}_{rev} (or \dot{W}) may not be wholly available for consumption (Bejan (1988)). If the system boundary with the atmosphere (at pressure p_o) is such that it undergoes a change in volume, then work is done against the atmosphere or by the atmosphere on the system, this work component being represented by $p_o dV/dt$.

We then define the remainder of available work as the *Exergy*, \dot{E}_w , given by

$$\dot{E}_w = \dot{W} - p_o \frac{dV}{dt} \quad (3.15)$$

or
$$\underbrace{\dot{E}_w}_{\substack{\text{Combined exergy} \\ \text{(flow/non flow)}}} = \frac{-d}{dt} [E - T_o S + p_o V] + \sum \left(1 - \frac{T_o}{T_i} \right) \dot{Q}_i + \sum_{in} \dot{m} (h_t - T_o s) - \sum_{out} \dot{m} (h_t - T_o s) - \underbrace{T_o \dot{S}_{gen}}_{\substack{\text{Exergy lost} \\ \text{through irreversibilities}}} \quad (3.16)$$

$\underbrace{\quad}_{\substack{\text{Intake of flow} \\ \text{energy via mass flow}}}$
 $\underbrace{\quad}_{\substack{\text{Discharge of flow} \\ \text{exergy via mass flow}}}$

Clearly, the maximum total exergy occurs in the limit of zero irreversibility or zero entropy generation, with the last term $T_o \dot{S}_{gen}$ equal to zero.

Here, since the system so far considered is a general one, containing both flow and non flow (cumulative) elements, the exergy term is a combined exergy being the sum of flow and non flow components. Equation (3.16) allows us to introduce definitions of the individual flow and non flow availability and exergy terms, in both extensive and intensive forms.

We define the argument of the first term as the non flow availability (intensive A, intensive a),

$$\begin{aligned} A &= E - T_o S + p_o V \\ a &= e - T_o s + p_o v \end{aligned} \quad (3.17)$$

in extensive and intensive forms respectively.

Clearly, once the atmospheric condition has been defined, which is central anyway to the numerical definition of internal energy e and entropy s , the availability is a state thermodynamic property. The general condition is of course that the "o" state is arbitrarily defined in which case the availability is not a state property (see Hayward 1980).

The second term is the sum of *available work (or exergy) contents of the heat transfer interactions*, denoted by $(\dot{E}_Q)_z$, noting that for each interaction the available work is that of the (reversible) Carnot cycle.

The argument of each of the third terms is defined as the flow availability (B, b):

$$\begin{aligned}
 B &= H_t - T_o S \\
 b &= h_t - T_o s \\
 &= h + \frac{u^2}{2} + gz - T_o s \\
 &= (h - T_o s) + \frac{u^2}{2} + gz
 \end{aligned} \tag{3.18}$$

and thus we can express the generalised equation (3.16) as

$$\dot{E}_w = -\frac{dA}{dt} + \sum_{i=1}^n (\dot{E}_Q)_i + \sum_{in} \dot{m} b - \sum_{out} \dot{m} b - T_o \dot{S}_{gen} \tag{3.19}$$

Apart from the special cases of regenerators, both static and rotary, and operational transients in conventional exchangers, heat exchangers are designed and operated in steady state conditions. We thus continue the investigation with this assumption.

Steady flow exergy processes

Steady flow processes include most power, refrigeration and chemical process operations, and also periodic (cyclic) operation if parameters do not change from one period to the next. With zero time derivatives, equation (3.18) becomes

$$\dot{E}_w = \sum_{i=1}^n (\dot{E}_Q)_i + \sum_{in} \dot{m} b + \sum_{out} \dot{m} b - T_o \dot{S}_{gen} \tag{3.20}$$

For r unmixed streams, since these constitute the majority of power and refrigeration applications, this becomes

$$\dot{E}_w = \sum_{i=1}^n (\dot{E}_Q)_i + \sum_{k=1}^r [(\dot{m} b)_{in} - (\dot{m} b)_{out}] - T_o \dot{S}_{gen} \tag{3.21}$$

Invoking now the definition of flow exergy as the reversible energy available for a given flow with no heat interactions other than that of the final one,

$$\begin{aligned}\dot{E}_w &= \sum_{i=l}^n (B - B_o)_{k,in} - \sum_{k=l}^r (B - B_o)_{k,out} \\ &= \sum_{k=l}^r (\dot{m} b - \dot{m} b_o)_{k,in} - \sum_{k=l}^r (\dot{m} b - \dot{m} b_o)_{k,out}\end{aligned}\quad (3.22)$$

and since by definition

$$(\dot{m} b_o)_{k,in} = \dot{m} (k_{t,o} - T_o s_o)_{k,in} = \dot{m} (k_{t,o} - T_o s_o)_{k,out} \quad (3.23)$$

we have

$$\begin{aligned}\text{total flow exergy } \dot{E}_{w,rev} &= \sum_{k=l}^r (B_{k,in} - B_{k,out}) \\ \text{and } &= \sum [(\dot{m} b)_{k,in} - (\dot{m} b)_{k,out}]\end{aligned}\quad (3.24)$$

$$\text{with } E_x = B - B_o = H_t - H_{t,o} - T_o (S - S_o) \quad (\text{extensive})$$

$$\text{and } e_x = b - b_o = h_t - h_{t,o} - T_o (s - s_o) \quad (\text{intensive}) \quad (3.25)$$

as individual stream exergy identities.

We note in passing that at the atmospheric condition, used as previously mentioned for the "Zero State" basis for the state properties h , s , e , etc., the function

$$a_o = e_o - T_o s_o + p_o v_o \quad (3.26)$$

becomes identical to the Helmholtz function evaluated at the zero state, and when we exclude potential energy and kinetic energy components from h_t , we have

$$b_o = h_o - T_o s \quad (3.27)$$

which is equal to the Gibbs function evaluated at zero state. Since also in general $h = e + pv$, the Gibbs function and Helmholtz functions are identical at this state (although at no other state).

The general form of flow exergy given by equation 3.25 can be expressed in more usable forms (Bejan (1988)) by, for an incompressible liquid with specific heat c and density constant:

$$e_x = cT_o \left(\frac{T}{T_o} - 1 - \ln \frac{T}{T_o} \right) + \frac{p - p_o}{\rho} \quad (3.28)$$

and for an ideal gas with constant c_p and R :

$$e_x = c_p T_o \left(\frac{T}{T_o} - 1 - \ln \frac{T}{T_o} \right) + RT_o \ln \frac{p}{p_o} \quad (3.29)$$

The inter-relationships between availabilities and exergies for nonflow and flow process are summarised in Table 3.1. Non-flow parameters, although not used for heat exchangers, are included for completeness.

Here, the overbars denote the molar form of the intensive quantity. Note also that forms such as \dot{E} , denote rate terms in the conventional way: $\dot{E}_x = dE_x / dt = \dot{m}e_x$.

Table 3.1 Availability and Exergy terms

Name	Nonflow		Flow	
	Symbol	Equation (intensive form)	Symbol	Equation (intensive form)
Availability	A, a	$a = e - T_o s + p_o v$	B, b	$b = h_t - T_o s$
Exergy (thermomechanical or physical)	Ξ, ξ	$\xi = a - a_o$	E_x, e_x	$e_x = b - b_o$

APPLICATION OF EXERGY ANALYSIS TO HEAT EXCHANGERS

As mentioned in the introduction to this chapter, heat exchangers have two functions in systems: to *conserve thermal energy* (basically by recovering heat, a first law function), and to *enable the operation of power and refrigeration systems*.

Many systems, of course, have both functions operating (in other words the interchange of heat and work), each with its heat exchanger(s).

Clearly there are differences in how the exergy situation is looked at in these situations, but in all cases there is exergy exchanged between the streams. Most heat exchangers have only two streams, but some, in gas separation (cryogenic) duties, have several. In view of this, Sekulic (1990) has suggested a rational definition of a heat exchanger as:

“... a device which provides for a change of the mutual thermal (exergy) levels between two or more fluids in thermal contact without external heat and work interactions”.

It may be argued that an exergetic analysis of the first function (heat recovery) is unnecessary as power production or refrigeration is not involved. However, power for both streams is consumed, with its exergy flows, so that a combined first and second law, or exergy approach is still valid, especially if system optimisation is applied.

Basics of entropy generation

For the first and second law analysis of heat exchangers it is convenient to work in terms of the rate of entropy generation, and make further interpretation using the results as obtained.

We start with the first and second law statements for a one-dimensional heat transfer duct as given by Bejan [1978], referring to Figure 3.2:

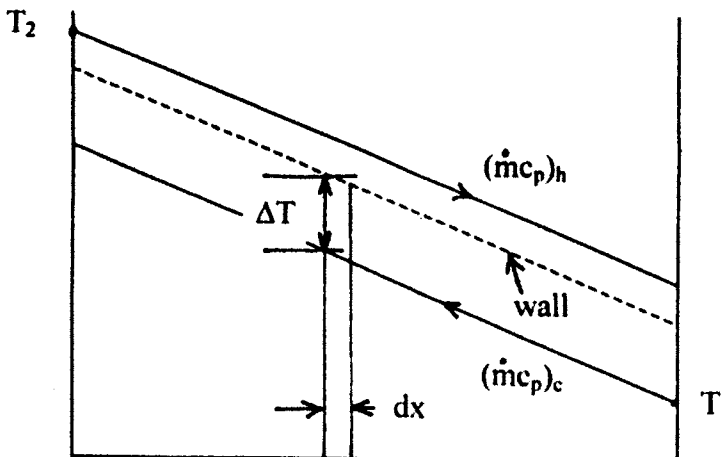


Figure 3.2 Elemental surface in heat exchanger

$$1\text{st law: } \dot{m}dh = q'dx \quad (3.30)$$

where q' is the lengthwise rate of heat transfer $q' = d\dot{Q}/dx$

From equation (3.3), with the conditions $\dot{W} = 0, \dot{Q}_o = 0$ (no work and no heat loss to or gain from the environment), and assuming steady state flow, the second law statement is

$$\int d\dot{S}_{gen} = \int \frac{d\dot{Q}}{T \pm \Delta T} + \dot{m}s_{in} - \dot{m}s_{out} \geq 0 \text{ for each side,} \quad (3.31)$$

or, in differential form,

$$d\dot{S}_{gen} = \frac{d\dot{Q}}{T \pm \Delta T} + \dot{m}ds \geq 0 \text{ for each side,} \quad (3.32)$$

with the \pm sign depending on which of the hot or cold streams is considered.

The canonical thermodynamic relationship for entropy is

$$dh = Tds + \frac{dp}{\rho}, \quad (3.33)$$

$$\text{giving } \frac{dh}{dx} = T \frac{ds}{dx} + \frac{1}{\rho} \frac{dp}{dx}. \quad (3.34)$$

Linking 3.30, 3.32 and 3.34 gives, for the cold fluid,

$$\dot{S}'_{gen} = \frac{d\dot{S}_{gen}}{dx} = \frac{q'\Delta T}{T^2(1+\tau)} + \frac{\dot{m}}{\rho T} \left(-\frac{dp}{dx} \right) \quad (3.35)$$

where $\tau = \Delta T / T$, the dimensionless temperature difference.

In many cases, the contribution of the pressure drop terms is very small in comparison with that of the temperature rise: this is specially the case when incompressible liquids are the heat transfer media (assumed to be both fluids).

The simplification involved in this assumption of $\Delta p = 0$ gives rise to expressions which illustrate clearly the main trends of second law performance.

The heat transfer gradient is given by

$$q' = \alpha p_s \Delta T \quad (3.36)$$

where p_s is the surface perimeter, and making the temporary use of α for heat transfer coefficient to avoid confusion with h (enthalpy). Then it is easily shown by substitution in equation (3.35) that for an incremental surface area ΔA_s , the incremental entropy generation $\Delta \dot{S}_{gen}$ is given by

$$\Delta \dot{S}_{gen} = \frac{\alpha \Delta A_s \tau^2}{1 + \tau} \quad (3.37)$$

Thus the entropy generation rate for the thermal component is proportional to the square of the dimensionless temperature difference τ , and is minimised when τ is minimised. The importance of a progressively reducing ΔT for cryogenic applications (low absolute temperature T) is clear, a point made clearly by Grossman and Kopp (1957) and reiterated by Smith (1997).

Considering now the general case for two streams in a heat exchanger (see Figure 3.2), with hot and cold inlet temperatures T_2 and T_1 respectively, we can write

$$d\dot{S}_{gen} = -\left(\frac{q' dx}{T(T + \Delta T)}\right)_1 + \left(\frac{q' dx}{T(T - \Delta T)}\right)_2 - \dot{m}_1 R_1 \frac{dp_1}{p_1} - \dot{m}_2 R_2 \frac{dp_2}{p_2}, \quad (3.38)$$

which becomes on integration, after some algebraic manipulation, for an ideal gas (since $dh = c_p dT$),

$$\dot{S}_{gen} = (\dot{m}c_p)_1 \ln\left(\frac{T_{1out}}{T_1}\right) + (\dot{m}c_p)_2 \ln\left(\frac{T_{2out}}{T_2}\right) + (\dot{m}R)_1 \ln\left(\frac{p_1}{p_{1out}}\right) + (\dot{m}R)_2 \ln\left(\frac{p_2}{p_{2out}}\right) \quad (3.39a)$$

For an incompressible liquid,

$$\begin{aligned} \dot{S}_{gen} = & (\dot{m}c)_1 \ln\left(\frac{T_{1out}}{T_1}\right) + (\dot{m}c)_2 \ln\left(\frac{T_{2out}}{T_2}\right) \\ & - \left(\frac{\dot{m}}{\rho}\right)_1 \left(\frac{\Delta p}{T_{in}}\right)_1 - \left(\frac{\dot{m}}{\rho}\right)_2 \left(\frac{\Delta p}{T_{in}}\right)_2 \quad (\Delta p \ll \rho c T_{in}) \end{aligned} \quad (3.39b)$$

These forms, which reflect the simple entropy change in an open system, arise because there is no heat transferred into or out of the system (the heat exchanger), assuming that it is thermally insulated from the surroundings. The individual streams, however, have heat flow \dot{Q}/T entropy terms, which affect their entropy analysis and optimisation, as will be shown later.

Initial observation of equation (3.39a) indicates that if the terminal temperatures T_1 , T_2 , T_{1out} , and T_{2out} are fixed by process considerations such as a pinch condition, which implies fixed driving temperature differences, then the first two terms are fixed. The pressure drop contributions, however, can be controlled by increasing the flow area in accordance with the core velocity equation (London, [1983]). This point will be further investigated later.

The subsequent analysis will be restricted to perfect gas flow on the basis that frictional entropy generation for liquids is very small in most situations, owing to the high density in the second two terms in equation 3.39b.

Some fundamental relationships linking entropy generation with heat exchange parameters are first re-examined for the case of zero pressure drop. Pressure drop is then taken into account in section 4, allowing for optimisation, or entropy minimisation analysis.

ZERO PRESSURE DROP

Balanced counterflow

We start with the case of balanced counterflow, referring to Figure 3.2, for which the performance is described by the ε -Ntu relationship

$$\varepsilon = \frac{T_{1out} - T_1}{T_2 - T_1} = \frac{T_2 - T_{2out}}{T_2 - T_1} = \frac{Ntu}{1 + Ntu}, \quad (3.40)$$

which gives (Bejan, [1980]),

$$\dot{S}_{gen} = \dot{m}c_p \ln \left[\frac{\left(1 + \frac{T_1}{T_2} Ntu\right) \left(1 + \frac{T_2}{T_1} Ntu\right)}{\left(1 + Ntu\right)^2} \right]. \quad (3.41)$$

The choice of the way of non-dimensionalising this equation has been discussed by the author (Hesselgreaves (2000)). The simplest way algebraically is to divide equation 3.41 by the heat capacity rate $\dot{m}c_p$, but this gives rise to interpretative difficulties, notably the 'entropy generation paradox' (Bejan

(1980)). The most logical way is to utilise the heat load \dot{Q} , since this characterises the *raison d'être* of the exchanger, together with a reference temperature. The most rational temperature to use in terms of exergy analysis would be the ambient T_0 , and we would thus non-dimensionalise equation 3.40 by \dot{Q} / T_0 . This approach is taken by Witte and Shamsundar [1983], and London and Shah [1983]. A disadvantage is that it introduces a further temperature (the ambient T_0) into the analysis, in addition to the terminal temperatures T_1 and T_2 , and complicates presentation. For a process situation there is normally one stream regarded as the process stream, and its inlet temperature would be the logical one to choose.

In the current approach we choose the cold stream as the process stream, and thus non-dimensionalise by \dot{Q} / T_1 . We accordingly call the resultant entropy generation number N_{s1} , to avoid confusion with Bejan's N_s based on $\dot{m}c_p$. Since the heat flow is

$$\dot{Q} = \dot{m}c_p \varepsilon (T_2 - T_1), \quad (3.42)$$

the entropy generation number becomes

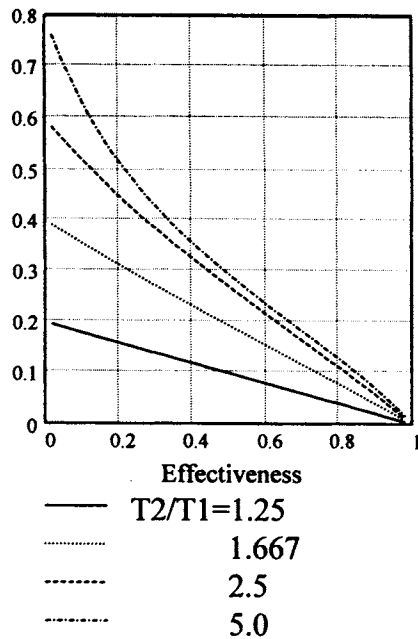
$$N_{s1} = \frac{T_1 \dot{S}_{gen}}{\dot{Q}} = \frac{1}{\varepsilon (T_2 / T_1 - 1)} \ln \left(\frac{(1 - T_2 Ntu / T_1)(1 + T_2 Ntu / T_1)}{(1 + Ntu)^2} \right) \quad (3.43)$$

$$= \frac{1}{\varepsilon (T_2 / T_1 - 1)} \ln \left(\left(1 + \varepsilon \left(\frac{T_2}{T_1} - 1 \right) \right) \left(1 - \varepsilon \left(1 - \frac{T_1}{T_2} \right) \right) \right) = \frac{N_s}{\varepsilon (T_2 / T_1 - 1)} \quad (3.44)$$

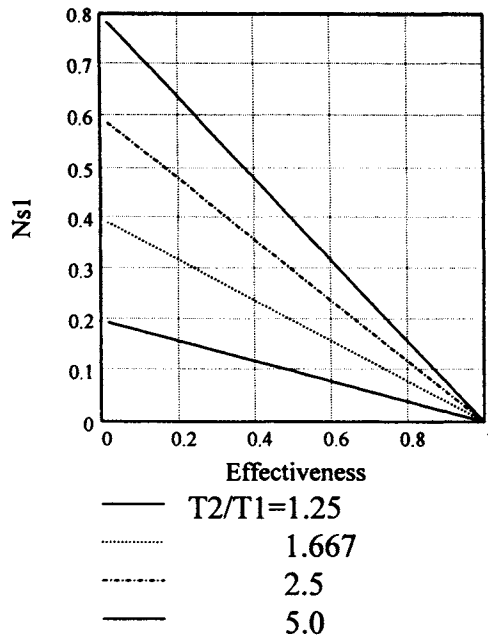
This function is shown in Figure 3.3, for the range of T_2/T_1 of 1.25, 1.6667, 2.5 and 5.

Thus for process situations in which the heat load \dot{Q} is given, the entropy generation rate (N_{s1}) decreases monotonically as ε tends to unity or Ntu tends to infinity. Note that the formulation of N_{s1} is such that for a given heat capacity rate $\dot{m}c_p$ and initial temperatures T_1 and T_2 , the specification of heat load \dot{Q} ($< \dot{Q}_{\max}$) directly determines ε and hence \dot{S}_{gen} , as is evident from equation (3.43) since all four terminal temperatures are then fixed. If \dot{Q} and temperature limits only are specified, the process designer has one degree of freedom ($\dot{m}c_p$ or ε), linked by equation (3.42).

Ns1



a) Exact solution
(Equation 3.44)



b) Approximate solution
(Equation 3.44b)

Figure 3.3 Entropy generation number for balanced counterflow

A simplification of equation (3.43) can be obtained by writing the operand of the logarithmic term as

$$\left[\frac{\left(1 + \frac{T_1}{T_2} Ntu \right) \left(1 + \frac{T_2}{T_1} Ntu \right)}{(1 + Ntu)^2} \right] = 1 + \frac{Ntu}{(1 + Ntu)^2} \left(\frac{T_2}{T_1} - 1 \right)^2 \left/ \left(\frac{T_2}{T_1} \right) \right. . \quad (3.45)$$

For small values of $\frac{Ntu}{(1 + Ntu)^2} \left(\frac{T_2}{T_1} - 1 \right)^2 \left/ \left(\frac{T_2}{T_1} \right) \right.$, valid for many (especially high Ntu) applications, a single term in the series expansion is adequate, giving

$$N_{s1} = \frac{T_1 \dot{S}_{gen}}{\dot{Q}} \approx (1 - \varepsilon) \left(1 - \frac{T_1}{T_2} \right), \quad (3.44b)$$

which simplifies to

$$N_{s1} = \frac{\Delta T}{T_2}, \quad (3.43c)$$

and gives the corresponding entropy generation rate

$$\dot{S}_{gen} = \frac{\dot{Q} \Delta T}{T_1 T_2}. \quad (3.46a)$$

This simple expression clearly relates the two- stream generation rate to that given in equation 3.36 for a single stream, bearing in mind that the heat flow \dot{Q} is itself proportional to ΔT . It is easily shown to correspond directly to Bejan's expression (Bejan (1977)) for a counterflow exchanger. Note also the strong analogy with the entropy generation rate (Bejan (1982, 1988) for heat being exchanged between two constant temperature reservoirs with the terminal temperatures T_1 and T_2 :

$$\dot{S}_{gen} = \frac{\dot{Q}(T_2 - T_1)}{T_1 T_2}. \quad (3.47)$$

These two situations are compared schematically in Figure 3.4.

Here, the only difference is the temperature gap between the 'streams', and the heat exchanger (equation 3.46a) has a lower entropy generation by a factor of $(1 + Ntu)$. Interestingly, the same ratio applies, inversely, to the heat conductance US , or thermal length, required for transfer of \dot{Q} . This is represented by the horizontal scale for the two cases, to give equal areas contained between the temperature distribution envelopes. The product $(US)_{min}$ is the value required to transmit \dot{Q} with the maximum possible temperature difference $(T_2 - T_1)$. This correspondence is a direct consequence of the linearisation of the entropy generation equation 3.43.

The form of equation 3.46a is also reflected later in our discussion of single stream optimisation.

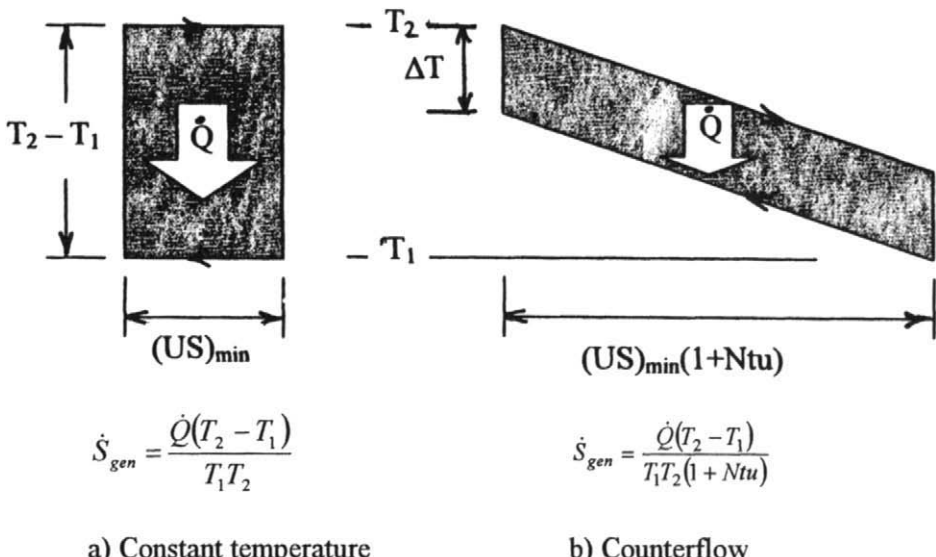


Figure 3.4 Constant temperature and counterflow heat exchangers, showing thermal lengths

The closeness of the linearisation expressed by equation 3.42b is evident in Figure. 3b, especially for low T_2/T_1 . Its usefulness is evident by noting that for $T_1 = 400K$, the ratio $T_2/T_1 = 1.6667$ corresponds to $T_2 = 666.7K$ - a substantial temperature span, and with negligible error in entropy generation calculation.

The design problem is simplified somewhat by writing the dimensionless heat flow as

$$B = \dot{Q} / \dot{m}c_p T_1 = \varepsilon(T_2/T_1 - 1), \quad (3.48)$$

since this is a function of specified process parameters, and expressing the temperature ratio T_2/T_1 in terms of B and ε . The new relationship then becomes

$$N_{s,1} = \frac{1}{B} \ln \left((1+B) \left(1 - \varepsilon \frac{B}{(\varepsilon+B)} \right) \right). \quad (3.49)$$

This is shown in Figure 3.5. Obviously, the upper temperature T_2 could have been used in non-dimensionalising the parameter B as well as the entropy parameter N_s .

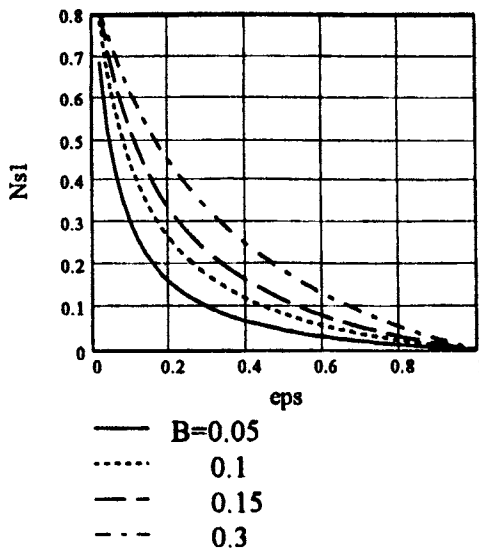


Figure 3.5 Entropy generation number N_{s1} in terms of Parameter B (balanced counterflow)

As mentioned by Witte and Shamsundar, the exergy loss is simply obtained by multiplying N_{s1} by T_0/T_1 . Witte and Shamsundar also observed that in many cases (e.g. Joule (or Brayton) cycle recuperators, feed preheat trains) the cold inlet temperature T_1 is very close to the environmental temperature T_0 , thus justifying the corresponding simplification in their analysis. The generality of $T_0 \neq T_1$ is retained in the present work.

A further observation on the present formulation (equation 3.44) is that N_{s1} can exceed unity. This corresponds to the point made by Bejan [1988] that Witte and Shamsundar's thermodynamic efficiency parameter $\eta = 1 - T_0 \dot{S}_{gen}/\dot{Q}$ can be negative in cryogenic operational conditions- a conceptually inconvenient result.

General analysis for exchangers with flow imbalance

In this case, characterised by $\dot{m}_1 \neq \dot{m}_2$, with the ratio of heat capacity rates $(cm)_{\min}/(cm)_{\max} = C_{\min}/C_{\max}$ denoted by C^* , the entropy generation rate becomes (Bejan [1977]), again neglecting the pressure drop contribution:

$$\dot{S}_{gen} = C_{\min} \ln\left(\frac{T_{1out}}{T_1}\right) + C_{\max} \ln\left(\frac{T_{2out}}{T_2}\right), \quad (3.50)$$

for the case with stream 2 having the larger heat capacity rate, giving

$$\frac{\dot{S}_{gen}}{C_{min}} = \left\{ \ln \left[1 + \varepsilon \left(\frac{T_2}{T_1} - 1 \right) \right] + \frac{1}{C^*} \ln \left[1 - C^* \varepsilon \left(1 - \frac{T_1}{T_2} \right) \right] \right\}, \quad (3.51)$$

$$\text{where } \varepsilon = \frac{T_{1out} - T_1}{T_2 - T_1} = \frac{1}{C^*} \frac{T_2 - T_{2out}}{T_2 - T_1}. \quad (3.52)$$

The entropy generation number N_{s1} then becomes

$$N_{s1} = \frac{T_1 \dot{S}_{gen}}{\dot{Q}} = \frac{T_1}{\varepsilon(T_2 - T_1)} \left\{ \ln \left[1 + \varepsilon \left(\frac{T_2}{T_1} - 1 \right) \right] + \frac{1}{C^*} \ln \left[1 - C^* \varepsilon \left(1 - \frac{T_1}{T_2} \right) \right] \right\} \quad (3.53)$$

$$\text{where } \dot{Q} = C_{min} (T_{1out} - T_1) = C_{max} (T_2 - T_{2out}) = \varepsilon C_{min} (T_2 - T_1). \quad (3.54)$$

Note that in the limit of the balanced counterflow case $C = 1$, this reduces to equation (3.44) with $\varepsilon = Ntu/(1 + Ntu)$. For the case of stream 1 having the larger heat capacity, the corresponding equation is

$$N_{s1} = \frac{T_1 \dot{S}_{gen}}{\dot{Q}} = \frac{T_1}{\varepsilon(T_2 - T_1)} \left\{ \frac{1}{C^*} \ln \left[1 + C^* \varepsilon \left(\frac{T_2}{T_1} - 1 \right) \right] + \ln \left[1 - \varepsilon \left(1 - \frac{T_1}{T_2} \right) \right] \right\} \quad (3.55)$$

$$\text{with } \dot{Q} = C_{max} (T_{1out} - T_1) = C_{min} (T_2 - T_{2out}). \quad (3.56)$$

In Figures 3.6 and 3.7 equations (3.53) and (3.55) are shown for $C^* = 0, 0.2, 0.5$ and 1.0 and $T_2/T_1 = 1.2$ and 1.5 in terms of effectiveness, illustrating the effect of whether the hot or cold stream has the highest heat capacity rate. All cases exhibit the lower limit of $N_{s1} = 1 - T_1/T_2$, and the curves shown correspond to the complement of Witte and Shamsundar's [1983] efficiency parameter with $T_1 = T_0$. It is clear that imbalance increases entropy generation, and that only in the balanced case does N_{s1} approach zero in the limit $\varepsilon \rightarrow 1$. The thermodynamic advantage of the hot stream having the highest heat capacity rate is also evident, as was observed by Witte and Shamsundar for their efficiency approach. Physically, this reflects the higher mean temperature of heat exchange.

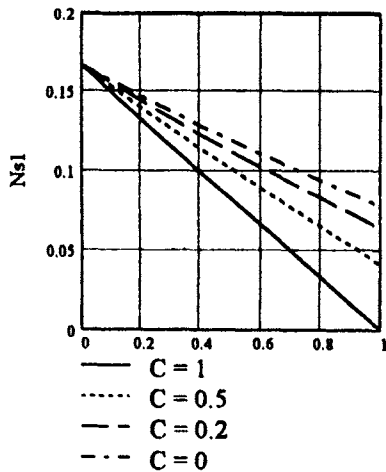


Figure 3.6a N_{s1} versus effectiveness,
 $T_2/T_1 = 1.2$.
 (hot stream highest mc_p)

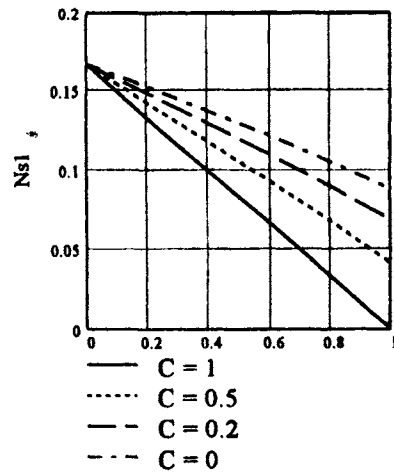


Figure 3.6b N_{s1} versus effectiveness,
 $T_2/T_1 =$ for $C^* = (1) 1.0,$
 $(2) 1.5, (3) 2, (4) 10001.2$,
 (cold stream highest mc_p)

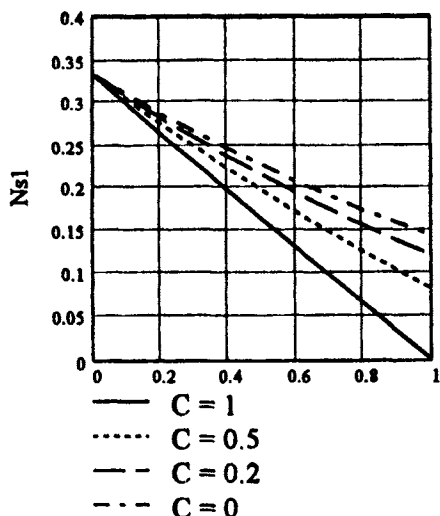


Figure 3.7a N_{s1} versus effectiveness,
 $T_2/T_1 = 1.5$.
 (hot stream highest mc_p)

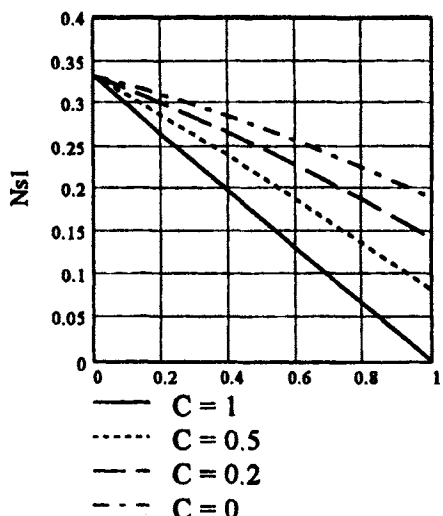


Figure 3.7b N_{s1} versus effectiveness,
 $T_2/T_1 = 1.5$.
 (cold stream highest mc_p)

Since the above formulations are in terms of the thermal effectiveness ε , they are perfectly general, and are independent of exchanger flow arrangements. Specific common arrangements are considered briefly below, in terms of the practically useful Ntu .

Unbalanced counterflow

The ε - Ntu relationship for this case (see also chapter 6) is given by

$$\varepsilon = \frac{1 - \exp(-Ntu(1 - C^*))}{1 - C^* \exp(-Ntu(1 - C^*))}, \quad (3.57)$$

giving N_{s1} - Ntu relationships from Equation 3.53 as shown in Figure 3.8, for temperature ratios T_2/T_1 of 1.2 and 1.5, for values of C^* of 0, 0.2, 0.5 and 1, the latter approximating to the condensing case of $C^* = 0$.

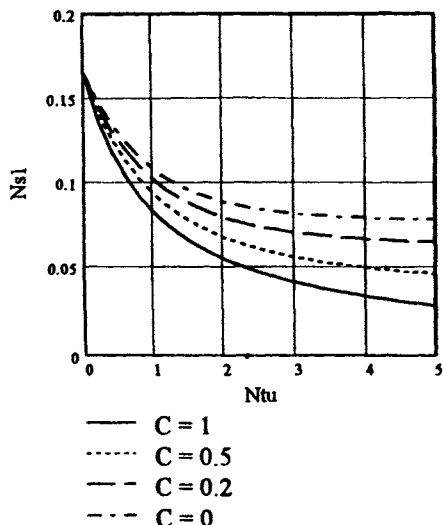


Figure 3.8a N_{s1} versus Ntu , $T_2/T_1 = 1.2$
(hot stream highest mc_p)

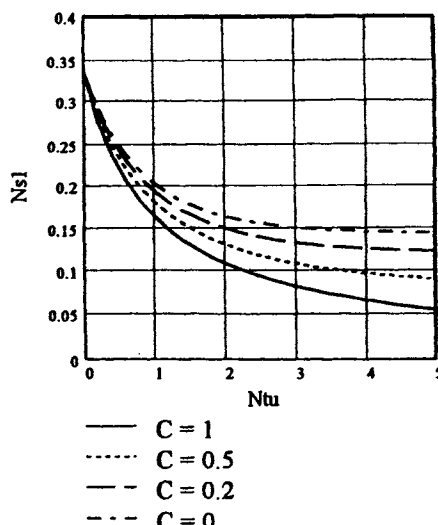


Figure 3.8b N_{s1} versus Ntu , $T_2/T_1 = 1.5$
(hot stream highest mc_p)

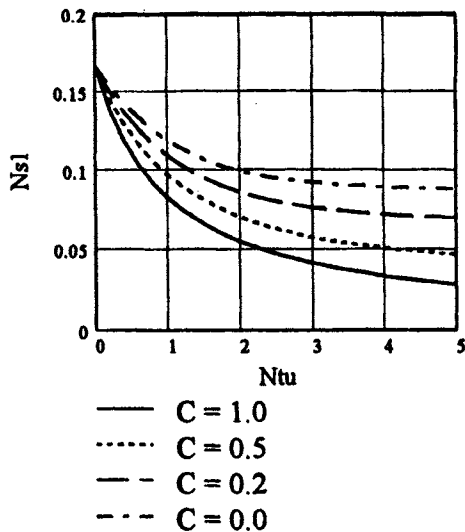


Figure 3.8c N_{s1} versus Ntu , $T_2/T_1 = 1.2$
(cold stream highest mc_p)

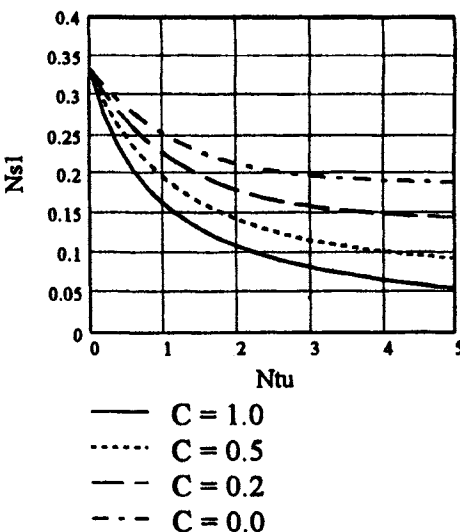


Figure 3.8d N_{s1} versus Ntu , $T_2/T_1 = 1.5$
(cold stream highest mc_p)

Cocurrent (parallel) flow

The ε - Ntu relationship for this case is given by

$$\varepsilon = \frac{1 - \exp(-Ntu(1 + C^*))}{1 + C^*}, \quad (3.58)$$

and the corresponding N_{s1} - Ntu relationship is shown in Figures 3.9 and 3.10, for the temperature ratios $T_2/T_1 = 1.2$ and 1.5 . It is clear that the effect of flow imbalance is minimal, reflecting the thermodynamic similarity of this configuration to that of condensation, with 0 (see below).

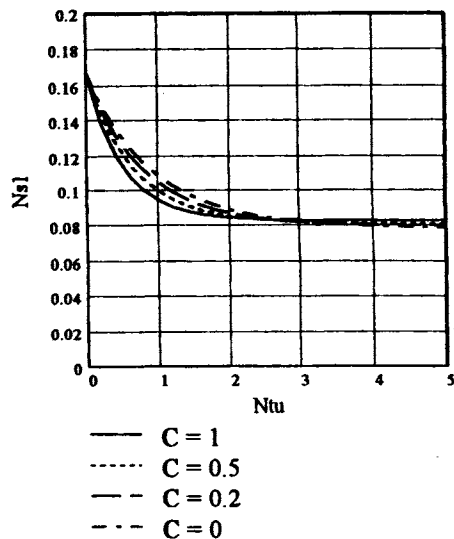


Figure 3.9 N_{sl} versus Ntu , $T_2/T_1 = 1.2$ (cocurrent flow)

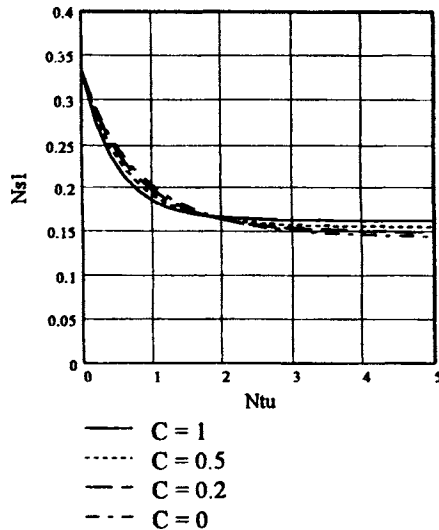


Figure 3.10 N_{sl} versus Ntu , $T_2/T_1 = 1.5$ (cocurrent flow)

Condensing on one side

For condensation, with $C^* = 0$, the ε - Ntu relationship is particularly simple:

$$\varepsilon = 1 - \exp(-Ntu). \quad (3.59)$$

Equation (3.53) simplifies to

$$N_{sl} = \frac{\ln\left(1 + \varepsilon \left(\frac{T_2}{T_1} - 1\right)\right)}{\varepsilon \left(\frac{T_2}{T_1} - 1\right)} - \frac{T_1}{T_2}, \quad (3.60)$$

and allows a relatively simple expression in terms of Ntu (Witte [1988]):

$$N_{sl} = \frac{\ln \left(1 + (1 - \exp(-Ntu)) \left(\frac{T_2}{T_1} - 1 \right) \right)}{(1 - \exp(-Ntu)) \left(\frac{T_2}{T_1} - 1 \right)} - \frac{T_1}{T_2}. \quad (3.61)$$

This is shown in Figure 3.11.

Evaporation on one side

For this case $C^* = 0$, the effectiveness relation is the same as for condensation, equation (3.58), and equation (3.54) gives on substitution

$$N_{sl} = \frac{\ln \left[1 - \varepsilon \left(1 - \frac{T_1}{T_2} \right) \right]}{\varepsilon \left(\frac{T_2}{T_1} - 1 \right)} + 1, \quad (3.62)$$

and in terms of Ntu:

$$N_{sl} = \frac{\ln \left(1 - (1 - \exp(-Ntu)) \left(1 - \frac{T_1}{T_2} \right) \right)}{(1 - \exp(-Ntu)) \left(\frac{T_1}{T_2} - 1 \right)} + 1. \quad (3.63)$$

This is shown in Figure 3.12. Comparing Figures 3.11 and 3.12, the strong difference between the two cases of condensation and evaporation as the temperature ratio T_2/T_1 is increased is clearly seen.

FINITE PRESSURE DROP

Optimisation based on local rate equation

We start with the basic equation (3.35) (Bejan [1978,1987]) for entropy production rate at a given point in the heat exchanger surface with a local bulk temperature T . A single stream only is examined.

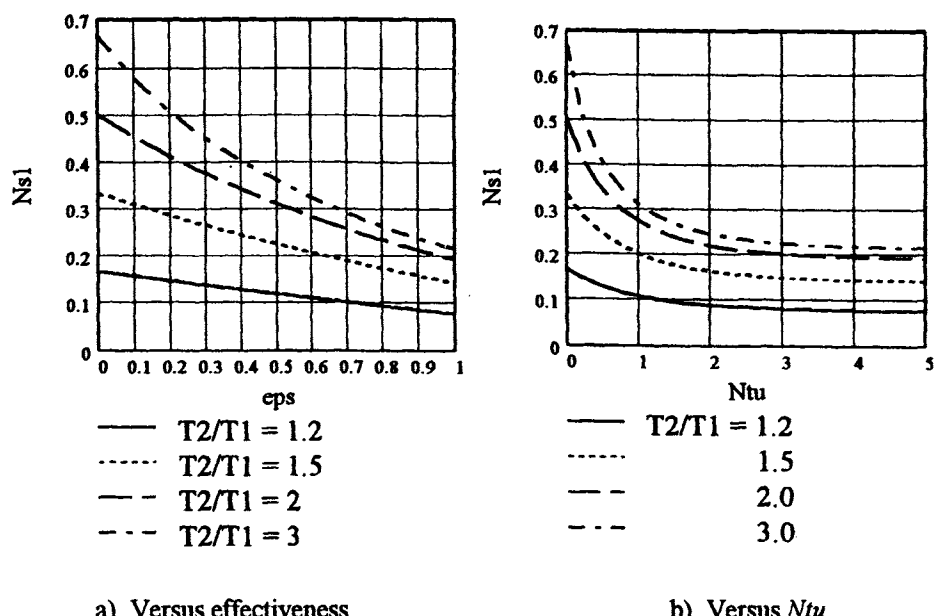


Figure 3.11 N_{s1} for condensation on one side ($T_2/T_1 = 1.2, 1.5, 2.0, 3.0$)

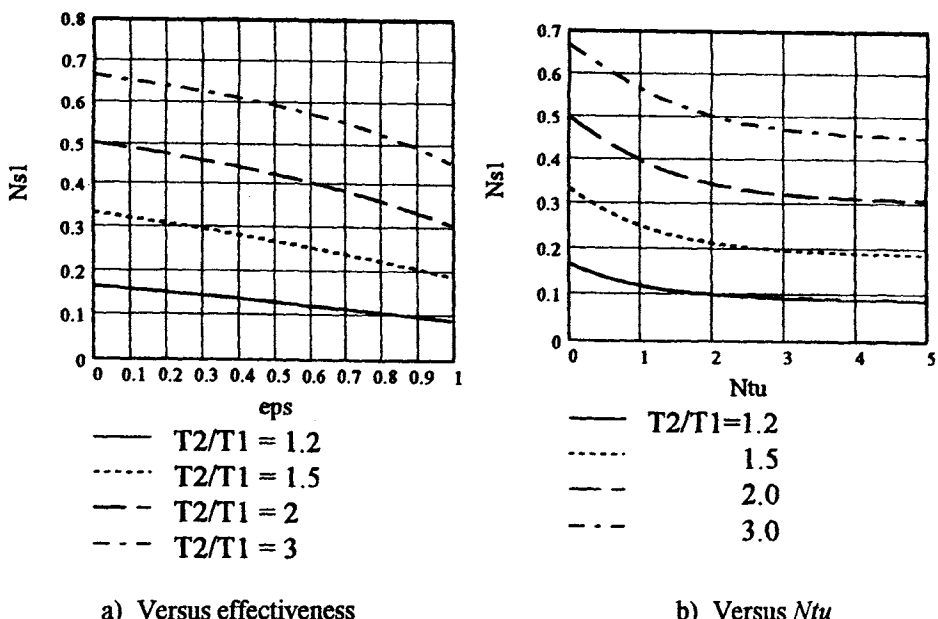


Figure 3.12 N_{s1} for evaporation on one side ($T_2/T_1 = 1.2, 1.5, 2.0, 3.0$)

Non-dimensionalising by q' / T gives

$$N_{s1} = \frac{T\dot{S}'_{gen}}{q'} = \frac{\tau}{1+\tau} + \frac{\dot{m}}{\rho q'} \left(-\frac{dp}{dx} \right). \quad (3.64)$$

Substituting from the following standard heat transfer and pressure drop equations for given surface parameters:

Heating rate:

$$q' = \alpha p_s \Delta T, \quad (3.65)$$

where p_s = perimeter of the surface, giving

$$q' = St c_p G p_s \Delta T = St G c_p T p_s \tau, \quad (3.66)$$

Pressure gradient:

$$\frac{dp}{dx} = \frac{2f}{d_h} \rho u^2 \quad (3.67)$$

yields, in terms of τ ,

$$N_{s1} = \left(\frac{f Re^2 \eta^2}{2 \rho^2 d_h^2 c_p T St} \right) \frac{1}{\tau} + \frac{\tau}{1+\tau}. \quad (3.68a)$$

Differentiation with respect to τ for minimum N_{s1} can be done because the term in parentheses is only a function of Re and the local temperature T . Expressing this term as A_2 , we have

$$N_{s1} = \frac{A_2}{\tau} + \frac{\tau}{1+\tau}, \quad (3.68b)$$

and differentiating for fixed Reynolds number gives a minimum at a value of τ denoted by τ_{opt}

$$\tau_{opt} = \frac{A_2^{1/2} + A_2}{1 - A_2} \approx A_2^{1/2} \text{ for the normally small } A_2. \quad (3.69)$$

The minimum value of N_s then becomes

$$N_{s1,\min} = \frac{2A_2^{1/2}}{1 + A_2^{1/2}} + \frac{A_2(1 - A_2^{1/2})}{1 + A_2^{1/2}} \approx 2A_2^{1/2} = 2\tau_{opt} \text{ for small } A_2. \quad (3.70)$$

Implicit in equation (3.70) is that contributions from the pressure drop and heat flow are equal at the optimum condition of $Be = 0.5$, which is consistent with Bejan's analysis for developing plate flow (Bejan [1982] and indirectly for counterflow heat exchangers (Bejan [1977])). The plate flow has a direct analogy with that of an offset strip fin heat exchanger surface.

Looking further at the parameter A_2 ,

$$A_2 = \frac{f}{2St} \frac{G^2}{\rho^2 c_p T} = \frac{f}{St} \frac{u^2}{2c_p T}. \quad (3.71)$$

For a perfect gas, the speed of sound a is given by

$$a^2 = (\gamma - 1)c_p T, \quad (3.72)$$

so equation (3.71) becomes

$$A_2 = \frac{f}{j} Pr^{2/3} \frac{\gamma - 1}{2} M^2 = \frac{f}{St} \frac{\gamma - 1}{2} M^2, \quad (3.73)$$

where M is the Mach number.

Noting that $\frac{\gamma - 1}{2} M^2$ is the incremental stagnation temperature due to velocity, since $\frac{T_s}{T} = 1 + \frac{\gamma - 1}{2} M^2$ for compressible one-dimensional flow,

with T_s being the stagnation temperature, the factor f/St in A_2 is a simple multiplier in this increment. It is readily shown that the present analysis is consistent with a development of the analysis of Shapiro [1953], presented in log-differential form, for a one-dimensional duct flow with friction and heat addition, in which the Reynolds analogy of $f/St = 2$ is assumed.

We now have

$$N_{s1,\min} = 2M \left(\frac{f}{j} \frac{Pr^{2/3}(\gamma - 1)}{2} \right)^{1/2}. \quad (3.74)$$

Thus $N_{s1,\min}$ is only related to the area goodness factor j/f and Mach number, for a given gas. For typical gas side velocities of the order of a few m/s, and speed of sound of say 200-300 m/s, a typical Mach number is of the order of 0.01, which gives a corresponding $N_{s1,\min}$ of the same order. The corresponding temperature difference is then a few degrees, being of order (0.01^*T K) . An alternative form of the minimum value, from equations (3.70) and (3.71), is

$$N_{s1,\min} = 2 \left(\frac{fPr^{2/3}}{j} \frac{\dot{m}^2}{2\rho^2 c_p T} \right)^{1/2} \frac{1}{A_c}. \quad (3.75)$$

The general rate equation, from equation (3.68) is, in terms of Mach number,

$$N_{s1} = \frac{T\dot{S}_{gen}}{q'} = \frac{f}{St} \frac{\gamma - 1}{2} M^2 \frac{1}{\tau} + \frac{\tau}{1 + \tau} \quad (3.76a)$$

for the conventional case, and

$$N_{s1} = \frac{T\dot{S}_{gen}}{q'} = \frac{kPr}{Nu} \frac{\gamma - 1}{2} M^2 \frac{1}{\tau} + \frac{\tau}{1 + \tau} \quad (3.76b)$$

for the fully developed laminar flow case. In both cases, the importance of the *area goodness factor* (j/f or Nu/k , respectively) in minimising entropy generation is clear.

For given process requirements of \dot{m} , ρ , and heating load rate q' , it is clear, as observed by Bejan [1977], that the minimum local entropy generation rate *relative to q'* can be made indefinitely small, by making the flow area A_c large enough (or the mass velocity small enough). This simultaneously reduces both the pressure drop and ΔT . The absolute generation rate is proportional to q' . Selection of G gives an optimum ΔT , which in conjunction with a specified q' determines the hydraulic diameter via equation 3.66, since $d_h = 4A_c/\rho_s$. Alternatively, selection of d_h and ΔT , the more usual scenario, determines the optimum G and also fixes q' . More generally, the above analysis shows that

the Mach number is the fundamental controlling parameter. Values for typical practical variations of A_2 and τ are shown in Figure 3.13, from equation (3.68).

It is clear from equations (3.74) and (3.75) that the shape of the $N_{s1,min}$ locus is linear with M or $1/A_c$ if f/j is constant, that is, independent of A_c and hence Re . In general f/j is a (usually weak) function of Re , as already remarked.

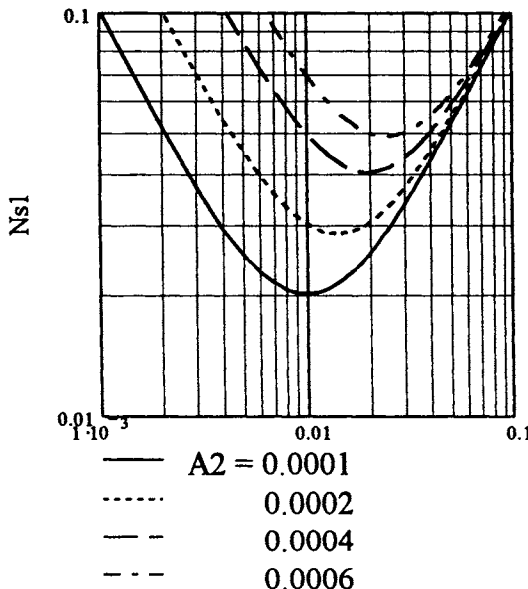


Figure 3.13 Parameter N_{s1} versus τ and A_2

Application of the rate equation to balanced counterflow

The analysis so far is based on a local rate process, and is thus valid for a given point (position, temperature, etc.) in a stream within a heat exchanger. We now develop its application to actual heat exchanger streams with temperature varying along the stream. Considering the rate equation (3.68), still for a single side,

$$\frac{d\dot{S}_{gen}}{dx} = \frac{q'}{T} \left[\frac{A_2}{\tau} + \tau \right] \text{ for small } \tau \quad (3.77)$$

$$\text{and } q' = -\dot{m} c_p \frac{dT}{dx} \quad (3.78)$$

we have, substituting for q' in (3.77),

$$\frac{d\dot{S}_{gen}}{dT} = \frac{\dot{m} c_p}{T} \left[\frac{A_2}{\tau} + \tau \right] \quad (3.79)$$

Recalling that from (3.71),

$$A_2 = \frac{f}{2St} \cdot \frac{G^2}{\rho^2 c_p T} = \frac{f}{2St} \cdot \frac{G^2 R^2 T}{p^2 c_p} \quad \text{for a perfect gas.} \quad (3.80)$$

Here, G^2 is fixed by the mass flow rate and throughflow area, which is normally constant, and $f/2St$ is only a weak function (in general) of Re (or density). In addition, the variation of absolute pressure p is normally small in comparison with that of temperature, as was shown by Hesselgreaves (2000), so we can put

$$A = \frac{A_2}{T} = \frac{f}{2St} \cdot \frac{G^2}{p^2 c_p} \cdot R^2 \quad [\text{where } A \text{ is very nearly constant}], \quad (3.81)$$

noting that A has dimensions of $1/T$. Thus we can re-formulate (3.79) as

$$\frac{d\dot{S}_{gen}}{dT} = -\dot{m} c_p \left[\frac{AT}{\Delta T} + \frac{\Delta T}{T^2} \right], \quad (3.82)$$

which now accounts correctly for the density variation.

$$\text{Thus } \dot{S}_{gen} = -\dot{m} c_p \left[\frac{A}{\Delta T} \int_{T_1}^{T_{1out}} T dT + \Delta T \int_{T_1}^{T_{1out}} \frac{dT}{T^2} \right], \quad (3.83)$$

for side 1, since ΔT is constant with flow length in a balanced exchanger.

Integrating,

$$\dot{S}_{gen} = -\dot{m} c_p \left[\frac{A}{2\Delta T} \left(T_{1out}^2 - T_1^2 \right) - \Delta T \left[\frac{1}{T_{1out}} - \frac{1}{T_1} \right] \right] \quad (3.84)$$

Putting $B_3 = \frac{\dot{m} c_p A}{2} (T_{1out}^2 - T_1^2)$ (3.85)

and $C_1 = -\dot{m} c_p \left[\frac{1}{T_{1out}} - \frac{1}{T_1} \right]$ (3.86)

we have $\dot{S}_{gen} = -\frac{B_3}{\Delta T} + C_1 \Delta T$ (3.87)

which is the generalised form of the basic rate equation (equation 3.66), for a single stream over its temperature range, noting that the temperature difference is stream to surface, rather than the normal stream to stream. Differentiation gives a minimum when

$$\Delta T^2 = \Delta T^{*2} = \frac{B_3}{C_1} = \frac{A}{2} (T_1 + T_{1out}) T_1 T_{1out} \quad (3.88)$$

and the minimum value is accordingly

$$\dot{S}_{gen, \min} = \frac{B_3}{\Delta T^*} + C_1 \Delta T^* = 2\sqrt{B_3 C_1} \quad (3.89)$$

with equal contributions from temperature difference and pressure drop as for the local case.

Note that in the limit of $T_{1out} \rightarrow T_1$, the optimum temperature difference converges to the 'local' value of

$$\Delta T = \tau T = T \sqrt{AT} = TA_2^{1/2} \quad . \quad (3.90)$$

The expansion of (3.89) gives

$$\dot{S}_{gen, \min} = 2\dot{m} c_p \left(\frac{f}{2St} \cdot \frac{G^2 R^2}{p^2 c_p} \right)_2^{\frac{1}{2}} (T_{1out} - T_1) \sqrt{\frac{(T_1 + T_{1out})}{2(T_1 T_{1out})}} \text{ (for one side)} \quad (3.91)$$

and for both sides:

$$\dot{S}_{gen, \min} = 2\dot{m} c_p \left(\frac{f}{2St} \cdot \frac{G^2 R^2}{p^2 c_p} \right)_1^{\frac{1}{2}} (T_{1out} - T_1) \sqrt{\frac{(T_1 + T_{1out})}{2(T_1 - T_{1out})}} + 2\dot{m} c_p \left(\frac{f}{2St} \cdot \frac{G^2 R^2}{p^2 c_p} \right)_2^{\frac{1}{2}} (T_2 - T_{2out}) \sqrt{\frac{(T_2 + T_{2out})}{2(T_2 - T_{2out})}} \quad (3.92)$$

In the limit of vanishingly small ΔT (Bejan's [1977] condition), $T_{2out} = T_1$ and $T_{1out} = T_2$, giving

$$\dot{S}_{gen, \min} = 2\dot{m} c_p (T_2 - T_1) \sqrt{\frac{(T_1 + T_2)}{2(T_1 T_2)}} \left[\left(\frac{f}{2St} \cdot \frac{G^2 R^2}{p^2 c_p} \right)_1^{\frac{1}{2}} + \left(\frac{f}{2St} \cdot \frac{G^2 R^2}{p^2 c_p} \right)_2^{\frac{1}{2}} \right] \quad (3.93)$$

Bejan's corresponding relationship for both sides is

$$\dot{S}_{gen, \min} = \frac{2\dot{m} c_p (T_2 - T_1)}{\sqrt{T_1 T_2}} \left[\left(\frac{f}{2St} \cdot \frac{G^2 R^2}{p^2 c_p} \right)_1^{\frac{1}{2}} T_{1ref}^{\frac{1}{2}} + \left(\frac{f}{2St} \cdot \frac{G^2 R^2}{p^2 c_p} \right)_2^{\frac{1}{2}} T_{2ref}^{\frac{1}{2}} \right] \quad (3.94)$$

where T_{1ref} and T_{2ref} are the implied reference temperatures pertaining to the definition by Bejan of dimensionless mass velocity g_1 as $g_1 = \frac{G}{(2\rho p)^{\frac{1}{2}}}$.

Inspection of equations (3.93) and (3.94) shows that Bejan's relationship and the more general one are in agreement if $T_{1ref} = T_{2ref} = (T_1 + T_2)/2$, by Bejan's assumption of infinitesimal ΔT . This applies if the density in g_1 is selected at the arithmetic mean temperature of both streams- a felicitous result.

For one side, the consequences of evaluating the entropy rate at a single terminal temperature instead of using the full optimum relationship are shown in Figure 3.14, in terms of the variable $t = T_{in}/T_{out}$ of the hot stream.

These equations can be used for optimising in the case of real balanced counterflow exchangers with 'long' duties, i.e. high temperature span.

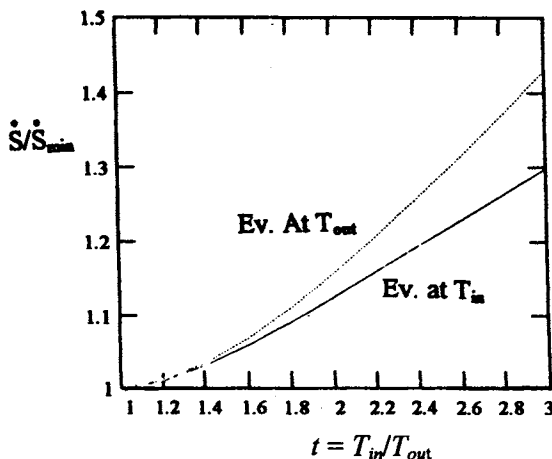


Figure 3.14 Relative entropy generation for evaluating equation (3.85) at terminal temperatures.

IMPLICATIONS OF THE ENTROPY MINIMISATION ANALYSIS FOR SELECTION AND DESIGN

It has been observed earlier in this chapter that if the terminal temperatures and mass flows of a heat exchanger are fixed, as is often the case, then the entropy production rate from the temperature driving potential is also fixed. The contribution from the pressure drop can be reduced indefinitely, in theory, by maximising the flow area, thereby minimising flow velocity (or mass velocity, or Mach number). The minimisation process then depends on replacing the constraint of fixed terminal temperatures of the second stream with that of fixing the heating rate or heating gradient. This constraint thus couples the flow area and temperature difference. In terms of a balanced counterflow heat exchanger the situation is shown schematically in Figure 3.15. This shows a hot stream which is to be cooled, with a given heat load, by a service stream with (a) high inlet temperature and (b) low inlet temperature, with consequent low and high ΔT . We will confine attention now to a single stream, with the ΔT referring to the stream- to surface difference.

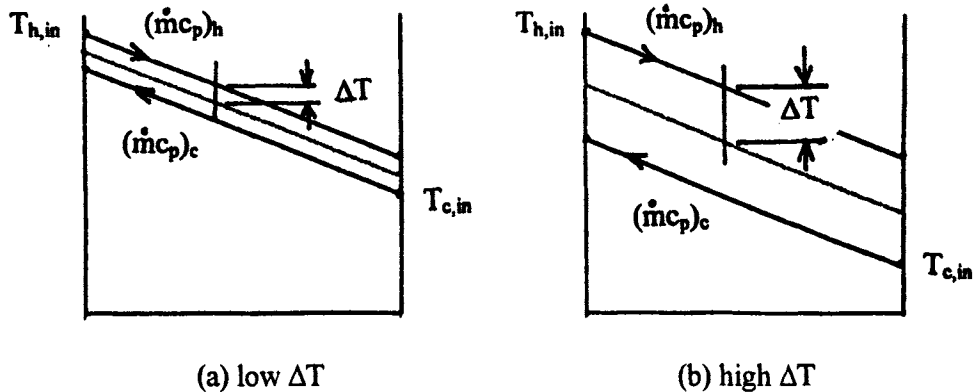


Figure 3.15 Counterflow options

Writing the heating rate as

$$q' = Stc_p G \frac{4A_c}{d_h} \Delta T = Stc_p \frac{4\dot{m}}{d_h} \Delta T = Stc_p \frac{4\dot{m}^2}{A_c \eta Re} \Delta T, \quad (3.95)$$

we see that specifying both the flow area A_c and heating rate necessarily implies fixing the Reynolds number and hence the hydraulic diameter and ΔT , since the Stanton number is a function of Reynolds number and A_c and ΔT are linked through equation 3.69. Alternatively, fixing the hydraulic diameter and heating rate determines the Reynolds number, flow area and ΔT . This is made clearer by re-writing equation 3.95, using 3.71, as

$$q' = \frac{4\eta Re}{\rho d_h} \left(\frac{f St}{2} \right)^{1/2} (c_p T)^{1/2}. \quad (3.96)$$

Since f and St are functions of Re equation 3.96 thus provides a direct inter-relationship of heating rate q' , Re and d_h . These relationships are best illustrated by means of an example.

These example cases clearly show the implications of choice of the hydraulic diameter of the surface. If this is high, then for a specified heating rate the operational temperature difference is high, with consequently a high entropy and exergy loss. Constraining the heating rate thus removes the freedom to reduce indefinitely the flow area and hence pressure drop, replacing this freedom with an optimisation, if chosen. The analysis allows us to examine the effects

for any specified duty of varying the temperature differences, or in other words, of the inlet temperature of the cold (service) stream.

Example 3.1 Consider the cooling of an air stream with the following specification:

Mass flow	$\dot{m} = 0.07 \text{ kg/s}$	Heating rate	$q' = 3000 \text{ W/m}$
Temperature	$T = 300 \text{ K}$	Surface characteristic, $St = 0.5Re^{-0.5}$	
Density	$\rho = 1.2 \text{ kg/m}^3$		$f/J = 5$
Viscosity	$\eta = 1.85 \times 10^{-5} \text{ Ns/m}^2$		
Thermal conductivity	$\lambda = 0.026 \text{ W/m}^2\text{K}$		
Prandtl No.	$Pr = 0.707$		
Specific heat	$c_p = 1005 \text{ J/kgK}$		

Option 1: specify flow area $A_c = 0.03 \text{ m}^2$, giving $G = 2.333 \text{ kg/m}^2\text{s}$

Then equation 3.71 gives the parameter A_2 :

$$A_2 = \frac{G^2}{\rho^2 c_p T} \left(\frac{f}{2St} \right) = \frac{2.33^2}{1.2^2 \times 1005 \times 300} \left(\frac{5 \times 0.707^{2/3}}{2} \right) = 2.481 \times 10^{-5}$$

Equation 3.69 gives the optimum ΔT :

$$\Delta T = A_2^{1/2} T = 0.00498 \times 300 = 1.494 \text{ K}.$$

Equation 3.95 gives the ratio Re/St :

$$\frac{Re}{St} = \frac{4c_p \dot{m}^2 \Delta T}{q' A_c \eta} = \frac{4 \times 1005 \times 0.07^2 \times 1.494}{3000 \times 0.03 \times 1.846 \times 10^{-5}} = 17713$$

Invoking the surface characteristic then gives

$$\frac{Re^{3/2}}{17713} = 0.5, \text{ and } Re = 427.8$$

The hydraulic diameter then becomes

$$d_h = \frac{\eta Re}{G} = \frac{1.846 \times 427}{2.333} = 0.00338 \text{ m, or } 3.38 \text{ mm}$$

The minimum entropy generation rate is, from equation 3.70

$$S' = \frac{N_{sl,min}q'}{T} = \frac{2\tau_{opt}q'}{T} = \frac{2A_2^{1/2}q'}{T} = \frac{2 \times 0.00498 \times 3000}{300} = 0.0996 \text{ W/mK},$$

and the exergy rate loss based on a 'dead' state temperature T_o of 25°C = 298K is

$$E'_x = T_o S' = 298 \times 0.0996 = 29.68 \text{ W/m}, \text{ one hundredth of the heat rate.}$$

Option 2: specify hydraulic diameter $d_h = 5.0 \text{ mm} = 0.005 \text{ m}$

We re-write equation 3.96 in a form to express q' in terms of d_h and Re , and inverting to give

$$Re \left(\frac{fSt}{2} \right)^{1/2} = \frac{q' \rho d_h^2}{4 \dot{m} \eta (c_p T)^{1/2}} = \frac{3000 \times 1.2 \times 0.005^2}{4 \times 0.07 \times 1.846 \times 10^{-5} \times (1005 \times 300)^{1/2}} = 31.71$$

The function of Re in parentheses is readily calculated to be

$$\left(\frac{fSt}{2} \right)^{1/2} = \frac{0.704}{Re^{1/2}},$$

$$\text{which gives } Re^{1/2} = \frac{31.71}{0.704} = 45.04, \text{ and } Re = 2029.$$

The flow area is simply given by

$$A_c = \frac{\dot{m} d_h}{Re \eta} = \frac{0.07 \times 0.005}{2029 \times 1.846 \times 10^{-5}} = 0.009345,$$

and the parameter A_2 is

$$A_2 = \left(\frac{f}{2St} \right) \frac{\dot{m}^2}{A_c^2 \rho^2 c_p T} = \frac{1.984 \times 0.07^2}{0.009345^2 \times 1.2^2 \times 1005 \times 300} = 0.0002645.$$

This gives $\tau = A_2^{1/2} = 0.0157$, and optimum temperature difference $\Delta T = T\tau = 4.71 \text{ K}$.

As for the first option, the entropy generation rate is given by

$$S' = \frac{N_{s1,\min} q'}{T} = \frac{2\tau_{opt} q'}{T} = \frac{2A_2^{1/2} q'}{T} = \frac{2 \times 0.0157 \times 3000}{300} = 0.314 W/mK.$$

This gives an exergy loss rate of

$$E'_x = T_o S' = 298 \times 0.314 = 93.57 W/m,$$

which is approximately one thirtieth of the heat rate.

APPLICATION TO HEAT EXCHANGER NETWORKS

Much has been written about the optimum design of heat exchanger networks, including its Second Law aspects (Chato and Damianides (1986), Hesselmann (1984)). A good description is given by Linnhoff et al. (1982). The basic principle is to arrange diagrammatically the various streams to be heated and those to be cooled into a Cold Composite stream and Hot Composite stream respectively, in the form of temperatures versus heat load. The composite streams are adjusted to have a minimum approach temperature difference at a certain point (see Figure 3.16, for a simple 3-stream system) called the *pinch*, and the minimum temperature difference ΔT_{\min} occurs in one of the heat exchangers used for the network. Also shown in Figure 3.16 is an alternative Cold Composite curve with a lower ΔT_{\min} . The differences on the load scale between the upper and lower terminal points represent the minimum hot utility (service) and the minimum cold utility respectively. The overlap between the curves on the load scale represents the heat recovery, which can be seen to increase as ΔT_{\min} is reduced. Clearly, each kink in the curve is associated with a change in heat capacity rate, so indicates the need for a further exchanger.

What is evident from the figure, and is of great significance for energy and exergy analysis, is that a reduction of ΔT_{\min} carries a double benefit, reducing both hot and cold utility requirements. This is particularly important in complex process systems involving mechanical energy recovery (gas turbine generators) on the one hand, and refrigeration on the other hand. It is in these cases that a full exergy analysis is necessary for optimisation, as distinct from a First Law (heat recovery) approach.

The advantage of achieving a low ΔT_{\min} in process networks is thus clear, even if, as for many cases, the pinch is 'sharp' enough to only require close approach temperatures in one exchanger. We have seen in equation 3.95 that for this one, a low ΔT requires a correspondingly low hydraulic diameter to achieve

a high heating rate. A lower heating rate (for the same final heat duty) would require a larger and possibly more expensive exchanger.

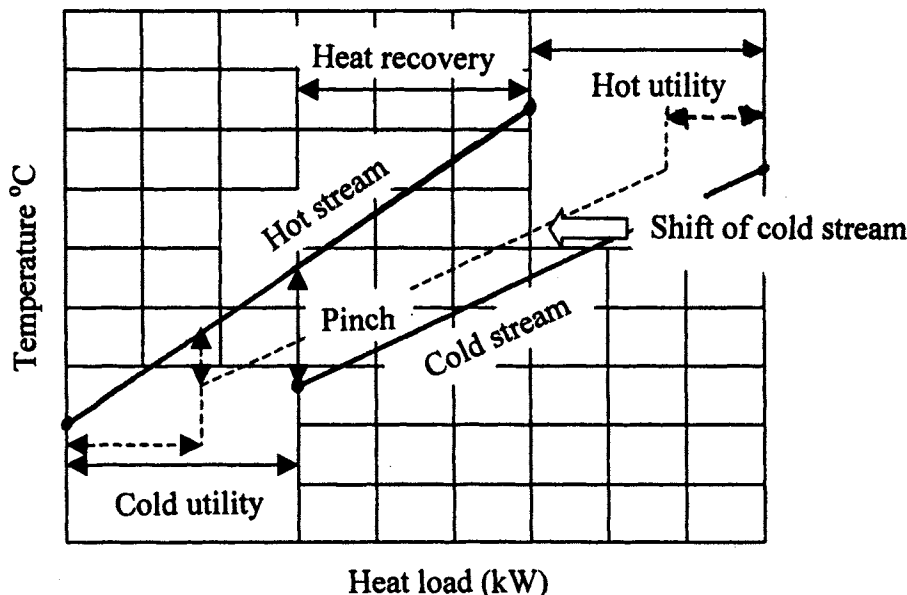


Figure 3.16 A simple 2-stream Composite Curve diagram

Finally, it should be re-iterated that the optimum analysis developed in this chapter only applies to ideal or near-ideal gas flows: for liquid flows the pressure drop component is nearly always negligible, and the temperature components only of entropy production are sufficient. Two-phase flows require special treatment: see Zubair et al. (1987).

References

Aherne, J.E., (1986), The Exergy Method of Energy Systems Analysis, John Wiley, New York.

Bejan, A., 1977, The Concept of Irreversibility in Heat Exchanger Design: Counterflow Heat Exchangers for Gas-Gas Applications. *J Heat Transfer*; 99: 374-380.

Bejan, A., 1978, General Criterion for Rating Heat Exchanger Performance. *Int. J. Heat Mass Transfer*; 21: 655-658.

Bejan, A., 1979, A Study of Entropy Generation in Fundamental Convective Heat Transfer. *J Heat Transfer*; 101: 718-725.

Bejan, A., 1980, Second Law Analysis in Heat Transfer. *Energy*; 5: 721-732

Bejan, A., 1982, Entropy Generation through Heat and Fluid Flow. New York : John Wiley.

Bejan, A., 1987, The Thermodynamic Design of Heat and Mass Transfer Processes and Devices. *Heat and fluid flow*; 8, 4.

Bejan, A., 1988, Advanced Engineering Thermodynamics. 1st ed. John Wiley, New York.

Bejan, A., 1996, Entropy Generation Minimization. Boca Baton: CRC.

Bejan, A., 1997, Advanced Engineering Thermodynamics. 2nd ed. John Wiley, New York.

Grossman, P. and Kopp, J., (1957), Zur gunstigen Wahl der temperaturdifferenz und der Wärmeübergangszahl in Wärmeaustauschern Kaltetechnic, 9(10), 306-308.

Linnhoff, B. et al, (1982), A user guide on Process Integration for the Effective Use of Energy, IChemE, Rugby.

London, A.L., 1983, Compact Heat Exchangers - Design Methodology. In: Kakac, S., Shah, R.K., Aung, W., editors. Low Reynolds Number Flow Heat Exchangers. Washington: Hemisphere.

London, A.L. and Shah, R.K., 1983, Costs of Irreversibilities in Heat Exchanger Design, *Heat Transfer Engineering*, 4, 59-73.

McClintock, F.A., 1951, The Design of Heat Exchangers for Minimum Irreversibility. Paper No 51-A-108, presented at the 1951 ASME Annual Meeting.

Nag, P.K. and De, S., 1996, Design and Operation of a Heat Recovery Steam Generator with Minimum Irreversibility, *Appl. Thermal Eng.* Vol.17 No.4, pp.385.

Sekulic, D.P., 1986, Entropy Generation in a Heat Exchanger. *Heat Transfer Engineering*, 7: 83-88.

Sekulic, D.P., 1990, A Reconsideration of the Definition of a Heat Exchanger, *Int. J. Heat Mass Transfer*, Vol.33, No.12, pp2748-2750.

Shapiro, A.H., 1953, *The Dynamics and Thermodynamics of Compressible Fluid Flow*, New York: Ronald.

Sjargut, J., Morris, D.R. and Steward, I.R., (1988), *Exergy Analysis of Thermal, Chemical and Metallurgical Processes*, Hemisphere, New York.

Smith, E.M., (1997) *Thermal Design of Heat Exchangers, a Numerical Approach*. John Wiley & sons, New York.

Witte, L.C. and Shamsundar, N., 1983, A Thermodynamic Efficiency Concept for Heat Exchange Devices. *J Eng for Power*, 105: 199-203.

Witte, L.C., 1988, The Influence of Availability Costs on Optimal Heat Exchanger Design. *ASME J. Heat Trans.* 110(4), 830-835.

Zubair, S.M., Kadaba, P.V. and Evans, R.B. (1987), Second Law Based Thermo-economic Optimisation of Two-Phase Heat Exchangers, *J. Heat Transfer*, 109: 287-294.

Chapter 4

SURFACE COMPARISONS, SIZE, SHAPE AND WEIGHT RELATIONSHIPS.

Science stops at the frontiers of logic, but nature does not – she thrives on ground as yet untrodden by theory.

C. G. Jung

INTRODUCTION

The purpose of this chapter is to build on and amplify the elements of compactness outlined in the Introduction (chapter 1) and to explore its implications for the size and shape of compact exchangers. For grasping the physical implications of compactness on size and shape, it is only necessary to consider one side. This can be justified on the grounds that there is usually one stream which is critical from, for example, the pressure drop requirement. The design requirement is specified by Number of Thermal Units (N), pressure drop and mass flow rate for the side considered. The latter two parameters also provide an equivalent specification of pumping power. The consequences for cross-sectional area, volume and weight are examined for different surfaces, including type and scale (represented by hydraulic diameter), and are developed in terms of comparison ratios for two surfaces. The analysis is given for two regimes, firstly the conventional regime based on the core velocity equation, for which turbulent or high transitional Reynolds numbers apply¹, and secondly for fully-developed laminar flow. Both approaches are developed for pure counterflow, which does not invalidate the general significance of the results for single or multi-pass cross-flow operation. Comparisons of some typical surfaces are then made, and indications are given for criteria for selection. Optimisation approaches are briefly discussed. More complete thermal design and analysis procedures are given in Chapter 6, whilst detailed performance correlations for different surfaces are discussed in Chapter 5.

¹ Note that many compact surfaces, especially those with periodically interrupted passages such as corrugations or offset strip fins, have effectively transitional flow at Reynolds numbers as low as about 300, so the conventional (j,f) approach following applies in these conditions. In many cases the flow on the surfaces and hence the form of j factor approximates closely to laminar developing flow on a flat plate.

CONVENTIONAL THEORY (THE CORE MASS VELOCITY EQUATION, AND GEOMETRICAL CONSEQUENCES)

For this approach the surface performance is assumed to be describable by Colburn j factor and Fanning friction factor f as functions of Reynolds number, as given for example by Kays and London (1984). The Colburn factor, often described by a simple power-law relationship, gives an approximate rationalisation of heat transfer coefficient over a wide range of Prandtl numbers. This will be valid for most high performance surfaces down to Reynolds numbers of about 400, but excludes laminar flows. The object of the analysis is to combine the heat transfer and pressure drop specification into forms that allow both for approximate sizing of the surface and for comparison of different surfaces. Some aspects are similar to those developed by Bruzzi and presented by Taylor (1990), and also by Polley (1991). The comparison aspects are also similar in form and implication to the Performance Evaluation Criteria (PEC) discussed by Webb (1994), and are closely equivalent to those thoroughly discussed by Cowell (1990).

Heat transfer

A specified heat load, \dot{Q} , is given by the heat transfer and rate equations for either side, as given in Chapter 1:

$$\dot{Q} = \alpha A_s \overline{\Delta T} = \dot{m} c_p (T_2 - T_1), \quad (4.1)$$

neglecting for convenience the influences of wall resistance and surface efficiency on h .

We now express α in terms of the dimensionless j factor by the definition

$$j = \frac{Nu}{Re Pr^{1/3}} = St Pr^{2/3}, \quad (4.2)$$

where Nu = Nusselt number

$$Nu = \frac{\alpha d_h}{\lambda}. \quad (4.3)$$

$$\text{Thus } \frac{\alpha d_h}{\lambda} = \frac{ud_h}{v} j Pr^{1/3},$$

$$\text{and } \alpha = \frac{\dot{m}}{\rho v} \lambda Pr^{1/3} \frac{j}{A_c}, \quad (4.4)$$

$$\text{where } u = \frac{\dot{m}}{\rho A_c}. \quad (4.5)$$

Manipulation of equations 4.1, 4.3 and 4.4 gives

$$j = \frac{A_c}{A_s} Pr^{2/3} N, \quad (4.6)$$

where $N = \text{NTU}$ (Number of Thermal Units)

$$= (T_2 - T_1) / \overline{\Delta T} \quad \text{for this case.}$$

Recalling now the definition of hydraulic diameter d_h as

$$d_h = \frac{4A_c L}{A_s} \quad (4.7)$$

we have an alternative equation

$$j = \frac{d_h}{4L} Pr^{2/3} N. \quad (4.8)$$

For given conditions the product $Pr^{2/3} N$ is fixed, so for two surfaces suffixed 1 and 2 to be compared,

$$\frac{L_1}{L_2} = \frac{d_{h,1} j_2}{d_{h,2} j_1}. \quad (4.9)$$

Thus flow length is directly proportional to hydraulic diameter, and inversely proportional to j factor, which is Reynolds number dependent. This is the first major result of the analysis, arising solely from the thermal requirement, showing that the flow length element of size and shape is reduced directly by reducing hydraulic diameter and increasing j factor. We note in passing that j factor rises

as Reynolds number decreases, which in turn is proportional to hydraulic diameter (see section 4.2.3).

Example 4.1

The required length for given conditions of Prandtl No = 0.7, N = 3.0, for a surface of hydraulic diameter $d_h = 2$ mm (= 0.002 m), and for a j factor of 0.015 (obtained at, say, $Re = 1000$), is, from equation 2.8, $L = 0.0788$ m. This is a relatively 'short' duty for a compact exchanger: note that if the hydraulic diameter were 20 mm, the corresponding length would be 0.788 m.

Pressure drop

Neglecting, for many practical exchangers, the relatively small contributions of entry and exit losses and flow acceleration, the pressure drop Δp of fluid through a surface is given in terms of the Fanning friction factor by

$$\Delta p = \frac{1}{2} \rho u^2 \frac{4L}{d_h} f. \quad (4.10)$$

From 4.5, substituting for the velocity u , we have

$$\frac{2\rho\Delta p}{\dot{m}^2} = f \frac{4L}{d_h A_c} = \text{constant for given conditions.} \quad (4.11)$$

Thus, again comparing two surfaces denoted by suffices 1 and 2, with given pressure drop

$$\frac{A_{c,1}^2}{A_{c,2}^2} = \frac{f_1 L_1 d_{h,2}}{f_2 L_2 d_{h,1}} \quad (4.12)$$

Thus if the thermal performance is ignored, the flow areas for two surfaces with similar friction factors are the same if the ratios L/d_h are the same.

Combined thermal and pressure drop comparison

As introduced in chapter 1, the *core mass velocity equation*, after London (1983), can be derived from equations 4.8 and 4.11:

$$\frac{2\rho\Delta p}{\dot{m}^2} = \frac{fPr^{2/3}N}{jA_c^2},$$

and

$$\frac{G^2}{2\rho\Delta p} = \frac{j/f}{Pr^{2/3}N}, \quad (4.13)$$

G being the mass velocity \dot{m}/A_c . As mentioned, G , and hence flow area, can be closely estimated from the design specification, and this equation, with the assumption of a typical value of j/f , is often used as a starting point for preliminary sizing.

Example 4.2

To illustrate the use of equation 4.13, take a gas of density 4kg/m^3 , with Prandtl number of 0.7, and operating conditions $N = 3$ (as for example 4.1), $\Delta p = 2000\text{Pa}$, and with a surface giving $j/f = 0.25$. Then equation 4.13 gives the group $\left(\frac{2\rho\Delta p}{Pr^{2/3}N}\right)^{1/2} = 82.25 \text{ kg/m}^2\text{s}$, $G = 41.13 \text{ kg/m}^2\text{s}$, and a gas throughflow velocity of 4.6m/s . The flow area is simply proportional to the required mass flow rate. Thus if $\dot{m} = 4.0 \text{ kg/s}$, the necessary flow area is 0.217 m^2 . For a square face and a typical porosity of 0.8, this gives side dimensions of 0.52m .

The basic elements of the effect of the surface on thermal design, embodied in equations 4.8 and 4.13 are, as mentioned in chapter 1:

- that flow length decreases as hydraulic diameter decreases
- that flow area is largely independent of hydraulic diameter

Thus if performance specification includes the pressure drop, as is normally the case, then increasing compactness only implies the reduction of flow length, with a change of shape, or aspect ratio, of the active block. [In practice, this reduction in flow length can make longitudinal conduction a problem to be taken into account, see chapter 6.]

In terms of surface comparison, again linking equations 4.9 and 4.11, we have

$$\frac{A_{c,1}}{A_{c,2}} = \left[\frac{f_1}{f_2} \cdot \frac{j_2}{j_1} \right]^{1/2}$$

$$= \left(\frac{j_2 / f_2}{j_1 / f_1} \right)^{1/2} \quad (4.14)$$

The form of equation 4.14 gives rise to the description of the ratio j/f as the *Flow Area Goodness Factor* (London (1964)). It is important in comparing surfaces in the task of determining the face area of automotive radiators, especially with modern constraints on frontal area (Cowell (1997)); a further important application is that of aerospace environmental control and other systems, in which severe space limitations are often applied.

The actual surface cross- sectional area, A_s , is linked to A_c by the porosity σ , so that

$$\frac{C_{s,1}}{C_{s,2}} = \frac{A_{c,1}\sigma_2}{A_{c,2}\sigma_2} = \frac{(j_2 / f_2)^{1/2} \sigma_2}{(j_1 / f_1)^{1/2} \sigma_1} \quad (4.15)$$

The exchanger (one-side) volume is given by $V = C_s L$ so that, linking equations 4.15 and 4.9,

$$\frac{V_1}{V_2} = \frac{C_{s,1}L_1}{C_{s,2}L_2} = \frac{(j_2^3 / f_2)^{1/2} d_{h,1} \sigma_2}{(j_1^3 / f_1)^{1/2} d_{h,2} \sigma_1}, \quad (4.16)$$

and the fluid inventory ratio $V_{i,1}/V_{i,2}$, important for safety audits when hazardous fluids are used, is

$$\frac{V_{i,1}}{V_{i,2}} = \frac{C_{s,1}L_1}{C_{s,2}L_2} = \frac{(j_2^3 / f_2)^{1/2} d_{h,1}}{(j_1^3 / f_1)^{1/2} d_{h,2}}. \quad (4.16a)$$

The material content, necessary for some exergy- related studies (see chapter 3), is given by $V_m = V(1-\sigma)$, so that

$$\frac{V_{m,1}}{V_{m,2}} = \frac{V_1(1-\sigma_1)}{V_2(1-\sigma_2)} = \frac{(j_2^3 / f_2)^{1/2} d_{h,1} \sigma_2 (1-\sigma_1)}{(j_1^3 / f_1)^{1/2} d_{h,2} \sigma_1 (1-\sigma_2)} \quad (4.17)$$

Thus, for two surfaces with comparable j/f ratios, both exchanger volume and material content are low when j is high, hydraulic diameter is low, and porosity is high.

Operating parameter

No indication is given in the above equations of the operating Reynolds number, with which j is a strong function and j/f is a weak function for most surfaces. The ratio of Reynolds number is given by

$$\frac{Re_1}{Re_2} = \frac{u_1 d_{h,1}}{u_2 d_{h,2}} = \left(\frac{j_1 / f_1}{j_2 / f_2} \right)^{1/2} \frac{d_{h,1}}{d_{h,2}}. \quad (4.18)$$

Equation 4.18 can be re-expressed as a criterion for equivalence of operating points:

$$\frac{Re_1}{d_{h,1}(j_1 / f_1)^{1/2}} = \frac{Re_2}{d_{h,2}(j_2 / f_2)^{1/2}}, \quad (4.19)$$

which is constant for a given specification, and can also be expressed in terms of prescribed NTU and pressure drop by

$$\frac{Re}{d_h(j/f)^{1/2}} = \frac{1}{\eta} \left(\frac{2\rho\Delta p}{Pr^{2/3} N} \right)^{1/2} \quad (4.20)$$

from equations 4.8 and 4.13. This equation is an alternative form of the mass velocity equation, but expressed in terms of Reynolds number instead of mass velocity. The function P_o forming the left hand side of equation 4.20,

$$P_o = \frac{Re}{d_h(j/f)^{1/2}} \quad (\text{dimensional, m}^{-1}) \quad (4.20a)$$

defined by equation 4.20a is denoted the Operating Parameter, and is a reduced Reynolds number, or more correctly a reduced throughflow velocity, since $Re = ud_h/v$. It links the overall performance requirements to the necessary Reynolds number. It is interesting to note that the velocity (see Martin (1999)) is often used as a guideline for 'economic' operation of heat exchanger surfaces, a point also implicated in the Second Law optimisation studies described in Chapter

3. Since j and f are functions of Re , the operating parameter P_o is also a unique function of Re , and thus can be plotted against Re for any given surface. As we observed earlier, j/f is not normally strongly Reynolds number sensitive, so the straightforward interpretation of this function is that the operating Reynolds number is close to directly proportional to hydraulic diameter. Thus, for example, a non-compact exchanger surface with a hydraulic diameter (typically a tube diameter) of 25 mm for a given duty would operate at a Reynolds number of about 25 times that of a compact surface of 1 mm hydraulic diameter. This has important implications for surface selection: typically a 1mm hydraulic diameter surface would operate in developing or fully developed laminar flow, whilst for the same duty a 25 mm surface would be in high transitional or turbulent flow.

The right hand side of equation 4.20 is correspondingly a function of prescribed operational variables $\rho, \eta, \Delta p, Pr$ and N , so that for a given specification P_o can be calculated, with clear implications for the relationship between size (hydraulic diameter) and performance (j, f). The advantage of this form is that for a surface with given hydraulic diameter, the Reynolds number is immediately derived fairly accurately for an approximate value of j/f . This gives a good pointer to the appropriateness of using the surface for this specification, since different surfaces vary in their performance over the frequently-used transitional range of $500 < Re < 5000$.

Example 4.3

Using the data of Example 4.2, and with a typical air value of viscosity η of 2.286×10^{-5} kg/ms (at 400K), the operating parameter P_o given by equation 4.20a becomes 3.598×10^6 , and for the typical surface characteristics of $j/f = 0.25$, $d_h = 0.001\text{m}$, the Reynolds number becomes 1799.

At this point it is worth noting that in most presentations of compact surface performance (e.g. Kays and London) the data are given as curves or tables of f and j factors versus Reynolds number for a fixed scale (hydraulic diameter, d_h) of surface, corresponding to the dimensions of an actual test surface. Since the f and j data are dimensionless, however, a given data set can be applied with equal validity to either reduced or enlarged scale (lower or higher hydraulic diameter), provided only that the scaling is applied to every dimension. This point was clearly made by Cowell (1990), but is not often recognised in design exercises quoted in the literature. This point is further discussed in the next section. This feature allows the designer to fine-tune, or optimise, the two sides of an exchanger, especially for example for counterflow designs in order to utilise pressure drop allowances fully. In the case of an extended surface such as a

plate-fin surface, fin efficiency calculations would naturally form a necessary part of a complete analysis. Further discussion on this is given in chapter 6.

Size and Shape Relationships

Face area

In absolute terms, the face area, or overall surface cross-sectional area can be derived from equations (4.8) and (4.11) to give:

$$C_s = \frac{A_c}{\sigma} = \frac{\dot{m}d_h^2}{4L\sigma} \frac{Pr^{2/3}N}{\eta jRe} = \frac{1}{\sigma} \left(\frac{f}{j} \right)^{1/2} \dot{m} \left(\frac{Pr^{2/3}N}{2\rho\Delta p} \right)^{1/2} = \frac{\dot{m}d_h}{\sigma\eta Re} \quad (4.21)$$

As mentioned above, the cross-sectional area, derived from the core mass velocity equation, is independent of scale (hydraulic diameter), except for a relatively small influence of Reynolds number.

The term $\dot{m} \left(\frac{Pr^{2/3}N}{2\rho\Delta p} \right)^{1/2}$ is purely a function of operating parameters, and is independent of the surface used.

Hence $\frac{1}{\sigma} \left(\frac{f}{j} \right)^{1/2} = C_s / \dot{m} \left(\frac{Pr^{2/3}N}{2\rho\Delta p} \right)^{1/2} = P_f$ can be used as a dimensionless face area parameter P_f , being simply the required face area divided by a function of heat-exchanger duty. Note that since the relationship is derived from the core mass velocity equation, the face area is largely independent of surface type.

Volume

The corresponding volume parameter can be derived from equations (4.21) and (4.8).

$$V = LC_s = \left(\frac{f}{j^3} \right)^{1/2} \frac{d_h}{\sigma} \frac{\dot{m}Pr N^{3/2}}{4(2\rho\Delta p)^{1/2}} \quad (\text{m}^3) \quad (4.22)$$

which can also be expressed as

$$V = \frac{d_h^2}{\sigma} \cdot \frac{\dot{m} Pr^{2/3} N}{4 j Re \eta} \quad (4.23)$$

This volume expression, also obtained by Cowell (1990), is remarkable because of the absence of direct dependency on either pressure drop or the surface friction factor, although the face area and length components are individually dependent. This arises mathematically because both pressure drop and friction constant terms cancel in multiplying flow area and length components. There is, however, an indirect dependence because the Reynolds number depends on pressure drop through the core mass velocity equation.

Alternatively, it is easily shown from equation 4.21 and by the definition of Reynolds number

$$Re = \frac{\dot{m} d_h}{\eta A_c} = \frac{G d_h}{\eta}, \quad (4.24)$$

where G is the mass velocity, that

$$L = \frac{d_h Pr^{2/3} N}{4 j} = \frac{\dot{m} Pr^{2/3} d_h^2 N}{4 A_c \cdot j Re \eta}, \quad (4.25)$$

and thus that the product $LA_c = \sigma V = \frac{d_h^2}{\eta} \left(\frac{\dot{m} Pr^{2/3} N}{4 j Re} \right)$ is independent of f and Δp .

Hence, from 4.22, the group

$$\frac{d_h}{\sigma} \left(\frac{f}{j^3} \right)^{1/2} = V / \frac{\dot{m} Pr N^{3/2}}{4(2\rho\Delta p)^{1/2}} = P_v \quad (\text{m}) \quad (4.26)$$

is a dimensional volume parameter which we shall call P_v as indicated.

This parameter thus gives a direct measure of overall compactness. Compactness is seen to have two components: that of geometry (hydraulic diameter and porosity), and that of performance (f / j^3) regardless of scale. It is the inverse of Polley's (1991) Volume Performance Index (VPI), a *high* value of which represents a low volume. Polley, however, compares surfaces on the

basis of VPI versus Reynolds number, which is less useful for comparison against a specific duty.

Example 4.4

Using the data of examples 4.1 and 4.2, with $j = 0.015$, $f = 4j = 0.06$, and taking a typical porosity of 0.8, equation 4.22 gives $P_v = \frac{d_h}{\sigma} \left(\frac{f}{j^3} \right)^{1/2} = 0.333$ (m), and $\frac{\dot{m}Pr N^{3/2}}{4(2\rho\Delta p)^{1/2}} = 0.0288$, and a volume of 0.0096 m³. This could have been determined more directly from the length and face area calculations.

It is now appropriate to examine relationships represented by equations 4.20 and 4.26 graphically for given surfaces.

Examination of equation 4.20 shows that the operating parameter P_o forming the left hand side is a unique function of Re for any given surface, being closely proportional to Re , but importantly, dependent on hydraulic diameter. The left-hand side of equation 4.24 is also a unique function of Reynolds number, so that a plot of the left-hand sides of these equations against each other (2.26 against 2.20) is unique for any surface. This enables direct comparisons to be made between surfaces for any given specification of Δp , mass flow, N (side Ntu), and the properties Pr , ρ and η . Note especially that surfaces for a given thermal specification cannot be compared validly on the basis of volume parameter $\frac{d_h}{\sigma} \left(\frac{f}{j^3} \right)^{1/2}$ as a function of Reynolds number: the comparison has to be made at the same value of P_o .

Comparisons of some typical compact surfaces on the basis of volume parameter versus operating parameter are given in Figure 4.1, in parallel with equivalent comparisons for laminar flow surfaces (ducts). The implications of these comparisons are discussed after the development of the laminar size relationships which follow this section.

Aspect ratio of block

Of interest for many applications is the shape of the heat exchanger block, which is best described by an aspect ratio parameter $L / C_s^{1/2}$. This is readily given by

$$\frac{L}{C_s^{1/2}} = \frac{\sigma^{1/2} d_h}{(j^3 f)^{1/4}} \frac{(Pr^{2/3} N)^{3/4}}{4m^{1/2}} (2\rho\Delta p)^{1/4} \quad (4.27)$$

It should be noted that this equation only gives the 'one side' values - in a counterflow heat exchanger the value of L would of course remain the same for the other stream but A_c and C_s would have different values depending on the second stream properties and the surface used. The overall cross-section would then be the sum of those pertaining to the two streams. For low values of $L/C_s^{1/2}$, it is clear that any distributor sections would have a significant effect on the actual shape.

Exchanger (side) weight

If the added component of side bars (see chapter 6) is ignored, the weight of a side is given by

$$W_s = \rho_m V (1 - \sigma) \quad (4.28)$$

when empty, where ρ_m is the material density, and

$$W_s = \rho_m V (1 - \sigma) + \sigma \rho V \quad (4.29)$$

when full of the working fluid of density ρ . Note that if ρ/ρ_m were small as would be the case with low- pressure gases, the last term in equation 4.27 would be negligible.

The above equations only apply of course to the main block: distributors and headers, especially for high- pressure duties, would add considerably to the side weight. Typically, the distributors (e.g. for a PFHE) have lengths each equal to 1/3 of the block width, so that for a block (side) aspect ratio of 3, the distributors add about 2/9ths (22%) to the volume and weight. Obviously, the higher the aspect ratio (or the higher the Ntu), the lower the relative incremental weight and pressure drop. Further aspects of distributors are discussed in chapter 6.

Pumping Power

For many gas- gas and gas- liquid applications, common in air conditioning, prime mover, gas processing and gas turbine power generation equipment, the pumping power is important in having a direct impact on the net efficiency of the plant (see also chapter 3).

From the pressure drop relationship given by equation 4.10, the pumping power \dot{W}_p becomes

$$\dot{W}_p = \frac{\dot{m} \Delta p}{\rho} = \frac{2 f \dot{m}^3 L}{\rho^2 A_c^2 d_h}, \quad (4.30)$$

which is fixed if the pressure drop is fixed. Substituting for L/d_h from equation 4.8 gives

$$\dot{W}_p = \frac{f}{j} \frac{1}{A_c^2} \frac{\dot{m}^3 Pr^{2/3} N}{2 \rho^2}, \quad (4.31)$$

a slightly different formulation from that Cowell (1990), who retained pressure drop and hence pumping power as variables in his comparison study. The last grouping in this equation is fixed by process requirements, so that if the pumping power is allowed to vary, for comparing of power requirements for different surfaces, we have

$$\frac{\dot{W}_{p,1}}{\dot{W}_{p,2}} = \frac{(f/j)_1}{(f/j)_2} \left(\frac{A_{c,2}}{A_{c,1}} \right)^2, \quad (4.32)$$

which is unity for equal powers, showing the importance of the area goodness parameter j/f its implications for flow area requirement. This point thus directly reflects the core mass velocity equation and its flow area relationship, equation (4.14)

LAMINAR FLOW ANALYSIS

When the operating Reynolds number is very low it is no longer physically realistic to assign single power- law relationships to j and f factors, especially when simple channel- type surfaces are used. In such conditions the performance is described by the laminar flow relationships characterised by constant Nusselt number and constant product fRe , and the corresponding absence of the Prandtl number dependence has some important consequences.

Heat transfer

Again, we start with equation 2.6

$$j = StPr^{2/3} = \frac{A_c}{A_s} Pr^{2/3} N, \quad (4.33)$$

and replacing the Stanton number by its relationship to Reynolds, Prandtl and Nusselt number

$$Nu = StPrRe \quad (4.34)$$

we obtain, with a little manipulation

$$Nu = \frac{PrRe_h N}{4L} \quad (4.35)$$

This result can be compared to equation 4.8 for the previous case: it is clear that now, the product $j/Pr^{2/3}$ has been replaced by $Nu/PrRe$, both being alternative forms of the Stanton number. Since, for fully developed laminar flow, Nu is a function only of the surface chosen and is independent of Re , and Pr is fixed by the specification, equation 4.24 gives the relationship between Re and d_h/L . For a specified d_h , therefore, L is proportional to Re , so that the lower the Re , the lower the flow length.

Example 4.5

Using the previous data ($Pr = 0.7$, $N = 3$, $d_h = 0.002\text{m}$), and for a rectangular passage with a typical T boundary condition of $Nu = 5$, $L = 0.00021Re$, so that, for example, for $Re = 1000$, $L = 0.21\text{m}$. This is considerably higher than the corresponding conventional case, reflecting the lower Nusselt number at this Re , but incorporation of the pressure drop below changes this situation.

Pressure drop

Starting again from equation 4.10, we note that for fully developed flow the product fRe is constant, and we denote it by (Gersten(1992))

$$k = fRe. \quad (4.36)$$

Like Nu , it is only a function of the surface shape. A similar analysis to the above gives corresponding expression to 4.11:

$$\frac{2\rho\Delta p}{\dot{m}^2} = \frac{k}{Re} \frac{4L}{d_h A_c^2} \quad (4.37a)$$

or

$$\frac{2\rho\Delta p}{\dot{m}} = \frac{4Lk\eta}{d_h^2 A_c}. \quad (4.37b)$$

For comparison of two surfaces independently of the thermal requirement,

$$\frac{A_{c,1}}{A_{c,2}} = \left(\frac{d_{h,2}}{d_{h,1}} \right)^2 \frac{k_1}{k_2} \frac{L_1}{L_2} \quad (4.38)$$

Combined heat transfer and pressure drop

A simple analysis using Nusselt number and $k = fRe$ gives corresponding core mass velocity equations

$$\frac{2\rho\Delta p}{\dot{m}^2} = \frac{NPr}{A_c^2} \frac{k}{Nu} \quad (4.39)$$

and

$$\frac{G^2}{2\rho\Delta p} = \frac{Nu/k}{NPr} \quad (4.40)$$

This is the laminar form of the core mass velocity equation.

The operating parameter P_o is readily derived from equation 4.40 and is

$$P_o = \frac{Re}{d_h (Nu/k)^{1/2}} = \frac{1}{\eta} \left(\frac{2\rho\Delta p}{Pr \cdot N} \right)^{1/2} \quad (4.41)$$

Note that in this case, in contrast to the conventional case, the operating parameter is identically proportional to Re , since both Nu and k are independent of Re by definition.

Example 4.6

Using the data of ex. 4.4, and taking a typical value of k (fRe) of 20, $G = 43.64 \text{ kg/m}^2\text{s}$, and $A_c = 0.29 \text{ m}^2$, and the throughflow velocity is 3.45 m/s. Note, as before, that this is unaffected by hydraulic diameter. The operating parameter P_o becomes $3.818E+6\text{m}^{-1}$, from equation 4.40.

Size and shape relationships

The face area and flow area are:

$$C_s = \frac{A_c}{\sigma} = \frac{\dot{m} d_h^2}{\sigma 4L \eta N u} \frac{PrN}{\eta N u} = \frac{\dot{m}}{\sigma} \left(\frac{k}{Nu} \right)^{1/2} \left(\frac{PrN}{2\rho \Delta p} \right)^{1/2}, \quad (4.42)$$

which gives a corresponding face area parameter P_f .

$$P_f = \frac{1}{\sigma} \left(\frac{k}{Nu} \right)^{1/2} = C_s / \dot{m} \left(\frac{PrN}{2\rho \Delta p} \right)^{1/2} \quad (4.43)$$

Comparison of two surfaces gives

$$\frac{C_{s,1}}{C_{s,2}} = \frac{\sigma_2}{\sigma_1} \left(\frac{k_1/Nu_1}{k_2/Nu_2} \right)^{1/2} \quad (4.44)$$

The volume is

$$V = \frac{d_h}{\sigma} \left(\frac{k}{Nu^3} \right)^{1/2} \frac{(PrN)^{3/2} \dot{m} Re}{4(2\rho \Delta p)^{1/2}} \quad (4.45)$$

(comparable to equation (4.22) for the conventional case).

Comparison of two surfaces gives

$$\frac{V_1}{V_2} = \frac{\sigma_2}{\sigma_1} \frac{d_{h,1}^2}{d_{h,2}^2} \frac{Nu_2}{Nu_1} \quad (4.46)$$

showing dependence only on hydraulic diameter and Nusselt number

The dimensional volume relationship simplifies to

$$V = \frac{d_h^2}{\sigma} \frac{\dot{m} Pr N}{4 Nu \eta} \quad (4.47)$$

This is the corresponding relationship to equation 4.23, and in a similar way, can be derived from equations 4.35 and 4.24:

$$L = \frac{Pr Red_h N}{4 Nu} = \frac{\dot{m} Pr d_h^2 N}{4 A_c \eta Nu}, \quad (4.48)$$

thus giving the product $LA_c = \sigma V = \frac{d_h^2}{\eta} \left(\frac{\dot{m} Pr N}{4 Nu} \right)$.

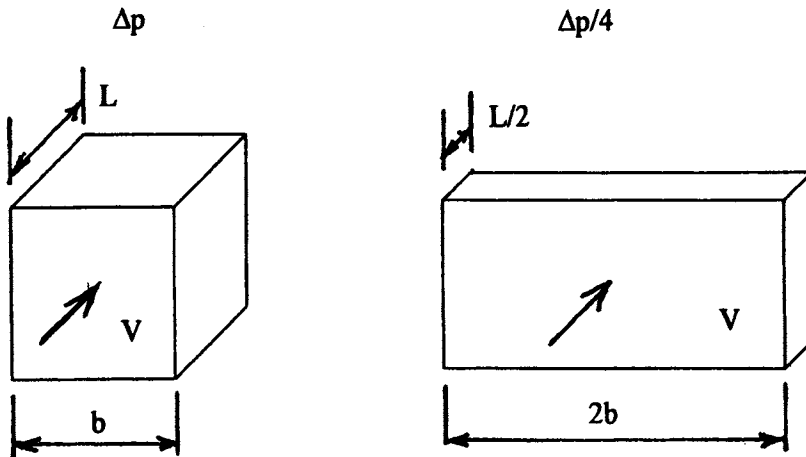
Thus for a high value of L/d_h^2 , both pressure drop and volume are high, and vice-versa. The volume has a very strong (square law) dependency on hydraulic diameter, illustrating the considerable advantage of compactness of surface. We have already observed that the flow (or face) area is independent of hydraulic diameter if the pressure drop is prescribed, so that the square law effect is entirely in the flow length, shown in equation 4.37b.

It should be noted for this case, in contradistinction to the conventional case, that within the inherent proviso of fully developed laminar flow, the volume is independent of pressure drop, since the Nusselt number Nu is independent of Reynolds number. However, the pressure drop does affect the shape (block aspect ratio) through the mass velocity equation.

Example 4.7

To illustrate the above observations, using the thermal requirements of the above examples ($N = 3$, $Nu = 5$, $fRe = 20$, $Pr = 0.7$, $m = 4\text{kg/s}$, $\eta = 2.286\text{E-}5 \text{ kg/ms}$) but with a hydraulic diameter of 0.001 m, the Reynolds number becomes 1909- just compatible with laminar flow! The flow area becomes, from equation 4.42, $A_c = 0.0917\text{m}^2$, the flow length $L = 0.2002\text{m}$, and the volume 0.023m^3 for a surface of porosity 0.8. If the specified pressure drop was reduced to a quarter of its previous value, that is to 500Pa, the required flow area would double, but the operating Reynolds number would halve, as would the flow length, leaving the

volume the same. This is illustrated schematically in the figure below, using a square initial face for simplicity



The corresponding aspect ratio of the surface is

$$\frac{L}{C_s^{1/2}} = \frac{\sigma^{1/2} d_h}{(Nu^3 k)^{1/4}} \frac{(PrN)^{3/4}}{\dot{m}^{1/2}} \left(\frac{\rho \Delta p}{128} \right)^{1/4} Re \quad (4.49)$$

Pumping power

The pumping power W_p corresponding to equation 4.31 is simply obtained as

$$W_p = \frac{k}{Nu} \frac{1}{A_c^2} \frac{\dot{m}^3 PrN}{2\rho^2}, \quad (4.50)$$

and for comparison of surfaces,

$$\frac{W_{p,1}}{W_{p,2}} = \frac{(k/Nu)_1}{(k/Nu)_2} \left(\frac{A_{c,2}}{A_{c,1}} \right)^2, \quad (4.51)$$

which, as for the conventional case (see equation 4.30), is unity for specified pressure drop.

COMPARISON OF COMPACT SURFACES

It is now appropriate to compare surface performances for both conventional and laminar flow surfaces, in terms of volume parameter versus operational parameter. Figures 4.1, 4.2 and 4.3 show comparisons of surfaces using data from surfaces tested by Kays and London (1984), for cross-sectional area and volume parameters respectively. As remarked earlier, each surface can be scaled, in theory, to any hydraulic diameter, so Figure 4.3 is presented to illustrate the effect of a common hydraulic diameter.

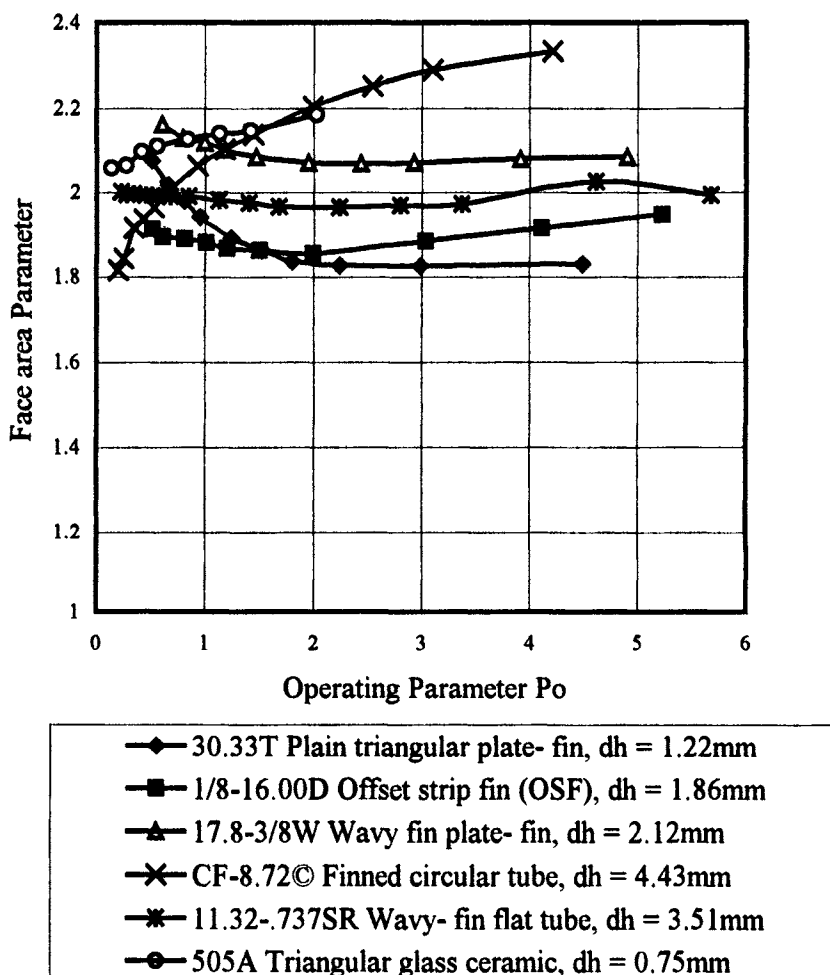


Figure 4.1 Face area parameter for a selection of surfaces from Kays and London (1984)

The face area parameter P_f (evaluated at a common value of $\sigma = 1$ in the absence of complete data for porosity), given by equations 4.21 and 4.32, compared in Figure 4.1, reflects the relatively low spread arising from the low variation of f/j , all data lying between 1.8 and 2.4. The low variation of this ratio with Reynolds number is also evident. The theoretical ideal of the Reynolds analogy ($f/j = 2$) would be represented by a value of the cross-sectional area parameter of $\sqrt{2} = 1.414$, for a porosity of unity. The comparison is equivalent to the *flow area goodness factor* comparison of Kays and London (1984).

The Volume Parameter, P_v , equation 4.26 is shown in Figure 4.2 for the same surfaces, based on the test hydraulic diameter for each case. The advantage of a low hydraulic diameter is clear, especially at low operating parameter, which itself implies a low hydraulic diameter for given thermal and pressure drop specification. Of note is the clear winner of the triangular duct surface, which has a linear relationship because of the fully-developed laminar flow.

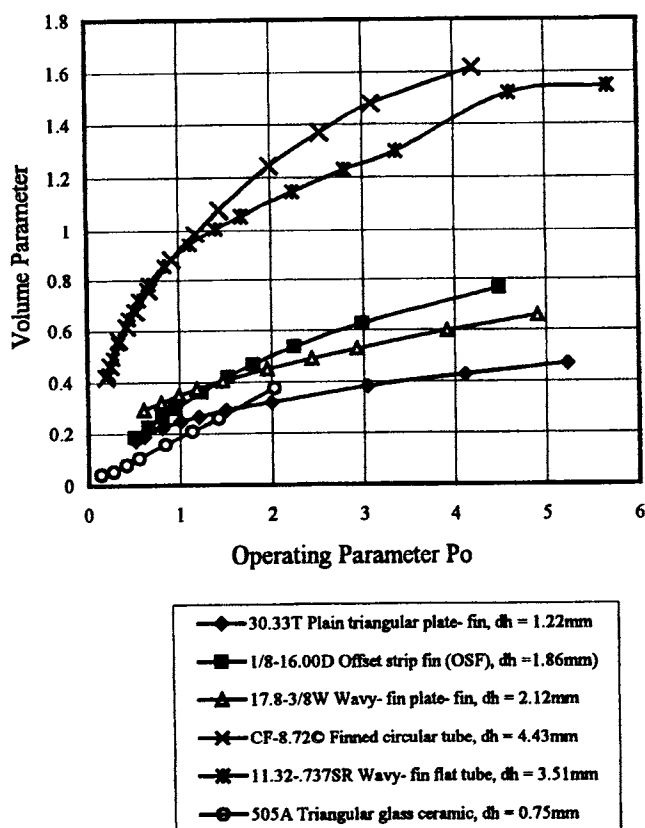


Figure 4.2 Volume parameter for a selection of surfaces, based on test hydraulic diameter

When we compare surfaces at a common hydraulic diameter (in sporting terms, a level playing field!), as shown in Figure 4.3, the situation is quite different. The common diameter chosen here is 1.5mm, typical of plate-fin surfaces. The most striking aspect of these results is that the *lowest* performers (highest volume) are now the continuous duct surfaces, which are also the *most compact* in their tested form. The surfaces with enhancement by boundary layer interruption are grouped fairly closely together, with the offset strip fin (OSF) the highest performer. The simple reason for this is that it has (a) the shortest re-start (fin) length, and (b) a fin which is thin enough not to have a dominating form drag. The relative performance at lower values of operating parameter is unclear, owing to the lack of data at low Reynolds number, but is unlikely to be very different.

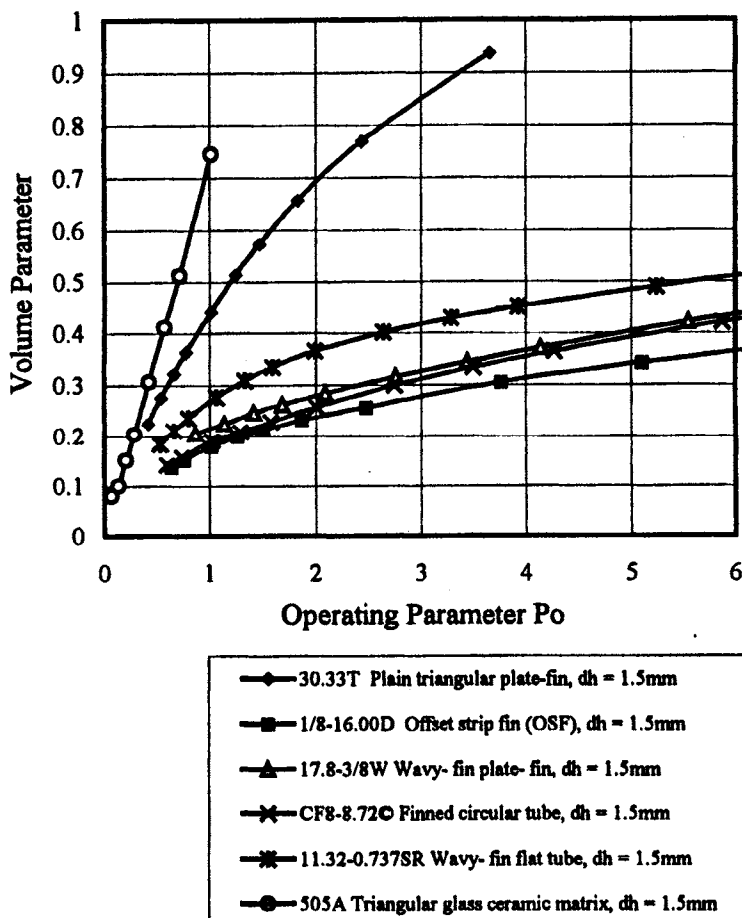


Figure 4.3 Volume Parameter based on common hydraulic diameter of 1.5 mm

The clear implication of the above observations is that where there is the option available for greater compactness, this is best accompanied by enhancement, that is, boundary layer interruption either by re-start as with an offset strip fin, or by secondary flow (wavy fin or dimpled plate/tube). It should be pointed out that the Kays and London (1984) data were produced using air ($Pr = 0.7$) as a working medium. Whilst the interrupted surface j vs. f data would be expected to be independent of Prandtl Number, even at low Re , the duct-type surfaces 30.33T and 505A would operate at a constant Nusselt Number at the laminar conditions (say $Re < 2000$), so the j vs. f data would be Prandtl number dependent. Thus for high Prandtl Number fluids the comparison would be *less* favourable to the duct surfaces, since $j = Nu/RePr^{1/3}$. Conversely, this approach emphasises the value of enhancement for high Prandtl Number fluids, confirming the argument made in chapter 1.

Not included in the above comparisons are some important classes of surface, especially the corrugated plate of the plate and frame type, the Printed Circuit Heat Exchanger (PCHE), and the slotted plate structure or the Marbond type. As a guideline a typical point estimated for a plate is shown on Figure 4.2, based on $Re = 1000$, $f/j = 10$ and the correlations given in chapter 5. The PCHE has a hydraulic diameter of approximately 2mm and typically has an enhanced (wavy) surface, but has a much lower porosity than other surfaces, so will have about twice the volume of an equivalent OSF surface. The slotted plate design has a hydraulic diameter of the order of 1mm, is enhanced by fins (in this case parallel to the separating plate, see chapter 2), and an intermediate porosity of about 0.6. It therefore will fall into the same band as the OSF design.

COMPARISON OF CONVENTIONAL AND LAMINAR APPROACHES

We can now clearly see, by comparing equations, the difference in design consequences between 'normal' and laminar flow approaches. It is clear that the choice of a very low, or micro- channel scale hydraulic diameter, will tend to necessitate a laminar approach in many conditions, as dictated by the operating Reynolds number (Equation 4.29). This argument is tempered by the observation that it has been shown to be worthwhile to interrupt the boundary layer even at low Reynolds number. The effective flow then becomes either of the developing laminar form or is 'tripped' into early turbulence.

The relationships developed in this chapter are shown in collected form in Table 4.1, which gives the parallel forms of sizing and related equations for the conventional and laminar cases. For some sizing parameters (flow area and flow length) alternative forms are given using different parameter groupings which may be appropriate for analysis purposes. All sizing parameters are given in two forms, one containing Reynolds number, which is itself a design variable. These

forms simply reflect the relationship between j and Nu , f and k ($= f\text{Re}$) with Reynolds and Prandtl numbers. Those containing Reynolds number are of less immediate value for sizing, but are included for completeness of the table and because they illustrate clearly the difference between laminar and conventional approaches. For example, the pressure drop is given firstly in the direct form dependent on (mass flow)², but independent of thermal parameters, and secondly in a form dependent on thermal parameters and independent of mass flow. It will be observed that the second conventional form is Reynolds number dependent whereas the first laminar form is Reynolds number dependent. This pattern is repeated for volume and shape (aspect ratio) relationships.

In summary, the real 'compactness' of a heat exchanger side is a function of two independent parameter groups: the hydraulic diameter (the main identifiable compactness parameter) combined with porosity, and the surface performance parameters j and f (conventional), and Nu and k (laminar). The third group in the equations contains the property and thermal specification parameters, which are fixed by the thermal requirement, although it should be noted that the pressure drop is often negotiable, and in complex systems should be incorporated in the second law optimisation process (chapter 3).

Table 4.1 One-side size and shape equations

	<u>General (common) relationships</u>	<u>Comments</u>
	$\alpha A_s \overline{\Delta T} = \dot{m} C_p (T_2 - T_1) = \dot{Q}$	Rate and heat transfer equation
	$Pe = Re Pr$	Peclet Number
	$Nu = St Pr Re = j Re Pr^{1/3} = \frac{\alpha d_h}{\lambda}$	Relating dimensionless parameters
	$St = \frac{\alpha}{Gc_p}$	Stanton Number
	$N = \overline{\Delta T} / (T_2 - T_1)$	One-side Number of Thermal Units (NTU)
	$d_h = \frac{4 A_c L}{S}$	Hydraulic diameter in terms of flow and surface areas
	$Re = \frac{\dot{m} d_h}{A_c \eta} = \frac{G d_h}{\eta}$	Reynolds Number in terms of mass flow rate and mass velocity

Table 4.1 contd.

<u>Conventional</u> j and f are functions of Re	<u>Laminar</u> (fully-developed) $K (=fRe)$, Nu are independent of Re	<u>Comments</u>
$j = St Pr^{\frac{1}{3}} = \frac{Nu}{Re Pr^{\frac{1}{3}}}$ $St = \frac{Nd_h}{4L}$	$Nu = Pr Re \frac{d_h \cdot N}{4L} = \frac{Pe d_h \cdot N}{4L} = \frac{Gz \cdot N}{4}$	<u>Heat Transfer</u> (specify N , Nu) Colburn analogy Stanton and Nusselt numbers
$2\rho \Delta p = \dot{m}^2 \frac{2f}{d_h} \cdot \frac{4L}{A_c^2}$ $= \left(\frac{4L}{d_h^2} \right)^2 \cdot \eta^2 Re^2 \left(\frac{jf}{Pr^{\frac{1}{3}} N} \right)$	$2\rho \Delta p = \dot{m}^2 \cdot \frac{k}{Re} \frac{4L}{d_h} \frac{1}{A_c^2}$ $= \left(\frac{4L}{d_h^2} \right)^2 \cdot \eta^2 \frac{kNu}{Pr N}$	<u>Pressure drop</u> (specify Δp , f , $k = fRe$) Dependent on mass flow (Laminar form Re dependent) Dependent on thermal requirement (Conventional form Re dependent)

Table 4.1 contd.

<u>Conventional</u>	<u>Laminar (fully-developed)</u>	<u>Comments</u>
$2\rho\Delta p = \dot{m}^2 \cdot \frac{f}{j} \cdot \frac{Pr^{2/3} N}{A_c^2}$ $\frac{G^2}{2\rho\Delta p} = \frac{j/f}{Pr^{2/3} N} = \frac{St/f}{N}$	$2\rho\Delta p = \dot{m}^2 \cdot \frac{k}{Nu} \cdot \frac{Pr N}{A_c^2}$ $\frac{G^2}{2\rho\Delta p} = \frac{Nu/k}{Pr N}$	<u>Combined heat transfer and pressure drop (HT & PD)</u> <u>Pressure drop</u> <u>Core mass velocity equation</u>
$A_c = \dot{m} \left(\frac{f}{j} \right)^{1/2} \left(\frac{Pr^{2/3} N}{2\rho\Delta p} \right)^{1/2}$ $A_c = \frac{\dot{m} d_h^2 Pr^{2/3} N}{4L\eta j Re} = \frac{\dot{m} d_h}{Re \eta}$ $C_s = \frac{A_c}{\sigma} = \frac{\dot{m} d_h^2 Pr^{2/3} N}{\sigma 4L\eta j Re}$ $= \frac{\dot{m}}{\sigma} \left(\frac{f}{j} \right)^{1/2} \left(\frac{Pr^{2/3} N}{2\rho\Delta p} \right)^{1/2}$	$A_c = \dot{m} \left(\frac{k}{Nu} \right)^{1/2} \left(\frac{Pr N}{2\rho\Delta p} \right)^{1/2}$ $A_c = \dot{m} \frac{d_h^2 Pr N}{4L\eta Nu} = \frac{\dot{m} d_h}{Re \eta}$ $C_s = \frac{A_c}{\sigma} = \frac{\dot{m} d_h^2 Pr N}{\sigma 4L \eta Nu}$ $= \frac{\dot{m}}{\sigma} \left(\frac{k}{Nu} \right)^{1/2} \left(\frac{Pr N}{2\rho\Delta p} \right)^{1/2}$	<u>Flow area (combined HT and PD)</u> Independent of hydraulic diameter d_h . (laminar form completely so) Showing how A_c , L and d_h are related. Conventional form Re dependent. <u>Face area</u> Form independent of Δp Conventional form Re Dependent Form independent of d_h (conventional form indirectly dependent)

Table 4.1 contd.

<u>Conventional</u>	<u>Laminar (fully-developed)</u>	<u>Comments</u>
$P_o = \frac{Re}{d_h (j/f)^{1/2}} = \frac{1}{\eta} \left(\frac{2\rho\Delta p}{Pr^{3/2} N} \right)^{1/2}$	$P_o = \frac{Re}{d_h (Nu/k)^{1/2}} = \frac{1}{\eta} \left(\frac{2\rho\Delta p}{Pr N} \right)^{1/2}$	<u>Operating Parameter P_o (combined HT and PD)</u> Showing how Reynolds Number is related to hydraulic diameter.
$V = C_s L = \frac{d_h}{\sigma} \left(\frac{f}{j^3} \right)^{1/2} \frac{\dot{m} Pr N^{3/2}}{4(2\rho\Delta p)^{1/2}}$ $= \frac{d_h^2}{\sigma} \frac{\dot{m} Pr^{3/2} N}{4j Re \eta}$	$V = C_s L = \frac{d_h}{\sigma} \left(\frac{k}{Nu^3} \right)^{1/2} \frac{\dot{m} (Pr N)^{3/2} Re}{4(2\rho\Delta p)^{1/2}}$ $= \frac{d_h^2 \dot{m} Pr N}{\sigma 4 Nu \eta}$	<u>Volume (combined HT and PD)</u> Laminar form Re dependent Conventional form Re dependent. Laminar form independent of pressure drop and friction factor coefficient k.
$\frac{L}{C_s^{1/2}} = \frac{\sigma^{1/2} d_h (Pr^{3/2} N)^{3/4}}{(j^3 f)^{1/4} 4 \dot{m}^{1/2}} (2\rho\Delta p)^{1/4}$ $= \frac{d_h^2 \sigma^{1/2} (Pr^{3/2} N)^{3/4} (2\rho\Delta p)^{3/4}}{(j f^3)^{1/4} 4 \dot{m}^{1/2} Re \eta}$	$\frac{L}{C_s^{1/2}} = \frac{\sigma^{1/2} d_h (Pr N)^{3/4}}{(Nu^3 k)^{1/4} 4 \dot{m}^{1/2}} (2\rho\Delta p)^{1/4} \cdot Re$ $= \frac{d_h^2 \sigma^{1/2} (Pr N)^{3/4} (2\rho\Delta p)^{3/4}}{(Nu k^3)^{1/4} 4 \dot{m}^{1/2} \eta}$	<u>Shape (aspect ratio) (combined HT and PD)</u> Laminar form Re dependent Conventional form Re dependent

Table 4.1 contd.

<u>Conventional</u>	<u>Laminar</u> (fully-developed)	<u>Comments</u>
$L = \frac{Pr^{\frac{2}{3}} N d_h}{4j}$ $= \frac{d_h^2}{4\eta Re} \left(\frac{2\rho \Delta p \cdot Pr^{\frac{2}{3}} N}{j_f} \right)^{\frac{1}{2}}$ $= \frac{\dot{m} d_h^2 Pr^{\frac{2}{3}} N}{4A_c \eta Re j}$	$L = \frac{Pr Re N d_h}{4 Nu}$ $= \frac{d_h^2}{4\eta} \left(\frac{2\rho \Delta p \cdot N Pr}{Nuk} \right)^{\frac{1}{2}}$ $= \frac{\dot{m} d_h^2 Pr N}{4A_c \eta Nu}$	<u>Flow Length</u> Form independent of cross sectional area. Conventional form Re dependent. Form independent of pressure drop. Conventional form Re dependent.

References

Cowell, T.A., A General Method for the Comparison of Compact Heat Transfer Surfaces, *Trans. ASME, Journal of Heat Transfer* , 112, 288-294, May 1990.

Cowell, T.A., and Achaichia, N., (1997), Compact Heat Exchangers for the Automobile Industry, *Proceedings of the International Conference on Compact Heat Exchangers for the Process Industries*, ed. R.K. Shah, Snowbird, Utah: Begell House, New York.

Gersten, K., (1992), Single Phase Fluid Flow: Ducts, in *Handbook of Heat Exchanger Design*, ed. Hewitt, Begell House, New York.

Kays, W.M. and London, A.L., (1984), *Compact Heat Exchangers*, third edition, McGraw Hill.

London, A.L., (1964), Compact Heat Exchangers: Part 2 - Surface Geometry, *Mechanical Engineering*, Vol. 86, 31-34.

London, A.L., (1983), Compact Heat Exchangers- Design Methodology, in *Low Reynolds Number Flow Heat Exchanger*, ed. Kakac, S., Shah, R.K. and Bergles, A.E., Hemisphere, New York.

Polley, G.T. (1991), Optimisation of Compact Heat Exchangers, in *Heat Exchange Engineering*, Vol. 2: *Compact Heat Exchangers, Techniques of Size Reduction*, Ellis Horwood, Chichester, U.K.

Taylor, M.A., (1987), *Plate-Fin Heat Exchangers - Guide to their Specification and use, HTFS*. (revised 1990)

Webb, R.L., (1994), *Principles of Enhanced Heat Transfer*, John Wiley, New York.

Chapter 5

SURFACE TYPES AND CORRELATIONS

Some of us should venture to embark on a synthesis of facts and theories, albeit with a secondhand and incomplete knowledge of some of them and at the risk of making fools of ourselves.

E. Schrödinger

INTRODUCTION

This chapter describes the principal surface types used in compact exchangers, and corresponding correlations are given. In view of the large range of graphical and raw data on surfaces given in the seminal work Kays and London (1984) it is not thought appropriate to repeat it here, but rather to provide, as far as possible, approximate algebraic correlations usable for computer-aided solutions. Where these are not available, tabular or graphical information is given. Graphical data for selected surfaces from Kays and London are provided for completeness and comparison purposes.

Unless otherwise indicated, the Reynolds numbers and Nusselt numbers given are based on the hydraulic diameter.

In the consideration of specific surfaces (such as those of Kays and London) and their f and j correlations, it should be noted that these correlations, being dimensionless, are independent of scale. This carries important implications, especially for any optimization process, that are not generally recognized. Thus the surfaces themselves can in theory be scaled up or down, provided that each dimension (fin thickness, length etc and hence hydraulic diameter) is scaled in the same proportion, and provided also (naturally!) that material is available in the appropriate sizes. In the design process, the fin efficiency calculations have to take into account the real fin dimensions. This allows the designer to achieve, for example, exact matching of pressure drop for both sides in counterflow exchangers for a given nominal surface designation, and in the process gives reduced size and weight. This point is illustrated in chapter 6 on design.

DUCTS

The continuous duct is perhaps the most important class of surface for compact exchangers, encompassing plain circular tubes to the very compact polygonal passages of gas turbine regenerator matrices. Some of the correlations

provide a generic base for other correlations, for example those of plate-fin surfaces.

Laminar flow

As the operational flow Reynolds number decreases as hydraulic diameter decreases, for given operational conditions, as described in chapter 4, the flow will increasingly tend towards a laminar condition. The critical Reynolds number for a laminar condition to prevail depends somewhat on the surface geometry itself, but it is generally safe to assume that it will apply for $Re < 2200$, provided that there is little inlet turbulence. Fully developed flow is considered first, then developing flow.

Fully developed laminar flow

Fully developed flow provides the limiting case for all solutions, in theory necessitating an infinite length to diameter ratio. The practical case of a finite ratio makes use of the fully developed solutions, often in a form of asymptotic combination. This is dealt with in the next section.

Precise solutions for a wide variety of continuous duct shapes have long been available, and have been comprehensively summarised by Shah and London (1984). Several of these shapes are characteristic of the static or rotary regenerators used for gas turbine power plant, for which a high thermal performance is essential, and for which the low aspect ratio (length/duct cross flow dimension) is of minor significance. The data are summarized in Table 5.1, adapted from Kakac et al. (1983), and show the (fully developed) Nusselt number for the major boundary conditions H_1 , H_2 and T (see footnote¹), together with the product fRe (= k). Also given are the ratio Nu/k (the area goodness factor, used in estimating the flow area and important in determining the minimum entropy generation, see chapter 3), the dimensionless incremental

¹ Boundary conditions and typical applications:

T	Constant temperature axially and circumferentially	Condensers and evaporators, and heat exchangers with very high C^*
H1	Axially constant wall heat flux with circumferentially constant wall temperature	Nuclear and electric resistance heating, nearly balanced counterflow exchangers, with very high heat wall conductivity
H2	Axially and circumferentially constant heat flux	As H1 but with very low wall conductivity, e.g. ceramic or polymer

pressure drop K_∞ for the developing length, and the corresponding dimensionless hydrodynamic entrance length L_{hy}^+ . These parameters are defined in the following section.

From the table, it is clear that the surfaces with highest Nu also have the highest ratios Nu/k, the infinite flat plate being the highest performer, and 'narrow' triangular sections being the worst. This is also reflected in their Second Law performance (see chapter 3).

Table 5.1 Laminar flow parameters for ducts

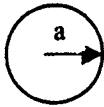
Geometry	Nu_{HI}	Nu_T	k (fRe)	$\frac{j_{HI} +}{f}$	$\sqrt{\frac{Nu_T}{k}}$	$\sqrt{\frac{Nu_{HI}}{k}}$	K_∞	L^+	$\sqrt{\frac{Nu_T^3}{k}}$	$\sqrt{\frac{Nu_{HI}^3}{k}}$
sine	3.014	2.390	12.630	0.269	0.435	0.489	1.739	0.040	1.040	1.472
triang	3.111	2.470	13.333	0.263	0.430	0.483	1.818	0.040	1.063	1.503
square	3.608	2.976	14.227	0.286	0.457	0.504	1.433	0.090	1.361	1.817
hex	4.002	3.340	15.054	0.299	0.471	0.516	1.335	0.086	1.573	2.063
rect2	4.123	3.391	15.548	0.299	0.467	0.515	1.281	0.085	1.584	2.123
circ	4.364	3.657	16.000	0.307	0.478	0.522	1.250	0.056	1.748	2.279
rect4	5.331	4.439	18.233	0.329	0.493	0.541	1.001	0.078	2.190	2.883
rect6	6.049	5.137	19.702	0.346	0.511	0.554	0.885	0.070	2.623	3.352
rect8	6.490	5.597	20.585	0.355	0.521	0.561	0.825	0.063	2.918	3.644
par	8.235	7.541	24.000	0.386	0.561	0.586	0.674	0.011	4.227	4.824
parlins	5.385	4.861	24.000	0.253	0.450	0.474	0.674	0.011	2.188	2.551
semicirc	4.089		15.780	0.292		0.509	1.440	0.090		2.081

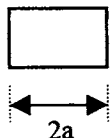
* for $Pr = 0.7$

It should be noted, especially for duct shapes with acute corners (e.g. triangular sections), that the consequences of the manufacturing process such as brazing material residing in the corners means that these are often effectively rounded, resulting in higher friction factors and higher Nusselt numbers (see Shah et al, 1983).

Algorithms for more generalized duct geometries to those above, including definitions of hydraulic diameter are given by Shah and Bhatti (1987), and extracts are as follows in Table 5.2.

Table 5.2 Fully developed friction factors and Nusselt numbers

Duct shape	Hydraulic diameter	Friction factors and Nusselt numbers
	<p>Circular: $d_h = 2a$</p>	$fRe = k = 16$ $Nu_T = 3.657$ $Nu_H = 4.3636$

Rectangular:

$$d_h = \frac{4ab}{a+b}$$

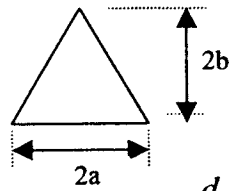
$$a^* = 2b/2a$$

$$fRe = 24(1 - 1.3553\alpha^* + 1.9467\alpha^{*2} - 1.7012\alpha^{*3} + 0.9564\alpha^{*4} - 0.2537\alpha^{*5})$$

$$Nu_T = 7.541(1 - 2.61\alpha^* + 4.97\alpha^{*2} - 5.119\alpha^{*3} + 2.702\alpha^{*4} - 0.548\alpha^{*5})$$

$$Nu_{H1} = 8.235(1 - 2.0421\alpha^* + 3.0853\alpha^{*2} - 2.4765\alpha^{*3} + 1.0578\alpha^{*4} - 0.1861\alpha^{*5})$$

$$Nu_{H2} = 8.2351(1 - 10.6044\alpha^* + 61.1755\alpha^{*2} - 155.18\alpha^{*3} + 176.92\alpha^{*4} - 72.9236\alpha^{*5})$$

Triangular (equilateral)

$$d_h = \frac{4b}{3}, \quad a = \frac{2b}{\sqrt{3}}$$

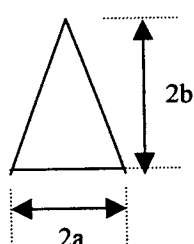
$$fRe = 40/3 = 13.3333$$

$$Nu_T = 2.49$$

$$Nu_{H1} = 28/9 = 3.1111$$

$$Nu_{H2} = 1.892$$

An example of experimental data for a triangular fin is given in Figure 5.1

Triangular (isosceles)

The most common geometry is that for $0 \leq \alpha^* \leq \infty$, giving the following relationships.

$$fRe = \frac{12(\alpha^{*3} + 0.2592\alpha^{*2} - 0.2046\alpha^* + 0.0552)}{\alpha^{*3}}$$

$$Nu_T = 0.943(\alpha^{*5} + 5.3586\alpha^{*4} - 9.2517\alpha^{*3}$$

$$- 11.9314\alpha^{*2} + 9.8035\alpha^* - 3.3754)/\alpha^{*5}$$

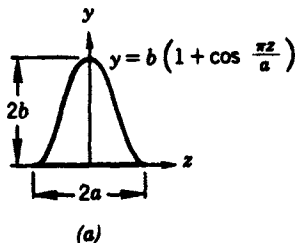
$$Nu_{H1} = 2.059(\alpha^{*5} + 1.2489\alpha^{*4} - 1.0559\alpha^{*3}$$

$$+ 0.2515\alpha^{*2} + 0.1520\alpha^* - 0.0901)/\alpha^{*5}$$

Triangular (contd.)

$$Nu_{H2} = 0.912(\alpha^{*3} - 13.3739\alpha^{*2} + 78.9211\alpha^{*} - 46.6239)/\alpha^{*3} \quad \text{for } 1 \leq \alpha^{*} < 8$$

$$d_h = \frac{4ab}{a + \sqrt{a^2 + 4b^2}}$$

Sine

The geometric data and fully-developed flow data for sine ducts are given in Tables 5.3 and 5.4 respectively.

For $0 \leq \alpha^{*} \leq 2$ the data can be approximated by:

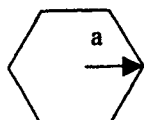
$$fRe = 9.5687(1 + 0.8772\alpha^{*} + 0.8619\alpha^{*2} - 0.8314\alpha^{*3} + 0.2907\alpha^{*4} - 0.338\alpha^{*5})$$

$$Nu_T = 1.1791(1 + 2.7701\alpha^{*} - 3.1901\alpha^{*2} - 1.995\alpha^{*3} - 0.4966\alpha^{*4})$$

$$Nu_{H1} = 1.9030(1 + 0.4556\alpha^{*} - 1.2111\alpha^{*2} - 1.6805\alpha^{*3} + 0.7724\alpha^{*4} - 0.1228\alpha^{*5})$$

$$Nu_{H2} = -0.0202(1 - 30.0594\alpha^{*} - 216.1635\alpha^{*2} + 244.3812\alpha^{*3} - 82.4951\alpha^{*4} + 7.6733\alpha^{*5}).$$

(Hydraulic diameter is defined within 1% by
 $d_h/2a = (1.0542 - 0.4670\alpha^{*} - 0.1180\alpha^{*2} + 0.1794\alpha^{*3} - 0.0436\alpha^{*4})\alpha^{*}$

Regular Polygonal

$$fRe = \left(\frac{n^2}{0.44 + n^2} \right)^4$$

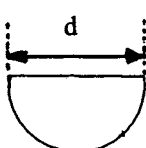
n = number of nodes: n = ∞ for circular, 3 for triangular.

$$Nu_{H1} = 0.1908 \left(1 + 7.9489n - 1.1383n^2 + 0.0712n^3 - 0.0016n^4 \right)$$

Regular Polygonal (contd.)

$$Nu_{H2} = -2.2578 \left(\begin{array}{l} 1 - 0.8051n + 0.0586n^2 \\ - 0.0007n^3 - 0.0002n^4 \\ + 0.000003n^5 \end{array} \right)$$

$d_h = 2a \cos\left(\frac{\pi}{n}\right)$, where a is the radius of the circumscribed circle

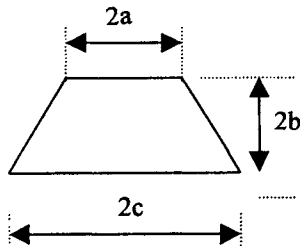
Semicircular segment

$$Re = 15.78$$

$$Nu_{H1} = 4.089$$

$$Nu_{H2} = 2.96$$

$$d_h = \frac{d}{(1 + 2/\pi)}$$

Trapezoidal duct

Provided that the included angle of the sides is greater than about 60° , and the ratio of short side to height is about unity, the following approximations can be used:

$$fRe = 14.2$$

$$Nu_{H1} = 3.4$$

$Nu_{H2} = 2.2, 2.8$ and 3.0 for $\phi = 60, 75$ and 85 degrees respectively

$$d_h = \frac{4b(a+c)}{a+c + \sqrt{(c-a)^2 + 4b^2}}$$

Table 5.3 Geometric data and fully-developed flow characteristics for sine duct.
 (from Shah and Bhatti (1987) in Handbook of Single Phase Convective
 Heat Transfer, Eds. Kakaç et al. Copyright © (John Wiley & Sons, Inc.)
 Reprinted by permission of John Wiley & Sons, Inc.])

$\frac{2b}{2a}$	$\frac{P}{2a}$	$\frac{D_h}{2a}$	$\frac{\bar{y}}{2a}$	$\frac{\bar{y}_{\max}}{2a}$	$\frac{u_{\max}}{u_m}$
∞	—	—	—	—	3.825
2	5.1898	0.77074	0.75000	0.46494	2.288
$\frac{3}{2}$	4.2315	0.70897	0.56250	0.40964	2.239
$\frac{1}{2}$	3.3049	0.60516	0.37500	0.33390	2.197
$\sqrt{3}/2$	3.0667	0.56479	0.32476	0.30773	2.191
$\frac{3}{4}$	2.8663	0.52332	0.28125	0.28205	2.190
$\frac{1}{2}$	2.4637	0.40589	0.18750	0.21347	2.211
$\frac{1}{4}$	2.1398	0.23366	0.09375	0.11926	2.291
$\frac{1}{8}$	2.0375	0.12270	0.04688	0.06173	2.357
0	2.0000	0.00000	0.00000	0.00000	2.400

Table 5.4 Fully-developed flow and heat transfer characteristics for sine duct.

$\frac{2b}{2a}$	$K(\infty)$	L_{hy}^+	$f \text{ Re}$	Nu_T	Nu_{H1}	Nu_{H2}	$T_{w,\max}^*$	$T_{w,\min}^*$
∞	3.218	0.1701	15.303	0.739	2.521	0	—	—
2	1.884	0.0403	14.553	—	3.311	0.95	2.92	0.002
$\frac{3}{2}$	1.806	0.0394	14.022	2.60	3.267	1.38	2.93	0.257
$\frac{1}{2}$	1.744	0.0400	13.023	2.45	3.102	1.55	2.17	0.398
$\sqrt{3}/2$	1.739	0.0408	12.630	—	3.014	1.47	2.58	0.396
$\frac{3}{4}$	1.744	0.0419	12.234	2.33	2.916	1.34	2.93	0.379
$\frac{1}{2}$	1.810	0.0464	11.207	2.12	2.617	0.90	3.65	0.266
$\frac{1}{4}$	2.013	0.0553	10.123	1.80	2.213	0.33	4.16	0.099
$\frac{1}{8}$	2.173	0.0612	9.743	—	2.017	0.095	4.31	0.030
0	2.271	0.0648	9.600	1.178	1.920	0	—	—

Developing laminar flow (entrance region effects)

In the entrance region of ducts the flow will start from a condition of the leading edge of an infinite flat plate- ignoring any separation arising from the finite thickness, with locally infinite Nusselt number and wall shear stress. It will then develop with influence from the duct walls until it is fully developed, and the centreline velocity is a maximum. So in real (finite length) heat transfer

ducts both friction and heat transfer parameters are higher than the fully developed values. In addition the heat transfer parameters in developing flow are affected by Prandtl number, in distinction to the fully developed case. These phenomena are described by the entrance length friction parameter K_∞ , and the hydrodynamic and thermal entrance lengths L_{hy} and L_{th} , together with their dimensionless versions L_{hy}^+ and L_{th}^* .

The dimensionless incremental pressure drop K_∞ is defined as that added to the fully developed value according to the equation

$$\Delta p = \left[\frac{4f_{fd}L}{d_h} + K_\infty \right] \frac{G^2}{2\rho} \quad (5.1)$$

where f_{fd} represents the fully developed Fanning friction factor. The increment K_∞ includes both the extra shear stress and the change in momentum flux arising from the transverse velocity distribution. Sometimes the 'apparent friction factor', f_{app} , to include the developing length L is used, such that

$$\Delta p = \left[\frac{4f_{app}L}{d_h} \right] \frac{G^2}{2\rho}, \quad (5.2)$$

where the pressure drop is calculated up to the developing length.

$$\text{Thus } K_\infty = (f_{app} - f_{fd}) \frac{4L}{d_h} \quad (5.3)$$

The hydrodynamic entrance length L_{hy} is defined as the axial, or flow distance at which 99% of the fully developed flow velocity is attained at the centreline of the duct. Its dimensionless version L_{hy}^+ is defined by

$$L_{hy}^+ = \frac{L_{hy}}{Red_h}. \quad (5.4)$$

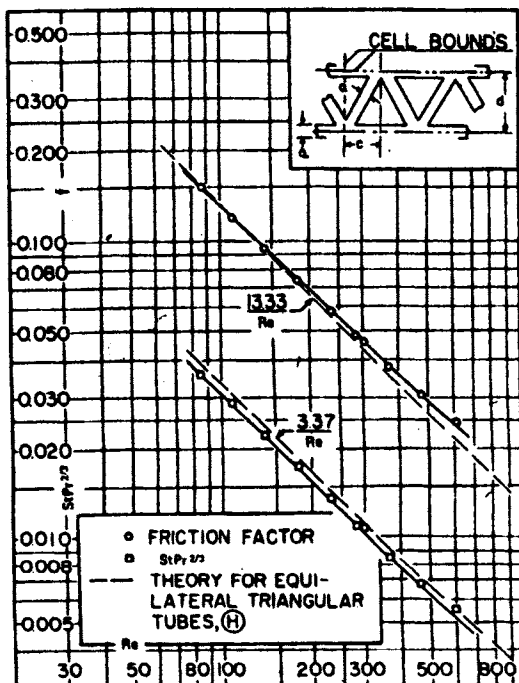
At a distance x less than L_{hy} , its dimensionless form x^+ is defined accordingly as

$$x^+ = \frac{x}{Red_h}. \quad (5.5)$$

For the case in which the flow length x is less than L_{hy} the parameter K_∞ cannot be used, and a parameter K_x is used, defined by

$$K_x = (f_{app} - f_{fd}) \frac{4x}{d_h} \quad (5.6)$$

The ratio K_x/K_∞ is shown as a function of x^+ for a number of duct shapes in Figure 5.1. It increases with x^+ and is asymptotic to unity at high x^+ . Examination of the curves shows that convergence is much faster for the parallel plate section than for those with acute corners.



Passage count = 526 per in² = 815,300 per m²

Porosity, $\rho = 0.794$

Flow passage hydraulic diameter, $4r_h = 0.00247 \text{ ft} = 0.753 \times 10^{-3} \text{ m}$

Cell height/width, $d/c = 0.731$

$L/4r_h = 101$

Total heat transfer area/total volume, $\alpha = 1285 \text{ ft}^2/\text{ft}^3 = 4216 \text{ m}^2/\text{m}^3$

Figure 5.1 Triangular duct surface: Glass ceramic matrix 505A (from Kays & London, Compact Heat Exchangers, 3rd Ed. 1998.

Copyright ©1984, McGraw-Hill Inc., reproduced by permission of Krieger Publishing company, Malabar, Florida, USA.)

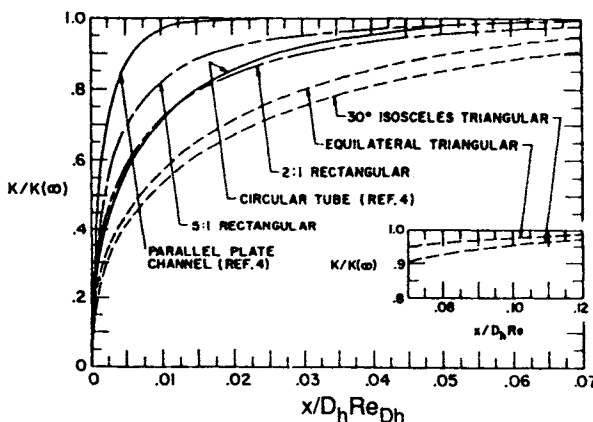
The thermal entrance length L_{th} is defined as the flow distance at which the local Nusselt number is 1.05 times the fully developed value, noting that Nu decreases with flow length.

Its dimensionless version L_{th}^* is defined by

$$L_{th}^* = \frac{L_{th}}{RePrd_h}. \quad (5.7)$$

The corresponding dimensionless thermal distance x^* is defined as

$$x^* = \frac{x}{RePrd_h}. \quad (5.8)$$



$K(\infty)$	CHANNEL
.65	PAR. PLATE
.96	5:1 RECT.
1.24	CIRC. TUBE
1.46	2:1 RECT.
1.67	EQUIL. TRI.
1.85	30° ISO. TRI.

Figure 5.2 Incremental pressure drop ratio K/K_∞ as a function of developing length.

(from Webb (1994), copyright © (John Wiley & Sons, Inc.). Reprinted by permission of John Wiley & Sons, Inc.)

It will be noted that x^* is related to the Graetz number² Gz used to describe developing flow:

$$Gz = RePr \frac{d_h}{x} = Pe \frac{d_h}{x} = \frac{1}{x^*} \quad (5.9)$$

The mean Nusselt number Nu_m over a developing length x with a developed velocity profile is shown for a variety of surfaces in Figure 5.2, for the constant temperature boundary condition, expressed as a ratio of Nu_m to its fully developed value.

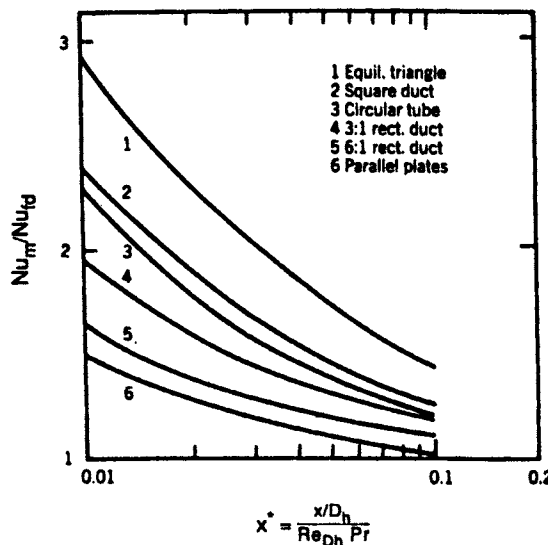


Fig 5.3 Ratio of Nusselt number Nu_T to fully developed Nu_T as function of developing length.

(from Webb (1994), copyright © (John Wiley & Sons, Inc.). Reprinted by permission of John Wiley & Sons, Inc.)

² Note that this form of Graetz number is different from that commonly used in chemical engineering, which we can call Gz_c . Here Gz_c is defined as

$$Gz_c = \frac{\dot{m}c_p}{\lambda x} = \frac{PrRep_s}{4x} = \frac{Pep_s}{4x},$$

where p is the perimeter of the surface. Thus for a circular tube

$$Gz_c = \frac{Ped}{x} \frac{\pi}{4} = \frac{Ped_h}{x} \frac{\pi}{4} = Gz \frac{\pi}{4}$$

The apparent advantage of the triangular and other acute-cornered shapes is more than countered by the fact that their fully developed Nu's are much lower, as shown in Table 5.1. What is not evident in the graph, however, is that as x^* tends to zero, all solutions tend to the developing value for a flat plate, given by Gnielinski (1983)

$$Nu_m = \frac{0.664}{Pr^{1/6} (x^*)^{1/2}}. \quad (5.10)$$

This arises simply because as the 'leading edge' is approached at low x , the influence of the duct shape disappears and the effective surface is that of an infinite (closed) length of plate. The flow is effectively fully developed from $x^* = 0.2$ onwards, with the acute cornered surfaces converging slowest. Thus if $Re = 1000$, and $Pr = 0.7$, this implies fully developed conditions from a length to diameter ratio of 140.

Recommended equations for mean Nusselt numbers for circular ducts are given by Gnielinski as the greater of:

$$Nu_{m,T} = \sqrt[3]{3.66^3 + 1.61^3 Gz} \quad (5.11)$$

$$Nu_{m,T} = 3.66 + \frac{0.19 Gz^{0.8}}{1 + 0.117 Gz^{0.467}} \quad (5.12)$$

$$\text{and} \quad Nu_{m,T} = \frac{0.664 Gz^{1/2}}{Pr^{1/6}} \quad (5.13)$$

for the constant temperature (T) condition, and the higher of

$$Nu_{m,H1} = \sqrt[3]{4.36^3 + 1.953^3 Gz} \quad (5.14)$$

$$Nu_{m,H1} = \frac{0.664 Gz^{1/2}}{Pr^{1/6}} \quad (5.15)$$

for the constant heat flux (H1) condition.

For the corresponding pressure drop, the recommended equation given by Shah and Bhatti (1987) is

$$\frac{\Delta p}{\frac{1}{2} \rho u^2} = 13.74 x^{+1/2} + \frac{1.25 + 64x^+ - 13.74x^{+1/2}}{1 + 0.00021x^{+2}}, \quad (5.16)$$

giving an effective Fanning friction factor for the dimensionless length x^+ as

$$fRe = \frac{1}{4x^+} \left[13.74x^{+1/2} + \frac{1.25 + 64x^+ - 13.74x^{+1/2}}{1 + 0.00021x^{+2}} \right]. \quad (5.17)$$

For rectangular section ducts, for simultaneously developing velocity and temperature boundary layers, which are more likely to be characteristic of real situations, the Nusselt numbers for $Pr = 0.7$ (for air) are approximated by the data of Wibulswas (1966) shown in Table 5.5. Data for square ducts ($a^* = 1$) with a range of Pr are given by Chandrupatla and Shastri (1978) in Table 5.6.

Table 5.5 Nusselt Numbers for simultaneously developing flow in rectangular ducts

(from Shah and Bhatti (1987) in *Handbook of Single Phase Convective Heat Transfer*, Eds. Kakaç et al. Copyright © (John Wiley & Sons, Inc.). Reprinted by permission of John Wiley & Sons, Inc.)

$\frac{1}{x^*}$	Nu _{x, H1}				Nu _{m, H1}				Nu _{m, T}				
	$\alpha^* = 1.0$	0.5	$\frac{1}{3}$	0.25	1.0	0.5	$\frac{1}{3}$	0.25	1.0	0.5	$\frac{1}{3}$	0.25	$\frac{1}{6}$
5	—	—	—	—	4.60	5.00	5.57	6.06	—	—	—	—	—
10	4.18	4.60	5.18	5.66	5.43	5.77	6.27	6.65	3.75	4.20	4.67	5.11	5.72
20	4.66	5.01	5.50	5.92	6.60	6.94	7.31	7.58	4.39	4.79	5.17	5.56	6.13
30	5.07	5.40	5.82	6.17	7.52	7.83	8.13	8.37	4.88	5.23	5.60	5.93	6.47
40	5.47	5.75	6.13	6.43	8.25	8.54	8.85	9.07	5.27	5.61	5.96	6.27	6.78
50	5.83	6.09	6.44	6.70	8.90	9.17	9.48	9.70	5.63	5.95	6.28	6.61	7.07
60	6.14	6.42	6.74	7.00	9.49	9.77	10.07	10.32	5.95	6.27	6.60	6.90	7.35
80	6.80	7.02	7.32	7.55	10.53	10.83	11.13	11.35	6.57	6.88	7.17	7.47	7.90
100	7.38	7.59	7.86	8.08	11.43	11.70	12.00	12.23	7.10	7.42	7.70	7.98	8.38
120	7.90	8.11	8.37	8.58	12.19	12.48	12.78	13.03	7.61	7.91	8.18	8.48	8.85
140	8.38	8.61	8.84	9.05	12.87	13.15	13.47	13.73	8.06	8.37	8.66	8.93	9.28
160	8.84	9.05	9.38	9.59	13.50	13.79	14.10	14.48	8.50	8.80	9.10	9.36	9.72
180	9.28	9.47	9.70	9.87	14.05	14.35	14.70	14.95	8.91	9.20	9.50	9.77	10.12
200	9.69	9.88	10.06	10.24	14.55	14.88	15.21	15.49	9.30	9.60	9.91	10.18	10.51
220	—	—	—	—	15.03	15.36	15.83	16.02	9.70	10.00	10.30	10.58	10.90

Table 5.6 Nusselt Numbers for simultaneously developing flow in square ducts Kakac 3.53

(from Shah and Bhatti (1987) in Handbook of Single Phase Convective Heat Transfer, eds. Kakaç et al. Copyright © (John Wiley & Sons, Inc.). Reprinted by permission of John Wiley & Sons, Inc.)

$\frac{1}{x^*}$	$Nu_{x, H1}$					$Nu_{m, H1}$				
	Pr = 0.0	0.1	1.0	10.0	∞	0.0	0.1	1.0	10.0	∞
200	14.653	11.659	8.373	7.329	7.269	21.986	17.823	13.390	11.200	11.103
133.3	12.545	9.597	7.122	6.381	6.331	19.095	15.391	11.489	9.737	9.653
100	11.297	8.391	6.379	5.816	5.769	17.290	13.781	10.297	8.823	8.747
80	10.459	7.615	5.877	5.480	5.387	16.003	12.620	9.461	8.181	8.111
50	9.031	6.353	5.011	4.759	4.720	13.622	10.475	7.934	7.010	6.949
40	8.500	5.883	4.683	4.502	4.465	12.647	9.601	7.315	6.533	6.476
25	7.675	5.108	4.152	4.080	4.048	10.913	8.043	6.214	5.682	5.633
20	7.415	4.826	3.973	3.939	3.907	10.237	7.426	5.782	5.347	5.301
10	7.051	4.243	3.687	3.686	3.686	8.701	5.948	4.783	4.580	4.549
0	7.013	3.612	3.612	3.612	3.612	7.013	3.612	3.612	3.612	3.612

For the limiting case of parallel plates ($a^* = 0$), a good approximation to the mean Nusselt number is given by Stephan (1957) for the (T) condition:

$$Nu_{m,T} = 7.55 + \frac{0.024x^{*-1.14}}{1 + 0.0358 \text{Pr}^{0.17} x^{*-0.64}} \quad (5.18)$$

Triangular ducts

For developing flow in triangular section ducts, the correlations recommended by Wibulswas and Tangsirimonkol (1978) quoted by Kakac et al (1987) are:

For an equilateral triangular and right-angled isosceles triangular duct

$$Nu_{m,T} = 0.44x^{*-0.66} \quad \text{for } 1.82 \times 10^{-3} < x^* < 3.33 \times 10^{-2} \quad (5.19)$$

and

$$Nu_{m,T} = 1.594x^{*-0.331} \quad \text{for } x^* > 3.33 \times 10^{-2}. \quad (5.20)$$

Tabulated data for equilateral triangular ducts are given in Table 5.7

Table 5.7 Nusselt Numbers (local and mean) for simultaneously developing flows for an equilateral triangular duct (Wibulswas, 1966) (from Shah and Bhatti (1987) in Handbook of Single Phase Convective Heat Transfer, Eds. Kakac et al. Copyright © (John Wiley & Sons, Inc.). Reprinted by permission of John Wiley & Sons, Inc.)

$\frac{1}{x^*}$	Nu _{x,T}			Nu _{m,T}			Nu _{x,HI}			Nu _{m,HI}		
	Pr = ∞	0.72	0	∞	0.72	0	∞	0.72	0	∞	0.72	0
10	2.57	2.80	3.27	3.10	3.52	4.65	3.27	3.58	4.34	4.02	4.76	6.67
20	2.73	3.11	3.93	3.66	4.27	5.79	3.48	4.01	5.35	4.76	5.87	8.04
30	2.90	3.40	4.46	4.07	4.88	6.64	3.74	4.41	6.14	5.32	6.80	9.08
40	3.08	3.67	4.89	4.43	5.35	7.32	4.00	4.80	6.77	5.82	7.57	9.96
50	3.26	3.93	5.25	4.75	5.73	7.89	4.26	5.13	7.27	6.25	8.20	10.65
60	3.44	4.15	5.56	5.02	6.08	8.36	4.49	5.43	7.66	6.63	8.75	11.27
80	3.73	4.50	6.10	5.49	6.68	9.23	4.85	6.03	8.26	7.27	9.73	12.35
100	4.00	4.76	6.60	5.93	7.21	9.98	5.20	6.56	8.81	7.87	10.60	13.15
120	4.24	4.98	7.03	6.29	7.68	10.59	5.50	7.04	9.30	8.38	11.38	13.82
140	4.47	5.20	7.47	6.61	8.09	11.14	5.77	7.50	9.74	8.84	12.05	14.46
160	4.67	5.40	7.88	6.92	8.50	11.66	6.01	7.93	10.17	9.25	12.68	15.02
180	4.85	5.60	8.20	7.18	8.88	12.10	6.22	8.33	10.53	9.63	13.27	15.50
200	5.03	5.80	8.54	7.42	9.21	12.50	6.45	8.71	10.87	10.02	13.80	16.00

An approximate correlation for friction factor can be given as

$$f \text{Re} = (fRe)_{f-d} + 2.5x^{+^{-1/2}}, \quad (5.21)$$

where $(fRe)_{f-d}$ is the fully developed value for each case. This agrees quite well with the graphical data presented by Kakac et al (1987).

Semicircular ducts

The developing flow Nusselt numbers for a semicircular duct, including the case of the base being insulated are shown in Table 5.8, from the data of Hong and Bergles (1974)

Table 5.8 Local Nusselt numbers for the thermal entrance region of a semicircular duct

(from Shah and Bhatti (1987) in Handbook of Single Phase Convective Heat Transfer, eds. Kakaç et al. Copyright © (John Wiley & Sons, Inc.). Reprinted by permission of John Wiley & Sons, Inc.)

x^*	$Nu_{x,Hi}$		x^*	$Nu_{x,Hi}$	
					
0.000458	17.71	17.43	0.0279	4.767	4.339
0.000954	13.72	13.41	0.0351	4.562	4.037
0.00149	11.80	11.37	0.0442	4.429	3.830
0.00208	10.55	10.08	0.0552	4.276	3.686
0.00271	9.605	9.141	0.0686	4.217	3.543
0.00375	8.475	8.127	0.0849	4.156	3.425
0.00493	7.723	7.375	0.105	4.124	3.330
0.00627	7.137	6.788	0.130	4.118	3.265
0.00777	6.556	6.312	0.159	4.108	3.208
0.00946	6.300	5.912	0.196	—	3.171
0.0128	5.821	5.368	0.241	—	3.161
0.0168	5.396	4.935	0.261	—	3.160
0.0217	5.077	4.579	∞	4.089	3.160

Turbulent and transitional flow in ducts

Circular duct: fully- developed and developing flow in smooth duct

Because of its wide use in heat exchangers, this is probably the most researched area of heat transfer. We give first, for completeness, the simplest and most commonly- used correlations, which are

$$(Blasius (1913)) \quad f = 0.0791 Re^{-0.25} \quad \text{recommended for } 4 \times 10^3 < Re < 10^5 \quad (5.22)$$

This correlation is within +2.7 and -1.4 % of the Techo et al correlation, for a circular duct.

$$(Dittus-Boelter (1930)) \quad Nu = 0.024 Re^{0.8} Pr^{0.4} \quad \text{for heating} \quad (5.23)$$

$$Nu = 0.026 Re^{0.8} Pr^{0.3} \quad \text{for cooling.} \quad (5.24)$$

These heat transfer correlations are no longer recommended for design use, as they can be seriously in error (greater than 20%) in some circumstances.

The recommended correlations giving an explicit relationship are:

Friction factor

Smooth duct:

$$(\text{Techo et al. (1965)}) \quad \frac{1}{\sqrt{f}} = 1.7372 \ln \left[\frac{Re}{1.964 \ln(Re) - 3.8215} \right] \quad (5.25)$$

(recommended for $10^4 < Re < 10^7$), or

$$(\text{Filonenko (1954)}) \quad \frac{1}{\sqrt{f}} = 1.56 \ln(Re) - 3.00 \quad (10^4 < Re < 10^7) \quad (5.26)$$

modified, see Martin (1996),

Rough duct:

$$(\text{Chen (1979)}) \quad \frac{1}{\sqrt{f}} = 3.48 - 1.7372 \ln \left[\frac{\epsilon}{a} - \frac{16.2426}{Re} \ln(A_1) \right] \quad (4000 < Re < 10^8) \quad (5.27)$$

$$\text{where } A_1 = \frac{(\epsilon/a)^{1.1098}}{6.0983} + \left(\frac{7.149}{Re} \right)^{0.8981} \quad (5.28)$$

$$(\text{Nikuradze (1933)}) \quad \frac{1}{\sqrt{f}} = 3.48 + 1.737 \ln \frac{\epsilon}{a} \quad (Re_\epsilon > 70.) \quad (5.29)$$

In the above, ϵ is the roughness height and a is the radius of the duct ($= d_h/2$).

It should be noted that a rough duct is unlikely to be found in a compact heat exchanger, since the surfaces are normally formed from well-rolled sheet. Roughness would, however, be introduced by surface fouling layers.

Nusselt Number

Smooth duct

(Gnielinski (1992))

$$(1) \quad Nu = \frac{(f/2)(Re - 1000)Pr}{1 + 12.7(f/2)^{1/2}(Pr^{2/3} - 1)} \left[1 + \left(\frac{d_h}{L} \right)^{2/3} \right] \quad (2300 < Re < 5 \times 10^4 \text{ and } 0.5 < Pr < 2000). \quad (5.30)$$

$$(2) \quad Nu = 0.0214(Re^{0.8} - 100)Pr^{0.4} \left[1 + \left(\frac{d_h}{L} \right)^{2/3} \right] \quad (10^4 < Re < 5 \times 10^6 \text{ and } 0.5 < Pr < 1.5) \quad (5.31)$$

$$(3) \quad Nu = 0.012(Re^{0.87} - 280)Pr^{0.4} \left[1 + \left(\frac{d_h}{L} \right)^{2/3} \right] \quad (3 \times 10^3 < Re < 10^6 \text{ and } 1.5 < Pr < 500) \quad (5.32)$$

In the above correlations the friction factor is calculated as needed from the Filonenko (modified) or Techo correlations, either of which are sufficiently accurate for practical purposes.

Fully developed, rough

Bhatti and Shah (1987) give

$$Nu = \frac{RePr(f/2)}{1 + \sqrt{f/2} \left(4.5Re_t^{0.2}Pr^{0.5} - 8.48 \right)} \quad (5.33)$$

for $0.5 < Pr < 10$, $0.002 < \epsilon/d_h < 0.05$ and $Re > 10^5$, and

$$Nu = \frac{(Re - 1000)Pr(f/2)}{1 + \sqrt{f/2} \left[(17.42 - 13.77Pr_t^{0.8})Re_t^{0.5} - 8.48 \right]} \quad (5.34)$$

for $0.5 < Pr < 5000$, $0.001 < \epsilon/d_h < 0.05$ and $Re > 2300$, with

$$Pr_t = 1.01 - 0.09 Pr^{0.36} \text{ for } 1 \leq Pr \leq 145$$

$$Pr_t = 1.01 - 0.11 \ln(Pr) \text{ for } 145 \leq Pr \leq 1800$$

$$Pr_t = 0.99 - 0.29 \ln(\ln(Pr))^{1/2} \text{ for } 1800 \leq Pr \leq 12500$$

Transitional Reynolds number flow regimes (ducts of all cross sections)

Plain ducts of the polygonal geometries tend to have fairly sharp transition between laminar and turbulent flows, depending of the free stream conditions at entry. Transition starts between $Re = 1000$ and $Re = 2000$, and is effectively complete (that is, with fully developed turbulent flow) at about $Re = 4000$. Circular ducts have rather later transition. Prediction of friction factors and Nusselt Numbers is uncertain in this transitional region. For friction factor, Bhatti and Shah (1987) recommend for a circular tube:

$$f = A + \frac{B}{Re^{1/m}}, \quad (5.35)$$

with $A = 0.0054$, $B = 2.3 \times 10^{-8}$, $m = -2/3$ for the Reynolds number range $2100 < Re < 4000$.

For heat transfer, Bhatti and Shah (1987) recommend

$$Nu^{10} = Nu_t^{10} + \left\{ \frac{\exp(2000 - Re)/365}{Nu_t^2} + \frac{1}{Nu_t^2} \right\}^{-5}, \quad (5.36)$$

where Nu_t is the fully-developed laminar value according to the thermal boundary condition (i.e. 3.657 and 4.364 for the T and H boundary conditions respectively), and

$$Nu_t = Nu_o + \frac{0.078(f/2)^{1/2} Re Pr}{(1 + Pr^{4/5})^{5/6}}, \quad (5.37)$$

with $Nu = 4.8$ and 6.3 for the T and H conditions respectively.

Gnielinski (1983) recommends that in the transitional regime, the highest value for Nu given by equations 5.10, 5.11 and 5.30 be used.

These relationships could be used for other duct shapes, in the absence of specific correlations. The physical reasoning behind this is simply that in fully turbulent flow the mixing is sufficiently strong that it reaches well into the corners or apices of a polygonal cross sectional duct, and thus the overall flow represented by the core velocity distribution is largely insensitive to shape. This will be more the case- for all shapes- as Reynolds number and hence turbulence increases, and less so for sharp or highly- cusped cross sections for which the turbulence is damped or 'squeezed out' near to the corners, as pointed out by Bhatti and Shah (1987).

PLATE FIN SURFACES

This surface type is by far the commonest of all compact types, being used for applications from aerospace air conditioning duties to oil refining. The four basic fin surfaces are illustrated in Figure 5.4.

Before describing the correlations it is necessary to define the surface geometry in a consistent way. The principal features and dimensions are shown in Figure 5.5.

The hydraulic diameter of plate- fin surfaces is defined by Manglic and Bergles (1990) as

$$d_h = \frac{4A_c}{A_s}, \quad \text{with lateral and vertical edges being accounted for,} \quad (5.38)$$

giving

$$d_h = \frac{4shl}{[2(sl + hl + t_f h) + t_f s]} \quad (5.39)$$

This formulation does take into account the flow constriction between the offset sections, so might not be as accurate as it might be in correlating pressure drop, especially for thick fins.

The porosity σ is an important geometrical parameter controlling core weight (see chapter 4), and is given by

$$\sigma = \frac{sh}{(s + t_f)(b + t)} = \frac{s(b - t_f)}{(s + t_f)(b + t)}. \quad (5.40)$$

Note that a more complex formulation is necessary for the porosity if a splitter plate configuration is used, to allow for the splitter plate having a different thickness to that of the separation plate.

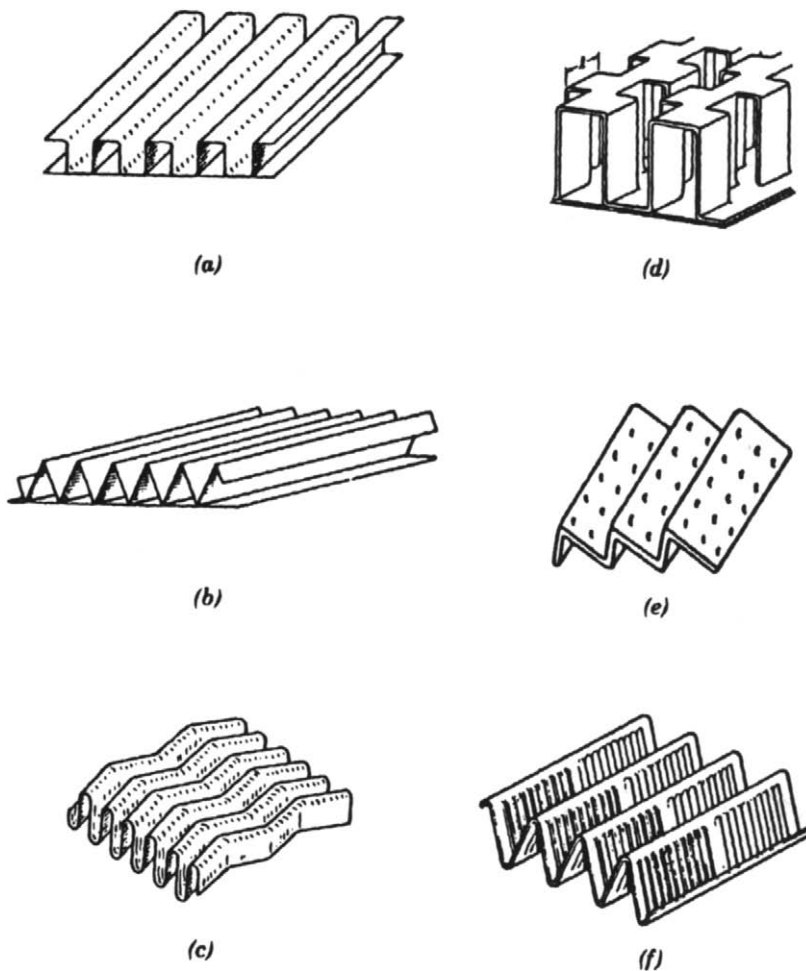


Figure 5.4 Plate fin surface types: (a) plain rectangular, (b) plain triangular, (c) Wavy, (d) offset strip (OSF), (e) perforated, (f) louvred.
(From Webb (1987) in *Handbook of Single Phase Convective Heat Transfer*,
Eds. Kakaç et al. Copyright © (John Wiley & Sons, Inc.). Reprinted by
permission of John Wiley & Sons, Inc.)

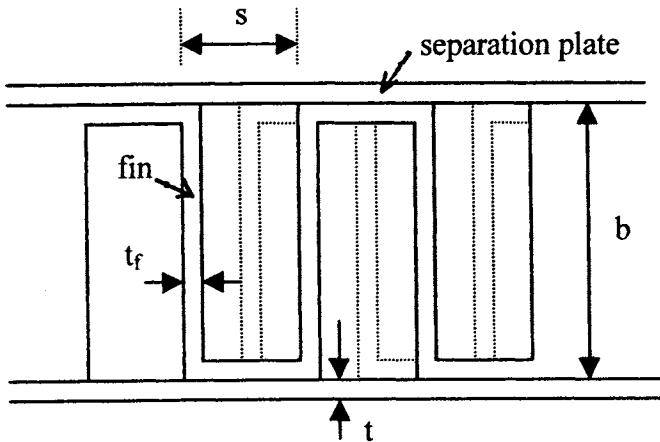


Figure 5.5 Basic geometry (schematic) of rectangular plate-fin surface (OSF shown dashed).

Dimensions	Symbol	Dimensionless ratios
Fin thickness	t_f	$\alpha = s/h$
Separation plate thickness	t	$\delta = t_f/l$
Hydraulic diameter	d_h	$\gamma = t_f/s$
Plate-gap (= distance between plate surfaces)	b	
Passage height ($= b - t_f$)	h	
Splitter plate thickness (if used)	t_s	
Fin spacing	s	
Fin (strip) length	l	

Plain fin (Rectangular, triangular and sine section shapes)

Data for a variety of plain fin surfaces are given in Kays and London (1984). In the absence of data for a specific geometry, the following correlations are recommended.

Laminar flow, fully developed and developing.

The values for f/Re and Nu for fully developed and developing laminar flow in the corresponding plain ducts should be used if there are no specific correlations available. These are given in Tables 5.1 and 5.2. It should be remembered that these values are for perfectly formed duct shapes. Real manufactured shapes will differ because of non-straight fins, and the presence of

braze fillets in the corners, the latter having the effect of reducing the flow area and surface area but of improving the Nu/Re ratio, as noted above.

Transitional and turbulent flow.

The Gnielinski correlation for circular ducts should be used, as recommended for non-circular channels.

Triangular plain fin

Data for a variety of triangular fin surfaces are given in Kays and London (1984), an example being shown in Figure 5.6. Comparison with the continuous duct triangular geometry of Figure 5.5 Shows the advantage of the developing flow condition of the fin surface.

If data for the required geometry are unavailable the following correlations are suggested.

For an equilateral triangular duct, Bhatti and Shah(1987) recommend, for fully-developed turbulent flow

$$f = \frac{0.0425}{Re^{0.2}} \quad (5.41)$$

and for $Pr = 0.7$ the present author suggests, based on the 2- heated side results of Altemani and Sparrow (1980):

$$Nu_{H1} = 0.028Re^{0.781} \quad (4000 < Re < 6 \times 10^4) \quad (5.42)$$

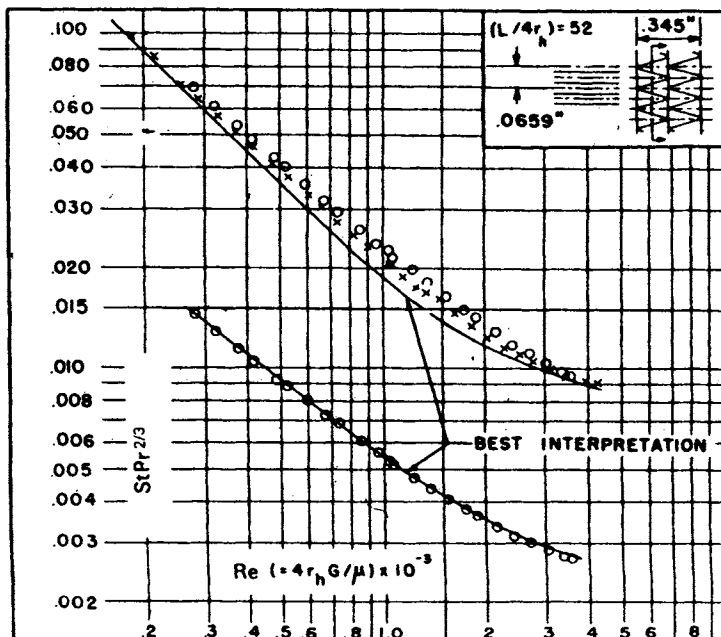
For isosceles triangular ducts, Bhatti and Shah (1987) recommend

$$f = \frac{C}{Re^{0.25}}, \quad (5.43)$$

where C is a function of the minimum (apex) angle 2ϕ (radians), given by

$$C = 0.060759 + 0.07863\phi - 0.078093\phi^2 - 0.202421\phi^3 + 0.28228\phi^4 \quad (5.44)$$

For the Nusselt Number, it is suggested that for triangular fins, unless there are specific experimental data, the Gnielinski correlation be used, factored by the ratio of $Nu/Nu_{(circular)}$ for the fully- developed laminar duct value for the appropriate boundary condition.



$$\text{Fin pitch} = 30.33 \text{ per in} = 1194 \text{ per m}$$

Plate spacing, $b = 0.345$ in = 8.763×10^{-3} m

Splitter symmetrically located

Fin length flow direction = 2.50 in = 63.5×10^{-3} m

Flow passage hydraulic diameter: $4r_1 = 0.0048$

Fin metal thickness = 0.004 in. aluminum = 0.101×10^{-3} in.

Splitter metal thickness = 0.006 in. $\approx 0.152 \times 10^{-3}$ m

Total heat transfer area/volume between plates, $\beta = 812.51 \text{ ft}^2/\text{ft}^3 = 2.666 \text{ m}^2/\text{m}^3$

Fin area (including spillover)/total area = 0.938

FIN area (including splitter)

Figure 5.6. Plain triangular fin surface 30.33T
 (from Kays & London, Compact Heat Exchangers, 3rd Ed. 1998.
 Copyright ©1984, McGraw-Hill Inc., reproduced by permission
 of Krieger Publishing company, Malabar, Florida, USA.)

Offset Strip Fin, OSF (also called serrated fin, or interrupted fin)

This form of fin surface is the highest performer, and hence has been the subject of most experimental research, starting with the extensive work of Kays

and London (1984). Although specific data sets are recommended if a particular defined surface is used, for exploratory and optimisation work generalised correlations are valuable. The most recent and accurate correlations are those of Joshi and Webb (1987), and Manglic and Bergles (1990).

The correlations recommended are those of Manglic and Bergles, and employ an asymptotic combination of individual correlations for the laminar and turbulent flow regimes. This avoids the need for calculating a critical Reynolds number and then choosing the corresponding high or low Reynolds number correlation:

Friction coefficient:

$$f = 9.6243 Re^{-0.7422} \alpha^{-0.1856} \delta^{0.3053} \gamma^{-0.2659} (1 + 7.669 \times 10^{-8} Re^{4.429} \alpha^{0.92} \delta^{3.767} \gamma^{0.236})^{0.1} \quad (5.45)$$

Heat transfer coefficient:

$$j = 0.6522 Re^{-0.5403} \alpha^{-0.1541} \delta^{-0.1409} \gamma^{-0.0678} (1 + 5.269 \times 10^{-5} Re^{1.34} \alpha^{0.504} \delta^{0.456} \gamma^{-1.055})^{0.1} \quad (5.46)$$

using the geometrical notation as above.

For estimation purposes the following simplified correlations could be used for OSF surfaces with high fin/total area and with thin fins (400 < Re < 3000):

$$j = 0.6 Re_l^{-0.5} = 0.6 Re_{dh}^{-0.5} \left(\frac{d_h}{l} \right)^{0.5} \quad (5.47)$$

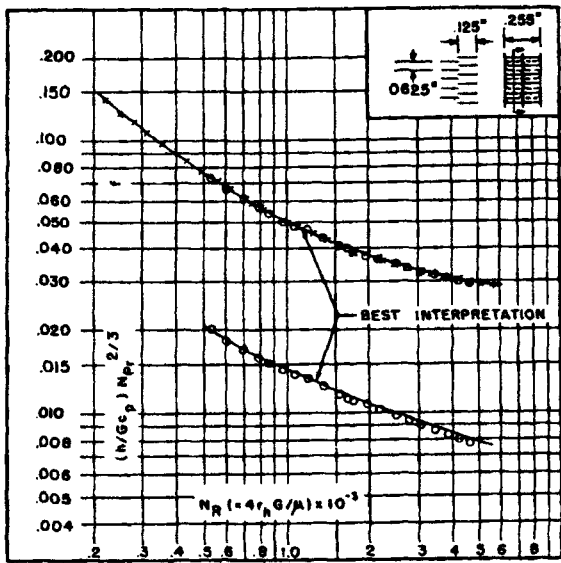
$$f = 4j \quad (5.48)$$

where l is the length of the strip.

Data for five OSF geometries from Kays and London (1984) are shown in Figures 5.7 to 5.10, selected for a range of hydraulic diameters and fin lengths.

Wavy (corrugated, or herringbone) fin

This fin, as reported by Webb (1994), is competitive with the OSF. The form can be either that of a folded fin strip between flat separating plates, with the corrugations being in the plane of the plates, or that of a corrugated fin interlaced by flat or round tubes. The length of each corrugation is typically less than that of the OSF fin length, and although there are no blunt leading edges to create wakes and form drag, there will be small dead zones in the bottom of each



Fin pitch = 16.00 per in.

Plate spacing, $b = 0.255$ in.

Splitter symmetrically located

Fin length flow direction = 0.125 in.

Flow passage hydraulic diameter, $4r_h = 0.006112$ ft

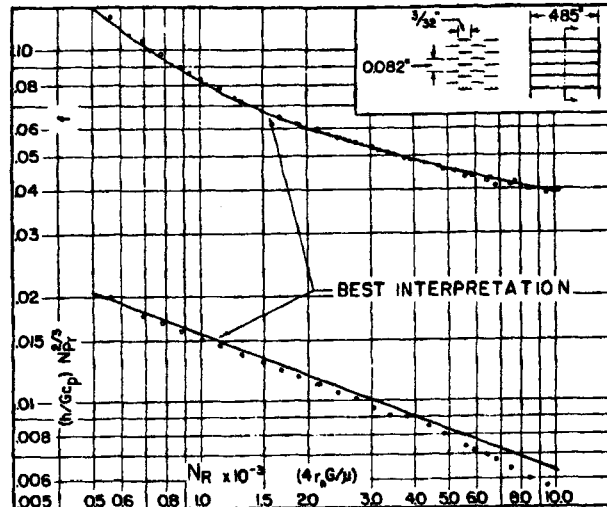
Fin metal thickness = 0.006 in., aluminum

Splitter metal thickness = 0.006 in.

Total heat transfer area/volume between plates, $\beta = 549.5 \text{ ft}^2/\text{ft}^3$

Fin area (including splitter)/total area = 0.845

Figure 5.7 OSF surface 3/32-12.22



Fin pitch = 12.22 per in.

Plate spacing, $b = 0.485$ in.

Fin length = 0.094 in.

Fins staggered symmetrically

Flow passage hydraulic diameter, $4r_h = 0.01120$ ft

Fin metal thickness = 0.004 in., copper

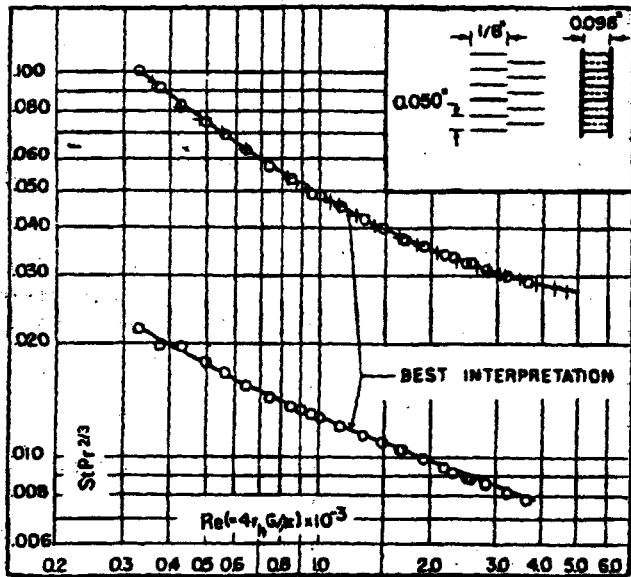
Total heat transfer area/volume between plates, $\beta = 340 \text{ ft}^2/\text{ft}^3$

Fin area/total area = 0.862

Note: Fin leading and trailing edges slightly scarfed from fin cutting operation. Friction factors may be lower with clean fins.

Figure 5.8 OSF surface 1/8-16D

(Both from Kays & London, Compact Heat Exchangers, 3rd Ed. 1998. Copyright ©1984, McGraw-Hill Inc., reproduced by permission of Krieger Publishing company, Malabar, Florida, USA.)



Fin pitch = 19.86 per in = 782 per m

Plate spacing, $b = 0.098 \text{ in} = 2.49 \times 10^{-3} \text{ m}$

Fin length = 0.125 in = $3.175 \times 10^{-3} \text{ m}$

Flow passage hydraulic diameter, $4r_h = 0.00508 \text{ ft} = 1.54 \times 10^{-3} \text{ m}$

Fin metal thickness = 0.004 in = $0.102 \times 10^{-3} \text{ m}$

Total heat transfer area/volume between plates, $\beta = 887 \text{ ft}^2/\text{ft}^3 = 2254 \text{ m}^2/\text{m}^3$

Fin area/total area = 0.785

Figure 5.9 OSF surface 1/8- 19.86)

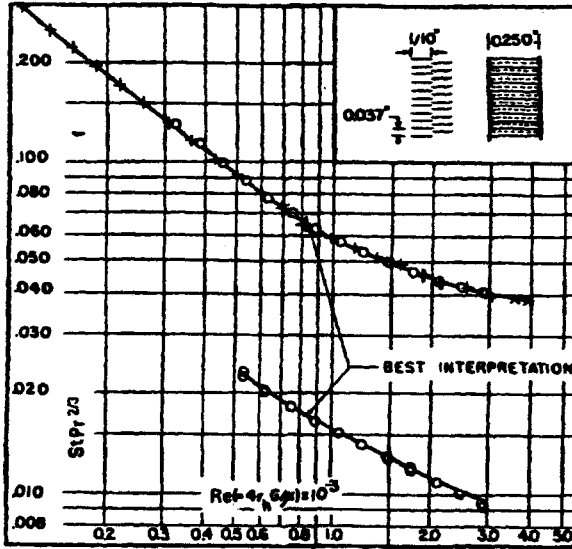


Figure 5.10 OSF surface 1/10- 27.03

(Both from Kays & London, Compact Heat Exchangers, 3rd Ed. 1998. Copyright ©1984, McGraw-Hill Inc., reproduced by permission of Krieger Publishing company, Malabar, Florida, USA.)

corrugation giving a higher mean velocity and associated skin friction. It is known that secondary flows (Goertler vortices) induced by the corrugations assist the augmentation in addition to the partial 'restarts' of the boundary layers. The basic form of the geometry is shown in Figure 5.11

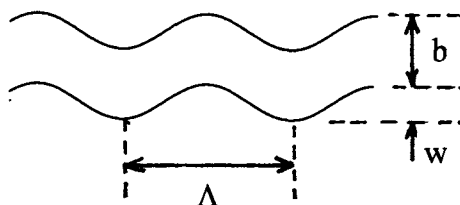


Fig 5.11 Schematic geometry of corrugated surfaces

There appear to be no general correlations available for these surfaces: a correlation which describes approximately a typical high performance surface such as 17.8- 3/8W of Kays and London (1984) is

$$f = 1.08 Re^{-0.425} \quad \text{for } 400 < Re < 3000. \quad (5.49)$$

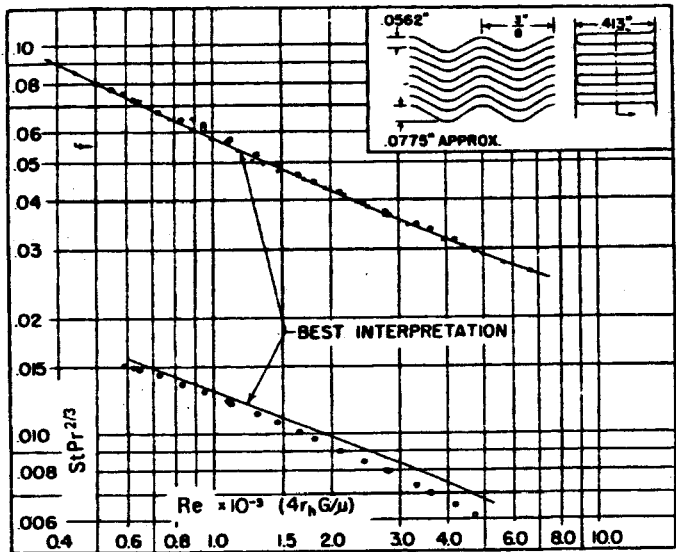
$$j = 0.24 Re^{-0.425}$$

The performance data for the above surface are shown in Figure 5.12, whilst data for the wavy fin with flat tubes (9.29-0.737-SR) are given in Figure 5.13.

An alternative correlation, which describes both the above and other data (for example Oyakawa & Shinzato (1989)), quite well, is, for $w/\Lambda = 0.25$,

$$\left. \begin{aligned} f &= 4.8 Re^{-0.36} \left(\frac{2b}{\Lambda} \right)^{1.5}, \\ j &= 0.4 Re^{-0.36} \left(\frac{2b}{\Lambda} \right)^{0.75} \end{aligned} \right\} \quad 10^4 < Re < 10^5 \quad (5.50)$$

$$\left. \begin{aligned} \text{and} \quad j &= 0.4 Re^{-0.4} \left(\frac{2b}{\Lambda} \right)^{0.75}, \\ f &= 5j \end{aligned} \right\} \quad 600 < Re < 3000 \quad (5.51)$$



Fin pitch = 17.8 per in = 701 per m

Plate spacing, $b = 0.413$ in = 10.49×10^{-3} m

Flow passage hydraulic diameter, $4r_h = 0.00696$ ft = 2.123×10^{-3} m

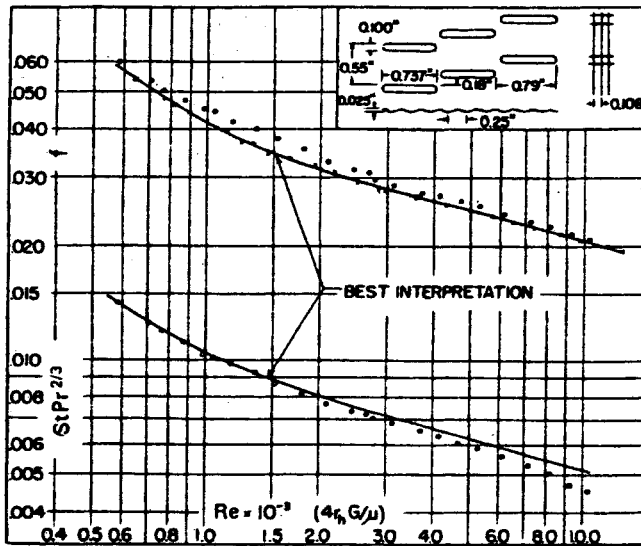
Fin metal thickness = 0.006 in, aluminum = 0.152×10^{-3} m

Total heat transfer area/volume between plates, $\beta = 514 \text{ ft}^2/\text{ft}^3 = 1,686 \text{ m}^2/\text{m}^3$

Fin area/total area = 0.892

Note: Hydraulic diameter based on free-flow area normal to mean flow direction.

Figure 5.12 Wavy surface 17.8- 3/8W



Fin pitch = 9.29 per in = 366 per m

Flow passage hydraulic diameter, $4r_h = 0.01352$ ft = 4.12×10^{-3} m

Fin metal thickness = 0.004 in, copper = 0.102×10^{-3} m

Free-flow area/frontal area, $\sigma = 0.788$

Total heat transfer area/total volume, $\alpha = 228 \text{ ft}^2/\text{ft}^3 = 748 \text{ m}^2/\text{m}^3$

Fin area/total area = 0.814

Figure 5.13 Wavy fin with flat tubes (9.29-0.737-SR)

(Both from Kays & London, Compact Heat Exchangers, 3rd Ed. 1998. Copyright ©1984, McGraw-Hill Inc., reproduced by permission of Krieger Publishing company, Malabar, Florida, USA.)

The latter friction factor correlation is conservative: an f/j ratio of 4 or lower is commonly achieved for high performance surfaces. It should be noted that both correlations only apply for wavy surfaces such as sinusoidal surfaces, that is, without sharp corners. If sharp corners are used (i.e. for triangular corrugations), the heat transfer can be increased by up to about 18%, but with a normally prohibitive friction factor penalty of 55 to 80 % (Sparrow & Hossfield, 1984)).

It should be noted that in the above correlations there is no indicated influence of the corrugation height- that is to accommodate how 'aggressive' the corrugation is. As corrugation, or wave, height to wavelength increases the separation zones in the troughs increase in relative size, giving rise to disproportionately high pressure drop.

Perforated fin

Perforated fins are used in the distributor sections of exchangers and also for boiling applications (see chapter 6). The perforations in distributors allow for lateral migration of flow (including the vapour phase), without the pressure drop penalty of the OSF. The interruptions given by them give a slight performance improvement per unit surface area, but offset by loss of surface area, and there is generally a higher friction factor. Shah (1975) has shown that there is a modest improvement of heat transfer for Reynolds numbers greater than 2000- suggesting that the onset of turbulence is brought forward. A reasonable assumption to use is that of the same j factor but 20% higher friction factor than that of the plain fin of the same nominal dimensions.

Louvred fin surfaces

This class of surface is an important one. The various forms of louvred fin flat- tube surface are shown in Figure 5.14 , the basic distinctions being between the geometries of a triangular fin and of a plate fin (with slotted tubes).

The fin is formed by a rolling process instead of the reciprocating press necessary for the OSF geometry. The manufacturing process makes it much cheaper to produce, and hence the form is widely used for mass production markets such as automotive heaters, radiators etc. The finning can be bonded to either separating plates as a form of conventional plate-fin surface, or to tubes. Although louvred fins are increasingly used with round tubes for air conditioning applications, the tubes themselves may not come under the strict definition of 'compact', the internal diameter usually being of 10mm or more. For the automotive and prime mover market the tubes are almost invariably flattened, and are compact, being 1-2mm wide.

The louvred fin has comparable or even superior performance to that of the OSF. This is thought to arise because in an OSF arrangement the flow length

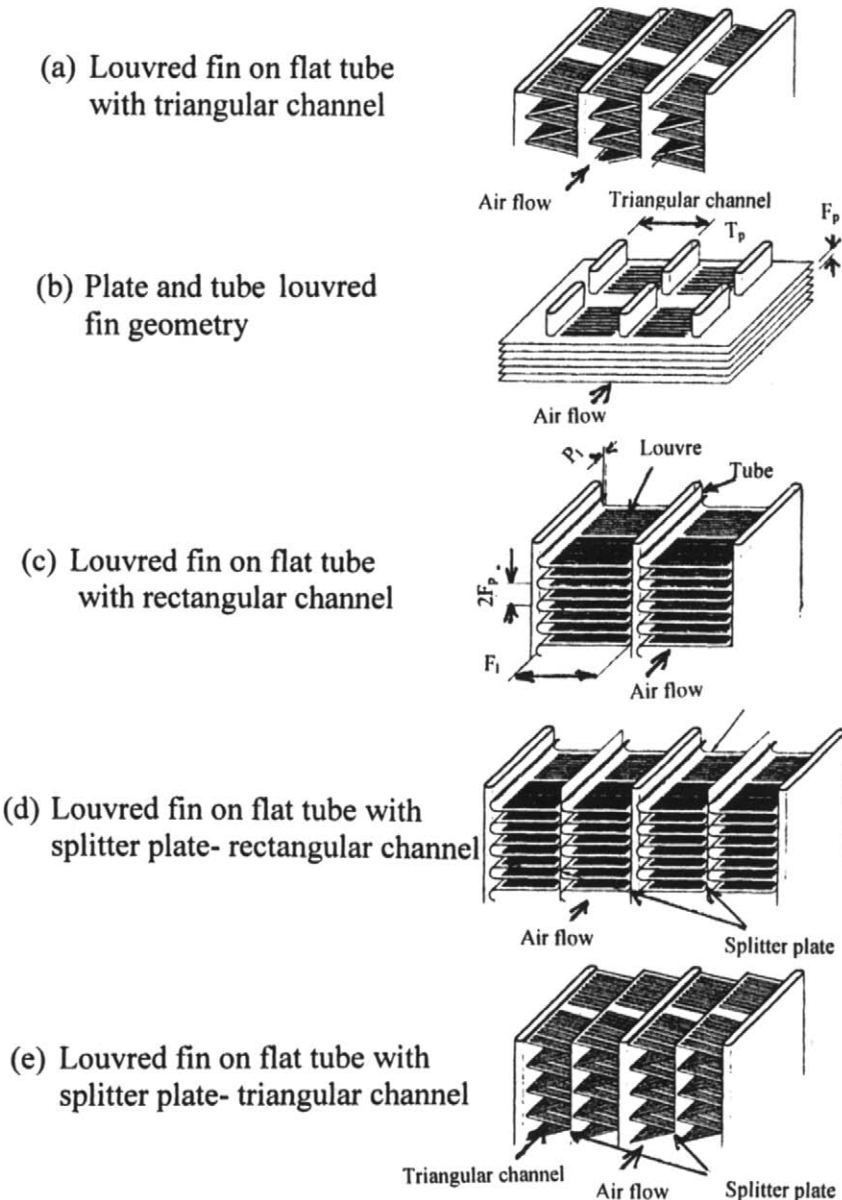
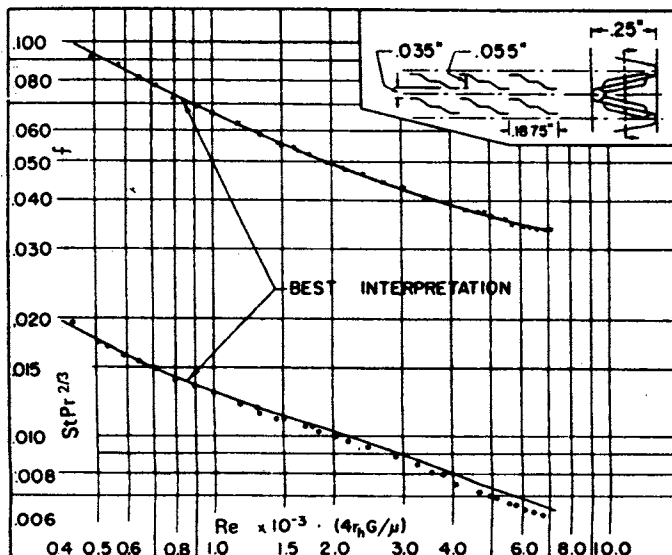


Fig 5.14 Forms of louvred fin-flat tube surface, from Chang et al. (2000), used with permission.

available for mixing of the fin wakes is only one fin length, whereas several fin lengths are characteristic of the flow in a louvred surface (in appropriate operating conditions, see below). Mixing is accordingly more complete between one fin and its downstream neighbour, giving a higher effective temperature difference.

Performance data for a variety of plate- and louvred fin surfaces are given in Kays and London (1984), and a typical example is shown in Figure 5.15.



Fin pitch = 11.1 per in = 437 per m

Plate spacing, $b = 0.250$ in = 6.35×10^{-3} m

Louver spacing = 0.1875 in = 4.763×10^{-3} m

Fin gap = 0.035 in = 0.89×10^{-3} m

Louver gap = 0.055 in = 1.4×10^{-3} m

Flow passage hydraulic diameter, $4r_h = 0.01012$ ft = 3.084×10^{-3} m

Fin metal thickness = 0.006 in, aluminum = 0.152×10^{-3} m

Total heat transfer area/volume between plates, $\beta = 367 \text{ ft}^2/\text{ft}^3 = 1,204 \text{ m}^2/\text{m}^3$

Fin area/total area = 0.756

Figure 5.15 Louvred plate-fin surface 3/16 11.1
 (from Kays & London, Compact Heat Exchangers, 3rd Ed. 1998.
 Copyright ©1984, McGraw-Hill Inc., reproduced by permission
 of Krieger Publishing company, Malabar, Florida, USA.)

The most comprehensive data for louvred plate-fin surfaces were compiled by Davenport (1980), for a Z-shaped triangular fin, other sources including Tanaka et al. (1984). Cowell, Heikal and Achaichia (1995) reviewed the data in

relation to the flow modelling: this is also discussed by Webb (1994). An important finding from recent research is that there is a distinct change in flow structure with Reynolds number based on louvre length. At low Reynolds number the flow bypasses the louvre passages and stays in the main fin passage, as shown in Figure 5.16, analogous to the flow in a 'stalled' compressor blade cascade. The heat transfer performance is then close to that of a plain duct, Figure 5.18, and the louvres are relatively ineffective. At higher Reynolds number there begins a progressive re-alignment of the flow through the louvre system, resulting in a distinct start of the boundary layer on each fin with the corresponding increase of heat transfer coefficient. Davenport's dimensional correlations are based on a triangular fin layout (Figure 5.17b) slightly different from the normal form of fin (Figure 5.14A), and are

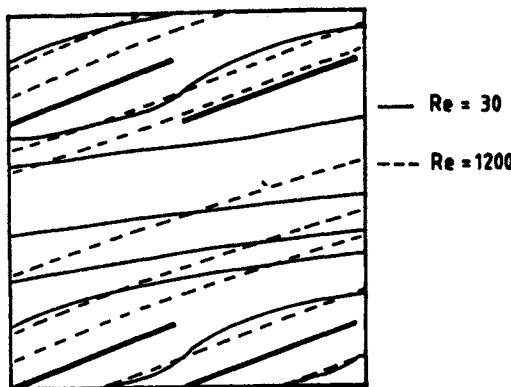


Figure 5.16 Streamlines at high and low Reynolds number in louvre array (Achaichia and Cowell (1988)), used with permission.

$$j = 0.249 Re_L^{-0.42} L_H^{0.33} (L_L/F_H)^{1.1} F_H^{0.26} \quad 300 < Re_L < 4000 \quad (5.52)$$

$$f = 5.47 Re_L^{-0.72} L_H^{0.37} (L_L/F_H)^{0.89} L^{0.2} F_H^{0.23} \quad 70 < Re_L < 900 \quad (5.53)$$

$$f = 0.494 Re_L^{-0.39} (L_H/L)^{0.33} (L_L/F_H)^{1.1} F_H^{0.46} \quad 1000 < Re_L < 4000 \quad (5.54)$$

where

L_H is the louvre height- the projected distance from the louvre edge to the base surface (see fig. 5.17a),

F is the fin pitch,

F_H is the fin height,

L_L is the louvre length (i.e the length of cuts from which the louvre is formed), and

L is the louvre pitch- or flow length, the distance between cuts in the base surface.

Clearly L_H and L are related, for thin, fins by

$$L_H = L \sin(\alpha). \quad (5.55)$$

The lower restriction on Reynolds number in Davenport's correlation was imposed because of inconsistencies arising from the change in flow structure mentioned above. To overcome this- an important consideration because of the trend towards lower louvre flow lengths- a method has been proposed by Achaichia and Cowell (1988) which correlates the change in mean flow angle β through the louvres and allows a good prediction down to $Re_L = 75$. The correlation is

$$\beta = 0.936 - (243/Re_L) - 1.76(F/L) + 0.995\alpha, \quad (5.56)$$

where β is the mean angle of flow and α is the louvre angle (both in degrees). It should be noted from Figure 5.17. that L , L_L and α are related geometrically by

$$L = L_L \cos \alpha. \quad (5.57)$$

Achaichia and Cowell (1988) showed that equation 5.57 yielded a relatively simple expression for Stanton number, re-expressed here as j - factor:

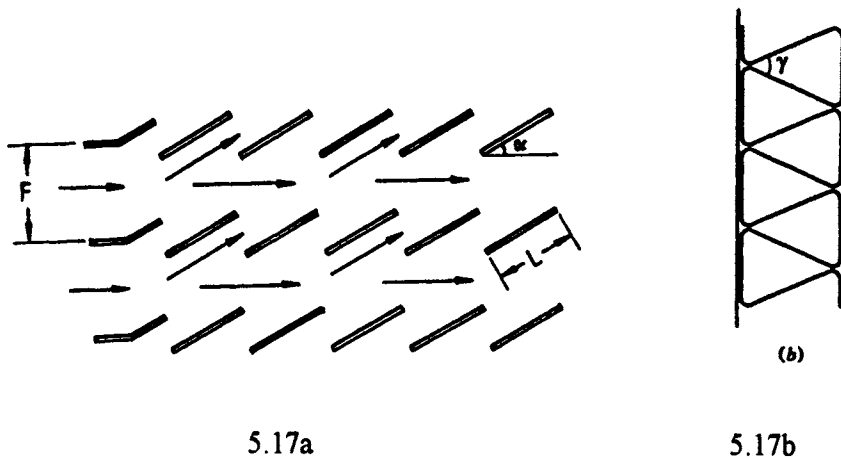
$$j = StPr^{2/3} = 1.18(\beta/\alpha)Re_L^{-0.58}Pr^{2/3} \quad (5.58)$$

As an example, for $Re_L = 200$, $Pr = 0.7$, $\alpha = 25^\circ$, $F = 3$ mm, $L = 2$ mm, equation 5.56 gives $\beta = 21.96$, and equation 5.59 gives $j = 0.038$.

It is often useful, for optimisation purposes, to evaluate the Reynolds number Re_L^* below which the j factor begins to flatten. Cowell et al. showed that this could be approximated well by

$$Re_L^* = 4860/[0.936 - 1.76(F/L) + 0.995\alpha]. \quad (5.59)$$

For the above example, $Re_L^* = 221$.



5.17a

5.17b

Figure 5.17 Form of louvred fin geometry tested by Davenport (1980)

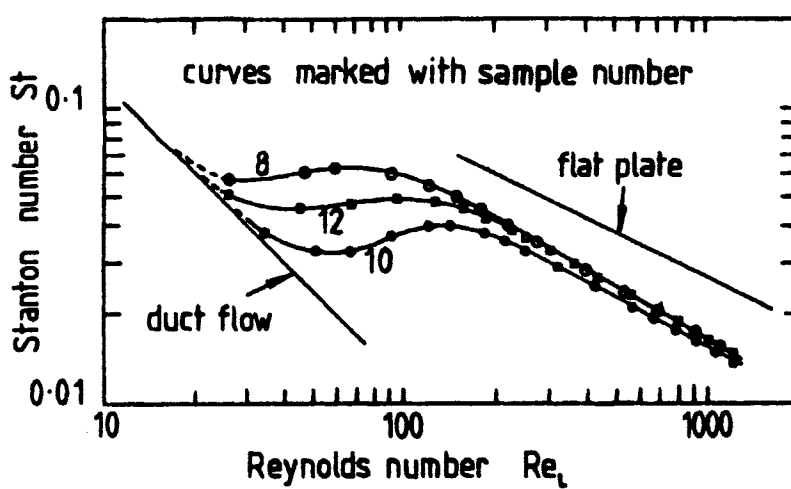


Figure 5.18 Deterioration of flat plate flow to duct flow (Achaichia and Cowell (1988)), used with permission.

A more recent, generalised pair of correlations which take account of all of the relevant geometrical variations are those of Chang and Wang (1997) and Chang et al. (2000). These also draw from a larger data set than any previous correlations and have a high accuracy. The geometrical data are given in Figure 5.19.

For the friction factor, Chang et al. (2000) give

$$f = f_1 f_2 f_3 \quad (5.60)$$

where

$$f_1 = 14.39 Re_{Lp}^{(-0.805 F_p / F_l)} (\ln(1.0 + (F_p / L_p)))^{3.04} \quad Re_{Lp} < 150 \quad (5.61)$$

$$f_1 = 4.97 Re_{Lp}^{0.6049 - 1.064 / \theta^{0.2}} (\ln((F_1 / F_p)^{0.5} + 0.9))^{-0.527} \quad 150 < Re_{Lp} < 5000 \quad (5.62)$$

$$f_2 = (\ln((F_1 / F_p)^{0.48} + 0.9))^{-1.435} (d_h / L_p)^{-3.01} (\ln(0.5 Re_{Lp}))^{-3.01} \quad Re_{Lp} < 150 \quad (5.63)$$

$$f_2 = ((d_h / L_p) \ln(0.3 Re_{Lp}))^{-2.966} (F_p / L_l)^{-0.7931(T_p / T_h)} \quad 150 < Re_{Lp} < 5000 \quad (5.64)$$

and

$$f_3 = (F_p / L_l)^{-0.308} (F_d / L_l)^{-0.308} (e^{-0.1167 T_p / d_m}) \theta^{0.35} \quad Re_{Lp} < 150 \quad (5.65)$$

$$f_3 = (T_p / d_m)^{-0.0446} \ln(1.2 + (L_p / F_p)^{1.4})^{-3.553} \theta^{-0.477} \quad 150 < Re_{Lp} < 5000 \quad (5.66)$$

83% of data were correlated to within $\pm 15\%$ by the above relationships

For the j factor, Chang et al. give

$$j = Re_{Lp}^{-0.49} \left(\frac{\theta}{90} \right)^{0.27} \left(\frac{F_p}{L_p} \right)^{0.14} \left(\frac{F_l}{L_p} \right)^{-0.29} \left(\frac{T_d}{L_p} \right)^{-0.23} \left(\frac{L_l}{L_p} \right)^{0.68} \left(\frac{T_p}{L_p} \right)^{-0.28} \left(\frac{\delta_f}{L_p} \right)^{-0.05} \quad (5.67)$$

which correlates 89% of data to within 15%:

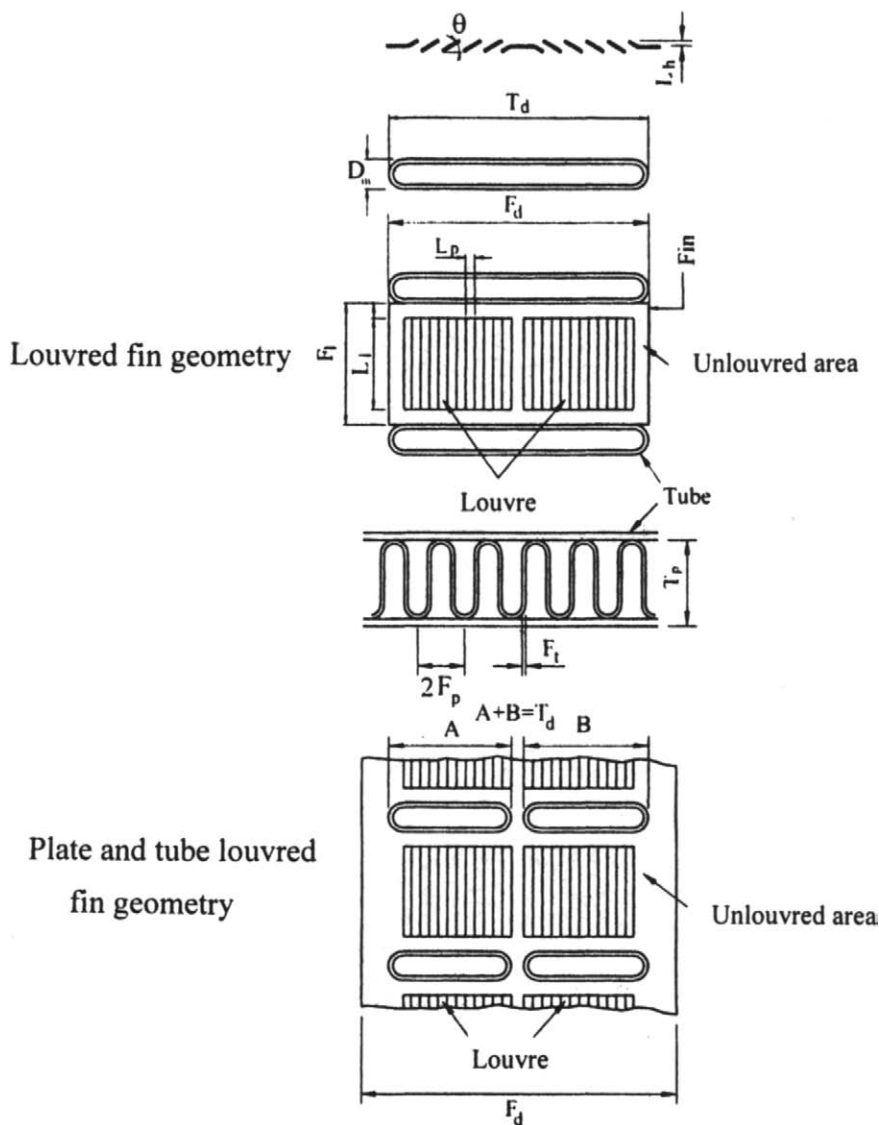


Figure 5.19 Geometrical data for Chang et al (2000) correlation, used with permission,

A less formidable approximation given by Chang et al. is

$$j = 0.425 Re_{Lp}^{-0.496} \quad (5.68)$$

which correlates 70% of the data within 15% and affirms the dominating flow model of simultaneously developing laminar flow on a flat plate (the louvre), which in isolation would give $j = 0.664 Re_{Lp}^{-0.5}$, the difference in initial constant reflecting (largely) the proportion of un-louvred surface.

Convex Louvre Fin

A more recently- developed form of louvre is that of the convex louvre fin, as described by Hatada and Senshu (1984), and shown in Figure 5.20.

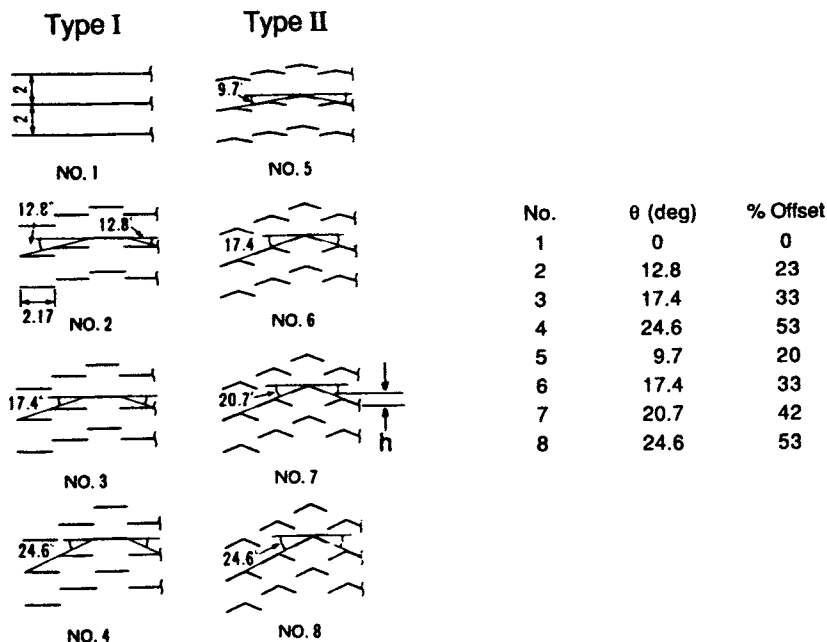


Figure 5.20 Fin geometries for convex louvre fin
(from Hatada and Senshu (1984)), reprinted from Webb (1994).
Copyright © (John Wiley & Sons, Inc.). Reprinted by permission
of John Wiley & Sons, Inc.)

The correlation given for their data is

$$j = 0.4529 Re_{dh}^{-0.433} \quad (5.69)$$

$$f = 2.233 Re_{dh}^{-0.4735}$$

with Re_{dh} based on hydraulic diameter and maximum throughflow velocity, and for a fin frequency of 500/m. other geometrical details are as shown in the figure.

PRESSED PLATE TYPE SURFACES

The best known example of pressed plate surface is that of the plate and frame exchanger, the plate (see chapter 2) of which employs a number of variants of a chevron- corrugated form. Variations are in both the form of chevron pattern and also the detailed shape of the corrugation itself. A typical corrugation shape is shown in Figure 5.21. An important parameter describing the corrugation form is the chevron angle ϕ , which, as shown in Figure 5.22, is the angle between the overall flow direction and the line of the corrugation troughs. Thus a 90 degree angle represents normal flow that is, directly across the corrugation, and 0 degrees represents flow along the corrugation. These limits are rarely applied because the pressure containment capability depends on the points of contact of the ridges: the density of these points is highest for a 45 degree angle.

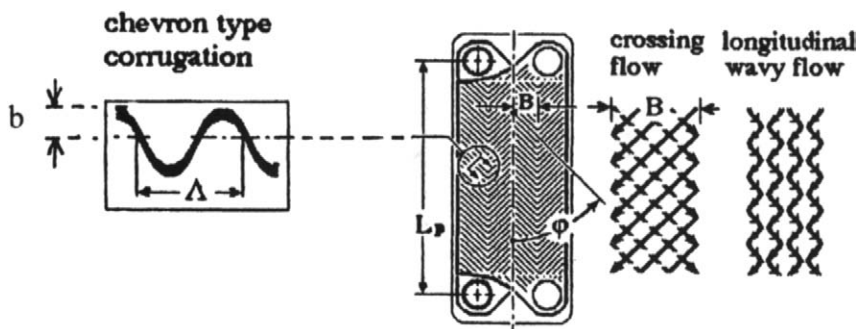


Fig. 5.21 Corrugation shape

Figure 5.22 Geometry of plate with chevron configuration, showing low ϕ (crossing flow) and high ϕ (wavy flow) patterns (from Martin (1995), with permission).

Because of the wide number of commercial variations, with differences in corrugation shape and aspect ratio (width to length ratio), accurate generalized correlations are not possible, and industry relies on specific experimental data for the performance, with most data sources being proprietary. Several representative sets of performance results have been published in the open literature (e.g. Shah et al (1988), Heavner et al (1993)), for typical chevron angles of 30-60 degrees. A good set of equations based on a sound mechanistic model of the flow is that given by Martin (1996, 1999). This uses the generalized Lévêque solution, which is related to the developing thermal boundary layer with a developed (parabolic) velocity profile on a flat plate. In this approach the Nusselt Number is expressed in terms of the friction factor. The friction factor is given as a function of the chevron angle ϕ as

$$\frac{1}{\sqrt{f}} = \frac{\cos \phi}{\sqrt{0.045 \tan \phi + 0.09 \sin \phi + f_0 / \cos \phi}} + \frac{1 - \cos \phi}{\sqrt{3.8 f_1}}, \quad (5.70)$$

where $f_0 = 16/Re$ for $Re < 2000$ (5.71)

$$f_0 = (1.56 \ln Re - 3.0)^{-2} \quad \text{for } Re \geq 2000 \quad (5.72)$$

which are the fully developed laminar and recommended turbulent (smooth) relationships for a circular duct: (the present author prefers $f_0 = 20/Re$ for the fully-developed laminar condition),

and $f_1 = 149/Re + 0.9625$ for $Re < 2000$ (5.73)

$$f_1 = 9.75/Re^{0.289} \quad \text{for } Re \geq 2000 \quad (5.74)$$

The Reynolds number is defined in terms of the hydraulic diameter

$$d_h = \frac{2b}{\Phi}, \quad (5.75)$$

with the area enhancement factor Φ defined as

$$\Phi(X) = \frac{1}{6} \left(1 + \sqrt{1 + X^2} + 4\sqrt{1 + X^2/2} \right), \quad (5.76)$$

and $X = \frac{2\pi b}{\Lambda}$, (5.77)

Λ being the wavelength of the corrugation (see Figure 5.22).

The velocity u in the Reynolds number is defined as

$$u = \frac{\dot{m}}{\rho b B_p}, \quad (5.78)$$

with B_p being the plate width.

The above correlation given by equations 5.71 is quoted by Martin (1999) as being accurate within -50% and $+100\%$ for the corrugation range $10-80^\circ$.

Once the friction factor is found, the Nusselt number is given by Martin as

$$Nu = 0.205 Pr^{1/3} \left(\frac{\eta_m}{\eta_w} \right)^{1/6} (f Re^2 \sin 2\phi)^{0.374} \quad (\text{liquids}) \quad (5.79)$$

and $Nu = 0.205 Pr^{1/3} (f Re^2 \sin 2\phi)^{0.374}, \quad (\text{gases}) \quad (5.80)$

which are accurate to $\pm 20\%$, also for the corrugation range $10-80^\circ$.

Example 5.1

For a Reynolds number of 1000, and with values of $b = 2\text{mm}$, $\lambda = 15\text{mm}$ and $\phi = 60$ degrees, these equations give $f = 0.24$, $Nu = 14.75$ and $j = 0.017$ for a Prandtl number of 0.7. The f/j ratio is accordingly 14.12.

For estimation purposes, the following approximate correlations can be used, based on the data summarised by Hessami (1999), and the trends observed by Focke et al. (1985).

$$j = 0.10 Re^{-0.333} (1 + 0.8(\phi - 30) / 30) \quad (5.81)$$

$$f = 0.63 Re^{-0.23} (1 + 9.0(\phi - 30) / 30) \quad (5.82)$$

with the chevron angle ϕ in degrees. These can be used in the range $1000 < Re < 15,000$. The j factor is largely compatible with the correlation given by Buonopane et al. (1963), of

$$Nu = 0.2536 Re^{0.65} Pr^{0.4} \quad (5.83)$$

An alternative definition of hydraulic diameter suggested by Shah and Focke (1988) is simply twice the plate spacing ($d_h = 2b$), since the developed surface approach used by Martin above is difficult to define for a general corrugation shape.

PLATE AND SHELL SURFACES

These surfaces are essentially in the form of the Chevron plate type described above. The distinction between the distributor and core heat transfer zones, however, is not clear because there is no section with constant flow area. In the absence of specific test information an estimate can be made for heat transfer by taking the effective surface of each plate as that of the rectangle between the nearest edges of the two ports and the edge of the plate, as shown in Figure 5.23. This zone can then be treated in the normal way, using, for example, equivalent dimensions as for the plate and frame approach above. Unless the plate corrugations are specifically developed to avoid preferential flow directly from port to port, however, this treatment is likely to over-predict the thermal performance, and a correction factor should be applied. A value of 0.7 is suggested for this. The pressure drop calculated on a similar basis should be treated with caution.

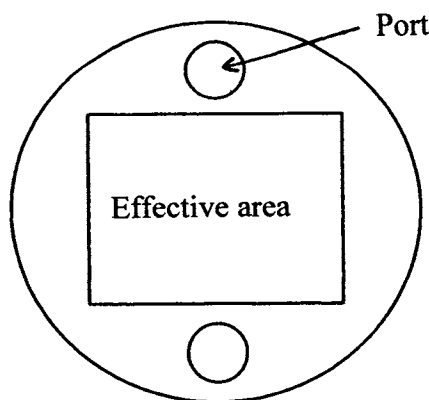


Figure 5.23 Effective surface for plate and shell exchanger

OTHER PLATE-TYPE SURFACES (WELDED PLATES ETC.)

Unless this type of surface is strongly corrugated, it can be treated adequately for scoping purposes as a plain duct of rectangular section with high aspect ratio (such as 8-1), and the corresponding fully-developed laminar or turbulent correlations applied as given above. The hydraulic diameter and flow

length should be applied as usual for developing flow. In the case of pressed plates with regular dimples or small corrugations for plate support, it is recommended that the lengthwise spacing "l" of these corrugations be used for the d_h/l correction in the Gnielinski correlation, in order to simulate the enhancement obtained.

Some highly structured pressed plate surfaces (for example the Compabloc type) have corrugation structures similar to PHE plates, and their performance characteristics are therefore comparable (Roussel (1993)).

PRINTED CIRCUIT HEAT EXCHANGER (PCHE) SURFACES

The basic shape of the PCHE duct closely approximates to a semicircle, as can be seen in Figure 2.12. Although straight channels are sometimes used, the predominant form is laterally corrugated.

Straight channels

For fully-developed laminar flows in a straight channel the following values given above can be used:

$$fRe = 15.78 \quad (5.84)$$

$$Nu_{HI} = 4.089. \quad (5.85)$$

For turbulent and transitional flow, the equation of Gnielinski (1983), equation 5.30 can be used with equation 5.86 for the extremes, with the equations 5.35-5.37 used with caution for transition.

For the corrugated channel for performance will be strongly dependent on the detailed form of the channel. The wavelength to width ratio of a typical channel is about 7. Relating this to the two-dimensional data of Oyakawa et al. (1989), the present author suggests the following approximation:

$$j = 0.125Re^{-0.36} \quad (5.86)$$

$$f = 11.0Re^{-0.53}$$

References

Achaichia, A. and Cowell, T.A., 1988, Heat Transfer and Flow Friction Characteristics of Flat Tube and Louvred Plate Fin Surfaces, *Exp. Thermal Fluid Sci.*, Vol. 1, pp147-157.

Atemani, C.A.C. and Sparrow, E.M., 1980, Turbulent Heat Transfer and Fluid Flow in an unsymmetrically Heated Triangular Duct, *J. Heat Transfer*, Vol. 102, pp. 590-597.

Bhatti, M.S. and Shah, R.K., 1987, Turbulent and Transition Flow Forced Convective Heat Transfer in Ducts, in *Handbook of Single Phase Convective Heat Transfer*, Wiley.

Blasius, H., 1913, Das Ähnlichkeitsgesetz bei Reibenvorgangen in Flüssigkeiten, *Forschg. Arb. Ing.-Wes.*, No. 131, Berlin.

Buonopane, R.A., Troup, R.A. and Morgan, J.C., 1963, Heat Transfer Design Method for Plate Heat Exchangers, *Chem. Eng. Prog.*, Vol. 59, No. 7, pp. 57-61.

Chandrupatla, A.R. and Sastri, V.M.K., 1978, Laminar Flow and Heat Transfer to a Non-Newtonian Fluid in an Entrance Region of a Square Duct with Prescribed Constant Axial Wall Heat Flux, *Numer. Heat Transfer*, Vol. 1, pp 243-254.

Chen, N.H., 1979, An Explicit Equation for Friction Factor in Pipe, *Ind. Eng. Chem. Fund.*, Vol. 18, pp. 297-297.

Cowell, T.A., Heikal, M.R. and Achaichia, A., 1995, Flow and Heat Transfer in Compact Louvred Fin Surfaces, *Experimental Thermal and Fluid Science*, 10: 192-199.

Davenport, C.J., 1980, Heat Transfer and Fluid Flow in Louvred Triangular Ducts, Ph.D Thesis, CNAA, Lanchester Polytechnic, Coventry, UK.

Dittus, P.W. and Boelter, L.M.K., 1930, Heat Transfer in Automobile Radiators of the Tubular Type, *Univ. Calif. Pub. Eng.*, Vol. 2 No. 13, pp 443-461; reprinted in *Int. Comm. Heat Mass Transfer*, Vol.12, pp. 3-22, 1985.

Filonenko, G.K., 1954, Hydraulic Resistance in Pipes (in Russian), *Teploenergetika*, Vol.1, No 4, pp 40-44

Focke, W.W., Zachariades, J., and Olivier, I., 1985, The Effect of the Corrugation Inclination Angle on the Thermohydraulic Performance of Plate Heat Exchangers, *Int. J. Heat Mass Transfer*, Vol. 28, pp 1469-1479.

Gnielinski, V. 1983, Forced Convection in Ducts, Section 2.5.1, *Heat Exchanger Design Handbook*, Ed. Hewitt et al., Hemisphere.

Hatada, T. and Senshu, T., (1984), Experimental Study on Heat Transfer Characteristics of Convex Louvre Fins for Air Conditioning Heat Exchangers, ASME Paper ASME 84-HT-74.

Heavner, R.L., Kumar, H. and Wannierachchi, A.S., 1993, Performance of an Industrial Plate Heat Exchanger: Effect of Chevron Angle, AICHE Symposium Series, No.295, Vol.89, Heat Transfer Atlanta, pp.262-267.

Hessami, M-A., 1999, The Effects of Corrugation Angle on Heat Transfer and Pressure Loss in a Cross-Corrugated Passage, in Compact Heat Exchangers and Enhancement Technology for the Process Industries, Banff, ed. Shah, R.K., Begell House.

Hong, S.W. and Bergles, A.E., 1974, Augmentation of Laminar Flow Heat Transfer in Tubes by Means of Twisted- Tape Inserts, Tech.Rep.HTL-5, ISU-ERI-AMES-75011, Eng.Res. Inst., Iowa State Univ., Ames.

Martin, H., 1996, A Theoretical Approach to Predict the Performance of Chevron-Type Plate Heat Exchangers. Chem. Egng. Process., Vol 35, pp.301-310.

Martin, H., 1999, Economic Optimisation of Compact Heat Exchangers, in Compact Heat Exchangers and Enhancement Technology for the Process Industries, Banff, ed. Shah, R.K., Begell House.

Nikuradse, J., 1933, Stormungsgesetze in Rauhen Rohren, Forsch. Arb. Ing.-Wes., No361; English translation, NACA TM 1292.

Oyakawa, K., Shinzato, T. and Mabuchi, I., 1989, The Effects of the Channel Width on Heat Transfer Augmentation in a Sinusoidal Wave Channel, JSME International Journal, Series II, Vol. 32 no.. 3, 403-410.

Roussel, C., (1993), The Welded and Corrugated Plate Heat Exchanger of the Compabloc Type, in Heat Exchanger Technology, Recent Developments, eds. Marvillet & Vidil, Seminar 33, Eurotherm, Paris, France.

Shah, R.K., 1975, Perforated Heat Exchanger Surfaces: Part 2- Heat Transfer and Flow Friction Characteristics. ASME Paper 75-WA/HT9.

Shah, R.K. and Focke, W.W., 1988, Plate Heat Exchangers and their Design Theory, in Heat Exchanger Equipment Design, Hemisphere.

Sparrow, E.M. and Hossfeld, L.M., 1984, Effect of Rounding of Protruding Edges on Heat Transfer and Pressure Drop in a Duct. *Int. J Heat Mass Transfer*, 27, 10, 1715-1723.

Stephan, K, 1959, Wärmeübergang und Druckabfall bei nicht ausgebildeter Laminar- Stromung in Rohren und in ebenen Spatten, *Chem.-Ing.-Tech.*, Volume. 31, 773-778.

Tanaka, T., Itoh, M., Kudoh, M. and Tomika, A., 1984, Improvement of Compact Heat Exchangers with Inclined Louvred Fins, *Bull. JSME* 27, (224), pp. 219-226.

Techo, R., Tickner, R.R. and James, R.E., 1965, An Accurate Equation for the Computation of the Friction Factor for Smooth Pipes for the Reynolds Number, *J. Appl. Mech.*, Vol. 32, p443.

Webb, R. L., 1994, *Principles of Enhanced Heat Transfer*, John Wiley & Sons, New York.

Wibulwas, P., 1966, *Laminar Flow Heat Transfer in Non-Circular Ducts*, Ph.D Thesis, London Univ.

Wibulwas, P. and Tangsirimonkol, P., 1978, Laminar and Transition Forced Convection in Triangular Ducts with Constant Wall Temperature , Unpublished paper, London University.

Chapter 6

THERMAL DESIGN

*Genius which means the transcendental capacity
of taking trouble, first of all.*

Thomas Carlyle

INTRODUCTION

This chapter gives an introduction to compact heat exchanger design and in particular how the size and shape of the exchanger are affected by the thermal requirements

Most compact heat exchangers are formed of layers of plates or finned channels of fixed length and width. The surface shape of the plate or it's finning determines the surface performance, which is described by non-dimensional heat transfer coefficient and friction factor relationships. Thus a feature of design is to determine a channel size and then find the number of layers to meet the duty. For the specialised cases of plate and frame exchangers and other welded plate products, the plate sizes are already specified in ranges by the manufacturers. The design problem is then confined to selecting the most appropriate size and the number of plates. This *selection* process is readily achieved by adaptation of the procedure given here, and thermal design of new plates could be approximated (complete design needing data on the thermal and pressure drop performance of the distributor sections).

In the following development it is assumed for the sake of brevity that the fluid properties are constant throughout the exchanger, and are evaluated for each stream at an appropriate mean temperature. An outline of the approach for a more realistic situation which allows for property variation is also given.

The main methods of heat exchanger design and analysis are those of the Logarithmic Mean Temperature Difference (LMTD) method, the Effectiveness-Number of Transfer Units (ϵ - Ntu) method, and the P- Ntu method, the latter being a variant of the ϵ - Ntu method, specifically developed for shell and tube exchangers, and which indeed preceded the ϵ - Ntu method (Shah (1983)). The methods can be shown to be mathematically equivalent to each other. In the description here for single-phase flows the major attention is confined to the ϵ - Ntu method as it has distinct advantages in some aspect of design and analysis,

and is also physically easier to understand and interpret. An outline of the LMTD method is also given.

Boiling and condensing flows in compact passages are the subject of increasing research attention, stimulated partly by their long term application in cryogenic duties, and partly by the outstanding success of the brazed plate heat exchanger in low to medium power (to 100kW) refrigeration systems. A summary of the design method and recommended correlations is given. Finally, the approach for designing exchangers with endothermic or exothermic reaction is outlined.

The methods described here will be adequate for most practical design purposes. For rapid design, and for some scoping or comparison purposes, the method of Polley et al. (1991) can be used: this makes use of single power law relationships of Colburn j factor and friction factor with Reynolds number. A much more comprehensive treatment of the core design is given by Smith (1997).

FORM OF SPECIFICATION

A heat exchanger by definition exchanges heat, or, more generally, exergy (Sekulic (1990)) between two or more streams. In process applications with two streams one stream, the process stream, may be heated or cooled by a service or utility stream. The process stream flow rate, its upstream and downstream temperatures (or heat load), and allowable pressure drop are often specified closely. In these cases the service stream may only have its inlet temperature specified, for example, and part of the design problem is to find the most economic value for its flow rate and for the heater/ cooler. More often heat is to be exchanged between two process streams of given flow rates and given inlet temperatures, and the minimum approach or "pinch" temperature (see below) is an important design criterion.

Pressure drop of either or both streams may be specified. In some cases there may be a pressure drop availability in a stream, arising from process requirements, which can be "used up" by the heat exchanger. More often the allowable pressure drop is determined by system constraints such as the available pump head. For gas streams this can be critical, and the corresponding pumping power is often a limiting factor; this is rarely the case with liquid streams. For certain applications a full thermodynamic second law analysis of the system is necessary to determine the economic relationship between size, thermal duty and pressure drop, as outlined in chapter 3.

BASIC CONCEPTS AND INITIAL SIZE ASSESSMENT

When the thermal and pressure drop specification has been fixed, it is possible to ascertain quickly whether the most appropriate flow configuration is that of crossflow, counterflow, or often multipass overall counterflow arrangements. We will examine first the effectiveness design approach, and then the Log Mean Temperature Difference (LMTD) approach.

The effectiveness method

For each stream, the rate equation is, for hot and cold streams respectively,

$$\begin{aligned}\dot{Q} &= \dot{m}_h c_{p,h} (T_{h,out} - T_{h,in}) \\ \text{and} \\ \dot{Q} &= \dot{m}_c c_{p,c} (T_{c,out} - T_{c,in}).\end{aligned}\tag{6.1}$$

The product $\dot{m}c$, is often denoted C for convenience, the highest and lowest between the two streams being C_{\max} and C_{\min} . The *ratio of stream capacity rates* is denoted C^* , given by

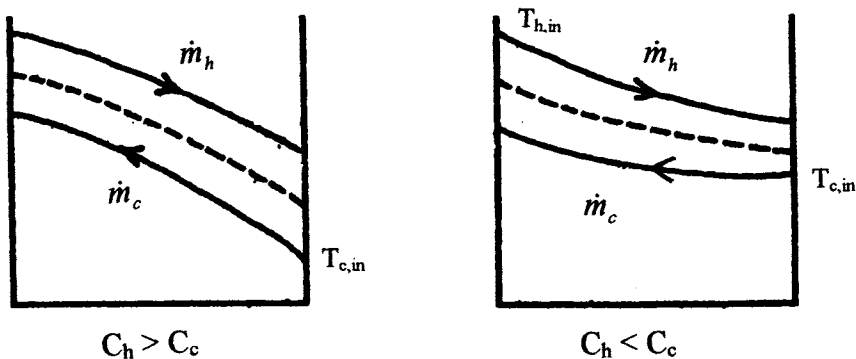
$$C^* = \frac{C_{\min}}{C_{\max}}.\tag{6.2}$$

Typical temperature distributions for common arrangements are shown in Figure 6.1. Note that the curvature changes according to whether C_h or C_c is the C_{\min} stream. If C^* is unity, the exchanger is said to be *balanced*, a condition often approached in gas turbine recuperators, and the distributions would be straight and parallel, provided that the heat transfer coefficients were constant along the length. Representative surface temperature distributions are also shown: these will be closer to the hot stream temperatures if the heat transfer coefficient is higher for the hot stream, a point which will be further developed later.

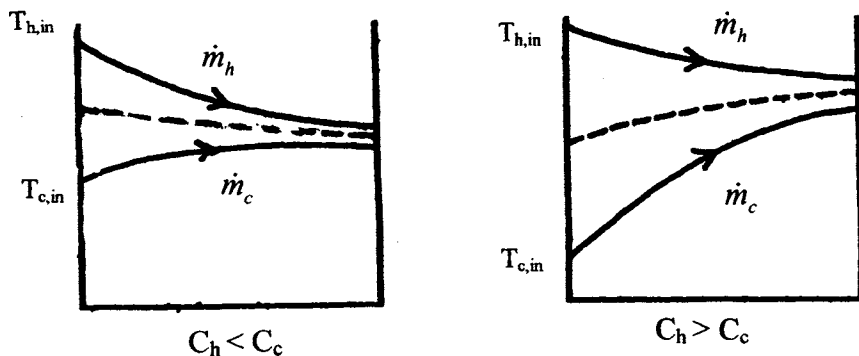
The maximum possible heat exchanged between the streams, \dot{Q}_{\max} , is given by

$$\dot{Q}_{\max} = C_{\min} (T_{h,i} - T_{c,i}),\tag{6.3}$$

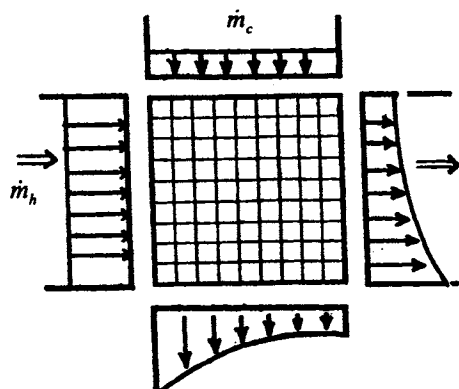
which represents the idealised performance with infinite surface area. This is best described physically with the aid of the idealised temperature distribution diagrams shown in Figure 6.2



(a) Counterflow



(b) Parallel flow



(c) Crossflow (unmixed)

Figure 6.1 Typical temperature distributions in heat exchangers

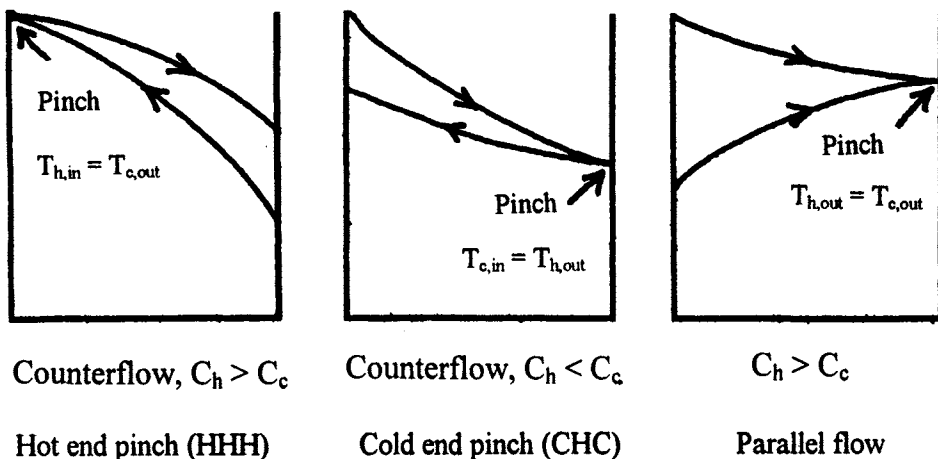


Figure 6.2 Idealised temperature distributions showing the pinch

Clearly the maximum heat transferred is obtained when the stream of lowest heat capacity rate has an outlet temperature equal to the inlet temperature (for a counterflow configuration) of the other stream. For the parallel flow arrangement, the state is reached when both streams attain the same temperature at outlet. In all cases the state corresponds to a theoretically infinite surface area. The point of equal temperatures is called the *pinch point* or simply the *pinch*. In this ideal case it corresponds to zero temperature difference, but in general, especially in the process industries, the *pinch* refers to the minimum temperature difference in the heat exchanger, also referring to the minimum in a heat exchanger network (see chapter 3). It is important for energy targeting.

An acronym for remembering which end of the heat exchanger the pinch is at can be given as:

HHH = Hot fluid has Highest heat capacity rate \rightarrow Hot end pinch

CHC = Cold fluid has Highest heat capacity rate \rightarrow Cold end pinch

From this definition of \dot{Q}_{max} the heat exchanger *effectiveness*, ε , can be given as

$$\varepsilon = \frac{\dot{Q}}{\dot{Q}_{max}} = \frac{C_h(T_{h,i} - T_{h,o})}{C_{min}(T_{h,i} - T_{c,i})} = \frac{C_c(T_{c,o} - T_{c,i})}{C_{min}(T_{h,i} - T_{c,i})}, \quad (6.4)$$

where C_c and C_h are the cold stream and hot stream heat capacity rates respectively, one of which will be C_{min} unless the exchanger is balanced.

Thus the *effectiveness* of the exchanger to be designed can be determined directly from the terminal temperatures, if these are given, and the stream parameters.

The other major relationship needed for this stage is that of the heat exchange equation. This is given by

$$\dot{Q} = (UA_s) \Delta T_m \quad (6.5)$$

where ΔT_m is a suitably averaged temperature difference between streams, usually expressed as the Log Mean Temperature Difference (LMTD) multiplied by a correction factor which depends on the flow configuration, and UA_s is the product of overall heat transfer coefficient and reference surface area¹. This product is often called the heat transfer conductance.

Defining the Number of Transfer Units (Ntu) for the exchanger as

$$Ntu = \frac{UA_s}{C_{mn}}, \quad (6.6)$$

which is a measure of the 'thermal length' of the exchanger (see chapter 4), it can be shown that the effectiveness ϵ is a function of Ntu and C^* , the form of function depending on the flow configuration. The most common are counterflow and crossflow (both streams unmixed) and these are shown below.

For computer-aided design purposes, algebraic relationships are needed, and a selection for the most commonly used configurations is given in Table 6.1.

Figure 6.3 gives a graphic illustration of how the Ntu, giving the product of required area and heat transfer coefficient, is related to the effectiveness, determined by the specified temperatures, and the capacity rate ratio C^* . It is clear from these figures that the configuration makes little difference to the effectiveness if either C^* is low, ($C^* < 0.25$ for example), or Ntu is low (e.g. $Ntu < 1$), the latter implying of course that effectiveness is low. Hence, because of its simplicity, a crossflow design is most appropriate for these cases, most often applying to liquid/gas exchangers, for which the gas side heat transfer coefficient is low and dominates the overall UA_s . If C^* is higher than about 0.25, and especially if the required effectiveness is high ($\epsilon > 0.8$), a counterflow configuration will usually give the most economic design. Figure 6.3c shows that for multipass cross-counterflow the pure counterflow value of effectiveness is

¹ Note that any such value of overall coefficient U has to be uniquely associated with its reference surface area A , but the product UA_s is independent of reference area, having dimensions W/K or kW/K .

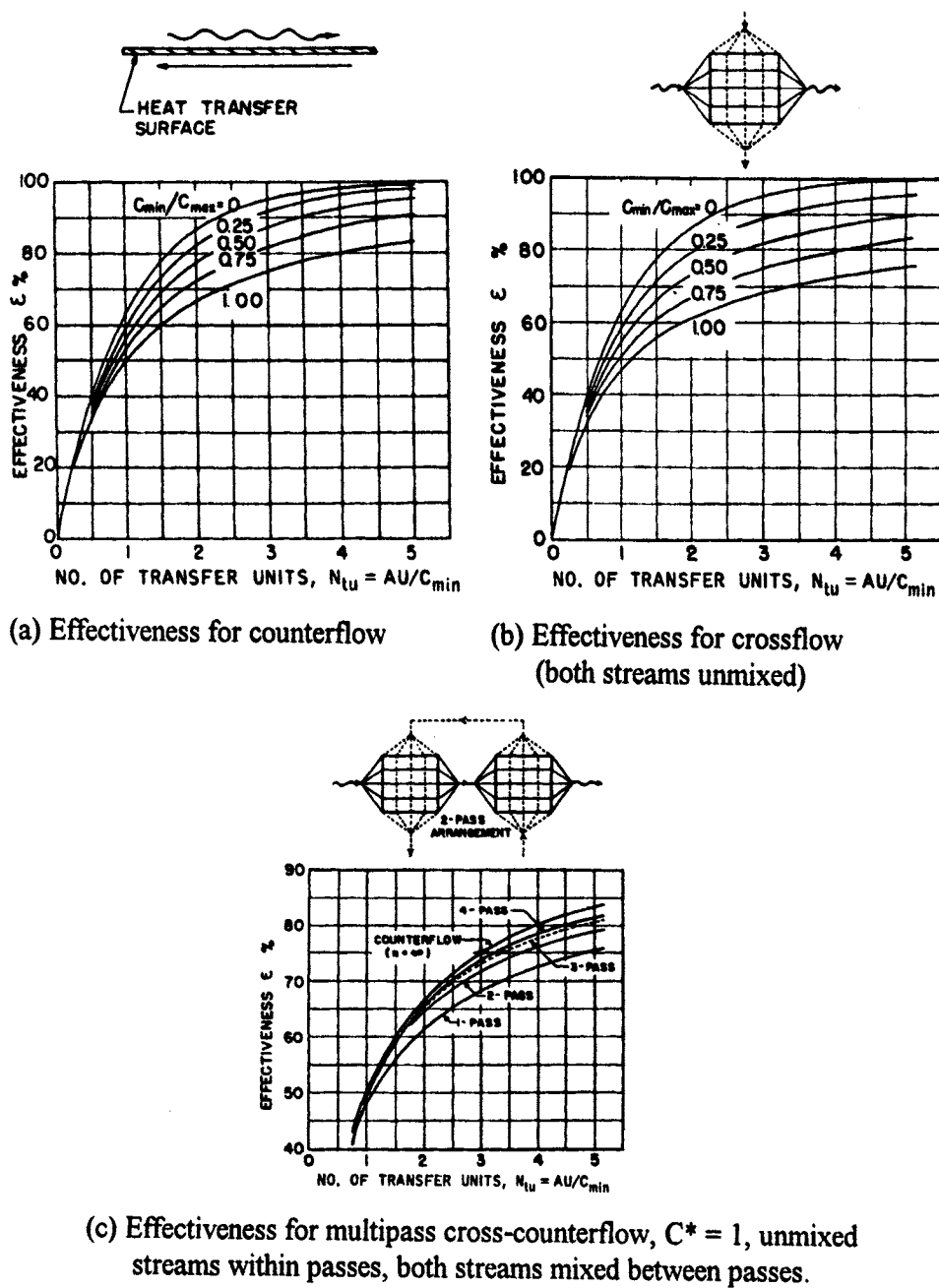


Figure 6.3 Effectiveness versus N_{tu} curves for simple configurations
(From Kays and London Compact Heat Exchangers, 3rd Ed. 1998.

Copyright © 1984, McGraw-Hill Inc., reproduced by permission of Krieger Publishing Company, Malabar, Florida, USA.

closely approached for 3 or more passes, and this is often preferred over the pure counterflow configuration because porting is easier and cheaper (see section on distributors below).

Table 6.1 Effectiveness- Ntu relationships

Counterflow

$$\varepsilon = \frac{1 - \exp(-Ntu(1 - C^*))}{1 - C^* \exp(-Ntu(1 - C^*))}$$

(Asymptotic value = 1 as $Ntu \rightarrow \infty$, for all C^*)

Unmixed crossflow
(approximation from Kays and Crawford (1993))

$$\varepsilon = 1 - \exp\left(\left(\exp\left(-Ntu^{0.78} C^*\right) - 1\right) Ntu^{0.22} / C^*\right)$$

(Asymptotic value = 1 as $Ntu \rightarrow \infty$, for all C^*)

Parallel, or cocurrent flow

$$\varepsilon = \frac{1 - \exp(-Ntu(1 + C^*))}{1 + C^*}$$

(Asymptotic value = $1/(1+C^*)$, for all C^*)

Crossflow, $C_{\min \text{ unmixed}}$

$$\varepsilon = \frac{1}{C^*} \left[1 - \exp\left\{ -C^* [1 - \exp(-Ntu)] \right\} \right]$$

(Asymptotic value = $[1 - \exp(-C^*)]/C^*$ as $Ntu \rightarrow \infty$)

Crossflow, $C_{\max \text{ unmixed}}$

$$\varepsilon = 1 - \exp\left\{ -\frac{1}{C^*} \left[1 - \exp(-NtuC^*) \right] \right\}$$

(Asymptotic value = $[1 - \exp(-1/C^*)]$ as $Ntu \rightarrow \infty$)

Crossflow, both fluids mixed

$$\varepsilon = \frac{1}{\frac{Ntu}{1 - \exp(-Ntu)} + \frac{NtuC^*}{1 - \exp(-NtuC^*)} - 1}$$

(Asymptotic value = $1/(1+C^*)$, for all C^*)

Multipass overall counterflow, fluids mixed between passes

$$\varepsilon = \frac{\left(\frac{1 - \varepsilon_p C^*}{1 - \varepsilon_p} \right)^n - 1}{\left(\frac{1 - \varepsilon_p C^*}{1 - \varepsilon_p} \right)^n - C^*}$$

with n = number of identical passes (i.e. each pass having the same ε_p)
 ε_p = effectiveness of each pass (as a function of $Ntu_p = Ntu/n$)

and

$$\varepsilon_p = \frac{\left(\frac{1 - \varepsilon C^*}{1 - \varepsilon} \right)^{1/n} - 1}{\left(\frac{1 - \varepsilon C^*}{1 - \varepsilon} \right)^{1/n} - C^*}$$

(Limiting value = $\varepsilon_{\text{counterflow}}$, as $n \rightarrow \infty$).

Multipass overall parallel flow, fluids mixed between passes:

$$\varepsilon = \frac{1}{1 + C^*} \left[1 - \left\{ 1 - (1 + C^*) \varepsilon_p \right\}^n \right]$$

All configurations, $C^* = 0$ (for pure condensation and evaporation):

$$\varepsilon = 1 - \exp(-Ntu).$$

Inverse relationships

In scoping calculations the terminal temperatures are often specified, and these directly determine the effectiveness ε . It is then helpful to be able to express Ntu explicitly in terms of ε instead of the vice-versa relationships above. This then gives the overall conductance UA_s , and is directly equivalent to the LMTD method discussed next. Some expressions for simple flow configurations are given in Table 6.2.

Table 6.2 Inverse (Ntu- ϵ) relationships

Counterflow:	$Ntu = \frac{1}{C^* - 1} \ln\left(\frac{\epsilon - 1}{C^* \epsilon - 1}\right)$
Counterflow ($C^* = 1$) :	$Ntu = \frac{\epsilon}{1 - \epsilon}$
Parallel flow:	$Ntu = \frac{-\ln[1 - (1 + C^*)\epsilon]}{1 + C^*}$
Crossflow:	
C_{\max} mixed, C_{\min} unmixed	$Ntu = -\ln\left[1 + \frac{1}{C^*} \ln(1 - C^* \epsilon)\right]$
C_{\max} unmixed, C_{\min} mixed	$Ntu = \frac{-1}{C^*} \ln[1 + \ln(1 - \epsilon)]$
All configurations, $C^* = 0$:	$Ntu = -\ln(1 - \epsilon)$

A further aspect strongly affecting counter- versus crossflow choice is that of pressure drop. These points are further explored in the discussion on mass velocity equation below.

The LMTD Method

This approach utilises the commonly- available knowledge (or specification) of the terminal temperatures. It is easily shown that it is mathematically compatible with the effectiveness- Ntu method, the working equations of one being derivable from those of the other. The method includes design and rating options. These, and the basic analytical approach, are fully treated by Smith (1997). Only a summary will be presented here.

The LMTD design method

The design or sizing problem involves the selection of the heat load \dot{Q} , the inlet temperatures and the two mass flow rates (of the specified fluids), or a

combination with allows the derivation of all four terminal temperatures, as shown in Figure 6.1. At this stage the configuration is not important. The method is predominantly used for the design of shell and tube exchangers (which may be compact- see Figure 1.5).

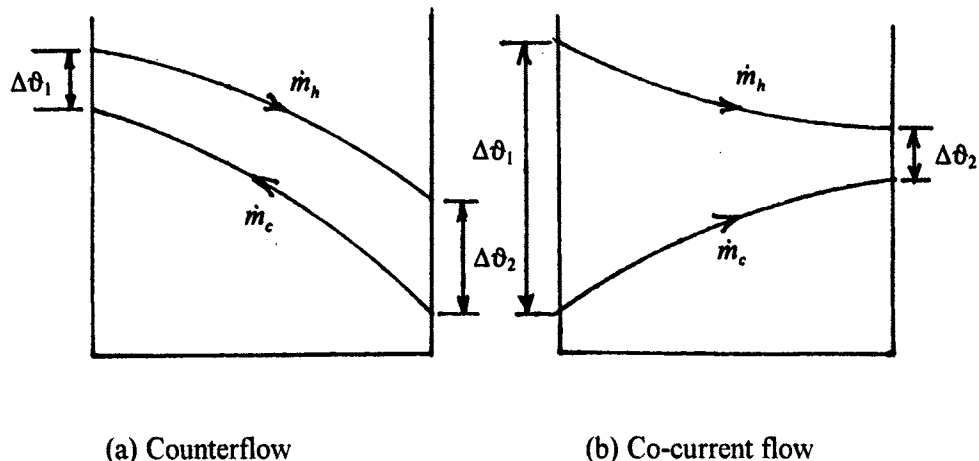


Figure 6.4 Temperature profiles

The essential equation is the heat transfer equation 6.5. The assumption made, as for the effectiveness method, is that the heat transfer coefficients of both sides are constant along the exchanger (or a chosen segment of it if necessary). By consideration of heat flows along the exchanger length it is easily shown that the appropriate mean temperature difference in this equation is

$$\Delta T_{lm} (= \text{LMTD}) = \frac{\Delta \theta_1 - \Delta \theta_2}{\ln(\Delta \theta_1 / \Delta \theta_2)}, \quad (6.7)$$

the $\Delta \theta$ s being the terminal temperature differences regardless of configuration, as shown in Figure 6.4.

For simple exchangers (pure counterflow, pure co-current flow), the required conductance then follows directly:

$$UA_s = \frac{\dot{Q}}{\Delta T_{lm}}. \quad (6.8)$$

For other configurations the LMTD is still used and calculated as if for pure counterflow, but with a correction factor F to reflect the departure from counterflow:

$$\dot{Q} = F(UA_s) \Delta T_{lm} \quad (6.9)$$

Note that F does not represent the effectiveness of the exchanger, so that a high value (close to unity) is not necessarily indicative of a high effectiveness, but merely shows how close the performance is to that of a counterflow exchanger (Shah (1983)) for the specified operating conditions. Although analytical expressions for F for some configurations are available (Shah (1983)), it is usual to use charts.

The use of F for shell and tube design necessitates the introductions of two new variables, which, in contrast to the effectiveness approach, distinguish between shellside and tube side streams. The heat capacity rates are denoted C_s and C_t for shell and tube sides correspondingly, and an effectiveness parameter P is defined as

$$P = \frac{C_{\min}}{C_t} \varepsilon \quad (6.10)$$

so that $P = \varepsilon$ for $C_t = C_{\min}$,
and $P = \varepsilon C^*$ for $C_t = C_{\max}$.

The other parameter needed is the heat capacity rate ratio R , defined as

$$R = \frac{C_t}{C_s}, \quad (6.11)$$

so that $R = C^*$ for $C_t = C_{\min}$,
and $R = 1/C^*$ for $C_t = C_{\max}$.

It is also convenient to define an additional Number of Transfer Units, Ntu , as the overall conductance divided by the tube side heat capacity rate:

$$Ntu_T = \frac{UA_s}{C_t}. \quad (6.12)$$

Thus the relationship between Ntu_T and Ntu based on C_{\min} is (Shah (1983)),

$$Ntu_T = Ntu \frac{C_{\min}}{C_T}, \quad (6.13)$$

and $Ntu_T = Ntu$ for $C_T = C_{\min}$,
 $Ntu_T = Ntu C^*$ for $C_T = C_{\max}$.

Then F can be expressed in terms of R and P by

$$F = \frac{1}{Ntu_T(1-R)} \ln \left[\frac{1-RP}{1-P} \right] \text{ for } R \neq 1 \quad (6.14)$$

$$F = \frac{P}{Ntu_T(1-P)} \quad \text{for } R = 1, \quad (6.15)$$

If equations 6.8 to 6.11 are used for parallel flow it is necessary to use the following expression for F (yielding the Ntu), since for this configuration the LMTD is defined in terms of the inlet and outlet terminal temperature differences of each stream:

$$F = \frac{R+1}{R-1} \frac{\ln[(1-RP)/(1-P)]}{\ln[1-(1+R)P]}. \quad (6.16)$$

In terms of effectiveness ε and C^* , using equations 6.9, 6.14 and 6.15 above,

$$F = \frac{Ntu_{cf}}{Ntu} \quad (6.17)$$

where Ntu_{cf} is the corresponding value for pure counterflow;

$$F = \frac{1}{Ntu(1-C^*)} \ln \left(\frac{1-C^*\varepsilon}{1-\varepsilon} \right) \quad \text{for } C^* \neq 1 \quad (6.18)$$

$$F = \frac{\varepsilon}{Ntu(1-\varepsilon)} \quad \text{for } C^* = 1. \quad (6.19)$$

Thus in design for most configurations other than pure counterflow and parallel flow, the required Ntu, giving UA_s , can only be found implicitly by solving iteratively for F : for a crossflow exchanger with one fluid mixed and for 1-2 parallel counterflow with shell fluid mixed an explicit relation between Ntu and ϵ allows a corresponding direct solution for Ntu in terms of P and R . Figure 6.5 shows this F - P relationship. Shah (1983) recommends that exchanger designs should avoid the steep (high Ntu) regions of the graph, for good utilisation of surface area, and in addition that F should not be less than the value F_{\min} superimposed on the figure in order to avoid a temperature cross in this arrangement.

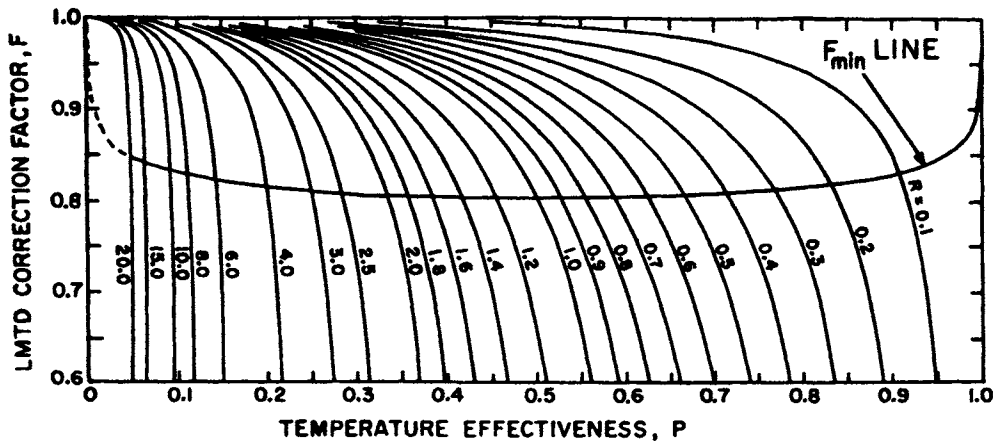


Figure 6.5 Correction factor (F) versus P curves for a 1-2 parallel-counter flow exchanger
(Shah (1983) with permission)

Overall conductance

For either effectiveness or LMTD approaches it is now necessary to expand on the formation of overall conductance UA_s . This is defined in terms of the individual heat transfer coefficients α and areas A_s as

$$\frac{1}{UA_s} = \frac{1}{(\eta_o \alpha A_s)_h} + \frac{1}{(\eta_o \alpha_f A_s)_h} + \frac{t}{\lambda_m A_{sw}} + \frac{1}{(\eta_o \alpha A_s)_c} + \frac{1}{(\eta_o \alpha_f A_s)_h}, \quad (6.20)$$

which is the sum of the reciprocals of the hot stream, wall and cold stream, and fouling or scale conductances on both sides, or simply the sum of the component *heat transfer resistances*. It is convenient to write

$$R_{f,h} = \frac{1}{(\eta_o \alpha_f A_s)_h} \text{ and } R_{f,c} = \frac{1}{(\eta_o \alpha_f A_s)_c} \quad (6.21)$$

for the fouling resistances, related to the fouling thicknesses by:

$$R_{f,h} = \left(\frac{t_f / \lambda_f}{\eta_o A_s} \right)_h \text{ and } R_{f,c} = \left(\frac{t_f / \lambda_f}{\eta_o A_s} \right)_c, \quad (6.22)$$

where the t_f s and λ_f s are the fouling thicknesses and conductivities respectively (see chapter 7 for a discussion of fouling resistances). Note that there is an implicit assumption here that the fouling layers are uniform on the surface(s), which may be far from reality. However, the instances in which a highly non-uniform distribution is expected may well be known to the experienced designer, and can therefore be taken into account. Normally the error incurred in the assumption is relatively small.

If there are no fouling layers equation 6.20 simplifies to

$$\frac{1}{UA} = \frac{1}{(\eta_o \alpha A_s)_h} + R_w + \frac{1}{(\eta_o \alpha A_s)_c}, \quad (6.23)$$

where the wall resistance is

$$R_w = \frac{t}{\lambda_m A_w} \text{ for a plane wall, and} \quad (6.24a)$$

$$R_w = \frac{\ln(d_o/d_i)}{2\pi\lambda_w L N_T} \text{ for a circular tube,} \quad (6.24b)$$

where the $d_{o,i}$ are the outer and inner tube diameters, L is the tube length and N_T is the number of tubes in the exchanger. For thin-walled tubes a satisfactory approximation to this case is

$$R_w = \frac{t_w}{\lambda_m A_m}, \quad (6.24c)$$

where t_w is the tube wall thickness ($= (d_o - d_i)/2$) and A_m is the area evaluated at the arithmetic mean diameter ($A_m = \pi L N_T (d_o + d_i)/2$).

It is clear that the resistances operate in a similar way to electrical resistances in series, the temperature difference being the driving potential, directly analogous to the voltage, and the heat flow, constant through each resistance, analogous to the current, as shown in Figure 6.6.

Note that only in the case of one-dimensional heat flow, that is, with constant area conductive path, is the *heat flux* constant: an important point for heat exchangers but not normally for the electrical analogy.

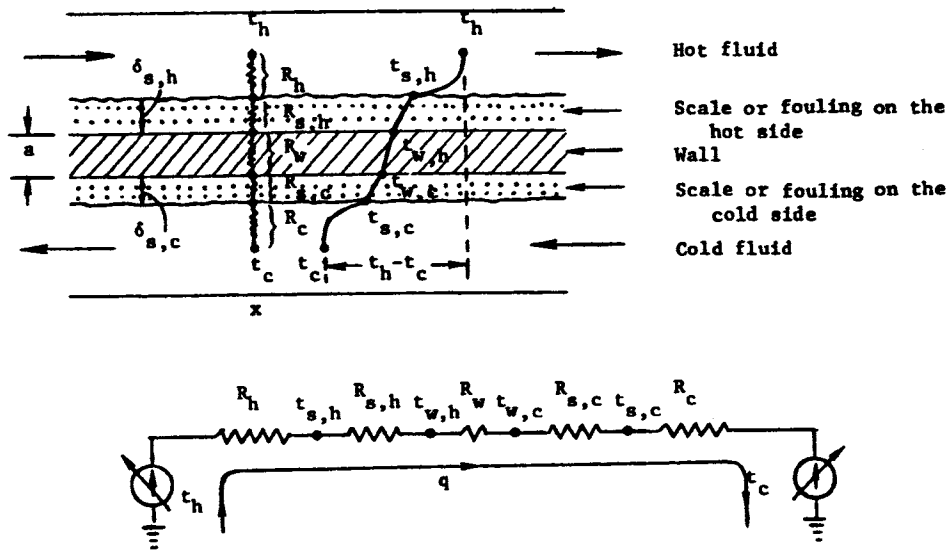


Figure 6.6 Heat transfer resistance analogy
(Shah (1983) with permission)

In many cases the wall resistance is negligible, but with increasing use being made of stainless steels, titanium and nickel alloys, all of which have low conductance, in process exchangers, it is becoming increasingly significant and should be included in the overall Ntu calculation. It can be the dominating resistance for polymer exchangers.

The surface effectivenesses η_o are typically of the order of 0.8 and this value can be used for the first scoping calculation.

The resistance of the largest stream dominates the overall resistance. As mentioned above, if one side is a gas stream, its conductance is likely to be lowest and the resistance highest. This arises because typical heat transfer coefficients (α) for low pressure gases are in the region 50-100 W/m²K, whereas liquid side coefficients are typically 2000-5000 W/m²K. Further details of the relative influence of resistances are given in Berntsson et al (1995). A low coefficient α is usually compensated for by an increase in surface area A_s on that side, in order to obtain a better balanced design, that is, to have closer to equal resistances. This helps to achieve an economic overall design, and explains the practice of combining a plain tube (inside) for liquid flows with a finned or extended surface on the air side of air conditioning and related exchangers. Note that the balancing referred to here is not the same as the balance of heat capacity rates, which is only a function of specified stream variables.

Equation 6.20 above can be expressed in terms of the individual side Ntus ($N_{h,c}$) by

$$Ntu = \frac{1}{C_{min}} \left[\frac{1}{1/(\eta_o \alpha A_s)_h + R_{f,h} + R_w + R_{f,c} + 1/(\eta_o \alpha A_s)_c} \right], \text{ or} \quad (6.25)$$

$$\frac{1}{Ntu} = \frac{1}{N_h (C_h / C_{min})} + \frac{1}{N_c (C_c / C_{min})}, \quad (6.26)$$

neglecting the wall term,

$$\text{where the } N_{h,c}\text{'s are } N_{h,c} = \frac{\eta_o \alpha_{h,c} A_{h,c}}{C_{h,c}}. \quad (6.27)$$

Wall temperature

It is often necessary to know the wall temperature in an application, especially in areas of food processing- to prevent food degradation by excessively high temperatures, or where one stream in the exchanger is a particularly viscous fluid. High temperature applications also require this information for stress calculations. By equating the heat flow through the resistances, it is easily shown (Shah (1983)) that

$$\dot{Q} = \frac{T_h - T_{w,h}}{R_h + R_{f,h}} = \frac{T_{w,c} - T_c}{R_c + R_{f,c}} \quad (6.28)$$

and if the wall resistance is small, so that $T_{w,h} = T_w = T_{w,c}$,

$$T_w = \frac{T_h + \left(\frac{R_h + R_{f,h}}{R_c + R_{f,c}} \right) T_c}{1 + \left(\frac{R_h + R_{f,h}}{R_c + R_{f,c}} \right)}. \quad (6.29)$$

For clean fluids the fouling resistances $R_{f(h,c)}$ are negligible, giving

$$T_w = \frac{T_h/R_h + T_c/R_c}{1/R_h + 1/R_c} = \frac{(\eta_o \alpha A_s)_h T_h + (\eta_o \alpha A_s)_c T_c}{(\eta_o \alpha A_s)_h + (\eta_o \alpha A_s)_c}. \quad (6.30)$$

The wall temperature clearly approaches the hot or cold stream temperature if there is a large mis-match of conductances, represented by $(\eta_o \alpha A_s)_h / (\eta_o \alpha A_s)_c \gg 1$ or $(\eta_o \alpha A_s)_h / (\eta_o \alpha A_s)_c \ll 1$ respectively. This condition is approached of course in many low-pressure gas to condensing or evaporating liquid applications.

We can now consider the design of the individual side, which involves linking the thermal and pressure drop requirements in the *core mass velocity equation* introduced in chapter 4.

The core mass velocity equation

For the side chosen we now drop the suffix h or c, and the N's in the following equations are simply N_h , N_c as discussed above.

The core mass velocity equation is, from chapter 4:

$$\frac{2\rho\Delta p}{\dot{m}^2} = \frac{fPr^{2/3}N}{jA_c^2}, \quad \text{and} \quad \frac{G^2}{2\rho\Delta p} = \frac{j/f}{Pr^{2/3}N}, \quad (4.13)$$

G being the mass velocity. For laminar flows

$$\frac{2\rho\Delta p}{\dot{m}^2} = \frac{NPr}{A_c^2} \frac{k}{Nu}, \quad \text{and} \quad \frac{G^2}{2\rho\Delta p} = \frac{Nu/k}{PrN}, \quad (4.28)$$

where the friction factor is given by $f = k / Re$. (4.34)

As noted earlier, for given conditions of Pr , N , ρ and Δp , it is clear that G is only a function of j/f , or Nu/k , and most importantly is independent of the hydraulic diameter of the surface. The ratio j/f is only a weak function of Reynolds number, being of the order of 0.2 to 0.3 for most compact surfaces. Thus G , and hence flow area A_c , can be closely estimated from the design specification. Note the difference in Prandtl number exponent.

The operating Reynolds number, with which j/f is a weak function and j is a strong function (see chapter 4) for most surfaces, is, in terms of prescribed side NTU and pressure drop:

$$\frac{Re}{d_h(j/f)^{1/2}} = \frac{1}{\eta} \left(\frac{2\rho\Delta p}{Pr^{2/3}N} \right)^{1/2}, \quad \text{or} \quad \frac{Re}{d_h(Nu/k)^{1/2}} = \frac{1}{\eta} \left(\frac{2\rho\Delta p}{PrN} \right)^{1/2} \quad (\text{laminar}) \quad (6.31)$$

If G has already been calculated as above, we can put simply

$$Re = \frac{Gd_h}{\eta} \quad (6.32)$$

Note that this estimation of G effectively determines the throughflow velocity, which is also reflected in equation 6.32, since this velocity is proportional to Re/d_h . The velocity is, in addition, responsible for determining the controllable entropy generation rate (see chapter 3), and features in economic optimisation (Martin (1999)).

Face area, volume and aspect ratio

The surface cross-sectional area is linked to the surface porosity σ and is, for conventional and laminar approaches:

$$C_s = \frac{A_c}{\sigma} = \frac{\dot{m}}{\sigma} \left(\frac{f}{j} \right)^{1/2} \left(\frac{Pr^{2/3}N}{2\rho\Delta p} \right)^{1/2}, \quad (\text{or } C_s = \frac{A_c}{\sigma} = \frac{\dot{m}}{\sigma} \left(\frac{k}{Nu} \right)^{1/2} \left(\frac{PrN}{2\rho\Delta p} \right)^{1/2}) \quad (6.33)$$

If the operating Reynolds number has already been calculated, C_s is simply given by

$$C_s = \frac{\dot{m}d_h}{\sigma\eta Re} \quad (6.34)$$

The corresponding volumes, for conventional and laminar cases, are:

$$V = LC_s = \frac{d_h}{\sigma} \left(\frac{f}{j^3} \right)^{1/2} \left(\frac{\dot{m}PrN^{3/2}}{4(2\rho\Delta p)^{1/2}} \right), \text{ or} \quad)$$

$$V = LC_s = \frac{d_h}{\sigma} \left(\frac{k}{Nu^3} \right)^{1/2} \left(\frac{\dot{m}(PrN)^{3/2} Re}{4(2\rho\Delta p)^{1/2}} \right). \quad) \quad (6.35)$$

In each case, the last parameter in parentheses is a function of the specification and is fixed, so the remainder thus gives a direct measure of the influence of the surface on overall compactness. As discussed in Chapter 4, the two practical components of compactness are those of geometry (hydraulic diameter and porosity) and that of performance (f/j^3 or k/Nu^3) regardless of scale (although scale enters the former parameter via the operating parameter and Re).

The shape of each block side is described by the aspect ratio parameter $L/C_s^{1/2}$, given by:

$$\frac{L}{C_s^{1/2}} = \frac{\sigma^{1/2} d_h (Pr^{2/3} N)^{3/4}}{\left(j^3 f \right)^{1/4} 4\dot{m}^{1/2}} (2\rho\Delta p)^{1/4}, \text{ or} \quad \frac{L}{C_s^{1/2}} = \frac{\sigma^{1/2} d_h (PrN)^{3/4}}{\left(Nu^3 k \right)^{1/4} \dot{m}^{1/2} \eta} \left(\frac{2\rho\Delta p}{128} \right)^{1/4} \quad (6.36)$$

(conventional)

(laminar)

In a counterflow heat exchanger the value of L would be the same for both streams but A_c and C_s would have different values depending on the second stream specification and the surface used. The overall cross-section would then be the sum of those pertaining to the two streams, so that if the streams were of similar flows (fluids and flow rates) the sides would be balanced and the cross section would be twice that for each side. It is clear that the aspect ratio gives a secondary indication of the likely flow arrangement: if the aspect ratio is significantly greater than 1, the preferred arrangement will be counterflow. Exchangers with unbalanced flows, for example for most liquid to low pressure gas applications, yield very different flow lengths for each side, so pointing towards a crossflow arrangement as the optimum.

DETAILS OF THE DESIGN PROCESS

The effect of temperature-dependent fluid properties

The basic design processes described in this chapter make the implicit assumption that physical properties are uniform throughout the exchanger, since, for example, Reynolds number is assumed to be constant in a given passage or duct; but Re depends on viscosity, which in turn depends on temperature. A mean temperature for the evaluation of fluid properties is usually utilised, and for most purposes the arithmetic mean of inlet and outlet temperatures for each side is adequate. For exchangers with $C^* > 0.5$ Shah (1988) recommends $T_{m,cm\min} = T_{m,cm\max} \pm \Delta T_{lm}$, where ΔT_{lm} is the log-mean temperature difference based on terminal temperatures, with the plus sign being used if the C_{\min} side is hot, otherwise the minus sign. The arithmetic mean is used for the C_{\max} side. The density for friction calculations (especially for a gas) should be evaluated after the mean pressure has been calculated, using the gas law, as recommended by Smith (1997).

The above mean property evaluation temperature will serve well for calculation of the heat transfer and friction parameters in cases for which the driving temperature differences are small, in other words for $T_{bulk} \approx T_{wall}$. Fortunately this is commonly the case, low temperature differences being characteristic of compact exchangers. For larger driving temperature differences, the effect depends on whether the stream is a gas (or vapour) or a liquid one. Commonly-used corrections are of the following form (Kays and Crawford (1993)).

For gases, a *temperature* correction is applied:

$$\frac{Nu}{Nu_{cp}} = \frac{St}{St_{cp}} = 1 \quad (6.37)$$

$$\text{and } \frac{f}{f_{cp}} = \left(\frac{T_w}{T_m} \right) \quad (6.38)$$

For liquids, a *viscosity* correction is applied:

$$\frac{Nu}{Nu_{cp}} = \frac{St}{St_{cp}} = \left(\frac{\eta_w}{\eta_m} \right)^{-0.14} \quad (6.39)$$

$$\text{and } \frac{f}{f_{cp}} = \left(\frac{\eta_w}{\eta_m} \right)^{0.5} \text{ for } \frac{\eta_w}{\eta_m} > 1, \quad (6.40)$$

$$\frac{f}{f_{cp}} = \left(\frac{\eta_w}{\eta_m} \right)^{0.58} \text{ for } \frac{\eta_w}{\eta_m} < 1, \quad (6.41)$$

where the suffix cp refers to the property evaluated at the mean temperature defined above, and suffix w refers to the wall temperature. Local wall temperatures can be evaluated by means of equation 6.29 or 6.30.

The above allowance for mean property evaluation is sometimes not adequate because properties may vary in a non-linear way in the temperature range involved. This can particularly be the case when one of the fluids is an oil, with high temperature dependence on viscosity. High Ntu applications may involve a high temperature range. In these cases it is necessary to segment the exchanger into cells, and evaluate mean properties for each cell. This can readily be done if the design process is on a spreadsheet, for example, with a matrix of spreadsheet cells for each exchanger cell, and using an appropriate algorithm locally for those properties subject to variation. Such a procedure is essential for exchangers with these 'long' duties, especially for those used for cryogenic or gases separation plant, and gas turbine recuperators.

Fin efficiency and surface effectiveness

Fin efficiency is defined as the ratio of actual heat flow of the fin to that which would be obtained with a fin of constant temperature uniformly equal to the base surface temperature, that is, with one with infinite thermal conductivity. It is readily found by consideration of the heat flow within the fin together with that from the fin surface (an example of a *conjugate* problem). The fin efficiency η_f for a fin of constant rectangular section (see Figure 6.7) and with constant heat transfer coefficient α over the surface is given by

$$\eta_f = \frac{\tanh(ml)}{ml}, \quad (6.42)$$

where m is a dimensional (L^{-1}) function given by

$$m = \sqrt{\frac{2\alpha}{\lambda_m t_f}} \left(1 + \frac{t_f}{l_f} \right), \quad (6.43)$$

l is the fin length (especially for a triangular fin) or height, l_f is the fin (flow) length, and t_f is fin thickness. This function (equation 6.42) is shown in Figure 6.8, which also shows the corresponding relationships for fins on circular tubes with different radius ratios.

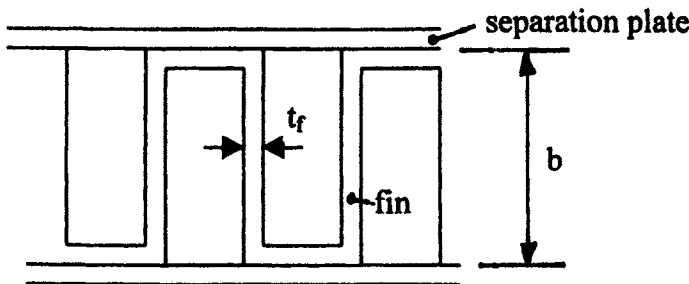


Figure 6.7 Schematic of rectangular fin.

In the case of a plate-fin (PFHE) surface with a rectangular fin, the fin height l used is, from symmetry considerations, the half- height of the effective gap, which is the plate separation b minus the fin thickness t_f .

$$l = 0.5(b - t_f) \quad (6.44)$$

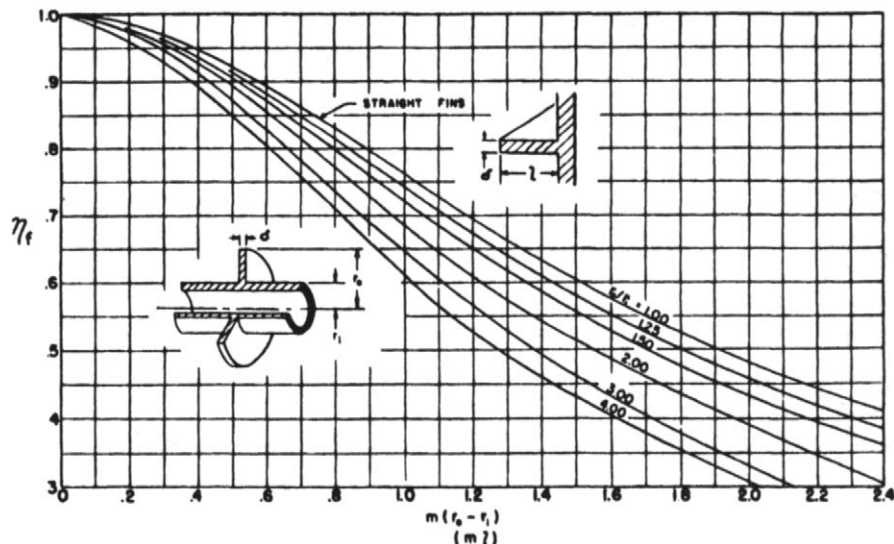


Figure 6.8 Heat transfer effectiveness of straight and circular fins (from Kays & London, Compact Heat Exchangers, 3rd Ed. 1998, Copyright ©1984 McGraw-Hill Inc., reproduced by permission of Krieger Publishing company, Malabar, Florida, USA.)

If the ratio of fin surface area to total area is given as A_f/A_s , the surface effectiveness η_o is defined as the ratio of actual heat flow on the total (that is, primary plus secondary) to the ideal heat flow obtained if both primary and secondary surfaces were at the same temperature. It is easily shown that η_o is given by

$$\eta_o = 1 - (1 - \eta_f) \frac{A_f}{A_s} \quad (6.45)$$

The assumption here is that primary and secondary surfaces have the same heat transfer coefficient. Both this assumption and that of uniform coefficient are strictly invalid, the coefficient being very low (in fact tending to zero) in the corner regions where the fin is joined to the primary or base surface. This is especially the case with fully-developed laminar flow, but is progressively less significant as Reynolds number increases. With high fins of high density, that is, with a high aspect ratio duct shape, the whole primary surface may have a low heat transfer coefficient.

For moderate (e.g. gas side) heat transfer coefficients and for the commonly-used aluminium or especially copper fins, both fin efficiency and surface effectiveness are close to unity, and values of 0.8 or 0.9 are often used for scoping designs. Thus the inevitable error arising from the above assumptions is of minor importance in these cases. In addition, in heat exchanger design practice, the error in most cases is smaller than that of, for example, pressure drop estimation, and the simple relationships above are usually used without modification.

In plate-fin arrangements with mismatched heat capacity rates, it is often necessary to provide much more flow area on one side (usually a low-pressure gas side) to achieve good heat transfer balancing. Double or multiple banking is used for this purpose, as shown in Figure 6.9.

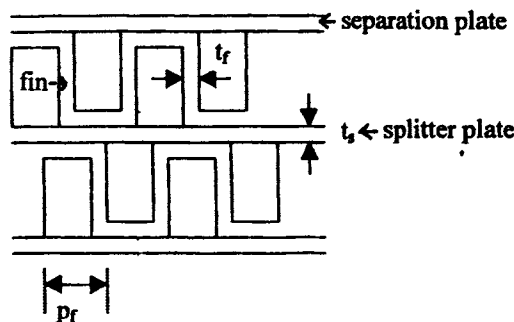


Figure 6.9 Double-banked fin geometry

The relationships for fin efficiency for a symmetrical double-banked arrangement are given by Shah (1985) as

$$\eta_f = \frac{E_1 l_1 + E_2 l_2}{l_1 + l_2} \frac{1}{1 + m_1^2 E_1 E_2 l_1 l_2}, \quad (6.46)$$

$$\text{where } E_1 = \frac{\tanh(m_1 l_1)}{m_1 l_1}, \quad (6.47)$$

with $l_1 = b - t_f + t_s/2$, and $l_2 = p_f/2$, p_f being the fin pitch and t_s being the splitter plate thickness.

Layer stacking and banking factor

In a two- stream exchanger the stacking arrangement is normally simple, good practice being to have the outer layers containing the cold stream to reduce or eliminate the insulation requirements. This results in unequal numbers of hot and cold streams. Sometimes, however, to achieve a well-balanced design it is necessary to have either equal stream numbers, giving one hot outer layer, or unequal numbers the 'wrong' way, with both outer layers hot. In the first, ideal, case, with cold (C) and hot (H) layers in a typical form such as CHCHCHC, the outer C layers receive heat from one side only, in which case their effective fin height is doubled. A banking factor B is defined as

$$B = \left(\frac{\text{effective fin height}}{\text{true fin height}} \right)^2 \quad (6.48)$$

which allows the use of l as the true fin height (Taylor 1990) in equation 6.44 which then becomes

$$m = \sqrt{\frac{2Ba}{\lambda_m t_f}} \left(1 + \frac{t_f}{l_f} \right). \quad (6.43b)$$

Thus at the centre of a block, the banking factor B = 1 (unity), whereas at the outer layers B = 4, giving twice the effective fin height l in equation 6.43. Taylor (1990) recommends that a mean value of 2.25 be used for the block as a whole.

For a double- banked stacking arrangement such as

CHC CHC CHC CHC CHC

there is clear thermal symmetry with no heat flow between the adjacent C streams of each group CHC, and banking factors B of 1 for the H stream and 4 for the C streams will apply.

As mentioned earlier, the PCHE surface is normally treated sufficiently accurately as all-primary, although it is in reality a variable-area all-secondary surface with very thick fins. Certain proprietary surfaces such as the MarbondTM and G-pak[®] slotted-plate structures have secondary and tertiary surfaces, which need special analysis.

Entry and Exit Losses

In the application of friction factor data for surfaces it is implicitly assumed that the pressure drop of each flow is entirely within the matrix. In reality the flows experience abrupt contractions at entry and expansions at exit to the core, from the headers or ducts. These give rise to net increases in pressure drop which are usually small, being of the order of 10% or less for a long duty. For 'short, fat' duties, (i.e. low pressure drop gas duties), these extra losses should be accounted for. Kays and London (1984) gives calculation processes based on systematic tests of a wide range of cores with different porosities.

The basic model of pressure development through a general core is shown in Figure (6.10).

The total pressure drop of a side with straight ducts as shown is

$$\frac{\Delta p}{p} = \frac{G^2}{2} \frac{1}{p_i \rho_i} \left[(1 - \sigma^2 + K_c) + f \frac{4L}{d_h} \rho_i \left(\frac{1}{\rho_m} \right) + 2 \left(\frac{\rho_i}{\rho_o} - 1 \right) - (1 - \sigma^2 - K_e) \frac{\rho_i}{\rho_o} \right], \quad (6.49)$$

with the four terms being the entrance effect, core friction, acceleration and exit effect respectively. The contraction and expansion loss coefficients K_c and K_e are given graphically for parallel plates and square plate-fin surfaces in Figure 6.11. Triangular fins have very similar values to the latter.

Equation 6.49 allows for density changes, which are important for long gas duties but are small for liquids and short gas duties such as in air conditioning and related applications. The mean density can be given by

$$\left(\frac{1}{\rho} \right)_m = \frac{1}{2} \left(\frac{1}{\rho_i} + \frac{1}{\rho_o} \right) \quad (6.50)$$

This will apply for gas duties with a linear temperature distribution ($C^* = 1$), and for liquid duties. For gases with other values of C^* a log-mean temperature

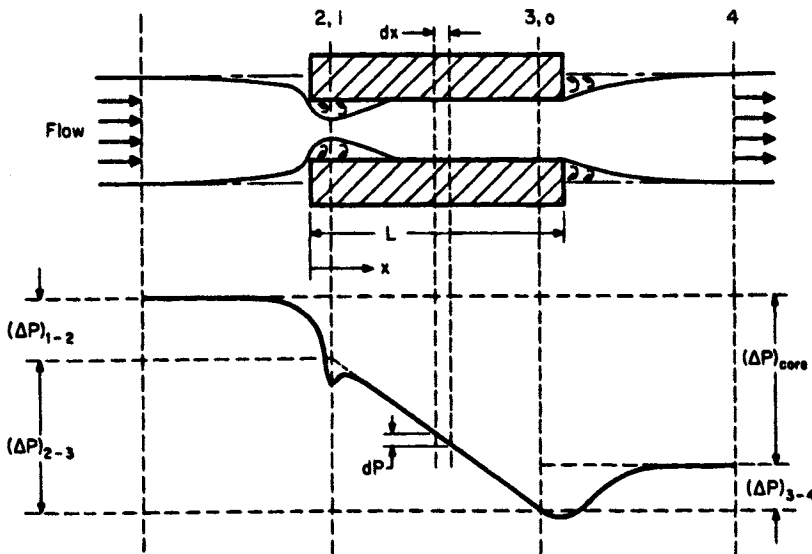


Figure 6.10 Pressure development in one core passage of a plate-fin heat exchanger

(from Shah, R.K.(1985), Compact Heat Exchangers, Part 3 of Handbook of Heat Transfer Applications, ed. Rohsenow, Hartnett and Ganic. Reproduced with permission of The McGraw-Hill Companies.)

T_{lm} should be used together with the mean pressure and the perfect gas law to derive the (log mean) density:

$$\left(\frac{1}{\rho}\right)_m = \frac{R}{p_{ave}} T_{lm}. \quad (6.51)$$

An alternative approach to entry and exit losses is given by Dubrovsky and Vasiliev (1988), using the analytical results of Idel'chik (1986). This approach, which was shown to be of good accuracy for offset strip fin surfaces, is recommended because it avoids the use of graphs- a feature of the Kays and London method.

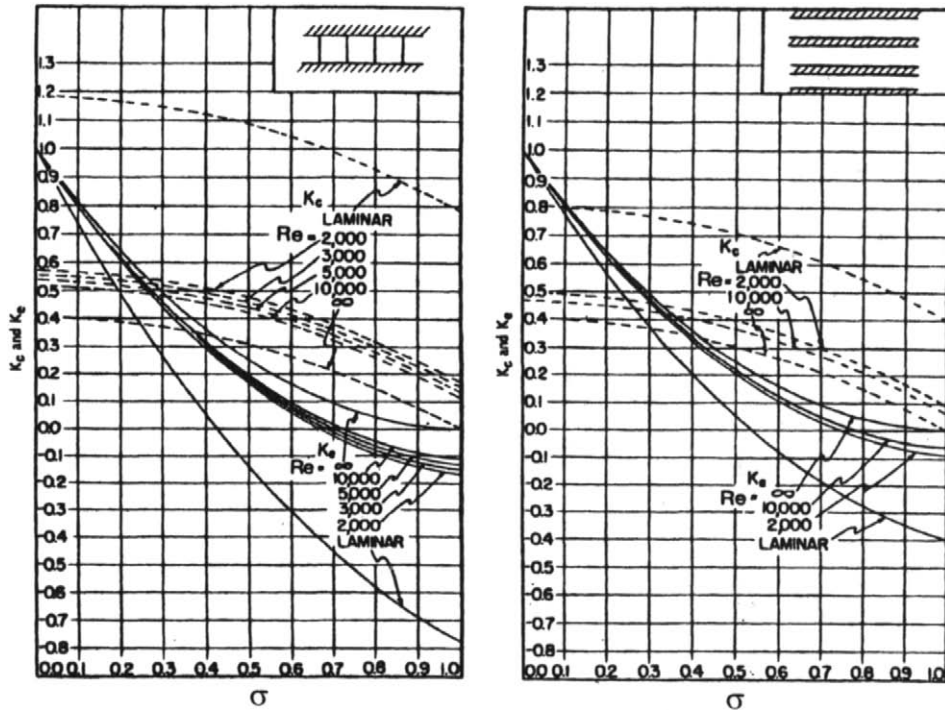
The entry loss coefficient is

$$\xi_{en} = 0.5(1 - \sigma) \quad (6.52)$$

and the exit loss coefficient is

$$\xi_{ex} = (1 - \sigma)^2, \quad (6.53)$$

where the loss coefficients ξ replace the first and last terms in equation 6.49



(a) Multiple-tube flat-duct

(b) Multiple square-tube

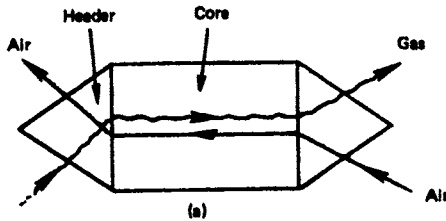
Figure 6.11 Entry and exit loss coefficients,
with abrupt entrance and Expansion

(from Kays and London, Compact Heat Exchangers, 3rd Ed. 1998,
copyright © (1984), reproduced by permission of Krieger Publishing
Company, Malabar, Florida, USA.)

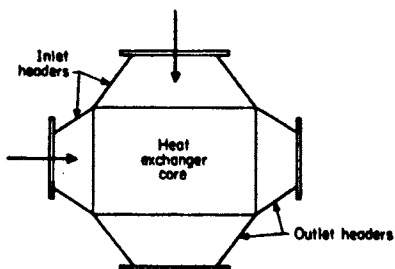
Thermal-hydraulic design of headers and distributors

Principles of selection

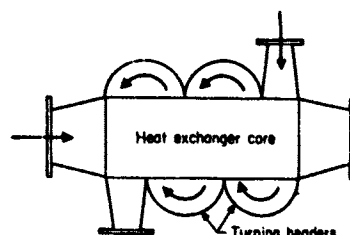
Heat exchangers are connected to their hot and cold streams by means of header systems and/ or distributors, headers being external to the heat exchanger block and distributors usually internal to it, except in the specialised case of refrigerant distributors for evaporator coils. Sometimes when blocks are connected in parallel, an external manifold system is used. A selection of headers and distributors is shown in Figure 6.12.



(a) Counterflow with crossflow header



(b) Crossflow, normal entry



(c) Multipass cross-counterflow with turning headers

Figure 6.12 Header and distributor types
 (from Shah, R.K.(1985), Compact Heat Exchangers, Part 3 of Handbook of Heat Transfer Applications, ed. Rohsenow, Hartnett and Ganic. Reproduced with permission of The McGraw-Hill Companies.)

It is a central problem to the heat exchanger designer to ensure that each stream flows as uniformly as possible into the active part of the block (that is, with equal throughflow velocity across the block face).

In the case of plate and frame and plate and shell exchangers the nozzle connections are normal to the plane of the plates, so each fluid has to be guided to and from the nozzle openings by distributor sections of channels pressed into the plates, as shown in (a). These channels usually have periodic gaps in them to allow equalisation of pressure, to assist obtaining an even flow distribution across the main exchanger block.

Plate-fin exchangers have external header tanks with nozzles welded into them. Because the internal flow is normally in the counterflow configuration, internal distributors are required since one stream must be taken in/out in at least partial crossflow. Some of the distributor configurations used for this purpose are shown in Figure 6.13 others being given by Taylor (1990).

By the use of a combination of Side- Entry (a) or (b), End Entry (Left or Right) and End Entry (Central), up to 5 streams can be accommodated for an all-counterflow configuration. It is clear from the two forms of Side-Entry that the mitred form is superior in having both a higher flow area in the distributor section, giving lower pressure drop, and also a longer thermal section. It also avoids the dead zone as shown. A disadvantage is that it is more expensive since both thermal and distributor sections have to be cut diagonally, which is difficult to accomplish cleanly with offset strip fin corrugations (Taylor (1990)). The End Entry (central) distributor has better distribution than the side entry ones, partly because of its symmetry and partly because the effective passage width is higher, giving lower pressure drop.

The inherent hydraulic problem, common to all configurations, is that the effective sections are triangular, so that the channels have (usually linearly) varying lengths, and hence varying pressure drops. Although gaps in the finning to allow pressure equalization are not in general possible (because they could cause stress concentrations), equalization of pressure is often attained to some degree by the use of perforated finning. Ideally the finning could be made of variable fin spacing to give a constant L/d_h and hence approximately equal pressure drop, but this is not usually practical. A common solution is to configure the exchanger flows for a 'Z' pattern, Figure 6.13, so that all flow paths have equal lengths through the whole exchanger. This of course requires that the pipework connections be on opposite sides of the exchanger, which can be expensive: an alternative is to have a 'C' pattern (Figure 6.13), with connections on the same side, but this means unequal flow lengths and perhaps unacceptable maldistribution.

For many applications involving air or gas flows with short, fat cores (gas turbine recuperators, vehicle and aerospace air conditioning); external (oblique flow) headers are used in a folded core arrangement as shown in Figure 6.14.

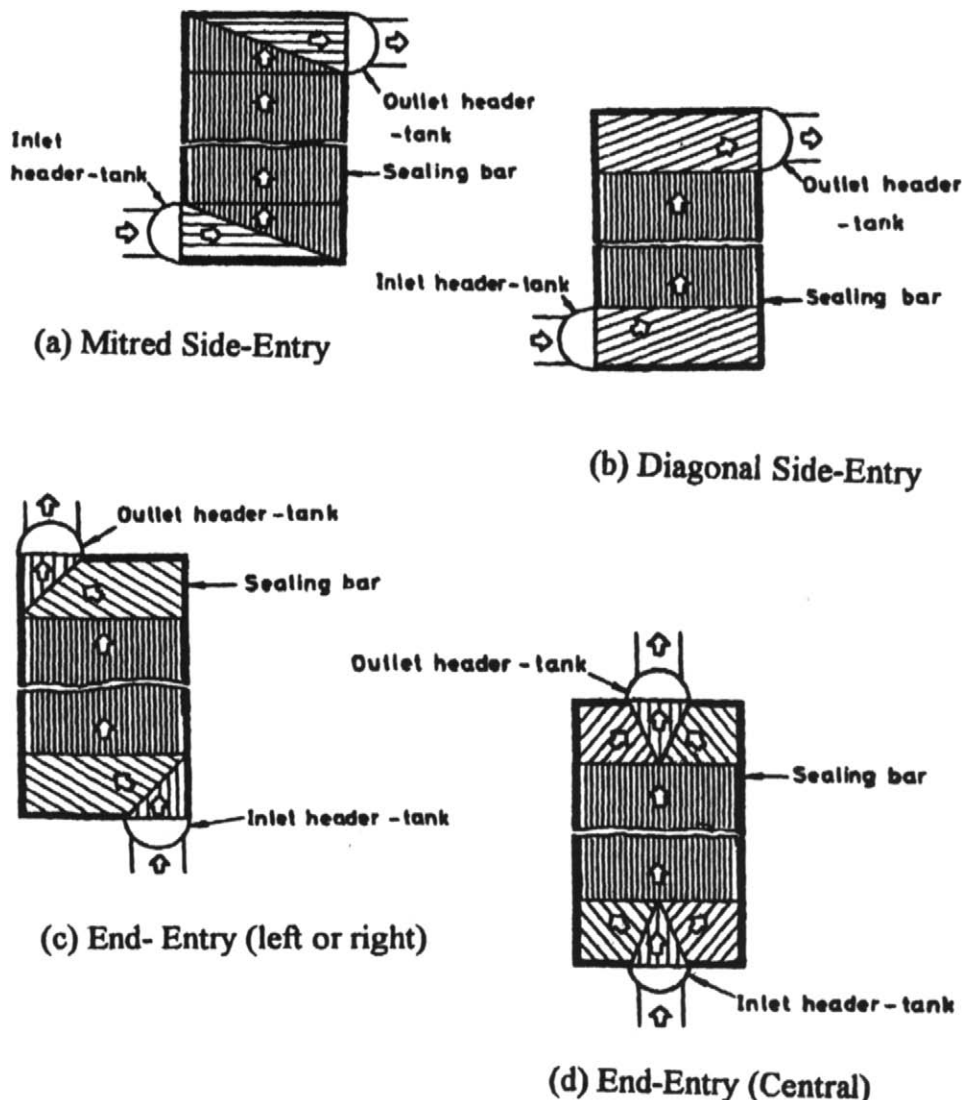


Figure 6.13 Distributors for plate-fin exchangers
(from Taylor (1987), used with permission, HTFS.)

It is noteworthy that the optimum design of header duct shape to obtain uniform flow through the core is the same as that for an array of inclined filters (Moody (1971)), which compact exchangers are sometimes accused (unfairly) of being! This ideal duct shape for the present wider application depends on

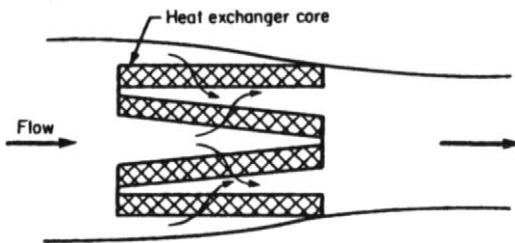


Figure 6.14 Folded core header arrangement for "short, fat" exchanger (from Shah, R.K.(1985), Compact Heat Exchangers, Part 3 of Handbook of Heat Transfer Applications, ed. Rohsenow, Hartnett and Ganic. Reproduced with permission of The McGraw-Hill Companies.)

whether the flow exits on the same or opposite side to the inlet into a rectangular exit header, or alternatively has a free discharge. These configurations are shown in Figure 6.15.

The ideal shapes are given by London et al. (1968) as:

$$\text{Same side exit: } \frac{y}{y_o} = 0.636 \left(\frac{\rho_o}{\rho_i} \right)^{1/2} \quad (6.54)$$

where ρ_i and ρ_o are the inlet and outlet densities respectively. Note that this is a constant width (y), or a box- section, header shape.

$$\text{Opposite side exit: } \frac{y}{y_o} = \frac{1 - X^*}{\left[\left(\rho_i / \rho_o \right) \left(\pi^2 / 4 \right) X^{*2} + \left(y_o / y_i \right) \right]^{1/2}} \quad (6.55)$$

$$\text{Free discharge: } \frac{y}{y_o} = 1 - X^* \quad (6.56)$$

Pressure drop in headers

It is clear from the variation in inlet duct constriction that the same side exit configuration has the lowest mean velocity and hence the lowest total pressure drop (excluding the core). Shah (1985) gives factors of 2.47, 0.59 and 1 velocity

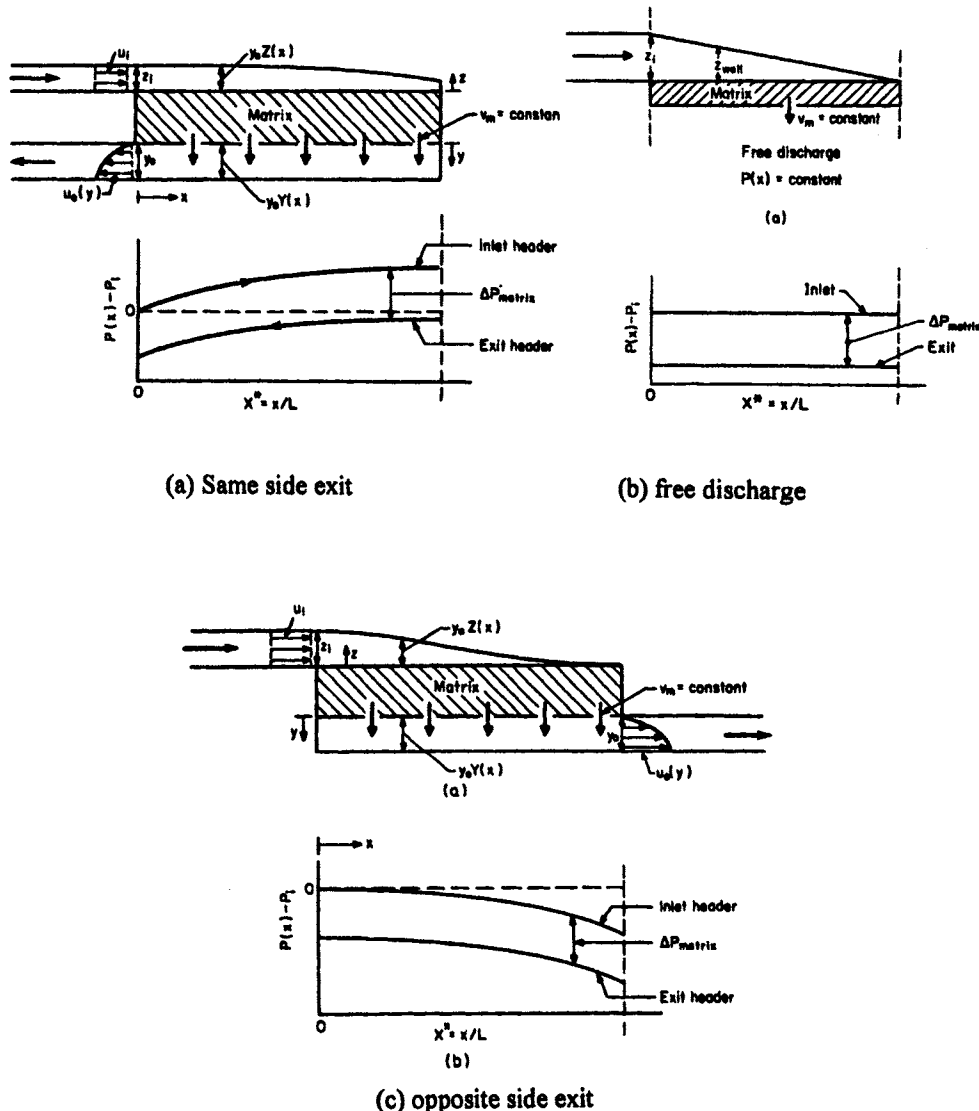


Figure 6.15 External header configurations
 (from Shah, R.K.(1985), Compact Heat Exchangers, Part 3 of Handbook of Heat Transfer Applications, ed. Rohsenow, Hartnett and Ganic. Reproduced with permission of The McGraw-Hill Companies.)

head of the inlet flow $\rho v_i^2 / 2$, for the same side, opposite side and free discharge exit respectively, for equal inlet and outlet header widths y_i and y_o .

Other forms of distributor

Two-phase distributors for all kinds of compact heat exchangers are a specialised problem, and different manufacturers have different approaches. Taylor (1990) gives some typical examples for PFHEs.

In the case of Printed Circuit Heat Exchangers (PCHEs), as shown in fig. 6.16 the distributor channels are chemically etched into the plates in the same process as the thermal section. Great care is taken to ensure that the channel lengths are equal, since the option for inter-connection of the channels for pressure equalisation is not available.

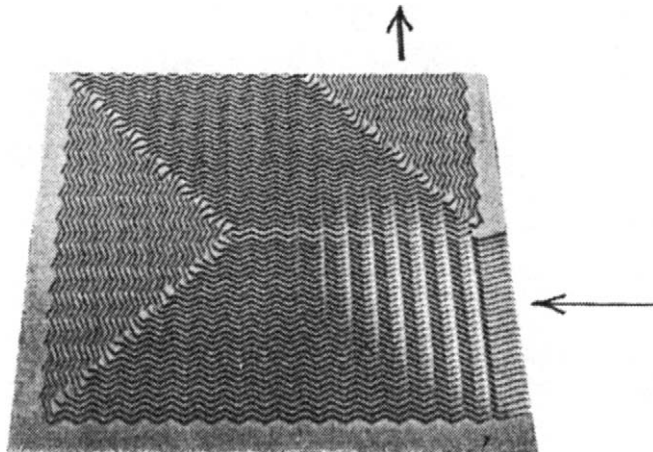


Figure 6.16 Typical distributor design for PCHE
(courtesy Heatic)

For the slotted fin plates of the Marbond™ type, the structure allows for either isolated channels or inter-connected ones depending on the application, as does that of the plate of the PHE.

As pointed out by Taylor (1990), the distributor contribution can dominate the overall pressure loss. This arises largely because the flow area available is much smaller than that of the thermal section. For this reason great caution should be exercised in choosing configurations requiring distributors in applications for which gas or vapour flows are used.

Attention here is focussed on the estimation of the pressure drop; the contribution to thermal performance is often ignored as being very small, and acts as a margin for error. A proviso for this is that the relative pressure drop component of the distributor is likely to be highest for short (low Ntu) duties, for

which the thermal contribution may not be negligible. Kays and Crawford (1993) give a method of analysis for counterflow with crossflow headers.

Friction loss in distributors

The single-phase friction component of pressure drop is calculated in the same way as that of the main surface:

$$\Delta p_d = 4 f_d \left(\frac{l_d}{d_{h,d}} \right) \frac{G_d^2}{2\rho}, \quad (6.57)$$

where the suffix d refers to the distributor. The length l_d is the mean channel length of the finning, and G_d is based on the available flow area.

Momentum losses

Momentum losses occur whenever there is a change in velocity due to a flow area change (e.g. at entry to a distributor), or a sudden change of direction, such as from a mitre to the thermal section of a PFHE. Taylor (1990) recommends the following methods of calculation of these losses:

$$\Delta p = \frac{G_d^2}{2\rho} + (K_u - 1) \left(\frac{G_u^2}{2\rho} \right), \quad (6.58)$$

where G is the upstream mass velocity and K is the loss coefficient, the subscripts u and d referring to upstream and downstream respectively.

The effect of longitudinal conduction

Longitudinal conduction takes place in both the walls of a heat exchanger and in the fluids themselves.

In the fluids, it can be ignored if the Peclet Number ($Pe = RePr$) is greater than 10 and the reduced flow length $x^* \geq 0.005$ (Shah and London (1978)). Clearly, in liquid metals with high conductivity and low Prandtl number it has to be accounted for, and analytical methods are given by Roetzel (1993), in these papers the effect being called 'dispersion', making the analogy with mass diffusion.

In the following discussion only the case of two fluid single pass configurations will be considered.

In the heat exchanger walls, conduction acts as a heat bypass and reduces the effective Ntu- and hence effectiveness, although without actual heat loss.

Infinite wall conductivity

A striking illustration of its effect can be gained by taking an extreme example of infinite wall conductivity in a counterflow exchanger, shown schematically in Figure 6.17, for balanced flow ($C^* = 1$), with the wall at constant temperature. The ideal case is also shown, and it is assumed that the nominal Ntu is the same for each case.

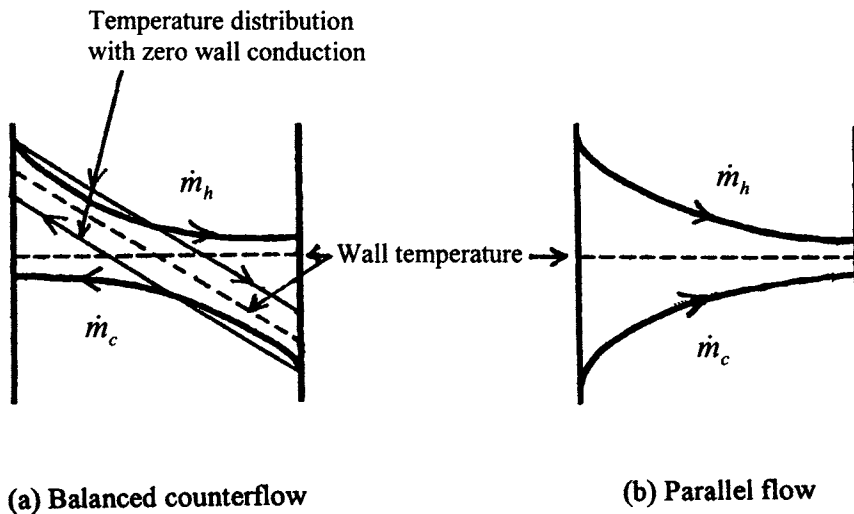


Figure 6.17 Temperature distributions with longitudinal wall conduction (infinite wall conductivity).

Analysis

We suppose that the inlet temperatures are $T_{h,in}$ and $T_{c,in}$ for hot and cold streams respectively. The individual side Ntus, $Ntu_h = Ntu_c = 2Ntu$ are given by

$$Ntu_c = \frac{\alpha_c A}{C_c} \quad (6.59)$$

Since we have assumed effectively infinite wall conductivity, the wall temperature T_w must be uniform and equal to $T_w = (T_{h,in} + T_{c,in})/2$ for this case, making the two sides identical and allowing us to analyse one side, say the hot side, only. We put the actual outlet temperature as $T_{h,out}$, and the outlet

temperature without wall conduction as $T_{h,out}^*$, as shown in Figure 6.17. Then the following relationships are readily derived:

$$Ntu_h = \ln \left(\frac{T_{h,in} - T_w}{T_{h,out} - T_w} \right), \quad (6.60)$$

$$T_{h,out}^* = \frac{T_{h,in} + \frac{Ntu_h}{2} T_{c,in}}{1 + Ntu_h/2}, \quad (6.61)$$

$$\varepsilon = \frac{\dot{Q}}{\dot{Q}_{max}} = \frac{1 - \exp(-Ntu_h)}{2}, \quad (6.62)$$

$$\varepsilon^* = \frac{N}{2 + N}, \quad (\text{optimum, non-conducting}) \quad (6.63)$$

$$\frac{\dot{Q}}{\dot{Q}^*} = \frac{\varepsilon}{\varepsilon^*} = \frac{(1 - \exp(-Ntu_h))}{2} \frac{(2 + N)}{N},$$

(ratio of actual to non-conducting heat flow) (6.64)

These relationships are shown in Figure 6.18. Note that the heat flow limitation is mathematically and physically identical to the case of parallel flow (see Table 6.1 above), because for $C^*=1$ for this case the wall temperature is constant. The only difference is that the temperature distributions in the latter case are symmetrically placed about the wall temperature. In the case of $Ntu \rightarrow \infty$ the heat flow tends to half of the ideal, but the effect at low Ntu (below about 2) is small. Because of the absence of sensitivity to flow direction, the analysis applies equally to all flow configurations. This also applies to the more general case of $C^* \neq 1$, the only change being that T_w depends on C^* . The balanced parallel flow case is shown in Figure 6.17; here, the conducting and non-conducting situations are identical.

Clearly, from the above analysis, the effect of longitudinal conduction is zero in the cases of condensation and evaporation (the (T) boundary condition), with the condensation temperature being identical to the wall temperature.

Finite wall conductivity

The wall conduction effect for a finite, rather than infinite, wall conductivity is dependent on the parameter P_λ ¹, defined by

$$P_\lambda = \frac{\lambda_w A_w / L}{C_{\min}}, \quad (6.65)$$

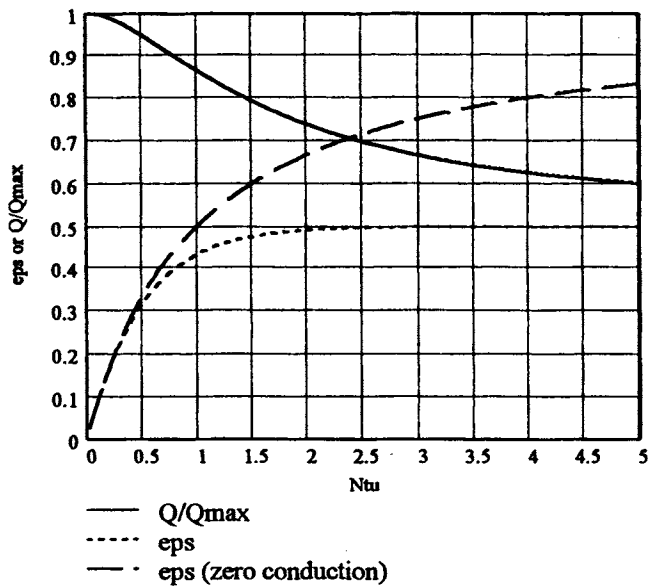


Figure 6.18 Ratio of heat flows, with effectiveness for zero and infinite wall conductivity.

Multiplication of top and bottom by the ideal terminal temperature change, which for a balanced counterflow exchanger is the same for both fluids and wall, this represents the ratio of wall heat flow to fluid heat flow, or, in other words a heat bypass ratio. The higher the value of P_λ , or the higher the wall conductivity, the thicker the wall, and the lower the flow length (i.e. with low hydraulic diameter), the more serious is the conduction effect. We would thus expect the problem to become more important as compact heat exchangers become more widely used, and as compactness increases (hydraulic diameter decreases). Since for compact exchangers the porosity is normally in the range 0.7-0.85, the wall area A_w is proportional to the flow area, so that the core *aspect ratio* (see chapter

¹ The parameter is normally denoted λ , but this symbol is already in use for thermal conductivity.

4) is a controlling parameter for counterflow arrangements. Conditions of high P_λ occur most often in cryogenic applications, where high effectiveness exchangers are used with aluminium fabrication. They are also important in the design of gas turbine regenerators (Shah (1988)). Both applications involve gas or vapour flows (low C_{\min}).

The following approaches are recommended by Shah (1994) using the analysis of (Kroeger (1967)) for the appropriate flow arrangements, in terms of loss of effectiveness:

Counterflow for the special case of $C^* = 1$ only

$$1 - \varepsilon = \frac{1}{1 + \gamma Ntu} \quad (6.66)$$

where the parameter γ is given by

$$\gamma = \frac{1 + P_\lambda \left\{ P_\lambda Ntu / (1 + P_\lambda Ntu) \right\}^{1/2}}{1 + P_\lambda Ntu} \quad (6.67)$$

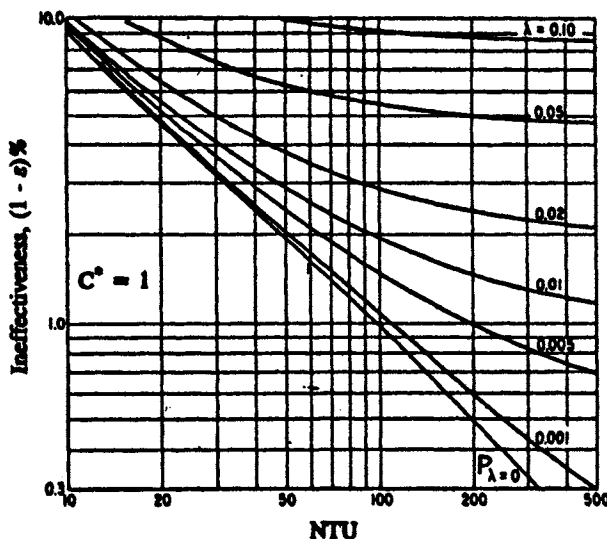


Figure 6.19 Ineffectiveness as a function of Ntu and conduction parameter P_λ (Kroeger (1967)).

These relationships are reasonably valid for $0.1 \leq (\eta_0 h A_s)^* \leq 10$ and $Ntu > 3$, where $(\eta_0 h A_s)^*$ is the ratio of thermal conductances in the two streams $(\eta_0 h A_s)_s / (\eta_0 h A_s)_h$. Kroeger's more accurate results are shown graphically in Figure 6.19. It is instructive to examine the results also on a conventional effectiveness- Ntu graph, and this is shown on Figure 6.20 for representative values of P_λ . The limiting curves correspond to the normal (non- axially conducting wall) counterflow case, and the parallel flow equivalent (constant temperature wall) respectively. Clearly, even for quite low values of P_λ , the effect on ϵ is sufficiently large that it needs to be taken into account at high Ntu, where a small degradation of ϵ necessitates a high increment of Ntu. The above formulae agree well with the more accurate results for values of P_λ up to the practical limit of about 1, but do not predict the limiting case of infinite P_λ well, as can be seen. Kroeger's results are also inaccurate at this limit.

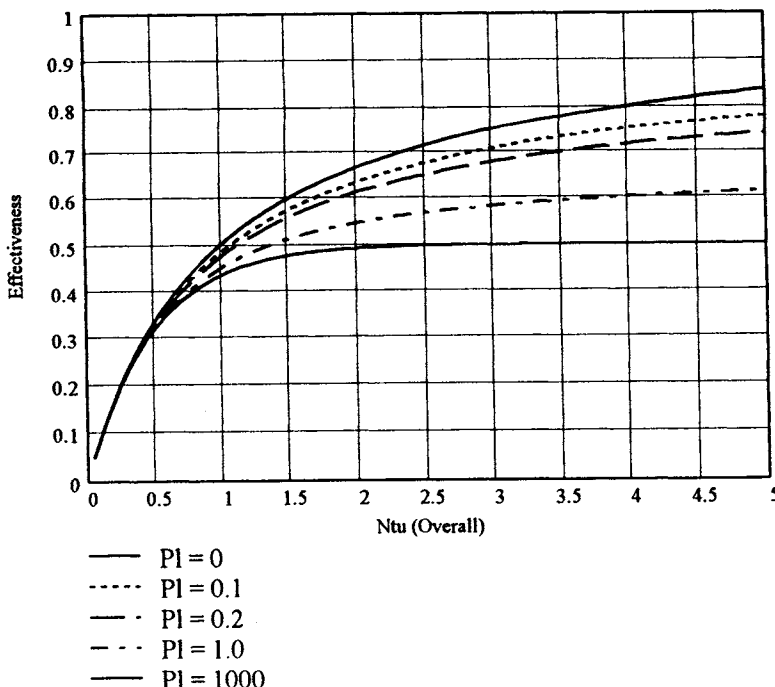


Figure 6.20 Effectiveness with longitudinal conduction, counterflow, $C^* = 1$.

For the more general case of $C^* < 1$, Kroeger's approximations, which are sufficiently accurate for most purposes, are

$$1 - \varepsilon = \frac{1 + C^*}{\varphi \exp(r_1) - C^*}, \quad (6.68)$$

where $r_1 = \frac{(1 - C^*)Ntu}{1 + P_\lambda Ntu C^*}.$ (6.69)

The values of the parameter φ in equation 6.68, as calculated by Kroeger (1967), are shown graphically in Figure 6.21

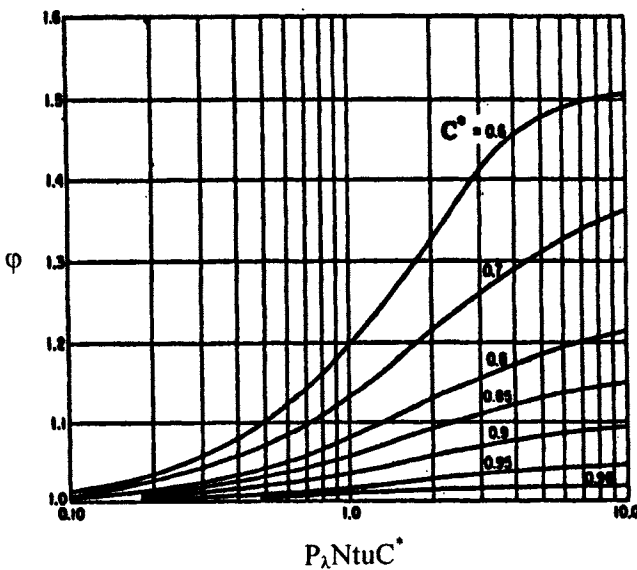


Figure 6.21 The function φ in equation 6.68 for calculation of ineffectiveness of a counterflow exchanger (Kroeger (1967)).

Example

A plate-fin heat exchanger has continuous (plain) aluminium fins on both sides, a length L of 1m, a porosity σ of 0.8 and a face area $C_s = 0.5\text{m}^2$. The thermal conductivity λ_w is $190\text{W/m}^2\text{K}$. Gases each of density $\rho = 1.2\text{ kg/m}^3$ and specific heat c_p of 1kJ/kgK flow in counterflow with a velocity u of 3m/s.

Then the parameter P_λ is

$$P_\lambda = \frac{C_s \sigma (1 - \sigma) \lambda_w}{L \rho \rho u_p C_s \sigma / 2} = \frac{2(1 - \sigma) \lambda_w}{L \rho \rho u_p} = \frac{2 \times (1 - 0.8) \times 190}{1 \times 1.2 \times 3 \times 1000} = 0.0211$$

(Notice that P_λ can be expressed in this case in terms of the mass velocity G ($= \rho u$)).

For an Ntu of 4 the ideal (zero conduction) case would give an effectiveness of 0.80. To achieve this value with the above value of P_λ would require an Ntu from equation 6.66 of 4.33- a substantial increase in surface area. Because this increase in turn changes P_λ , the correction has to be iterated.

Parallel flow

In a parallel flow exchanger the temperature distribution in the wall is fairly flat regardless of both the stream conductance ratio $(\eta_0 h A_s)^*$ or the heat capacity rate ratio C^* . Because of this the wall conduction is negligible and no allowance is normally needed.

Crossflow

The flows in most compact crossflow exchangers are exactly or are very close to unmixed, and as such this case has received most attention. Because of the two-dimensional nature of the temperature distribution, the actual temperature gradients are higher than those of a counterflow unit, but since crossflow exchangers are generally designed for much lower effectiveness and hence lower Ntus the loss of effectiveness is usually small.

The case of an unmixed- unmixed crossflow exchanger has been investigated numerically by Chiou (1976, 1978, 1980). Shah (1994) presented his results in terms of the parameters $P_{\lambda,c}$, $P_{\lambda,h}$, $(\eta_0 \alpha A_s)_c$, $(\eta_0 \alpha A_s)_h$, C_c , C_h and Ntu in Table 6.3 It is clear that in most cases the effect can be ignored: Shah (1994) gives the main trends for the exceptions.

For a more advanced treatment Smith (1997) gives a numerical approach, which examines the inlet faces only, as indicative of the worst conditions. This enables the solution of the full set of equations solved by Kroeger, aimed at evaluating the reduction of LMTD, thus giving a correction for use in design. This approach would be adaptable, in a fuller treatment, to the case of varying conditions through the exchanger.

Multipass Heat Exchangers

Although wall conduction in these exchangers has not been studied in detail, owing to their complexity, the fact that in an overall counterflow arrangement- the most likely to arise- the individual pass Ntus are likely to be modest and the effects should be relatively small. This should apply even for a high overall Ntu, and the effects should be readily calculable by a stepwise process using the individual pass Ntus (Shah (1994)).

The effect of non- uniformity of manufacture of heat exchanger passages

In the manufacture of plate- fin surfaces, especially the so- called deepfold corrugations intended to model as closely as possible the 'ideal' form of surface- that of infinite parallel plates (see chapter 5), it has been found (Mondt (1990), London (1970)) that distortions often occur. These have the form of non- uniform fin spacing, recurved fin shape, or an open fin, as shown schematically in Figure 6.22. Thus some channels will be wider, and some narrower, than their design or nominal values.

The consequence of these non- uniformities is twofold: a reduction in Ntu, and a reduction in pressure drop, both arising from the fluid taking preferential flow paths through the wider channels. Shah (1985) gives some indicative numerical data.

Mondt (1990) showed results of tests designed to correlate these performance effects with a statistical measurement of the non- uniformity of prepared heat cores, finding reasonable agreement.

The problem is only likely to arise to any serious extent in the manufacture and utilisation of high aspect ratio finned surfaces of the kind described, which are characteristic of gas turbine and related applications. It should be noted that the ideal thermal requirement for a long length of fin of low flow length (high aspect ratio) is achieved without serious non-uniformity problems by the louvred fin, flat tube surface (Figure 5.14b) much used for automotive and related applications

DESIGN FOR TWO- PHASE FLOWS

Compact surfaces are increasingly used for boiling and condensing duties in the process industries. Aluminium plate- fin exchangers have been used extensively for gas separation for fifty years, and their use in applications such as ethylene production and petroleum refining is becoming increasingly common. Compact exchangers have also a long history in aircraft environmental control

Table 6.3 Reduction in effectiveness of crossflow exchanger due to longitudinal conduction (from Shah (1994), with permission, for $C_e/C_h = 0.5$).

$\frac{A_e}{A_h}$	$\frac{(n_{o,h})_h}{(n_{o,h})_e}$	$\frac{\lambda_h}{\lambda_e}$	$\frac{h}{h_e}$	ϵ		$\Delta\epsilon/\epsilon$					
				0.0000	0.0400	0.0600	0.0800	0.1000	0.2000	0.4000	
0.5	0.5	0.5	1.00	0.5477	0.0072	0.0101	0.0127	0.0150	0.0245	0.0369	
			2.00	0.7329	0.0128	0.0190	0.0237	0.0271	0.0444	0.0674	
			4.00	0.8706	0.0191	0.0271	0.0343	0.0469	0.0673	0.1018	
			6.00	0.9248	0.0218	0.0318	0.0393	0.0470	0.0700	0.1186	
			8.00	0.9526	0.0226	0.0324	0.0413	0.0496	0.0832	0.1275	
			10.00	0.9687	0.0236	0.0326	0.0418	0.0504	0.0857	0.1324	
			30.00	1.0000	0.0093	0.0165	0.0254	0.0344	0.0756	0.1330	
			100.00	1.0000	0.0052	0.0122	0.0205	0.0294	0.0714	0.1307	
			1.00	0.5477	0.0092	0.0114	0.0134	0.0210	0.0302	0.0302	
			2.00	0.7329	0.0121	0.0170	0.0214	0.0254	0.0413	0.0616	
0.5	0.5	1.0	4.00	0.8706	0.0181	0.0257	0.0327	0.0391	0.0649	0.0988	
			6.00	0.9248	0.0205	0.0294	0.0376	0.0452	0.0760	0.1160	
			8.00	0.9526	0.0213	0.0308	0.0396	0.0478	0.0815	0.1262	
			10.00	0.9687	0.0213	0.0310	0.0401	0.0486	0.0841	0.1215	
			30.00	1.0000	0.0090	0.0159	0.0247	0.0337	0.0753	0.1229	
			100.00	1.0000	0.0050	0.0118	0.0201	0.0290	0.0712	0.1306	
			1.00	0.5477	0.0087	0.0092	0.0114	0.0134	0.0207	0.0291	
			2.00	0.7329	0.0118	0.0167	0.0211	0.0251	0.0411	0.0612	
			4.00	0.8706	0.0172	0.0247	0.0316	0.0379	0.0641	0.0907	
			6.00	0.9248	0.0194	0.0289	0.0361	0.0437	0.0749	0.1166	
0.5	0.5	2.0	8.00	0.9526	0.0201	0.0293	0.0390	0.0462	0.0803	0.1260	
			10.00	0.9687	0.0200	0.0285	0.0385	0.0470	0.0838	0.1213	
			30.00	1.0000	0.0075	0.0153	0.0240	0.0330	0.0748	0.1229	
			100.00	1.0000	0.0047	0.0115	0.0208	0.0286	0.0710	0.1307	
			1.00	0.5477	0.0113	0.0156	0.0194	0.0228	0.0355	0.0395	
			2.00	0.7329	0.0168	0.0264	0.0322	0.0393	0.0626	0.0904	
			4.00	0.8706	0.0268	0.0370	0.0475	0.0564	0.0905	0.1313	
			6.00	0.9248	0.0300	0.0424	0.0535	0.0637	0.1029	0.1580	
			8.00	0.9526	0.0305	0.0440	0.0559	0.0667	0.1093	0.1599	
			10.00	0.9687	0.0300	0.0442	0.0565	0.0677	0.1131	0.1652	
0.5	0.5	1.0	30.00	1.0000	0.0143	0.0264	0.0390	0.0513	0.1036	0.1691	
			100.00	1.0000	0.0100	0.0213	0.0337	0.0461	0.0990	0.1696	
			1.00	0.5477	0.0093	0.0120	0.0150	0.0185	0.0290	0.0382	
			2.00	0.7329	0.0166	0.0233	0.0292	0.0345	0.0548	0.0787	
			4.00	0.8706	0.0244	0.0346	0.0437	0.0521	0.0846	0.1241	
			6.00	0.9248	0.0276	0.0394	0.0500	0.0590	0.0982	0.1453	
			8.00	0.9526	0.0287	0.0412	0.0527	0.0622	0.1051	0.1564	
			10.00	0.9687	0.0287	0.0416	0.0535	0.0646	0.1085	0.1620	
			30.00	1.0000	0.0135	0.0285	0.0390	0.0506	0.1020	0.1681	
			100.00	1.0000	0.0097	0.0208	0.0331	0.0451	0.0993	0.1670	
0.5	0.5	2.0	1.00	0.5477	0.0093	0.0115	0.0142	0.0166	0.0291	0.0340	
			2.00	0.7329	0.0116	0.0212	0.0267	0.0317	0.0500	0.0736	
			4.00	0.8706	0.0244	0.0346	0.0437	0.0521	0.0846	0.1241	
			6.00	0.9248	0.0276	0.0394	0.0500	0.0590	0.0982	0.1453	
			8.00	0.9526	0.0287	0.0412	0.0527	0.0622	0.1051	0.1564	
			10.00	0.9687	0.0287	0.0416	0.0535	0.0646	0.1085	0.1620	
			30.00	1.0000	0.0135	0.0285	0.0390	0.0506	0.1020	0.1681	
			100.00	1.0000	0.0097	0.0208	0.0331	0.0451	0.0993	0.1670	
			1.00	0.5477	0.0113	0.0156	0.0194	0.0228	0.0355	0.0395	
			2.00	0.7329	0.0156	0.0212	0.0267	0.0317	0.0500	0.0736	
0.5	0.5	1.0	4.00	0.8706	0.0267	0.0336	0.0415	0.0483	0.0721	0.0961	
			6.00	0.9248	0.0402	0.0356	0.0460	0.0502	0.1266	0.1619	
			8.00	0.9526	0.0443	0.0416	0.0474	0.0548	0.1353	0.1827	
			10.00	0.9687	0.0437	0.0462	0.0493	0.0562	0.1221	0.1744	
			30.00	1.0000	0.0266	0.0453	0.0631	0.0794	0.1414	0.2096	
			100.00	1.0000	0.0212	0.0396	0.0576	0.0744	0.1405	0.2217	
			1.00	0.5477	0.0111	0.0156	0.0182	0.0218	0.0301	0.0385	
			2.00	0.7329	0.0245	0.0336	0.0415	0.0483	0.0721	0.0961	
			4.00	0.8706	0.0337	0.0406	0.0517	0.0617	0.1107	0.1512	
			6.00	0.9248	0.0403	0.0363	0.0503	0.0627	0.1278	0.1757	
0.5	0.5	2.0	8.00	0.9526	0.0420	0.0391	0.0472	0.0574	0.1365	0.1804	
			10.00	0.9687	0.0422	0.0400	0.0475	0.0587	0.1413	0.1856	
			30.00	1.0000	0.0235	0.0446	0.0618	0.0781	0.1397	0.2054	
			100.00	1.0000	0.0207	0.0309	0.0502	0.0736	0.1304	0.2125	
			1.00	0.5477	0.0111	0.0156	0.0182	0.0218	0.0301	0.0385	
			2.00	0.7329	0.0207	0.0207	0.0256	0.0417	0.0636	0.0863	
			4.00	0.8706	0.0315	0.0443	0.0536	0.0657	0.1038	0.1456	
			6.00	0.9248	0.0361	0.0314	0.0469	0.0769	0.1217	0.1704	
			8.00	0.9526	0.0383	0.0547	0.0653	0.0825	0.1314	0.1844	
			10.00	0.9687	0.0389	0.0568	0.0714	0.0852	0.1368	0.1924	
0.5	0.5	1.0	30.00	1.0000	0.0243	0.0427	0.0604	0.0766	0.1385	0.2040	
			100.00	1.0000	0.0201	0.0302	0.0562	0.0739	0.1378	0.2077	

Table 6.3 contd.

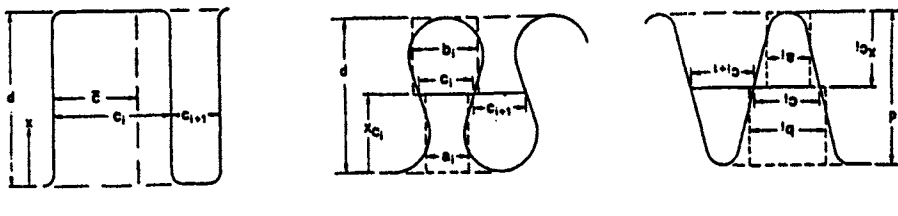
$$C_v/C_h = 1.0$$

$\frac{\lambda_c}{\lambda_h}$	$\frac{(n_0 \text{ha})_h}{(n_0 \text{ha})_c}$	$\frac{\lambda}{\lambda_h}$	e	$\Delta e/e$						
				0.0000	0.0400	0.0600	0.0800	0.1000	0.2000	0.4000
0.5	0.5	1.0	1.00	0.4764	0.0102	0.0125	0.0170	0.0202	0.0330	0.0480
			2.00	0.6147	0.0173	0.0247	0.0323	0.0373	0.0621	0.0930
			4.00	0.7231	0.0277	0.0393	0.0499	0.0556	0.0862	0.1468
			6.00	0.7729	0.0416	0.0490	0.0619	0.0736	0.1196	0.1760
			8.00	0.8021	0.0508	0.0581	0.0705	0.0827	0.1242	0.1949
			10.00	0.8238	0.0646	0.0617	0.0774	0.0914	0.1448	0.2083
			20.00	0.9229	0.0761	0.1013	0.1223	0.1404	0.2058	0.2754
			30.00	0.9476	0.0891	0.1158	0.1377	0.1563	0.2219	0.2928
			100.00	0.9476	0.0891	0.1158	0.1377	0.1563	0.2219	0.2928
			1.00	0.4764	0.0102	0.0143	0.0180	0.0213	0.0341	0.0480
0.5	1.0	2.0	2.00	0.6147	0.0192	0.0258	0.0327	0.0391	0.0643	0.0959
			4.00	0.7231	0.0284	0.0404	0.0512	0.0621	0.1002	0.1491
			6.00	0.7729	0.0353	0.0499	0.0630	0.0749	0.1213	0.1779
			8.00	0.8021	0.0404	0.0589	0.0716	0.0848	0.1356	0.1965
			10.00	0.8238	0.0466	0.0624	0.0782	0.0924	0.1462	0.2096
			20.00	0.9229	0.0763	0.1013	0.1226	0.1407	0.2053	0.2750
			30.00	0.9476	0.0891	0.1158	0.1377	0.1564	0.2221	0.2933
			100.00	0.9476	0.0891	0.1158	0.1377	0.1564	0.2221	0.2933
			1.00	0.4764	0.0115	0.0162	0.0204	0.0241	0.0367	0.0550
			2.00	0.6147	0.0194	0.0276	0.0359	0.0419	0.0669	0.1026
1.0	0.5	1.0	4.00	0.7231	0.0294	0.0418	0.0530	0.0632	0.1036	0.1525
			6.00	0.7729	0.0368	0.0516	0.0644	0.0766	0.1239	0.1816
			8.00	0.8021	0.0411	0.0578	0.0728	0.0862	0.1377	0.1968
			10.00	0.8238	0.0451	0.0633	0.0793	0.0936	0.1486	0.2115
			20.00	0.9229	0.0764	0.1017	0.1229	0.1419	0.2097	0.2765
			30.00	0.9476	0.0893	0.1160	0.1379	0.1566	0.2223	0.2943
			100.00	0.9476	0.0893	0.1160	0.1379	0.1566	0.2223	0.2943
			1.00	0.4764	0.0126	0.0190	0.0227	0.0280	0.0436	0.0609
			2.00	0.6147	0.0238	0.0336	0.0423	0.0501	0.0803	0.1154
			4.00	0.7231	0.0368	0.0530	0.0653	0.0773	0.1239	0.1753
1.0	1.0	2.0	6.00	0.7729	0.0456	0.0637	0.0797	0.0940	0.1472	0.2070
			8.00	0.8021	0.0529	0.0723	0.0909	0.1087	0.1624	0.2270
			10.00	0.8238	0.0571	0.0790	0.0979	0.1145	0.1751	0.2416
			20.00	0.9229	0.0940	0.1223	0.1473	0.1677	0.2377	0.3090
			30.00	0.9476	0.1080	0.1385	0.1532	0.1840	0.2546	0.3273
			100.00	0.9476	0.1080	0.1385	0.1532	0.1840	0.2546	0.3273
			1.00	0.4764	0.0132	0.0193	0.0228	0.0266	0.0412	0.0567
			2.00	0.6147	0.0238	0.0331	0.0417	0.0493	0.0766	0.1128
			4.00	0.7231	0.0368	0.0517	0.0650	0.0769	0.1228	0.1742
2.0	0.5	1.0	6.00	0.7729	0.0458	0.0637	0.0797	0.0940	0.1472	0.2070
			8.00	0.8021	0.0529	0.0723	0.0909	0.1087	0.1624	0.2270
			10.00	0.8238	0.0571	0.0790	0.0979	0.1143	0.1749	0.2407
			20.00	0.9229	0.0940	0.1223	0.1473	0.1677	0.2377	0.3090
			30.00	0.9476	0.1080	0.1385	0.1532	0.1840	0.2546	0.3270
			100.00	0.9476	0.1080	0.1385	0.1532	0.1840	0.2546	0.3273
			1.00	0.4764	0.0136	0.0199	0.0227	0.0280	0.0436	0.0609
			2.00	0.6147	0.0238	0.0336	0.0423	0.0501	0.0803	0.1154
			4.00	0.7231	0.0368	0.0530	0.0653	0.0773	0.1239	0.1753
2.0	1.0	2.0	6.00	0.7729	0.0458	0.0637	0.0797	0.0940	0.1472	0.2070
			8.00	0.8021	0.0529	0.0723	0.0909	0.1087	0.1624	0.2270
			10.00	0.8238	0.0571	0.0790	0.0979	0.1143	0.1749	0.2407
			20.00	0.9229	0.0940	0.1223	0.1473	0.1677	0.2377	0.3090
			30.00	0.9476	0.1080	0.1385	0.1532	0.1840	0.2546	0.3273
			100.00	0.9476	0.1080	0.1385	0.1532	0.1840	0.2546	0.3273
			1.00	0.4764	0.0178	0.0232	0.0295	0.0330	0.0490	0.0652
			2.00	0.6147	0.0327	0.0449	0.0552	0.0643	0.0959	0.1326
			4.00	0.7231	0.0512	0.0702	0.0863	0.1002	0.1491	0.1991
2.0	2.0	1.0	6.00	0.7729	0.0630	0.0857	0.1049	0.1213	0.1779	0.2344
			8.00	0.8021	0.0716	0.0958	0.1178	0.1356	0.1965	0.2560
			10.00	0.8238	0.0792	0.1052	0.1274	0.1462	0.2096	0.2708
			20.00	0.9229	0.1226	0.1566	0.1834	0.2053	0.2758	0.3405
			30.00	0.9476	0.1707	0.1727	0.1799	0.2231	0.2933	0.3619
			100.00	0.9476	0.1707	0.1727	0.1799	0.2231	0.2933	0.3619
			1.00	0.4764	0.0178	0.0232	0.0295	0.0330	0.0490	0.0652
			2.00	0.6147	0.0313	0.0432	0.0533	0.0621	0.0938	0.1324
			4.00	0.7231	0.0499	0.0695	0.0844	0.0982	0.1468	0.1971
			6.00	0.7729	0.0619	0.0844	0.1033	0.1196	0.1760	0.2320
2.0	2.0	2.0	8.00	0.8021	0.0706	0.0936	0.1164	0.1342	0.1949	0.2540
			10.00	0.8238	0.0774	0.1041	0.1262	0.1430	0.2063	0.2690
			20.00	0.9229	0.1223	0.1583	0.1831	0.2039	0.2734	0.3401
			30.00	0.9476	0.1702	0.1723	0.1797	0.2219	0.2926	0.3600
			100.00	0.9476	0.1702	0.1723	0.1797	0.2219	0.2926	0.3600

Table 6.3 contd.

$$C_c/C_b = 2.0$$

$\frac{\lambda_c}{\lambda_b}$	$\frac{(n_0 h_0)}{h}$	$\frac{\lambda}{h}$	ϵ	$\Delta\epsilon/\epsilon$						
				0.0000	0.0000	0.0000	0.1000	0.2000	0.4000	
0.5	0.5	0.5	1.00	0.5477	0.0062	0.0000	0.0111	0.0131	0.0210	0.0301
			2.00	0.7329	0.0113	0.0162	0.0207	0.0240	0.0417	0.0636
			4.00	0.8706	0.0169	0.0245	0.0315	0.0381	0.0657	0.1030
			6.00	0.9248	0.0193	0.0281	0.0363	0.0441	0.0769	0.1217
			8.00	0.9526	0.0201	0.0394	0.0383	0.0457	0.0825	0.1304
			10.00	0.9687	0.0200	0.0397	0.0389	0.0476	0.0852	0.1368
			30.00	1.0000	0.0076	0.0155	0.0243	0.0335	0.0769	0.1386
			100.00	1.0000	0.0049	0.0117	0.0281	0.0391	0.0729	0.1370
			1.00	0.5477	0.0078	0.0109	0.0137	0.0162	0.0235	0.0360
			2.00	0.7329	0.0125	0.0193	0.0245	0.0292	0.0462	0.0721
0.5	1.0	0.5	4.00	0.8706	0.0194	0.0279	0.0357	0.0429	0.0723	0.1107
			6.00	0.9248	0.0217	0.0313	0.0403	0.0486	0.0827	0.1279
			8.00	0.9526	0.0224	0.0323	0.0420	0.0508	0.0876	0.1365
			10.00	0.9687	0.0222	0.0323	0.0422	0.0514	0.0897	0.1411
			30.00	1.0000	0.0082	0.0164	0.0233	0.0349	0.0781	0.1397
			100.00	1.0000	0.0052	0.0122	0.0207	0.0327	0.0726	0.1384
			1.00	0.5477	0.0182	0.0243	0.0280	0.0223	0.0379	0.0485
			2.00	0.7329	0.0163	0.0233	0.0294	0.0351	0.0577	0.0859
			4.00	0.8706	0.0222	0.0317	0.0403	0.0483	0.0803	0.1206
			6.00	0.9248	0.0243	0.0348	0.0445	0.0534	0.0933	0.1353
0.5	2.0	0.5	8.00	0.9526	0.0246	0.0357	0.0455	0.0551	0.0931	0.1424
			10.00	0.9687	0.0244	0.0354	0.0457	0.0552	0.0946	0.1459
			30.00	1.0000	0.0090	0.0174	0.0265	0.0368	0.0734	0.1216
			100.00	1.0000	0.0053	0.0127	0.0212	0.0304	0.0744	0.1205
			1.00	0.5477	0.0083	0.0115	0.0142	0.0166	0.0251	0.0340
			2.00	0.7329	0.0158	0.0232	0.0267	0.0317	0.0589	0.0736
			4.00	0.8706	0.0223	0.0319	0.0407	0.0487	0.0807	0.1203
			6.00	0.9248	0.0254	0.0366	0.0470	0.0565	0.0949	0.1424
			8.00	0.9526	0.0265	0.0386	0.0498	0.0602	0.1021	0.1541
			10.00	0.9687	0.0266	0.0391	0.0508	0.0617	0.1060	0.1600
0.5	1.0	0.5	30.00	1.0000	0.0128	0.0246	0.0371	0.0494	0.1021	0.1676
			100.00	1.0000	0.0093	0.0203	0.0326	0.0451	0.0950	0.1670
			1.00	0.5477	0.0093	0.0128	0.0186	0.0205	0.0280	0.0382
			2.00	0.7329	0.0146	0.0232	0.0292	0.0343	0.0548	0.0787
			4.00	0.8706	0.0244	0.0346	0.0437	0.0532	0.0944	0.1241
			6.00	0.9248	0.0276	0.0394	0.0500	0.0598	0.0983	0.1453
			8.00	0.9526	0.0287	0.0412	0.0527	0.0632	0.1051	0.1564
			10.00	0.9687	0.0287	0.0416	0.0535	0.0646	0.1086	0.1626
			30.00	1.0000	0.0135	0.0255	0.0380	0.0504	0.1028	0.1683
			100.00	1.0000	0.0097	0.0208	0.0331	0.0456	0.0933	0.1570
0.5	2.0	0.5	1.00	0.5477	0.0113	0.0195	0.0294	0.0220	0.0355	0.0498
			2.00	0.7329	0.0180	0.0264	0.0323	0.0393	0.0626	0.0904
			4.00	0.8706	0.0268	0.0378	0.0475	0.0580	0.0963	0.1312
			6.00	0.9248	0.0309	0.0424	0.0525	0.0637	0.1028	0.1500
			8.00	0.9526	0.0309	0.0440	0.0539	0.0657	0.1049	0.1530
			10.00	0.9687	0.0309	0.0443	0.0535	0.0657	0.1118	0.1653
			30.00	1.0000	0.0143	0.0264	0.0390	0.0513	0.1036	0.1693
			100.00	1.0000	0.0100	0.0213	0.0327	0.0461	0.0959	0.1594
			1.00	0.5477	0.0115	0.0232	0.0302	0.0207	0.0391	0.0371
			2.00	0.7329	0.0211	0.0268	0.0354	0.0411	0.0612	0.0825
0.5	1.0	0.5	4.00	0.8706	0.0316	0.0439	0.0546	0.0641	0.0987	0.1368
			6.00	0.9248	0.0361	0.0507	0.0636	0.0749	0.1156	0.1623
			8.00	0.9526	0.0368	0.0510	0.0639	0.0757	0.1166	0.1630
			10.00	0.9687	0.0365	0.0511	0.0639	0.0750	0.1173	0.1636
			30.00	1.0000	0.0240	0.0426	0.0592	0.0748	0.1129	0.1944
			100.00	1.0000	0.0201	0.0376	0.0550	0.0710	0.1107	0.1931
			1.00	0.5477	0.0215	0.0252	0.0382	0.0210	0.0302	0.0299
			2.00	0.7329	0.0214	0.0291	0.0357	0.0413	0.0616	0.0841
			4.00	0.8706	0.0327	0.0450	0.0536	0.0649	0.0988	0.1365
			6.00	0.9248	0.0376	0.0522	0.0649	0.0760	0.1160	0.1618
0.5	2.0	0.5	8.00	0.9526	0.0388	0.0559	0.0679	0.0803	0.1266	0.1758
			10.00	0.9687	0.0385	0.0551	0.0692	0.0830	0.1213	0.1836
			30.00	1.0000	0.0240	0.0426	0.0592	0.0748	0.1129	0.1944
			100.00	1.0000	0.0201	0.0380	0.0553	0.0713	0.1106	0.1931
			1.00	0.5477	0.0227	0.0373	0.0313	0.0245	0.0359	0.0308
			2.00	0.7329	0.0227	0.0310	0.0352	0.0444	0.0673	0.0939
			4.00	0.8706	0.0343	0.0469	0.0570	0.0673	0.1018	0.1464
			6.00	0.9248	0.0393	0.0541	0.0669	0.0780	0.1186	0.1635
			8.00	0.9526	0.0393	0.0573	0.0711	0.0832	0.1275	0.1762
			10.00	0.9687	0.0384	0.0584	0.0729	0.0857	0.1324	0.1837
			30.00	1.0000	0.0254	0.0433	0.0602	0.0756	0.1330	0.1948
			100.00	1.0000	0.0205	0.0383	0.0553	0.0714	0.1307	0.1952



(a) Non-uniform fin spacing

(b) Recurved fin

(c) Open fin

Figure 6.22 Schematics of non-uniform fin passages (from London (1970))

Boiling

There are two principal mechanisms of boiling, those of nucleate boiling and convective boiling. The heat transfer coefficients characteristic of nucleate boiling are very high, but normally only for relatively high driving temperature differences (or wall superheats), for example of the order of 10K. This is overcome in many applications, particularly refrigeration, by the use of so-called high flux surfaces, which trap superheated liquid within their structure and reduce the required wall superheat. Convective boiling relies on the normal convective mechanism of heat transfer with the phase change occurring by evaporation at the liquid-vapour interface. This process is augmented by the increased velocity of the bulk flow caused by the lower density of the vapour component.

In compact exchangers there is little scope (or need at present) for incorporating high flux surfaces. Provided that the fluid velocity is not too high, lateral bubble growth and the convective augmentation are sufficiently high that the typical temperature differences are adequately low, being of the order of 1 to 2K for cryogenic systems.

For quality (the mass ratio of vapour to total flow) between 0 and 0.95, a commonly-used assumption is that the two mechanisms operate simultaneously. At any point the two-phase flow augments or enhances the heat transfer as mentioned above. Conversely, the nucleate boiling component is suppressed by the convection, since superheated liquid is removed from the surface. The Chen (1966) superposition correlation for local convective boiling is widely used in direct or adapted form to describe this combination, and is

$$\alpha = F\alpha_l + S\alpha_{nb} \quad (6.70)$$

where α_l^1 is the heat transfer coefficient for liquid flowing alone (that is, if the liquid component was flowing by itself), F is the two- phase enhancement factor, α_{nb} is the nucleate boiling heat transfer coefficient, and S is the suppression factor, introduced to account for the removal by convection of the superheated liquid required for nucleation.

The liquid coefficient α_l is calculated using the appropriate single- phase correlation for the surface, based on a Reynolds number for the liquid component flowing alone, Re_l , defined in terms of quality x_g by

$$Re_l = \frac{G(1-x_g)d}{\eta_l} \quad (6.71)$$

The quality x_g is defined as the proportion of total flow rate as vapour at any station. It thus increases from near-zero to 1 in an evaporator.

An important parameter with a controlling role in describing the effects of two phase flows is the Lockhart- Martinelli (1949) parameter X , which is defined as the ratio of liquid to vapour pressure gradients, with the assumption that each phase flows alone in the channel:

$$X = \frac{(dp/dx)_l}{(dp/dx)_v} \quad (6.72)$$

The parameter takes different forms depending on the assumed or measured flow regime of each phase. The most common assumption is that both phases are turbulent, giving rise to the subscript "tt" for liquid and vapour phases respectively (the others being, for completeness, lt , ll and tl , l denoting laminar). The general form is given as

$$X = \left(\frac{\rho_g}{\rho_l} \right)^{0.5} \left(\frac{\eta_l}{\eta_g} \right)^{n/2} \left(\frac{(1-x_g)}{x_g} \right)^{(1-n/2)} \quad (6.73)$$

where x_g is the local quality and n is index of Reynolds number in the single- phase frictional correlation $f = ARe^{-n}$ for the surface considered. Thus for

¹ The suffices l for the liquid phase and g for the gas (vapour) phase are used here. Other works and some data representations have suffices f (fluid) for the liquid phase and v for the vapour phase. A common combination is f, g .

turbulent flows of both components the index n will be approximately 0.2, whilst for fully developed laminar flow $n = 1$. Taylor (1990) uses an alternative form of X , readily derivable from equation 6.73:

$$X = \left(\frac{f_l \rho_g}{f_g \rho_l} \right)^{0.5} \frac{(1 - x_g)}{x_g} \quad (6.74)$$

where f_l and f_g are the friction factors for liquid and vapour phases respectively, and recommends that F should be set to 1 when $X > 10.5$. This form avoids the assumption implicit in equation 6.73 that the Reynolds number exponents for friction factor are the same for each component. In practice, for compact surfaces, it is wise to calculate the component Reynolds numbers since the flows may well span different regimes with different Re indices. The form 6.74 is thus preferable.

The convective heat transfer enhancement factor F was correlated by Butterworth (1979) in terms of X_{tr} as

$$F = 2.35(0.213 + 1/X_{tr})^{0.736}. \quad (6.75)$$

If the Chen correlation (equation 6.70) is used, it is pointed out by Hewitt et al. (1994) that the nucleate boiling component should be calculated using the Forster- Zuber (1955) correlation in conjunction with the suppression factor given below (equation 6.80):

$$\alpha_{nb} = \frac{0.00122 \Delta T_{sat}^{0.24} \Delta p_{sat}^{0.75} c_{pl}^{0.45} \rho_l^{0.49} \lambda_l^{0.79}}{\sigma^{0.5} h_{lg}^{0.24} \eta_l^{0.29} \rho_g^{0.24}}, \quad (6.76)$$

where ΔT_{sat} and Δp_{sat} are the wall superheat and corresponding saturation pressure difference respectively, other parameters being, in consistent (SI) units:

σ = surface tension

c_{pl} = liquid specific heat

ρ_l = liquid density

ρ_g = vapour density

λ_l = liquid thermal conductivity

η_l = liquid dynamic viscosity

h_{lg} = latent heat

Several alternative correlations for the nucleate boiling coefficient are available. The simplest, and one of the most reliable for application to compact surfaces (Cornwell and Kew (1999)), is given by Cooper (1984). This is based on reduced pressure, and is given by

$$\alpha_{nb} = 55 p_r^{0.12} (-\log_{10} p_r)^{-0.55} M^{-0.5} q^{0.67}, \quad (6.77)$$

where p_r is the reduced pressure p/p_c , with p_c being the critical pressure, M being the molecular weight and q the heat flux.

Cornwell and Kew recommend that for compact passages the Cooper correlation be used as the starting point for design.

For plate-fin exchangers Feldman et al. (1996) correlated both perforated and OSF surfaces ($dh = 2.06\text{mm}$, R114) well by a Chen-type approach with the Lockhart – Martinelli parameter in the laminar (liquid phase) – turbulent (vapour phase) form, and with the corresponding multiplier:

$$F = 1 + 1.8 X_{lt}^{-0.79} \quad (6.78)$$

The OSF data correlated well with the convective component only. The perforated fin data correlated with an approach which took the greater of the Cooper correlation (α_{nb} , with $S = 1$) and the convective term $F\alpha_l$.

Mandrusiak and Carey (1989) correlated OSF data using R113 with the superposition model, equation 6.70, by

$$F = \left(1 + \frac{28}{X_{lt}} \right)^{0.372}, \quad (6.79)$$

with the suppression factor of Bennett and Chen (1980). The simple correlation of Butterworth (1979) could be used instead:

$$S = \frac{1}{1 + 2.53 \times 10^{-6} Re_s^{1.17}}, \quad (6.80)$$

where Re_s is a two phase Reynolds number given by

$$Re_s = Re_l F^{1.25} \quad (6.81)$$

Some researchers give an asymptotic version of equation 6.70 to account for a smooth transition between the nucleate boiling and the several convective mechanisms. However, there is insufficient systematic evidence over the variety of surface types and scales to justify such an approach at present.

When the flow gap (tube diameter or half of hydraulic diameter) is less than the departure diameter of the equilibrium vapour bubble, the bubble is invariably 'squeezed'. Many researchers (Kew (1995), Cornwell and Kew (1995), Kew and Cornwell (1995), Rampisela et al. (1993)) have found that this *confinement* normally acts to augment the heat transfer. The mechanism is largely that of reduction of thickness of the liquid layer between the bubble and the surface, caused by the high lateral growth rate of the bubble. A proviso is that confinement can in some circumstances lead to intermittent dryout at relatively low heat fluxes if it prevents the re-wetting of the surface (Kew (2000)). For circular and rectangular ducts, tested with R12 and R134a, Tran et al. (1997) developed a correlation to account for bubble confinement. In terms of the Confinement number Co (which is the inverse of the square root of the Bond Number), they give:

$$Nu = 770(BoRe,Co)^{0.62} \left(\frac{\rho_g}{\rho_l} \right)^{0.279} \quad (6.82)$$

where the Boiling number Bo is

$$Bo = \frac{q}{h_{fg} G}, \quad (6.83)$$

where q is the heat flux, and the confinement number is

$$Co = \frac{\left[\frac{\sigma}{g(\rho_l - \rho_g)} \right]^{0.5}}{d_h}. \quad (6.84)$$

Thus when the confinement number Co is greater than 0.5 (Cornwell and Kew (1995)), the confinement process has a significant effect on the heat transfer. Note that the Tran et al. correlation is independent of quality, since they found little effect of quality over the normal range.

Much of the published experimental information has been obtained, for both heat transfer and pressure drop, using single channels. Cornwell and Kew (1999)

point out that multiple channel exchanger surfaces may well perform better than single channels because of the lower adverse influence of flow instability caused by liquid slugs. Use of the single channel correlations would then be conservative.

For flow quality higher than 0.95 the heat transfer is largely that of pure vapour, and the appropriate single phase correlation should be used with the saturated vapour properties (Taylor (1990)). This may not apply to evaporation in plate exchangers in which the active part of the surface is probably maintained at a wet condition by the high flow turbulence.

Example 6.1 Calculate the convective boiling coefficient for Benzene in the following conditions:

Physical property data

(from Appendix 5)	Temperature T_{sat}	400K
Molecular weight		78.108 kg/kmol
Liquid:	density	ρ_l 767 kg/m ³
	specific heat	c_{pl} 2.08 kJ/kgK
	viscosity	η_l 205x10 ⁻⁶ Ns/m ²
	thermal conductivity	λ_l 0.119 W/mK
	surface tension	σ 15.5x10 ⁻³ N/m
	latent heat	h_{lg} 364.2 kJ/kg
	saturation pressure	p_{sat} 354 kPa
	critical pressure	p_{crit} 4924 kPa
	Prandtl number	Pr_l 3.583
Vapour density		ρ_g 8.87 kg/m ³
	specific heat	c_{pg} 1.53 kJ/kgK
	viscosity	η_g 10.7x10 ⁻⁶ Ns/m ²
	Universal gas constant	R 8314.3kJ/kmolK
Operational and surface data		
	mass flux	G 100kg/m ³
	quality	x_g 0.5
	Wall superheat	ΔT_{sat} 4K
	hydraulic diameter	d_h 0.002m
	corrugated plate fin	
	surface described by	$j = 0.24Re^{-0.425}, f = 1.08Re^{-0.425}$

Calculation: First evaluate the saturated pressure difference from the Clausius- Clapeyron equation:

$$\Delta p_{sat} = p_{sat} \left\{ \exp \left[\frac{h_{lg} M}{R} \left(\frac{1}{T_{sat}} - \frac{1}{T_{wall}} \right) \right] - 1 \right\}$$

$$\Delta p_{sat} = 354 \left\{ \exp \left[\frac{364.2 \times 10^3 \times 78.108}{8314.3} \left(\frac{1}{400} - \frac{1}{404} \right) \right] - 1 \right\}$$

$$\Delta p_{sat} = 3.129 \times 10^4 \text{ Pa}$$

Evaluate the Forster-Zuber nucleate boiling coefficient using equation 6.76:

$$\alpha_{fz} = \frac{0.00122 \times 4^{0.24} \times (3.129 \times 10^4)^{0.75} \times (2.08 \times 10^3)^{0.45} \times 767^{0.49} \times 0.119^{0.79}}{(15.5 \times 10^{-3})^{0.5} \times (364.2 \times 10^3)^{0.24} \times (205 \times 10^{-6})^{0.29} \times 8.87^{0.24}}$$

$$\alpha_{fz} = 1.552 \times 10^3 \text{ W/m}^2 \text{ K}$$

For convective boiling, first evaluate the Lockhart- Martinelli parameter X, from 6.73: since the friction factor Reynolds number exponent is $n = 0.5$, this is

$$X = \left\{ \left(\frac{1 - x_g}{x_g} \right)^{1-n/2} \left(\frac{\rho_v}{\rho_l} \right)^{0.5} \left(\frac{\eta_l}{\eta_v} \right)^{n/2} \right\} = 0.201$$

then evaluate the convective enhancement factor F from 6.75:

$$F = 2.35 \left(\frac{1}{X} + 0.213 \right)^{0.736} = 7.883.$$

Calculate the single-phase (liquid) heat transfer coefficient from the j factor correlation given:

$$Nu = j Re_l Pr_l^{0.3333} = 0.24 Re_l^{0.575} Pr_l^{0.3333} = 12.903$$

$$\alpha_l = \frac{Nu \lambda_l}{d_h} = 767.73 \text{ W/m}^2 \text{ K},$$

and the augmented convective coefficient is

$$\alpha_c = F\alpha_l = 6052 \text{W/m}^2\text{K}$$

Procedure for suppression factor S

Calculate the liquid- alone Reynolds number, with overall Reynolds number first:

$$Re = \frac{Gd_h}{\eta}, \text{ and } Re_l = Re(1 - x) = 487.8.$$

Two phase Reynolds number for suppression from 6.81

$$Re_s = Re_l F^{1.25} = 6443$$

Now evaluate the suppression factor S, from 6.80:

$$S = \frac{1}{1 + 2.53 \times 10^{-6} \times Re_s^{1.17}} = 0.932$$

Hence the Chen correlation gives, for this case

$$\alpha_{Chen} = F\alpha_l + S\alpha_{fz} = 6052 + 0.932 \times 1552 = 7499 \text{W/m}^2\text{K}$$

(For comparison, the methods of Feldman, Mandrusiak and Carey, and Tran et al. give values of 5669, 4826 and 8884W/m²K respectively: this level of variation is not untypical of presently available methods)

Condensation

The mechanisms of condensation in compact exchangers (Thonon and Chopard, (1995)) are essentially those of gravity- controlled film condensation, for which a Nusselt- type theory applies, and a shear- controlled process in which convective mechanisms dominate. Compact exchangers have an advantage again, in general, in that the condensate drainage process is augmented by surface tension drawing the liquid into the corners of the surface, which act as preferred drainage paths and thinning the liquid layer on the active surface. The orientation (horizontal or vertical downflow) is clearly important, as emphasised by Srinivasan and Shah (1995), who gave the following table of typical parameters:

Table 6.4 Flow parameters in compact condensers (Srinivasan and Shah (1995))

Condenser Type	Application	Range of G kg/m ² s	Re_1	Re_2	We_1	We_2	Bo	D_b mm
Plate-fin	Cryogenic main condensers (nitrogen)	15-50	0-1000	0-12,000	0-0.75	0-25	1.0-10.0	1.5-3.0
Flat tube and corrugated fin	Automotive A/C condensers (R-134a refrigerant)	10-120	0-1000	0-12,000	0-1.0	0-60	0.8-20.0	1.0-3.0
Plate-and-frame	Energy conversion devices/ chemical process systems	2-40	0-1200	0-30,000	0-0.80	0-450	3.0-12.0	2.0-8.0
Printed circuit	Chemical process systems	2-20	0-600	0-15,000	0-0.30	0-200	3.0-12.0	1.2-1.5
Shell-and-tube	Powerplant (steam-water)	20-500	0-20,000	0-50,000	0-100	0-5000	3.0-85.0	12.7-25.4

Mass fluxes are typically lower than those encountered in conventional tubular condensers.

In the absence of proven general correlations, it is recommended that the method of Taylor (1990) for PFHEs be applied, which simply augments the liquid-only coefficient α_l by the Boyko and Krushilin (1967) shear factor, an adaptation of the homogeneous two-phase multiplier. This gives the overall coefficient α_c as:

$$\alpha_c = \alpha_l \left(1 + x_g \left(\frac{\rho_l}{\rho_g} - 1 \right) \right)^{1/2}. \quad (6.85)$$

For a first approximation a mean value of half the end values for a range of quality x_g can be used (Hewitt et al. (1994)).

When a finned surface is used for condensing, it is important (Shah (1985)) for care to be used in the fin efficiency calculation, since the heat transfer coefficients are very high (implying low fin efficiency). There will also be a considerable deterioration on progression downstream, owing to the accumulation of condensate. Because of this it is normal to segment the analysis or design of a condenser, 100 stages being typically reported for large duties.

Two-phase pressure drop

Whilst heat transfer performance can be measured or inferred locally, only the overall pressure drop across the surface can normally be measured, except in experimental facilities. Since the quality varies with progression downstream, it is necessary to integrate any correlation, which depends on quality over the heat exchanger length to compare with measurements.

Pressure drop correlations are generally accepted to be valid without modification for both boiling and condensation duties.

Moriyama and Inouie (1992) and other researchers have shown that for flows in narrow channels the Chisholm (1967) correlation for friction multiplier gives good results:

$$\phi_l^2 = 1 + \frac{C}{X_{it}} + \frac{1}{X_{it}^2}, \quad (6.86)$$

where

$$\phi_l^2 = \frac{(dp/dx)}{(dp/dx)_l}, \quad (6.87)$$

and $(dp/dx)_l$ is the local liquid-only pressure gradient. If the heat flux is constant with length, the quality x_g varies linearly with length and the above equation with $C = 0$ can be integrated to give an overall friction multiplier:

$$\phi_{lo}^2 = 1 - \frac{\rho_l \eta_g}{\rho_g \eta_l} \left[\frac{\ln(1 - x_{g,out})}{x_{g,out}} + 1 \right] \quad (6.88)$$

where $x_{g,out}$ is the exit quality.

In most applications the term including the parameter C should be retained, which prevents the straightforward integration as above. Instead, the friction multiplier can be based simply on exit quality, which gives a conservative result. There are insufficient experimental data for general conclusions to be made for the value of C . Moriyama and Inoue (1992) found that setting the parameter C to zero gave good results for their very narrow (0.11mm) gaps. This trend was also confirmed by the present author (Hesselgreaves (1997)) with perforated plate surfaces with small hydraulic diameters (about 0.3mm); for higher hydraulic diameter (1.18mm) a value of C of 5 gave improved results. Palm and Thonon (1999) suggest a value of 3 for plate exchangers (hydraulic diameter about 4mm) with refrigerants. Sterner and Sundén (1997) found a dependence on liquid-only Reynolds number from a series of tests with commercial plate exchangers using ammonia. The values derived were higher than others reported here but interestingly showed a significant reduction for lower hydraulic diameter. Cornwell and Kew (1999) observed that the two-phase multiplier ϕ was relatively insensitive to C but a value of 12 gave good agreement for 5.0mm diameter tubes. An extensive series of tests with tubes, rectangular channels and trapezoidal

channels by Holt et al. (1997) suggested a hydraulic diameter- related value of C given by the dimensional formula:

$$C = 21(1 - \exp(-0.135d_h)), \quad (6.89)$$

which gives a reasonable fit to most of the available data, as shown in Figure 6.22

THE DESIGN PROCESS

We now have the tools with which to approach a given design problem. Traditionally, heat exchanger analysis is treated in two separate ways, most often called the *design problem* and the *rating problem*. These are normally treated separately, with distinct *batch*, or once-through computer programs. Because of the speed and power of modern computing techniques, however, it is possible to combine these approaches effectively, both to yield a satisfactory design and also to indicate its sensitivity to geometric and operational changes. Thus off- design performance can be calculated immediately, a significant advantage if some specified performance parameters are negotiable. The approach presented here can be applied readily in a spreadsheet program. The basic process is that a *scoping* size is established with the aid of the core mass velocity equation for each side. At this point the flow configuration (that is, counterflow, crossflow or multipass) is decided, and the compatibility of dimensions between the two sides

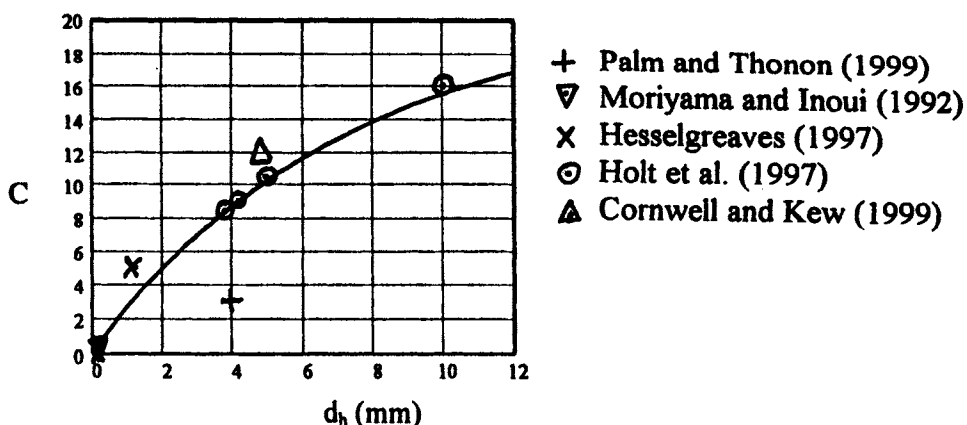


Figure 6.23 Correlation of Holt et al.(1997) of Chisholm's C parameter with hydraulic diameter, with additional data

is established. It should be pointed out that an experienced designer will often

know closely from the specification which configuration is called for, to meet the imposed constraints. The design is then *rated*, and changes made to the geometry until the rated performance meets the required performance, including pressure drop for both sides. Depending on the flexibility allowed for surface variation, the latter can be met exactly for both counter- and crossflow arrangements. The choice of counter- or crossflow depends largely on the first stage. The following outline gives the basic process: some details of practical variations such as two-phase flows and longitudinal wall conduction have already been mentioned and can be allowed for by appropriate algorithms and segmentation as necessary.

The options for configuration are shown schematically in Figure 6.24.

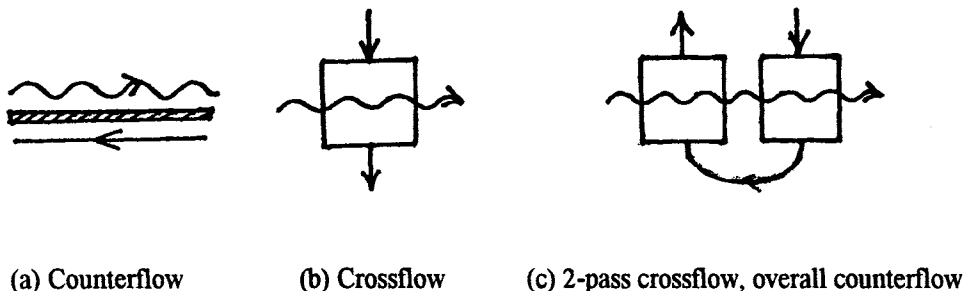


Figure 6.24 Flow stream configurations

Stage 1: Scoping size

1. From the thermal specification and equation 6.4 calculate the thermal effectiveness ϵ .
2. From $\dot{m}c_p$, for both sides with knowledge of fluids used, make an interim decision about whether a counter- or crossflow arrangement is best. Calculate the ratio of heat capacity rates C^* .
3. From the appropriate ϵ -Ntu chart or formula estimate the overall Ntu.
4. From Ntu estimate side N's as starting values. If heat exchanger is approximately balanced, e.g. liquid to liquid, take $N=2\text{Ntu}$; if liquid- gas take $N=1.1\text{Ntu}$ for gas side, $N=10C^*\text{Ntu}$ for liquid side. In general, if one side is estimated, the other follows from equation 6.26.
5. From N, Δp and mean properties, estimate G from equation 4.13 or 4.40, and hence A_c for each side.
6. From the first choice of surfaces, especially hydraulic diameter d_h (see chapter 2 for exchanger type, and chapter 5 for corresponding surface),

calculate Re , and consequently j or Nu , and f for each side from correlation or data.

7. From equation 4.25 or 4.48 calculate the length L for each side.

This completes the initial scoping. The next stage is basically a rating stage, but conducted iteratively to converge on a satisfactory design for the option chosen.

Stage 2.

A. Counterflow design.

- C1. Take the geometric mean of the two lengths from 7 above. We now have the first estimation of length and flow areas. Use these as starting values for optimisation using an iterative rating process.
- C2 From Re , f and j (Nu) for each side calculate Δp from equation 4.10, α from 4.3 and N from equation 4.8. The surface effectiveness η_o should then be calculated, if relevant from 6.45.
- C3. Calculate Ntu from 4.8, and ϵ from chart or formula for counterflow (Table 6.1).
- C4. Calculate P_λ from 6.65, and assess whether a wall conduction correction is needed. If so, calculate the corrected ϵ from equation 6.68 and 6.69. Any allowance for non-uniformity of surface should also be incorporated at this stage.
- C5. Compare ϵ with desired ϵ from step 1.
- C6. Change geometric variables (A_c for either side, flow length or surface d_h), recalculate G from step 5 if necessary and repeat stages C2- C4 until satisfactory convergence of ϵ and Δps is obtained. Note that if specific surfaces, with given hydraulic diameters, are chosen, then precise matching of Δp is rarely possible. There is usually one side that is critical (for example the gas side if the exchanger is a gas-liquid one), and this is met as precisely as possible, with the other Δp normally being lower than specified. Because the width of the core must be the same for each side, and the number of layers equal or differing by 1, the flow areas must be very nearly in the same ratio as the layer height. This requirement provides some initial guidance for the choice of surfaces. Put simply, for most process liquid pairs with similar properties, the higher the ratio {mass flow/pressure drop^{1/2}}, the higher is the ideal ratio of layer heights, from the mass velocity equation. Sometimes good matching requires the expedient of a double- banked surface, if a plate- fin (PFHE) exchanger is used. This ensures a closer match of Δps and avoids wasted surface, weight and cost.

C7. Arrange the shape of the overall face area (combined sides) to be close to square, with the constraint of an integral number of layers for each side. Most often the outer side is the cold side, to minimise heat loss to the environment. If either side is adjacent to the outside (top and bottom), this side has one more layer than the other, and this needs to be taken account of as discussed above, including allowance for the single- side heat transfer of the end layers, especially if the number is small. The actual block dimensions follow from knowledge of surface heights and porosities.

B. Crossflow design

X1. Perform step 1 for the appropriate crossflow arrangement. Compact surfaces are usually effectively unmixed on both sides: an approximate relationship that is close enough for most purposes is given in Table 6.1. Alternatively a chart can be used.

X2. Perform steps 2 to 7 for each side to give flow areas and lengths.

X3. Perform step C2 to give G , Re and N for each side, with chosen surfaces.

X4. Perform step C3 to give Ntu for exchanger, and ϵ from crossflow chart/ estimation.

X5. Compare ϵ with desired ϵ .

X6. Adjust geometry as for C5 until performance is satisfactory. It will be noted that for a crossflow heat exchanger matrix the length of one side provides one dimension (the width) for the flow area on the other side, taking into account surface porosity. Since a chosen surface has a given channel height, the requirement for an integer number of channels of each side stipulates that the lengths acceptable are in discrete steps rather than continuously variable: these are readily found. The step immediately higher than that calculated in X2 is appropriate (in practise the number of layers is selected). Further adjustment may then be necessary. Allowance must be made for the ineffective zones in each layer caused by the edge bars of the adjacent layers.

Entry and exit losses: these arise from the abrupt expansion and contraction of flow from the matrix and are usually small. Kays and London (1984) gives calculation processes.

C. Multipass crossflow, overall counterflow configuration.

This is often a viable alternative to a pure counterflow design for a high Ntu , since distributor sections are not required, the fluid entry to both sides being by headers, which are relatively cheap to manufacture, and which have low pressure drop.

For the simplest approach we assume that the passes are geometrically identical and with identical fluid properties. We also assume that each fluid is mixed between passes. Then the f and j factors and the Ntu s are the same, so the individual Ntu_p is $1/n$ of the overall Ntu , for n passes. Each flow is also the same for each pass, and the pass effectiveness ϵ_p is also the same.

Shah (1988) gives further details, and also a method for the case of unmixed flow between passes.

- M1. Guess a starting value of Ntu (overall). This could be estimated from the required effectiveness ϵ using the relationship for pure counterflow, in Table 6.2
- M2. Select number of passes, n .
- M3. Evaluate the value of ϵ_p using the multipass equation in Table 6.1 and with these values of n and C^* .
- M4. Determine the first approximation to intermediate temperatures (between passes) from simultaneous solution of the effectiveness equations 6.4, using this ϵ_p .
- M5. Evaluate mean physical properties for each pass.
- M6. The procedure for single pass crossflow design is then followed, using the selected surfaces for each pass. Each pass is taken to be identical.
- M7. The actual value of Ntu for each pass is then evaluated, from the geometric and thermal values for the two sides. The total pressure drop, over all passes, is also calculated for each side.
- M8. From the Ntu , calculate a new ϵ_p and hence intermediate and final temperatures.
- M9. Iterate dimensions (layer numbers and widths) until thermal and pressure drop requirements are met.

D) Design process for two-phase flows

The general process for these exchangers involves evaluating the proportions of the surface length required for preheating, superheating and/or subcooling either end of the saturated region. These lengths are treated separately as for single-phase flows, for liquid or vapour as appropriate. Taylor (1990) gives detailed procedures. It should be noted that when designing for convective boiling, the pure vapour calculation should be performed for the final 5% of the surface length, since the wall is often effectively dry even though the bulk fluid is still such that the mean quality has not attained unity. The length for the preheat section is determined by a straightforward heat balance.

For the saturated region, the simple effectiveness- Ntu relationships for zero heat capacity ratio can be used, with perhaps a small allowance for the progressive loss of saturation temperature caused by the two-phase pressure drop.

Final block sizes (all configurations)

The thermal performance determined from the above procedures refers of course to the active thermal zone, that is the wetted zone including distributors. It should be noted, and allowed for in the final design, that the area occupied by the edge bars of a plate fin block contributes to the pressure drop but not to the thermal performance. Thus in a crossflow configuration the active length for pressure drop for one side is the active width plus twice the width of the edge bars of the other side, and vice versa.

Example of thermal design

A design is required for the following specification:

	Side 1	Side 2
Fluid	Water	Methyl alcohol
Inlet temperature (°C)	60	28
Outlet temperature (°C)	40	48
Mass flow rate (kg/s)	10	16.24
Pressure drop (kPa)	10 (this side critical)	5

Mean properties

Specific heat c_p kJ/kgK	4.182	2.575
Dynamic viscosity η kg/ms	544E-6	475E-6
Thermal conductivity λ W/mK	.643	0.209
Density ρ kg/m ³	1000	770
Prandtl number Pr	3.54	5.87

Stage 1: scoping size

- Effectiveness $\varepsilon = \frac{C_c(T_{c,o} - T_{c,i})}{C_{\min}(T_{h,i} - T_{c,i})} = \frac{10 \times 4.182(60 - 40)}{16.24 \times 2.575(60 - 28)} = 0.625$
- Since heat capacity rates are identical, $C^* = 1.0$, and effectiveness is fairly high, choose a counterflow design.

3. For balanced counterflow $Ntu = \epsilon/(1+\epsilon) = 1.667$
4. Take N (each side) = $2 \times 1.667/0.7 = 4.77$, allowing for surface effectiveness of 0.7.
5. Take starting value of j/f of 0.25. From equation 4.13 the mass velocity is given by $\frac{G^2}{2\rho\Delta p} = \frac{j/f}{Pr^{2/3}N}$, giving

$$G_1 = \sqrt{\frac{2 \times \rho \times \Delta p \times j/f}{Pr^{2/3}N}} = \sqrt{\frac{2 \times 1000 \times 10000 \times 0.25}{3.54^{2/3} \times 4.77}} = 672 \text{ kg/m}^2\text{s.}$$

Flow area $A_1 = 0.0149 \text{ m}^2$.

Similarly $G_2 = 503 \text{ kg/m}^2\text{s}$, and $A_{c2} = .0323 \text{ m}^2$.

6. Since liquids are used, one of which is water, a stainless steel surface is most likely to be appropriate, with low fin efficiency. Low fin height and a thicker fin are accordingly necessary. This qualifies a design based on published data such as those of Kays and London (1998), which refer mainly to aluminium surfaces. Representative stainless steel surfaces are thus used here. Take hydraulic diameters d_{h1} and d_{h2} each as 0.002 m. Then from 4.24, $Re_1 = (Gd_h/\eta)_1 = 3528$, and $Re_2 = 2118$. High performance surfaces will have typical values of $j = 0.09$ and $.01$ respectively, with $j/f = .25$ each, at these Reynolds numbers, allowing for the thicker fins.
7. From equation 4.8, $L_1 = d_h * Pr^{2/3}N/4j = 0.61 \text{ m}$, and similarly $L_2 = 0.77 \text{ m}$

Stage 2 Counterflow design

- C1. For compliance with the critical pressure drop, select $L = 0.61 \text{ m}$
- C2. The water side pressure drop is automatically met at 10 kPa. The methyl alcohol pressure drop is given by equation 4.10:

$$\Delta p_2 = (2G^2 \times L \times f/\rho/d_h)_1 = 4008 \text{ Pa}$$
. This is well within the allowable value. Take surface effectiveness at 0.7 for each side. Then the effective N values are given by

$$N_1 = 4 \times L \times j \times \eta_1 / (Pr^{2/3}d_h) = 3.31$$
, and $N_2 = 2.624$, which gives the new $Ntu = 1.464$.

C3 to C5. The calculated value of overall Ntu is below the required value of 1.667, so the flow length should be increased by perhaps 15%. In addition the water side flow area will need to increase by about 8% to accommodate the pressure drop requirement. Further detailed convergence would normally be undertaken to take into account full surface effectiveness calculations.

Block dimensions

The final length $0.61 \times 1.15 = 0.7$ m. Core flow areas are $0.0149 \times 1.08 = 0.0161$ m² (water side), and $.0323$ m² (methyl alcohol side), and if typical values of porosity of 0.7 are taken, then the total face area is $(0.0161+0.0323)/0.7 = 0.069$ m², giving for example a square side of 0.263 m. The number of layers would depend on the detailed surface geometry. For this counterflow arrangement the flow distributors would need to be taken into account in the pressure drop calculation, and would add to the total weight and length.

The block weight without distributors would be 113 kg

THERMAL DESIGN FOR HEAT EXCHANGER REACTORS

In the growing pursuit of Process Intensification (PI) in the chemical process industries it is becoming desirable to achieve heat exchange and chemical reaction in one unit (Butcher and McGrath (1993), Phillips and et al. (1997), Arakawa et al (1998)). The purpose is twofold, one being simply to save equipment (and with it fluid inventory, important for safety and environmental considerations), the other being that the heat of reaction, either exothermic or endothermic, can be removed or added during the reaction process. In this way the temperature of the reactants can be closely controlled, which has substantial benefits for by-product production. It has been shown (Edge et al. (1997)) that very significant reduction in by-product production can be obtained by custom-designed heat exchanger reactors. The danger of runaway reactions is also almost completely avoided.

In the following discussion we will use the terminology that a flow rate of a reactant (usually of relatively low flow compared with the primary flow) is injected into the primary flow, with which it reacts. The secondary flow is a service flow from the point of view of the unit, although it may also be a process fluid.

The simplest form of heat exchanger reactor is one in which the reactant is injected at entry to the exchanger (for example into the inlet manifold or header). It is usually assumed that the exchanger removes or supplies only the heat of

reaction and no further sensible heat. Thus the temperature at inlet of the primary stream (before reaction commences) and its final temperature are equal, and we call this the nominal temperature. This is ideally the temperature defined by optimum reaction kinetics. The consequent temperature distribution along the exchanger length depends on the speed of reaction together with the mixing characteristics of the exchanger primary flow surface. Two possibilities are illustrated diagrammatically in Figures 6.25 and 6.26. For this purpose we assume that the reaction is exothermic.

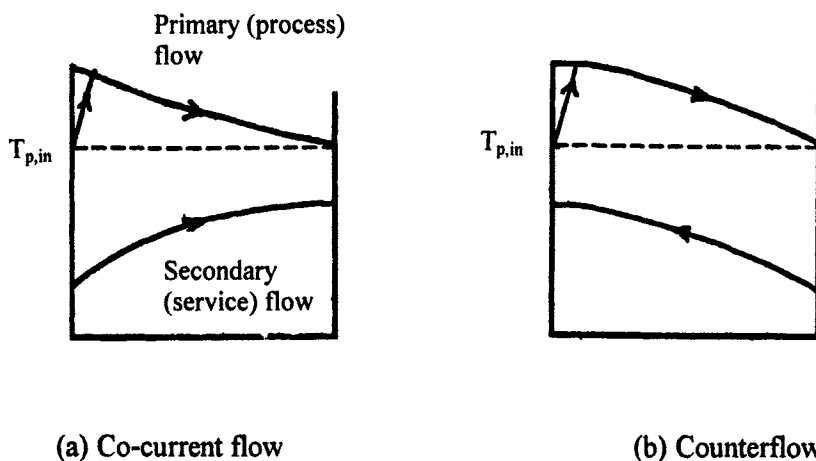


Figure 6.25 Temperature profiles for instantaneous reaction and mixing

In Figure 6.25 the reaction is instantaneous, with instantaneous mixing with the primary flow, and with a consequent instantaneous temperature rise. The performance is then identically that of a conventional (sensible heat) exchanger with the peak temperature T^* determined by the heat of reaction and thermal equilibrium with the primary stream. The subsequent temperature profile of the reacting (primary) flow stream depends on the flow arrangement. If this is co-current (Figure 6.25(a)) then the temperature falls rapidly with distance since the initial temperature difference is high: in a counterflow arrangement (Figure 6.25(b)) the fall is more gradual, as shown: it is linear if the heat capacity rates are equal. From the point of view of by-product generation the co-current arrangement is clearly preferable, although the required surface area will be higher, to attain the nominal starting temperature of the primary flow.

If the reaction is not instantaneous, but takes place at a rate such that it is completed exactly at the end of the exchanger- the other limiting condition is reached. For a reaction rate which is constant with length- the simplest condition, the temperature profiles will be as shown in Figure 6.26, showing again the cases

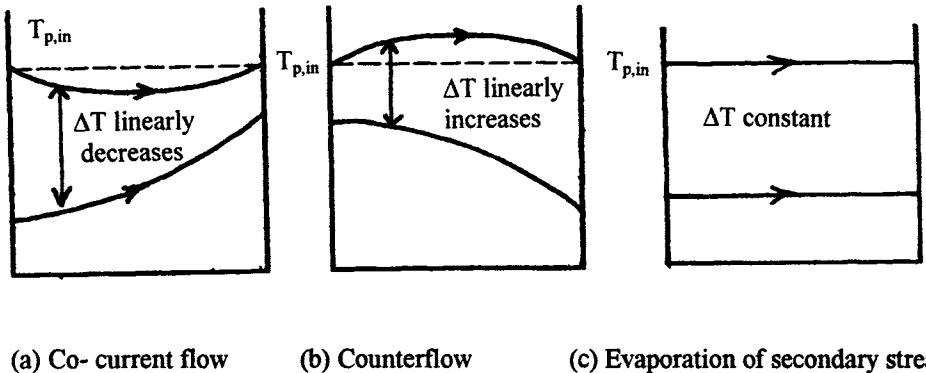


Figure 6.26 Temperature profiles for constant rate

of co-current and counterflow conditions. In the case of co-current flow the primary stream with its reactant drops below the nominal temperature, and for the counterflow case it rises above it: in both configurations the final temperature is the same as the nominal temperature, for an idealised design.

It is clear from the latter cases of linearly-distributed reaction that the primary, reacting stream could be maintained at the nominal temperature if the secondary flow were also at constant temperature, since the driving temperature difference would be constant. The heat removal rate would thus match that of the heat release. This would correspond to an evaporating secondary flow.

In a real reacting situation neither of the above ideal cases would occur, although they may be approached closely in some processes. The heat exchanger reactor designer has to consider both a non-uniform rate of heat release, and also the probable requirement for progressive injection of reactant into the primary stream in order to attain a primary stream temperature close to the temperature of reaction. This is a specialised design problem.

MECHANICAL ASPECTS OF DESIGN

Pressure containment

Pressure containment is achieved by the tension in the fins of a plate-fin heat exchanger, by spot or edge welding in welded plate exchangers, and on the contacting plate to plate surface of diffusion bonded exchangers. In addition to the finning, the edge bars take both normal and lateral stresses. For duties involving substantial pressures, the width of the edge bars is made approximately

equal to the plate spacing. Lower widths may be used for near-atmospheric pressures. Taylor (1990) gives a method of design stress calculation for the finning of a plate-fin surface, with relation to the figure below, which also shows schematic PCHE and tubular surfaces.

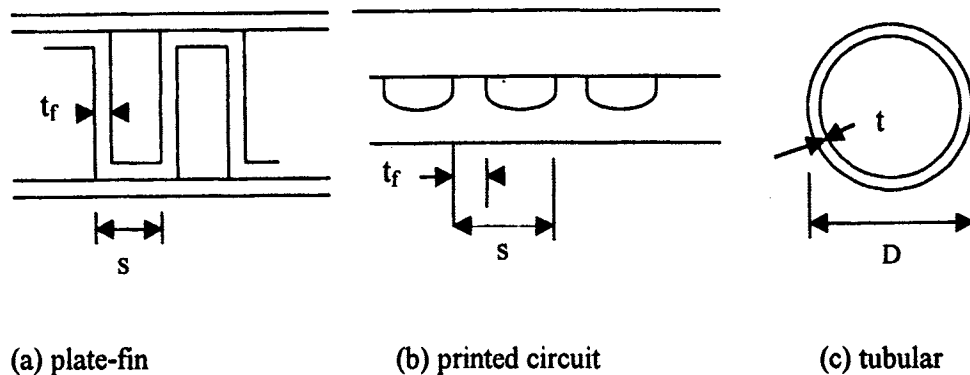


Figure 6.27 Schematics of surfaces for pressure containment

Suppose the pressure differential between streams is δp , the fin thickness is t_f and fin density N (fins/m). Then for both the plate-fin (PFHE) and Printed Circuit (PCHE) surface types the stress E (Pa or kPa) in the fin is given by

$$E = \delta p \left(\frac{1}{N} - \frac{1}{t_f} \right) / t_f = \delta p \left(\frac{1}{N t_f} - 1 \right). \quad (6.90)$$

For given pressure differential, therefore, the stress reduces as the product Nt increases. This product is often simply called the "N-t" value of a surface to denote its pressure containment potential. In practice it is related to the yield stress of the material by an appropriate factor of safety (for example in a design code for the exchanger type) to give a maximum allowable pressure difference.

For circular tubes, the corresponding hoop stress (for a thin-walled tube) is given by

$$E = \frac{\delta p}{2} \left(\frac{D-t}{t} \right) = \frac{\delta p}{2} \left(\frac{D}{t} - 1 \right). \quad (6.91)$$

It is clear from the above relationships that pressure containment capability is independent of scale, since in the PFHE case, equation 6.86, the product Nt does not change, and in the tubular case, the product D/t does not change – in both

cases provided that all dimensions are equally scaled. Thus the more compact the surface is, the lower is the required material thickness to contain a given pressure. This implies that the porosity requirement for stressing purposes is independent of scale. In practice, however, realistic allowance must be made for the possibility of loss of material through corrosion and erosion. This puts lower limits on the separating plate thickness, as does the handling aspect for large block dimensions.

For aluminium alloys the allowable tensile stress is given by Taylor (1990) as approximately 2/3 of the yield stress, giving the allowable stress as 24 MPa. A corresponding value for the yield stress of 316L austenitic stainless steel is 234 MPa, giving an operating stress limit of 156 MPa.

The pressure containment capability of plate-type exchangers (welded plate, brazed plate) depends on their detailed plate patterns and bonding mechanisms, and hence is specific to each manufacturer. Some operational information is given in Chapter 2.

Strength of bonds

The above arguments are only valid, of course, if the fin to separating plate (PFHE), or the plate to plate (PCHE) bonds are at least as strong as the parent metal for which the yield strength is used. For the high silicon brazing alloys used in aluminium brazing this is valid for a good braze (Shah (1990)) for temperatures of up to 150°C, the normal operating limit for aluminium alloys. (Taylor (1990) gives 250°C as a limit for certain aerospace applications). In addition there is normally a fillet of brazing metal at the fin-plate interface of greater effective thickness than the fin, thus reducing the local stress. Corresponding arguments can be made for the brazing alloys used for stainless steel PFHEs, provided that the stringent requirements of preparation of the matrix and for temperature control are met (Shah (1990)). It has also been demonstrated that the bond strength of commercial PCHE structures, which are diffusion-bonded, is that of the parent metal, because of the crystal grain growth across the interface during bonding.

REFERENCES

Bennett, D.L. and Chen, J.C. (1980), Forced Convective Boiling in Vertical Tubes for Saturated Pure Components and Binary Mixtures, *AIChE Journal*, Vol. 26, No 3, pp 454-461.

Berntsson, T., Franck, P-A. Hilbert, L., and Horgby, K. (1995), Learning from Experiences with Heat Exchangers in Aggressive Environments, CADDET Analysis Series No. 16, CADDET, Sittard, Netherlands.

Butterworth, D. (1979), The Correlation of Cross Flow Pressure Drop Data by Means of Permeability Concept, Report AERE-R9435, Atomic Energy Research Establishment, Harwell.

Chen, J.C., (1966), Correlation for Boiling Heat Transfer to Saturated Fluids in Convective Flow, Ind. Eng. Chem. Proc. Des., 5, 322.

Chiou, J.P., (1976), Thermal Performance Deterioration In Crossflow Heat Exchanger due to Longitudinal Heat Conduction in the Wall, ASME paper No. 76-WA/HT-8

Chiou, J.P. (1978), The Effect of Longitudinal Heat Conduction on Crossflow Heat Exchanger, ASME J Heat Transfer, 100, 436-441.

Chiou, J.P., (1980), The Advancement of Compact Heat Exchanger Theory Considering the Effects of Longitudinal Heat Conduction and Flow Non-Uniformity, in Compact Heat Exchangers: History, Technological Advancement and Mechanical Design Problems, HTD. Volume 10, 101-121, ASME, New York.

Cooper, M.K., (1984), Saturated Nucleate Pool Boiling: a Simple Correlation, 1st. U.K. National Heat Transfer Conference, Vol. 2, pp785-793.

Cornwell, K and Kew, P.A., (1995), Evaporation in Microchannel Heat Exchangers, Paper C510/117, 4th UK National Heat Transfer Conference, Manchester, MEP.

Cornwell, K and Kew, P.A., (1999), Compact Evaporators, in Convective Flow and Pool Boiling, Proceedings of the International Engineering Foundation 3rd Conference, Irsee, Germany: Taylor and Francis.

Edge, A.M., Pearce, I. And Phillips, C.H., (1997), Compact Heat Exchangers as Chemical Reactors for Process Intensification (PI), Proc. 2nd Int. Conf. on Process Intensification in Practice, Antwerp.

Feldman, A., Marvillet, Ch., and Lebouche, M., (1996), An Experimental Study of Boiling in Plate Fin Heat Exchangers, Proc. 2nd European Thermal- Sciences and 14th UIT National Heat Transfer Conference, 445-450, Eds. Celata et al., Edizioni ETS, Pisa.

Forster, H.K. and Zuber, N., (1955), Dynamics of Vapour Bubbles and Boiling Heat Transfer, AIChE J., 1, 531.

Hesselgreaves, J.E., (1997), Single Phase and Boiling Performance of a Novel Highly Compact Heat Exchanger Surface, 5th UK National Heat Transfer Conference, London.

Hewitt, G.F., Bott, T.R. and Shires, G.L., (1994), Process Heat Transfer, Begell House & CRC Press.

Holt, A.J., Azzopardi, B.J. and Biddulph, M.W., (1997) Two- Phase Pressure Drop and Void Fraction in Channels, 5th UK National Conference on Heat Transfer, IChem E , London.

Idel'chik, (1986), Handbook of Hydraulic Resistance, 2nd. Edn., Hemisphere, New York

Kays, W.M and Crawford, M.E., (1993) Convective Heat and Mass Transfer, 3rd edn., McGraw Hill.

Kays, W.M and London, A.L. (1984), Compact Heat Exchangers, 3rd edn., McGraw Hill.

Kew, P.A., (1995), Boiling in Narrow Channels, Ph.D thesis, Heriot- Watt University, Edinburgh, UK.

Kew, P.A. and Cornwell, K., (1995), Confined Bubble Flow and Boiling in Narrow Channels, 10th Int. Heat Transfer Conf., Brighton, UK.

Kew, P.A., (2000), Private communication.

Kroeger, P.G. (1967), Performance Deterioration in High Effectiveness Heat Exchangers due to Axial Heat Conduction Effects, in Advances in Cryogenic Engineering, Volume.12, 363-372.

Lockhart, R.W. and Martinelli, R.C. (1949), Proposed Correlation of Data for Isothermal Two-Phase Two-Component Flow in a Pipe, *Chem. Eng. Prog.*, 45, 39.

London, A.L., (1970), Laminar Flow Gas Turbine Regenerators- The influence of Manufacturing Tolerances, *ASME J Eng. for Power*, 92, Series A, (1), 46-56f

London, A.L. Klopfer, G., and Wolf, S. (1986), Oblique Flow Headers for Heat Exchangers, *J. Eng. Power*, vol. 90A, pp271-286.

Martin, H. (1999), Economic Optimisation of Compact Heat Exchangers, *Proceedings of the International Conference on Compact Heat Exchangers and Enhancement Technology for the Process Industries*, Banff; Begell House, New York.

Mondt, J.R., (1990), Highlights from thirty years of research to develop compact heat exchangers with emphasis on interactions between General Motors and Stanford University. In *Compact Heat Exchangers, A Festschrift for A.L. London*, Ed. Shah et al, Hemisphere, New York.

Moody, G.W., (1971), Boundary Wall Shapes for Uniform Flow through an Inclined Filter, *NEL Report No 487*, Dept. of Trade and Industry, London.

Moriyama, K. and Inoue, A. (1992), The Thermohydraulic Characteristic of Two- Phase Flow in Extremely Narrow Channels (The frictional Pressure Drop and Void Fraction of Adiabatic Two-Component Two-Phase Flow), *Heat Transfer- Japanese Research*, 21, (8).

Palm, B. and Thonon, B., (1999), Thermal and Hydraulic Performances of Compact Heat Exchangers for Refrigeration Systems, *Proceedings of the International Conference on Compact Heat Exchangers and Enhancement Technology for the Process Industries*, Banff; Begell House, New York.

Phillips, C.H., Lauschke, G. and Peerhossaini, H., (1997), Intensification of Batch Chemical Process by using Integrated Chemical Reactor- Heat Exchangers, *Applied Thermal Engineering*, vol. 17 nos. 8-10, pp809-824.

Polley, G.T., Panjeh Shahi, M.H., and Picon Nunez, M., (1991), Rapid Design Algorithms for Shell- and -Tube and Compact Heat Exchangers, *Trans. IChemE*, Vol.69 Part A.

Rampisela, P., Berthold, G., Marvillet, Ch. and Bandelier, P. (1993), Enhanced Boiling in Very Confined Channels, Proc. 1st. Int. Conf. on Aerospace Heat Exchanger Technology, Palo Alto, CA., Elsevier.

Roetzel, W. and Luo, X., (1993), Pure Crossflow with Longitudinal Dispersion in One Fluid, Proc. 1st. Int. Conf. on Aerospace Heat Exchanger Technology, Palo Alto, CA., Elsevier.

Shah, R K (1983), Heat Exchanger Basic Design Methods, in Low Reynolds Number Flow Heat Exchangers, ed. Kakac, S., Shah, R. K. and Bergles, A.E., Hemisphere.

Sekulic, D.P. (1990), Reconsideration of the Definition of a Heat Exchanger, Int.J.Heat Mass Transfer, Vol. 33, no. 12, 2748-2750.

Shah, R.K. (1985), Compact Heat Exchangers, Part 3 of Handbook of Heat Transfer Applications, ed. Rohsenow, Hartnett and Ganiç, McGraw Hill, New York.

Shah, R.K. (1988), Plate- Fin and Tube- Fin Heat Exchanger Design Procedures, in Heat Transfer Equipment Design, ed. R.K. Shah, E.C. Subbarao, and R A Mashelkar, Hemisphere.

Shah, R.K. (1990), Brazing of Compact Heat Exchangers, In Compact Heat Exhangers: A Festschrift for A.L. London, Hemisphere, New York.

Shah, R.K. (1994), A Review of Longitudinal Wall Heat Conduction in Recuperators, Jnl. Energy, Heat and Mass Transfer, 16, pp 881-888.

Shah, R.K and London, A.L. (1978), Laminar Flow Forced Convection in Ducts, Supplement 1 to Advances in Heat Transfer, Academic Press, New York.

Smith, E.M., (1997), Thermal Design of Heat Exchangers, a Numerical Approach, John Wiley and Sons, New York.

Srinivasan, V. and Shah, R.K., (1995), Condensation in Compact Heat Exchangers, Eurotherm Seminar 47: Heat Transfer in Condensation, Ed. Marvillet and Vidil, Paris, France, Elsevier.

Sterner, D. and Sundén, B., (1997), Performance of some Plate- and Frame Heat Exchangers as Evaporators in a Refrigeration System, 5th UK National Heat Transfer Conference, London.

Taylor, M.A. (1990), Plate-Fin Heat Exchangers: Guide to their Specification and Use. HTFS, Harwell, UK.

Thonon, B., and Chopard, F. (1995), Condensation in Plate Heat Exchangers: Assessment of a Design Method, Eurotherm Seminar 47: Heat Transfer in Condensation, Ed. Marvillet and Vidil, Paris, France, Elsevier.

Tran, T.N., Wambganss, M.W., Chyu, M.-C. and France, D.M., (1997), A Correlation for Nucleate Flow Boiling in Small Channels, Proceedings of the Int. Conf. On Compact Heat Exchangers for the Process Industries, Snowbird, Utah, Begell House, New York

Chapter 7

COMPACT HEAT EXCHANGERS IN PRACTICE

(D. A. Reay and J. E. Hesselgreaves)

At the end of its analysis physics is no longer sure whether what is left in its hands is pure energy or, on the contrary, thought.

P. Teilhard de Chardin

In this Chapter, a number of factors affecting, ultimately, the long-term satisfactory operation of compact heat exchangers are discussed. Having decided upon the type of heat exchanger to be used in a particular situation (an exercise which will have already considered some aspects of fouling), the installation of the unit must be carried out, and guidance given to those involved in the operation and maintenance of the unit. Fouling, and to a lesser extent corrosion, and their minimisation remain key priorities during the life of many heat exchangers, particularly those in arduous process industry duties, and these aspects should never be neglected during the life of the unit.

The Chapter is mainly targeted towards process applications, although some of the principles are relevant to all applications of compact heat exchangers.

The factors to be considered, including those necessarily affecting system design, are set out in the following order:

- Installation
- Commissioning
- Operation
- Maintenance:
 - General factors
 - Fouling & corrosion
- Design approaches to reduce fouling
- Fouling factors.

INSTALLATION

Many of the features of compact heat exchangers which affect installation will no doubt have been considered during the specification stage. In some cases

there may be a need for instrumentation which monitors the performance of the compact heat exchanger continuously, because of its higher sensitivity to some changes in conditions than, say, standard shell and tube units. This will have been considered before installation, but correct location is of course important. In the case of compact heat exchangers, the provision of on-line pressure drop monitoring will provide a useful guide to the build up of fouling, which will of course be reflected in an increase in pressure drop across the unit.

Where fouling is of particular concern, insofar as it could affect the time the heat exchanger spends on line, the use of two identical heat exchangers in parallel should be considered. Then, if one becomes partially blocked, the other unit can be brought into service during cleaning of the fouled unit, without significant process interruption. It must be remembered that the cost of production lost due to the need to shut a stream while a heat exchanger is cleaned, or worse, can greatly outweigh the extra cost of a second heat exchanger in a parallel bypass stream.

There are substantial differences between installations where an old heat exchanger is being replaced by a new one, or a new one added to an existing plant – retrofitting – than where a completely new plant is being constructed with compact heat exchangers as part of this new installation. An aspect of retrofitting sometimes overlooked is the need to either replace or at least fully clean pipework upstream of the new heat exchanger. (Of course, owing to size differences, the pipes immediately local to the new heat exchanger will need replacing). Compact units, being susceptible to particulates in the fluid stream, require much better control of upstream conditions than a conventional shell and tube heat exchanger, or other types with large passages. Even in an all-new plant, debris may get into pipework during plant construction, which could affect subsequent compact heat exchanger performance. ALPEMA¹ makes specific recommendations for the start up of brazed plate-fin heat exchangers, concerning purging and cool-down (where used in cryogenic duties), to clean the unit, prevent freezing, and preserve its integrity.

The installer who is used to making substantial provision of space for bundle removal in conventional shell and tube heat exchanger installations will find that on an all-new installation, the amount of space required for removal of the core during maintenance will be substantially less². Lifting gear needs will also be different, and it will have become evident during the design and specification of

¹ ALPEMA is The Brazed Aluminium Plate-Fin Heat Exchanger Manufacturers' Association (see ref. 14).

² Note that not all compact heat exchangers have cores which can be removed for mechanical cleaning, for example. Where brazing or diffusion bonding is used, alternatives should be considered – see section on fouling.

the installation that the options for location of the heat exchanger will have increased owing in part to its lower weight for a given duty.

Installation is frequently carried out while other activities are under way in the locality. It may seem obvious, but compact heat exchangers need to be protected from adverse conditions during installation and commissioning. Ingress of dust could be disastrous, and the introduction of any fluid which is not that anticipated within process operation could also create problems, such as corrosion. Obviously if the plant is located on-shore, but near the sea, a salt-laden atmosphere would be damaging to an aluminium plate-fin heat exchanger, for example.

Bott (1990), in his *Fouling Notebook*, highlights problems which might occur if hydraulic testing (carried out on site prior to commissioning) is not properly implemented. Some corrosion control by inhibitors, for example, is recommended immediately following the test, and good quality water should of course be used for the hydraulic test itself. It may be that the inhibitor will be left in the heat exchanger for some time, prior to final installation and commissioning.

Of course, as pointed out by Bott, the heat exchanger should be thoroughly checked on its arrival at the site, to make sure that all components and the whole assembly meet the specification requested.

COMMISSIONING

It is particularly important to be careful when commissioning a compact heat exchanger installation. As mentioned earlier, if the installation is a retrofitted one, all pipework accessing the heat exchanger(s) should be fully cleaned. Heat exchangers with small passages, particularly those where access for cleaning is difficult, are particularly sensitive to operation outside their design envelope, in terms of temperature and velocity of the fluid(s) passing through the heat exchanger. High temperature can change the nature of the fluid at the heat exchanger wall/fluid interface, leading to fouling which would not, under normal circumstances, be anticipated, (see later in this Chapter). If the velocity of the fluid passing thought the unit is reduced during commissioning, well below that to prevent deposition of particulates on surfaces, for example, accelerated fouling can occur and some deposits which were not anticipated when the heat exchanger was specified may be found difficult to remove. Beyond the commissioning stage, of course, similar difficulties might arise during start up of the whole process plant, where conditions through the heat exchanger may be substantially different to those normally encountered during steady state operation. (An analogy may be made with a car engine clean-up system, where the cold engine can affect catalyst performance due to increased throughput of unburned hydrocarbons, for example).

Many compact heat exchanger types are still relatively new in some market sectors. It is therefore essential for even large user companies to make full use of the experience of the heat exchanger vendor gained during installation and commissioning at other sites. Even if the vendor was not directly involved, the contractor will no doubt have provided some feedback, particularly if any problems had been encountered. 'Learning from the experience of other' (Reay, 1999) is a key recommendation for anyone contemplating using heat exchanger equipment.

OPERATION

The operation of compact heat exchangers requires a degree of control over conditions which tends to be greater than that exercised with conventional shell and tube heat exchangers. This arises from the faster transient conditions consequent on the lower fluid inventory of compacts. Some may find that this limits the flexibility of the overall installation, but as long as the user is aware of the operating parameters of the process streams when he is making the selection of the heat exchanger and associated plant, this should not be a problem. Indeed, some types of compact heat exchanger are specifically designed to be expanded or reduced in size to cope with differing process conditions over the life of a plant. The gasketed plate heat exchanger is one such example. Tight design can affect the performance of the heat exchanger where a reduction in stream velocity might occur, for example. The effect this might have has already been highlighted in the section on commissioning above.

A perhaps obvious aspect of compact heat exchanger operation is the need to ensure that operators have the necessary training to address any problems which might arise, and are conversant with cleaning procedures, the handling needs of particular types of surface and/or materials, and the degree of tightness when installing gaskets, for example.

If one is concerned about possible failure of any heat exchanger, due to pressure rupture, excessive temperatures affecting gasket material, or fouling leading to complete blockage, the main way to ensure that damage limitation is fully implemented is to *monitor*, preferably continuously, critical factors such as stream temperatures and pressure drop across the sides (there may be more than two streams) of the heat exchanger.

An aspect of operation which cannot readily be anticipated is a change in the nature of the product which is being processed in the plant of which the compact heat exchangers are essential components. While it may be acceptable, albeit with some change in overall heat transfer coefficients, to change the material going through a shell and tube heat exchanger having tubes of 19 mm internal diameter, to do the same with a printed circuit unit with an hydraulic diameter of

channels of 2-3 mm is to increase the degree of risk substantially. As with all of the advice given, it is assumed that reputable plant operators will be aware of such hazards and avoid them. There will, however, be those who remain ignorant, and one can in such cases only point out potential sources of erroneous judgement!

MAINTENANCE

In this Section, the maintenance of compact heat exchangers is discussed. Because fouling (and corrosion) are factors of compact units (apart from their small size) most regularly mentioned whenever these heat exchanger types are considered, it is important to discuss in some detail the types of fouling mechanisms, some of which are directly associated with corrosion, which can occur. Even more significant is a description of the techniques used to overcome the several forms of fouling which can occur in 'conventional' or compact heat exchangers.

Thus, following a general discussion of maintenance aspects of compact units, a sub-section is devoted to a description of fouling mechanisms, and solutions for overcoming fouling, in particular in compacts.

Maintenance – General Factors

In many cases, maintenance of compact heat exchangers can be easier than that of larger conventional shell and tube units. As an example, consider the volume differences between a shell and tube unit with provision for removing the whole tube bundle, and a welded plate heat exchanger of the same duty. In the former case, a distance equivalent to the whole heat exchanger length should be provided downstream of one of the end covers for bundle removal, while for the plate unit a distance, either vertically or horizontally, of about 30% of that needed for the shell and tube unit is necessary for an identical operation. While on-shore such space considerations may not be critical, on an off-shore platform the cost of platform space is such that reduced space needs are dominant in equipment selection.

The reduced volume of the compact core also has other advantages – it can be readily shipped off site for maintenance and/or cleaning, for example. An important aspect of maintenance sometimes neglected by users is associated with gaskets. Where these are used, for example between plates, uniform gasket compression should be ensured. In recent years, the original equipment manufacturers have also become concerned about the use of 'cheaper' gaskets which are not approved by the heat exchanger supplier. As in many other sectors of industry, 'bogus' spare parts are a serious problem affecting service reliability,

and companies should never contemplate sacrificing the perhaps higher cost of spares from a reputable company in order to seemingly save capital expenditure. The pitfalls of doing this are obvious.

Maintenance of the heat exchanger is useless if carried out in isolation. A heat exchanger is but one component of a process stream, and associated with the heat exchanger will be controls, valves, filters and sensors, such as pressure transducers and thermocouples. Checking of the calibration of equipment which is used to monitor the performance of the heat exchanger is essential – this goes without saying – but it is also vitally important, as mentioned in the section on ‘operation’, to ensure that such equipment is used during heat exchanger running. If monitoring equipment is in place, but is neglected, no-one other than the site person responsible can be blamed for the consequences of failure. The cleaning of filters is a regular maintenance operation, not to be forgotten. If the pressure drop across the heat exchanger is being monitored (as it should be), the location of the pressure tappings may be such that the filters are included in the pressure drop being measured; if they are outside the region between tappings, a second pressure drop monitoring system covering the upstream filters, could be usefully installed.

Preventative maintenance is designed, of course, to reduce the chances of breakdown in any of the components making up a process stream. However, contingency plans should always be present in case failure of the whole, or part, of a heat exchanger does occur while on line. The remedial action may involve directing the process stream(s) through an adjacent second heat exchanger, (installed for such an eventuality), or blocking off the offending layers in the compact heat exchanger.

Maintenance - Fouling and Corrosion

Fouling, while perceived as one of the limitations affecting increased use of CHEs, can be addressed in a number of ways to minimise its effect on the system, and on the CHE in particular, (Reay, 1995). In this sub-section the mechanisms of fouling which may occur in CHEs (and of course in other types of heat exchanger) are described, and solutions put forward. There are also a number of heat exchanger types, not all of them CHEs, which are designed specifically to handle fouled process streams. These are briefly discussed at the end of this sub-section. For those wanting a more detailed treatment of fouling in heat exchangers, a recent text by Bott (1995) is recommended.

The principal types of fouling are:

- Crystallisation or precipitation fouling
- Particulate fouling or silting

- Biological fouling
- Corrosion fouling
- Chemical reaction fouling
- Freezing or solidification fouling

Crystallisation or precipitation fouling

This occurs when a solute in the fluid stream is precipitated and crystals are formed, either directly on the heat transfer surface, or in the fluid, to be subsequently deposited on the surface. When the fluid concerned is water, and calcium or magnesium salts are deposited, the mechanism is frequently referred to as scaling. Waxes can also precipitate out as temperatures of fluids are reduced through the heat exchanger.

Scaling is a function of wall temperature and possibly also of kinetics. The wall temperature profile through most compact heat exchangers is well-defined relative to that in shell and tube units, and it is suggested (Clarke, 1994) that a less conservative view of scaling should be taken with CHEs, and any permissible increase in the outlet temperature of sea water, when used as a coolant, would be welcomed because of the associated reduction it brings in pump sizes, etc.

It is important to note that there are a number of compounds, known as inverse solubility salts, which exhibit a reduction in solubility with increasing temperature. These include calcium carbonate and magnesium silicate. In these cases, identification of the *highest* cooling water temperature likely to occur in a heat exchanger with narrow channels is therefore important for determining the water treatment strategy.

In general, crystallisation or precipitation fouling is avoided either by pre-treatment of the fluid stream (e.g. by acid addition to cooling water to remove carbonate) or by the continuous addition of chemicals that reduce or eliminate deposit formation. There are positive indications that the addition of appropriate particles into the fluid stream - seeding or germination - can be effective in minimising deposition on heat transfer surfaces, (Grillot, 1997). Additives can be used to minimise waxing, but environmental pressures are increasingly mitigating against excessive use of chemical treatments. Mechanical cleaning methods such as high pressure lances are unlikely to be usable in compact heat exchangers because of the small passage sizes and their sometimes tortuous flow paths. These features make it difficult to clean any passages which are completely blocked. Note that care should be taken to ensure that cleaning chemicals are compatible with materials of construction, including brazes, gaskets etc.

Recently, electromagnetic descaling technology – sometimes called physical water conditioning by the equipment suppliers, which is extensively promoted for

scale prevention in water-carrying pipes to inhibit calcium carbonate deposition on the surfaces, has been examined as a protective measure to inhibit heat exchanger fouling. The work indicates that the method can be effective for both inverse solubility salts and those exhibiting normal solubility characteristics, such as silica. Most of the scale inhibitors which are marketed extensively for pipe scale control use a controlled electromagnetic field through which the water stream passes, affecting the size and structure of mineral crystals within the stream. This reduces their ability to adhere to each other, and to the pipe or heat exchanger surfaces, thus reducing the propensity to scale.

Although patents were taken out on the concept as early as 1895, companies such as Hydromag (UK) state that a considerable amount of time has been expended on achieving the correct field strength in combination with positioning of the lines of the magnetic field with regard to the direction of the water stream. Although more strictly categorised as a device for the prevention of scaling, rather than one for removing it once it builds up, the system has to date been of particular value in calorifiers and humidifiers. It has also been used effectively in cooling/'clean in place'/washdown systems in, for example, breweries. The units are largely maintenance-free, and can be cleaned by polarity reversal. Throughputs, in terms of water flow rate, are typically 0.1 – 30 l/s for a single unit.

Data specific to the used of such scale reduction techniques on compact heat exchangers are sparse, but tests have been reported arising out of a research project in the USA (Cho, 1997). Here it was proposed that the electromagnetic descaling unit, located upstream of the plate heat exchanger, led to agitation of the charged mineral (calcium and bicarbonate) ions, resulting in them colliding with one-another and thereafter precipitating. Once the dissolved ions are converted to insoluble crystals, the level of super-saturation of the water greatly decreases, preventing new scale deposits forming on the surfaces of the heat exchanger. The cited paper reports on field trial on an Alfa Laval heat exchanger with titanium plates. A 7% brine solution was cooled by river water, and scaling, which occurred on both sides of the heat exchanger, had resulted in a 10% reduction in the 'U' value every week. This necessitated regular acid cleaning. However, the electromagnetic descaling system eliminated degradation in performance during the trial period of 16 weeks.

Of potential use in compact heat exchangers is a new method of minimising scaling. This is based on surface treatment, similar to that used to create surfaces for drop-wise condensation promotion. Research at the University of Surrey in the UK has shown that surface modifications of a metallurgical nature, such as ion implantation and magnetron sputtering can lead to a greater than 70% reduction in the growth of crystalline deposits and an even greater reduction in bacteria adhesion. The treatment should be readily applicable to the plates of

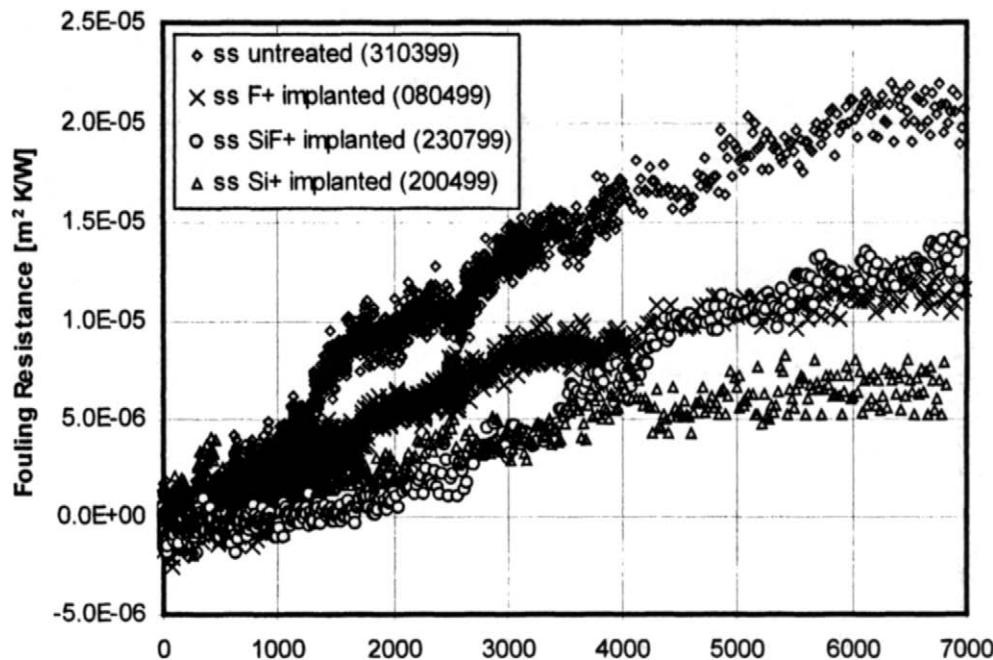


Figure 7.1 Effect of Ion Implantation (F^+ , Si^+ and SiF^+ Ions) on the Variation of Fouling Resistance with Time

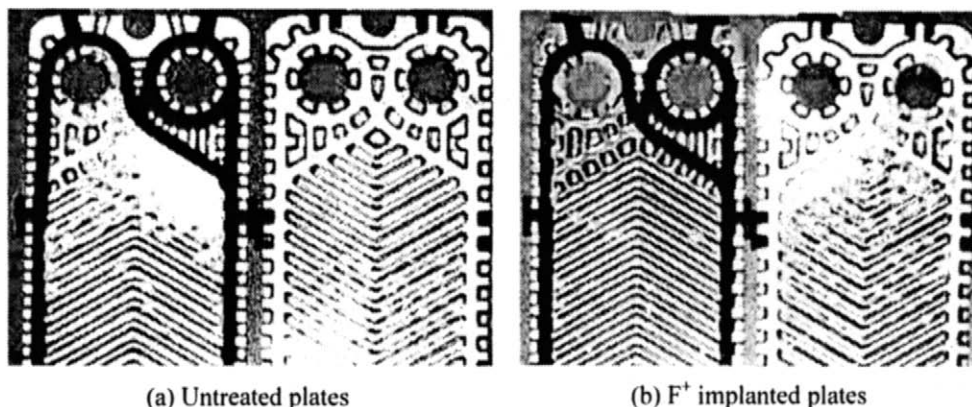


Figure 7.2 Photographs showing the fouling layers on untreated and Ion implanted plates

compact heat exchangers before they are assembled, and the surface treatment is also believed to offer resistance to corrosion and erosion, (Müller-Steinhagen and Zhao, 1997) (Figures 7.1 and 7.2).

Recent data suggest that considerable differences in fouling propensity are exhibited, depending upon the ions which are attached to the surface of the exchanger *via* ion implantation. Si and F, for example, can demonstrate reductions in fouling resistance of over 50% compared to the untreated surface, while implantation of hydrogen had an adverse effect on r_f . The sputtering of amorphous carbon reduced fouling by calcium sulphate, and Ni as a component had the effect, it was suggested, of possibly increasing the solubility of calcium sulphate.

Many of these procedures act also to minimise corrosion. It was found that several coatings tested on equipment provided by a major petrochemical company met the criterion of corrosion rates less than 0.1 mm/year.

Particulate fouling (silting)

Silting is the deposition of solid particles on a surface – the phrase ‘silted up’ is commonly used to describe a pipe or channel which has a thick covering of particles at one or more locations. Small particles can be harder to remove than larger ones, as the forces holding them together and to the surface can be greater. Much has been written about electrophoretic and thermophoretic effects in attracting small particles to surfaces, and these forces do play a role in many particulate fouling events. However, these, and other temperature-driven effects are less in compact heat exchangers because of the (generally) lower temperature differences.

Particulates by themselves are not too difficult to remove. Problems arise when the particulates are combined with other fouling mechanisms, in particular tar formation. Then removal needs more drastic measures, such as chemical/solvent treatment.

Pure particulate fouling can be reduced by using high fluid velocities, except in cases where an adhesive component may be mixed with the particles. The effect of velocity on fouling resistance under particulate fouling conditions is graphically illustrated in Figure 7.3, for a PHE, (Karabelas, 1997). Filtration of particles can be applied and for CHEs a suitable strainer can be installed upstream. Severe pressure pulses, such as obtained by rupture of a bursting disc, can also remove fouling. For gasketed PHEs, it is suggested (Bowes, 1997) that steel/stainless steel brushes be avoided when cleaning opened exchanger plates, nylon brushes being recommended, with water. For greasy deposits, kerosene can be used, together with brushing. In welded plate heat exchangers, vacuum cleaning of the inlet headers is recommended.

For those with an interest in the detail of fouling mechanisms, Karabelas *et al* (1997) have studied this aspect with a view to improving design standards for novel and conventional heat exchangers. Fouling data are given for plate heat exchangers with various corrugation angles and particles of mean diameter 5 mm. The results showed that fouling is adhesion -controlled and that the maximum

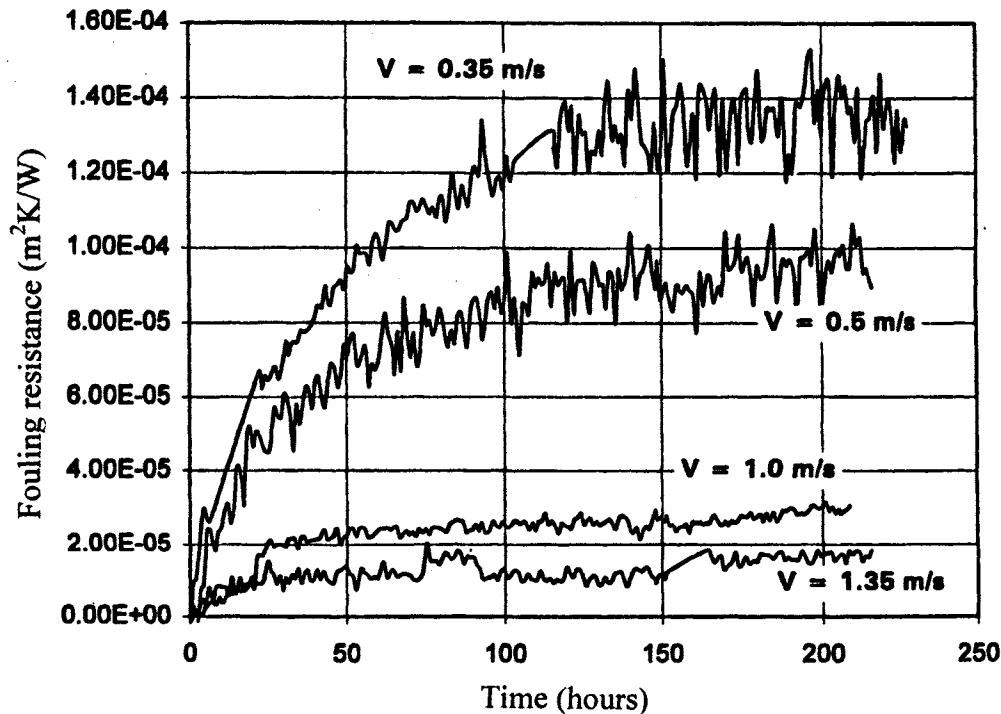


Figure 7.3 Effect of flow velocity on the fouling resistance evolution of a 30° corrugation angle plate heat exchanger fabricated by Vicarb

fouling resistance is almost one order of magnitude less than the TEMA³ recommendations. The corrugated surface geometry common to such

³ TEMA is the Tubular Exchanger Manufacturers' Association

compact heat exchanger plates assisted particle detachment from the surfaces, the geometry leading to tangential hydrodynamic forces. Data obtained for specific particle sizes revealed a distribution of adhesive strengths which are strongly influenced by the acidity (pH) level.

Biological fouling

Biological fouling is caused by the deposition and growth of organisms on surfaces. Bacteria are the organisms most likely to cause problems in CHEs, and their presence can also assist corrosion by, for example, reducing sulphate to hydrogen sulphide, which is corrosive to common stainless steels and many other materials.

The best control method, especially for closed systems, is treatment with biocides. Non-oxidising biocides are normally alternated to prevent the development of resistance, and may kill the bacteria but not remove the biofilm. Some biocides have detergent properties which can disrupt the film. Chlorine and ozone are oxidising biocides, which kill the bacteria and oxidise the film. High concentrations may be necessary for them to be fully effective, but the smaller volume and fluid inventory in a CHE, compared to shell and tube heat exchangers, helps to minimise the quantities needed. The chemical diffuses to the biofilm, and in narrow channels this should be relatively rapid.

Applicable not just to biological fouling is an innovative method for fouling inhibition patented by workers in the UK. The company Applied Coolant Technologies has recently presented data on what it calls the 'micro-mechanical approach to fouling'. The concept uses micro-fibres, of an insoluble polymer, which are added to a circulating cooling water stream. The fibres are typically 250 µm in length, with a diameter of 12 µm. In the first experiments on a closed system – a car engine cooling water circuit – it was shown that fouling inside the engine and radiator was prevented and cavitation was also reduced.

More recently, a project supported by the UK Government under the Energy Efficiency Best Practice Programme has allowed the quantification of biofouling inhibition using these fibres to be carried out. In tests undertaken in the Department of Chemical Engineering at the University of Birmingham, (data yet to be published in report form) the impact of 'microflos' as the method is known, on biological fouling in cooling water systems was studied. Fibre density effects were studied, with fibre parts per million of 100 and 200 being used. It was found that the effectiveness was a strong function of water velocity, with complete biofouling control being achieved at velocities of 1.6 m/s or higher. The quality of the surface of the heat exchanger was also significant. The effectiveness of the method was demonstrated by taking out the fibres after 15 days of continuous successful inhibition of biological growth, and observing growth recommence.

Plans are in hand at the time of writing to use the method in a number of heat exchanger types, and to counter inorganic fouling. Other reports (Müller-Steinhagen, 1997) suggest that the addition of wood pulp fibres can also have a dramatic effect on reducing scale deposits.

At this time, more rigorous analyses are required of the effect of fibre addition, and the type of fibre, on the fouling mechanisms, both for scaling and biological fouling, but the data to date shows that a promising technique may be evolving.

Another recent approach to biological fouling minimisation is to use tube inserts, of the type made by Cal Gavin Ltd., the 'HiTRAN' element. While data on the trials are not yet published, there seems to be no reason to doubt that benefits will accrue to the use of these tube inserts, although of course in many applications the tubes will be somewhat larger than those associated with compact heat exchangers.

Corrosion fouling

Chemical reactions involving the heat transfer surface, or the carrying of corrosion products from other parts of the system, to be left on the heat transfer surface, lead to corrosion fouling. The formation of deposits can by itself lead to corrosion underneath them, for example as the result of formation of electrolytic oxygen concentration cells.

To avoid this type of fouling, construction materials which are resistant to corrosion should be selected. This is routinely done, of course, by the heat exchanger vendors, but there always remains the possibility that the user may change process streams passing through the heat exchanger. Where polymers may be appropriate to counter corrosion, a recent US Gas Research Institute report (Ball *et al*, 1996) gives much background on types of polymer, operating limits etc. Alternatively, inhibitors can be used. Cathodic protection can lead to cathodic scales being formed if hard water/brines are the flow streams. Several types of compact heat exchanger have no dissimilar metals within them, thus making the likelihood of corrosion attack more predictable. Nevertheless, if there is a possibility of a stainless steel unit being stored for a period in a salt air environment, the surfaces should be protected to avoid stress corrosion cracking, (Allan *et al*, 1995).

It should be noted that corrosion products could be significant in fouling whilst not endangering the exchanger from the point of view of leaks or pressure containment.

Chemical reaction fouling

Chemical reaction fouling arises from reactions between constituents in the process fluid, leaving viscous or solid layers on the heat transfer surface. The latter is not involved in the reaction. Polymerisation reactions are commonly associated with this form of fouling, and if the deposit turns from a tar to a hard coke, removal is very difficult. Recently, a new type of chemical reaction fouling will need to be examined - in this case in heat exchanger-reactors. Comparatively little quantitative data exist to date, but it is evident that if by-products of a reaction are produced within such units, or if the reaction is not closely controlled, the implications for fouling would be important. The converse is also potentially possible, whereby a reaction (primary or secondary) may take place which would involve and remove a product or by-product which would otherwise foul the exchanger.

For heat exchangers alone, careful control of fluid and heat transfer surface temperatures, and reductions in residence time at the higher temperatures which enhance this type of fouling, should minimise it. A number of the benefits of compact heat exchangers described in this book will help to control chemical reaction fouling in compact heat exchangers, where it may not be so easy in larger channel systems, because of the inherently good temperature control and low residence times.

Freezing or solidification fouling

If the temperature of a fluid passing through a heat exchanger becomes too low, the fluid can solidify at the heat transfer surface.

Control of this form of fouling is relatively easy, and only requires a rise in temperature to melt any deposits. In compact heat exchangers, the generally lower metal mass and low quantities of fluid make this quite a rapid process.

The type of fouling depends in certain cases on whether the stream being studied is the 'hot' or 'cold' one, and also upon the direction of heat flow. Particulate fouling of course is not necessarily influenced by temperature, but obviously freezing or solidification fouling tends to occur on the side from which excessive heat is being removed. This may be the hot or cold stream, depending upon the solidification temperature of the process fluid.

Scaling is a difficult area - because, as mentioned above, of the presence of some inverse solubility salts, which precipitate out as the water becomes warmer. Other crystals of course precipitate on cooling. Biological growth tends to accelerate, to a certain limit, with temperature.

Corrosion fouling is normally associated with increasing temperature of a process stream, the reaction proceeding more rapidly as the fluid becomes

warmer. However, those who maintain condensing economisers (normally not classed as compact heat exchangers) will advise caution when shutting down the plant. If an acid condensate – as occurs in such economisers on the gas side) – is left on the surfaces of the heat exchanger during a shut down period, although the temperature may be atmospheric ambient, some nice pockets of corrosion will be found on inspection some days or weeks later!

Chemical reaction fouling tends to be associated with increasing temperatures in the stream receiving the heat.

Heat Exchangers Designed to Handle Fouling

There are many heat exchangers which are designed specifically to handle fouled streams. The spiral heat exchanger is perhaps the main type of compact unit which is marketed specifically for streams such as those carrying sludge, followed by the plate and frame unit, which has a versatility in fouling duties difficult to rival by other 'mainsteam' compacts.

The ability of a heat exchanger to handle particulates is often a function of the gap available for passage through the unit of such particulates. Manufacturers of welded (and other) plate heat exchangers offer 'wide gap' variants which are specifically designed to handle fouled streams on one or more sides. An example, the Barriquand 'Platular' welded plate heat exchanger (see Chapter 2) has removable headers, as well as wide plate gaps, to allow ready access to the core for cleaning. Typical applications would be in the sugar industry and as a top condenser on a distillation column.

Other units which would not normally have a role in clean streams are available. These include:

- Scrapped surface heat exchangers - in which intermittent or continuous scraping of the heat transfer surfaces is carried out to maintain clean conditions.
- Fluidised bed heat exchangers - here the abrasive effect of fluidised particles in the fluid stream keep heat transfer surfaces free of fouling.
- Tube inserts (see short discussion in the biological fouling section above) - as well as enhancing heat transfer, these devices can be used inside tubes to reduce fouling.
- The INNEX shell and tube heat exchanger - PTFE rods inside each tube can freely move, impact with the tube walls minimising the chance of fouling building up.
- Stream additives - particles of many types can be introduced into the stream either to clean intermittently or continuously - e.g. sponge balls, sand, PVC, and fibres, as discussed earlier in this Chapter.

- External devices such as sootblowers, sonic horns etc. can be used to force particles off heat transfer surfaces.

Applications of Compact Heat Exchangers and Fouling Possibilities

The types of compact heat exchangers used in various sectors of industry do vary, depending upon the sector experience and degree of confidence. To a considerable degree the confidence is based upon a knowledge of fouling. In Table 7.1, the compact heat exchangers most commonly used in a variety of sectors, and two generic unit operations (refrigeration and prime movers) are identified, and comments made on the types of fouling likely to be encountered.

Table 7.1 Comments on Fouling in a Number of Sectors Commonly Using Compact Heat Exchangers

Sector/Application	Type of Heat Exchanger	Comments on Fouling
Chemicals & petrochemicals	Plate & frame heat exchanger	Because of the great variety in terms of process streams within this sector, each application and heat exchanger type should be examined independently. The plate & frame, spiral and compacts retaining a shell, such as the plate & shell hx, are more likely to be used where fouling is anticipated within the exchanger.
	Brazed plate heat exchanger	
	Welded plate heat exchanger	
	Spiral heat exchanger	
	Plate-fin heat exchanger	
	Printed circuit heat exchanger	
	Compact shell & tube heat exchanger	
	Compact types retaining a shell	
Cryogenics	Plate-fin heat exchanger Printed circuit heat exchanger	One characteristic, apart from the low temperature operation, which sets cryogenic applications apart from most others is that the streams are likely to be clean. Impurities in gases can occur, for example mercury, but this impinges more on materials selection than fouling.

Food & drink	Plate & frame heat exchanger Welded plate heat exchanger Compact types retaining a shell	The processing of food and drink is a vast application area for some types of compact heat exchangers. Cleanliness is of course critical, and the ability to use heat exchangers which can be cleaned, and which are made using stainless steel, tends to limit the choice. The plate & frame unit is the most commonly used, because it is easy to dismantle, is flexible, and is well known in the sector. Crystalline, biological fouling and silting are common types of fouling associated with the sector.
Paper & board	Plate & frame heat exchanger Spiral heat exchanger	Particulates, specifically fibres, are the principal contaminant in this sector, which is not a major user of compacts.
Textiles & fabric care	Plate & frame heat exchanger Spiral heat exchanger	The textile industry produces large quantities of warm effluent, contaminated with dyes and fibres. It is therefore important to use compacts which can be opened up for cleaning. The sector also uses specially-designed heat exchangers with rotating surfaces for such effluents, mainly for recovering heat in liquid-liquid duties.
Oil & gas processing	Plate & frame heat exchanger Brazed plate heat exchanger Welded plate heat exchanger Plate-fin heat exchanger Printed circuit heat exchanger	Often situated off-shore, in arduous environments, corrosion fouling can be a common problem. Waxing is countered by having sections of the heat exchanger steam-heated, for example. Compacts are routinely used nowadays for compressed gas duties, and the new types such as the PCHE have excellent high pressure capability.

Prime movers	Plate & frame heat exchanger Brazed plate heat exchanger Plate-fin heat exchanger Compact shell & tube heat exchanger	The increasing variety of prime movers (reciprocating gas or Diesel engines, gas turbines, steam turbines, Stirling engines etc.) have brought renewed interest in compact heat exchangers for a variety of duties. Recuperation based on heat recovery from exhaust gases is common using compact heat exchangers. Here corrosion might occur if the gases are cooled to too low a temperature (below the acid dewpoint). Particulate fouling may exist, depending upon the fuel. In gas turbine intercoolers, the gases tend to be clean, however. The main problem in gas turbines is not associated with fouling, but with thermal stresses, (see Chapter 6).
Refrigeration	Plate & frame heat exchanger Brazed plate heat exchanger Plate-fin heat exchanger Printed circuit heat exchanger	Where liquids are the heat source/sink, fouling can be more of a problem. Scaling, particulates and, on the secondary side, where cooling water or other fluids may be used with less known specifications, even biological fouling could occur. Thus access for cleaning is important.

In the last few years, there has been increasing interest in using 'natural' refrigerants, such as ammonia, hydrocarbons, CO_2 and air. Ammonia is toxic, hydrocarbons are flammable and CO_2 may be operating at or around its critical point, with relatively high pressures. All of these features make compact heat exchangers, in conjunction with other 'compact' units to reduce fluid inventories, desirable. However, while the refrigerant will be clean, the fluid on the secondary circuit may not be.

DESIGN APPROACHES TO REDUCE FOULING

Principles of exchanger- pumping system interaction

Heat exchangers in process, environmental and power systems almost always involve pumps, fans or compressors to provide the pressure differential across them (in addition of course to that needed for the pipework or ducting system). For most efficient operation of the plant the pumps etc. are normally designed or specified to operate at their best efficiency point, illustrated schematically by the intersection of the load curve (heat exchanger resistance) with the pump characteristic in Figure 7.3 (a).

It is assumed for simplicity that the system consists only of the pump and exchanger, the resistance of pipework being ignored. The pump of Figure 7.3(a) has a moderately flat characteristic, and the development of fouling can be represented by the progression from load curve 1 (clean) to load curve 2. Two observations can be made, firstly that the efficiency falls from the design maximum, and secondly that there is a significantly reduced flow through the exchanger. This is clearly much more important as the characteristic approaches the stall point.

The pump in Figure 7.3(b) has a much higher characteristic gradient, and the load curve intersection is at a higher flow than that of the best efficiency point. The exchanger flow is the same as that of the first case, Figure 7.3(a). In the progression of fouling the efficiency rises initially, to its maximum, and then falls slightly. Thus during the cycle between cleaning operations the pump efficiency

maintains high. What is perhaps more important is that the reduction in flow is much smaller because of the steepness of the characteristic.

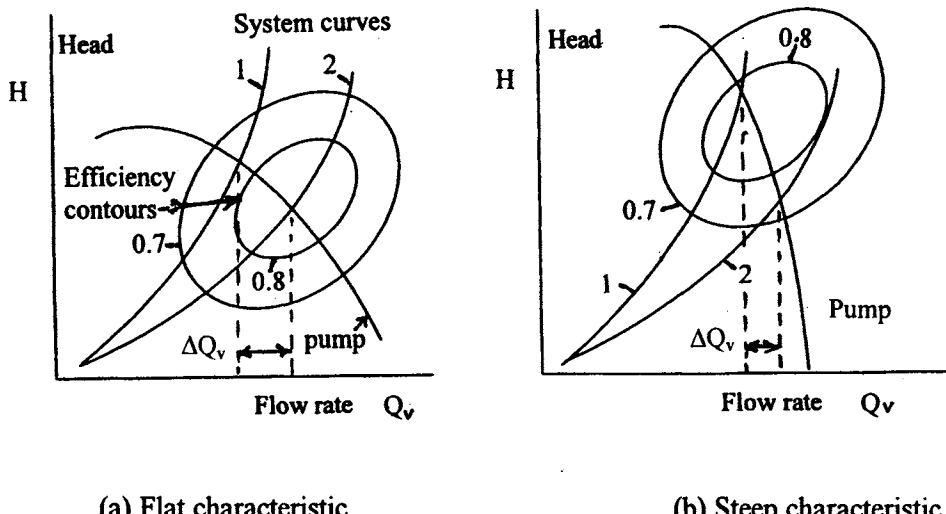


Figure 7.4 Schematics of pump- heat exchanger interactions, with fouling

Clearly there are complex inter-relationships between the various parameters of pump characteristic shape, fouling type and surface type. If the surface is compact, then any given fouling deposit will have a strong influence on pressure drop (Cowell and Cross (1981)). In this case the loss of flow in a practical system will dominate the effect on thermal performance. It has been shown in a simple analysis (Hesselgreaves (1992)) that depending on the interaction of these relationships there could be an initial rise both in fluid velocity and heat flow. This was shown to be dependent on a parameter P formed as the ratio of pump characteristic gradient at operating point and the head/ flow of the operating point itself:

$$P = \frac{(dH/dQ_v)_{pump}}{(H/Q_v)_{hx}} \quad (7.1)$$

Thus case (a) above has a lower value of P to that of case (b) and is more susceptible to the effects of fouling. Other factors involved are of course the surface geometry and the design flow condition (i.e. laminar or turbulent).

There are three options open for the pumping system designer to minimise the effects of fouling, regardless of the heat exchanger selection. The first is to

specify a pump *type* (i.e. whether centrifugal, mixed, or axial) with an inherently steep characteristic. The principal factor determining this is the pump *specific speed*, or *type number*, defined in non-dimensional form by

$$N_s = \frac{\omega Q^{1/2}}{(gH)^{3/4}}, \quad (7.2)$$

where Q is the volumetric flow rate in m^3/s , ω is the rotational speed in rad/s and H is the developed head in m . The higher the specific speed, the higher is the characteristic gradient (Stepanoff (1948)). For best efficiency, as specific speed increases, the typical shape of the impeller progresses from centrifugal ($N_s < 1$) through mixed flow ($1 < N_s < 3$) to axial flow type ($N_s > 3$). For given conditions of H and Q , however, the process engineer may be limited in choice of speed by the cost of motor/gearbox combinations. Similar arguments apply to fans for gas applications, steepness of characteristic increasing progressively from radial bladed centrifugal (flattest), through forward curved, then backward curved centrifugal, to axial flow types (steepest) (Perry and Green (1984)).

The second option is to specify the pump to have its best efficiency point (that is, its design point) at a higher head and lower flow than that of the heat exchanger specification, so that it operates further along its characteristic as in case (b) above. The third option is for the actual hydraulic design of a given type of pump, which may be relevant for large duties, for which a pump is specifically designed rather than bought "off the shelf". The characteristic of a given type can be made steeper, at a possible slight penalty of efficiency, by increasing the solidity of the blade system. This is achieved either by increasing the blade number, or by increasing the blade chord. A further option is to increase the hub ratio (axial pump) (Stepanoff (1948)). Combinations of these measures could be applied. The effect is to reduce the sensitivity to change of incidence, or flow, on the head generated.

The effect of fouling and the heat exchanger surface on thermal performance

The above observations have important implications for the fouling performance. Since there are many reference works on fouling mechanisms and their effects (Panchal et al. (1997), Bryers (1983), Somerscales et al. (1981)), a detailed description is not necessary here, but some comments are appropriate. Firstly, it is commonly mentioned (for example in tests on vehicle radiator matrices (Cowell and Cross (1981))) that for moderate fouling the heat transfer performance is often closely maintained provided that the flow is constant. This was thought to arise because the fouling deposit was almost entirely confined to the front face of the exchanger matrix, the internal surface remaining largely

clean. The latter is largely because the thermophoretic (temperature gradient-driven) effect is away from the surface, and any deposit is dried by the surface heat and cannot stick. Maintenance of performance has also been observed with frosting fouling, which in contrast is fairly evenly disposed on the surface. In this case of course the fouling is mass transfer-driven. Increased surface velocity with consequent higher heat transfer coefficient is thought to be responsible for the increase in heat load. The increase in roughness may also have some significance. This increase to some extent offsets the heat transfer resistance of the fouling (frosting) layer, where there is one. The second point is that, if the foulant is of a particulate nature, its deposition will be strongly dependent on the flow velocity (see Figure 7.3): If this rises above a threshold value, removal (re-entrainment) forces due to fluid shear will offset the deposition rate, and the exchanger will self-clean to an extent. This gives rise to the asymptotic fouling performance often experienced.

The surface geometry has a significant effect on fouling, which needless to say is interactive with the operational conditions. Excellent surveys of the interactions are given by Panchal and Rabas (1999) for process exchangers, and by Marner (1997) for gas-side fouling of compact exchangers. Clearly if the operational conditions are such that mass transfer or thermophoretic effects dominate, then there will be a fouling deposition rate largely independent of the surface type. Thus a narrow passage (low hydraulic diameter) is likely to fill rapidly. In compensation, a low hydraulic diameter is normally associated with a low driving temperature difference, and hence low mass transfer driving potential and fouling rate. Since the driving potential is often known with some accuracy to the process engineer, some constructive trade-off analysis could be done (at least in theory) to evaluate the best hydraulic diameter. Mass transfer-driven deposits are often well-bonded to the surface, and are not in general amenable to cleaning simply by increasing the flow velocity, either naturally by flow passage constriction or by flushing. An example of such a deposit type is that on a diesel exhaust recuperator on a power generation set. Important in the latter and other combustion-related heat recovery applications is the onset of the acid dewpoint of the products, which corresponds to a step change in deposit rate, and is often associated with corrosion (Isdale et al. (1983)).

Similar arguments regarding trade-off could apply to scaling-type fouling. This is also driven by the temperature gradient between the bulk fluid and the surface, which is reduced (indirectly) by a low hydraulic diameter surface.

FOULING FACTORS

The thermal effect of fouling on performance is normally expressed as an extra resistance, or fouling factor R_f ($\text{m}^2\text{K/W}$), which is the inverse of a heat transfer

coefficient. This resistance is added to the film and wall resistances in the design process, giving an increased surface area to compensate for the fouling. Tables of recommended fouling factors for shell- and tube exchangers are published by the TEMA and other bodies.

The danger of blindly applying the quoted values R_f for compact exchangers has been clearly demonstrated (for example by Bott (1990)). This arises because the over-design gives rise to lower clean flow velocities, with then allow greater precipitation and fouling rates. Alternative values for plate exchangers are given by Panchal and Rabas (1999) as shown in Table 7.2

Table 7.2 Fouling factors for PHEs compared with TEMA values
(from Panchal and Rabas (1999), reproduced by permission
of Begell House, inc.)

Process Fluid	R_f - PHE $\text{m}^2 / \text{K kW}$	R_f - TEMA $\text{m}^2 / \text{K kW}$
Water		
Soft	0.018	0.18-0.35
Cooling tower water	0.044	0.18-0.35
Seawater	0.026	0.18-0.35
River water	0.044	0.35-0.53
Lube oil	0.053	0.36
Organic solvents	0.018-0.053	0.36
Steam (oil bearing)	0.009	0.18

For general compact surfaces, perhaps a more rational approach is to consider the fouling resistance in terms of its two components of (mean) thickness and conductivity. The thickness affects both the flow resistance (pressure drop) and thermal resistance, but is in theory independent of type of deposit, although the surface roughness affects the friction. The conductivity affects only the thermal resistance but depends on the type of deposit. The thermal resistance is given by

$$R_f = \frac{t_f}{\lambda_f}, \quad (7.3)$$

where t_f is the thickness, and λ_f is the conductivity of the fouling layer.

Some typical values of conductivity for various deposits are shown in Table 7.3, adapted from data given by Marner and Suitor (1987). The operating temperatures and measured thicknesses are also shown.

Table 7.3 Conductivities of various deposits
 (from Marner and Suitor (1987), in Handbook of Single Phase Convective Heat Transfer, Eds. Kakaç et al. Copyright © John Wiley & Sons, Inc., Reprinted by permission of John Wiley & Sons, Inc.)

Reference	Type of Deposit	Temperature, K	Thickness, mm	Density, kg/m ³	Thermal Conductivity, W/(m · K)	Relative Roughness
Chow et al. [49]	MHD seed slag	700–810	2.6–9.5	—	0.33–0.40	—
Weight [50]	Coal-fired boiler	673–1373	—	—	0.1–10.0	—
Characklis [51]	Biofilm	—	0.4–5.0	—	—	0.003–0.157
Characklis [52]	Biofilm	—	—	—	0.57–0.71	—
Lister [53]	Calcium carbonate	—	1.65–2.62	—	2.6	0.0001–0.0006
Sherwood et al. [54]	Calcium carbonate	—	—	—	2.26–2.93	—
	Calcium sulfate	—	—	—	2.31	—
	Calcium phosphate	—	—	—	2.60	—
	Magnesium phosphate	—	—	—	2.16	—
	Magnetic iron oxide	—	—	—	2.88	—
	Analcite	—	—	—	1.27	—
	Biofilm	—	—	—	0.63	—
Raask [55]	Coal-fired boiler	500–1200	0–50	500	0.03–3.0	—
Pritchard [56]	Calcium carbonate	—	—	—	1.6	—
Rogalski [47]	Oil-fired diesel exhaust	—	—	—	0.0353–0.047	—
Wagoner et al. [57]	Coal-fired boiler	889	—	—	0.0520	—
	Biofilm	300–301	—	10–40	0.17–1.08	—
	Calcium phosphate	310	0.25	—	1.0	—

CONVERSION FACTORS

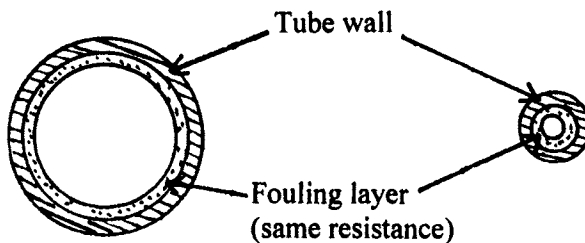
$$T_F = 1.8(T_K - 273) + 32 \quad 1 \text{ kg/m}^3 = 0.0624 \text{ lb}_m/\text{ft}^3$$

$$1 \text{ mm} = 0.00394 \text{ in.} \quad 1 \text{ W/(m · K)} = 0.578 \text{ Btu}/(\text{hr} \cdot \text{ft} \cdot {}^\circ\text{F})$$

It is probable that the conductivity for a given deposit varies as the deposit grows: there is a tendency for the density of a deposit to increase with time, owing to mass transfer through the layer. This is analogous to the known densification of frosting layers on evaporators with time. The conductivity then rises with density.

If we thus regard a fouling factor to represent a given thickness (by implication a notional thickness after which cleaning is implemented), we can relate this point to a pressure drop criterion. Thus, taking a 25mm diameter tube, the quoted TEMA fouling factor for cooling water is 0.18 to 0.35m²/kWK, and taking a mean value of 0.27 with a typical value of conductivity of calcium carbonate of 2.5W/mK, the layer thickness implied is 0.675mm. If this thickness is deposited on a tube of 25mm internal diameter, as shown schematically in

2mm diameter tube, the effective diameter becomes $2 - 1.35 = 0.65\text{mm}$, giving a pressure drop increase of 946%.



(a) 25mm diameter tube (b) 2mm diameter. Tube
(the same fouling factor for each)

Figure 7.5 The consequence of not scaling a fouling factor (schematic)

The absurdity of this example is clear. It would seem, therefore, that one logical approach would be to scale the fouling factor, and by implication, the allowable fouling thickness, by the hydraulic diameter of the surface considered. This would automatically give the same proportional increase in pressure drop, with its corresponding relative reduction in flow and change of heat load.

The suggestion is, therefore, that the TEMA or similar fouling factors, which can be presumed to be based on a notional internal tube diameter of 25mm, are scaled down by the ratio $25/d_h$, where d_h is the hydraulic diameter, in mm, of the exchanger surface under consideration. This approach is broadly compatible with the quoted values of R_f for the PHE given in Table 7.2, with a typical value of d_h of 5mm.

A further stage might be to include the effects of velocity and geometry. Thomas (1998) has shown that the asymptotic fouling factors for PHEs is a strong function of velocity, reducing markedly as velocity increases; there was also a strong reduction observed as corrugation angle increased from 30 to 60°. These considerations would apply especially to particulate fouling.

For mass-transfer driven fouling, it is likely that the driving temperature difference (ΔT), which often controls the mass transfer, would also be an important factor in determining the asymptotic fouling resistance. Compact exchangers often have lower ΔT s than shell and tube exchangers, so we would expect lower fouling factors to apply for these cases.

References

Allan, S.J. et al, 1995, The Effect of Salt on Steels and Protective Coatings. GEC Journal of Research, Vol. 12, No. 2.

Anon., 1994, The Standards of the Brazed Aluminium Plate-Fin Heat Exchanger Manufacturers' Association. ALPEMA.

Ball, D.A. et al, 1996, Development of a Technology Base for Application of Plastics to Condensing Heat Exchangers. GRI Final Report, GRI-96/0451, Gas Research Institute, Chicago.

Bott, T.R., 1990, Fouling Notebook. The Institution of Chemical Engineers, Rugby, U.K.

Bott, T.R., 1995, Fouling of Heat Exchangers. Chemical Engineering Monograph Vol. 26, Elsevier Science, Amsterdam.

Bowes, G., 1997, Cleaning of heat transfer equipment. Proc. Seminar 'Focus on Fouling', Institute of Petroleum, London.

Bryers, R.W., (ed.), (1983), Fouling of Heat Exchanger Surfaces, Engineering Foundation, New York.

Cho, Y.I. et al, 1997, Use of Electronic Descaling Technology to Control Precipitation Fouling in Plate and Frame Heat Exchangers. In: Compact Heat Exchangers for the Process Industries, Begell House, New York, pp. 267-273.

Clarke, R.H., 1994, Fouling - a Factor within Control for Compact Heat Exchangers Offshore. Proc. Gas Processors' Association Meeting, Aberdeen, UK.

Cowell. T.A. and Cross, D.A. (1981), Airside Fouling of Internal Combustion Engine Radiators, SAE Transactions, Vol. 89, pp3179-3188.

Grillot, J.M., 1997, Compact Heat Exchangers Liquid-Side Fouling. Applied Thermal Engineering, Vol. 17, Nos. 8-10, pp. 717-726.

Hesselgreaves, J.E. (1992), The Effect of System Parameters on the Fouling Performance of Heat Exchangers. Proc. 3rd. UK. National Heat Transfer Conf. Incorporating 1st European Conf on Thermal Sciences, Inst. Chem Eng. Rugby, UK.

Isdale, J.D., Scott, A.C. and Cartwright, G. (1983), Report on Fouling in Diesel Exhausts, prepared for International Energy Conservation in Heat Transfer and Heat Exchangers, National Engineering Laboratory, Glasgow, Scotland.

Karabelas, A.J. et al, 1997, Liquid-Side Fouling of Heat Exchangers. An Integrated R&D Approach for Conventional and Novel Designs. Applied Thermal Engineering, Vol. 7, Nos. 8-10, pp. 727-737.

Marner, W.J. (1997), Gas-Side Fouling in Compact Heat Exchangers, Proc. International Conference on Compact Heat Exchangers for the Process Industries, Snowbird, Utah. Begell House, New York.

Marner, W.J and Suttor, J.W. (1987), Fouling with Convective Heat Transfer, in Handbook of Single Phase Convective Heat Transfer, Ed. Kakaç, Shah & Aung, John Wiley, New York.

Muller-Steinhagen, H., 1997, Recent Developments in Fouling Mitigation. Proc. Seminar 'Focus on Fouling', Institute of Petroleum, London.

Muller-Steinhagen, H. and Zhao, Q., 1997, Investigation of Low Fouling Surface Alloys made by Ion Implantation Technology. Chem. Engng. Sci., Vol. 52, No. 19, pp. 3321-3332.

Panchal, C., Bott, T.R., Somerscales, E. and Toyama, S. (eds.), (1997), Fouling Mitigation of Industrial Heat Exchangers, Begell House, New York.

Panchal, C.H. and Rabas, T.J. (1999) Fouling Characteristics of Compact Heat Exchangers and Enhanced Tubes, Proc. International Conference on Compact Heat Exchangers and Enhancement Technology for the Process Industries, Banff, Canada. Begell House, New York.

Perry, R.H. and Green, D., (1984), Perry's Chemical Engineer's Handbook, sixth edn., McGraw-Hill, New York

Reay, D.A., 1999, Learning from Experiences with Compact Heat Exchangers. CADDET Analysis Series No. 25, CADDET, Sittard, The Netherlands.

Reay, D.A., 1995, Fouling of Compact Heat Exchangers. Proc. Seminar 'Developments in Energy Efficient Technologies for the Refining and Petrochemicals Industries'. Institute of Petroleum, London.

Stepanoff, A.J. (1948), Centrifugal and Axial Flow Pumps, John Wiley, New York.

Somerscales, E.F.C. and Knudsen, J.G., (1981) Fouling of Heat Transfer Equipment, Hemisphere, Washington.

Thomas, B., (1998), Compact Heat Exchangers Applied to Industrial and Environment Processes. Eurotherm Seminar 62 "Heat Transfer in Evaporation and Condensation".

Appendix 1 Nomenclature

a	speed of sound (m/s)
a	radius or dimension of duct (chap 5) (m)
a^*	$=2a/2b$
a_o	Helmholz function (chap 3) (J/kg)
A	parameter (dimensional) (eqn. 3.81) (1/T)
A_1	parameter
A_2	parameter defined by eqns. 3.68, 3.77
A_s	surface area (m^2)
A_c	flow area (m^2)
b	duct dimension (chap 5) (m)
b	effective plate gap (chap 5) (m)
b	specific availability (chap 3) (J/kg)
b_o	Gibbs function (chap 3) (J/kg)
B	availability (chap 3) (J)
B	banking factor (eqn. 6.48)
B	plate width (chap 5) (m)
B	dimensionless heat flow (eqn. 24)
Be	Bejan number (chap 3)
Bi	Biot number = $\alpha b/\lambda_m$
Bo	boiling number
B_0	dimensionless parameter (Bejan, eqn. 73)
B_1	dimensionless parameter (eqn. 64)
B_2	dimensionless parameter (eqn. 68)
B_3	dimensionless parameter (eqn. 82)
c	duct dimension (chap 5) (m)
c	specific heat (incompressible substance) (J/kgK)
c_p	specific heat at constant pressure (J/kgK)
C	heat capacity rate (W/K)
C	constant in Chisholm two- phase multiplier (eqn. 6.87, 6.90)
Co	confinement number
C_d	drag coefficient
C_s	face area (m^2)
C_1	constant (eqn. 3.86)
C^*	ratio of heat capacity rates
d_h	hydraulic diameter (m)
D	tube outside diameter (m)
e_x	flow exergy (J/kg)
E	internal energy (J)
E	stress in fin (eqn. 6.91) (Pa or kPa)
$E_{1,2}$	fin efficiencies for double-banked plate- fin arrangement (eqn. 6.47)

\dot{E}_w	exergy (rate) (W)
f	Fanning friction factor
$f_{1,3}$	friction components (eqn 5.43)
f_{app}	apparent friction factor (eqn. 5.2)
f_{fd}	fully- developed friction factor
F	LMTD correction factor (chap 6)
F	two- phase heat transfer enhancement factor (eqn. 6.71)
F_H	fin height of louvred surface (m)
g	gravitational constant (m/s ²)
g_1	dimensionless mass velocity (Bejan)
G	mass velocity (kg/m ² s)
G_z	Graetz number = $RePrd_h/L$
h	specific enthalpy (chap 3) (J/kg)
h	passage height (chap 5) (m)
h_{lg}	latent heat of vaporisation (J/kg)
H	enthalpy (J)
H	pump or fan head (chap 7) (m)
j	Colburn factor
k	= fRe , for fully- developed laminar duct flow
$K_{c,e}$	contraction and expansion loss coefficients (eqn. 6.49)
K_x	dimensionless incremental pressure drop
K_{∞}	dimensionless incremental pressure drop
l	length (height) of fin in efficiency formula (eqn. 6.42) (m)
l_f	length of strip (fin) (m)
L	flow length, louvre pitch (m)
L_{hy}	hydraulic entrance length (see chap 5) (m)
L_H	louvre height (above fin surface) (m)
L_{hy}^+	dimensionless entrance length
L_L	louvre length (m)
L_{th}^*	thermal entrance length (m)
L_{th}^*	dimensionless thermal entrance length
m	fin efficiency parameter (eqn. 6.43) (m ⁻¹)
\dot{m}	mass flow rate (kg/s)
M	Mach number
M	molecular weight (kg/kmol)
n	number of nodes of polygonal duct
N	Ntu for one side
N	number of fins/unit length (eqn. 6.91) (m ⁻¹)
N_s	specific speed of pump or fan (eqn. 7.2)
N_t	number of tubes in exchanger (chap 6)
Ntu	number of thermal units
N_s	entropy generation number based on heat capacity rate

N_{s1}	entropy generation number based on heat flow
Nu	Nusselt number
p	pressure (Pa)
p_c	critical pressure (Pa)
p_f	fin pitch (m)
p_r	reduced pressure (Pa)
p_{sat}	saturation pressure (Pa)
P	effectiveness parameter (chap 6)
P	pump/system interaction parameter (eqn. 7.1)
Pr	Prandtl number
P_f	face area parameter
P_λ	longitudinal wall conduction parameter (eqn. 6.66)
P_o	operating parameter (m^{-1})
P_v	volume parameter (m)
p_s	perimeter (m)
Q_v	volume flow rate of pump or fan (chap 7) (m^3/s)
\dot{Q}	heat flow (W)
q	heat flux (W/m^2)
q'	heat gradient (W/m)
r_0	inner radius of tube (m)
R	ideal gas constant (J/kgK)
R	capacity rate ratio (chap 6)
Re	Reynolds number
R_f	fouling resistance (m^2K/W)
R_w	wall resistance (m^2K/W)
s	fin spacing (i.e. space between fins) (m)
s	specific entropy (chap 3) (J/kgK)
S	entropy (chap 3) (J/K)
S	nucleate boiling suppression factor (eqn. 6.71 and 6.81)
St	Stanton number
S'	entropy gradient (J/mK)
\dot{S}_{gen}	entropy generation rate (W/K)
t	dimensionless temperature ratio T_{in}/T_{out} (chap 3)
t	separation plate thickness (m)
t_f	fin thickness (m)
t_s	splitter plate thickness (m)
t_w	tube wall thickness (m)
T	absolute temperature (K)
u	velocity (m/s)
U	overall heat transfer coefficient

V	volume of one side
w	height of corrugation (m)
W_s	weight of core side (chap 4)
\dot{W}_p	pumping power
x	axial distance (m)
x	transverse distance across header face (fig 6.15) (m)
x^+	dimensionless length from leading edge (eqn. 5.5)
x^*	dimensionless thermal length from leading edge (eq. 5.8)
x_g	quality (eqn. 6.72) ($= \dot{m}_g / \dot{m}$)
X	parameter defined by eqn. 5.77
X	Lockhart- Martinelli parameter (eqn. 6.72)
X^*	dimensionless transverse distance across header face (eqn. 6.55, 6.56)
y	shape co-ordinate of header (eqn. 6.54 et seq.) (m)
y_o	maximum depth of header (eqn. 6.54 et seq.) (m)

Greek symbols

α	heat transfer coefficient (W/m ² K)
β	surface area density (m ⁻¹)
γ	conduction parameter (eqn. 6.67, 6.68)
ϵ	effectiveness
η	dynamic viscosity (Ns/m ² = kg/ms = Pas)
η_f	fin efficiency
η_o	surface effectiveness
λ	thermal conductivity (W/mK)
Λ	pitch (wavelength) or corrugated channel (m)
$\xi_{en,ex}$	entry and exit loss coefficients (eqn.6.52,6.53)
ρ	density (kg/m ³)
σ	porosity (largely chap 4)
σ	surface tension (chap 6) (N/m)
τ	dimensionless temperature difference $\Delta T/T$
ϕ	chevron angle (chap 5) (degrees)
ϕ_l^2	two- phase friction multiplier (eqn. 6.87)
Φ	area enhancement factor (chap5)
ω	rotational speed of pump or fan (eqn 7.2) (rad/s)

Subscripts

1	cold stream (chap 3)
2	hot stream (chap 3)
in	inlet

out	outlet
c	cold stream
d	distributor (eqn. 6.57)
f	fouling (according to context)
f	fin
h	hot stream
l	liquid (eqn. 6.71 et seq.)
lt	laminar in liquid phase, turbulent in vapour phase (eqn. 6.78)
m	mean
min	minimum
max	maximum
opt	optimum
out	outlet or exit value
ref	reference
S	shell
tt	turbulent in both liquid and vapour phases
T	tube
w	wall

Superscripts

*	non-conducting (eqn. 6.64)
---	----------------------------

Appendix 2 Conversion Factors

Mass m	$1 \text{ kg} = 2.2046 \text{ lb}$	$1 \text{ lb} = 0.4536 \text{ kg}$
Density ρ	$1 \text{ kg/m}^3 = 0.06243 \text{ lb/ft}^3$	$1 \text{ lb/ft}^3 = 16.018 \text{ kg/m}^3$
Length	$1 \text{ m} = 3.2828 \text{ ft}$	$1 \text{ ft} = 0.3048 \text{ m}$
	$1 \text{ mm} = 0.03937 \text{ in}$	$1 \text{ in} = 25.4 \text{ mm}$
Volume	$1 \text{ m}^3 = 35.315 \text{ ft}^3$	$1 \text{ ft}^3 = 0.028317 \text{ m}^3$
Time	$1 \text{ s} = 1 \text{ min}/60 = 1\text{hr}/3600$	
Temperature	$1 \text{ K} (\text{°C}) = 1.8 \text{ R} (\text{°F})$	$1 \text{ R} = 0.55555 \text{ K}$
Force	$1 \text{ N} = 1 \text{ kgm/s}^2$	$1 \text{ lbf} = 32.174 \text{ lbft/s}^2$
	$1 \text{ N} = 0.22481 \text{ lbf}$	$1 \text{ lbf} = 4.4482 \text{ N}$
Pressure p	$1 \text{ Pa} = 1 \text{ N/m}^2 = 1.4503 \times 10^{-4} \text{ lbf/in}^2$	$1 \text{ lbf/in}^2 = 6894.8 \text{ Pa}$
	$1 \text{ bar} = 10^5 \text{ N/m}^2 \text{ (or Pa)} = 14.5 \text{ lbf/in}^2 = 750 \text{ mmHg} = 10.20 \text{ mH}_2\text{O}$	
Energy and Exergy	$1 \text{ J} = 1 \text{ Nm} = 0.73756 \text{ ftlbf}$	$1 \text{ ftlbf} = 1.35582 \text{ J}$
	$1 \text{ kJ} = 0.9478 \text{ Btu}$	$1 \text{ Btu} = 1.0551 \text{ kJ}$
Specific Energy (u, h)	$1 \text{ kJ/kg} = 0.42992 \text{ Btu/lb}$	$1 \text{ Btu/lb} = 2.326 \text{ kJ/kg}$
Power	$1 \text{ W} = 1 \text{ J/s} = 3.413 \text{ Btu/h}$	$1 \text{ Btu/h} = 0.293 \text{ W}$
	$1 \text{ kW} = 737.6 \text{ ftlbf/s}$	$1 \text{ hp} = 550 \text{ ftlbf/s}$
	$1 \text{ kW} = 1.341 \text{ hp}$	$1 \text{ hp} = 0.7457 \text{ kW}$
Specific Heat	$1 \text{ kJ/kgK} = 0.238846 \text{ Btu/lbR}$	$1 \text{ Btu/lbR} = 4.1868 \text{ kJ/kgK}$
(c, R, s)	$1 \text{ kcal/kgK} = 1 \text{ Btu/lbR}$	
Thermal Conductivity (λ)	$1 \text{ kW/mK} = 577.8 \text{ Btu/ft hR}$	$1 \text{ Btu/ft hR} = 0.0017307 \text{ kW}$

Heat Transfer $1 \text{ kW/m}^2\text{K} = 176.1 \text{ Btu/ft}^2\text{hR}$ $1 \text{ Btu/ft}^2\text{hR} = 0.005679 \text{ kW/m}^2\text{K}$
Coefficient (α)

Dynamic $1 \text{ kg/ms} = 1 \text{ Ns/m}^2 = 1 \text{ Pas} = 10 \text{ poise}$

Viscosity (η) $= 2419 \text{ lb/ft h}$ $1 \text{ lb/ft h} = 0.0004134 \text{ kg/ms}$

Kinematic $1 \text{ m}^2/\text{s} = 38750 \text{ ft}^2/\text{h}$

Viscosity (ν) $1 \text{ ft}^2/\text{h} = 0.25806 \times 10^{-4} \text{ m}^2/\text{s}$

Appendix 3 Software Organisations and Awareness Groups

The following organisations conduct research into compact heat exchangers, and offer software for design, or are concerned with promoting the interests of those connected with all aspects of design, manufacture and operation. A short description of activities is given for each in the following pages.

ALPEMA

ESDU

GRETh

HEXAG

HTFS

HTRI

NLAHX

ALPEMA**(Brazed Aluminium Plate-Fin Heat Exchanger Manufacturers' Association)**

The major manufacturers of brazed aluminium plate-fin heat exchangers started meeting in 1989 and formed a formal association at the end of 1991. The association was registered in Japan and Europe in 1992. The first edition of the ALPEMA standards was published in 1994. Membership is open to quality manufacturers of BAHXs of over 200 kg used primarily in cryogenic applications. Members must agree to comply with the ALPEMA Constitution and Standards, play an active role in the Association and be able to demonstrate a satisfactory level of QA.

ALPEMA was formed to

- promote the broader use of brazed aluminium plate-fin heat exchangers (BAHXs) in existing and new markets
- harmonise the standards concerning their general design, construction and application
- promote and improve the safety and quality of BAHXs at manufacture and in service
- promote R&D on BAHXs.

www.aeat.co.uk/pes/alpema

Contact David Butterworth

ESDU (Engineering Sciences Data Unit)

ESDU has issued a number of design guides (Data Items) relating to heat exchangers including Items on heat exchanger effectiveness (including compact configurations) and process integration with particular reference to the energy recovery in heat exchanger trains.

In process design, having established the overall heat recovery network the next step (preceding detailed design considerations) is to select the types of heat exchanger. For any given duty, several types will often be suitable, often including one or more types of compact exchanger. However, without access to reliable selection and costing information for a wide range of exchangers at this initial process design stage, process engineers often find it difficult to specify exchanger types other than those with which they are familiar. This leads to many lost opportunities to use perfectly suitable, cheaper compact alternatives.

In collaboration with heat exchanger manufacturers and end users, ESDU have developed a series of Data Items on the selection and costing of heat exchangers. Guidance is given on the selection of types of exchanger that are feasible for given duties, and cost data based on manufacturers' own costing methods allows rapid estimates of their costs. Final selection can then be made, usually based on economic factors (that is the capital and operating costs). Ideally, the operating costs (mainly maintenance and pumping costs) and capital costs should be balanced to give a minimum annual cost for the exchanger. More usually, the "allowable pressure drop" across the exchanger is specified by the process designer and this allows no scope for optimisation, the capital cost being the only consideration taken into account by the process engineer.

The criteria on which selection of heat exchangers is made include the thermal and hydraulic requirements., compatibility with fluids and operating conditions, maintenance, availability, economic factors, space and weight and fouling propensity. Detailed descriptions are provided for a wide range of exchanger types including the most common compact types.

ESDU are continuing the process of developing new selection and costing information, and updating the existing data. This work is available as part of ESDU's Process and Environmental Technology series. Further information on this work is available from ESDU at www.esdu.com.

Simon J. Pugh, Head of Thermofluids Group, ESDU International plc,
27 Corsham St, London N1 6UA, UK. www.esdu.com
sjpugh@esdu.com : tel +44 (207) 566 5709 : fax (207) 490 2701

GRETh

GRETh (Research Group on Heat Exchangers) was created, in 1983 by the French Agency for Energy Management (A.F.M.E.) and the French Atomic Energy Commission (C.E.A.), to provide assistance, in the area of RTD, to manufacturers, engineering companies and users of heat exchangers. It was recognised in France that the heat exchanger is an essential element in any energy management policy, because a considerable proportion of the thermal energy in industrial processes is transferred through such equipment. Apart from a few big companies, heat exchanger manufacturers are often SME's (more than one hundred in France) and GRETh carries out RTD on heat exchangers that could not be carried out by these firms since they are small and scattered. The staff at GRETh (50 persons) is composed of engineers, technicians, professors and post-graduate students.

GRETh runs a club of industrial partners with more than 100 members in Europe including large companies to SME's. All European companies may become members of GRETh. The services offer to the members are :

- access to the RTD results carried out at GRETh ;
- a technical handbook which is continuously updated ;
- direct access to the industrial test rigs ;
- access to heat exchanger sizing and simulation software ;
- technical meetings and training courses ;
- confidential research.

The GRETh RTD activities concerns single and two-phase heat transfer intensification, improvement of industrial processes, high temperature heat transfer, environmental protection and sustainable technologies. GRETh has a strong technology transfer activity, which includes the diffusion of software for heat exchanger design, publications in scientific and engineering reviews, the organisation of seminars and short courses.

Some research activities relevant to compact exchangers are summarised in the following pages.

For more information contact Bernard Thonon at

CEA-Grenoble

Greth

17 rue des martyrs

38054 Grenoble Cedex 9

France

tel : 33 476 88 30 79

fax : 33 476 88 51 72

e-mail : thonon@cea.fr

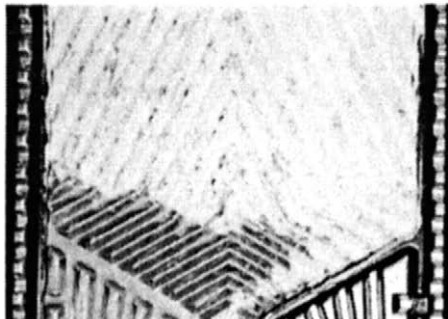
web site : www.greth.org

Compact heat exchangers

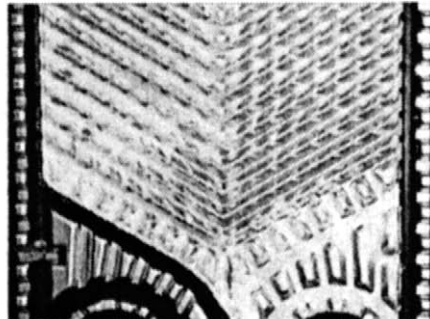
Fouling of heat exchangers

Fouling is highly detrimental to thermohydraulic performance and must be well understood if the heat exchange capability of practical equipment needs to be accurately predicted. In water cooling applications, particulate and precipitation fouling are frequently responsible for the decrease of the heat transfer performance. Enhanced heat transfer surfaces provide higher heat transfer coefficients than conventional plain tubes and will be more sensitive to fouling. Furthermore, the fouling margin implies extra surface area, which generally costs more than for plain stainless steel or copper tubes. In consequence, some specific recommendations need to be given for both fouling resistance values and operating conditions. Mitigation of fouling of enhanced heat exchangers must be taken into account at the design stage, and should include several factors such as the operating conditions, transient and start-up procedures, maintenance capabilities...

In consequence, factors affecting the fouling rate must be studied for different enhanced geometries (low-finned tubes, structured surfaces, plate heat exchangers, etc.) under controlled flow and fouling conditions. The present knowledge on fouling and the complexity of the mechanisms encountered does not allow the development of predictive tools which could be incorporated in the process control systems, but long term studies should be devoted to this topic.



View of the deposit (30° corrugation angle at a velocity of 0.5 m/s)



View of the deposit (60° corrugation angle at a velocity of 0.5 m/s)

Two-phase flow and heat transfer of high performance heat exchangers

The performance capabilities of enhanced heat exchangers are such that temperature approaches down to 1°C can be reached. This high thermal effectiveness requires accurate design tools for the design of the heat exchangers, and it is still necessary to obtain heat transfer and pressure drop correlations. Most of the research, carried out on enhanced geometries use model fluids (i.e. refrigerants for phase change heat transfer), and these fluids are generally not representative of industrial processes. Nevertheless, studies with model fluids are still useful to understand the basic mechanisms occurring.

In order to develop and validate design tools for enhanced heat exchangers in the process industry, it is necessary to obtain the performance with fluids which are representative of actual processes such as hydrocarbons. Furthermore, the size of the tested equipment should be significantly representative of industrial equipment. In regard to these conditions, there are only very few data available in the open literature of studies which are devoted to heat transfer into process equipment.

Greth is involved in several projects involving compact heat exchangers applied to the process industry. Condensation and evaporation of pure or mixture of hydrocarbons is studied on pilot units with actual flow conditions. In parallel with these tests under controlled conditions, field tests are carried out to validate the design methods developed previously.

Heat exchangers for gas or liquid waste treatments

Within the new environmental requirements gas or liquid waste treatments become fundamental and several aspects must be taken into account. The treatment of gaseous effluents (VOC's) is either realised by combustion at high temperature, absorption or condensation at low temperatures. Generally, the treatment is realised in a two stages process which associates two different techniques. From the view point of heat transfer, one of the problems is the knowledge of the effluent composition, which is generally not known precisely or which can change with time. This lack of information does not enable an effective design, and very often the equipment does not match the environmental requirements. To obtain a better sizing for VOC equipment, heat and mass transfer aspects must be studied under representative flow conditions. For instance, it has been observed that condensation of VOC's could be either in mist or film depending on the gas composition.

Recently, Greth has commissioned a new test rig devoted to VOC's treatment. This test rig can handle any type of VOC's with a flow rate of 500 m³/h of effluent to be treated and temperatures ranging from ambient to cryogenic. This test rig is used either to test single components such as condensers or full size equipment.

HEXAG

Heat Exchanger Action Group

HEXAG is a group of organisations involved in the manufacture and use of heat exchangers or with interests in the further development of heat exchanger technology. Currently there are some 300 members from a range of organisations.

HEXAG provides a regular forum for the interchange of information on all aspects of advances in heat exchanger technology. This encourages collaboration between manufacturers, users and researchers in the further development of advanced exchangers and helps to stimulate the industrial use of the technology. The group provides industry with information which enables them to make informed decisions on supporting development activities and on the application of advanced exchangers. The transfer of information between members is achieved through regular meetings of the group, through a newsletter and through a newsgroup.

HEXAG is funded by the Department of Trade & Industry under its Programme for Supporting Technology Transfer.

Contact Details

Further information on HEXAG, contact:

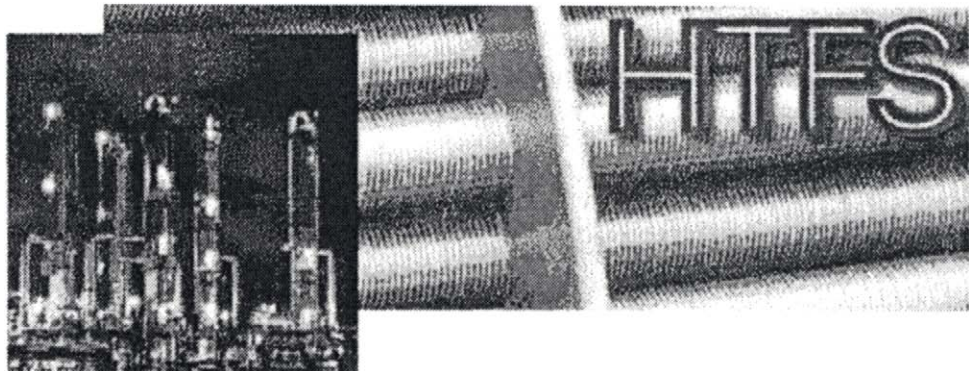
p.a.kew@hw.ac.uk

or:

David Reay,
HEXAG Co-ordinator,
PO Box 25, Whitley Bay,
Tyne & Wear, UK NE26 1QT.
Tel: 0191 251 2985 Fax: 0191 252 2229
Email: DAREay@aol.com

HTFS

(Heat Transfer and Fluid Flow Service)



- **Are heat transfer systems designs increasing your costs?**
- **Are your design engineers working at their full potential?**
- **Are you maximising the return on engineering software investments?**

The purpose of HTFS is to increase the profitability of our customers by providing state of the art knowledge of all Heat Transfer and Fluid systems. We primarily transfer this knowledge, which has been accumulated since 1968, through software, research papers and training.

As well as leasing or purchasing our software you can join others in guiding software development, oversee extensive research programmes and access the results via membership of the Research network. This special partnership between HTFS and its customers ensures that our software anticipates your business needs.

HTFS Research

The special partnership between HTFS and its customers via the research network ensures that our software anticipates your business needs. Open literature methods can work for simple cases, but are inadequate for the complete range of today's exacting design problems that include complex processes, such as boiling liquids and condensing vapours, in addition to single-phase fluids. This means RESEARCH. This research is incorporated into our software as calculation methods and is available to all members of the HTFS Research network through research papers and reports which enable detailed process understanding.

The research covers the following areas:

- Shell & tube heat exchangers
- Crossflow heat exchangers
- Furnaces 7 fired heaters
- Compact heat exchangers

Over two thirds of our 250 software customers are also members of the Research network. These customers have a close involvement in directing our research and the evolution of our products.

The Research Network on-line via the Web, makes this information even more accessible to those throughout your organisation involved in this area of work.

Research Network

The Research Network provides members with online access to a number of features including:

- **HTFS Discussion Forum** for members to exchange views online.
- **HTFS Research portfolio** including: the **HTFS Handbook**, a comprehensive reference to heat exchanger theory and practice; **HTFS Design Reports**, detailed derivation and comparisons of design methods; validation of design procedures and description of the technical methods used in the HTFS programs; **HTFS Research Papers** generated from our extensive research programme over the last 30 years.
- **Run HEAd online** to select the best heat exchanger type for a given process application, based on cost and technical suitability, and provides detailed information on design, manufacture and operation.
- **Download DEVIZE** to guide the engineer through the thermal design of shell and tube heat exchangers using a graphical, interactive and highly visual engineering approach.

- **HTFS HEATFLO** – a bibliographic reference database containing references to over 90,000 high quality experimental and theoretical research papers in the field of applied heat transfer and fluid flow relevant to the needs of the chemical process and power industries.

Benefits of membership

- Access to the latest information being generated by our heat transfer research program.
- Access to a quarterly current awareness bulletin, HTFS Digest, listing the latest papers on heat transfer published in the open literature.
- Access to over 50 HTFS Design Reports capturing the knowledge of over 30 years experience and explaining the models behind the software.
- Access to the HTFS Handbook, an invaluable tool for any heat transfer engineer.
- Access HTFS Research Volumes outlining the research performed over the last 30 years.
- Access to leading heat transfer specialists to help troubleshoot on plant and design issues.
- Participation in Review Panels in Europe and US co-ordinated by our heat transfer experts to provide input to our research & development program.
- Networking with other practitioners of heat transfer at our European, Japanese or North American annual meetings, courses or the HTFS Forum on-line.

HTFS Research Facilities for Compact Heat Exchangers

Plate-fin heat exchanger

Measurement of single phase and boiling heat transfer and pressure drop for single and multi-component hydrocarbons and a range of fin types at pressures up to 10 bar and temperatures from -5°C to 150°C .

Plate & Frame Heat Exchanger Rig

Measurement of single phase and boiling heat transfer and pressure drop for single and multi-component hydrocarbons and a range of plate types.

HTFS Software for Compact Heat Exchangers

HTFS Program MUSE for Plate-fin Heat Exchangers

HTFS software for performance simulation of compact, multistream plate-fin heat exchangers. This program can handle up to 15 process streams, in single phase, boiling or condensing, and any complexity of exchanger inlet and outlet geometry, including thermosyphon reboilers. Distributor pressure drop calculations are available and thermal conduction effects can be calculated. Research-validated fin performance correlations are built into the software for cases without manufacturers' data. Graphical capabilities are provided for input and output review and links to process simulators and physical properties packages are included.

MUSE has a variety of calculation options (and includes or will include options currently or previously not available).

HTFS Program APLE for Plate Heat Exchangers

Software for design, checking and simulation of plate heat exchangers, either gasketed plate and frame or brazed plate of the type used for general heating and cooling duties, including vaporization and condensation. The program can handle non Newtonian fluids. Co- or counter current exchangers are modelled with single or multiple passes and special attention is given to checking for the effects on performance of maldistribution.

Compact Heat Exchanger Research

Research in the compact heat exchangers area is driven by two main factors. Firstly, there is an urgent need to obtain reliable information about the heat transfer and pressure drop characteristics of the compact exchanger channels for single phase and two-phase duties. Secondly, as these channels are small, non-circular and often very complex, the fluid flow and heat transfer phenomena are very different to those well understood phenomena occurring in large diameter tubes. Therefore, there is a need to obtain better understanding of the underlying physics of these phenomena in the compact exchanger channels. Currently the HTFS research in this area covers -

- * Plate heat exchangers
- * Plate-fin heat exchangers

Plate Heat Exchangers

Boiling and condensation studies are undertaken in full industrial size plate heat exchangers using four plates to provide three flow channels for detailed investigation. Here the main emphasis is on making a large number of measurements of temperature and pressure at several locations, including inside of the plate channels, so that very detailed local thermal-hydraulic information is obtained.

This information is subsequently used to validate and develop boiling and condensation correlations, which are specific to plate heat exchanger channels. Many times these heat transfer experiments are supplemented by flow visualisation studies carried out with a transparent plastic replica of plate channels to obtain visual information on flow distribution within the cross corrugated channels of these exchangers.

Plate-fin Heat Exchangers

Heat transfer and pressure drop characteristics of various types of fin used in plate-fin heat exchangers are studied under flow boiling conditions over a wide range of pressure, heat flux, mass flux and vapour qualities. In these experiments, a rectangular test-section containing many different types of fin-pad is used, employing a large number of thermocouples for measuring wall and bulk fluid temperature at many different points along the test-section. Both absolute and differential pressures are also measured at a number of locations. Current experiments concentrate on hydrocarbon fluids.

These data together with the past data obtained with cryogenic fluids provide a large database for validating and developing the correlations which are specific to plate-fin passages.

AEA Technology Engineering Software www.software.aeat.com
<http://www.software.aeat.com>

Dr Vishwas V Wadekar <mailto:Vishwas.Wadekar@software.aeat.com>
<mailto:Vishwas.Wadekar@software.aeat.com>
Principal Scientist
HTFS, Building 392.7
Harwell, Oxfordshire,
OX11 0RA, UK

Tel: +44 1235 434249
Fax: +44 1235 831981

Heat Transfer Research, Inc.

Worldwide Headquarters

1500 Research Parkway, Suite 100
College Station, Texas 77842
USA

Phone: +1-979-260-6200
Fax: +1-979-260-6249
E-mail: HTRI@HTRI.net
Website: www.HTRI-net.com

European Office

The Surrey Technology Centre
40 Occam Road
The Surrey Research Park
Guildford, Surrey GU2 7YG
United Kingdom

Phone: +44-1483-845100
Fax: +44-1483-845101
E-mail: HTRI.Europe@HTRI.net

Introduction

Heat Transfer Research, Inc. (HTRI) is an international consortium founded in 1962 that conducts research on industrial-scale units and provides software tools for design, rating, and simulation of process heat transfer equipment. HTRI's software is based on its proprietary research data as well as other data available in the literature. HTRI also produces a wide range of technical publications in the following research areas:

- boiling
- condensing
- extended surfaces
- fouling
- non-tubular and compact heat exchangers
- shellside flow
- flow-induced vibration

HTRI software products include the following:

ACE Design, rating, and simulation of air-cooled heat exchangers, economizer bundles, and air preheaters

FH Simulation of fired heaters

IST Design, rating, and simulation of single- and two-phase shell-and-tube heat exchangers, including kettle and thermosiphon reboilers, falling film evaporators, and reflux condensers

PHE	Design, rating, and simulation of plate heat exchangers
VIB	Rigorous analysis of flow-induced vibration in a heat exchanger bundle
Xtlo	Graphical standalone rigorous tube layout software; also part of IST

HTRI also provides an educational version of a single-phase shell-and-tube heat exchanger program (ST Educational), which can be used for teaching at educational institutions.

Compact Heat Exchangers

Experimental Research Unit

HTRI has a single-phase experimental unit with two plate-and-frame heat exchangers, one welded plate heat exchanger, and one spiral plate heat exchanger.

The experimental unit has a design pressure of 11.4 bar and can operate at flow rates up to 136 m³/h with fluid viscosities up to 250 cP. The compact heat exchangers in this rig include:

Plate-and-frame heat exchanger (Alfa Laval Thermal Inc.)

Plate-and-frame heat exchanger (Tranter PHE, Inc.)

Compabloc® welded plate heat exchanger (Alfa Laval Vicarb)

HTRI has acquired isothermal, heat transfer, and port flow maldistribution data with various types of plates and fluid mixtures. This has resulted in generalized correlations to predict the pressure drop and heat transfer performance in plate heat exchangers.

PHE software

HTRI's PHE software designs, rates, and simulates the performance of plate heat exchangers. Plate groups are calculated individually using local physical properties and process conditions.

PHE handles single-phase, no-phase-change liquids, in laminar and turbulent flow. Geometries handled include those common to most commercially available plate heat exchangers.

- Chevron angles from 0 to 90 degrees
- Any number of plates
- One or two different plates
- Up to six passes
- Many commercial plate geometries available in databank

Technical Publications

HTRI has published several proprietary reports on plate heat exchangers, including experimental data and analysis for pressure drop and heat transfer performance.

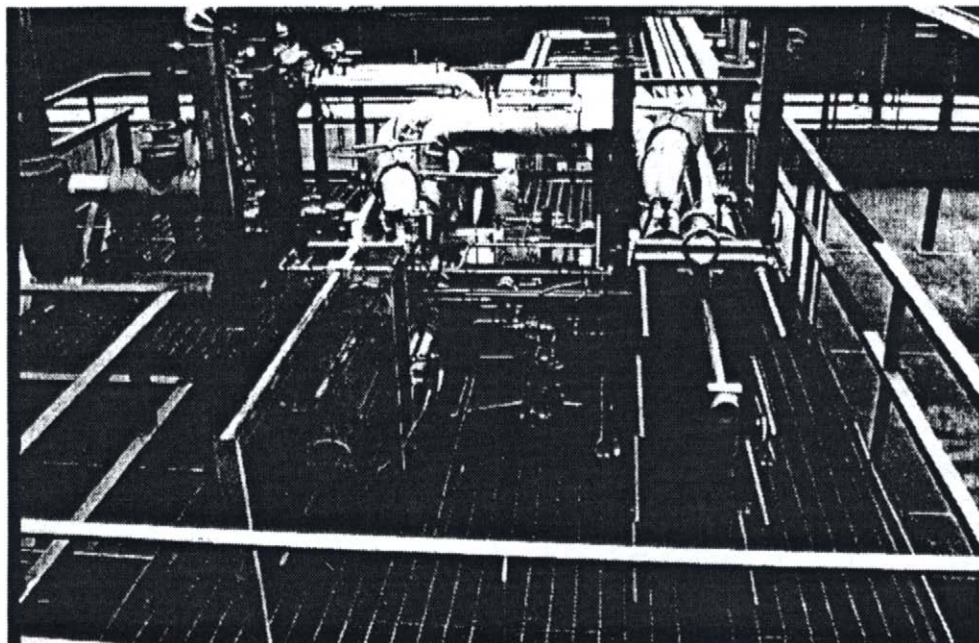


Figure 1. HTRI Single Phase Experimental Unit (2 PHEs, 1 Welded Plate Heat Exchanger and one Spiral Heat Exchanger).

NLAHX, Nederlandse Advanced Heat Exchanger (NOVEM) working party.

Mission:

To stimulate the use of advanced heat transfer equipment in order to improve the process efficiency by making use of better heat transfer to save energy.

Chairman: Bert Boxma
e-mail : bert.boxma@nl.abb.com

Participating organisations:

End users:

SHELL Global Solution

Dow Chemical

DSM

General Electric Plastic

ESSO

NAM

Nerefco

AKZO

Engineering contractors:

ABB Lummus Heat Transfer

Fluor Daniel

Jacobsen Eng.

Raytheon

Suppliers:

ABB Lummus Heat Transfer

Alfa Laval

Bronswerk

Institutes:

ECN

TUT

TNO MEP

Activities:

Regular meetings every 2-3 months. Exchange information generated from the Task-forces and invite organisations/suppliers for presentations.

Task Forces:

1. Heat Exchanger selection.
2. Heat Exchangers in gas service.
3. Fouling in Heat Exchangers.
4. Internet.

NOVEM will provide for every working party a homepage where the activities will be listed:

Agenda of the next meeting, Minutes of Meeting, Seminars and Internet hot-links to HTRI, HTFS, ESDU, HEXAG, GRETH and others.

Operational Feed-back and Lessons Learned data bank will be integrated.

The Task Force members will concentrate on their specific subjects and report back at the meeting.

The subsidy links by using advanced heat exchanged technology will be integrated e.g. Novem, Senter, TENDEM and SPIRIT.

Database and hotlink to suppliers of advanced heat transfer equipment.

Appendix 4 List of Manufacturers

This list is adapted from that given in the CADDET Analysis Series No.25: Learning from Experiences with Compact Heat Exchangers, is reproduced by permission of CADDET Energy Efficiency.

4.1 Plate-and-Frame Heat Exchangers

Alfa-Laval THERMAL Ltd

Theta House, Doman Road, Camberley, GU15 3DN, UK

Tel.: +44-1276-63383, Fax: +44-1276-413603

(Also in USA as Alfa Laval Thermal Inc., 5400 International Trade Drive, Richmond, VA 23231, USA

Tel.: +1-804-2225300, Fax: +1-804-2361360)

APV UK

PO Box 4, Gatwick Road, Crawley, West Sussex, RH10 2QB, UK

Tel.: +44-1293-527777, Fax: +44-1293-552640

GEA Ecoflex GmbH

Voss-Str. 11/13, D-31157 Sarstedt, Germany

Tel.: +49-5066/601-0, Fax: +49-5066/601-106

Agent: Maxicause Ltd

PO Box 3000, Littlehampton, West Sussex, BN17 6TP, UK

Tel.: +44-1903-731666, Fax: +44-1903-733020

Irish & Associates Heat Exchanger products

5454 Able Court, Mobile, AL 36693, USA

Tel.: +1-334-6611414, Fax: +1-334-6610749

JM Heat Exchangers

9 Albion Place, South Parade, Doncaster, DN1 2EG, UK

Tel.: +44-1302-360169, Fax: +44-1302-329608

Kundinger Fluid Power Inc

32388 Edwards, PO Box 71590, madison Heights, MI 48071, USA

Tel.: +1-248-5891885, Fax: +1-248-5885699

ReHeat AB

PO Box 3546, S-183 03 Taby, Sweden

Tel.: +46-8-7567315, Fax: +46-8-7562020

Sabroe + Soby Koleteknik A/S
Sortevej 30, PO Box 121, 8543 Hornslet, Denmark
Tel.: +45-8699-4433, Fax: +45-8699-4170

Sudmo (UK) Ltd
8 De Salis court, Hampton Lovett, Droitwich, Worcs., WR9 0NX, UK
Tel.: +44-1905-797280, Fax: +44-1905-797281

SWEP International AB
Box 105, S-261 22 Landskrona, Sweden.
Tel.: +46-418-54000, Fax: +46-418-29295
(also in UK as: SWEP Ltd, Chobham Ridges, The Maultway,
Camberley, Surrey, GU15 1QE, UK
Tel.: +44-1276-64221, Fax: +44-1276-64344)

Thermowave GmbH
Eichenweg 4, D-06536 Berga, Germany
Tel.: +49-34651/418-0, Fax: +49-34651/418-13

VICARB S.A.
Rue du Rif Tronchard, 38120 Fontanil Cornillon, France
Tel.: +33-76565050, Fax: +33-76757909

York International A/S
Aage Grams vej 1,6500 Vojens, Denmark
Tel.: +45-7420-4080, Fax: +45-74204040

4.2 Plate Heat Exchangers (Brazed)

Alfa Laval Thermal Ltd (Contact as in 4.1)

APV Heat Exchangers (Contact as in 4.1)

EJ Bowman (Birmingham) Ltd
Chester Street, Birmingham, B6 4AP, UK
Tel.: +44-121-3595401, Fax: +44-121-3597495

Centri Force Engineering Co. Ltd
1-7 Montrose Avenue, Hillington Industrial Estate,
Glasgow, G52 4DX, UK
Tel.: +44-141-8823351, Fax: +44-141-8829965

Funke Wärmeaustauscher Apparatebau GmbH
Postfach 40, 3212 Gronau (Leine), Germany
Tel.: +49-5182-5820, Fax: +49-5182-58248

GEA Ecoflex (Contact as in 4.1)

HRS Process Engineering Ltd
10-12 Caxton Way, Watford Business Park, Watford,
Hertfordshire, WD1 8UA, UK
Tel.: +44-1923-336327, Fax: +44-1923-230266

Kundinger Fluid Power Inc (Contact as in 4.1)

Sentry Equipment Corporation (Contact as in 4.1)

Sudno (UK) Ltd (Contact as in 4.1)

SWEP International AB (Contact as in 4.1)

4.3 Plate Heat Exchangers (Welded)

Alfa Laval Thermal Ltd (Contact as in 4.1)

APV Heat Exchangers (Contact as in 4.1)

Barriquand Exchangeurs
Export Office, 114 rue Celestin Demblon, 4630 Soumange, Belgium
Tel.: +32-41-774249, Fax: +32-41-77497

Biwater Heat Exchangers
Johnson-Hunt Ltd, Astley Street, Dukinfield, Cheshire, SK16 4QT, UK
Tel.: +44-161-3300234, Fax: +44-161-3309417

Centri Force Engineering Co. Ltd (Contact as in 4.2)

Hunt Thermal Engineering Ltd
Astley Street, Dukinfield, Cheshire, SK16 4QT, UK
Tel.: +44-161-334400, Fax: +44-161-3309417

Irish & Associates Heat Exchanger Products (Contact as in 4.1)
(Agents for Barriquand)

Packinox SA

Tour Fiat, Cedex 16, 92084 Paris la Defense, France
Tel.: +33-1-47963434, Fax: +33-1-47963440

*VICARB SA (Contact as in 4.1)***4.4 Spiral Heat Exchangers***Alfa Laval Thermal Ltd (Contact as in 4.1)**GEA Canzler GmbH*

Kolber Landstrasse 332, 52351 Düren, Germany
Tel.: +49-2421-7051, Fax: +49-2421-705280

Kapp Netherlands BV

Mailbox 960, Spijkenisse, 3200 AX, The Netherlands
Tel.: +31-181-690113, Fax: +31-181-690114

Occo Coolers Ltd

7 The Town Hall, Beaconsfield, Bucks., HP9 2PP, UK
Tel.: +44-1494-673458, Fax: +44-1494-677060

Radscan AB

PO Box 3011, S-611 03 Nykoping, Sweden
Tel.: +46-155-268030, Fax: +46-155-212155

Shipco AS

Ostre Strandgate 13SA, 4610 Kristiansand, Norway
Tel.: +47-38023207

4.5 Plate-Fin Heat Exchangers*Allied Signal Aerospace Company*

2525 West 190th Street, PO Box 2960, Torrance,
California 90509, USA
Fax: +1-310-5122607

ALTEX International

2191 Ward Avenue, La Crosse, Wisconsin 54601, USA
Tel.: +1-608-787-3333, Fax: +1-608-7872141

Chart Heat Exchangers Ltd

Industrial Heat Exchangers Group, Wobaston Road, Fordhouses,
Wolverhampton, WV10 6QJ, UK

Tel.: +44-1902-397777, Fax: +44-1902-397792

Colibri bv

Tentstraat 5, 6291 BC Vaals, The Netherlands

Tel.: +31-43-3066277, Fax: +31-43-3065797

Kobe Steel Ltd

2-3-1 Shinhma, Arai-cho, Takasago-Shi, Hyogo-Ken, 676 Japan

Tel.: +81-794-457334, Fax: +81-794-457239

Linde AG

Dr-Carl-von-Linde Str. 6-14, D 82049 Hollriegelskreuth,
Near Munich, Germany

Tel.: +49-80-7445-0, Fax: +49-89-74454955

Nordon Cryogenie

25, rue du Fort, BP 87, 88194 Golbey Cedex, France

Tel.: +33-29-680065, Fax: +33-29-313621

Normalair-Garrett Ltd

Yeovil, Somerset, BA20 2YD, UK

Tel.: +44-1935-75181, Fax: +44-1935-27600

Rolls Laval Heat Exchangers Ltd

PO Box 100, Ettinshall, Wolverhampton, WV4 6JX, UK

Tel.: +44-1902-343353

(Marketed by Alfa Laval Thermal – see 4.1)

Serck Aviation Ltd

Warwick Road, Birmingham, B11 2QY, UK

Tel.: +44-121-6931300, Fax: +44-121-7666013

Sumitomo Precision Products Co.

1-10, Fuso-cho, Amagasaki, Hyogo, 660 Japan

Tel.: 81-6-489-5875, Fax: 81-489-5879

4.6 Printed Circuit Heat Exchangers*Heetric Ltd*

46 Holton Road, Holton Heath, Poole, Dorset, BH16 6LT
Tel.: +44-1202-627000, Fax: +44-1202-632299

4.7 MARBOND™ Heat Exchangers and Heat Exchanger/Reactors

Chart Heat Exchangers (Contact as in 4.5)

4.8 Laminar Flow Heat Exchangers*CPI*

Engineering Division, Unit U, Riverside Estate, Fazeley, Tamworth,
Staffordshire, B78 3RW, UK
Tel.: +44-1827-261291, Fax: +44-1827-261102

4.9 Compact Shell-and-Tube Heat Exchangers*ABB Lummus Heat Transfer BV*

Oostduinlaan 75, 2596 JJ The Hague, The Netherlands
Tel.: +31-70-37330 91, Fax: +31-70-3733193

Associated Heat Engineering plc

Unit 2C Hunting Gate, East Portway, Andover,
Hampshire, SP10 3LF, UK
Tel.: +44-1264-334423, Fax: +44-1264-334417

EJ Bowman (Birmingham) Ltd (Contact as in 4.2)

Britannia Heat Transfer

Units 1 & 2, Station Road, Coleshill, Birmingham, B46 1JT, UK
Tel.: +44-1675-466060, Fax: +44-1675-467675
(Including specialised Materials)

Brown Fintube UK Ltd

Wimborne, BH21 5YA, UK
Tel.: +44-1258-840776, Fax: +44-1258-840961
(Also in USA as Brown Fin Tube Company, 12602 FM 529, Houston,
Texas 77041, USA)

ESKLA

Stadhouderslaan 66, 3116 HS Schiedam, The Netherlands

Tel.: +31-10-4736001

(Fluidised bed heat exchanger for fouling reduction)

Normalair-Garret Ltd (Contact as in 4.5)

Polymer Exchangers

Hollins Lane, Tilstock, Whitchurch, Shropshire, SY13 3NU, UK

Tel.: +44-1948-880627, Fax: +44-1948-880330

Serck Aviation (Contact as in 4.5)

Serck Heat Transfer

Warwick Road, Birmingham, B11 2QY, UK

Tel.: +44-121-7666666, Fax: +44-121-766-6014

4.10 'Prime Surface' Recuperators***Solar Turbines Inc***

220 Pacific Highway, PO Box 85376, San Diego,

California 92186, USA

Fax: +1-619-5442681

4.11 Compact Types Retaining a 'Shell'

APV Heat Exchangers (Contact as in 4.1)

(Plate + shell heat exchanger)

Vahterus

Pruukintie 7, FIN-23600 Kalanti, Finland

Tel.: +358-2-8427000, Fax: +358-2-8427029

(Plate + shell heat exchanger)

Wijbenga BV

Burg. Hondelinkstraat 3, 4153 VC Beesd, The Netherlands

Tel.: +31-3458-1549, Fax: +31-3458-2524

4.12 Tube Inserts (For heat transfer enhancement)***Cal Gavin Ltd***

Station Road, Alcester, Warwickshire, B49 5ET, UK

Tel.: +44-1789-400401, Fax: +44-1789-400411

Specialist Heat Exchangers

White Leather Square, Billingborough, Sleaford,
Lincolnshire, NG34 0QP, UK

Tel.: +44-1529-240686, Fax: +44-1529-240353

Tube Fins Ltd

Unit N, Riverside Estate, Fazeley, Tamworth,
Staffordshire, B78 3SD, UK

Tel.: +44-1827-251234, Fax: +44-1827-286612

4.13 Miscellaneous Types

ABB Lummus Heat Transfer BV (Contact as in 4.9)

(Also in USA ABB Lummus Heat Transfer Inc., 1515 Broad Street,
Bloomfield, NJ 07003, USA)

(Helical baffled shell and tube heat exchangers)

Cominco Engineering Services

Suite 160, 340 Midpark Way S.E., Calgary, Alberta, T2X 1P1, Canada
Tel.: +1-403-2543500, Fax: +1-403-2543501

(Bulk, etc.)

Saddleback Aerospace

5318 E. 2nd St., 154 Long Beach, CA 90803, USA

Tel.: +1-310-9300700, Fax: +1-310-9300031

(Laminated foil heat exchangers – liquid-liquid & liquid-gas)

ScanPress A/S

Vejlevej 158, DK-870 Horsens, Denmark

Tel.: +45-7564-1999, Fax: +45-7564-1977

(Plate gas-gas heat exchangers)

Sleegers Engineering Inc

649 Third Street, London, Ontario, N5V 2CA, Canada

Tel.: +1-519-6857444, Fax: +1-519-6852882

(Various types, including in exotic metals)

Sandex A/S

Jernet 9, DK-6000 Kolding, Denmark

Tel.: +45-7554-2855, Fax: +45-7553-8968

(Plate gas-gas heat exchangers)

Technova Inc

1459 Hebert Street, Drumondville, Quebec, J2C 2A1, Canada

Tel.: +1-819-4725454, Fax: +1-819-4724989

(Stainless steel heat exchangers for the process industries)

Thermo Design Engineering Ltd

PO Box 5557 STN. "L", Edmonton, Alberta, T6C 4E9, Canada

Tel.: +1-403-4406064, Fax: +1-403-4401657

(Modular skid-mounted units for gas processing plants)

Appendix 5 Physical Properties**5.1 Thermophysical properties of gases**

Air
Carbon monoxide (CO)
Carbon dioxide (CO₂)
Helium (He)
Hydrogen (H₂)
Nitrogen (N₂)
Oxygen (O₂)
Water Vapour
Air – Standard Atmosphere

5.2 Thermophysical properties of saturated liquids

Water
Ethylene Glycol
Glycerine
1-2 Butadiene
Air
Argon
Benzene
Butane
Carbon dioxide
Dowtherm A
Dowtherm J
Ethane
Ethanol
Ethylene
Helium
Hydrogen
Methane
Methanol
Nitrogen
Oxygen
Pentane
Propane
Toluene

5.3 Thermophysical properties of refrigerants

Ammonia R717 (NH₃)
Refrigerant R134a
Refrigerant R22

5.4 Thermophysical properties of fuels and oils

Engine oil (unused)
JP4 Aviation fuel
Hydraulic oil
Paraffin (kerosene)
Petrol (gasolene)

5.5 Thermophysical properties of metals**5.6 Thermophysical properties of nonmetallic solids****5.7 Mechanical properties of ferrous alloys****5.8 Mechanical properties of non-ferrous alloys****5.9 Mechanical properties of ceramic materials****5.10 Mechanical properties of polymers**

For sources and acknowledgements of the data in these appendices see pages 388 and 389.

5.1 Thermophysical Properties of Gases at Atmospheric Pressure*

T (K)	ρ (kg/m ³)	c_p (kJ/kgK)	$\eta \cdot 10^7$ (Ns/m ²)	$\nu \cdot 10^6$ (m ² /s)	$\lambda \cdot 10^3$ (W/mK)	$\delta \cdot 10^6$ (m ² /s)	Pr
Air							
100	3.5562	1.032	71.1	2.00	9.34	2.54	0.786
150	2.3364	1.012	103.4	4.426	13.8	5.84	0.758
200	1.7458	1.007	132.5	7.590	18.1	10.3	0.737
250	1.3947	1.006	159.6	11.44	22.3	15.9	0.720
300	1.1614	1.007	184.6	15.89	26.3	22.5	0.707
350	0.9950	1.009	208.2	20.92	30.0	29.9	0.700
400	0.8711	1.014	230.1	26.41	33.8	38.3	0.690
450	0.7740	1.021	250.7	32.39	37.3	47.2	0.686
500	0.6964	1.030	270.1	38.79	40.7	56.7	0.684
550	0.6329	1.040	288.4	45.57	43.9	66.7	0.683
600	0.5804	1.051	305.8	52.69	46.9	76.9	0.685
650	0.5356	1.063	322.5	60.21	49.7	87.3	0.690
700	0.4975	1.075	338.8	68.10	52.4	98.0	0.695
750	0.4643	1.087	354.6	76.37	54.9	109	0.702
800	0.4354	1.099	369.8	84.93	57.3	120	0.709
850	0.4097	1.110	384.3	93.80	59.6	131	0.716
900	0.3868	1.121	398.1	102.9	62.0	143	0.720
950	0.3666	1.131	411.3	112.2	64.3	155	0.723
1000	0.3482	1.141	424.4	121.9	66.7	168	0.726
1100	0.3166	1.159	449.0	141.8	71.5	195	0.728
1200	0.2902	1.175	473.0	162.9	76.3	224	0.728
1300	0.2679	1.189	496.0	185.1	82	238	0.719
1400	0.2488	1.207	530	213	91	303	0.703
1500	0.2322	1.230	557	240	100	350	0.685
1600	0.2177	1.248	584	268	106	390	0.688
1700	0.2049	1.267	611	298	113	435	0.685
1800	0.1935	1.286	637	329	120	482	0.683
1900	0.1833	1.307	663	362	128	534	0.677
2000	0.1741	1.337	689	396	137	589	0.672
2100	0.1658	1.372	715	431	147	646	0.667
2200	0.1582	1.417	740	468	160	714	0.655
2300	0.1513	1.478	766	506	175	783	0.647
2400	0.1448	1.558	792	547	196	869	0.630
2500	0.1389	1.665	818	589	222	960	0.613
3000	0.1135	2.726	955	841	486	1570	0.536

5.1 contd.

T (K)	ρ (kg/m ³)	c_p (kJ/kgK)	$\eta \cdot 10^7$ (Ns/m ²)	$\nu \cdot 10^6$ (m ² /s)	$\lambda \cdot 10^3$ (W/mK)	$\delta \cdot 10^6$ (m ² /s)	Pr
Carbon Monoxide (CO)							
200	1.6888	1.045	127	7.52	17.0	9.63	0.781
220	1.5341	1.044	137	8.93	19.0	11.9	0.753
240	1.4055	1.043	147	10.5	20.6	14.1	0.744
260	1.2967	1.043	157	12.1	22.1	16.3	0.741
280	1.2038	1.042	166	13.8	23.6	18.8	0.733
300	1.1233	1.043	175	15.6	25.0	21.3	0.730
320	1.0529	1.043	184	17.5	26.3	23.9	0.730
340	0.9909	1.044	193	19.5	27.8	26.9	0.725
360	0.9357	1.045	202	21.6	29.1	29.8	0.725
380	0.8864	1.047	210	23.7	30.5	32.9	0.729
400	0.8421	1.049	218	25.9	31.8	36.0	0.719
450	0.7483	1.055	237	31.7	35.0	44.3	0.714
500	0.67352	1.065	254	37.7	38.1	53.1	0.710
550	0.61226	1.076	271	44.3	41.1	62.4	0.710
600	0.56126	1.088	286	51.0	44.0	72.1	0.707
650	0.51806	1.101	301	58.1	47.0	82.4	0.705
700	0.48102	1.114	315	65.5	50.0	93.3	0.702
750	0.44899	1.127	329	73.3	52.8	104	0.702
800	0.42095	1.140	343	81.5	55.5	116	0.705
Carbon Dioxide (CO₂)							
280	1.9022	0.830	140	7.36	15.20	9.63	0.765
300	1.7730	0.851	149	8.40	16.55	11.0	0.766
320	1.6609	0.872	156	9.39	18.05	12.5	0.754
340	1.5618	0.891	165	10.6	19.70	14.2	0.746
360	1.4743	0.908	173	11.7	21.2	15.8	0.741
380	1.3961	0.926	181	13.0	22.75	17.6	0.737
400	1.3257	0.942	190	14.3	24.3	19.5	0.737
450	1.1782	0.981	210	17.8	28.3	24.5	0.728
500	1.0594	1.02	231	21.8	32.5	30.1	0.725
550	0.9625	1.05	251	26.1	36.6	36.2	0.721
600	0.8826	1.08	270	30.6	40.7	42.7	0.717
650	0.8143	1.10	288	35.4	44.5	49.7	0.712
700	0.7564	1.13	305	40.3	48.1	56.3	0.717
750	0.7057	1.15	321	45.5	51.7	63.7	0.714
800	0.6614	1.17	337	51.0	55.1	71.2	0.716

5.1 contd.

T (K)	ρ (kg/m ³)	c_p (kJ/kgK)	$\eta \cdot 10^7$ (Ns/m ²)	$\nu \cdot 10^6$ (m ² /s)	$\lambda \cdot 10^3$ (W/mK)	$\delta \cdot 10^6$ (m ³ /s)	Pr
Helium (He)							
100	0.4871	5.193	96.3	19.8	73.0	28.9	0.686
120	0.4060	5.193	107	26.4	81.9	38.8	0.679
140	0.3481	5.193	118	33.9	90.7	50.2	0.676
160	—	5.193	129	—	99.2	—	—
180	0.2708	5.193	139	51.3	107.2	76.2	0.673
200	—	5.193	150	—	115.1	—	—
220	0.2216	5.193	160	72.2	123.1	107	0.675
240	—	5.193	170	—	130	—	—
260	0.1875	5.193	180	96.0	137	141	0.682
280	—	5.193	190	—	145	—	—
300	0.1625	5.193	199	122	152	180	0.680
350	—	5.193	221	—	170	—	—
400	0.1219	5.193	243	199	187	295	0.675
450	—	5.193	263	—	204	—	—
500	0.09754	5.193	283	290	220	434	0.668
550	—	5.193	—	—	—	—	—
600	—	5.193	320	—	252	—	—
650	—	5.193	332	—	264	—	—
700	0.06969	5.193	350	502	278	768	0.654
750	—	5.193	364	—	291	—	—
800	—	5.193	382	—	304	—	—
900	—	5.193	414	—	330	—	—
1000	0.04879	5.193	446	914	354	1400	0.654

5.1 contd.

<i>T</i> (K)	<i>ρ</i> (kg/m ³)	<i>c_p</i> (kJ/kgK)	<i>η · 10⁷</i> (Ns/m ³)	<i>ν · 10⁶</i> (m ³ /s)	<i>λ · 10³</i> (W/mK)	<i>δ · 10⁶</i> (m ³ /s)	<i>Pr</i>
Hydrogen (H₂)							
100	0.24255	11.23	42.1	17.4	67.0	24.6	0.707
150	0.16156	12.60	56.0	34.7	101	49.6	0.699
200	0.12115	13.54	68.1	56.2	131	79.9	0.704
250	0.09693	14.06	78.9	81.4	157	115	0.707
300	0.08078	14.31	89.6	111	183	158	0.701
350	0.06924	14.43	98.8	143	204	204	0.700
400	0.06059	14.48	108.2	179	226	258	0.695
450	0.05386	14.50	117.2	218	247	316	0.689
500	0.04848	14.52	126.4	261	266	378	0.691
550	0.04407	14.53	134.3	305	285	445	0.685
600	0.04040	14.55	142.4	352	305	519	0.678
700	0.03463	14.61	157.8	456	342	676	0.675
800	0.03030	14.70	172.4	569	378	849	0.670
900	0.02694	14.83	186.5	692	412	1030	0.671
1000	0.02424	14.99	201.3	830	448	1230	0.673
1100	0.02204	15.17	213.0	966	488	1460	0.662
1200	0.02020	15.37	226.2	1120	528	1700	0.659
1300	0.01865	15.59	238.5	1279	568	1955	0.655
1400	0.01732	15.81	250.7	1447	610	2230	0.650
1500	0.01616	16.02	262.7	1626	655	2530	0.643
1600	0.0152	16.28	273.7	1801	697	2815	0.639
1700	0.0143	16.58	284.9	1992	742	3130	0.637
1800	0.0135	16.96	296.1	2193	786	3435	0.639
1900	0.0128	17.49	307.2	2400	835	3730	0.643
2000	0.0121	18.25	318.2	2630	878	3975	0.661

5.1 contd.

T (K)	ρ (kg/m ³)	c_p (kJ/kgK)	$\eta \cdot 10^7$ (Ns/m ²)	$\nu \cdot 10^6$ (m ² /s)	$\lambda \cdot 10^3$ (W/mK)	$\delta \cdot 10^6$ (m ² /s)	Pr
Nitrogen (N₂)							
100	3.4388	1.070	68.8	2.00	9.58	2.60	0.768
150	2.2594	1.050	100.6	4.45	13.9	5.86	0.759
200	1.6883	1.043	129.2	7.65	18.3	10.4	0.736
250	1.3488	1.042	154.9	11.48	22.2	15.8	0.727
300	1.1233	1.041	178.2	15.86	25.9	22.1	0.716
350	0.9625	1.042	200.0	20.78	29.3	29.2	0.711
400	0.8425	1.045	220.4	26.16	32.7	37.1	0.704
450	0.7485	1.050	239.6	32.01	35.8	45.6	0.703
500	0.6739	1.056	257.7	38.24	38.9	54.7	0.700
550	0.6124	1.065	274.7	44.86	41.7	63.9	0.702
600	0.5615	1.075	290.8	51.79	44.6	73.9	0.701
700	0.4812	1.098	321.0	66.71	49.9	94.4	0.706
800	0.4211	1.22	349.1	82.90	54.8	116	0.715
900	0.3743	1.146	375.3	100.3	59.7	139	0.721
1000	0.3368	1.167	399.9	118.7	64.7	165	0.721
1100	0.3062	1.187	423.2	138.2	70.0	193	0.718
1200	0.2807	1.204	445.3	158.6	75.8	224	0.707
1300	0.2591	1.219	466.2	179.9	81.0	256	0.701
Oxygen (O₂)							
100	3.945	0.962	76.4	1.94	9.25	2.44	0.796
150	2.585	0.921	114.8	4.44	13.8	5.80	0.766
200	1.930	0.915	147.5	7.64	18.3	10.4	0.737
250	1.542	0.915	178.6	11.58	22.6	16.0	0.723
300	1.284	0.920	207.2	16.14	26.8	22.7	0.711

5.1 contd.

T (K)	ρ (kg/m ³)	c_p (kJ/kgK)	$\eta \cdot 10^7$ (Ns/m ²)	$\nu \cdot 10^6$ (m ² /s)	$\lambda \cdot 10^3$ (W/mK)	$\delta \cdot 10^6$ (m ² /s)	Pr
Oxygen (O₂) (continued)							
350	1.100	0.929	233.5	21.23	29.6	29.0	0.733
400	0.9620	0.942	258.2	26.84	33.0	36.4	0.737
450	0.8554	0.956	281.4	32.90	36.3	44.4	0.741
500	0.7698	0.972	303.3	39.40	41.2	55.1	0.716
550	0.6998	0.988	324.0	46.30	44.1	63.8	0.726
600	0.6414	1.003	343.7	53.59	47.3	73.5	0.729
700	0.5498	1.031	380.8	69.26	52.8	93.1	0.744
800	0.4810	1.054	415.2	86.32	58.9	116	0.743
900	0.4275	1.074	447.2	104.6	64.9	141	0.740
1000	0.3848	1.090	477.0	124.0	71.0	169	0.733
1100	0.3498	1.103	505.5	144.5	75.8	196	0.736
1200	0.3206	1.115	532.5	166.1	81.9	229	0.725
1300	0.2960	1.125	588.4	188.6	87.1	262	0.721
Water Vapor (Steam)							
380	0.5863	2.060	127.1	21.68	24.6	20.4	1.06
400	0.5542	2.014	134.4	24.25	26.1	23.4	1.04
450	0.4902	1.980	152.5	31.11	29.9	30.8	1.01
500	0.4405	1.985	170.4	38.68	33.9	38.8	0.998
550	0.4005	1.997	188.4	47.04	37.9	47.4	0.993
600	0.3652	2.026	206.7	56.60	42.2	57.0	0.993
650	0.3380	2.056	224.7	66.48	46.4	66.8	0.996
700	0.3140	2.085	242.6	77.26	50.5	77.1	1.00
750	0.2931	2.119	260.4	88.84	54.9	88.4	1.00
800	0.2739	2.152	278.6	101.7	59.2	100	1.01
850	0.2579	2.186	296.9	115.1	63.7	113	1.02

5.1 contd.

Properties of the atmosphere

Geometric altitude, m	Temperature, K	Pressure, Pa	Density, kg/m ³	Viscosity, η Pa · s	Thermal Conductivity, mW/(mK)	Speed of Sound, m/s
0	288.2	1.01325	+05	1.225 +00	17.89	25.36
250	286.5	9.836	+04	1.196 +00	17.82	25.23
500	284.9	9.546	+04	1.167 +00	17.74	25.11
750	283.3	9.263	+04	1.139 +00	17.66	24.97
1,000	281.7	8.988	+04	1.112 +00	17.58	24.85
1,250	280.0	8.719	+04	1.085 +00	17.50	24.72
1,500	278.4	8.456	+04	1.058 +00	17.42	24.59
3,000	268.7	7.012	+04	9.093 -01	16.94	23.81
4,500	258.9	5.775	+04	7.770 -01	16.45	22.03
6,000	249.2	4.722	+04	6.601 -01	15.95	22.23
7,500	239.5	3.830	+04	5.572 -01	15.44	21.44
10,000	223.3	2.650	+04	4.135 -01	14.58	20.09
12,500	216.7	1.793	+04	2.884 -01	14.22	19.53
15,000	216.7	1.211	+04	1.948 -01	14.22	19.53
17,500	216.7	8.182	+03	1.316 -01	14.22	19.53
20,000	216.7	5.529	+03	8.891 -02	14.22	19.53
25,000	221.6	2.549	+03	4.008 -02	14.48	19.95
30,000	226.5	1.197	+03	1.841 -02	14.75	20.36
45,000	264.2	1.491	+02	1.966 -03	16.71	23.45
60,000	247.0	2.196	+01	3.097 -04	15.84	22.06
75,000	208.4	2.388	+00	3.992 -05	13.76	18.83

5.2 Thermophysical properties of saturated liquids

Thermophysical Properties of Saturated Water

Temperature, <i>T</i> (K)	Pressure, <i>P</i> (bars) ³	Specific Volume (m ³ /kg)		Heat of Vaporiza- tion, <i>H_v</i> (kJ/kg)		Specific Heat (kJ/kg) <i>c_{sp}</i>	Viscosity (Ns/m ²) <i>η</i> · 10 ⁶	<i>n</i> · 10 ⁴	Thermal Conductivity (W/mK) <i>λ</i> · 10 ⁴	<i>λ_c</i> · 10 ⁴	Prandtl Number <i>Pr_f</i>	Prandtl Number <i>Pr_s</i>	Surface Tension, σ · 10 ⁴ (N/m)	Expansion Coefficient, β · 10 ⁶ (K ⁻¹)	Temper- ature, <i>T</i> (K)
		<i>v_f</i> · 10 ³	<i>v_s</i>	<i>H_v</i> (kJ/kg)	<i>c_{sp}</i>										
273.15	0.00611	1.000	206.3	2502	4.217	1.854	1750	8.02	569	18.2	12.99	0.815	75.5	-68.05	273.15
275	0.00697	1.000	181.7	2497	4.211	1.855	1652	8.09	574	18.3	12.22	0.817	75.3	-32.74	275
280	0.00990	1.000	130.4	2485	4.198	1.858	1422	8.29	582	18.6	10.26	0.825	74.8	46.04	280
285	0.01387	1.000	99.4	2473	4.189	1.861	1225	8.49	590	18.9	8.81	0.833	74.3	114.1	285
290	0.01917	1.001	69.7	2461	4.184	1.864	1080	8.69	598	19.3	7.56	0.841	73.7	174.0	290
295	0.02617	1.002	51.94	2449	4.181	1.868	959	8.89	606	19.5	6.62	0.849	72.7	227.5	295
300	0.03531	1.003	39.13	2438	4.179	1.872	855	9.09	613	19.6	5.83	0.857	71.7	276.1	300
305	0.04712	1.005	29.74	2426	4.178	1.877	769	9.29	620	20.1	5.20	0.865	70.9	320.6	305
310	0.06221	1.007	22.93	2414	4.178	1.882	695	9.49	628	20.4	4.62	0.873	70.0	361.9	310
315	0.08132	1.009	17.82	2402	4.179	1.888	631	9.69	634	20.7	4.16	0.883	69.2	400.4	315
320	0.1053	1.011	13.98	2390	4.180	1.895	577	9.89	640	21.0	3.77	0.894	68.3	436.7	320
325	0.1351	1.013	11.06	2378	4.182	1.903	528	10.09	645	21.3	3.42	0.901	67.5	471.2	325
330	0.1719	1.016	8.82	2366	4.184	1.911	489	10.29	650	21.7	3.15	0.908	66.6	504.0	330
335	0.2167	1.018	7.09	2354	4.186	1.920	453	10.49	656	22.0	2.88	0.916	65.8	535.5	335
340	0.2713	1.021	5.74	2342	4.188	1.930	420	10.69	660	22.3	2.66	0.925	64.9	566.0	340
345	0.3372	1.024	4.683	2329	4.191	1.941	389	10.89	668	22.6	2.45	0.933	64.1	595.4	345
350	0.4163	1.027	3.846	2317	4.195	1.954	365	11.09	668	23.0	2.29	0.942	63.2	624.2	350
355	0.5100	1.030	3.180	2304	4.199	1.968	343	11.29	671	23.3	2.14	0.951	62.3	652.3	355
360	0.6209	1.034	2.645	2291	4.203	1.983	324	11.49	674	23.7	2.02	0.960	61.4	697.9	360
365	0.7514	1.038	2.212	2278	4.209	1.999	306	11.69	677	24.1	1.91	0.969	60.5	707.1	365
370	0.9040	1.041	1.861	2265	4.214	2.017	289	11.89	679	24.5	1.80	0.978	59.5	728.7	370
373.15	1.0133	1.044	1.679	2257	4.217	2.029	279	12.02	680	24.8	1.76	0.984	58.9	750.1	373.15
375	1.0815	1.045	1.574	2252	4.220	2.036	274	12.09	681	24.9	1.70	0.987	58.6	761	375
380	1.2869	1.049	1.337	2239	4.226	2.057	260	12.29	683	25.4	1.61	0.999	57.6	788	380
385	1.5233	1.053	1.142	2225	4.232	2.080	248	12.49	685	25.8	1.53	1.004	56.6	814	385

5.2 contd.

Thermophysical Properties of Saturated Water

Temper- ature, <i>T</i> (K)	Pressure, <i>P</i> (bars) ^b	Specific Volume (m ³ /kg)		Heat of Vapor- ization, <i>H_f</i> (kJ/kg)		Specific Heat (kJ/kg)		Viscosity (Ns/m ²)		Thermal Conductivity (W/mK)		Prandtl Number	Surface Tension, $\sigma \cdot 10^4$ (N/m)	Expansion Coeffi- cient, $\beta \cdot 10^6$ (K ⁻¹)	Temper- ature, <i>T</i> (K)
		<i>v_r</i> · 10 ³	<i>v_s</i>	<i>c_{fr}</i>	<i>c_{ss}</i>	<i>η_r · 10⁶</i>	<i>η_s · 10⁶</i>	$\lambda_r \cdot 10^3$	$\lambda_s \cdot 10^3$	<i>P_r</i>	<i>P_s</i>				
390	1.794	1.058	0.980	2212	4.239	2.104	237	12.69	686	26.3	1.47	1.013	55.6	841	390
400	2.455	1.067	0.731	2183	4.256	2.158	217	13.05	688	27.2	1.34	1.033	53.6	896	400
410	3.302	1.077	0.553	2153	4.278	2.221	200	13.42	688	28.2	1.24	1.054	51.5	952	410
420	4.370	1.088	0.425	2123	4.302	2.291	185	13.79	688	29.8	1.16	1.075	49.4	1010	420
430	5.699	1.099	0.331	2091	4.331	2.369	173	14.14	685	30.4	1.09	1.10	47.2		430
440	7.333	1.110	0.261	2039	4.36	2.46	162	14.50	682	31.7	1.04	1.12	45.1		440
450	9.319	1.123	0.208	2024	4.40	2.56	152	14.85	678	33.1	0.99	1.14	42.9		450
460	11.71	1.137	0.167	1989	4.44	2.68	143	15.19	673	34.6	0.95	1.17	40.7		460
470	14.55	1.152	0.136	1951	4.48	2.79	136	15.54	667	36.3	0.92	1.20	38.5		470
480	17.90	1.167	0.111	1912	4.53	2.94	129	15.88	660	38.1	0.89	1.23	36.2		480
490	21.83	1.184	0.0922	1870	4.59	3.10	124	16.23	651	40.1	0.87	1.25	33.9		490
500	26.40	1.203	0.0766	1825	4.66	3.27	118	16.59	642	42.3	0.86	1.28	31.6		500
510	31.66	1.222	0.0631	1779	4.74	3.47	113	16.95	631	44.7	0.85	1.31	29.3		510
520	37.70	1.244	0.0523	1730	4.84	3.70	108	17.33	621	47.5	0.84	1.35	26.9		520
530	44.58	1.268	0.0443	1679	4.95	3.96	104	17.72	608	50.6	0.85	1.39	24.5		530
540	52.38	1.294	0.0375	1622	5.08	4.27	101	18.1	594	54.0	0.86	1.43	22.1		540
550	61.19	1.323	0.0317	1564	5.24	4.64	97	18.6	580	58.3	0.87	1.47	19.7		550
560	71.08	1.355	0.0269	1499	5.43	5.09	94	19.1	563	63.7	0.90	1.52	17.3		560
570	82.16	1.392	0.0228	1429	5.68	5.67	91	19.7	548	76.7	0.94	1.59	15.0		570
580	94.51	1.433	0.0193	1353	6.00	6.40	88	20.4	528	76.7	0.99	1.68	12.8		580
590	108.3	1.482	0.0163	1274	6.41	7.35	84	21.5	513	84.1	1.05	1.84	10.5		590
600	123.5	1.541	0.0137	1176	7.00	8.75	81	22.7	497	92.9	1.14	2.15	8.4		600
610	137.3	1.612	0.0115	1068	7.85	11.1	77	24.1	467	103	1.30	2.60	6.3		610
620	159.1	1.705	0.0094	941	9.35	15.4	72	25.9	444	114	1.52	3.46	4.5		620
625	169.1	1.778	0.0085	858	10.6	18.3	70	27.0	430	121	1.65	4.20	3.5		625

T (K)	ρ (kg/m ³)	c_p (kJ/kg · K)	$\eta \cdot 10^2$ (Ns/m ²)	$\nu \cdot 10^6$ (m ² /s)	$\lambda \cdot 10^3$ (W/mK)	$\alpha \cdot 10^7$ (m ² /s)	Pr	$\beta \cdot 10^3$ (K ⁻¹)
Ethylene Glycol [C₂H₄(OH)₂]								
273	1,130.8	2.294	6.51	57.6	242	0.933	617	0.65
280	1,125.8	2.323	4.20	37.3	244	0.933	400	0.65
290	1,118.8	2.368	2.47	22.1	248	0.936	236	0.65
300	1,114.4	2.415	1.57	14.1	252	0.939	151	0.65
310	1,103.7	2.460	1.07	9.65	255	0.939	103	0.65
320	1,096.2	2.505	0.757	6.91	258	0.940	73.5	0.65
330	1,089.5	2.549	0.561	5.15	260	0.936	55.0	0.65
340	1,083.8	2.592	0.431	3.98	261	0.929	42.8	0.65
350	1,079.0	2.637	0.342	3.17	261	0.917	34.6	0.65
360	1,074.0	2.682	0.278	2.59	261	0.906	28.6	0.65
370	1,066.7	2.728	0.228	2.14	262	0.900	23.7	0.65
373	1,058.5	2.742	0.215	2.03	263	0.906	22.4	0.65
Glycerin [C₃H₈(OH)₃]								
273	1,276.0	2.261	1,060	8,310	282	0.977	85,000	0.47
280	1,271.9	2.298	534	4,200	284	0.972	43,200	0.47
290	1,265.8	2.367	185	1,460	286	0.955	15,300	0.48
300	1,259.9	2.427	79.9	634	286	0.935	6,780	0.48
310	1,253.9	2.490	35.2	281	286	0.916	3,060	0.49
320	1,247.2	2.564	21.0	168	287	0.897	1,870	0.50

5.2 contd.

1,2-BUTADIENE

Chemical formula: $\text{CH}_2\text{CH}=\text{C}=\text{CH}_2$
 Molecular weight: 54.09
 Normal boiling point: 284.0 K
 Melting point: 137.0 K

Critical temperature: 443.7 K
 Critical pressure: 4 500 kPa
 Critical density: 246.8 kg/m³

T_{sat} , K	284.0	300	315	330	345	360	375	390	400	443.7	
p_{sat} , kPa	101.3	189	265	445	661	945	1 310	1 770	2 140	4 500	[46, 76]
ρ_{g} , kg/m ³	651	643	625	605	585	563	537	507	485	246.8	[46]
ρ_{g} , kg/m ³	2.32	4.04	6.43	9.80	14.4	20.7	29.2	40.7	50.8	246.8	[62]
h_{g} , kJ/kg	-197	-166	-131	-94	-57	-19	19	61	88	255	[67]
h_{g} , kJ/kg	237	257	275	293	311	327	341	354	359	255	[46, 62, 69]
$\Delta h_{\text{g},\text{g}}$, kJ/kg	434	423	406	387	368	346	322	293	271		[46]
$c_{p,\text{g}}$, kJ/(kg K)	2.20	2.24	2.30	2.41	2.49	2.60	2.72	2.87	3.01		[46]
$c_{p,g}$, kJ/(kg K)	1.48	1.56	1.65	1.75	1.87	2.01	2.18	2.43	2.68		[46, 62]
η_{g} , $\mu\text{Ns/m}^2$	200	185	170	150	134	116	100	85	76	43	[46, 33]
η_{g} , $\mu\text{Ns/m}^2$	7.40	7.78	8.27	8.76	9.26	9.77	10.4	11.0	11.5	43	[46, 14]
λ_{g} , (mW/m ²)/(K/m)	126	119	113	107	102	98	93	88	82	49	[34]
λ_{g} , (mW/m ²)/(K/m)	12.5	14.1	15.8	17.5	19.3	21.2	23.3	25.6	27.3	49	[68, 22]
Pr_{g}	3.62	3.48	3.46	3.38	3.27	3.08	2.92	2.77	2.79		[12]
Pr_{g}	0.88	0.86	0.86	0.88	0.90	0.93	0.97	1.04	1.13		[12]
σ , mN/m	18.0	15.7	13.9	12.1	10.4	8.65	7.00	5.30	4.10		[46]
$\beta_{\text{e},\text{g}}$, kK ⁻¹	1.71	1.89	2.10	2.35	2.66	3.77	4.11	4.85	5.74		[10]

5.2 contd.

AIR

Chemical formula: N₂ (78.1%); O₂ (20.9%); Ar (0.9%)

Molecular weight: 28.96

Normal boiling point: 78.9 K

Melting point: ?

Critical temperature: 132.6 K

Critical pressure: 3 769 kPa

Critical density: 313 kg/m³

<i>T</i> _{sat} , K	78.9	85	90	95	100	110	115	120	125	132.6	
<i>p</i> _{sat} , kPa	101.3	192	304	457	662	1 260	1 670	2 160	2 740		[52]
<i>p</i> _{con} , kPa	0.721	1.45	2.40	3.75	6.60	11.2	15.2	20.1	26.1	37.69	[52]
<i>ρ</i> _g , kg/m ³	876	847	822	796	768	705	669	627	569		[52]
<i>ρ</i> _g , kg/m ³	3.27	6.26	9.98	15.2	22.4	45.1	62.8	87.3	123	313	[52]
<i>h</i> _g , kJ/kg	-124.6	-113.1	-103.5	-93.5	-83.3	-61.9	-50.3	-37.5	-22.0		[52]
<i>h</i> _g , kJ/kg	76.9	81.6	84.8	87.4	89.3	90.1	88.4	84.8	78.2	37.4	[52]
<i>Δh</i> _{g,2} , kJ/kg	201.5	194.7	188.3	180.9	172.6	152.0	138.7	122.3	100.2		[52]
<i>c</i> _{p,g} , kJ/(kg K)	1.87	1.91	1.94	1.99	2.05	2.14	2.48	2.92	4.59		[1]
<i>c</i> _{p,g} , kJ/(kg K)	1.05	1.07	1.09	1.13	1.26	1.56	1.92	2.46	3.38		[1]
<i>η</i> _g , μNs/m ²	183	142	116	97	82	63	55	48	41		[1]
<i>η</i> _g , μNs/m ²	5.6	6.0	6.4	6.8	7.3	8.5	9.0	9.8	10.9		[1]
<i>λ</i> _g , (mW/m ²)/(K/m)	148	137	128	120	111	94	85	77	66		[1]
<i>λ</i> _g , (mW/m ²)/(K/m)	7.4	7.8	8.4	9.2	10.1	12.5	13.9	15.2	17.4		[1]
<i>Pr</i> _g	2.31	1.98	1.76	1.61	1.51	1.43	1.60	1.82	2.85		[12]
<i>Pr</i> _g	0.79	0.82	0.83	0.84	0.91	1.06	1.24	1.59	2.12		[12]
<i>σ</i> , mN/m	9.64	8.29	7.26	6.22	5.22	3.34	2.45	1.62	0.88		[54]
<i>β</i> _{g,2} , kK ⁻¹	5.5	6.0	6.6	7.3	8.4	12.5	16.0	21.5	33.0		[10]

5.2 contd.

ARGON

Chemical formula: Ar
 Molecular weight: 39.944
 Normal boiling point: 87.29 K
 Melting point: 83.78 K

Critical temperature: 150.86 K
 Critical pressure: 4 898 kPa
 Critical density: 536 kg/m³

T_{sat}, K	87.29	94.4	101.4	108.5	115.5	122.6	129.7	136.7	143.8	150.9	[1]
$p_{\text{sat}}, \text{kPa}$	101.3	201.6	362.2	601.5	938.2	1 393	1 987	2 738	3 702	4 898	[1]
$\rho_{\text{g}}, \text{kg/m}^3$	1 393	1 348	1 301	1 251	1 197	1 137	1 068	986.7	877.6	535.6	[1]
$\rho_{\text{g}}, \text{kg/m}^3$	5.78	10.9	18.6	30.2	46.4	68.9	100.2	146.8	222.4	535.6	[1]
$h_{\text{g}}, \text{kJ/kg}$	-116.1	-108.8	-101.1	-92.9	-84.2	-74.9	-64.5	-53.0	-40.2	-2.4	[1]
$h_{\text{g}}, \text{kJ/kg}$	43.5	45.8	47.6	48.7	49.0	48.2	46.0	41.7	33.3	-2.4	[1]
$\Delta h_{\text{fg}}, \text{kJ/kg}$	159.6	154.6	148.9	141.6	133.2	123.1	110.6	94.7	73.5	[1]	
$c_{\text{p},\text{g}}, \text{kJ/(kg K)}$	1.083	1.168	1.200	1.218	1.257	1.358	1.559	1.923	2.011	[3, 9]	
$c_{\text{p},\text{g}}, \text{kJ/(kg K)}$	0.548	0.569	0.626	0.665	0.745	0.866	1.067	1.509	2.951	[9]	
$\eta_{\text{g}}, \mu\text{Ns/m}^2$	260.5	211.9	176.6	150.8	131.1	116.1	101.7	84.2	63.9	27.9	[4]
$\eta_{\text{g}}, \mu\text{Ns/m}^2$	7.43	8.04	8.69	9.39	10.2	10.5	12.1	13.6	15.8	27.9	[4]
$\lambda_{\text{g}}, (\text{mW/m}^2)/(\text{K/m})$	123.2	114.9	106.5	98.7	90.1	81.1	71.9	63.4	53.6	30	[2]
$\lambda_{\text{g}}, (\text{mW/m}^2)/(\text{K/m})$	6.09	6.63	7.23	7.92	8.70	9.67	11.1	12.9	15.4	30	[9]
Pr_{g}	2.29	2.15	1.99	1.86	1.83	1.94	2.21	2.55	2.40	[12]	
Pr_{g}	0.67	0.69	0.75	0.79	0.87	0.94	1.16	1.59	3.03	[12]	
$\sigma, \text{mN/m}$	14.50	12.77	11.28	9.35	7.73	6.18	4.71	3.34	2.61	1.75	[6]
$\beta_{\text{e},\text{g}}, \text{K}^{-1}$	4.58	5.01	5.50	6.41	7.80	9.61	12.6	16.8	23.7	41.8	[10]

BENZENE

Chemical formula: C_6H_6
 Molecular weight: 78.108
 Normal boiling point: 353.25 K
 Melting point: 278.7 K

Critical temperature: 562.6 K
 Critical pressure: 4 924 kPa
 Critical density: 301.6 kg/m³

	353.3	375	400	425	450	475	500	525	550	562.6	
T_{sat}, K	353.3	375	400	425	450	475	500	525	550	562.6	[1]
$p_{\text{sat}}, \text{kPa}$	101.3	191	354	607	975	1 484	2 166	3 060	4 218	4 924	[1]
$\rho_{\text{g}}, \text{kg/m}^3$	823	798	767	735	699	660	615	559	475	304	[1]
$\rho_{\text{g}}, \text{kg/m}^3$	2.74	4.90	8.87	14.8	23.6	36.1	54.2	82.0	133	304	[1]
$h_{\text{g}}, \text{kJ/kg}$	-154.3	-113.0	-62.1	-8.9	47.5	106.8	169.7	238.6	322.8	432.6	[1]
$h_{\text{g}}, \text{kJ/kg}$	243.4	270.3	302.1	334.8	367.9	400.7	432.3	460.4	478.5	432.6	[1]
$\Delta h_{\text{g},\text{f}}, \text{kJ/kg}$	397.7	383.3	364.2	343.7	320.4	293.9	262.6	221.8	155.7		[1]
$c_{p,\text{f}}, \text{kJ/(kg K)}$	1.88	1.98	2.08	2.20	2.32	2.45	2.60	2.83			[1]
$c_{p,\text{g}}, \text{kJ/(kg K)}$	1.29	1.40	1.53	1.67	1.81	2.01	2.32	2.73			[4, 20]
$\eta_{\text{f}}, \mu\text{Ns/m}^2$	321	258	205	166	138	116	97.9	80.7	59.6		[1]
$\eta_{\text{g}}, \mu\text{Ns/m}^2$	9.26	9.87	10.7	11.5	12.5	13.7	15.0	16.8	19.1		[1]
$\lambda_{\text{f}}, (\text{mW/m}^2)/(\text{K/m})$	131	126	119	112	106	100	93.5	87.1	77.4	62.6	[2]
$\lambda_{\text{g}}, (\text{mW/m}^2)/(\text{K/m})$	14.8	17.1	19.8	23.0	26.7	31.0	35.7	41.1	50.2	62.6	[2, 22]
\Pr_{f}	4.61	4.05	3.58	3.26	3.02	2.84	2.75	2.62			[12]
\Pr_{g}	0.81	0.82	0.83	0.84	0.85	0.89	0.97	1.12			[12]
$\sigma, \text{mN/m}$	21.2	18.5	15.5	12.7	9.89	7.26	4.80	2.55	0.65		[6]
$\beta_{\text{e},\text{f}}, \text{kK}^{-1}$	1.15	1.37	1.67	2.02	2.49	3.13	4.32	6.98	16.0		[10]

5.2 contd.

BUTANE

Chemical formula: $\text{CH}_3\text{CH}_2\text{CH}_2\text{CH}_3$

Molecular weight: 58.12

Normal boiling point: 272.66 K

Melting point: 134.82 K

Critical temperature: 425.16 K

Critical pressure: 3 796 kPa

Critical density: 225.3 kg/m³

T_{sat} , K	273.15	289	305	321	337	353	369	385	405	425.16	
p_{sat} , kPa	103	184	304	469	706	1 023	1 526	1 925	2 739	3 797	[56]
ρ_{g} , kg/m ³	603	587	571	551	529	504	475	441	388	225.3	[46]
ρ_{g} , kg/m ³	2.81	4.81	7.53	11.6	17.4	25.1	35.6	51.3	80.7	225.3	[56]
h_{g} , kJ/kg	-1 194	-1 158	-1 121	-1 081	-1 040	-997	-945	-896	-821	-665	[56]
h_{g} , kJ/kg	-809	-789	-769	-747	-725	-706	-681	-663	-648	-665	[56]
$\Delta h_{\text{g},\text{f}}$, kJ/kg	385	369	352	334	315	291	264	233	173		[46]
$c_{p,\text{g}}$, kJ/(kg K)	2.34	2.47	2.59	2.68	2.80	2.95	3.11	3.36	3.80		[46]
$c_{p,\text{g}}$, kJ/(kg K)	1.67	1.76	1.88	2.00	2.15	2.33	2.62	3.03	4.76		[56]
η_{g} , $\mu\text{Ns/m}^2$	206	179	154	131	112	95	80	65	51		[4]
η_{g} , $\mu\text{Ns/m}^2$	7.35	7.81	8.32	8.87	9.44	10.20	11.25	12.77	16.30		[4]
λ_{g} , (mW/m ²)/(K/m)	114.6	109.8	104.9	100.1	95.1	90.4	85.5	80.7	74.6	48.7	[2]
λ_{g} , (mW/m ²)/(K/m)	13.69	15.19	16.82	18.57	20.47	22.49	24.69	27.24	31.2	48.7	[2]
Pr_{g}	4.20	4.02	3.80	3.51	3.30	3.11	2.89	2.72	2.59		[12]
Pr_{g}	0.90	0.90	0.93	0.96	1.00	1.06	1.19	1.42	2.48		[12]
σ , mN/m	14.8	12.8	11.0	9.10	7.29	5.54	4.03	2.75	1.34		[46]
$\beta_{\text{e},\text{g}}$, kK^{-1}	1.73	2.01	2.37	2.80	3.45	4.31	7.31	9.87	10.0		[10]

CARBON DIOXIDE

Chemical formula: CO_2
 Molecular weight: 44.011
 Normal boiling point: 194.65 K
 Melting point: 216.55 K

Critical temperature: 304.19 K
 Critical pressure: 7 382 kPa
 Critical density: 468 kg/m^3

T_{sat}, K	216.55	230	240	250	260	270	280	290	300	304.19	[1]
$p_{\text{sat}}, \text{kPa}$	518	891	1 282	1 787	2 421	3 203	4 159	5 315	6 712	7 382	[1]
$\rho_g, \text{kg/m}^3$	1 179	1 130	1 089	1 046	998	944	883	805	676	468	[1]
$\rho_g, \text{kg/m}^3$	15.8	20.8	32.7	45.9	63.6	88.6	121	172	268	468	[1]
$h_g, \text{kJ/kg}$	-206.2	-181.5	-162.5	-142.6	-121.9	-99.6	-75.7	-47.6	-10.8	42.8	[1]
$h_g, \text{kJ/kg}$	141.1	148.5	151.7	151.1	148.6	142.9	134.9	122.8	96.3	42.8	[1]
$\Delta h_{g,g}, \text{kJ/kg}$	347.3	330.0	314.2	293.7	270.5	242.5	210.6	170.4	107.1		[1]
$c_{p,g}, \text{kJ/(kg K)}$	2.15	2.08	2.09	2.13	2.24	2.42	2.76	3.63	7.69		[9, 1]
$c_{p,g}, \text{kJ/(kg K)}$	0.89	0.98	1.10	1.20	1.42	1.64	1.94	3.03	9.25		[9, 1]
$\eta_g, \mu\text{Ns/m}^2$	250	200	166	138	117	102	90.8	79.0	59.6	31.6	[9, 4]
$\eta_g, \mu\text{Ns/m}^2$	11.0	12.0	12.7	13.5	14.3	15.2	16.5	18.7	22.8	31.6	[4]
$\lambda_g, (\text{mW/m}^2)/(\text{K/m})$	177	160	146	134	122	110	98	86.1	74.1	47.5	[1, 2]
$\lambda_g, (\text{mW/m}^2)/(\text{K/m})$	11.5	12.9	14.2	15.7	17.4	19.7	22.9	28.0	39.2	47.5	[9]
Pr_g	3.04	2.60	2.38	2.19	2.15	2.24	2.56	3.33	6.19		[12]
Pr_g	0.85	0.91	0.98	1.03	1.17	1.27	1.40	2.02	5.38		[12]
$\sigma, \text{mN/m}$	17.1	13.8	11.4	9.16	7.02	5.01	3.19	1.61	0.33		[6]
$\beta_{e,g}, \text{K}^{-1}$	2.86	3.60	4.18	4.91	6.00	7.63	10.2	18.2	57		[29]

5.2 contd.

DOWTHERM A

Chemical formula: $(C_6H_5)_2O$ (73.5%); $(C_6H_5)_2$ (26.5%)

Molecular weight: 166

Normal boiling point: 530.25 K

Melting point: 285.15 K

Critical temperature: 770.15 K

Critical pressure: 3 134 kPa

Critical density: 315.5 kg/m³

T_{sat} , K	530.25	555	580	605	630	655	680	700	730	770.15	
p_{sat} , kPa	101.3	170.4	270	411	600	848	1 170	1 470	2 040	3 134	[108]
ρ_g , kg/m ³	851.9	826	799	770	740	706	670	637	573	315.5	[108]
ρ_g , kg/m ³	3.96	6.47	10.0	15.2	22.0	31.8	45.1	60.1	100	315.5	[108]
h_g , kJ/kg	465	522	580	642	703	769	835	890	970		[108, 39]
h_g , kJ/kg	761	806	850	897	942	990	1 035	1 070	1 110		[108, 39]
$\Delta h_{g,l}$, kJ/kg	296	284	270	255	239	221	200	180	140		[108, 39]
c_p,g , kJ/(kg K)	2.24	2.32	2.40	2.47	2.53	2.59	2.69	2.83	3.26		[108, 39]
c_p,g , kJ/(kg K)	1.83	1.91	1.97	2.03	2.10	2.16	2.24	2.34	2.54		[108, 39]
η_g , $\mu\text{Ns/m}^2$	273	236	206	180	160	145	132	124	115		[108, 110]
η_g , $\mu\text{Ns/m}^2$	10.1	10.6	11.2	11.7	12.2	12.7	13.3	13.9	14.5		[108, 93, 110]
λ_g , (mW/m ²)/(K/m)	112	109	106	103	100	97	94	91	88		[108, 93]
λ_g , (mW/m ²)/(K/m)	20.4	22.6	24.8	27.2	29.8	32.6	35.6	38.8	42.0		[108, 93]
Pr_g	5.46	5.02	4.66	4.32	4.05	3.87	3.78	3.86	4.26		[12]
Pr_g	0.91	0.90	0.89	0.87	0.86	0.84	0.84	0.84	0.88		[12, 93]
σ , mN/m											[83]
$\beta_{e,g}$, kK^{-1}	1.20	1.33	1.50	1.70	2.02	2.41	2.93	3.73	6.85		[10]

DOWTHERM J

Chemical formula: $C_{10}H_{14}$

Molecular weight: 134

Normal boiling point: 454.26 K

Melting point: < 235.37 K

Critical temperature: 656.15 K

Critical pressure: 2 837 kPa

Critical density: 273.82 kg/m³

T_{sat} , K	454.26	480	500	520	540	560	580	600	620	656.15	
p_{sat} , kPa	101.3	187	279	351	536	804	1 070	1 460	1 870	2 837	[109]
ρ_g , kg/m ³	729.3	705.3	683.5	660.9	636.6	609.5	580.8	545.4	505.3	273.8	[109]
ρ_g , kg/m ³	3.75	6.70	9.79	14.2	20.3	28.7	39.5	63.9	96.4	273.8	[109]
h_g , kJ/kg	330	394	444	497	552	609	665	721	779		[109, 110]
h_g , kJ/kg	635	684	721	760	799	838	876	910	937		[109, 110]
$\Delta h_{g,2}$, kJ/kg	305	290	277	263	247	229	211	189	158		[109, 110]
$c_{p,g}$, kJ/(kg K)	2.40	2.51	2.58	2.66	2.75	2.84	2.95	3.08	3.25		[109, 110]
$c_{p,g}$, kJ/(kg K)	1.91	2.00	2.06	2.12	2.17	2.24	2.29	2.34	2.39		[109, 100]
η_g , $\mu\text{Ns/m}^2$	172	149	133	121	109	101	93	85	78		[109, 100]
η_g , $\mu\text{Ns/m}^2$	8.60	9.05	9.40	9.75	10.10	10.45	10.80	11.15	11.40		[109, 93]
λ_g , (mW/m ²)/(K/m)	118.5	117.0	115.6	114.2	111.8	110.4	109.0	107.6	106.2		[109]
λ_g , (mW/m ²)/(K/m)											[83]
Pr_g	3.48	3.20	2.97	2.82	2.68	2.60	2.52	2.43	2.39		[12]
Pr_g											[83]
σ , mN/m											[83]
$\beta_{e,g}$, K^{-1}	1.20	1.46	1.64	1.73	2.20	2.76	3.54	4.69	7.52		[10]

5.2 contd.

ETHANE

Chemical formula: CH_3CH_3

Molecular weight: 30.068

Normal boiling point: 184.52 K

Melting point: 89.88 K

Critical temperature: 305.5 K

Critical pressure: 4 913 kPa

Critical density: 212 kg/m³

	184.52	200	210	230	240	260	270	280	290	300	[1]
$p_{\text{sat}}, \text{kPa}$	101	217	334	700	968	1 712	2 208	2 801	3 510	4 365	[1]
$\rho_{\text{g}}, \text{kg/m}^3$	546.45	529.10	516.79	489.71	474.60	440.14	419.81	396.35	364.56	316.25	[1]
$\rho_{\text{g}}, \text{kg/m}^3$	2.04	4.09	6.21	12.75	17.56	31.65	42.03	55.96	77.10	119.18	[1]
$h_{\text{g}}, \text{kJ/kg}$	399.52	437.50	462.53	515.34	541.41	598.79	629.79	663.10	700.28	753.08	[1]
$h_{\text{g}}, \text{kJ/kg}$	889.19	903.74	912.82	929.18	935.72	943.27	943.23	941.14	930.10	892.31	[1]
$\Delta h_{\text{g},\text{0}}, \text{kJ/kg}$	489.67	466.24	450.29	414.84	394.31	344.48	313.44	278.04	229.82	139.23	[1]
$c_{\text{p},\text{g}}, \text{kJ/(kg K)}$	2.42	2.48	2.54	2.66	2.70	3.00	3.18	3.42	3.80	[3, 5]	
$c_{\text{p},\text{g}}, \text{kJ/(kg K)}$	1.40	1.48	1.54	1.70	1.79	2.13	2.42	2.94	3.31	9.51	[11]
$\eta_{\text{g}}, \mu\text{Ns/m}^2$	168	139	124	99.4	88.8	70.8	61.6	54.0	46.0	36.1	[4]
$\eta_{\text{g}}, \mu\text{Ns/m}^2$	6.00	6.59	7.03	7.89	8.42	9.85	10.9	12.1	14.2	19.0	[4, 15]
$\lambda_{\text{g}}, (\text{mW/m}^2)/(\text{K/m})$	157	146	140	126	117	99.2	92.1	83.9	76.0	67.4	[7]
$\lambda_{\text{g}}, (\text{mW/m}^2)/(\text{K/m})$	8.6	10.3	11.5	14.1	15.5	18.6	20.7	22.8	26.1	32.0	[2, 14]
Pr_{g}	2.59	2.37	2.26	2.10	2.05	2.14	2.12	2.2	2.23		[12]
Pr_{g}	0.98	0.95	0.94	0.95	0.97	1.13	1.27	1.56	1.80	5.64	[12]
$\sigma, \text{mN/m}$	15.86	13.28	11.71	8.51	6.85	4.28	3.14	2.00	1.14	0.43	[6]
$\beta_{\text{e},\text{g}}, \text{kK}^{-1}$	2.01	2.31	2.58	3.32	3.80	5.46	6.67	9.40	15.9	96.2	[10]

5.2 contd.

ETHYLENE

Chemical formula: $\text{H}_2\text{C:CH}_2$

Molecular weight: 28.052

Normal boiling point: 169.43 K

Melting point: 104 K

Critical temperature: 282.65 K

Critical pressure: 5 060 kPa

Critical density: 220 kg/m³

T_{sat}, K	169.43	183	193	203	213	223	233	243	263	281	[9]
$p_{\text{sat}}, \text{kPa}$	101.3	213	341	518	755	1 063	1 453	1 938	3 240	4 899	[9]
$\rho_{\text{g}}, \text{kg/m}^3$	567.92	547.95	532.88	517.17	500.61	482.84	463.41	441.61	385.64	287.43	[9]
$\rho_{\text{g}}, \text{kg/m}^3$	2.09	4.24	6.60	9.81	14.01	19.47	26.58	36.12	69.58	152.70	[9]
$h_{\text{g}}, \text{kJ/kg}$	-662.49	-624.50	-600.49	-578.48	-552.50	-526.51	-498.48	-468.50	-396.51	-301.15	[9]
$h_{\text{g}}, \text{kJ/kg}$	-179.97	-163.61	-155.64	-151.12	-145.06	-141.54	-140.04	-140.71	-152.62	-213.38	[9]
$\Delta h_{\text{g},\text{g}}, \text{kJ/kg}$	482.52	460.89	444.85	427.36	407.44	384.97	358.44	327.79	243.89	94.56	[9]
$c_{p,\text{g}}, \text{kJ/(kg K)}$	2.32	2.46	2.54	2.61	2.67	2.73	2.80	2.93	3.89		[9]
$c_{p,\text{g}}, \text{kJ/(kg K)}$	1.31	1.35	1.40	1.47	1.56	1.67	1.82	2.02	2.91		[9]
$\eta_{\text{g}}, \mu\text{Ns/m}^2$	162.0	138.5	124.1	112.1	102.6	94.4	86.4	77.6	55.9	28.7	[4]
$\eta_{\text{g}}, \mu\text{Ns/m}^2$	6.04	6.56	6.96	7.37	7.81	8.29	9.82	9.44	11.30	16.25	[9]
$\lambda_{\text{g}}, (\text{mW/m}^2)/(\text{K/m})$	192	178	168	158	147	137	126	116	94.7	77.0	[2]
$\lambda_{\text{g}}, (\text{mW/m}^2)/(\text{K/m})$	6.44	7.62	8.62	9.71	11.0	12.4	14.0	15.9	21.9		[9]
Pr_{g}	1.96	1.91	1.88	1.85	1.86	1.88	1.92	1.96	2.30		[12]
Pr_{g}	1.23	1.16	1.13	1.11	1.10	1.11	1.14	1.20	1.50		[12]
$\sigma, \text{mN/m}$	16.46	13.99	12.23	10.52	8.88	7.29	5.78	4.35	1.80	0.16	[6]
$\beta_{\text{e},\text{g}}, \text{kK}^{-1}$	2.52	2.83	3.12	3.47	3.88	4.50	5.40	6.70	10.4		[10]

5.2 contd.

ETHYLENE

Chemical formula: $\text{H}_2\text{C:CH}_2$

Molecular weight: 28.052

Normal boiling point: 169.43 K

Melting point: 104 K

Critical temperature: 282.65 K

Critical pressure: 5 060 kPa

Critical density: 220 kg/m³

T_{sat}, K	169.43	183	193	203	213	223	233	243	263	281	[9]
$p_{\text{sat}}, \text{kPa}$	101.3	213	341	518	755	1 063	1 453	1 938	3 240	4 899	[9]
$\rho_{\text{g}}, \text{kg/m}^3$	567.92	547.95	532.88	517.17	500.61	482.84	463.41	441.61	385.64	287.43	[9]
$\rho_{\text{g}}, \text{kg/m}^3$	2.09	4.24	6.60	9.81	14.01	19.47	26.58	36.12	69.58	152.70	[9]
$h_{\text{g}}, \text{kJ/kg}$	-662.49	-624.50	-600.49	-578.48	-552.50	-526.51	-498.48	-468.50	-396.51	-301.15	[9]
$h_{\text{g}}, \text{kJ/kg}$	-179.97	-163.61	-155.64	-151.12	-145.06	-141.54	-140.04	-140.71	-152.62	-213.38	[9]
$\Delta h_{\text{g},\text{g}}, \text{kJ/kg}$	482.52	460.89	444.85	427.36	407.44	384.97	358.44	327.79	243.89	94.56	[9]
$c_{p,\text{g}}, \text{kJ/(kg K)}$	2.32	2.46	2.54	2.61	2.67	2.73	2.80	2.93	3.89		[9]
$c_{p,\text{g}}, \text{kJ/(kg K)}$	1.31	1.35	1.40	1.47	1.56	1.67	1.82	2.02	2.91		[9]
$\eta_{\text{g}}, \mu\text{Ns/m}^2$	162.0	138.5	124.1	112.1	102.6	94.4	86.4	77.6	55.9	28.7	[4]
$\eta_{\text{g}}, \mu\text{Ns/m}^2$	6.04	6.56	6.96	7.37	7.81	8.29	9.82	9.44	11.30	16.25	[9]
$\lambda_{\text{g}}, (\text{mW/m}^2)/(\text{K/m})$	192	178	168	158	147	137	126	116	94.7	77.0	[2]
$\lambda_{\text{g}}, (\text{mW/m}^2)/(\text{K/m})$	6.44	7.62	8.62	9.71	11.0	12.4	14.0	15.9	21.9		[9]
Pr_{g}	1.96	1.91	1.88	1.85	1.86	1.88	1.92	1.96	2.30		[12]
Pr_{g}	1.23	1.16	1.13	1.11	1.10	1.11	1.14	1.20	1.50		[12]
$\sigma, \text{mN/m}$	16.46	13.99	12.23	10.52	8.88	7.29	5.78	4.35	1.80	0.16	[6]
$\beta_{\text{e},\text{g}}, \text{kK}^{-1}$	2.52	2.83	3.12	3.47	3.88	4.50	5.40	6.70	10.4		[10]

HELIUM

Chemical formula: He
 Molecular weight: 4.002 6
 Normal boiling point: 4.21 K
 Melting point: 0.95 K

Critical temperature: 5.19 K
 Critical pressure: 290 kPa
 Critical density: 69.3 kg/m³

	4.21	4.3	4.4	4.5	4.6	4.7	4.8	4.9	5.0	5.19	[1]
T_{sat}, K	4.21	4.3	4.4	4.5	4.6	4.7	4.8	4.9	5.0	5.19	[1]
$p_{\text{sat}}, \text{kPa}$	101.3	111	120	132	144	157	169	184	199	229	[1]
$\rho_{\text{g}}, \text{kg/m}^3$	125.0	123.6	122.0	119.5	117.0	114.4	111.0	106.5	101.0	69.3	[1]
$\rho_{\text{g}}, \text{kg/m}^3$	11.58	12.43	13.13	14.12	15.07	16.08	16.95	18.08	19.16		[111]
$h_{\text{g}}, \text{kJ/kg}$	0.00	0.42	0.50	0.53	0.57	0.62	0.69	0.82	1.02		[95]
$h_{\text{g}}, \text{kJ/kg}$	20.9	20.72	20.20	19.33	18.57	17.42	16.29	14.62	13.62		[85]
$\Delta h_{\text{g},\text{L}}, \text{kJ/kg}$	20.9	20.3	19.7	18.8	18.0	16.8	15.6	13.8	12.0		[1]
$c_{p,\text{L}}, \text{kJ/(kg K)}$	4.48	4.77	5.11	5.53	5.94	6.57	7.53	9.08	11.5		[1]
$c_{p,\text{g}}, \text{kJ/(kg K)}$	5.19	5.19	5.19	5.19	5.19	5.19	5.19	5.19	5.19		[30, 92]
$\eta_{\text{g}}, \mu\text{Ns/m}^2$	36.5	36.3	36.1	36.0	35.8	35.5	35.4	35.1	34.9		[25]
$\eta_{\text{g}}, \mu\text{Ns/m}^2$	1.09	1.11	1.13	1.16	1.18	1.20	1.22	1.25	1.27	1.31	[4, 93]
$\lambda_{\text{g}}, (\text{mW/m}^2)/(\text{K/m})$	31.2	32.4	33.9	35.4	37.0	38.7	40.5	42.3	44.3		[7]
$\lambda_{\text{g}}, (\text{mW/m}^2)/(\text{K/m})$	8.3	8.45	8.60	8.79	8.95	9.1	9.28	9.43	9.62		[31, 93]
Pr_{g}	5.23	5.37	5.44	5.62	5.75	6.19	6.58	7.95	9.06		[12]
Pr_{g}	0.68	0.68	0.68	0.68	0.68	0.68	0.68	0.69	0.69		[12, 93]
$\alpha, \text{mN/m}$	0.111	0.099	0.087	0.075	0.063	0.061	0.040	0.028	0.019		[6]
$\beta_{\text{e},\text{L}}, \text{kK}^{-1}$	117	144	177	214	256	306	384	528	806		[10]

5.2 contd.

HYDROGEN

Chemical formula: H_2
 Molecular weight: 2.016 0
 Normal boiling point: 20.38 K
 Melting point: 13.95 K

Critical temperature: 33.23 K
 Critical pressure: 1 316 kPa
 Critical density: 31.6 kg/m³

T_{sat}, K	20.38	21	23	25	27	29	30	31	32	33.23	
$p_{\text{sat}}, \text{kPa}$	101.3	121	204	321	479	685	808	946	1 100	1 316	[1]
$\rho_g, \text{kg/m}^3$	71.1	70.4	67.9	65.0	61.6	57.4	54.9	51.7	47.5	31.6	[1]
$\rho_g, \text{kg/m}^3$	1.31	1.56	2.49	3.88	5.81	8.60	10.5	13.0	16.6	31.6	[1]
$h_g, \text{kJ/kg}$	262	268	291	317	348	384	406	431	463	561	[1]
$h_g, \text{kJ/kg}$	718	721	729	732	730	719	710	694	671	561	[1]
$\Delta h_{g,p}, \text{kJ/kg}$	456	453	438	415	382	335	304	263	208		[1]
$c_{p,g}, \text{kJ/(kg K)}$	9.74	10.2	11.8	13.7	16.4	21.1	25.5	33.8	55.8		[1]
$c_{p,g}, \text{kJ/(kg K)}$	11.7	11.9	13.0	14.6	17.5	23.3	28.9	39.7	69.1		[1]
$\eta_g, \mu\text{Ns/m}^2$	12.7	12.0	10.5	9.05	7.84	6.76	6.27	5.67	5.00	3.38	[1]
$\eta_g, \mu\text{Ns/m}^2$	1.12	1.17	1.30	1.43	1.56	1.74	1.86	2.00	2.19	3.38	[1]
$\lambda_g, (\text{mW/m}^2)/(\text{K/m})$	119	121	126	127	122	112	106	100	91	60	[3]
$\lambda_g, (\text{mW/m}^2)/(\text{K/m})$	16.3	16.9	19.2	22	25	29	31	35	40	60	[3]
\Pr_g	1.04	1.02	0.99	0.98	1.05	1.27	1.51	1.92	3.07		[12]
\Pr_g	0.80	0.82	0.88	0.95	1.09	1.40	1.73	2.27	3.78		[12]
$\sigma, \text{mN/m}$	1.92	1.81	1.47	1.13	0.796	0.483	0.333	0.207	0.106		[1]
$\beta_{e,g}, \text{K}^{-1}$	15.9	16.8	20.6	26.3	35.1	52.0	68.4	95.3	172.9		[10]

METHANE^aChemical formula: CH₄

Molecular weight: 16.042

Normal boiling point: 111.42 K

Melting point: 90.66 K

Critical temperature: 190.55 K

Critical pressure: 4 641 kPa

Critical density: 162 kg/m³

T_{sat} , K	111.42	120	130	140	150	160	170	180	185	190	
p_{sat} , kPa	101	192	367	638	1 033	1 588	2 338	3 288	3 854	4 552	[1]
ρ_{g} , kg/m ³	424.3	412.0	396.7	379.8	361.0	339.3	312.3	271.9	240.0	182.0	[1]
ρ_{g} , kg/m ³	1.79	3.26	5.95	10.03	16.08	25.03	38.57	59.14	76.28	120.9	[1]
h_{g} , kJ/kg	716.3	747.0	784.1	821.9	860.0	901.4	948.4	1 011.1	1 057.0	1 133.4	[1]
h_{g} , kJ/kg	1 228.1	1 241.8	1 255.7	1 267.2	1 274.9	1 277.6	1 273.3	1 258.9	1 245.0	1 203.2	[1]
$\Delta h_{\text{g},\text{f}}$, kJ/kg	511.8	494.8	471.8	445.3	414.9	376.2	324.9	247.8	188	69.8	[1]
$c_{p,\text{g}}$, kJ/(kg K)	3.43	3.53	3.63	3.77	3.94	4.12	5.16	7.45	11.3	70.5	[3, 9]
$c_{p,g}$, kJ/(kg K)	2.07	2.11	2.19	2.33	2.53	2.90	3.62	5.95	6.33	277.5	[1, 11]
η_{g} , $\mu\text{Ns/m}^2$	106.5	86.05	71.65	61.26	52.24	44.54	37.69	30.98	26.92	19.34	[1]
η_{g} , $\mu\text{Ns/m}^2$	4.49	4.84	5.28	5.74	6.27	6.89	7.69	8.89	9.84	12.96	[1]
λ_{g} , (mW/m ²)/(K/m)	193	178	163	148	133	118	103	88	80	73	[2]
λ_{g} , (mW/m ²)/(K/m)	12.1	12.9	16.4	19.6	23.0	27.6	33.7	39.9	45.3	62.0	[9]
\Pr_{g}	1.88	1.70	1.60	1.56	11.55	1.56	1.89	2.62	3.80	18.8	[12]
\Pr_{g}	0.77	0.79	0.71	0.68	0.69	0.72	0.83	1.33	1.38	58.01	[12]
σ , mN/m	13.5	11.5	9.28	7.22	5.31	3.58	2.06	0.81	0.33	0.01	[6]
$\beta_{\text{e},\text{g}}$, K^{-1}	2.27	3.46	4.37	5.18	6.58	8.87	14.2	32.8	58.6	385	[10]

^aSee page 5.5.1-3 for definition of symbols and page 5.5.1-2 for discussion of interpolation methods.

5.2 contd.

METHANOL (METHYL ALCOHOL)

Chemical formula: CH_3OH

Molecular weight: 32.00

Normal boiling point: 337.85 K

Melting point: 175.15 K

Critical temperature: 513.15 K

Critical pressure: 7 950 kPa

Critical density: 275 kg/m³

T_{sat}, K	337.85	353.2	373.2	393.2	413.2	433.2	453.2	473.2	493.2	511.7	[1]
$p_{\text{sat}}, \text{kPa}$	101.3	178.4	349.4	633.3	1 076	1 736	2 678	3 970	5 675	7 775	[1]
$\rho_{\text{g}}, \text{kg/m}^3$	751.0	735.5	714.0	690.0	664.0	634.0	598.0	553.0	490.0	363.5	[1]
$\rho_{\text{g}}, \text{kg/m}^3$	1.222	2.084	3.984	7.142	12.16	19.94	31.86	50.75	86.35	178.9	[1]
$h_{\text{g}}, \text{kJ/kg}$	0.0	45	108	176	249	328	413	506			[84]
$h_{\text{g}}, \text{kJ/kg}$	1 101	1 115	1 130	1 144	1 171	1 171	1 169	1 151			[104]
$\Delta h_{\text{g},\text{g}}, \text{kJ/kg}$	1 101	1 070	1 022	968	922	843	756	645	482		[105]
$c_{\text{p},\text{g}}, \text{kJ/(kg K)}$	2.88	3.03	3.26	3.52	3.80	4.11	4.45	4.81			[6]
$c_{\text{p},\text{g}}, \text{kJ/(kg K)}$	1.55	1.61	1.69	1.83	1.99	2.20	2.56	3.65	5.40		[3]
$\eta_{\text{g}}, \mu\text{Ns/m}^2$	326	271	214	170	136	109	88.3	71.6	58.3	41.6	[1, 20, 106]
$\eta_{\text{g}}, \mu\text{Ns/m}^2$	11.1	11.6	12.4	13.1	14.0	14.9	16.0	17.4	20.1	26.0	[4, 21]
$\lambda_{\text{g}}, (\text{mW/m}^2)/(\text{K/m})$	191.4	187.0	181.3	178.5	170.0	164.0	158.7	153.0	147.3	142.0	[2]
$\lambda_{\text{g}}, (\text{mW/m}^2)/(\text{K/m})$	18.3	20.6	23.2	26.2	29.7	33.8	39.4	46.9	60.0	98.7	[2, 22, 107]
Pr_{g}	5.13	4.67	4.15	3.61	3.34	2.82	2.56	2.42			[12]
Pr_{g}	0.94	0.91	0.90	0.92	0.94	0.97	1.04	1.35	1.81		[12]
$\sigma, \text{mN/m}$	18.75	17.5	15.7	13.6	11.5	9.3	6.9	4.5	2.1	0.09	[1]
$\beta_{\text{e},\text{g}}, \text{kK}^{-1}$	0.42	1.20	1.69	2.00	2.49	3.15	4.21	6.40	17.2		[10]

NITROGEN

Chemical formula: N₂
 Molecular weight: 28.016
 Normal boiling point: 77.35 K
 Melting point: 63.15 K

Critical temperature: 126.25 K
 Critical pressure: 3 396 kPa
 Critical density: 304 kg/m³

T_{sat}, K	77.35	85	90	95	100	105	110	115	120	126	[1]
$p_{\text{sat}}, \text{kPa}$	101.3	290	360	540	778	1 083	1 467	1 940	2 515	3 357	[1]
$\rho_g, \text{kg/m}^3$	807.10	771.01	746.27	719.42	691.08	660.5	626.17	583.43	528.54	379.22	[1]
$\rho_g, \text{kg/m}^3$	4.621	9.833	15.087	22.286	31.989	44.984	62.578	87.184	124.517	237.925	[1]
$h_g, \text{kJ/kg}$	-120.8	-105.7	-95.6	-85.2	-74.5	-63.8	-51.4	-38.1	-21.4	17.4	[1]
$h_g, \text{kJ/kg}$	76.8	82.3	85.0	86.8	87.7	87.4	85.6	81.8	74.3	49.5	[1]
$\Delta h_{g,q}, \text{kJ/kg}$	197.6	188.0	180.5	172.2	162.2	150.7	137.0	119.9	95.7	32.1	[1]
$c_{p,g}, \text{kJ/(kg K)}$	2.064	2.096	2.140	2.211	2.311	2.467	2.711	3.180	4.347	[9]	
$c_{p,g}, \text{kJ/(kg K)}$	1.123	1.192	1.258	1.350	1.474	1.666	1.975	2.586	4.136	[9]	
$\eta_g, \mu\text{Ns/m}^2$	163	127	110	97.2	86.9	78.5	70.8	59.9	48.4	19.1	[4]
$\eta_g, \mu\text{Ns/m}^2$	5.41	5.60	6.36	6.80	7.28	7.82	8.42	9.25	10.68	19.1	[4, 9]
$\lambda_g, (\text{mW/m}^2)/(\text{K/m})$	136.7	122.9	112.0	104.0	95.5	88.0	80.2	70.4	62.8	52.8	[1, 9]
$\lambda_g, (\text{mW/m}^2)/(\text{K/m})$	7.54	8.18	9.04	9.77	10.60	11.69	14.50	20.76	30.91	51.11	[9]
\Pr_g	2.46	2.17	2.10	2.07	2.10	2.20	2.39	2.71	3.35	[12]	
\Pr_g	0.81	0.82	0.89	0.94	1.01	1.11	1.15	1.16	1.43	[12]	
$\sigma, \text{mN/m}$	8.85	7.20	6.16	4.59	3.67	2.79	1.98	1.18	0.52	0.01	[27, 28]
$\beta_{e,g}, \text{kK}^{-1}$	5.65	6.46	7.26	8.47	9.69	12.1	15.7	23.0	37.5	[10]	

5.2 contd.

OXYGEN

Chemical formula: O_2
 Molecular weight: 32.00
 Normal boiling point: 90.18 K
 Melting point: 54.35 K

Critical temperature: 154.77 K
 Critical pressure: 5 090 kPa
 Critical density: 405 kg/m³

T_{sat}, K	90.18	97	104	111	118	125	132	140	146	154	[1]
$p_{\text{sat}}, \text{kPa}$	101.3	196	352	583	908	1 348	1 924	2 782	3 591	3 939	[1]
$\rho_{\text{g}}, \text{kg/m}^3$	1 135.72	1 102.05	1 065.07	1 025.64	982.32	934.58	880.28	808.41	737.56	557.10	[1]
$\rho_{\text{g}}, \text{kg/m}^3$	4.48	8.23	14.14	22.79	35.03	52.05	75.81	116.12	163.34	304.41	[1]
$h_{\text{g}}, \text{kJ/kg}$	-133.4	-122.1	-110.3	-98.2	-85.4	-71.8	-57.8	-38.9	-23.2	10.6	[1]
$h_{\text{g}}, \text{kJ/kg}$	78.9	83.8	88.0	91.2	93.3	93.9	92.8	88.4	81.4	56.7	[1]
$\Delta h_{\text{g},\text{g}}, \text{kJ/kg}$	212.3	205.9	198.3	189.4	178.7	165.7	150.1	127.3	104.6	46.1	[1]
$c_{p,\text{g}}, \text{kJ/(kg K)}$	1.63	1.66	1.70	1.76	1.86	2.00	2.22	2.63	3.28		[1]
$c_{p,\text{g}}, \text{kJ/(kg K)}$	0.96	1.00	1.05	1.12	1.23	1.36	1.68	2.27	3.63		[9]
$\eta_{\text{g}}, \mu\text{Ns/m}^2$	195.83	161.75	136.55	116.80	101.20	89.00	80.15	69.66	60.65	42.48	[9]
$\eta_{\text{g}}, \mu\text{Ns/m}^2$	6.85	7.50	8.35	9.36	10.6	11.24	13.35	15.8	18.5	26.9	[9]
$\lambda_{\text{g}}, (\text{mW/m}^2)/(\text{K/m})$	148	139	130	121	111	102	92.5	82.0	71.2		[1]
$\lambda_{\text{g}}, (\text{mW/m}^2)/(\text{K/m})$	8.5	9.5	10.5	11.7	13.4	14.8	16.9	20.1	23.6	35.2	[9]
Pr_{g}	2.16	1.93	1.79	1.70	1.70	1.75	1.92	2.23	2.79		[12]
Pr_{g}	0.77	0.79	0.84	0.90	0.97	1.03	1.33	1.78	2.85	19.93	[12]
$\sigma, \text{mN/m}$	13.19	11.53	9.88	8.27	6.71	5.20	3.77	2.23	1.18	0.40	[6]
$\beta_{\text{e},\text{g}}, \text{kK}^{-1}$	4.26	4.71	5.39	6.30	7.38	9.65	11.9	17.6	29.0	545.0	[10]

PENTANE

Chemical formula: $\text{CH}_3(\text{CH}_2)_2\text{CH}_3$

Molecular weight: 72.151

Normal boiling point: 309.2 K

Melting point: 143.4 K

Critical temperature: 469.6 K

Critical pressure: 3 369 kPa

Critical density: 273.3 kg/m³

	309.2	335	350	365	380	395	410	425	440	469.6	[1]
ρ_s , kg/m ³	610.2	582.9	566.0	548.0	528.9	507.9	484.1	456.5	423.5	280.9	[1]
ρ_g , kg/m ³	3.00	6.36	9.41	13.51	18.99	26.11	36.21	49.73	68.96	184.1	[1]
h_g , kJ/kg	319.8	383.8	423.3	458.2	504.7	546.6	588.5	637.3	686.2	846.7	[15]
h_g , kJ/kg	678.0	721.1	744.3	767.6	790.8	814.1	837.4	855.9	876.9	846.7	[15]
$\Delta h_{g,0}$, kJ/kg	358.2	337.3	321.0	309.4	286.1	267.5	248.9	218.6	190.7		[15]
$c_{p,0}$, kJ/(kg K)	2.34	2.52	2.62	2.72	2.82	2.94	3.06	3.20	3.44		[55, 58]
$c_{p,g}$, kJ/(kg K)	1.79	1.96	2.05	2.16	2.28	2.48	2.66	2.96	3.37		[46, 20]
η_g , $\mu\text{Ns}/\text{m}^2$	196	159	140	123	108	95	83	72	60		[1]
η_g , $\mu\text{Ns}/\text{m}^2$	6.9	7.6	8.1	8.5	9.0	9.5	10.2	11.1	12.4		[1]
λ_g , (mW/m ²)/(K/m)	107	98	93	88	83	79	75	71	69	47	[46]
λ_g , (mW/m ²)/(K/m)	16.7	19.3	21.0	22.8	24.8	26.7	29.0	31.7	34.9	47	[46]
\Pr_g	4.29	4.09	3.94	3.80	3.67	3.53	3.36	3.16	2.84		[12]
\Pr_g	0.74	0.77	0.79	0.81	0.83	0.88	0.94	1.03	1.19		[12]
σ , mN/m	14.3	11.3	9.7	8.1	6.7	5.2	3.8	2.8	1.6		[51]
$\beta_{e,0}$, kK^{-1}	1.40	1.93	2.21	2.52	2.92	3.54	4.48	5.95	15.5		[10]

5.2 contd.

PROPANE

Chemical formula: $\text{CH}_3\text{CH}_2\text{CH}_3$

Molecular weight: 44.094

Normal boiling point: 231.10 K

Melting point: 85.47 K

Critical temperature: 370.00 K

Critical pressure: 4 264 kPa

Critical density: 225 kg/m³

T_{sat}, K	231.1	248.06	259.83	275.24	291.83	317.42	330.70	351.23	359.61	367.18	
$p_{\text{sat}}, \text{kPa}$	101	203	304	507	810	1 520	2 026	3 039	3 545	4 052	[1]
$\rho_{\text{g}}, \text{kg/m}^3$	582	562	549	528	504	460	434	381	347	300	[1]
$\rho_{\text{g}}, \text{kg/m}^3$	2.42	4.63	6.77	11.0	17.5	33.9	47.1	80.4	104	150	[1]
$h_{\text{g}}, \text{kJ/kg}$	421.2	459.7	485.2	522.5	563.1	631.8	672.8	745.7	781.7	829.0	[1]
$h_{\text{g}}, \text{kJ/kg}$	847.4	866.7	879.2	895.6	911.0	929.5	937.4	942.4	934.9	915.6	[1]
$\Delta h_{\text{g},\text{f}}, \text{kJ/kg}$	426.2	407.0	394.0	373.1	347.9	297.7	264.6	196.7	153.2	86.6	[1]
$c_{p,\text{g}}, \text{kJ/(kg K)}$	2.24	2.32	2.38	2.47	2.58	2.78	3.27	4.27	6.62		[1, 3]
$c_{p,\text{g}}, \text{kJ/(kg K)}$	1.37	1.51	1.65	1.88	2.27	3.37	4.14	6.16	7.01	11.42	[1, 9, 11]
$\eta_{\text{g}}, \mu\text{Ns/m}^2$	208.7	177.4	154.9	134.5	114.7	85.7	72.4	51.2	41.0	25.4	[4]
$\eta_{\text{g}}, \mu\text{Ns/m}^2$	6.0	7.0	7.3	7.5	8.5	9.6	10.3	12.1	14.9	20.1	[4]
$\lambda_{\text{g}}, (\text{mW/m}^2)/(\text{K/m})$	134	124	117	108	99	84	76	64	59		[6]
$\lambda_{\text{g}}, (\text{mW/m}^2)/(\text{K/m})$	10.7	12.8	14.1	15.9	17.8	21.7	23.9	28.1	31.0	36.1	[2, 14]
Pr_{g}	3.49	3.26	3.15	3.08	2.99	2.84	3.07	3.41	4.60		[12]
Pr_{g}	0.77	0.83	0.85	0.89	1.08	1.49	1.78	2.65	3.37	6.36	[12]
$\alpha, \text{mN/m}$	15.5	14.25	13.2	9.5	7.5	4.6	3.0	1.4	1.0	0.4	[6]
$\beta_{\text{g},\text{f}}, \text{kK}^{-1}$	2.01	2.21	2.45	2.90	3.60	5.19	6.52	15.2	23.7		[10]

TOLUENE

Chemical formula: $C_6H_5CH_3$

Molecular weight: 92.134

Normal boiling point: 383.78 K

Melting point: 178.16 K

Critical temperature: 594.0 K

Critical pressure: 4 050 kPa

Critical density: 290 kg/m³

T_{sat}, K	383.78	400	425	450	475	500	525	550	575	594.0	[1]
$p_{\text{sat}}, \text{kPa}$	101.3	158	285	487	776	1 230	1 820	2 570	3 450	4 050	[1]
$\rho_{\text{g}}, \text{kg/m}^3$	778	760	733	702	670	632	590	541	469	290	[1, 77]
$\rho_{\text{g}}, \text{kg/m}^3$	2.91	4.42	7.88	13.2	20.9	32.2	48.8	74.3	120.8	290	[62]
$h_{\text{g}}, \text{kJ/kg}$	336	381	432	488	551	604	667	734	808	899	[15]
$h_{\text{g}}, \text{kJ/kg}$	695	725	762	797	832	866	901	932	948	899	[15]
$\Delta h_{\text{g},\text{f}}, \text{kJ/kg}$	359	344	330	309	281	262	234	198	140		[15]
$c_{\text{p},\text{f}}, \text{kJ/(kg K)}$	1.81	1.88	1.96	2.07	2.21	2.38	2.59	2.86	3.34		[5]
$c_{\text{p},\text{g}}, \text{kJ/(kg K)}$	1.13	1.18	1.25	1.33	1.42	1.54	1.71	2.04	3.33		[63, 62]
$\eta_{\text{g}}, \mu\text{Ns/m}^2$	251	220	183	153	134	118	104	92	82	50	[1, 25]
$\eta_{\text{g}}, \mu\text{Ns/m}^2$	9.0	9.5	10.1	10.7	11.4	12.5	13.7	15.0	17.2	50	[1, 14]
$\lambda_{\text{g}}, (\text{mW/m}^2)/(\text{K/m})$	113	108	103	98	92	86	79	72	65	37.8	[1, 7]
$\lambda_{\text{g}}, (\text{mW/m}^2)/(\text{K/m})$	11.1	12.3	14.2	16.0	17.8	19.8	21.9	24.4	27.8	37.8	[64, 22]
Pr_{g}	4.02	3.83	3.48	3.23	3.22	3.27	3.41	3.65	4.21		[12]
Pr_{g}	0.92	0.91	0.89	0.89	0.91	0.97	1.07	1.25	2.06		[12]
$\sigma, \text{mN/m}$	18.0	16.3	13.8	11.4	8.99	6.74	4.62	2.66	0.95		[65]
$\beta_{\text{e},\text{g}}, \text{kK}^{-1}$	1.38	1.43	1.67	2.07	2.52	3.11	3.98	6.15	14.3		[10]

5.3 Thermophysical Properties of refrigerants

Ammonia (NH₃), Saturated Vapour

<i>T</i> (K)	<i>ρ</i> (kg/m ³)	<i>c_p</i> (kJ/kgK)	<i>η · 10⁷</i> (Ns/m ³)	<i>v · 10⁶</i> (m ² /s)	<i>λ · 10³</i> (W/mK)	<i>δ · 10⁶</i> (m ³ /s)	<i>Pr</i>
300	0.6894	2.158	101.5	14.7	24.7	16.6	0.887
320	0.6448	2.170	109	16.9	27.2	19.4	0.870
340	0.6059	2.192	116.5	19.2	29.3	22.1	0.872
360	0.5716	2.221	124	21.7	31.6	24.9	0.872
380	0.5410	2.254	131	24.2	34.0	27.9	0.869
400	0.5136	2.287	138	26.9	37.0	31.5	0.853
420	0.4888	2.322	145	29.7	40.4	35.6	0.833
440	0.4664	2.357	152.5	32.7	43.5	39.6	0.826
460	0.4460	2.393	159	35.7	46.3	43.4	0.822
480	0.4273	2.430	166.5	39.0	49.2	47.4	0.822
500	0.4101	2.467	173	42.2	52.5	51.9	0.813
520	0.3942	2.504	180	45.7	54.5	55.2	0.827
540	0.3795	2.540	186.5	49.1	57.5	59.7	0.824
560	0.3708	2.577	193	52.0	60.6	63.4	0.827
580	0.3533	2.613	199.5	56.5	63.8	69.1	0.817

Ammonia, Saturated Liquid

<i>T</i> (°C)	<i>ρ</i> (g/cm ³)	<i>c_p</i> (kJ/kg · K)	<i>η</i> (kg/s · m)	<i>v</i> (cm ² /s)	<i>λ</i> (W/m · K)	<i>δ</i> (cm ² /s)	<i>Pr</i>
-50	0.704	4.46	3.06×10^{-4}	4.35×10^{-3}	0.547	1.74×10^{-3}	2.50
-25	0.673	4.49	2.58×10^{-4}	3.84×10^{-3}	0.548	1.81×10^{-3}	2.12
0	0.640	4.64	2.39×10^{-4}	3.73×10^{-3}	0.540	1.82×10^{-3}	2.05
25	0.604	4.84	2.14×10^{-4}	3.54×10^{-3}	0.514	1.76×10^{-3}	2.01
50	0.564	5.12	1.86×10^{-4}	3.30×10^{-3}	0.476	1.65×10^{-3}	2.00

Refrigerant 134a (1, 1, 1, 2 – tetrafluoroethane)

Source: ASHRAE

Temp ^a °C	Pressure MPa	Density kg/m ³	Enthalpy kJ/kg				Specific Heat c _p kJ/(kg·K)		Velocity of Sound m/s	Viscosity μPa·s		Thermal Cond mW/(m·K)		Surface Tension mN/m	Temp °C
			Liquid	Vapor	Liquid	Vapor	Vapor	Liquid		Liquid	Vapor	Liquid	Vapor		
-30.00	0.08436	1385.9	161.10	380.45	1.260	0.771	145.	430.4	9.62	107.3	9.16	16.13	30.00		
-28.00	0.09268	1380.0	163.62	381.70	1.264	0.778	145.	418.0	9.71	106.3	9.35	15.83	28.00		
-26.07b	0.10132	1374.3	166.07	382.90	1.268	0.784	146.	406.4	9.79	105.4	9.52	15.54	26.07		
-26.00	0.10164	1374.1	166.16	382.94	1.268	0.785	146.	406.0	9.79	105.4	9.53	15.53	26.00		
-24.00	0.11127	1368.2	168.70	384.19	1.273	0.791	146.	394.6	9.88	104.5	9.71	15.23	24.00		
-22.00	0.12160	1362.2	171.26	385.43	1.277	0.798	146.	383.6	9.96	103.6	9.89	14.93	22.00		
-20.00	0.13268	1356.2	173.82	386.66	1.282	0.805	146.	373.1	10.05	102.6	10.07	14.63	20.00		
-18.00	0.14454	1350.2	176.39	387.89	1.286	0.812	146.	363.0	10.14	101.7	10.24	14.33	18.00		
-16.00	0.15721	1344.1	178.97	389.11	1.291	0.820	147.	353.3	10.22	100.8	10.42	14.04	16.00		
-14.00	0.17074	1338.0	181.56	390.33	1.296	0.827	147.	344.0	10.31	99.9	10.59	13.74	14.00		
-12.00	0.18516	1331.8	184.16	391.55	1.301	0.835	147.	335.0	10.40	99.0	10.76	13.45	12.00		
-10.00	0.20052	1325.6	186.78	392.75	1.306	0.842	147.	326.3	10.49	98.0	10.93	13.16	10.00		
-8.00	0.21684	1319.3	189.40	393.95	1.312	0.850	147.	318.0	10.58	97.1	11.10	12.87	8.00		
-6.00	0.23418	1313.0	192.03	395.15	1.317	0.858	147.	309.9	10.67	96.2	11.28	12.58	6.00		
-4.00	0.25257	1306.6	194.68	396.33	1.323	0.866	147.	302.2	10.76	95.3	11.45	12.29	4.00		
-2.00	0.27206	1300.2	197.33	397.51	1.329	0.875	147.	294.7	10.85	94.3	11.62	12.00	2.00		
0.00	0.29269	1293.7	200.00	398.68	1.335	0.883	147.	287.4	10.94	93.4	11.79	11.71	0.00		
2.00	0.31450	1287.1	202.68	399.84	1.341	0.892	147.	280.4	11.03	92.5	11.96	11.43	2.00		
4.00	0.33755	1280.5	205.37	401.00	1.347	0.901	147.	273.6	11.13	91.6	12.13	11.14	4.00		
6.00	0.36186	1273.8	208.08	402.14	1.353	0.910	147.	267.0	11.22	90.7	12.31	10.86	6.00		
8.00	0.38749	1267.0	210.80	403.27	1.360	0.920	147.	260.6	11.32	89.7	12.48	10.58	8.00		
10.00	0.41449	1260.2	213.53	404.40	1.367	0.930	146.	254.3	11.42	88.8	12.66	10.30	10.00		
12.00	0.44289	1253.3	216.27	405.51	1.374	0.939	146.	248.3	11.52	87.9	12.84	10.02	12.00		
14.00	0.47276	1246.3	219.03	406.61	1.381	0.950	146.	242.5	11.62	87.0	13.02	9.74	14.00		
16.00	0.50413	1239.3	221.80	407.70	1.388	0.960	146.	236.8	11.72	86.0	13.20	9.47	16.00		
18.00	0.53706	1232.1	224.59	408.78	1.396	0.971	146.	231.2	11.82	85.1	13.39	9.19	18.00		
20.00	0.57159	1224.9	227.40	409.84	1.404	0.982	145.	225.8	11.92	84.2	13.57	8.92	20.00		

b = boiling point. Critical temp = 101.03°C

5.3 contd.

Refrigerant 22 (CHClF₂), Saturated Vapour at 1 atm.

T (K)	ρ (kg/m ³)	c_p (kJ/kgK)	η (kg/sm)	ν (cm ² /s)	λ (W/mK)	δ (cm ² /s)	Pr
250	4.320	0.587	1.09×10^{-5}	0.025	0.008	0.032	0.80
300	3.569	0.647	1.30×10^{-5}	0.036	0.011	0.048	0.77
350	3.040	0.704	1.51×10^{-5}	0.050	0.014	0.065	0.76
400	2.650	0.757	1.71×10^{-5}	0.065	0.017	0.085	0.76
450	2.352	0.806	1.90×10^{-5}	0.081	0.020	0.105	0.77
500	2.117	0.848	2.09×10^{-5}	0.099	0.023	0.128	0.77

Refrigerant 22 (CHClF₂), Saturated Liquid^a

T (K)	p (bar)	ρ (g/cm ³)	c_p (kJ/kg · K)	η (kg/sm)	ν (cm ² /s)	λ (W/mK)	δ (cm ² /s)	Pr
180	0.037	1.545	1.058	6.47×10^{-5}	4.19×10^{-4}	0.146	8.93×10^{-4}	0.47
200	0.166	1.497	1.065	4.81×10^{-5}	3.21×10^{-4}	0.136	8.53×10^{-4}	0.38
220	0.547	1.446	1.080	3.78×10^{-5}	2.61×10^{-4}	0.126	8.07×10^{-4}	0.32
240	1.435	1.390	1.105	3.09×10^{-5}	2.22×10^{-4}	0.117	7.62×10^{-4}	0.29
260	3.177	1.329	1.143	2.60×10^{-5}	1.96×10^{-4}	0.107	7.04×10^{-4}	0.28
280	6.192	1.262	1.193	2.25×10^{-5}	1.78×10^{-4}	0.097	6.44×10^{-4}	0.28
300	10.96	1.187	1.257	1.98×10^{-5}	1.67×10^{-4}	0.087	5.83×10^{-4}	0.29
320	18.02	1.099	1.372	1.76×10^{-5}	1.60×10^{-4}	0.077	5.11×10^{-4}	0.31
340	28.03	0.990	1.573	1.51×10^{-5}	1.53×10^{-4}	0.067	4.30×10^{-4}	0.36

5.4 Properties of fuels and oils

Fuels, Liquids at $p \approx 1 \text{ atm}^*$

T (°C)	ρ (g/cm^3)	c_p (kJ/kgK)	η (kg/sm)	ν (cm^3/s)	λ (W/mK)	δ (cm^2/s)	Pr
Gasoline (Petro)							
20	0.751	2.06	5.29×10^{-4}	7.04×10^{-3}	0.1164	7.52×10^{-4}	9.4
50	0.721	2.20	3.70×10^{-4}	5.13×10^{-3}	0.1103	6.97×10^{-4}	7.4
100	0.681	2.46	2.25×10^{-4}	3.30×10^{-3}	0.1005	6.00×10^{-4}	5.5
150	0.628	2.74	1.56×10^{-4}	2.48×10^{-3}	0.0919	5.34×10^{-4}	4.6
200	0.570	3.04	1.11×10^{-4}	1.95×10^{-3}	0.0800	4.62×10^{-4}	4.2
Kerosene (Paraffin)							
20	0.819	2.00	1.49×10^{-3}	1.82×10^{-2}	0.1161	7.09×10^{-4}	25.7
50	0.801	2.14	9.56×10^{-4}	1.19×10^{-2}	0.1114	6.50×10^{-4}	18.3
100	0.766	2.38	5.45×10^{-4}	7.11×10^{-3}	0.1042	5.72×10^{-4}	12.4
150	0.728	2.63	3.64×10^{-4}	5.00×10^{-3}	0.0965	5.04×10^{-4}	9.9
200	0.685	2.89	2.62×10^{-4}	3.82×10^{-3}	0.0891	4.50×10^{-4}	8.5
250	0.638	3.16	2.01×10^{-4}	3.15×10^{-3}	0.0816	4.05×10^{-4}	7.8

JP-4 Fuel

$T, ^\circ\text{C}$	$\rho, \text{kg}/\text{m}^3$	$\eta, \text{Pa} \cdot \text{s}$	$\nu, \text{m}^2/\text{s}$	$C_p, \text{kJ}/(\text{kgK})$	$\lambda, \text{W}/\text{mK}$	Pr
-15	802	15.3 -04	19.1 -07	1.858	14.1 -02	20
0	789	11.2 -04	14.2 -07	1.926	14.0 -02	15
15	776	86.8 -05	11.2 -07	1.995	13.8 -02	13
30	763	70.1 -05	91.9 -08	2.063	13.7 -02	11
45	750	58.6 -05	78.2 -08	2.132	13.6 -02	9
60	737	50.4 -05	68.4 -08	2.201	13.5 -02	8
75	724	44.4 -05	61.3 -08	2.269	13.3 -02	8

5.4 contd.

Engine Oil, unused

T, °C	ρ , kg/m ³	η , Pa.s	v, m ² /s	C_p , kJ/kgK	λ , W/mK	Pr
0	898	38.3 -01	42.7 -04	1.788	14.7 -02	46 540
15	889	10.6 -01	12.0 -04	1.845	14.5 -02	13 530
30	881	36.9 -02	41.9 -05	1.905	14.3 -02	4 912
45	872	15.3 -02	17.5 -05	1.969	14.1 -02	2 130
60	863	73.2 -03	84.8 -06	2.035	14.0 -02	1 065
75	855	39.4 -03	46.1 -06	2.101	13.8 -02	598
100	840	17.2 -03	20.5 -06	2.214	13.6 -02	280
125	826	91.5 -04	11.1 -06	2.328	13.4 -02	159
150	811	56.4 -04	69.5 -07	2.440	13.2 -02	104

Hydraulic Fluid (MIL-H-5606) at 1bar

T, °C	ρ , kg/m ³	η , Pa · s	v, m ² /s	C_p , kJ/(kgK)	λ , W/mK	Pr
-15	879	70.6 -03	80.3 -06	1.737	12.7 -02	962
0	868	34.2 -03	39.4 -06	1.788	12.6 -02	483
15	858	19.2 -03	22.4 -06	1.845	12.4 -02	286
30	847	12.2 -03	14.4 -06	1.905	12.1 -02	192
45	836	84.4 -04	10.1 -06	1.969	11.7 -02	143
60	826	63.0 -04	76.3 -07	2.035	11.2 -02	114
75	815	49.9 -04	61.2 -07	2.101	10.8 -02	97

5.5 Thermophysical properties of metals

Appendix 5.5 Thermophysical properties of metals

Composition	Melting Point (K)	Properties at Various Temperatures (K)												
		Properties at 300 K					λ (W/mK)/ c_p (J/kgK)							
		ρ (kg/m ³)	c_p (J/kgK)	λ (W/mK)	$\alpha \cdot 10^6$ (m ² /s)	100	200	400	600	800	1000	1200	1500	2000
Aluminum Pure	933	2702	903	237	97.1	302 482	237 798	240 949	231 1033	218 1146				
Alloy 2024-T6 (4.5% Cu, 1.5% Mg, 0.6% Mn)	775	2770	875	177	73.0	65 473	163 787	186 925	186 1042					
Alloy 195, Cast (4.5% Cu)		2790	883	168	68.2			174	185	—				
Beryllium	1550	1850	1825	200	59.2	990 203	301 1114	161 2191	126 2604	105 2823	90.8 3018	78.7 3227	3519	
Bismuth	545	9780	122	7.86	6.59	16.5 112	9.62 120	7.04 127						
Boron	2573	2500	1107	27.0	9.76	190 128	55.5 600	16.8 1463	10.6 1892	9.60 2160	9.85 2338			
Cadmium	594	8650	231	96.8	48.4	203 198	99.3 222	94.7 242						
Chromium	2118	7160	449	93.7	29.1	159 192	111 384	90.9 484	80.7 542	71.3 581	65.4 616	61.9 682	57.2 779	49.4 937
Cobalt	1769	8862	421	99.2	26.6	167 236	122 379	85.4 450	67.4 503	58.2 550	52.1 628	49.3 733	42.5 674	
Copper Pure	1358	8933	385	401	117	482 252	413 356	393 397	379 417	366 433	352 451	339 480		
Commercial bronze (90% Cu, 10% Al)	1293	8900	420	52	14		42 785	52 460	59 545					
Phosphor gear bronze (89% Cu, 11% Sn)	1104	8780	355	54	17		41	65	74					
Cartridge brass (70% Cu, 30% Zn)	1188	8530	380	110	33.9	75	93	137	149					
Constantan (35% Cu, 45% Ni)	1493	8920	384	23	6.71	17 237	19 362	395 425						
Germanium	1211	5360	322	59.9	34.7	232 190	96.8 290	43.2 337	27.3 348	19.8 357	17.4 375	17.4 395		

Composition	Melting Point (K)	Properties at Various Temperatures (K)											
		Properties at 300 K					$\lambda (W/mK)/c_p (J/kgK)$						
		ρ (kg/m ³)	c_p (J/kgK)	λ (W/mK)	$\alpha \cdot 10^6$ (m ² /s)	100	200	400	600	800	1000	1200	1500
Gold	1336	19300	129	317	127	327 109	323 124	311 131	298 135	284 140	270 145	255 155	
Iridium	2720	22500	130	147	50.3	172 90	153 122	144 133	138 139	132 144	126 153	120 161	111 172
Iron Pure	1810	7870	447	80.2	23.1	134 216	94.0 384	69.5 490	54.7 574	43.3 680	32.8 975	28.3 509	32.1 654
Armcu (99.75% pure)	7870	447	72.7	20.7		95.6 215	80.6 384	65.7 490	53.1 574	42.2 680	32.3 975	28.7 609	31.4 634
Carbon steels													
Plain carbon (Mn \leq 1%, Si \leq 0.1%)	7854	434	60.5	17.7				56.7 487	48.0 559	39.2 685	30.0 1169		
AISI 1010	7832	434	63.9	18.8				58.7 487	48.8 559	39.2 685	31.3 1168		
Carbon-silicon (Mn \leq 1%, 0.1% $<$ Si \leq 0.6%)	7817	446	51.9	14.9				49.8 501	44.0 582	37.4 699	29.3 971		
Carbon-manganese- silicon (1% $<$ Mn \leq 1.65%, 0.1% $<$ Si \leq 0.6%)	8131	434	41.0	11.6				42.2 487	39.7 559	35.0 685	27.6 1090		
Chromium (low) steels													
$\frac{1}{2}$ Cr- $\frac{1}{2}$ Mo-Si (0.18% C, 0.65% Cr, 0.23% Mo, 0.6% Si)	7822	444	37.7	10.9				38.2 492	36.7 575	33.3 688	26.9 969		
1 Cr- $\frac{1}{2}$ Mo (0.16% C, 1% Cr, 0.54% Mo, 0.39% Si)	7858	442	42.3	12.2				42.0 492	39.1 575	34.5 688	27.4 969		
1 Cr-V (0.2% C, 1.02% Cr, 0.15% V)	7836	443	48.9	14.1				46.8 492	42.1 575	36.3 688	28.2 969		

Composition	Melting Point (K)	Properties at Various Temperatures (K)												
		Properties at 300 K				$\lambda (W/mK)/c_p (J/kgK)$								
		ρ (kg/m ³)	c_p (J/kgK)	λ (W/mK)	$\alpha \cdot 10^6$ (m ² /s)	100	200	400	600	800	1000	1200	1500	2000
Stainless steels														
AISI 302		8055	480	15.1	3.91			17.3	20.0	22.8	25.4			
AISI 304	1670	7900	477	14.9	3.95	9.2	12.6	16.6	19.8	22.6	25.4	28.0	31.7	606
AISI 316		8238	468	13.4	3.48	272	402	515	557	582	611	640	682	
AISI 347		7978	480	14.2	3.71			15.2	18.3	21.3	24.2			
Lead	601	11340	129	35.3	24.1	39.7	36.7	34.0	31.4					
Magnesium	923	1740	1024	156	87.6	169	159	153	149	146				
Molybdenum	2894	10240	251	138	53.7	179	143	134	126	118	112	105	98	90
Nickel Pure	1728	8900	444	90.7	23.0	164	107	80.2	65.6	67.6	71.8	76.2	82.6	
Nichrome (80% Ni, 20% Cr)	1672	8400	420	12	3.4	232	383	405	592	530	562	594	616	
Inconel X-750 (73% Ni, 15% Cr, 6.7% Fe)	1665	8510	439	11.7	3.1	8.7	10.3	13.5	17.0	20.5	24.0	27.6	33.0	
Niobium	2741	8570	265	53.7	23.6	55.2	52.6	55.2	58.2	61.3	64.4	67.5	72.1	79.1
Palladium	1827	12020	244	71.8	24.5	76.5	71.6	73.6	79.7	86.9	94.2	102	110	
Platinum Pure	2045	21450	133	71.6	25.1	77.5	72.6	71.8	73.2	75.6	78.7	82.6	89.5	99.4
Alloy 60Pt-40Rh (60% Pt, 40% Rh)	7900	16630	162	47	17.4	100	123	136	141	146	152	157	163	179

5.5 contd.

Composition	Melting Point (K)	Properties at Various Temperatures (K)													
		Properties at 300 K						$\lambda(\text{W/mK})/c_p(\text{J/kgK})$							
		ρ (kg/m ³)	c_p (J/kgK)	λ (W/mK)	$\alpha \cdot 10^6$ (m ² /s)	100	200	400	600	800	1000	1200	1500		
Rhenium	3453	21100	136	47.9	16.7	58.9 97	51.0 127	46.1 139	44.2 145	44.1 151	44.6 156	45.7 162	47.8 171	51.9 186	
Rhodium	2236	12450	243	150	49.6	186 147	154 220	146 253	136 274	127 293	121 311	116 327	110 349	112 376	
Silicon	1685	2330	712	148	19.2	884 259	264 556	98.9 790	61.9 867	42.2 913	31.2 946	25.7 967	22.7 992		
Silver	1235	10500	235	429	174	444 187	430 225	425 239	412 250	396 242	379 277	361 292			
Tantalum	3269	16600	140	57.5	24.7	59.2 110	57.5 133	57.8 144	58.6 146	59.4 149	60.2 152	61.0 155	62.2 160	64.1 172	65.6 189
Thorium	2023	11700	118	54.0	39.1	59.8 99	54.6 112	54.5 124	55.8 134	56.9 145	56.9 156	58.7 167			
Tin	505	7310	227	66.6	40.1	85.2 188	73.3 213	62.2 243							
Titanium	1953	4500	522	21.9	9.32	30.5 300	24.3 465	20.4 551	19.4 591	19.7 633	20.7 675	22.0 620	24.5 686		
Tungsten	3660	19300	132	174	68.3	208 87	186 122	159 137	137 142	125 145	118 148	113 152	107 157	100 167	95 176
Uranium	1406	19070	116	27.6	12.5	21.7 94	25.1 108	29.6 125	34.0 146	38.8 176	43.9 180	49.0 161			
Vanadium	2192	6100	489	30.7	10.3	35.8 258	31.3 430	31.3 515	33.3 540	35.7 563	38.2 597	40.8 645	44.6 714	50.9 867	
Zinc	693	7140	389	116	41.8	117. 297	118. 367	111. 402	103. 436						
Zirconium	2125	6370	278	22.7	12.4	33.2 205	25.2 264	21.6 300	28.7 322	21.6 342	23.7 362	26.0 344	28.8 344	33.0 344	

5.6 Thermophysical properties of nonmetallic solids

Composition	Melting Point (K)	Properties at Various Temperatures (K)												
		Properties at 300 K					λ (W/mK)/ c_p (J/kgK)							
		ρ (kg/m ³)	c_p (J/kgK)	λ (W/mK)	$\alpha \cdot 10^6$ (m ² /s)	100	200	400	600	800	1000	1200	1500	2000
Aluminum oxide, sapphire	2323	3970	765	46	15.1	450	82	324	18.9	13.0	10.5	—	—	—
Aluminum oxide, polycrystalline	2323	3970	765	36.0	11.9	133	55	940	1110	1180	1225	—	—	—
Beryllium oxide	2725	3000	1030	272	88.0	—	—	940	1110	1180	1225	—	—	—
Boron	2573	2500	1105	27.6	9.99	190	52.5	18.7	11.3	8.1	6.3	5.2	—	—
Boron fiber epoxy (30% vol) composite	590	2000	—	—	—	—	—	1490	1880	2135	2350	2555	—	—
k, \parallel to fibers				2.29	—	—	2.10	2.23	2.28	—	—	—	—	—
k, \perp to fibers				0.59	—	—	0.37	0.49	0.60	—	—	—	—	—
c_p			1122	—	—	—	364	757	1431	—	—	—	—	—
Carbon	—	—	—	—	—	—	—	—	—	—	—	—	—	—
Amorphous	1500	1950	—	1.60	—	—	0.67	1.18	1.89	2.19	2.37	2.53	2.84	3.48
Diamond, type IIa insulator	—	3500	509	2300	—	10000	4000	1540	—	—	—	—	—	—
Graphite, pyrolytic	2273	2210	—	—	1950	4970	3230	1390	892	667	534	448	357	262
$k \parallel$ to layers				5.70	—	16.8	9.23	4.09	2.68	2.01	1.60	1.34	1.08	0.81
k, \perp to layers				—	—	136	411	992	1406	1650	1793	1890	1974	2043
Graphite fiber epoxy (25% vol) composite	450	1400	709	—	—	—	—	—	—	—	—	—	—	—
k, \parallel heat flow				—	—	—	—	—	—	—	—	—	—	—
k, \parallel to fibers				11.1	—	—	5.7	8.7	13.0	—	—	—	—	—
k, \perp heat flow				—	—	—	—	—	—	—	—	—	—	—
k, \perp to fibers				0.87	—	—	0.46	0.68	1.1	—	—	—	—	—
c_p				—	—	—	337	642	1216	—	—	—	—	—
Pyroceram, Corning 9606	1623	2600	935	3.98	1.89	5.25	4.78	3.64	3.28	3.08	2.96	2.87	2.79	—
				—	—	—	908	1038	1122	1197	1264	1498	—	—

5.6 contd.

Composition	Melting Point (K)	Properties at 300 K						Properties at Various Temperatures (K)																	
		ρ (kg/m ³)	c_p (J/kgK)	λ (W/mK)	$\alpha \cdot 10^6$ (m ² /s)	100		200		400		600		800		1000		1200		1500		2000		2500	
						100	200	400	600	800	1000	1200	1500	2000	2500	100	200	400	600	800	1000	1200	1500	2000	2500
Silicon carbide	3100	3160	675	490	230	—	—	—	—	880	1050	1135	1195	1243	1310	87	58	30	—	—	—	—	—	—	—
Silicon dioxide, crystalline (quartz)	1883	2630				10.4	39	16.4	7.6	3.0	4.2														
						6.21	20.8	9.5	4.70	3.4	3.1														
			c_p	745			—	—	885	1075	1250														
Silicon dioxide, polycrystalline (fused silica)	1883	2220	745	1.38	0.834	0.69	1.14	1.51	1.75	2.17	2.87														4.00
Silicon nitride	2173	2400	691	16.0	9.65	—	—	13.9	11.3	9.88	8.76	8.00	7.16	6.20											
Sulfur	392	2070	708	0.206	0.141	0.165	0.185	403	606	778	937	1063	1155	1226											
Thorium dioxide	3573	9110	235	13	6.1	—	—	10.2	6.6	4.7	3.68	3.12	2.73	2.5											
						255	274	285	295	303	315	330													
Titanium dioxide, polycrystalline	2133	4157	710	8.4	2.8	—	—	7.01	5.02	3.94	3.46	3.28	3.05	2.80	2.55	2.30	2.15	2.00	1.85	1.70	1.55	1.40	1.25	1.10	1.00

5.7 Mechanical properties of ferrous alloys

Material	Density (g/cm^3)	Modulus of Elasticity ($\text{psi} \times 10^6$ (GPa))	Yield Strength [$\text{psi} (\text{MPa})$]	Tensile Strength [$\text{psi} (\text{MPa})$]	Ductility (%EL in 2 in.)	Poisson's Ratio	Electrical Conductivity [$(\text{O}-\text{m})^{-1} \times 10^7$]	Thermal Conductivity [W/m-K]	Coefficient Of thermal Expansion [$(^\circ\text{C})^{-1} \times 10^{-6}$]	Melting Temperature or Range ($^\circ\text{C}$)
Iron	7.87	30 (207)	19 (130)	38 (260)	45	0.29	10	80	11.8	1538
Gray cast iron	7.15	Variable	—	18 (125)	—	Variable	~1	46	10.8	•
Nodular cast iron	7.12	24 (165)	40 (275)	60 (415)	18	0.28	~1.5	33	11.8	•
Malleable cast iron	7.20–7.45	25 (172)	32 (220)	50 (345)	10	0.26	0.25–0.35	51	11.9	•
Low-carbon steel (1020)	7.86	30 (207)	43 (295)	57 (395)	37	0.30	5.9	52	11.7	1495–1520
Medium-carbon steel (1040)	7.85	30 (207)	51 (350)	75 (520)	30	0.30	5.8	52	11.3	1495–1505
High-carbon steel (1080)	7.84	30 (207)	55 (380)	89 (615)	25	0.30	5.6	48	11.0	1385–1475
Stainless steels										
Ferritic, type 446	7.50	29 (200)	50 (345)	80 (552)	20	0.30	1.5	21	10.4	1425–1510
Austenitic, type 316	8.00	28 (193)	30 (207)	80 (552)	60	0.30	1.4	16	16.0	1370–1400
Martensitic, type 410	7.80	29 (200)	40 (275)	70 (483)	30	0.30	1.8	25	9.9	1480–1530

• Dependent on composition.

5.8 Mechanical properties of non-ferrous alloys

Material	Density (g/cm ³)	Modulus of Elasticity [psi×10 ⁶ (GPa)]	Yield Strength [ksi(MPa)]	Tensile Strength [ksi(MPa)]	Ductility (%EL in 2 in.)	Poisson's Ratio	Electrical Conductivity [(Ω-m) ⁻¹ ×10 ⁶]	Thermal Conductivity (W/m-K)	Coefficient Of thermal Expansion ([°C] ⁻¹ ×10 ⁻⁶)	Melting Temperature or Range (°C)
Aluminum (>99.5)	2.71	10 (69)	2.5 (17)	8 (55)	25	0.33	36	231	23.6	646-657
Aluminum alloy 2014	2.80	10.5 (72)	14 (97)	27 (186)	18	0.33	29	192	22.5	507-638
Copper (99.95)	8.94	16 (110)	10 (69)	32 (220)	45	0.35	58	398	16.5	1085
Brass (70Cu-30Zn)	8.53	16 (110)	11 (75)	44 (303)	68	0.35	16	120	20.0	915-955
Bronze (92Cu-8Sn)	8.80	16 (110)	22 (152)	55 (380)	70	0.35	7.5	62	18.2	880-1020
Magnesium (>99)	1.74	6.5 (45)	6 (41)	24 (165)	14	0.29	17.5	122	27.0	650
Molybdenum (>99)	10.22	47 (324)	82 (565)	95 (635)	35	—	19.2	142	4.9	2610
Nickel (>99)	8.90	30 (207)	20 (138)	70 (483)	40	0.31	11.8	80	13.3	1454
Silver (>99)	10.49	11 (76)	8 (55)	18 (125)	48	0.37	56	418	19.0	961
Titanium (>99)	4.51	15.5 (107)	35 (240)	48 (330)	30	0.34	2.0	17	9.0	1670

Room-Temperature Properties in an Annealed State

5.9 Mechanical properties of ceramic materials

Material	Density (g/cm^3)	Modulus of Elasticity [$\text{psi} \times 10^6$ (GPa)]	Poisson's Ratio	Approximate Hardness (Knoop)	Modulus of Rupture [$\text{ksi} (\text{MPa})$]	Electrical Resistivity ($\Omega \cdot \text{m}$)	Thermal Conductivity (W/m·K)	Coefficient Of thermal Expansion [$(^\circ\text{C})^{-1} \times 10^{-6}$]	Melting Temperature or Range [$^\circ\text{C} (^\circ\text{F})$]
Alumina (Al_2O_3)	3.97	57 (393)	0.27	2100	40–80 (275–550)	$>10^{12}$	30	8.8 ^a	2050 (3720)
Magnesia (MgO)	3.58	30 (207)	0.36	370	15 ^b (105)	$>10^{12}$	48	13.5 ^a	2850 (5160)
Spinel (MgAl_2O_4)	3.55	36 (284)	—	1600	12–32 ^b (83–220)	—	15.0 ^a	7.6 ^a	2135 (3875)
Zirconia ^c (ZrO_2)	5.56	22 (152)	0.32	1200	20–35 ^b (138–240)	—	2.0	10.0 ^a	2500–2600 (4530–4710)
Fused silica (SiO_2)	2.2	11 (75)	0.16	500	16 (110)	$>10^{18}$	1.3	0.5 ^a	—
Soda-lime glass	2.5	10 (69)	0.23	550	10 (69)	$>10^{18}$	1.7	9.0 ^a	—
Borosilicate glass	2.23	9 (62)	0.20	—	10 (69)	$\sim 10^{13}$	1.4	3.3 ^a	—
Silicon carbide (SiC)	3.22	60 (414)	0.19	2500	65–75 ^b (450–520)	$\sim 10^{-2}$	90	4.7	2300–2500 ^c (4170–4530)
Silicon nitride (Si_3N_4)	3.44	44 (304)	0.24	2200	60–80 ^b (414–580)	$>10^{12}$	16–33 ^a	3.6 ^a	~1900 ^c (3450)
Titanium carbide (TiC)	4.92	67 (462)	—	2600	40–65 ^b (275–450)	$\sim 10^{-6}$	17.2	7.4	3160 (5720)

^a Mean value taken over the temperature range 0–1000°C.

^b Sintered and containing approximately 5% porosity.

^c Stabilized with CaO .

^d Mean value taken over the temperature range 0–300°C.

^e Sublimes.

Data are for Fully Dense Materials and at Room Temperature

unless noted otherwise.

5.10 Mechanical properties of polymers

Name/Repeat Unit	State	Density (g/cm ³)	Tensile Modulus [As(GPa)]	Tensile Strength at Break [As(MPa)]	Elongation At Break (%)	T _g (°C)	T _m (°C)	Thermal Conductivity (W/m·K)	Electrical Resistivity (Ω·m)	Coefficient Of Thermal Expansion [(°C) ⁻¹ ·10 ⁻⁴]
Thermoplastics										
Polyethylene [−CH ₂ − CH ₂] _n	High density, 70–80% crystalline	0.952–0.965 (1.07–1.09)	155–158 (22–31)	3.2–4.5 (22–31)	10–1200	−90	130–137	0.48	10 ¹¹ –10 ¹⁷	60–110
	Low density, 40–50% crystalline	0.917–0.932 (0.17–0.28)	25–41 (8.3–31.0)	1.2–4.5 (8.3–31.0)	100–650	−110	98–115	0.33	10 ¹¹ –10 ¹⁷	100–220
Polytetrafluoroethylene [−CF ₂ − CF ₂] _n	50–70% crystalline	2.14–2.20 (0.40–0.55)	58–80 (14–34)	2.0–5.0 (14–34)	200–400	−90	327	0.25	>10 ¹⁶	70–120
Polyvinyl chloride [−CH ₂ − CH − Cl] _n	Highly amorphous	1.30–1.58 (2.4–4.1)	350–600 (41–52)	6.0–7.5 (41–52)	40–80	75–105	212	0.18	—	50–100
Polypropylene [−CH ₂ − CH − CH ₃] _n	50–60% crystalline	0.90–0.91 (1.14–1.55)	165–225 (31–41)	4.5–6.0 (31–41)	100–600	−20	168–175	0.12	>10 ¹¹	80–100
Polystyrene [−CH ₂ − CH − C ₆ H ₅] _n	Amorphous	1.04–1.05 (2.28–3.28)	330–475 (36–52)	5.2–7.5 (36–52)	1.2–2.5	74–105	—	0.13	>10 ¹⁴	50–83
Polymethyl methacrylate [−CH ₂ − C(=O) − C ₂ H ₅ − O − CH ₃] _n	Amorphous	1.17–1.20 (2.24–3.24)	325–470 (48–76)	7–11 (48–76)	2–10	85–105	—	0.21	>10 ¹²	50–90

5.1.0 contd.

Name/Repeat Unit	State	Density (g/cm ³)	Tensile Modulus λ ₁₁ (GPa)	Tensile Strength at Break λ ₁₁ (MPa)	Elongation At Break (%)	T _g (°C)	T _m (°C)	Thermal Conductivity (W/m-K)	Electrical Resistivity (Ω-m)	Coefficient Of Thermal Expansion (°C) ⁻¹ ×10 ⁶
Nylon 6,6 Poly(hexamethylene adipamide)	30–40% crystalline	1.13–1.15	230–550 (1.58–3.79)	11–13.7 (76–94)	15–300	57	255–265	0.24	10 ¹¹ –10 ¹³	80
Polyethylene terephthalate (PET, a polyester)	0–30% crystalline	1.29–1.40	400–600 (2.76–4.14)	7.0–10.5 (48–72)	30–300	73–80	245–265	0.14	10 ¹¹	65
Polycarbonate (Polybisphenol-A carbonate)	Amorphous	1.20	345 (2.38)	9.5 (65.5)	110	150	—	0.20	10 ¹⁵	68
Thermosets										
Epoxy	Complex network, amorphous	1.11–1.40	350 (2.41)	4.0–13.0 (28–90)	3–6	—	—	0.19	~10 ¹⁴	45–65
Phenolic	Complex network, amorphous	1.24–1.32	400–700 (2.76–4.83)	5–9 (34–62)	1.5–2.0	—	—	0.15	10 ⁹ –10 ¹⁰	68
Polyester	Complex network, amorphous	1.04–1.46	300–640 (2.07–4.41)	6–13 (41–90)	<2	—	—	0.19	10 ¹¹	55–100

Sources and acknowledgements of property data

5.1 Properties of gases

Data for air, carbon monoxide, carbon dioxide, helium, hydrogen, nitrogen, oxygen and water vapour are from Incropera & de Witt: Fundamentals of Heat and Mass Transfer, 4th Edn., © 1996 John Wiley & Sons, Inc., reprinted with permission of John Wiley & Sons, Inc.

Data for air – Standard Atmosphere, are from Kays and Crawford: Convective Heat and Mass Transfer, © 1993 McGraw Hill, reprinted with permission of the McGraw Hill Companies, Inc.

5.2 Properties of liquids

Data for water, ethylene glycol and glycerine are from Incropera & de Witt: Fundamental of Heat and mass Transfer, 4th Edn., © 1996 John Wiley & Sons, Inc., reprinted with permission of John Wiley & sons, Inc.

All other liquid data are from Hewitt: Handbook of Heat Exchanger Design, © 1992 Begell House, reprinted with permission of Begell House, Inc.

5.3 Properties of refrigerants

Data for R22 are from Bejan: Heat Transfer: ©1993 by John Wiley & sons, Inc., reprinted with permission of John Wiley & Sons, Inc.

Data for R134a were compiled from ASHRAE data.

Data for Ammonia vapour are from Kays and Crawford: Convective Heat and Mass Transfer, © 1993 McGraw Hill, reprinted with permission of the McGraw Hill Companies, Inc.

Data for Ammonia liquid are from Bejan: Heat Transfer: ©1993 by John Wiley & sons, Inc., reprinted with permission of John Wiley & Sons, Inc.

5.4 Properties of fuels and oils

Data for gasoline and kerosene are from Bejan: Heat Transfer: ©1993 by John Wiley & sons, Inc., reprinted with permission of John Wiley & Sons, Inc.

Data for JP4 Hydraulic fluid and Engine Oil (unused) from Kays & London: Compact Heat Exchangers, 3rd Edn. 1998, © 1984 McGraw Hill Inc., reproduced by permission of Krieger Publishing company, Malabar, Florida, USA.

5.5 Thermal properties of metals, and

5.6 Thermophysical properties of nonmetallic solids

are from Incropera & de Witt: Fundamental of Heat and Mass Transfer, 4th Edn., © 1996 John Wiley & Sons, Inc., reprinted with permission of John Wiley & Sons, Inc.

5.7 Mechanical properties of ferrous alloys,

5.8 Mechanical properties of non-ferrous alloys,

5.9 Mechanical properties of ceramic materials, and

5.10 Mechanical properties of polymers

are from Callister, Materials Science and Engineering © 1994, John Wiley & Sons, Inc., reprinted with permission of John Wiley & Sons, Inc.

INDEX

- Acid**
 - condensing, 289
 - dew point, 296
- Additives**, 289
- Adhesion**
 - of particles, 284
- Aerospace**, 79
- Air**
 - properties, 342, 348, 353
- Air conditioning**, 230
- Alfa Laval**, 282
- ALPEMA**, 276, 312
- Aluminium**, 28, 268
- Ammonia**
 - Properties, 372
- Analysis**
 - balanced flows, 96, 112 et seq.
 - comparison of laminar etc., 146 et seq.
 - exergy, 83 et seq.
 - heat exchanger
 - design process, 257 et seq.
 - design for fouling, 289 et seq., 293 et seq.
 - imbalance of flow, 101
 - laminar flow, 137 et seq.
 - second law, 83
- Applications**, 1, 27 et seq., 156, 184, 290 et seq.
- aerospace, 79
- air conditioning, 1, 79 et seq., 230
- automotive, 79
- breweries, 282
- calorifiers, 282
- diesel recuperator, 296
- gas turbines, 2, 230
- sugar industry, 289
- Applied Coolant Technologies**, 286
- Area**
 - face, 133, 135, 143
- goodness factor**, 130, 144
- surface**, et seq., 9, 19 et seq., 36, 95, 177, 184, 203, 205, 206, 214 et seq., 242, 265, 297
- Argon**
 - properties, 354
- Aspect ratio**, 7 135
- Atmosphere**
 - properties, 348
- Automotive**, 1, 79
- Balanced flow**
 - analysis, 96, 112 et seq.
- Barriquand**, 289
- Benzene**
 - properties, 355
- Biocides**, 286
- Biological fouling**, 286 et seq.
- Biot number**, 20
- Boiling**, 20, 202, 247 et seq.
- Bond strength**, 268
- Boundary layer**, 17 et seq., 65, 146, 167, 182, 187
- Brazed plate heat exchanger**, 1, 57 et seq.
- Brazing**, 28, 29
- Brazing alloys**, 268
- Breweries**, 282
- 1-2 Butadiene**
 - properties, 352
- Butane**
 - properties, 356
- Calculations**
 - area (flow), 129
 - exergy analysis, 118
 - length, 128
 - operating parameter, 132
 - volume, 135
- Cal Gavin**, 18
- Calorifiers**, 282

- Carbon dioxide
 - properties, 343, 357
- Carbon monoxide
 - properties, 343
- Cathodic protection, 287
- Ceramics
 - properties, 385
- Chart-Pak, 71
- Chemical reaction fouling, 288
- Chemicals and petrochemicals, 290
- Cocurrent heat exchanger
 - analysis, 105, 204 et seq.
- Colburn factor, 4, 126
- Commissioning, 277
- Compacbloc heat exchanger, 43 et seq.
- Compact heat exchangers (see also heat exchangers)
 - core mass velocity, 126
 - correlations, 155
 - design, 201, 257 et seq.
 - entropy minimisation, 107 et seq.
 - heat transfer, 126 et seq.
 - sizing, 125 et seq.
 - surface comparison, 143 et seq.
 - types, 27 et seq., 155 et seq
- Compactness
 - basic aspect, 3 et seq., 13 et seq.
- Compact shell and tube exchanger, 63 et seq.
- Compacplate heat exchanger, 43 et seq.
- Composite curves, 120 et seq.
- Condensation, 20 et seq., 106, 202, 254 et seq.
 - dropwise, 282
 - acid, 289, 296
- Condensers, 32
 - flow parameters I, 255
- Conduction
 - in wall, 235 et seq.
- Control
- of conditions, 278
- Convective boiling
 - example, 247 et seq.
- Convex louvre fin, 192
- Core mass velocity, 126 et seq.
- Correlations
 - surfaces, 155 et seq.
- Corrosion, 280 et seq., 287, 296
- Corrugations, 179, 193
- Cost, 74 et seq.
- Counterflow heat exchanger
 - analysis, 96 et seq., 204 et seq., 239 et seq., 259 et seq.
- Crossflow heat exchanger, 204 et seq., 242 et seq.
- Cryogenics, 290
- Crystallisation fouling, 281
- Deposits, 298
- Descaling, 281
- Design methods
 - approach to design problem, 257 et seq.
 - E-NTU, 203 et seq.
 - fouling reduction, 293 et seq.
 - LMTD, 203, 210 et seq.
 - mechanical, 266 et seq.
- Diameter
 - hydraulic, 3, 117 et seq., 143
- Diesel recuperator
- Differential pressures, 266
- Diffusion bonding, 2, 35 et seq.
- Dip brazing, 31
- Distributors
 - thermal-hydraulic design, 229 et seq.
 - types, 229 et seq.
- Dittus-Boelter, 170
- Dowtherm A
 - properties, 358
- Dowtherm J
 - properties, 359
- Dropwise condensation, 282

- Ducts (as surfaces), 155 et seq.
 - circular, 157, 170 et seq.
 - entrance effects, 161 et seq.
 - friction factors, 157, 170
 - hydraulic diameter, 157
 - Nusselt number, 157, 172
 - semicircular, 169, 170
 - triangular, 158, 159, 168
 - turbulent/transitional flow, 168 et seq.
- Effectiveness**
 - heat exchanger, 97 et seq., 203 et seq.
 - inverse relationships, 209, 210
 - method, 203
- Electromagnetic descaling, 281
- Energy Efficiency Programme, 286
- Energy recovery
 - mechanical, 120
- Enhancement, 14 et seq.
- Entrance effects, 161 et seq.
 - losses, 226
- Entrance length
 - hydrodynamic, 162
 - thermal, 164
- Entropy, 84
 - generation, 93
 - minimisation, 107 et seq.
- ESDU, 313
- Ethane,
 - properties, 360
- Ethanol
 - properties, 361
- Ethylene glycol
 - properties, 351
- Ethylene
 - properties, 362
- Evaporation, 107 et seq.
- Exergy
 - analysis, 83 et seq.
 - application to exchangers, 92
 - definition, 88
- steady flow processes, 90
- Exit losses, 226 et seq.
- Exothermic reactions, 23
- Face area, 133, 143
- Fanning, 7, 126
- Ferrous alloys
 - properties, 383
- Fins, function of, 19 et seq.
 - plain, 177
 - offset strip fin, 178
 - wavy, 178
 - louvred, 184
 - convex louvred, 192
- Fin efficiency, 23, 222 et seq.
- Flow area
 - goodness factor, 111, 130, 143
 - imbalance, 101 et seq.
- Flow mixing, 17 et seq.
- Fluid inventory, 130
- Fluidised bed exchanger, 298
- Food and drink, 291
- Fouling, 276 et seq., 289 et seq.
 - biological, 286 et seq.
 - chemical reaction, 288 et seq.
 - crystallisation, 281 et seq.
 - effects, 295 et seq.
 - factors, 296 et seq.
 - reduction, 281 et seq.
 - scaling, 299
- Freezing, 288
- Friction factor, 7, 126, 157 et seq.
 - in ducts, 170 et seq.
 - louvred fins, 186 et seq.
 - offset strip fin (OSF), 178 et seq.
 - pressed plates, 194
 - wavy fins, 182 et seq.
- Friction losses
 - in distributor, 235
- Fuels
 - properties, 375
- Fully developed laminar flow, 156

- Gas turbines, 3
 - recuperators, 194
- Gasolene
 - properties, 375
- Gibbs function, 91
- Glass ceramic matrix, 163
- Glycerine
 - properties, 351
- Goodness factor, 111, 130, 143
- Graetz number, 17, 165
- GRETh, 24
- Headers
 - design, 229 et seq.
- Heat exchangers (see also 'Compact heat exchangers')
 - aspect ratio, 135
 - as reactor, 23 et seq., 69 et seq., 264 et seq.
 - cocurrent, 105 et seq., 204 et seq.
 - commissioning, 277
 - compact
 - design, 116 et seq., 257 et seq., 289 et seq.
 - entropy minimisation, 116 et seq.
 - condensation, 106 et seq.
 - corrosion, 280 et seq.
 - cost, 74
 - countercurrent, 96 et seq., 117, 204 et seq.
 - crossflow 204 et seq.
 - distributors, design of, 229 et seq.
 - effectiveness, 97 et seq., 203
 - enhancement, 14 et seq.
 - evaporation, 107 et seq.
 - exergy
 - face area, 133, 143
 - fluid inventory, 130
 - fouling, 28 et seq.
 - headers, design of, 229 et seq.
 - heat transfer in, 126 et seq., 137
 - hydraulic diameter, 117 et seq., 143
 - installation, 275 et seq.
 - laminar flow, 137
 - maintenance, 275 et seq.
 - material content, 20, 130
 - networks, 120
 - operation, 278
 - operating parameter, 131 et seq.
 - porosity, 130
 - pumping power, 136, 142
 - reliability, 74
 - sizing, 125 et seq., 140 et seq.
 - surfaces 143 et seq., 155 et seq.
 - thermal design, 201 et seq.
 - types, 143 et seq.
 - brazed plate, 1, 57 et seq.
 - marbond, 146,
 - microchannel, 146
 - PCHE, 35 et seq., 146, 197, 234
 - plate-fin, 143 et seq.
 - plate and frame, 193
 - plate and shell, 196
 - shell and tube, 13, 15
 - welded plate, 196 et seq.
 - weight, 136 et seq.
 - volume, 130, 133 et seq.
- Heat transfer
 - coefficient, 4 et seq.
 - enhancement, 14 et seq.
 - in exchangers, 126 et seq.
- Helium,
 - properties, 344, 363
- Helmholz function, 91
- HEXAG, 319
- HITRAN, 287
- HTFS, 320
- HTRI, 325
- Hydraulic diameter, 3, 117 et seq., 143, 157, 174

- Hydraulic testing, 277
- Hydrodynamic entrance length, 162
- Hydrogen
 - properties, 345, 364
- Hydromag (UK), 282
- INNEX, 289
- Installation, 275 et seq.
- Inventory (of fluid), 130
- Inverse relationships, 209
- Ion implantation, 282
- JP-4 fuel
 - properties, 375
- j factor, 4, 178 et seq.
- Kerosene
 - properties, 375
- Laminar flow
 - analysis, 6
 - comparison with conventional approach, 146 et seq.
 - entrance effects, 161 et seq.
 - examples, 138 et seq.
 - in ducts, 156 et seq.
- Length (flowpath), 128
- LMTD method, 210 et seq.
- Longitudinal conduction, 235 et seq.
- Losses
 - entry, 226 et seq.
 - exit, 226 et seq.
 - friction, 235
 - momentum, 235
- Lost work, 86 et seq.
- Louvred fins, 2, 184 et seq.
- Maintenance, 279 et seq.
- Manufacture
 - non-uniformity effects, 243
- Marbond, 24, 38 et seq., 69 et seq., 146, 234
- Material content
 - of exchanger, 20, 130
- Materials, 19, 27 et seq., 268, 287, 381
- Mechanical cleaning, 281
- Mechanical design, 266 et seq.
- Mechanical energy recovery, 120
- Metals
 - properties, 377
- Methane
 - properties, 365
- Methanol
 - properties, 366
- Micro-channel exchanger, 146
- Micro-fibres, 286
- Mixing, 17, 18
- Momentum losses, 235
- Monitoring
 - of performance, 278
- Multipass exchangers, 27 et seq.
 - design, 260 et seq.
 - wall conduction, 243
- Networks, 120 et seq.
- Nitrogen
 - properties, 346, 367
- NLAHX, 328
- Non-uniformity
 - of channels, 243, 247
- Nozzles, 230
- Nusselt number, 4
 - of ducts, 157, 172
 - pressed plates, 193
- Offset strip fin, 16, 178 et seq., 250 et seq.
- Oils
 - properties, 376
- Oil and gas processing, 291
- Operation of CHEs, 278
- Operating parameter, 131, 139 et seq.
 - example, 132

- Optimisation
 - via local rate equation, 107 et seq.
 - of surfaces, 22 et seq.
- Oxygen
 - properties, 346, 368
- Packinox exchanger, 48 et seq.
- Paper and board, 291
- Paraffin
 - properties, 375
- Particulate fouling, 284
 - adhesion, 286
- Passages
 - non-uniformities, 243, 247
- PCHE, 2, 35 et seq., 146, 197, 234, 267
- Peclet number, 235
- Pentane
 - properties, 369
- Perforated fin, 184, 247 et seq.
- Petrol
 - properties, 375
- Pinch, 205
- Plastic heat exchangers, 65 et seq.
- Plate-fin units, 27 et seq.
 - condensation in, 254 et seq.
 - distributors, 229 et seq.
 - fouling, 276
 - headers, 229 et seq.
 - hydraulic diameter, 174
 - pressure containment, 266 et seq.
 - surfaces, 174 et seq.
 - wall conduction, 235
- Plate and frame heat exchanger, 52 et seq.
- Plate heat exchangers, 1, 41 et seq., 193, 281 et seq.
- Plate and shell heat exchanger, 60 et seq.
 - surfaces, 196
- Platular exchange, 42 et seq.
- Polymerisation reactions, 288
- Polymers
 - properties, 386
 - (in exchangers), 64
- Porosity, 3, 130
- Porous surfaces, 20 et seq.
- Practical aspects, 275 et seq.
- Precipitation fouling, 281
- Pressed plate surfaces, 193
- Pressure containment, 266 et seq.
- Pressure drop
 - finite, 107 et seq.
 - in headers, 235 et seq.
 - laminar flow, 138
 - two-phase, 255 et seq.
 - zero analysis, 96 et seq.
- Prime mover applications, 79, 290
- Process integration, 2, 3
- Process intensification, 264
- Propane
 - properties, 370
- Properties
 - physical, 342 et seq.
- Pumping power, 136, 142
- Pumps, 293 et seq.
- Rate equation, 107 et seq.
- Reaction rates, 265
- Reactor heat exchangers, 2, 69 et seq.
 - fouling, 288
 - thermal design, 264 et seq.
- Recuperators, 2
- Refrigerants
 - Properties, 372-374
- Refrigeration applications, 79 et seq., 292
- Regenerators, 155
- Reliability, 74
- Retrofitting, 277
- Reynolds analogy, 16
- Ribs, 20 et seq.
- Rolls Laval exchanger, 39 et seq.

- Roughness, 20 et seq.
- Scaling, 8 et seq., 143, 288
- Scraped surfaces, 289
- Second Law analysis, 83
- Secondary surfaces (fins), 19, 177, 222
- Selection of surface, 74 et seq.
- Shape, 133 et seq.
- Shell and tube exchanger, 13, 63 et seq.
- Silting, 284
- Sizing of exchangers, 125 et seq., 133 et seq.
- Solder bonding, 31
- Solidification fouling, 288
- Soot blowers, 289
- Specific speed, 295
- Spiral exchanger, 61 et seq.
 - Recuperator, 2
- Stainless steel, 32 et seq., 268
- Stanton number, 4
- Stress corrosion cracking, 287
- Sugar industry, 289
- Superplastic forming, 39
- Surfaces
 - comparison, 143 et seq.
 - correlations, 155 et seq.
 - ducts, 155 et seq.
 - fins, 19 et seq.
 - optimisation, 22 et seq.
 - offset strip fin, 16, 17, 178, 250
 - plate-fin, 176 et seq.
 - plate and shell, 60, 196
 - pressed plate, 193 et seq.
 - selection, 74 et seq.
 - types, 155 et seq.
- Surface treatment, 282
- TEMA, 285, 297
- Testing (hydraulic), 277
- Textile applications, 291
- Thermal conductivity
- deposits, 298
- Thermal design, 201 et seq.
- Thermal entrance length, 164
- Thermodynamics
 - first Law, 84
 - second Law, 83
- Titanium, 39
- Toluene
 - properties, 371
- Transitional flow
 - in ducts, 170 et seq.
- Triangular ducts, 158, 163, 168
- Tube-fin exchanger, 34
- Tube inserts, 17, 18, 287, 289
- Turbulent flow
 - in ducts, 170 et seq.
- Two-phase flow
 - pressure drop, 255 et seq.
- Types of heat exchanger, 290 et seq.
 - Marbond, 146
 - micro-channel, 146
 - PCHE, 146
 - plate-fin, 28 et seq., 143 et seq.
 - plate and frame, 51 et seq.
 - plate and shell, 60 et seq.
 - shell and tube, 15, 63 et seq.
 - spiral, 61 et seq.
 - tube-fin, 34
 - tubular, 267
 - welded plate, 41 et seq.
- Types of surfaces, 155 et seq.
- University of Birmingham, 24, 286
- University of Newcastle, 24
- University of Surrey, 282
- Vacuum brazing, 57 et seq.
- Vicarb, 285
- Volume (of exchanger), 133, 135 et seq., 140
- Volume (of material), 22, 23, 130

Wall conductivity, 235 et seq.

Water

properties, 347, 349

Weight, 136, 264, 276

Welded plates, 1, 41 et seq., 196 et seq., 284

Wood pulp fibres, 287

Worked examples

convective boiling, 252 et seq.

exergy analysis, 118 et seq.

f/j for pressed plates, 195

flow area, 129

j-factor, 188, 195

laminar flow, 138, 140, 141

length calculation, 128

operating parameter, 132

thermal design, 262 et seq.

volume, 135

wall conduction, 241